

Overview

In most cases civil structures are placed on the ground. That segment of the structure which interfaces with the ground is called the foundation. In this chapter, we focus on a particular type of foundation called a shallow foundation. Shallow foundations are composed of footings which are plate type elements placed on the ground. Their function is to transmit the loads in the columns and walls to the ground. We describe the various types of shallow footings and identify the conditions under which each type is deployed. Then, we develop an analytical procedure for establishing the soil pressure distribution under a footing due to an arbitrary column loading. Given the soil pressure distribution, one can generate the shear and moment distribution in the footing and establish the peak values required for design. In this chapter, we describe how to determine these design values and also present various strategies for dimensioning shallow footings.

7.1 Introduction

7.1.1 Types of Foundations

Civil structures are viewed as having two parts. That part of the structure which is above ground is called the superstructure; the remaining part in contact with the ground is referred to as either the substructure or the foundation. Up to this point we have focused on the superstructure. Structural Engineers are responsible for the foundation design as well as the superstructure design. They are aided by Geotechnical Engineers who provide information on the soil properties such as the allowable soil bearing pressure at the site.

Figure 7.1 illustrates the different types of foundations. Shallow foundations are located near ground level. The structural loads are transferred directly to the soil

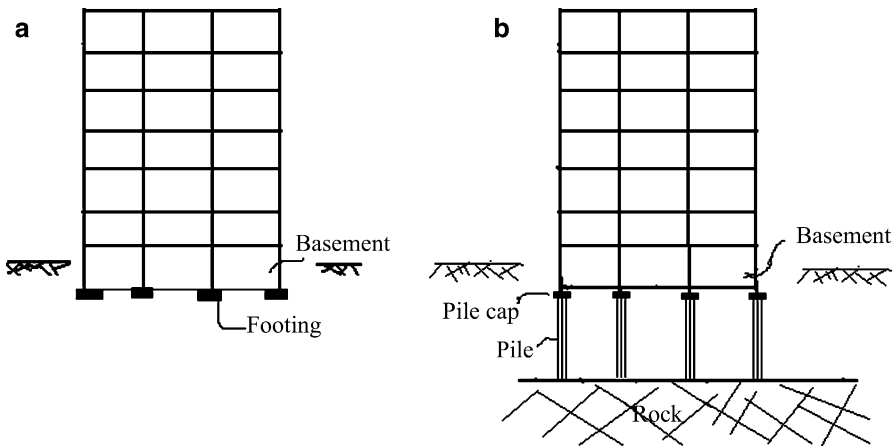


Fig. 7.1 Types of foundations. (a) Shallow foundation. (b) Deep foundation

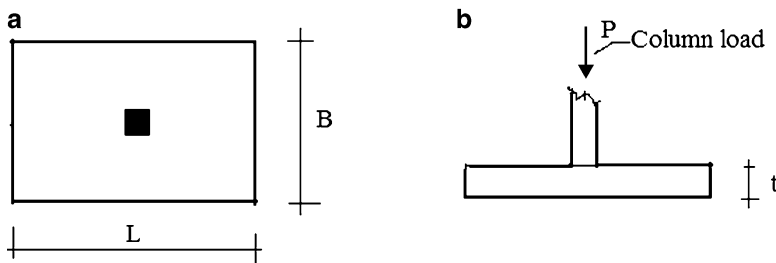


Fig. 7.2 Single footing—axial loading. (a) Plan. (b) Elevation

through plate type elements placed under the columns. These elements are called footings. This scheme is feasible only when the soil strength is adequate to resist the applied loading. If the soil near the surface is weak, it is necessary to transfer the loads to a deeper soil layer having adequate strength. Piles or caissons are typically used to transmit the loads through weak soil media. Basements which serve as underground parking facilities may also be incorporated in foundations.

7.1.2 Types of Shallow Foundations

A spread footing is a reinforced concrete plate type structural component that rests directly on the ground and supports one or more columns or walls. Different geometrical arrangements of footings are used, depending on the column spacing and soil strength. The simplest scheme is a single footing per column, shown in Fig. 7.2. One usually works with a square area. However, there sometimes are constraints such as proximity to a boundary line which necessitate shifting to a rectangular geometry. We describe later a procedure for determining the

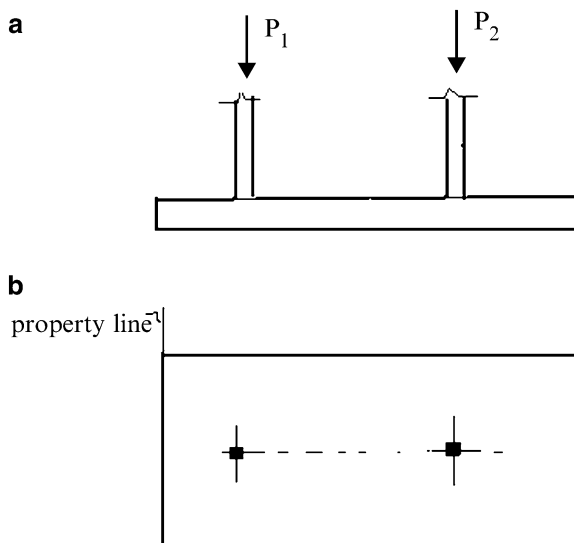


Fig. 7.3 Combined Footing layout. (a) Elevation. (b) Plan view

“dimensions” of the footing given certain geometric constraints. In what follows, we consider the column load to be an axial force. Later, we extend the analysis to deal with both axial force and bending moment.

When adjacent columns are located too close to each other such that their footings would overlap, or when one of the adjacent columns is located close to a property line, the adjacent footings are combined into a single “mega” footing, and this footing is designed to support the multiple column loads. Figure 7.3 illustrates this footing layout which is called a “*combined footing*.”

A different strategy is employed when the spacing between columns is large and one of the columns is located too close to a property line to support the entire column load with a single footing. It is necessary to shift some of the column load over to an adjacent footing by connecting the footings with a strap beam. This scheme is called a “*strap footing*” (see Fig. 7.4).

7.1.3 Soil Pressure Distribution

A vertical loading applied to the footing is resisted by soil pressure acting on the lower surface of the footing. The distribution of pressure depends on the type of soil at the site. Typical distributions for sand and clay type soils are shown in Fig. 7.5. In practice, we approximate the actual pressure distribution due to a concentric load with an “*average uniform*” distribution.

Depending on the column loading and the location of the column with respect to the centroid of the footing area, one of the distributions shown in Fig. 7.6a–c is normally assumed in order to establish the dimensions of the footing. A uniform

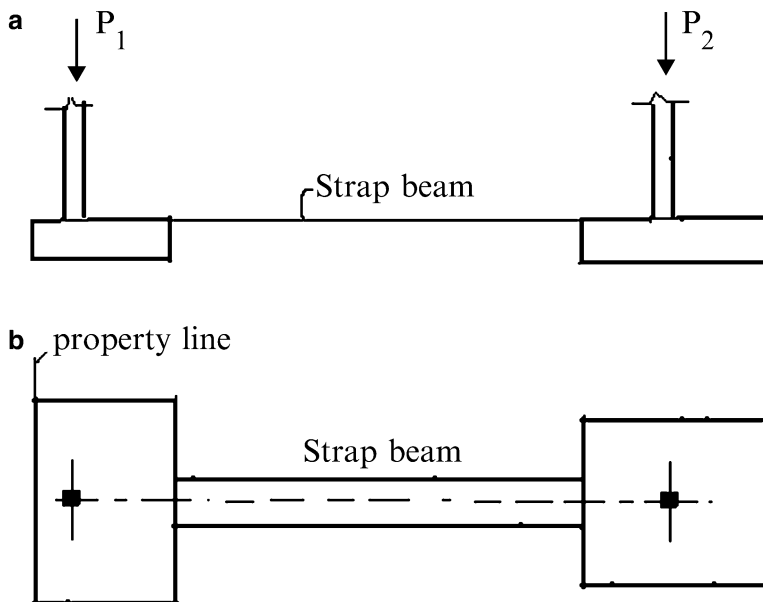


Fig. 7.4 Strap Footing layout. (a) Elevation. (b) Plan view

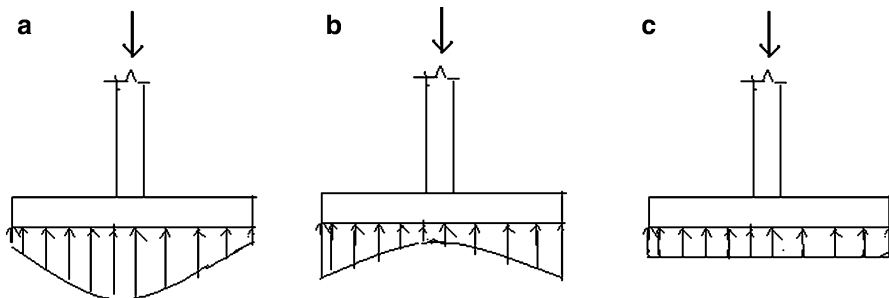


Fig. 7.5 Soil pressure distributions—concentric load. (a) Sandy soil. (b) Clayey soil. (c) Average soil pressure

distribution is the most desirable distribution. Since soil cannot resist tensile stress, one wants to avoid the case illustrated in Fig. 7.6c. We will describe a strategy for selecting the footing dimensions so as to avoid this situation in the following section.

The allowable pressure varies with the type of soil. Soil is a natural material in contrast to steel, which is manufactured with close quality control. Consequently, there is considerable variability in soil properties. We list typical allowable soil pressures for various types of soils in Table 7.1. These values are useful for estimating initial footing dimensions.

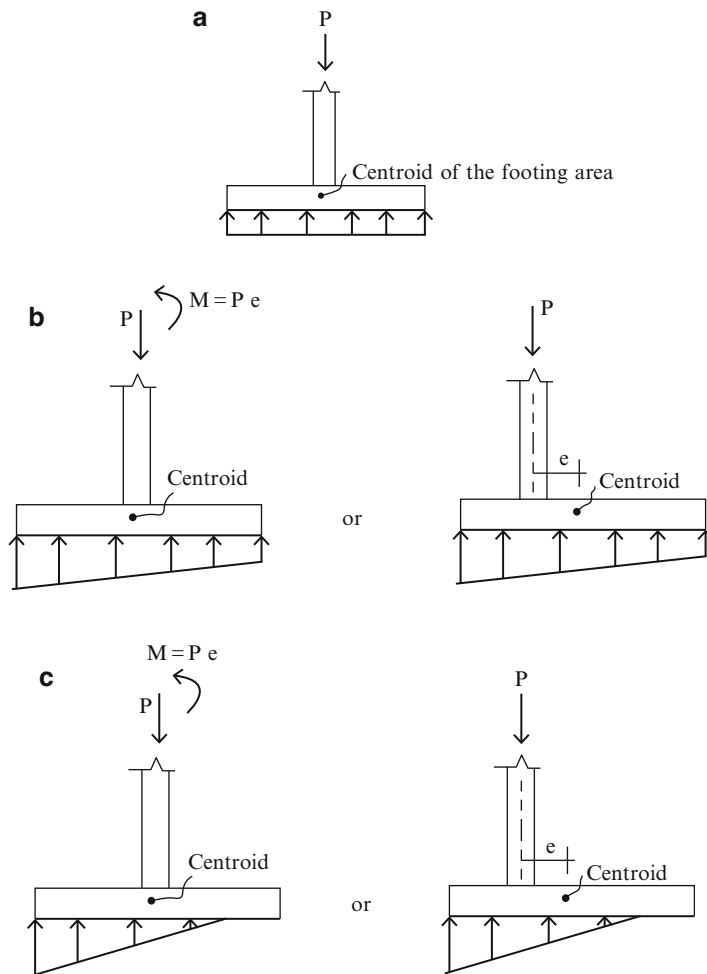


Fig. 7.6 Idealized pressure distributions. (a) Uniform. (b) Trapezoidal. (c) Triangular

Table 7.1 Allowable soil pressures—Reference Terzaghi and Peck [18]

Soil type	Allowable bearing pressure [kip/ft ² (kN/m ²)]
Compact coarse sand	8 (383)
Hard clay	8 (383)
Medium stiff clay	6 (287)
Compact inorganic sand	4 (191)
Loose sand	3 (144)
Soft sand/clay	2 (96)
Loose inorganic sand–silt mixture	1 (48)

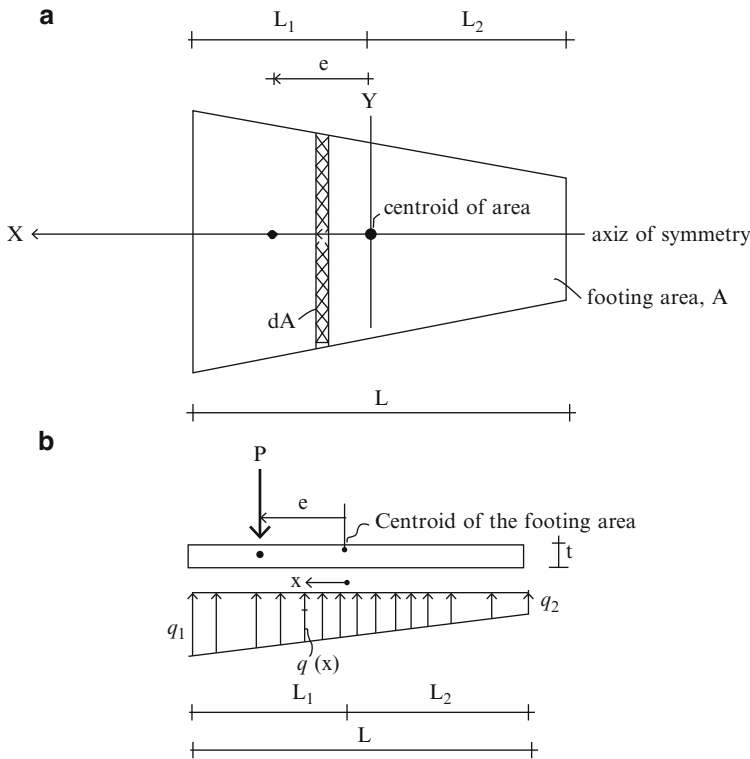


Fig. 7.7 Notation—Pressure distribution—single footing. (a) Plan. (b) Elevation

7.2 An Analytical Method for Evaluating the Soil Pressure Distribution under a Footing

We consider the single footing shown in Fig. 7.7. The force P represents the resultant of the column loading. We suppose it has an eccentricity e with respect to the centroid of the footing area. We also suppose the footing area is symmetrical with respect to the x axis and locate the area such that the column load is on the axis of symmetry. It follows that the pressure loading is symmetrical with respect to this axis. Taking the origin for x at the centroid of the footing area, we express the pressure as a linear function,

$$q(x) = b + ax \quad (7.1)$$

where a and b are unknown parameters. We determine these parameters by enforcing the equilibrium conditions for the footing.

Since x is measured from the centroid, the first moment of area vanishes. Then, $\int x dA = 0$. Requiring force and moment equilibrium to be satisfied, and noting that the column axial loading has an eccentricity, e , with respect to the centroid of the footing area, leads to the following expressions for b and a .

Vertical force equilibrium:

$$\begin{aligned} P &= \int q(x) dA = \int (b + ax) dA = b \int dA + a \int x dA = bA + 0 \\ &\quad \Downarrow \\ b &= \frac{P}{A} \end{aligned}$$

Moment equilibrium:

$$\begin{aligned} Pe &= \int q(x)x dA \\ &\quad \Downarrow \\ Pe &= \int (b + ax)x dA = b \int x dA + a \int x^2 dA = 0 + aI \\ &\quad \Downarrow \\ a &= \frac{Pe}{I} \end{aligned}$$

where I is the second moment of the footing area with respect to the Y -axis, $I = \int x^2 dA$. Substituting for a and b , (7.1) takes the form

$$q(x) = \frac{P}{A} + \frac{Pe}{I_y}x \quad (7.2)$$

The peak pressures are shown in Fig. 7.7b.

$$\begin{aligned} q_1 &= \left\{ \frac{P}{A} + \frac{(Pe)L_1}{I_y} \right\} \\ q_2 &= \left\{ \frac{P}{A} - \frac{(Pe)L_2}{I_y} \right\} \end{aligned} \quad (7.3)$$

One uses (7.3) to determine the pressure when the footing area is defined.

When the resultant acts at the centroid, $e = 0$ and the pressure distribution reduces to a uniform distribution.

$$q = q_1 = q_2 = \frac{P}{A} \quad (7.4)$$

When $e \neq 0$, the distribution is trapezoidal. As e increases, q_2 decreases. The critical state occurs when $q_2 = 0$. For this case (Fig. 7.8),

$$\begin{aligned} \frac{eL_2}{I_y} &= \frac{1}{A} \\ &\quad \Downarrow \\ e_{\text{critical}} &= \frac{I_y}{A} \frac{1}{L_2} \end{aligned} \quad (7.5)$$

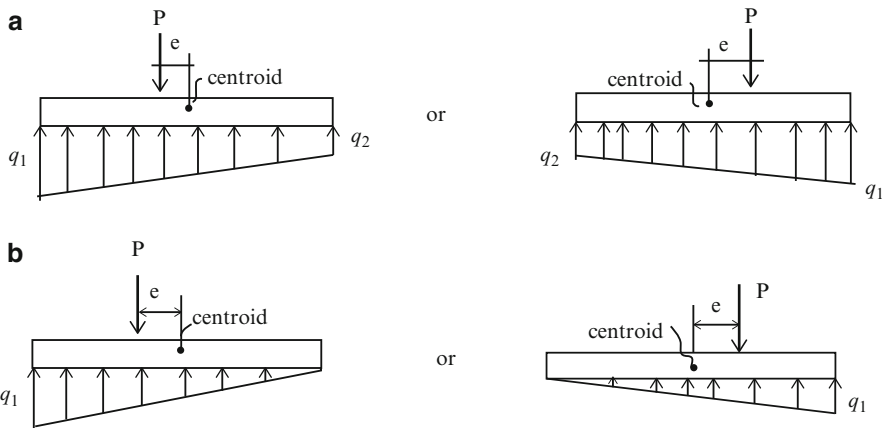


Fig. 7.8 Pressure distributions for $e \leq e_{\text{critical}}$. (a) $e < e_{\text{critical}}$. (b) $e = e_{\text{critical}}$

Applying this reasoning to a rectangular shape of width B and length L , and noting that

$$A = BL \quad I_y = \frac{BL^3}{12} \quad L_1 = L_2 = \frac{L}{2}$$

the expressions for the peak pressures take the form

$$\begin{aligned} q_1 &= \frac{P}{BL} + \frac{6Pe}{BL^2} \\ q_2 &= \frac{P}{BL} - \frac{6Pe}{BL^2} \end{aligned} \quad (7.6)$$

In this case, the critical value for e , which corresponds to either q_1 or q_2 equal to 0, is given by

$$e = e_{\text{critical}} = \frac{L}{6} \quad (7.7)$$

In order for the soil pressure to be compressive throughout the footing area, the point of application of the applied loading must be within a zone of width $L/3$ centered on the centroid. When loaded outside this region, (7.2) does not apply. In this case, the triangular distribution acting on a portion of the surface shown in Fig. 7.9d is used. The soil pressure adjusts its magnitude and extent such that the line of action of the resultant coincides with the line of action of the column force.

$$\begin{aligned} R &= P = q_1 \left(\frac{a}{2} B \right) \\ &\Downarrow \\ q_1 &= \frac{2P}{Ba} \end{aligned}$$

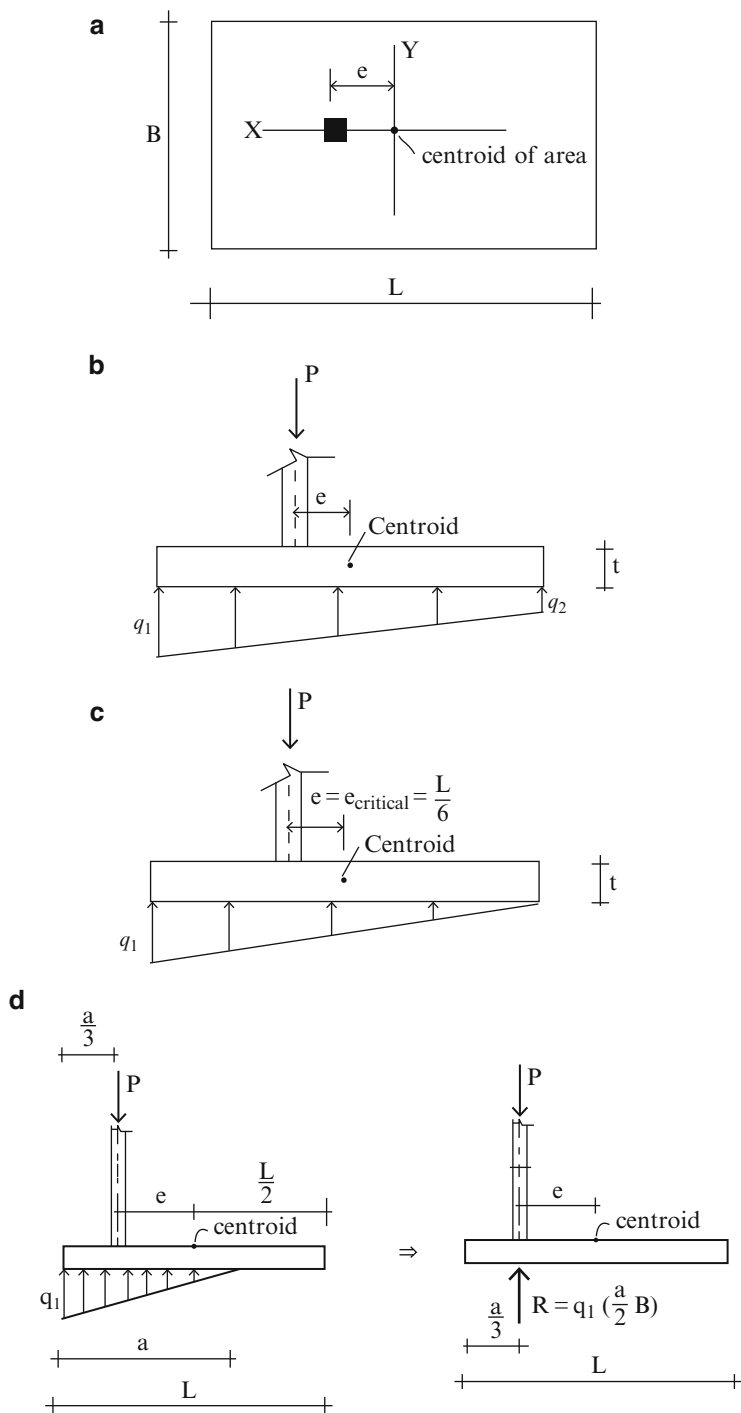


Fig. 7.9 (a) Plan—rectangular area. (b) Elevation $e < e_{\text{critical}}$. (c) Elevation $e = e_{\text{critical}}$. (d) Pressure distribution for $e > e_{\text{critical}}$

7.3 Dimensioning a Single Rectangular Footing

Normally, the column position is fixed by the geometry of the structure, and one can only adjust the location of the footing with respect to the column. We consider the case where the design goal is a uniform soil pressure. The optimal dimensions of the footing are achieved by locating the centroid of the footing on the line of action of the column force, i.e., by taking $e = 0$ in Fig. 7.7. The first choice is a square footing. If there is insufficient space in one direction, one can shift to a rectangular footing. If the design is still constrained by space restrictions, one can then follow a different strategy and work with a strap type footing which is discussed later.

We have shown that the soil pressure distribution is uniform for symmetrically positioned footings. The footing area is *determined using service loads*, P and the *effective soil pressure*, q_e which accounts for the weight of the footing and the soil above the footing. This notation is defined in Fig. 7.10. The relevant computations are

$$q_e = q_{\text{allowable}} - \gamma_{\text{conc.}} t - \gamma_{\text{soil}}(h - t) \approx q_{\text{allowable}} - \left(\frac{\gamma_{\text{conc.}} + \gamma_{\text{soil}}}{2} \right) h$$

$$A_{\text{required}} \geq \frac{P}{q_e} \rightarrow A = LB$$

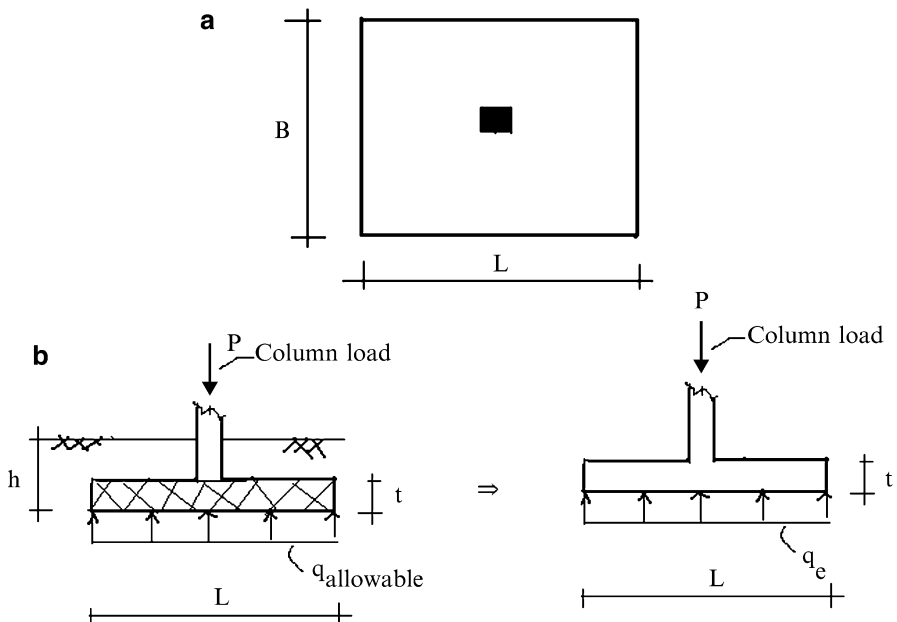


Fig. 7.10 Notation–effective soil pressure (q_e). (a) Plan. (b) Elevation

Current practice estimates the peak values of shear force and moment in the footing using the factored ultimate load P_u and determines the footing thickness and the required reinforcement steel area based on these values. Figure 7.11 illustrates this procedure for a single axial loaded footing. The expressions for the factored ultimate shear and moment are

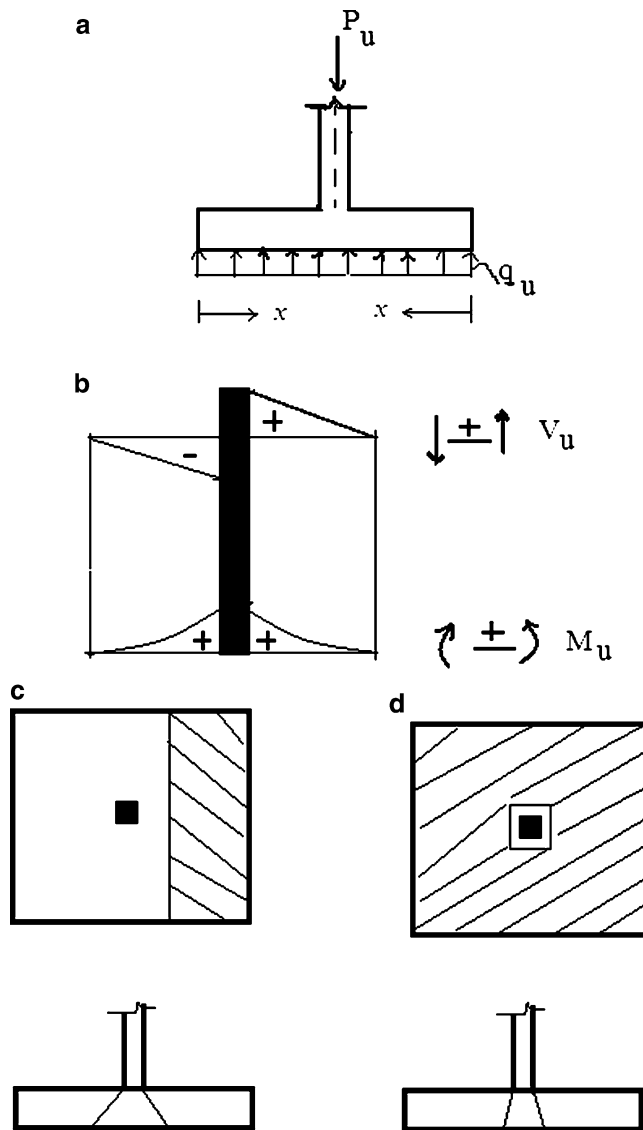


Fig. 7.11 Footing dimensioning process. (a) Factored soil pressure. (b) Shear and moment diagrams. (c) One way shear. (d) Punching shear

$$\begin{aligned} V_u(x) &= Bq_u x \\ M_u(x) &= \frac{Bq_u x^2}{2} \end{aligned} \quad (7.8)$$

where $q_u = \frac{P_u}{A}$. Positive bending moment requires reinforcing steel placed in two directions at the lower surface. One needs to check for two types of shearing actions, one way shear and punching shear. Figure 7.11 shows the location of the critical sections for shear. The distance parameter depends on the column type (steel, concrete). One needs to refer to the specific code for the value of the distance parameter.

Most footings are constructed using reinforced concrete. The location and magnitude of the steel reinforcement is dictated by the sense of the bending moment distribution (i.e., positive or negative). Noting that the function of the reinforcement is to provide the tensile force required by the moment, the moment diagrams shown in Fig. 7.11b require the reinforcement patterns defined in Fig. 7.12.

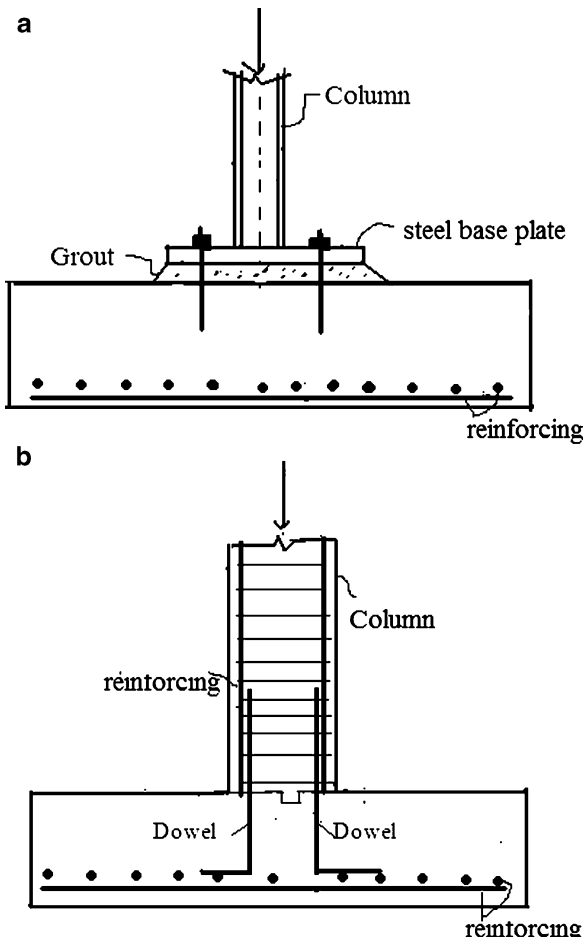


Fig. 7.12 Single Footing steel details. (a) Steel column. (b) Reinforced concrete column

The actual size/number of the rebar depends on the magnitude of the moment and particular design code used to dimension the member.

Figure 7.12 illustrates steel reinforcement for steel and concrete columns. A steel plate is welded to the base of a steel column, and anchored to the footing with bolts embedded in the concrete. Dowels are used to connect the longitudinal steel in the concrete column to the footing. Usually the column loading is purely axial and the support is considered to be simply supported. However, there are situations where moment as well as axial force is present in the column. The design strategy is the same for both cases.

Example 7.1 Single footing

Given: A 400 mm × 400 mm concentrically load column with axial dead load ($P_D = 890$ kN), and axial live load ($P_L = 1,070$ kN) to be supported on a shallow foundation. The effective soil pressure is $q_e = 165$ kN/m² (Figs. E7.1a, b).

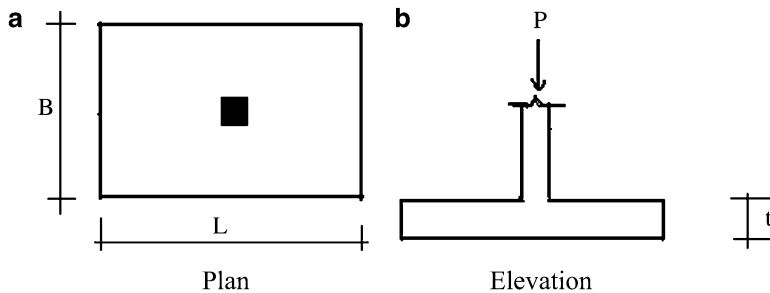


Fig. E7.1 Geometry and loading

Determine: The footing dimensions using service loads. Draw shear and moment diagrams using a factored load of $P_u = 1.2P_D + 1.6P_L$. Consider (a) A square footing, (b) A rectangular footing with $B = 3$ m.

Solution:

Footing dimensions

The required footing area is based on the service load and effective soil pressure.

$$P_{\text{service}} = (P_D + P_L) = 890 + 1,070 = 1,960 \text{ kN}$$

$$A_{\text{required}} = \frac{P_{\text{service}}}{q_e} = \frac{1,960}{165} = 11.88 \text{ m}^2$$

Assuming a square shape, the required dimension is $\sqrt{11.88} = 3.44 \text{ m}$

We use $L = B = 3.5 \text{ m}$.

Assuming a rectangular footing $B = 3 \text{ m}$, the required dimension is

$$L = \frac{11.88}{3} = 3.96 \text{ m. We use } L = 4 \text{ m}$$

Shear and moment distributions

The factored load is

$$P_u = 1.2P_D + 1.6P_L = 1.2(890) + 1.6(1,070) = 2,780 \text{ kN}$$

The corresponding factored soil pressure q_u and V_u, M_u are

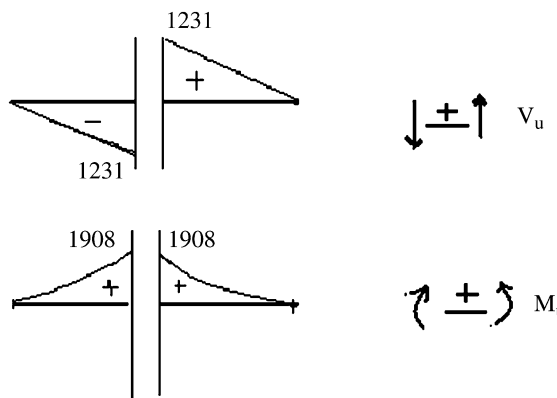
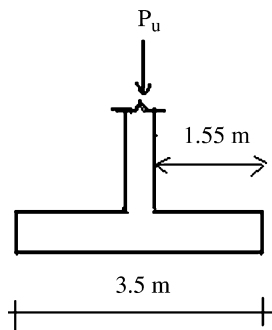
Square shape:

$$q_u = \frac{P_u}{LB} = \frac{2,780}{(3.5)(3.5)} = 226.94 \text{ kN/m}^2$$

$$V_{u\max} = 226.94 (3.5) (1.55) = 1,231 \text{ kN}$$

$$M_{u\max} = 226.94 (3.5) \frac{(1.55)^2}{2} = 1,908 \text{ kN m}$$

The shear and moment diagrams are plotted below.



Rectangular shape:

$$q_u = \frac{P_u}{LB} = \frac{2,780}{(3)(4)} = 231.67 \text{ kN/m}^2$$

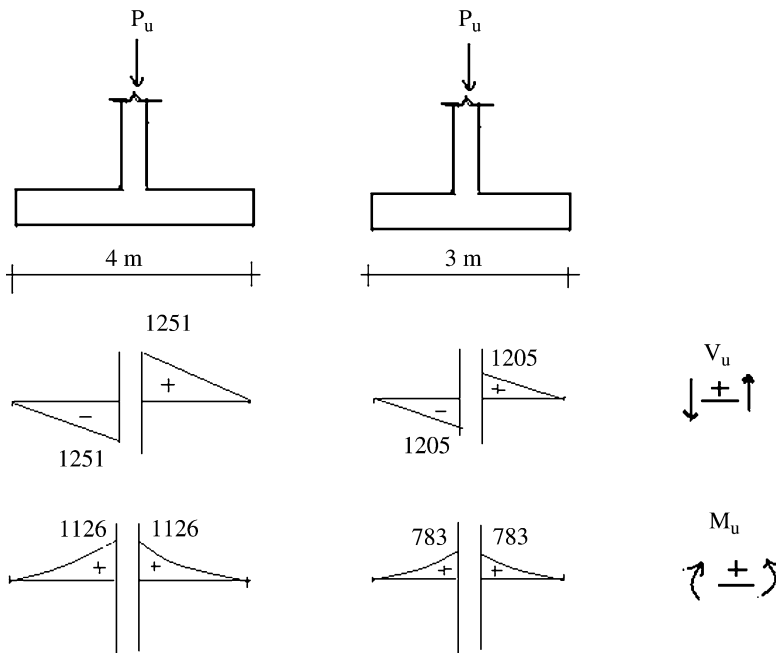
$$V_{u\max \text{ long}} = 231.67(3)(1.8) = 1,251 \text{ kN}$$

$$M_{u\max \text{ long}} = 231.67(3) \frac{(1.8)^2}{2} = 1,126 \text{ kN m}$$

$$V_{u\max \text{ short}} = 231.67(4)(1.3) = 1,205 \text{ kN}$$

$$M_{u\max \text{ short}} = 231.67(4) \frac{(1.3)^2}{2} = 783 \text{ kN m}$$

The shear and moment diagrams are plotted below.



Example 7.2 Dimensioning a footing under a column with eccentric loading.

Given: A 12 in. \times 12 in. column supporting the following loads: $P_D = 120$ kip, $P_L = 80$ kip, $M_D = 60$ kip ft, and $M_L = 40$ kip ft. The effective soil pressure is $q_e = 4.5$ kip/ ft^2 .

$$P = P_D + P_L = 120 + 80 = 200 \text{ kip}$$

$$M = M_D + M_L = 60 + 40 = 100 \text{ kip ft}$$

$$e = \frac{M}{P} = 0.5 \text{ ft}$$

Determine: Dimension square/rectangular footings for the following cases.

Case (a) the centerline of the column coincides with the centroid of the footing. M is counter clockwise (Fig. E7.2a).

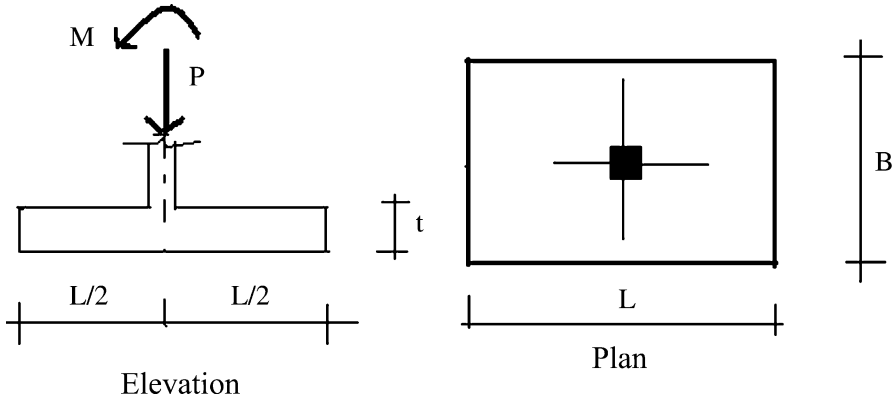


Fig. E7.2a Geometry and loading

Solution: Case (a)

Square footing ($L = B$): We use (7.6) and set $q_1 = q_e$

$$\frac{200}{L^2} + \frac{6(100)}{L^3} = 4.5 \Rightarrow L = 8 \text{ ft}$$

$$\text{For } L = B = 8 \text{ ft} \Rightarrow q_1, q_2 = 3.125 \pm 1.17 = \begin{cases} 4.3 \text{ kip}/\text{ft}^2 \\ 1.95 \text{ kip}/\text{ft}^2 \end{cases}$$

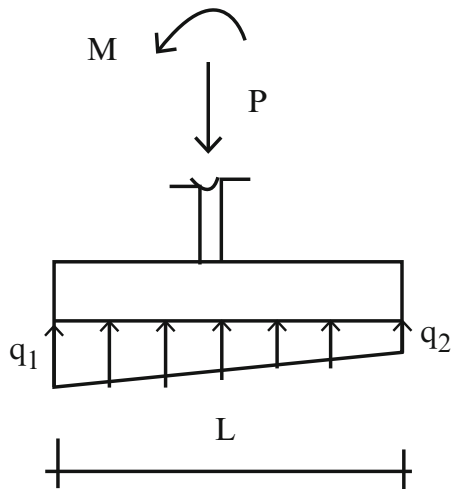
Rectangular footing: We take $B = 6$ ft. The pressure equation has the form

$$\frac{P}{6L} + \frac{6M}{6L^2} = q_e$$

$$\Downarrow$$

$$\frac{200}{6L} + \frac{6(100)}{6L^2} = 4.5 \Rightarrow L = 10 \text{ ft}$$

For $L = 10 \text{ ft}$ and $B = 6 \text{ ft} \Rightarrow q_1, q_2 = 3.33 \pm 1.0 = \begin{cases} 4.33 \text{ kip/ft}^2 \\ 2.33 \text{ kip/ft}^2 \end{cases}$



Case (b) the center line of the column is 3 ft from the property line. M is clockwise (Fig. E7.2b).

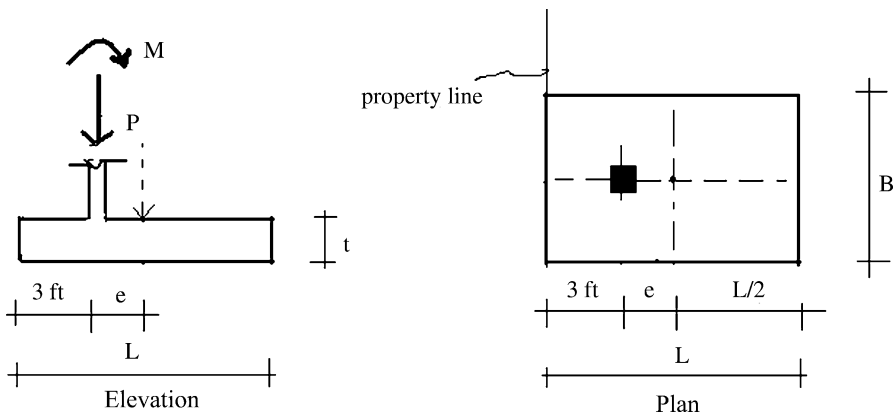


Fig. E7.2b Geometry and loading

Solution: Case (b) We position the centroid of the footing so that it is on the line of action of the resultant force. The location of the resultant is

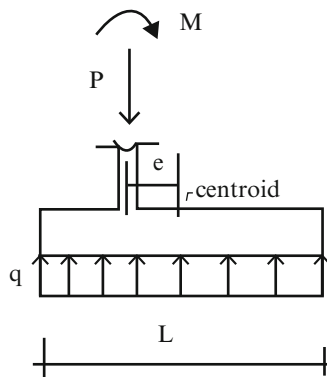
$$M_{\text{total}} = M - Pe = 100 - 200(e) = 0 \Rightarrow e = 0.5 \text{ ft}$$

Then

$$3 + e = \frac{L}{2} \Rightarrow L = 2(3 + e) = 7 \text{ ft}$$

$$q_1 = q_2 = \frac{P}{LB} \leq q_e \rightarrow B \geq \frac{200}{7(4.5)} = 6.35$$

$$\text{For } L = 7 \text{ ft and } B = 6.5 \text{ ft } \Rightarrow q_1 = q_2 = q = \frac{P}{LB} = \frac{200}{7(6.5)} = 4.39 \text{ kip/ft}^2$$



Case (c) the center line of the column is 3 ft from the property line. M is zero (Fig. E7.2c).

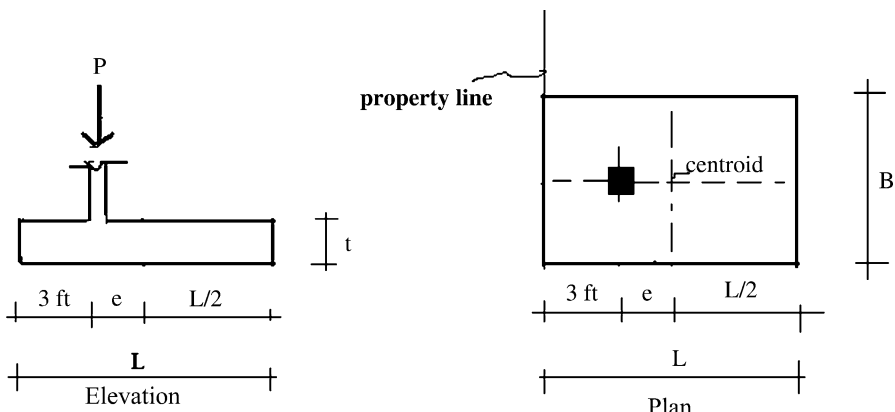
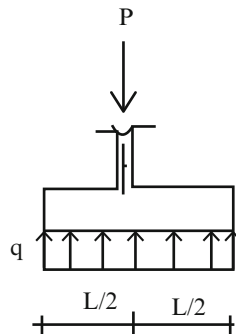


Fig. E7.2c Geometry and loading

Solution: Case (c) For this case, we locate the centroid on the center of the column. Then $e = 0$ and $L = 6.0$ ft. The area is determined with

$$q = q_1 = q_2 = \frac{P}{LB} \leq q_e \rightarrow B \geq \frac{200}{6(4.5)} = 7.4$$

Use $L = 6$ ft and $B = 7.5$ ft



Case (d) the center line of the column is 3 ft from the property line. M is counterclockwise (Fig. E7.2d).

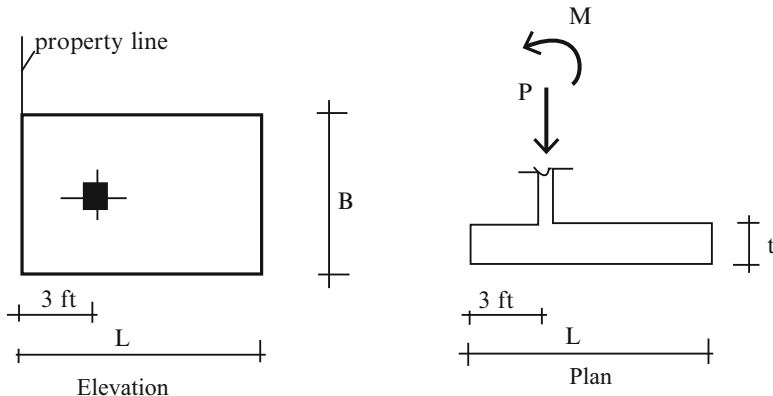
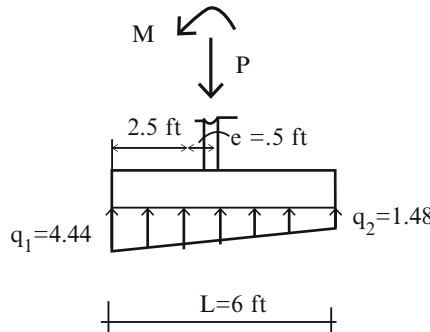


Fig. E7.2d Geometry and loading

Solution: Case (d) We decide to locate the centroid on the column line. Then $e = 0.5$ ft. This leads to the trapezoidal pressure distribution shown below. Taking $L = 6$ ft, and noting (7.3),

$$q_1 = \frac{200}{6B} + \frac{6(100)}{B(6)^2} \leq 4.5 \Rightarrow B \geq 11.1$$

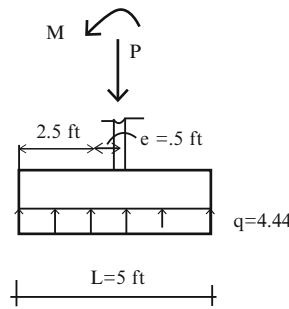
For $L = 6$ ft and $B = 11.25$ ft $\rightarrow q_1, q_2 = 2.96 \pm 1.48 = \begin{cases} 4.44 \text{ kip/ft}^2 \\ 1.48 \text{ kip/ft}^2 \end{cases}$



Another option is to take the centroid on the line of action of the resultant force. Then, $e = 0$ ft, $L = 5$ ft and (7.6) yields

$$\frac{200}{5B} = 4.5 \rightarrow B = 8.9$$

For $L = 5$ ft and $B = 9$ ft $q = q_1 = q_2 = \frac{200}{5(9)} = 4.44 \text{ kip/ft}^2$



7.4 Dimensioning Combined Footings

A combined footing has multiple column loads acting on a single area. This design is adopted when the column spacing is too small to allow for separate footings. Figure 7.13 illustrates the case of two columns. The analytical method described in Sect. 7.2 is also applicable here. One just has to *first replace the column loads with their resultant force*, and then apply (7.2) to determine the pressure distribution.

Specializing (7.2) for this case, and noting the notations defined in Fig. 7.13, the pressure distribution is given by

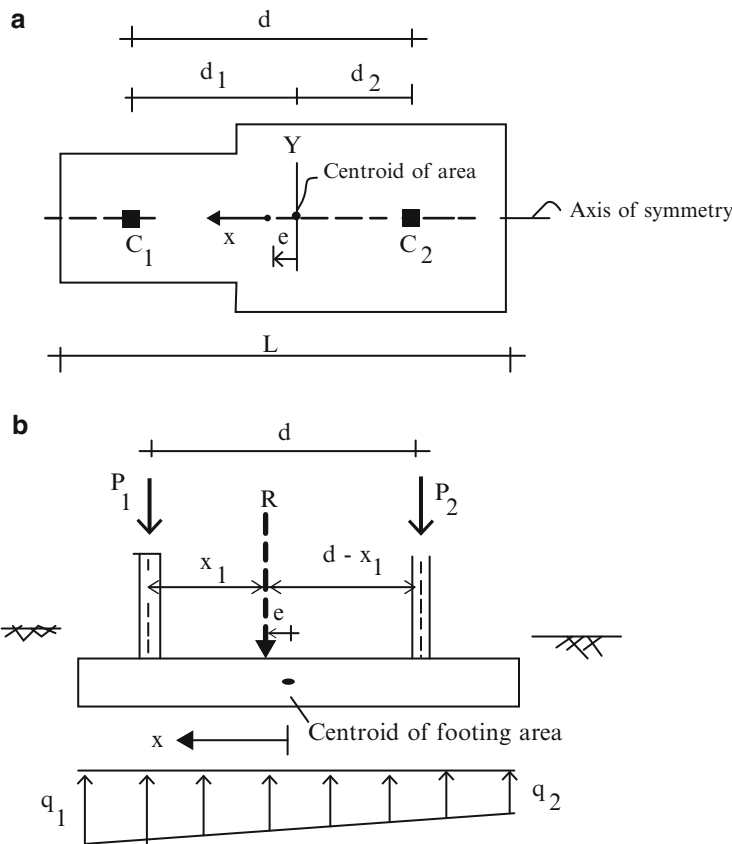


Fig. 7.13 Notation—combined footing. (a) Plan. (b) Elevation

$$q(x) = \frac{R}{A} + \left(\frac{Re}{I_y}\right)x \quad (7.9)$$

$$R = P_1 + P_2$$

where e is positive when R is located to the left of the centroid of the footing area.

The location of the resultant force can be determined by summing moments about the line of action of P_1

$$x_1 = \frac{P_2 d}{(P_1 + P_2)} \quad (7.10)$$

$$e = d_1 - x_1$$

It follows that *the soil pressure distribution is uniform when the centroid of the footing area is located on the line of action of the resultant force* (Fig. 7.14). For this case, $e = 0$ and $q = R/A$.

We compute the peak shear and moment, using factored loads. The position of the resultant with respect to the centroid may change when factored loads are used.

$$R_u = P_{1u} + P_{2u}$$

Then,

$$x_{1u} = d_1 - e_u = \frac{P_{2u}}{R_u} d \quad (7.11)$$

If $e_u \neq 0$, the distribution of pressure is trapezoidal, and we use (7.9) to find the corresponding peak pressures due to the factored loads.

The shear and moment diagrams corresponding to uniform soil pressure are plotted in Fig. 7.15b. Note that for this type of footing, the bending moment distribution in the footing in the longitudinal direction has *both positive and negative regions*. The peak moment values are

$$V_u = 0 \rightarrow Bq_u x_1 - P_{u1} = 0 \rightarrow x_1 = \frac{P_{u1}}{Bq_u}$$

$$\therefore M_{u\max}^- = Bq_u \frac{x_1^2}{2} - P_{u1}(x_1 - L_1)$$

$$M_{u\max}^+ = \text{larger of } \begin{cases} \frac{Bq_u}{2} \left(L_1 - \frac{a}{2}\right)^2 \\ \frac{Bq_u}{2} \left(L_1 + \frac{a}{2}\right)^2 - P_{u1} \left(\frac{a}{2}\right) \\ \frac{Bq_u}{2} \left(L_2 - \frac{b}{2}\right)^2 \\ \frac{Bq_u}{2} \left(L_2 + \frac{b}{2}\right)^2 - P_{u1} \left(\frac{b}{2}\right) \end{cases}$$

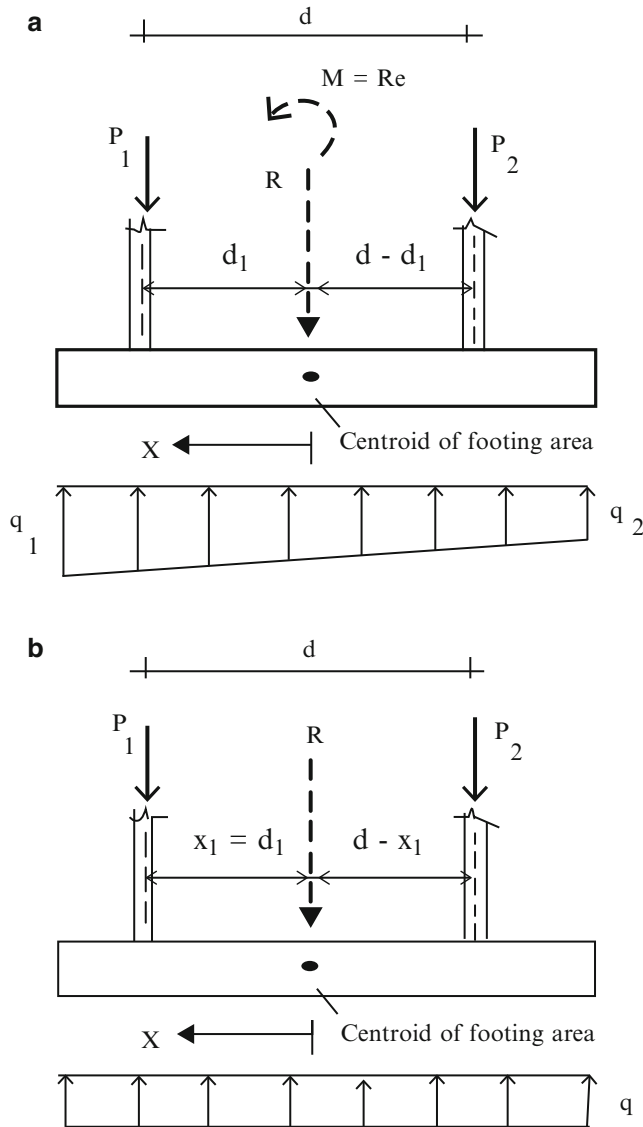


Fig. 7.14 Conditions for soil pressure distribution. (a) $e > 0$. (b) $e = 0$

Since the moment diagram for a combined footing generally has both positive and negative values, the steel placement pattern for a combined footing involves placing steel in the top zone as well as the bottom zone of the cross section. The required steel reinforcing patterns are shown in Fig. 7.15c, d. In general, the

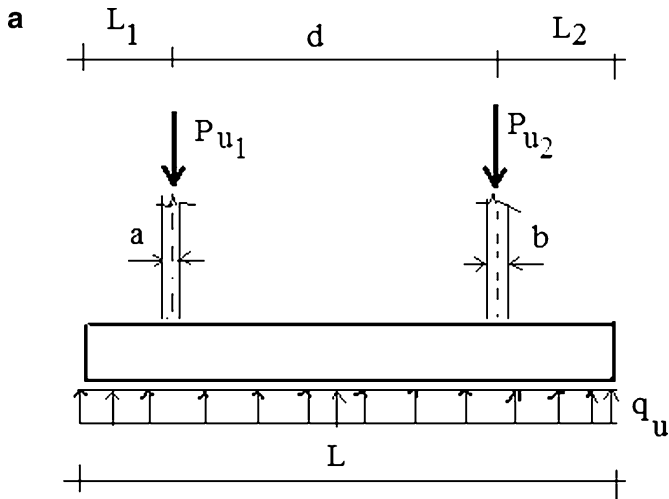


Fig. 7.15 (a) Rectangular footing with uniform ultimate soil pressure $e_u = 0$. (b) Shear and Moment diagrams $e_u = 0$. (c) Steel reinforcing pattern for longitudinal bending. (d) Steel reinforcing pattern for transverse bending

reinforcement pattern is two way. For the transverse direction, we treat the footing similar to the single footing and the steel for tension is placed at the lower surface.

Example 7.3 Dimensioning a combined footing

Given: A combined footing supporting two square columns. Column A is 400 mm \times 400 mm and carries a dead load of 700 kN and a live load of 900 kN. Column B is 500 mm \times 500 mm and carries a dead load of 900 kN and a live load of 1,000 kN. The effective soil pressure is $q_e = 160 \text{ kN/m}^2$ (Figs. E7.3a, b).

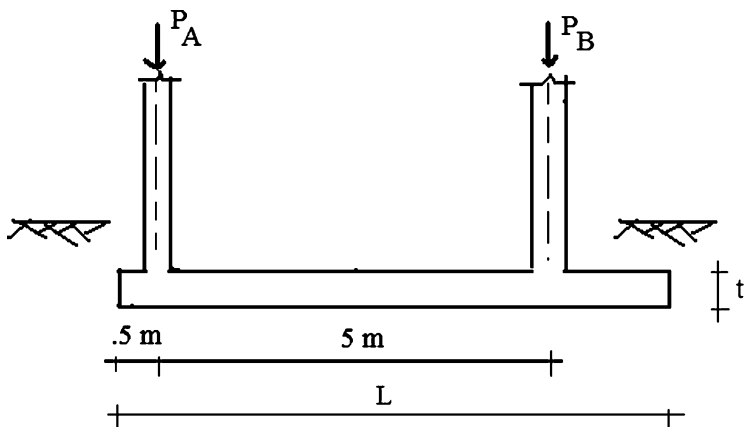


Fig. E7.3a Elevation

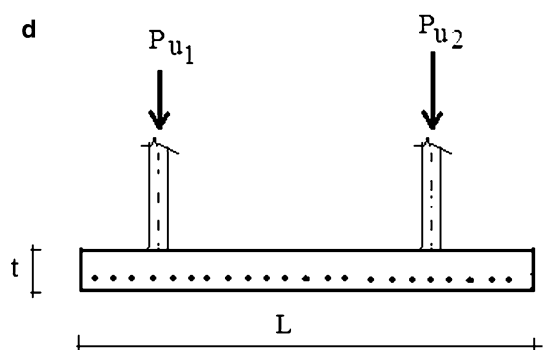
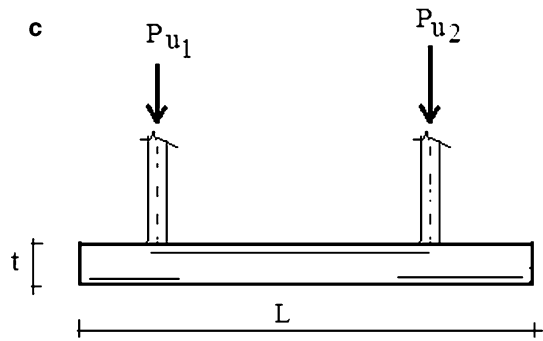
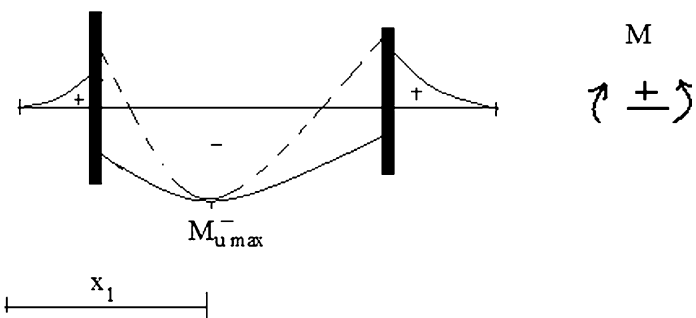
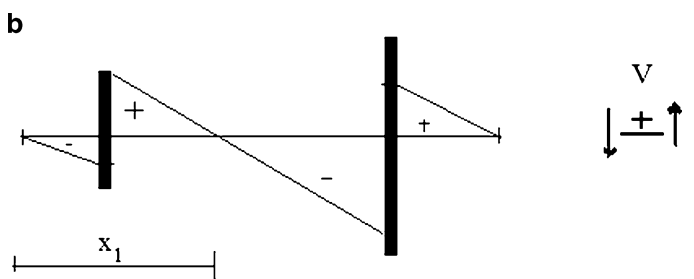


Fig. 7.15 (continued)

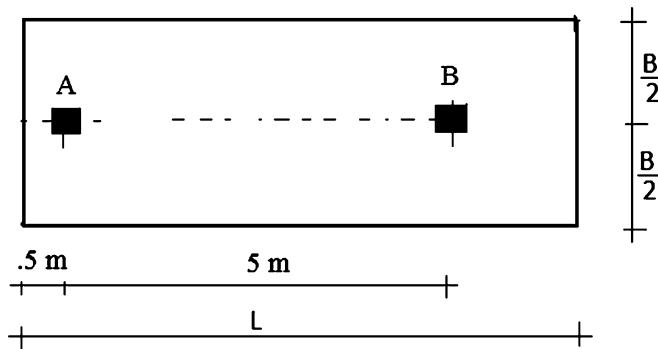


Fig. E7.3b Plan

Determine: The dimensions B and L for service load of $P = P_D + P_L$. Draw shear and moment diagrams for factored load of $P_u = 1.2P_D + 1.6P_L$.

Solution:

Step I : Locate the resultant force

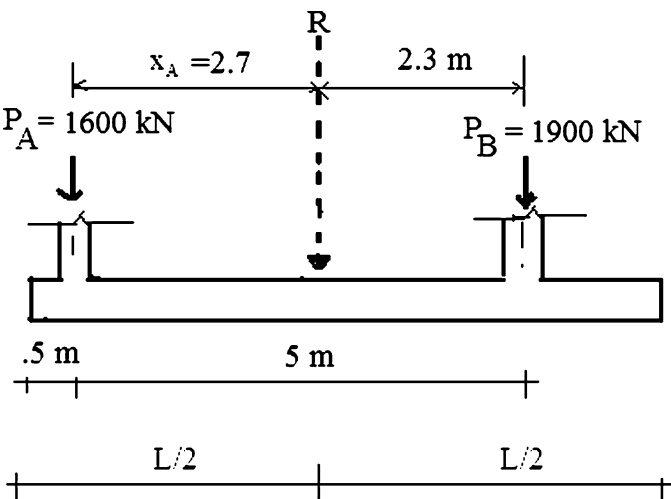
$$P_A = P_D + P_L = 700 + 900 = 1,600 \text{ kN}$$

$$P_B = P_D + P_L = 900 + 1,000 = 1,900 \text{ kN}$$

$$R = P_A + P_B = 3,500 \text{ kN}$$

$$x_A = \frac{1,900(5)}{3,500} = 2.7 \text{ m}$$

The resultant equals 800 kip located 8.8 ft from P_A .



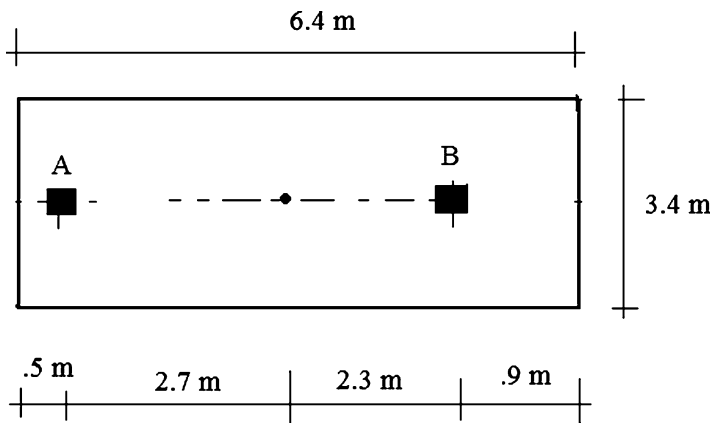
Step II: Select a rectangular geometry. We position the rectangle so that its centroid is on the line of action of the resultant. The design requirement is

$$\frac{L}{2} = x_A + 0.5 = (2.7) + 0.5 = 3.2$$

$$A_{\text{required}} = \frac{R}{q_e} = \frac{3,500}{165} = 21.2 \text{ m}^2$$

Take $L = 6.4 \text{ ft}$ and $B = 3.4 \text{ m} \rightarrow A = B \times L = 21.76 \text{ m}^2$

The final geometry is shown below



Step III: Draw the shear and moment diagrams corresponding to the factored loads $P_u = 1.2P_D + 1.6P_L$. We work with the soil pressure integrated over the width of the footing. This leads to the “total” shear and “total” moment. These distributions are plotted below. Note that we treat the column loads as concentrated forces. One can also model them as distributed loads over the width of the column.

$$P_{Au} = 1.2P_D + 1.6P_L = 1.2(700) + 1.6(900) = 2,280 \text{ kN}$$

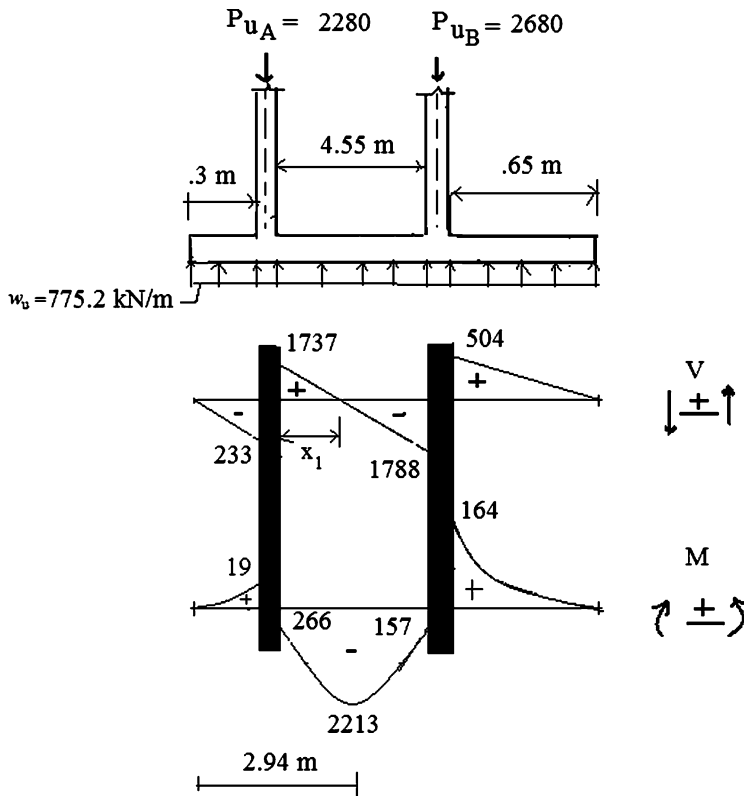
$$P_{Bu} = 1.2P_D + 1.6P_L = 1.2(900) + 1.6(1,000) = 2,680 \text{ kN}$$

The factored resultant acts 2.702 m from P_A . It follows that $e = 13 \text{ mm}$. We neglect this eccentricity and assume the pressure is uniform.

$$q_u = \frac{R_u}{A} = \frac{2,280 + 2,680}{6.4(3.4)} = 228 \text{ kN/m}^2$$

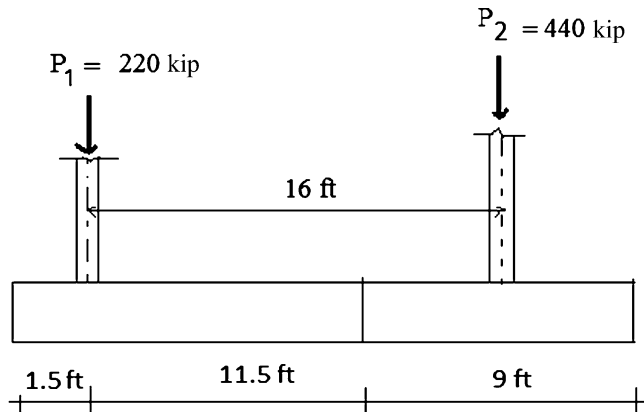
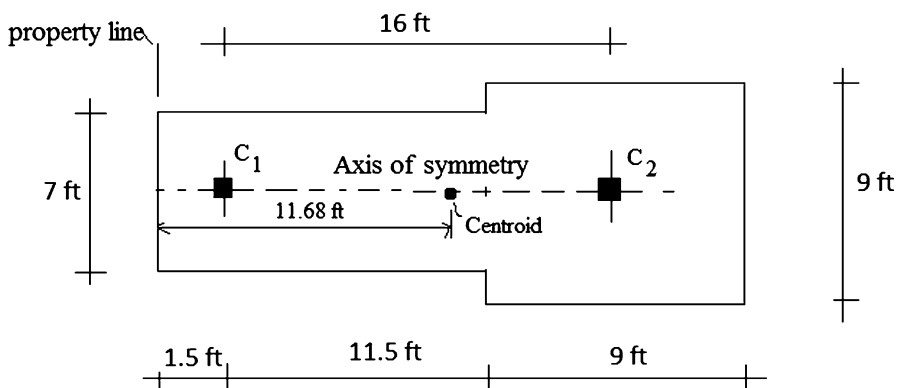
Then for $B = 3.4 \text{ m}$, $w_u = 228(3.4) = 775.2 \text{ kN/m}$

The shear and moment diagrams are plotted below.



Example 7.4

Given: A combined footing supporting two square columns. Column C_1 is 16 in. \times 16 in. and carries a service load of 220 kip. Column C_2 is 18 in. \times 18 in. and carries a service load of 440 kip. The effective soil pressure is $q_e = 3.5 \text{ kip/ft}^2$ (Figs. E7.4a, b).

**Fig. E7.4a** Elevation**Fig. E7.4b** Plan

Determine: The soil pressure distribution caused by the service loads P_1 and P_2 .

Solution:

Locate the centroid of the area

$$A = (9)(9) + (13)(7) = 172 \text{ ft}^2$$

$$L_1 = \frac{81(17.5) + 91(6.5)}{172} = 11.68 \text{ ft}$$

Locate the resultant force

$$R = P_1 + P_2 = 220 + 440 = 660 \text{ kip}$$

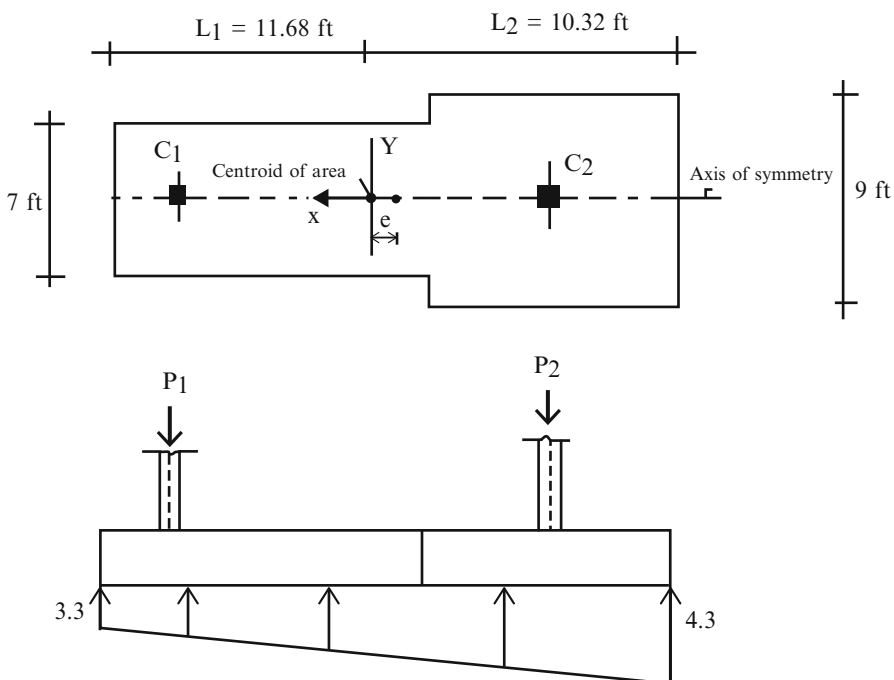
$$d_1 = \frac{P_2 d}{R} = \frac{440(16)}{660} = 10.67 \text{ ft}$$

$$e = 11.68 - (10.67 + 1.5) = -0.49 \text{ ft}$$

The peak pressures are

$$q_1 = \left\{ \frac{R}{A} + \frac{(Re)L_1}{I_y} \right\} = \frac{660}{172} + \frac{660(-.49)11.68}{7,014} = 3.3 \text{ kip}/\text{ft}^2$$

$$q_2 = \left\{ \frac{R}{A} - \frac{(Re)L_2}{I_y} \right\} = \frac{660}{172} - \frac{660(-.49)10.32}{7,014} = 4.3 \text{ kip}/\text{ft}^2$$



7.5 Dimensioning Strap Footings

Strap footings consist of individual footings placed under each column and connected together with a rigid beam to form a single unit. Figure 7.16 illustrates the geometric arrangement for two columns supported by two rectangular footings. The centroid for the interior footing (footing #2) is usually taken to be on the line of action of the interior column. The zone under the rigid beam is generally filled with a geo-foam material that has essentially no stiffness and provides negligible pressure on the beam. Therefore all of the resistance to the column loads is generated by the soil pressure acting on the individual footing segments.

We suppose the axis connecting the columns is an axis of symmetry for the area segments. The approach follows essentially the same procedure as employed for combined footings. Figure 7.17 defines the notation for this method.

First, we locate the resultant of the column loads.

$$x_1 = \frac{P_2}{R} d$$

$$R = P_1 + P_2$$

$$e = x_1 - d_1$$

Next, we take footing #2 to be located such that its centroid coincides with the line of action of load P_2 .

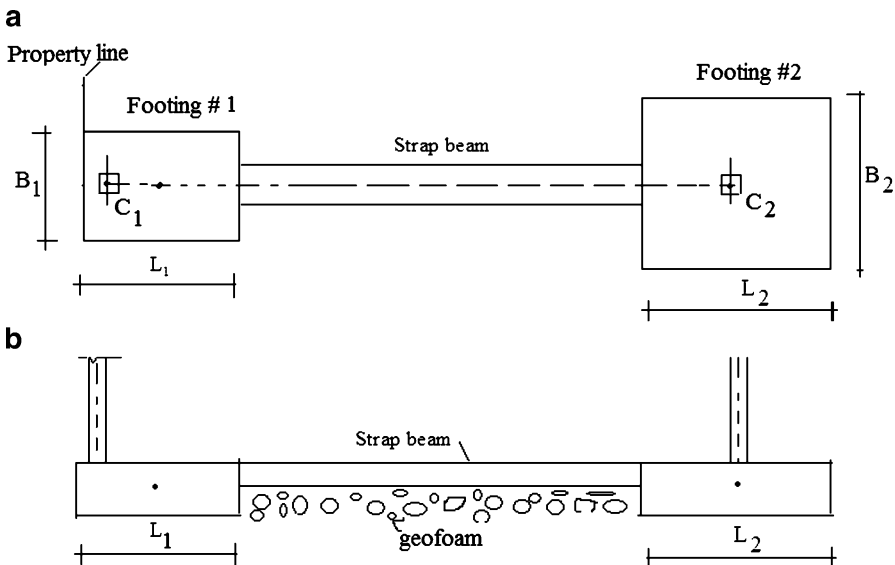


Fig. 7.16 Strap footing. (a) Plan. (b) Elevation

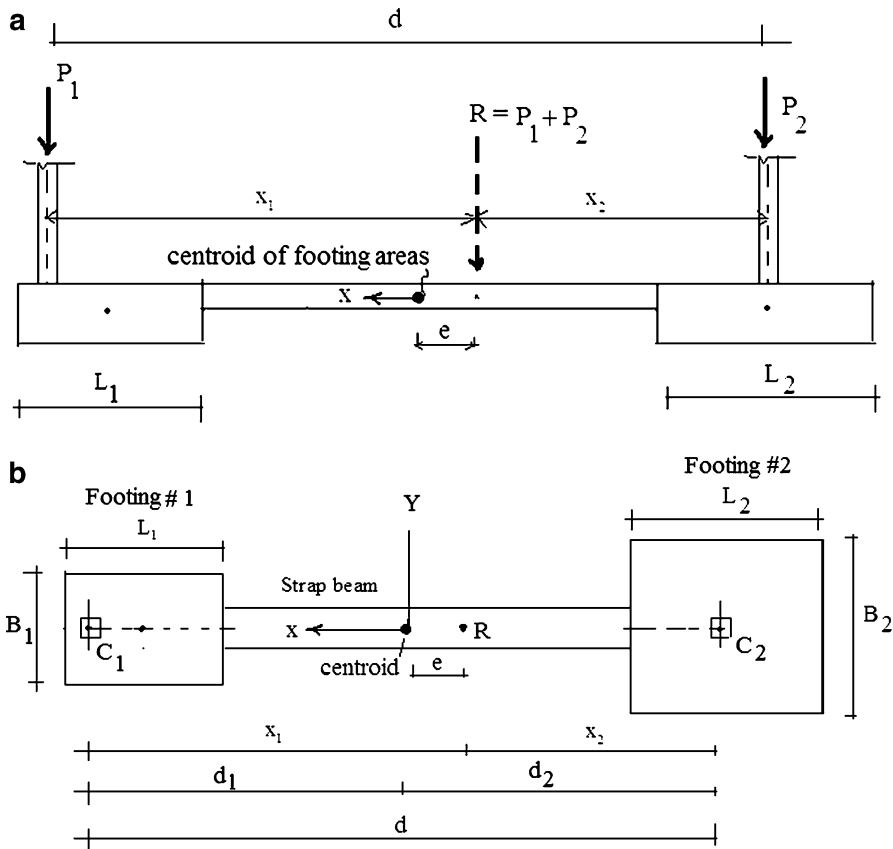


Fig. 7.17 Notation and pressure distribution for strap footing. (a) Elevation. (b) Plan

We locate the origin of the x axis at an arbitrary point on the axis of symmetry and use (7.1) to determine the soil pressure acting on the individual footings. We assume there is no soil pressure acting on the link member. Noting (7.1), the soil pressure is taken as

$$\begin{aligned} q(x) &= b + ax && \text{for footings \#1 and \#2} \\ q(x) &= 0 && \text{for the strap beam.} \end{aligned}$$

The coefficients are evaluated by *integrating over the footing areas*. Enforcing equilibrium leads to

$$\begin{aligned} R &= \int q(x) dA = b(A_1 + A_2) + a \left[\int_{A_1} x dA + \int_{A_2} x dA \right] \\ -Re &= \int xq(x) dA = b \left[\int_{A_1} x dA + \int_{A_2} x dA \right] + a \left[\int_{A_1} x^2 dA + \int_{A_2} x^2 dA \right] \end{aligned} \quad (7.12)$$

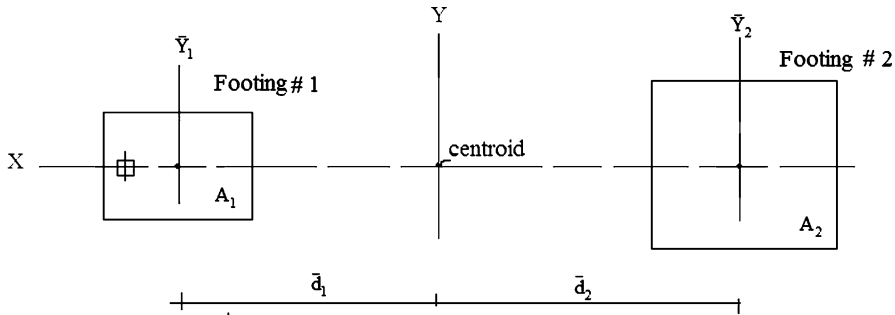


Fig. 7.18 Geometry—strap footing

Note that e is positive when to the right of the centroid (see Fig. 7.17b).

Now, we take the origin for x at the centroid of the combined section. Then $\int_{A_1} x \, dA + \int_{A_2} x \, dA = 0$ and (7.12) reduces to

$$\begin{aligned} R &= b(A_1 + A_2) \\ -Re &= a(I_1 + I_2) \end{aligned} \quad (7.13)$$

where $(I_1 + I_2)$ is sum of the second moments of area of the two footing cross sections about the y -axis through the centroid. Lastly, the pressure equation takes the form:

$$q(x) = \frac{R}{(A_1 + A_2)} - \frac{Re}{(I_1 + I_2)}x \quad (7.14)$$

where the I 's are computed using the parallel axis theorem. Noting Fig. 7.18, the I 's are computed using the following equations.

$$\begin{aligned} I_1 &= \bar{I}_{Y1} + A_1 \bar{d}_1^2 \\ I_2 &= \bar{I}_{Y2} + A_2 \bar{d}_2^2 \end{aligned}$$

We use (7.14) to determine the pressure for a given geometry and loading.

When dimensioning the footing, we locate the centroid of the combined footing area on the line of action of the resultant. This step results in a uniform pressure,

$$e = 0 \rightarrow q = \frac{R}{(A_1 + A_2)} = \frac{P_1 + P_2}{(A_1 + A_2)} \quad (7.15)$$

Given the effective soil pressure, we determine the total area with

$$A_1 + A_2 \geq \frac{P_1 + P_2}{q_e} \quad (7.16)$$

The solution procedure is as follows:

We assume the magnitude of either A_1 or A_2 and compute the other area with (7.16). Since we are locating footing #2 such that its centroid coincides with the line of action of P_2 , it follows from Fig. 7.17 that $x_2 \equiv d_2$. Then noting Fig. 7.18, $\bar{d}_2 \equiv d_2$. Lastly, we determined \bar{d}_1 with (7.17)

$$A_1\bar{d}_1 = A_2\bar{d}_2 \quad (7.17)$$

This equation correspond to setting $e = 0$.

An alternative design approach proceeds as follows. Consider Fig. 7.19. The resultants of the pressure distributions acting on the footings are indicated by R_1 and R_2 . Summing moments about the line of action of R_1 leads to

$$R_2 = P_2 - \frac{P_1 e_1}{d - e_1} \quad (7.18)$$

Summing forces leads to

$$R_1 + R_2 = P_1 + P_2$$

Then

$$R_1 = P_1 + \frac{P_1 e_1}{d - e_1} \quad (7.19)$$

Let

$$V = \frac{P_1 e_1}{d - e_1} \quad (7.20)$$

then

$$\begin{aligned} R_1 &= P_1 + V \\ R_2 &= P_2 - V \\ R &= R_1 + R_2 = P_1 + P_2 \end{aligned} \quad (7.21)$$

The quantity, V , is the shear force in the strap beam.

Once e_1 is specified, one can determine R_1 and R_2 . We also *assume* the soil pressure acting on the footing is constant and equal to the design pressure (q_e). Then,

$$\begin{aligned} A_{1\text{required}} &= \frac{R_1}{q_e} \\ A_{2\text{required}} &= \frac{R_2}{q_e} \end{aligned} \quad (7.22)$$

Typical reinforcing patterns for strap type footings are illustrated in Fig. 7.20.

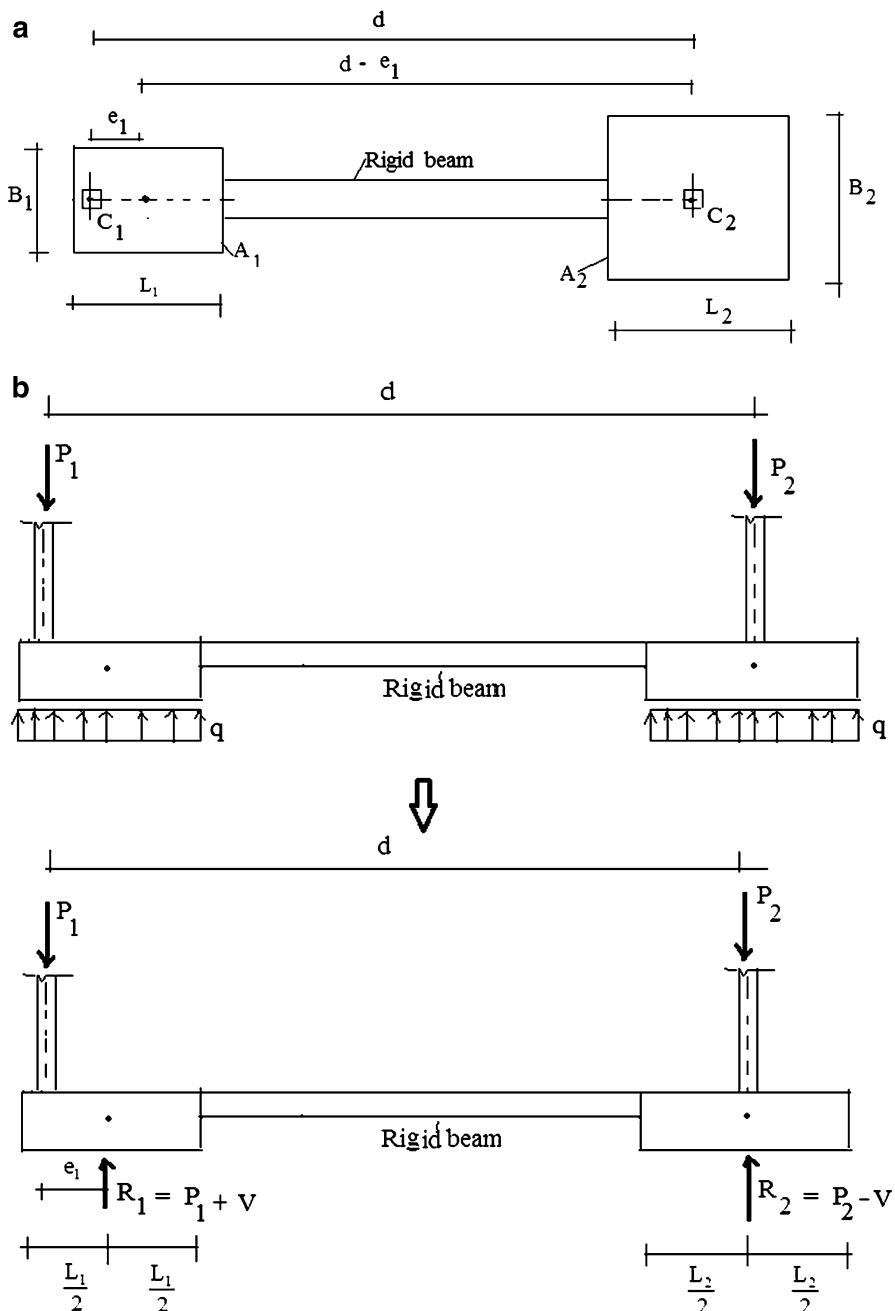
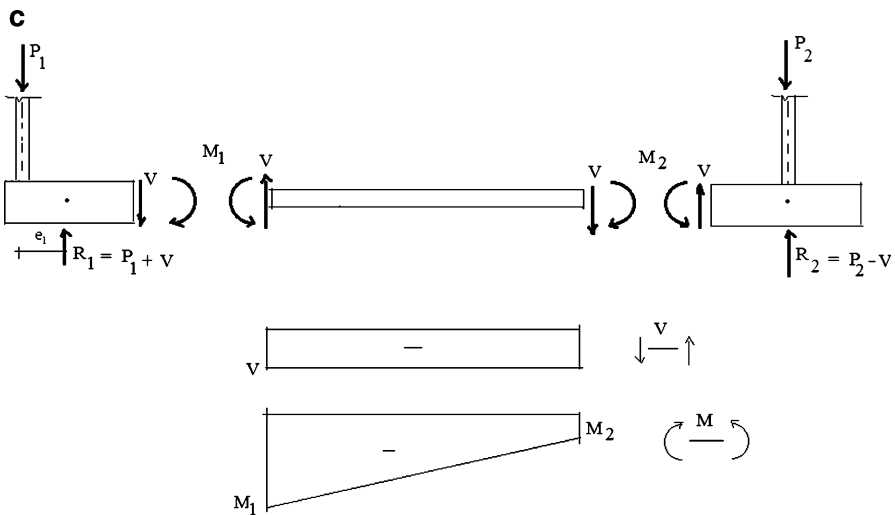


Fig. 7.19 Approximate strap footing analysis. (a) Plan. (b) Elevation

**Fig. 7.19** (continued)**Fig. 7.20** Typical reinforcing patterns

Example 7.5

Given: The eccentrically loaded footing A connected to the concentrically loaded footing B by strap beam as shown below. Assume the strap is placed such that it does not bear directly on the soil (Figs. E7.5a, b).

Determine: Determine the soil pressure profile under the footings.

Solution: Noting Fig. 7.17, the various measures are

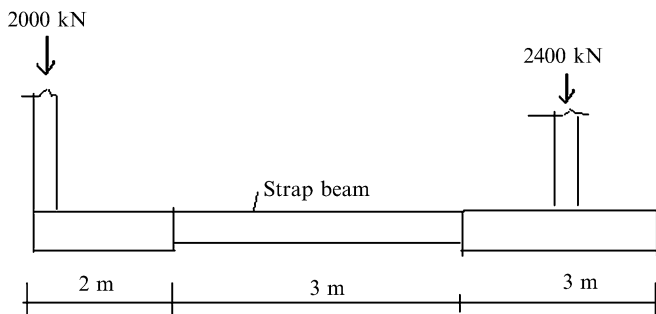


Fig. E7.5a (a) Elevation

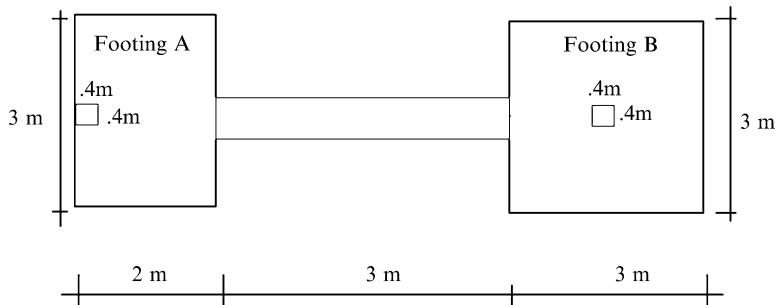


Fig. E7.5b (b) Plan

$$d_1 + 0.2 = \frac{6(1) + 9(6.5)}{15} = 4.3$$

$$x_1 = \frac{2,400(6.3)}{4400} = 3.436$$

$$e = 4.3 - 3.436 - 0.2 = 0.66 \text{ m}$$

$$R = 2,000 + 24,000 = 4,400 \text{ kN}$$

$$A_1 = 2(3) = 6 \text{ m}^2$$

$$A_2 = 3(3) = 9 \text{ m}^2$$

$$I_1 + I_2 = \frac{3(2)^3}{12} + 6(1)^2 + \frac{3(3)^3}{12} + 9(6.5)^2 = 395 \text{ m}^4$$

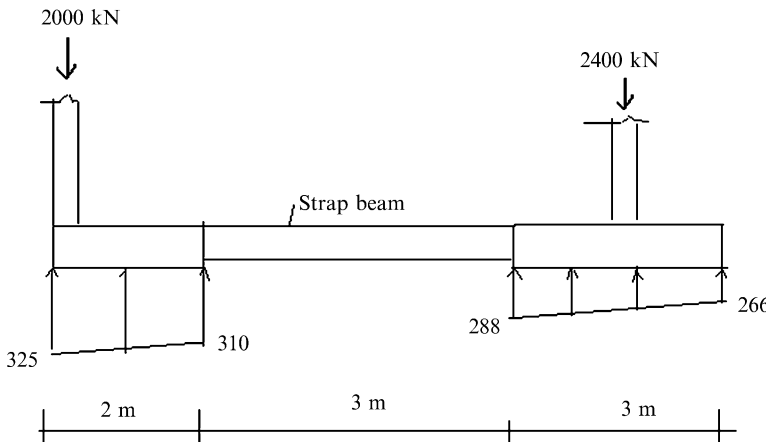
$$\begin{aligned} q(x) &= \frac{R}{(A_1 + A_2)} - \frac{Re}{(I_1 + I_2)}x \\ &= \frac{4,400}{15} - \frac{4,400(.66)}{395}x = 293.3 - 7.35x \\ &\therefore \end{aligned}$$

$$q(-4.3) = 325 \text{ kN/m}^2$$

$$q(-2.3) = 310 \text{ kN/m}^2$$

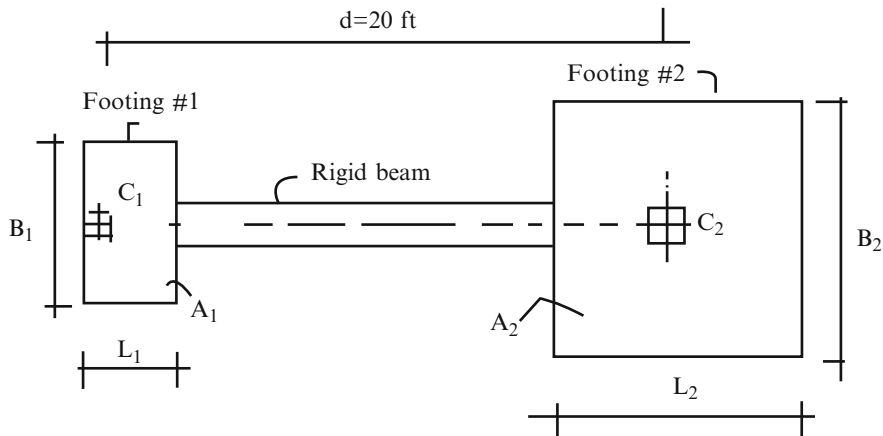
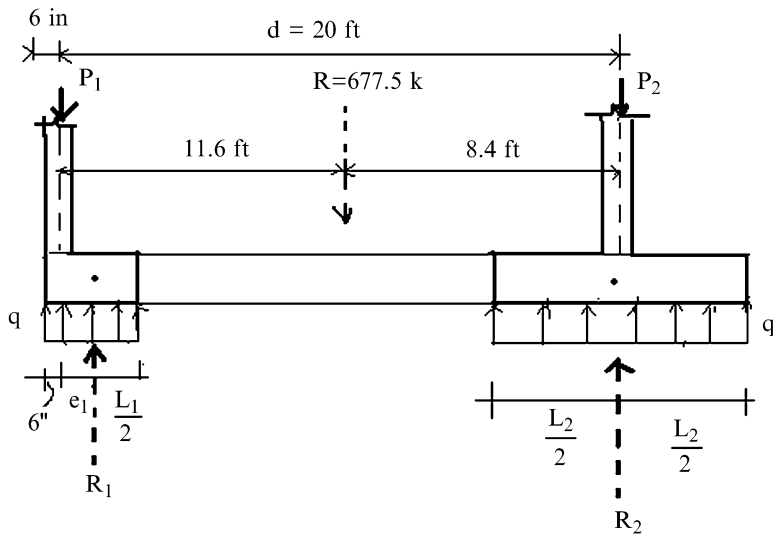
$$q(0.7) = 288 \text{ kN/m}^2$$

$$q(5.7) = 266 \text{ kN/m}^2$$



Example 7.6 Dimensioning a strap footing

Given: The exterior column C_1 is 12 in. \times 12 in. and carries a dead load of 160 kip and a live load of 130 kip. The interior column C_2 is 16 in. \times 16 in. and carries a dead load of 200 kip and a live load of 187.5 kip. The property line is at the edge of column #1 and the distance between the center lines of the columns #1 and #2 is 20 ft. The effective soil pressure is $q_e = 4.625 \text{ kip/ft}^2$ (Figs. E7.6a, b).

**Fig. E7.6a** Plan**Fig. E7.6b** Elevation

Determine: The dimensions of the footings for both columns using the two solution procedures described above.

Solution:

Procedure #1: The individual column loads are:

$$P_1 = 160 + 130 = 290 \text{ kip}$$

$$P_2 = 200 + 187.5 = 387.5 \text{ kip}$$

Next, we locate the resultant of the column loads.

$$R = P_1 + P_2 = 677.5 \text{ kip}$$

$$d_1 = x_1 = \frac{387.5}{667.5} (20) = 11.6 \text{ ft}$$

$$d_2 = x_2 = 20 - 11.6 = 8.4 \text{ ft}$$

Noting (7.16) we obtain:

$$A_1 + A_2 = \frac{677.5}{4.625} \geq 146.5 \text{ ft}^2$$

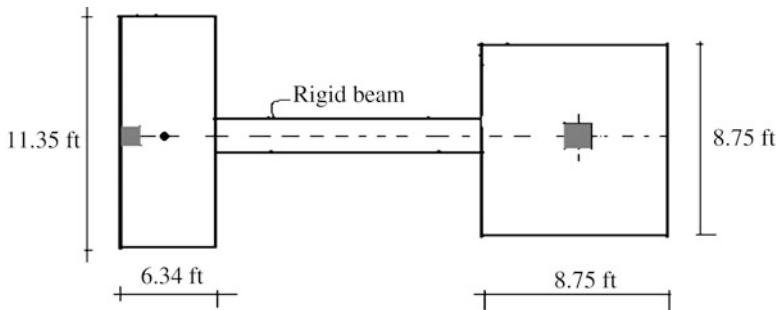
We take $A_2 = 76.56 \text{ ft}^2$. Then $A_1 \geq 69.94 \text{ ft}^2$. We select $A_1 = 72 \text{ ft}^2$
Noting (7.17),

$$\bar{d}_1 = \frac{A_2}{A_1} \bar{d}_2 = \frac{76.56}{72} (8.4) = 8.93 \text{ ft}$$

Then

$$\frac{L_1}{2} = e_1 + .5 = (11.6 - 8.93) + .5 = 3.17 \text{ ft}$$

The final dimensions are shown below.



Procedure #2: We illustrate the 2nd design approach here. We estimate A_1 by requiring the pressure under the footing#1 to be equal to q_e .

$$A_1 > \frac{P_1}{q_e} = \frac{290}{4.625} = 62.7 \text{ ft}^2$$

We take $L_1 = 6 \text{ ft}$ as a first estimate. Then, noting Fig. E7.6b

$$e_1 = \frac{L_1}{2} - .5 \approx 2.5 \text{ ft}$$

The remaining steps are listed below

$$V = \frac{P_1 e_1}{d - e_1} = \frac{290(2.5)}{20 - 2.5} = 41.43 \text{ kip}$$

$$R_1 = P_1 + V = 290 + 41.43 = 331.43 \text{ kip}$$

$$R_2 = P_2 - V = 387.5 - 41.43 = 346.07 \text{ kip}$$

$$A_{1_{\text{required}}} = \frac{331.43}{4.625} = 71.66 \text{ ft}^2 \Rightarrow B_1 = \frac{71.66}{6} = 11.94 \Rightarrow L_1 = 6 \text{ ft} \quad B_1 = 12 \text{ ft}$$

$$A_{2_{\text{required}}} = \frac{346.07}{4.625} = 74.82 \text{ ft}^2 \Rightarrow L_2 = B_2 = \sqrt{74.82} = 8.64 \Rightarrow B_2 = L_2 = 8.75 \text{ ft}$$

Repeating this computation for the ultimate loading case,

$$P_{1u} = 1.2P_D + 1.6P_L = 1.2(160) + 1.6(130) = 400 \text{ kip}$$

$$P_{2u} = 1.2P_D + 1.6P_L = 1.2(200) + 1.6(187.5) = 540 \text{ kip}$$

And assuming the same value for e leads to

$$V_u = \frac{P_{u1} e_1}{d - e_1} = \frac{400(2.5)}{17.5} = 57.14 \text{ kip}$$

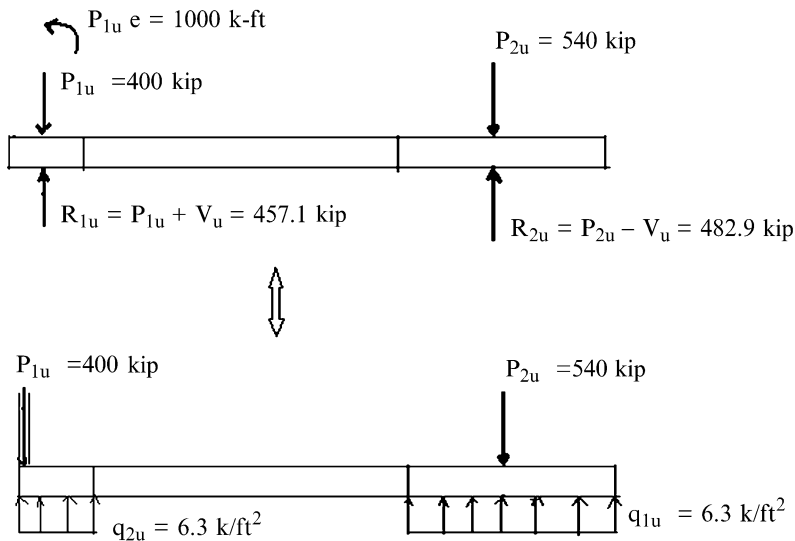
$$R_{1u} = P_{1u} + V_u = 400 + 57.14 = 457.14 \text{ kip}$$

$$q_{1u} = \frac{R_{1u}}{B_1 L_1} = \frac{457.14}{6(12)} = 6.35 \text{ kip}/\text{ft}^2$$

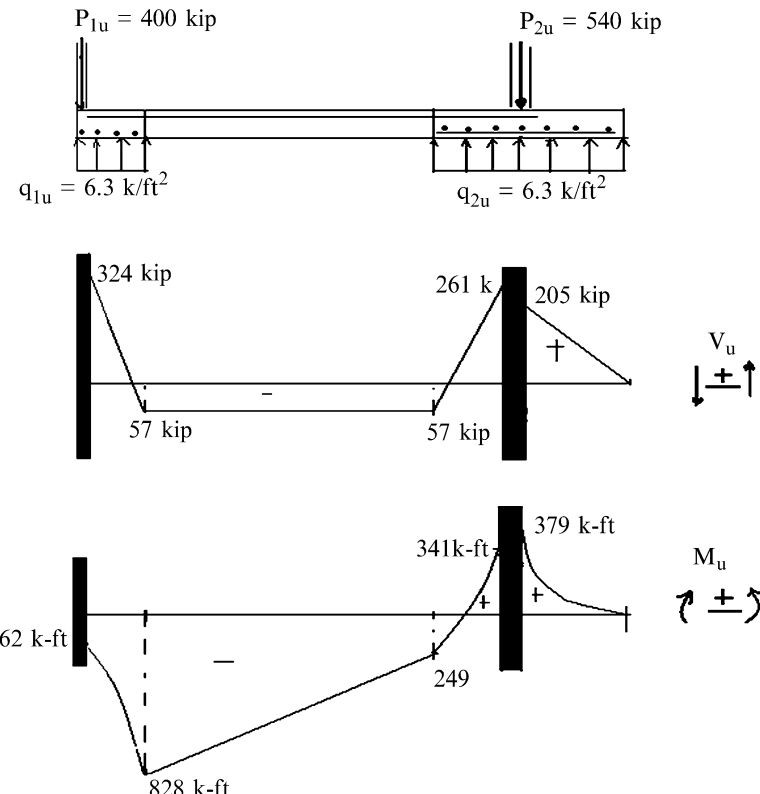
$$R_{2u} = P_{2u} - V_u = 540 - 57.14 = 482.86 \text{ kip}$$

$$q_{2u} = \frac{R_{2u}}{B_2 L_2} = \frac{482.86}{8.75(8.75)} = 6.31 \text{ kip}/\text{ft}^2$$

The corresponding forces are shown in the sketches below.



The shear and moment diagrams are plotted below.



7.6 Summary

7.6.1 Objectives of the Chapter

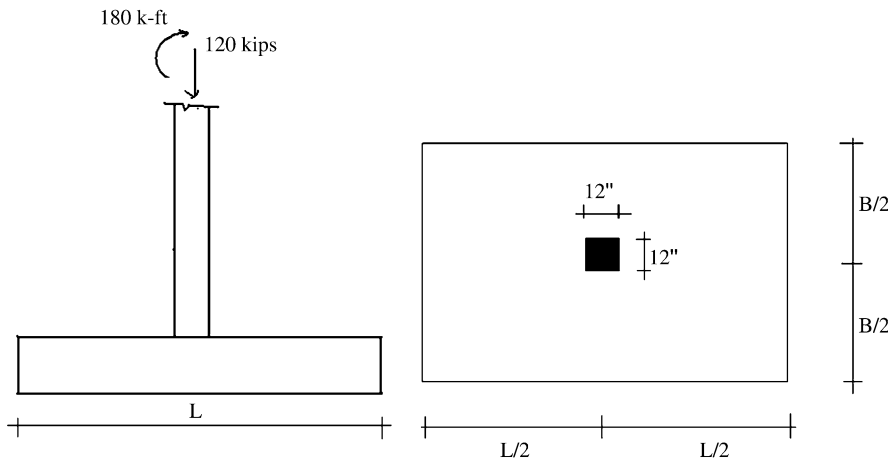
- To describe the various types of footings used in shallow foundations.
- To develop an analytical procedure for dimensioning footings.
- To develop a general analytical procedure for generating the shear and moment distribution in footings based on the assumption of a linear soil pressure distribution.
- To identify critical loading conditions which produce pressure loading distributions with high peak magnitudes.

7.7 Problems

Problem 7.1

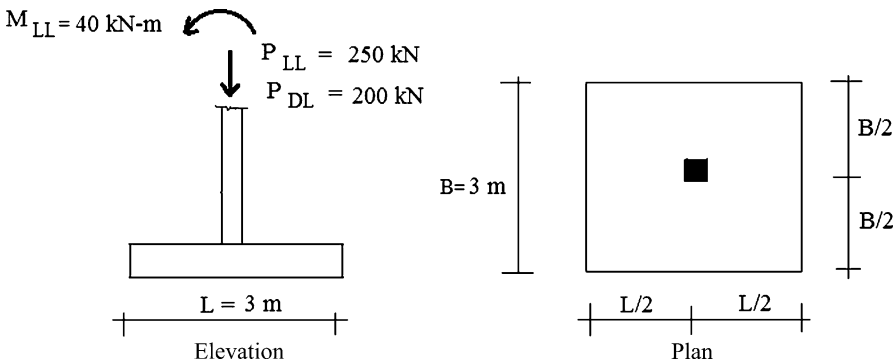
Consider the footing geometry shown below. Determine the soil pressure distribution corresponding to

- (a) $B = L = 8 \text{ ft}$
- (b) $L = 10 \text{ ft}, B = 5 \text{ ft}$

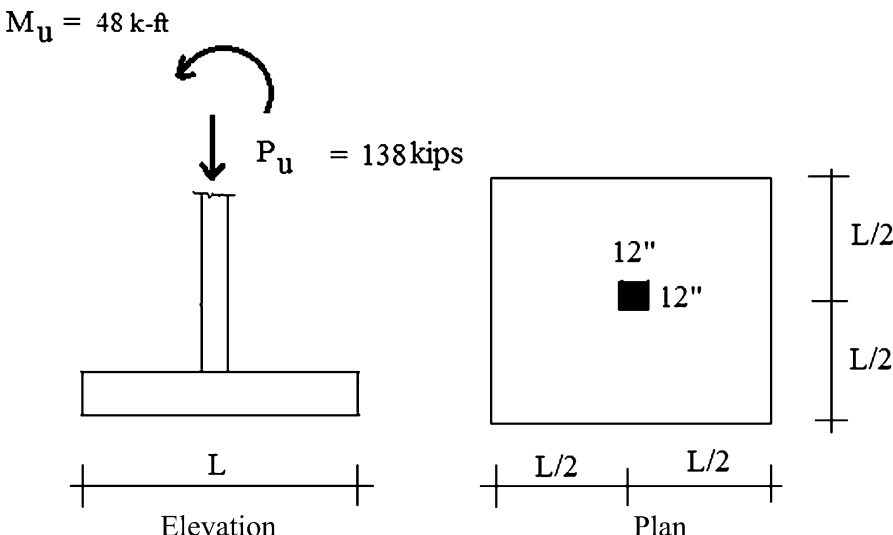


Problem 7.2

The plan view and elevation of a single footing supporting a 300 mm × 300 mm column is shown below. Determine the soil pressure distribution under the footing. Use a factor of 1.2 for DL and 1.6 for LL.

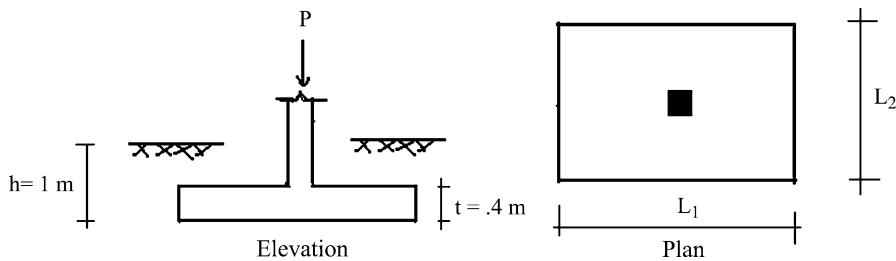
**Problem 7.3**

The plan view and elevation of a single footing supporting a column is shown below. The allowable soil pressure is 4,000 kip/ft². Determine the maximum allowable value for L .



Problem 7.4

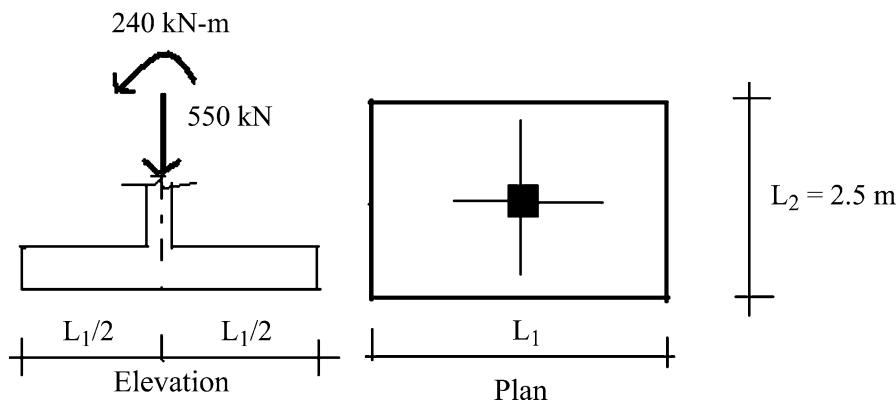
A 450 mm × 450 mm concentrically load column is to be supported on a shallow foundation. The base of the footing is 1 m below grade. Estimate the size of the footing using service loads. Draw shear and moment diagrams using a factor load of $P_u = 1.2P_D + 1.6P_L$. The allowable soil pressure is $q_{allowable} = 250 \text{ kN/m}^2$. $P_D = 1,000 \text{ kN}$ and $P_L = 1,400 \text{ kN}$. Consider: (a) A square footing ($L_1 = L_2 = L$) and (b) a rectangular footing with $L_2 = 2.5 \text{ m}$.



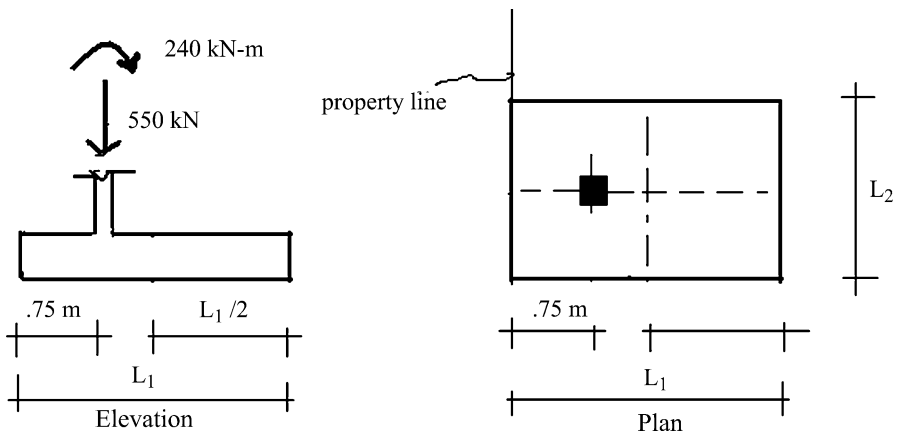
Problem 7.5

A 350 mm × 350 mm column is to be supported on a shallow foundation. Determine the dimensions (either square or rectangular) for the following conditions. The allowable soil pressure is $q_{allowable} = 180 \text{ kN/m}^2$.

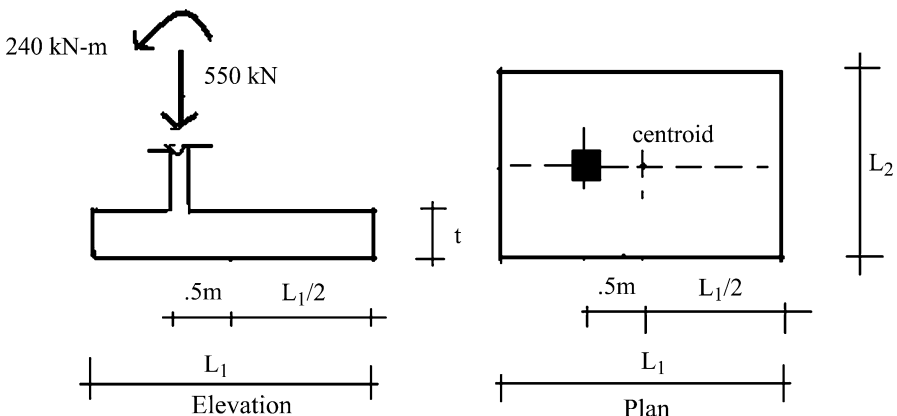
(a) The centerline of the column coincides with the centerline of the footing.



- (b) The center line of the column is 0.75 m from the property line.



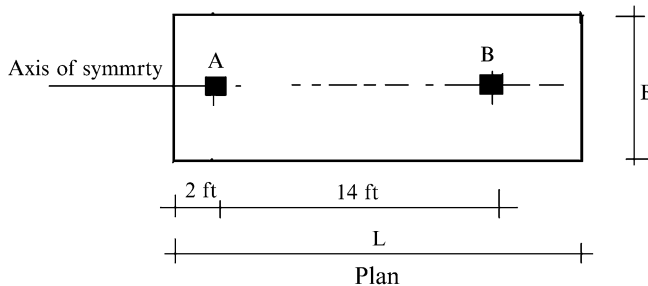
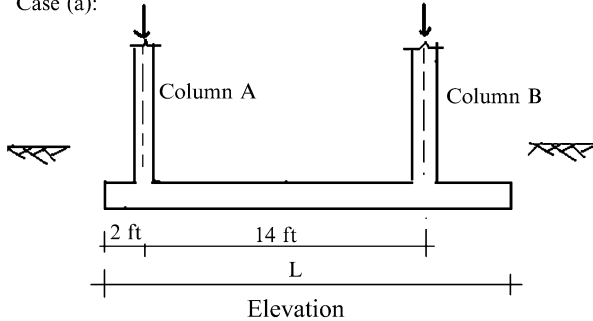
- (c) The center line of the column is 0.5 m from the centroid of the footing.



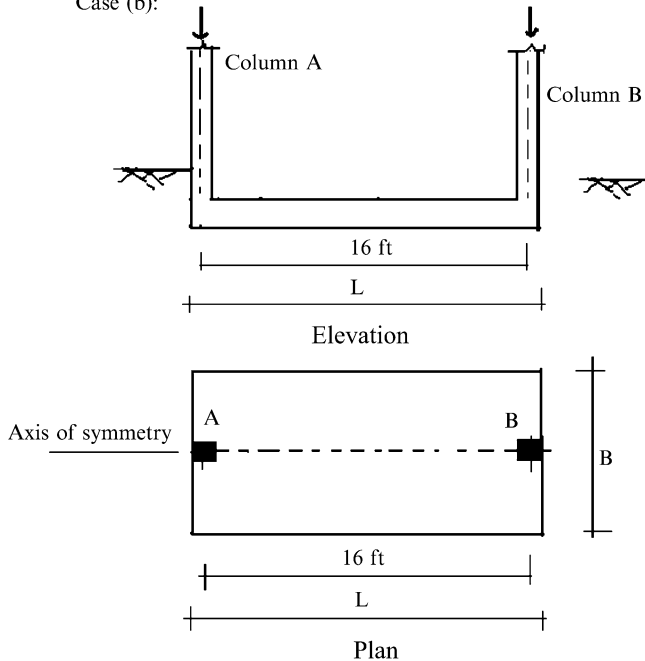
Problem 7.6

A combined footing supports two square columns: Column A is 14 in. \times 14 in. and carries a dead load of 140 kip and a live load of 220 kip. Column B is 16 in. \times 16 in. and carries a dead load of 260 kip and a live load of 300 kip. The effective soil pressure is $q_e = 4.5 \text{ kip}/\text{ft}^2$. Assume the soil pressure distribution is uniform. Determine the footing dimensions for the following geometric configurations. Establish the shear and moment diagrams corresponding to the factored loading, $P_u = 1.2P_D + 1.6P_L$.

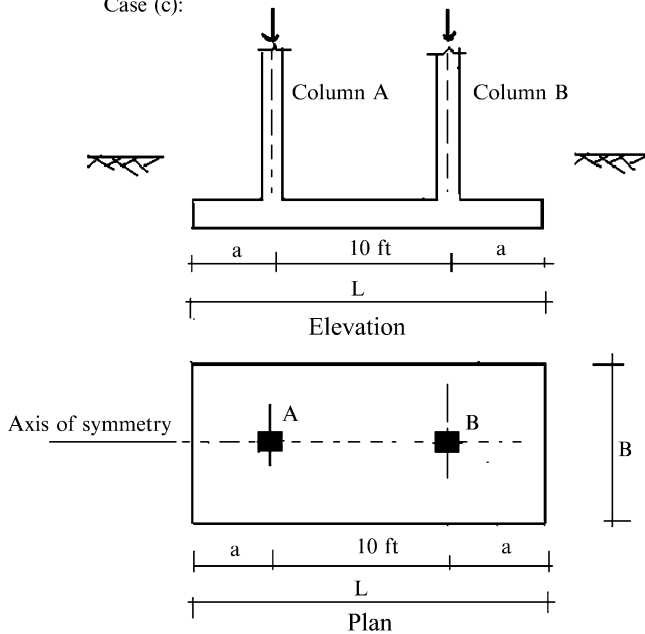
Case (a):



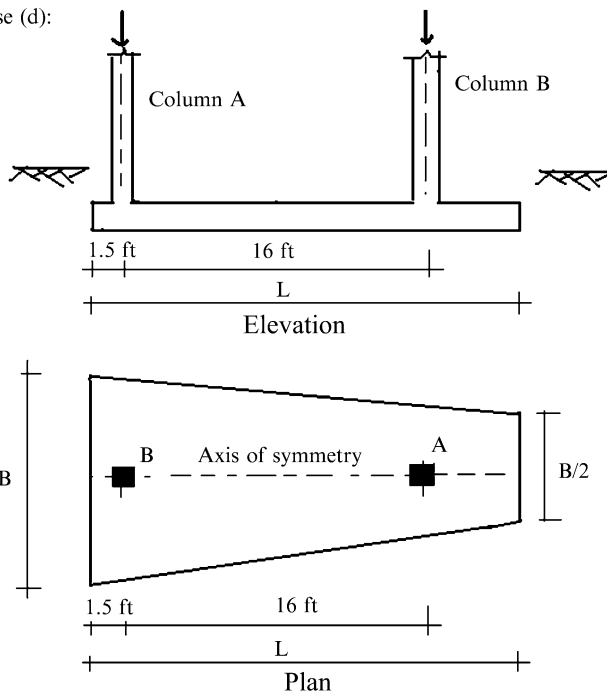
Case (b):



Case (c):

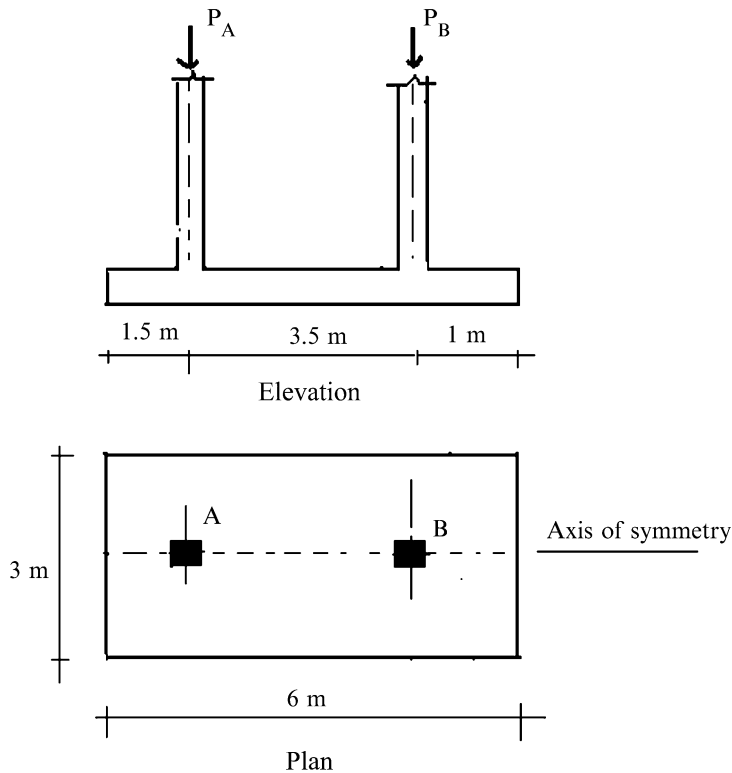


Case (d):



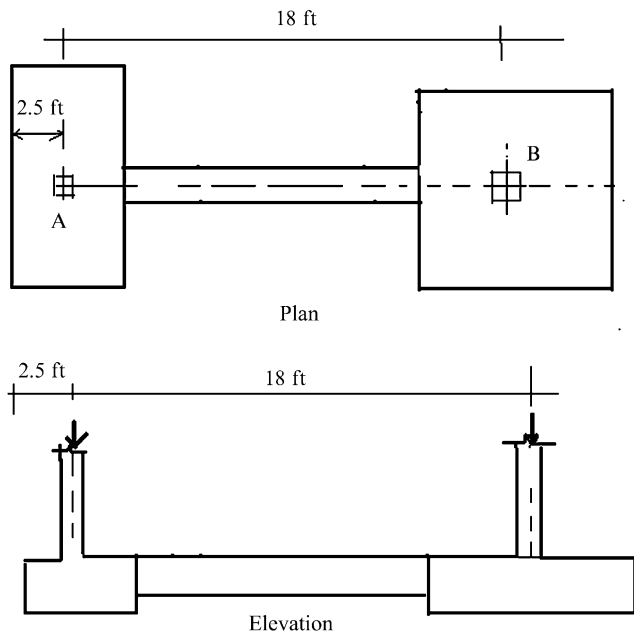
Problem 7.7

Column A is 350 mm \times 350 mm and carries a dead load of 1,300 kN and a live load of 450 kN. Column B is 450 mm \times 450 mm and carries a dead load of 1,400 kN and a live load of 800 kN. The combined footing shown below is used to support these columns. Determine the soil pressure distribution and the shear and bending moment distributions along the longitudinal direction corresponding to the factored loading, $P_u = 1.2P_D + 1.6P_L$.

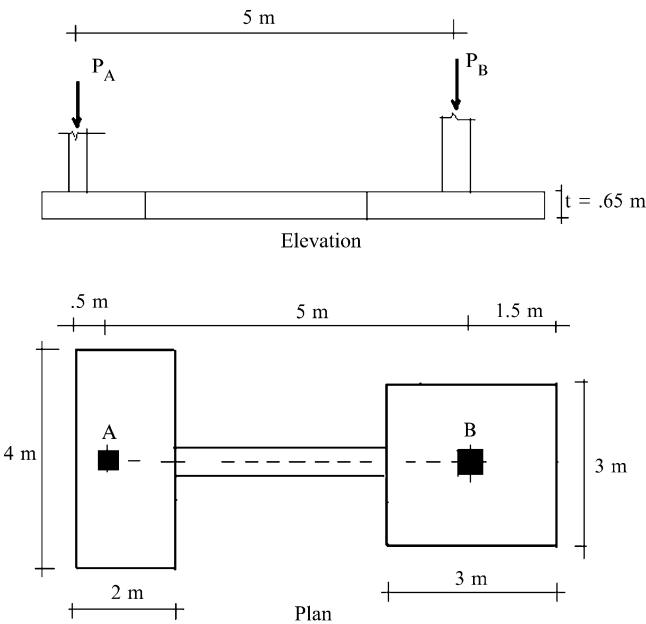


Problem 7.8

Dimension a strap footing for the situation shown. The exterior column A is 14 in. \times 14 in. and carries a dead load of 160 kip and a live load of 130 kip; the interior column B is 18 in. \times 18 in. and carries a dead load of 200 kip and a live load of 187.5 kip; the distance between the center lines of the columns is 18 ft. Assume the strap is placed such that it does not bear directly on the soil. Take the effective soil pressure as $q_e = 4.5 \text{ kip}/\text{ft}^2$. Draw shear and moment diagrams using a factored load of $P_u = 1.2P_D + 1.6P_L$.

**Problem 7.9**

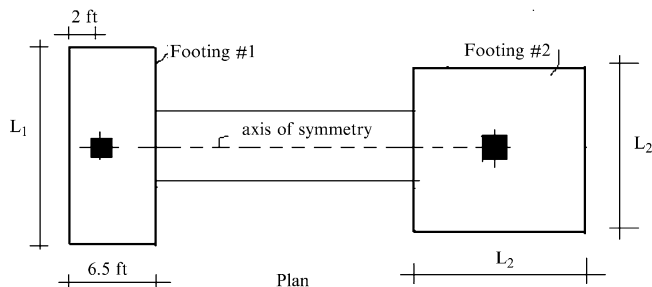
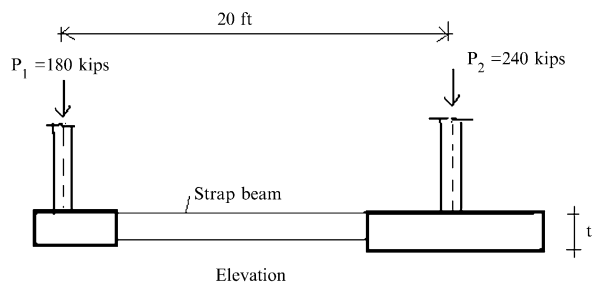
Column A is 350 mm \times 350 mm and carries a dead load of 1,300 kN and a live load of 450 kN. Column B is 450 mm \times 450 mm and carries a dead load of 1,400 kN and a live load of 800 kN. A strap footing is used to support the columns and the center line of Column A is 0.5 m from the property line. Assume the strap is placed such that it does not bear directly on the soil. Determine the soil pressure distribution and the shear and bending moment distributions along the longitudinal direction corresponding to the factored loading, $P_u = 1.2P_D + 1.6P_L$.



Problem 7.10

An exterior 18 in. \times 18 in. column with a total vertical service load of $P_1 = 180 \text{ kip}$ and an interior 20 in. \times 20 in. column with a total vertical service load of $P_2 = 240 \text{ kip}$ are to be supported at each column by a pad footing connected by a strap beam. Assume the strap is placed such that it does not bear directly on the soil.

- Determine the dimensions L_1 and L_2 for the pad footings that will result in a uniform effective soil pressure not exceeding $3 \text{ kip}/\text{ft}^2$ under each pad footing. Use $1/4 \text{ ft}$ increments.
- Determine the soil pressure profile under the footings determined in part (a) when an additional loading, consisting of an uplift force of 80 kip at the exterior column and an uplift force of 25 kip at the interior column, is applied.



Overview

Vertical wall type structures function as barriers whose purpose is to prevent a material from entering a certain space. Typical applications are embankment walls, bridge abutments, and as underground basement walls. Structural Engineers are responsible for the design of these structures. The loading acting on a retaining wall is generally due to the soil that is confined behind the wall. Various theories have been proposed in the literature, and it appears that all the theories predict similar loading results. In this chapter, we describe the Rankine theory that is fairly simple to apply. We present the governing equations for various design scenarios, and illustrate their application to typical retaining structures. The most critical concerns for retaining walls are *ensuring stability with respect to sliding and overturning, and identifying the regions of positive and negative moment in the wall segments*. Some of the material developed in Chap. 7 is also applicable for retaining wall structures.

8.1 Introduction

8.1.1 Types of Retaining Walls

Vertical retaining wall structures are used to form a vertical barrier that retains a fluid or other material such as soil. Figure 8.1 illustrates different types of vertical retaining wall structures. They are constructed using unreinforced concrete for gravity walls and reinforced concrete for cantilever walls and bridge abutments. The base of the wall/footing is placed below the frost level. The material behind the wall is called backfill and is composed of granular material such as sand.

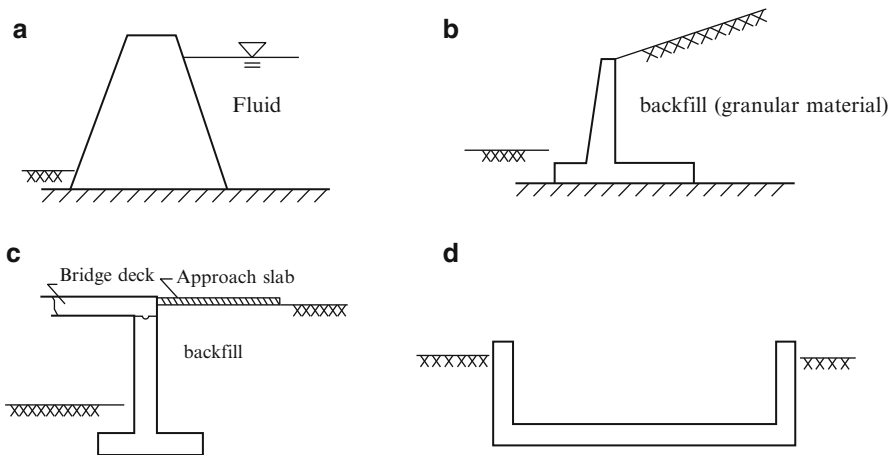


Fig. 8.1 Vertical retaining wall structures. (a) Gravity dam. (b) Cantilever retaining wall. (c) Bridge Abutment. (d) Underground basement

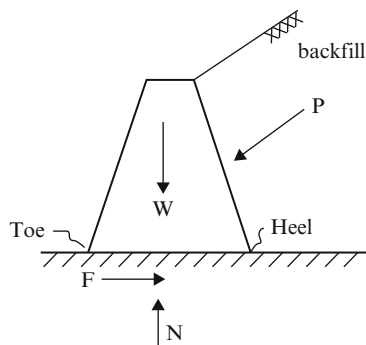


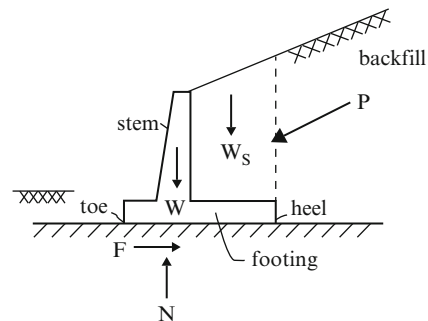
Fig. 8.2 Free body diagram—Gravity structure

8.1.2 Gravity Walls

A free body diagram of a gravity structure is shown in Fig. 8.2. The force acting on the structure due to the back fill material is represented by P ; the forces provided by the soil at the base are represented by the friction force F and the normal force N ; lastly the weight of the structure is represented by W . The end points of the base are called the “toe” and the “heel.” We observe that P tends to overturn the wall about its toe and also to slide the structure in the horizontal direction. The overturning tendency is resisted by the gravity force W which has a counterbalancing moment about the toe. Sliding is resisted by the friction which is proportional to the normal force. Therefore, since both resisting mechanisms are due to gravity, this type of structure is called a “Gravity” structure.

Of critical concern are the *sliding and overturning failure modes*. The key design parameter is the length of the base. We need to select this parameter such that the

Fig. 8.3 Free body diagram—Cantilever structure



factors of safety for sliding and overturning are sufficient to ensure global stability of the structure.

8.1.3 Cantilever Walls

The amount of concrete required for a gravity type wall increases with height. Therefore, in order to minimize the concrete volume, the cantilever type retaining wall geometry shown in Fig. 8.3 is used. A portion of the concrete wall is removed and a “footing” extending out from both the heel and toe is added. This change has a stabilizing effect in that the weight of the backfill above the footing, represented by W_s , now contributes to the counterbalancing moment and also to the normal force. The wall stem segment of a cantilever wall carries load through bending action whereas the gravity wall carries load primarily through *horizontal shear action*. These behavior modes dictate the type of construction.

Cantilever retaining walls, such as shown in Fig. 8.4, are reinforced concrete structures; gravity type walls tend to be unreinforced concrete. The key design issue is the width of the footing. This parameter is controlled by the requirements on the factors of safety with respect to overturning about the toe and sliding of the wall.

8.2 Force Due to the Backfill Material

8.2.1 Different Types of Materials

8.2.1.1 Fluid

We consider first the case where the backfill material is an ideal fluid. By definition, an ideal fluid has no shear resistance; the state of stress is pure compression. The vertical and horizontal pressures at a point z unit below the free surface are (see Fig. 8.5):

$$p_v = p_h = p = \gamma z \quad (8.1)$$

where γ is the weight density.

We apply this theory to the inclined surface shown in Fig. 8.6. Noting (8.1), the fluid pressure is normal to the surface and varies linearly with depth. The resultant force acts $H/3$ units up from the base and is equal to



Fig. 8.4 Cantilever wall construction

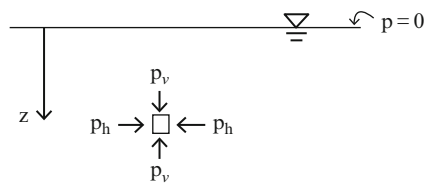


Fig. 8.5 Hydrostatic pressure

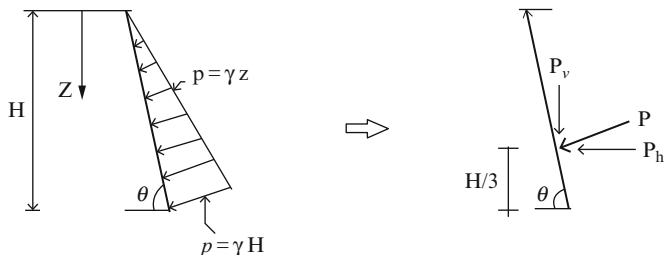


Fig. 8.6 Hydrostatic forces on an inclined surface

$$P = \frac{1}{2} p \frac{H}{\sin \theta} = \frac{1}{2} \gamma \left(\frac{H^2}{\sin \theta} \right) \quad (8.2)$$

Resolving P into horizontal and vertical components leads to

$$\begin{aligned} P_h &= P \sin \theta = \frac{1}{2} \gamma H^2 \\ P_v &= P \cos \theta = \frac{1}{2} \gamma H^2 \frac{1}{\tan \theta} \end{aligned} \quad (8.3)$$

Fig. 8.7 Granular material-stress state

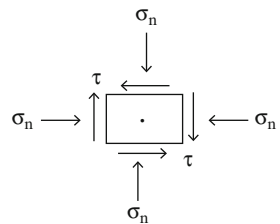


Fig. 8.8 Angle of repose

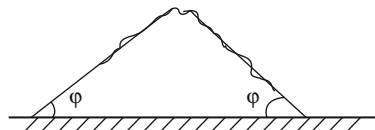
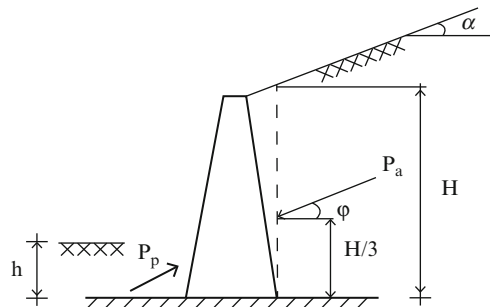


Fig. 8.9 Active and passive failure states



8.2.1.2 Granular Material

We consider next the case where the backfill behind the wall is composed of a granular material such as dry loose sand (Fig. 8.7). Loose sand behaves in a different manner than a fluid in that sand can resist shearing action as well as compressive action. The maximum shear stress for a sandy soil is expressed as

$$\tau = \sigma_n \tan \varphi$$

where σ_n is the normal stress and φ is defined as the internal friction angle for the soil. A typical value of φ for loose sand is approximately 30° . One can interpret φ as being related to the angle of repose that a volume of sand assumes when it is formed by dumping the sand loosely on the pile. Figure 8.8 illustrates this concept.

The presence of shear stress results in a shift in orientation of the resultant force exerted on the wall by the backfill. A typical case is shown in Fig. 8.9; P is assumed to act at an angle of φ' with respect to the horizontal, where φ' ranges from 0 to φ .

The magnitude of the soil pressure force depends on how the wall moved when the backfill was placed. If the wall moved away from the backfill (to the left in Fig. 8.9) the soil is said to be in an *active failure state*. The other extreme case is when the wall is pushed into the soil; the failure state is said to be in the *passive mode*. There is a significant difference in the force magnitudes corresponding to these states.

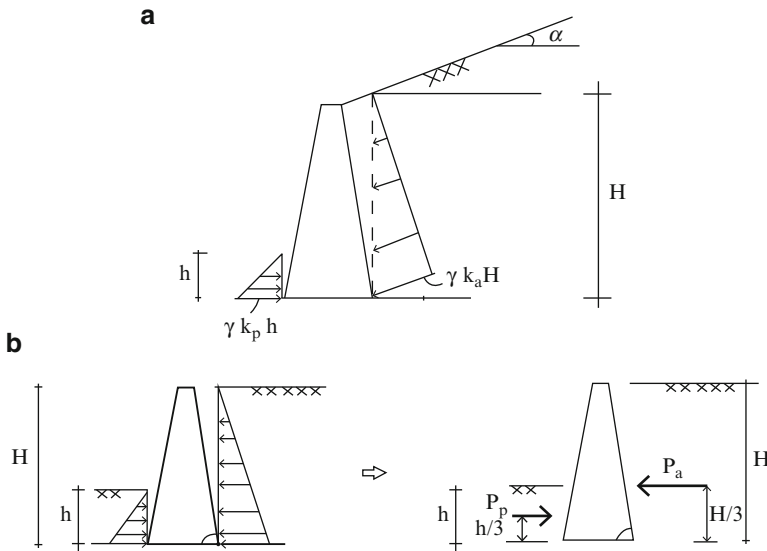


Fig. 8.10 (a) Soil pressure distribution for Rankine theory $\alpha \neq 0$. (b) Soil pressure distribution for Rankine theory $\alpha = 0$

In general, the active force is *an order of magnitude* less than the passive force. For the applications that we are considering, the most likely case is when the wall moves away from the soil, and therefore we assume “*active*” conditions. The downward component tends to increase the stability with respect to overturning about the toe and also increases the friction force.

Different theories for the soil pressure distribution have been proposed which relate to the choice of φ' . The Rankine theory assumes $\varphi' = 0$ (i.e., no shear stress), and the Coulomb theory assumes $\varphi' = \varphi$. Considering that there is significant variability in soil properties, both theories predict pressure distributions which are suitable for establishing the wall dimensions.

In what follows we present the key elements of the Rankine theory. There are many textbooks that deal with mechanics of soil. In particular we suggest Lamb and Whitman [20], Terzaghi and Peck [18], and Huntington [19].

8.2.2 Rankine Theory: Active Soil Pressure

Figure 8.10 defines the geometry and the soil pressure distribution. The pressure is applied to vertical surfaces through the heel and toe, and is assumed to vary linearly with depth as shown. The magnitude per unit wide strip in the longitudinal direction of the wall is defined by

$$\begin{aligned} P_a &= \frac{1}{2} \gamma H^2 k_a \\ P_p &= \frac{1}{2} \gamma h^2 k_p \end{aligned} \quad (8.4)$$

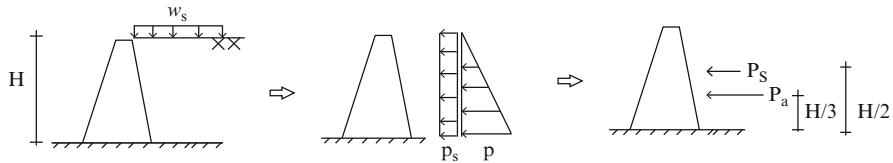


Fig. 8.11 Pressure distributions due to surcharge and active soil pressure

where γ is the unit weight of the soil backfill and k_a and k_p are defined as the active and passive soil pressure coefficients.

$$k_a = \cos \alpha \left\{ \frac{\cos \alpha - \sqrt{(\cos \alpha)^2 - (\cos \varphi)^2}}{\cos \alpha + \sqrt{(\cos \alpha)^2 - (\cos \varphi)^2}} \right\} \quad (8.5)$$

$$k_p = \frac{1 + \sin \varphi}{1 - \sin \varphi}$$

where φ is the internal friction angle and α is the angle of inclination for the backfill.

When the back fill is level, $\alpha = 0$ and k_a reduces to

$$k_a = \frac{1 - \sin \varphi}{1 + \sin \varphi} \quad (8.6)$$

In this case, both resultants are horizontal forces.

8.2.2.1 Soil Pressure due to Surcharge

When a surcharge is applied to the top of a backfill, additional soil pressure is developed. This pressure is assumed to be uniform over the depth. In the case of a uniform surcharge applied to a horizontal back fill, the *added* pressure is estimated as

$$p_s \approx k_a w_s \quad (8.7)$$

$$P_s \approx k_a w_s H$$

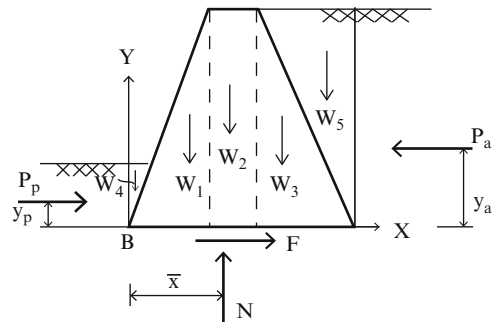
where k_a is defined by (8.6).

The soil pressure distributions due to the surcharge and the active soil pressure are illustrated in Fig. 8.11.

8.3 Stability Analysis of Retaining Walls

The key concerns for a retaining wall are overturning about the toe and sliding: In order to address these issues, one needs to determine the forces acting on the wall. This step requires that we carry out an equilibrium analysis.

Consider the typical gravity wall shown in Fig. 8.12. The weights of the wall and soil segments are denoted by W_j ; P_a and P_p represent the lateral soil pressure forces;

Fig. 8.12

N and F are the normal and tangential (friction) forces due to the soil pressure acting on the base. \bar{x} defines the line of action of the normal force acting on the base.

Summing forces in the vertical direction leads to

$$N = \sum W_j \quad (8.8)$$

Similarly, horizontal force summation yields

$$F = \sum P_i \quad (8.9)$$

The maximum horizontal force is taken as $F_{\max} = \mu N$. This quantity is used to define the factor of safety for sliding:

$$F.S._{\text{sliding}} = \frac{F_{\max}}{F} \quad (8.10)$$

where μ is a friction coefficient for the soil/base interface.

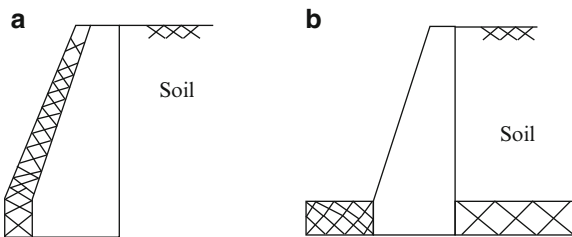
The line of action of N is found by summing moments about B.

$$\begin{aligned} N\bar{x} &= P_p y_p - P_a y_a + \sum W_j x_j = M_{\text{net}} \\ &\Downarrow \\ \bar{x}_1 &= \frac{M_{\text{net}}}{N} \end{aligned} \quad (8.11)$$

For stability respect to overturning, \bar{x} must be positive. A negative value of \bar{x} implies that the line of action of N lies outside the base. The safety measure for overturning is defined as the ratio of the resisting moment about the toe to the overturning moment.

$$F.S._{\text{overturning}} = \frac{M_{\text{resisting}}}{M_{\text{overturning}}} \quad (8.12)$$

Fig. 8.13 (a) Gravity wall and (b) cantilever retaining wall



Noting Fig. 8.12, this definition expands to

$$\text{F.S.}_{\text{overturning}} = \frac{P_p y_p + \sum W_j x_j}{P_a y_a} \quad (8.13)$$

Typical desired values are $\text{F.S.}_{\text{sliding}} > 1.5$ and $\text{F.S.}_{\text{overturning}} > 2$.

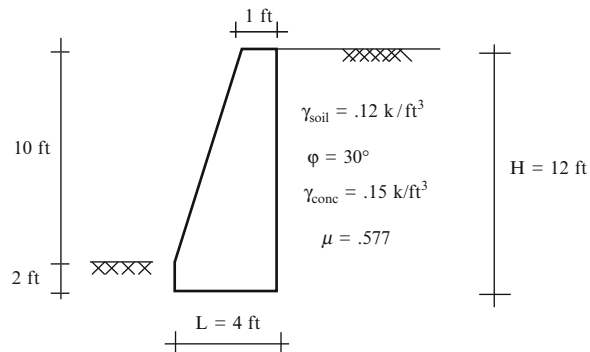
In order to increase the factors of safety against sliding and overturning one can either increase the width of the concrete wall, or one can add a footing extending out from the original base. These schemes are illustrated in Fig. 8.13.

Example 8.1 Gravity retaining wall analysis

Given: The concrete gravity wall and soil backfill shown in Fig. E8.1a.

Determine: The soil forces acting on the wall for active failure conditions based on the Rankine theory. Neglect the passive pressure acting on the toe.

Fig. E8.1a Wall geometry

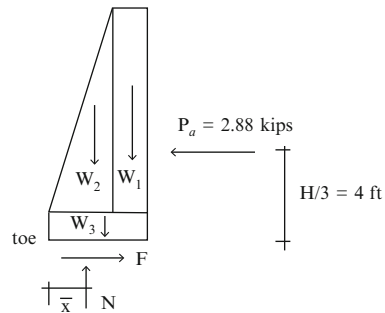


Solution:

$$\text{For } \varphi = 30^\circ, k_a = \frac{1 - \sin \varphi}{1 + \sin \varphi} = \frac{1}{3}$$

$$\text{Then } P_a = \frac{1}{2}(0.12)(12)^2 \left(\frac{1}{3}\right)(1 \text{ ft}) = 2.88 \text{ kip/ft of wall}$$

Fig. E8.1b Free body diagram



Next we compute the weight of the concrete wall segments per foot of wall. Noting Fig. E8.1b,

$$W_1 = (0.150)(10)(1)(1 \text{ ft}) = 1.5 \text{ kip}$$

$$W_2 = (0.150)\left(\frac{10}{2}\right)(3)(1 \text{ ft}) = 2.25 \text{ kip}$$

$$W_3 = (0.150)(4)(2)(1 \text{ ft}) = 1.2 \text{ kip}$$

Applying vertical force equilibrium yields

$$N = W_1 + W_2 + W_3 = 1.5 + 2.25 + 1.2 = 4.95 \text{ kip}$$

The factor of safety with respect to sliding is defined as the ratio of the maximum available friction force F_{\max} to the actual horizontal force.

$$F_{\max} = \mu N = 0.577(4.95) = 2.86 \text{ kip}$$

$$F.S.\text{,sliding} = \frac{\mu N}{P_a} = \frac{2.86}{2.88} = 0.99$$

The line of action of N is determined by summing moments about the toe. The factor of safety with respect to overturning is defined as the ratio of the resisting moment to the overturning moment, both quantities with respect to the toe.

$$M_{B_{\text{overturning}}} = P_a \left(\frac{H}{3}\right) = 2.88(4) = 11.52 \text{ kip ft}$$

$$M_{B_{\text{balancing}}} = W_1(3.5) + W_2(2) + W_3(2) = 1.5(3.5) + 2.25(2) + 1.2(2) = 12.15 \text{ kip ft}$$

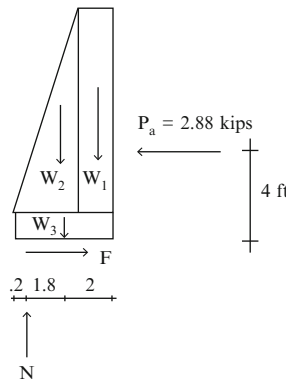
$$F.S.\text{,overturning} = \frac{M_{B_{\text{resisting}}}}{M_{B_{\text{overturning}}}} = \frac{12.15}{11.52} = 1.05$$

$$M_{B_{\text{net}}} = M_{B_{\text{overturning}}} - M_{B_{\text{resisting}}} = 0.63 \text{ kip ft clockwise}$$

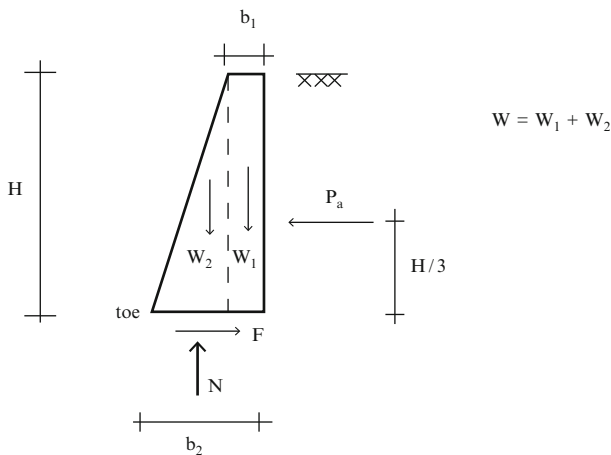
$$\bar{x} = \frac{M_{B_{\text{net}}}}{N} = \frac{0.63}{4.95} = 0.2 \text{ ft}$$

$$e = \frac{L}{2} - \bar{x} = 2 - 0.2 = 1.8 \text{ ft}$$

In order to increase the factors of safety the geometry needs to be modified.



The following procedure is useful for estimating appropriate values for b_1 and b_2 . Given the wall height, one can derive expressions for the factors of safety. The details are listed below.



$$W = \frac{(b_1 + b_2)}{2} H \gamma_c = N$$

$$P_a = k_a \left\{ \frac{1}{2} \gamma_s H^2 \right\}$$

$$F = P_a \quad \therefore F.S_{\text{sliding}} = \frac{\mu N}{F} = \frac{\mu N}{P_a}$$

↓

$$F.S_{\text{sliding}} = \left(\frac{\mu \gamma_c}{k_a \gamma_s} \right) \left(\frac{b_2}{H} \right) \left(1 + \frac{b_1}{b_2} \right)$$

$$M_{\text{overturning}} = \frac{H}{3} P_a = \frac{1}{6} k_a \gamma_s H^3$$

$$\begin{aligned} M_{\text{resisting}} &= \frac{2}{3} (b_2 - b_1) W_2 + \frac{2}{3} \left(b_2 - \frac{b_1}{2} \right) W_1 \\ &= \frac{H \gamma_c b_2^2}{3} \left\{ 1 - \frac{1}{2} \left(\frac{b_1}{b_2} \right)^2 + \frac{b_1}{b_2} \right\} \end{aligned}$$

$$\begin{aligned} F.S_{\text{overturning}} &= \frac{M_{\text{B}_{\text{resisting}}}}{M_{\text{B}_{\text{overturning}}}} = \frac{\frac{H \gamma_c b_2^2}{3} \left\{ 1 - \frac{1}{2} \left(\frac{b_1}{b_2} \right)^2 + \frac{b_1}{b_2} \right\}}{\frac{1}{6} k_a \gamma_s H^3} \\ &\downarrow \\ F.S_{\text{overturning}} &= \frac{2 \gamma_c}{k_a \gamma_s} \left(\frac{b_2}{H} \right)^2 \left\{ 1 - \frac{1}{2} \left(\frac{b_1}{b_2} \right)^2 + \frac{b_1}{b_2} \right\} \end{aligned}$$

One specifies the factor of safety with respect to overturning, and the ratio b_1/b_2 , and then computes the value for b_2/H . With b_2/H known, one checks for sliding and if necessary modifies the value of b_2/H .

Example 8.2

Given: The concrete gravity wall and soil backfill shown in Fig. E8.2a.

Determine: The required value for b_2 . Take the factors of safety for overturning and sliding to be equal to 2 and 1.5, respectively.

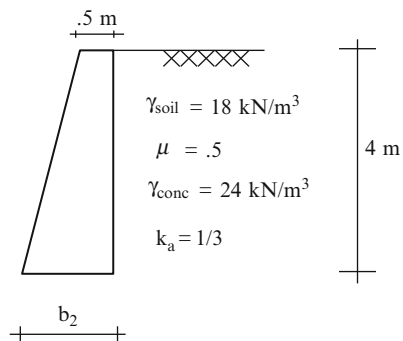


Fig. E8.2a

Solution: Given $b_1 = 0.5 \text{ m}$, $H = 4 \text{ m}$, F.S._{overturning} = 2, and F.S._{sliding} = 1.5 we will determine b_2 .

$$\text{F.S.}_{\text{overturning}} = \frac{2\gamma_c}{k_a\gamma_s} \left(\frac{b_2}{H} \right)^2 \left\{ 1 - \frac{1}{2} \left(\frac{b_1}{b_2} \right)^2 + \frac{b_1}{b_2} \right\}$$

$$\frac{2(24)}{\left(\frac{1}{3}\right)(18)} \left(\frac{b_2}{4} \right)^2 \left\{ 1 - \frac{1}{2} \left(\frac{0.5}{b_2} \right)^2 + \frac{0.5}{b_2} \right\} = 2$$

$$\therefore b_2^2 + 0.5b_2 - 4.125 = 0 \quad b_2 \text{ required} = 1.8 \text{ m}$$

$$\text{F.S.}_{\text{sliding}} = \left(\frac{\mu\gamma_c}{k_a\gamma_s} \right) \left(\frac{b_2}{H} \right) \left(1 + \frac{b_1}{b_2} \right)$$

$$1.5 = \frac{0.5(24)}{\left(\frac{1}{3}\right)(18)} \left(\frac{b_2}{4} \right) \left(1 + \frac{0.5}{b_2} \right) \quad b_2 \text{ required} = 2.5 \text{ m}$$

Use $b_2 = 2.5 \text{ m}$

8.4 Pressure Distribution Under the Wall Footing

We consider the footing defined in Fig. 8.13a. The pressure acting on the footing is assumed to vary linearly. There are two design constraints: firstly the peak pressures must be less than the allowable bearing pressure for the soil and secondly the pressure cannot be negative, i.e., tension. Noting the formulation presented in Sect. 7.2, the peak pressures are given by Equation (7.6) (we work with a unit width strip of the footing along the length of the wall, i.e., we take $B = 1$ and N as the resultant) which we list below for convenience.

$$\begin{aligned} q_1 &= \frac{N}{L} \left\{ 1 + \frac{6e}{L} \right\} \\ q_2 &= \frac{N}{L} \left\{ 1 - \frac{6e}{L} \right\} \end{aligned} \tag{8.14}$$

The second design constraint requires $|e| \leq L/6$ or equivalently, the line of action of N must be located within the middle third of the footing width, L . The first constraint limits the maximum peak pressure,

$$|q|_{\max} \leq q_{\text{allowable}}$$

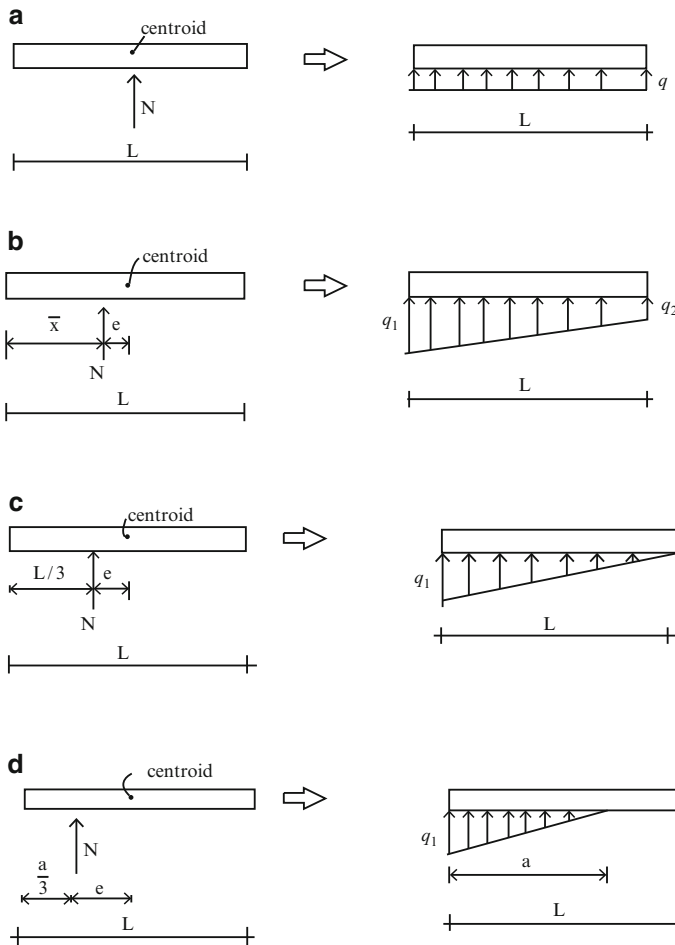


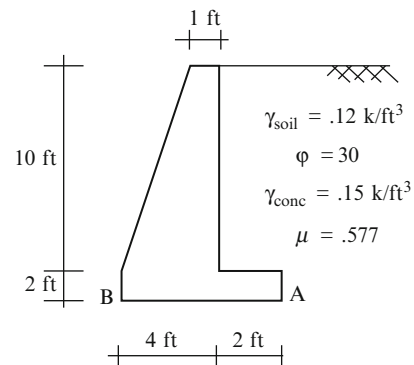
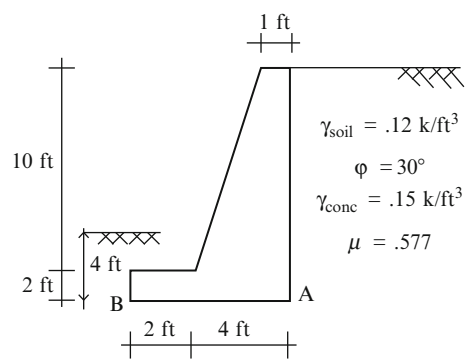
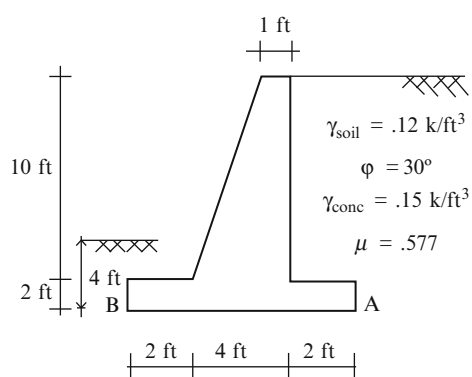
Fig. 8.14 Pressure distributions on footing/wall base. (a) $e = 0$. (b) $e < L/6$. (c) $e = L/6$. (d) $e > L/6$

where $q_{\text{allowable}}$ is the allowable soil pressure at the base of the wall. We note that the pressure distribution is uniform when N acts at the centroid of the footing area which, for this case, is the midpoint. Since e depends on the wall height and footing length, we define the optimal geometry as that combination of dimensions for which the soil pressure is *uniform*. Figure 8.14 shows the soil pressure distributions for various values of e . Note that the line of action of the resultant N always coincides with the line of action of the applied vertical load.

Example 8.3 Retaining wall with footing

Given: The walls defined in Figs. E8.3a–c. These schemes are modified versions of the wall analyzed in Example 8.1. We have extended the footing to further stabilize the wall.

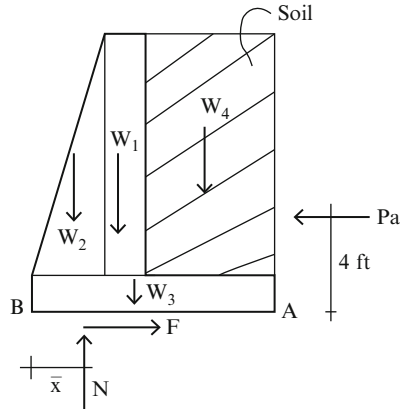
Determine: the location of the line of action of the normal bearing force based on the Rankine theory.

Fig. E8.3a Case "A"**Fig. E8.3b** Case "B"**Fig. E8.3c** Case "C"

Solution:

Case “A”: We work with the free body diagram shown in Fig. E8.3d. The vertical surface is taken to pass through the heel.

Fig. E8.3d



From Example 8.1:

$$W_1 = 1.5 \text{ kip} \quad W_2 = 2.25 \text{ kip} \quad P_a = 2.88 \text{ kip} \quad M_{B_{\text{overturing}}} = 11.52 \text{ kip ft}$$

The weight of the footing is

$$W_3 = (0.150)(6)(2)(1 \text{ ft}) = 1.8 \text{ kip}$$

The additional weight of soil is $W_4 = (0.120)(10)(4)(1 \text{ ft}) = 4.8 \text{ kip}$
Then

$$N = \sum W_i = W_1 + W_2 + W_3 + W_4 = 1.5 + 2.25 + 1.8 + 3.6 = 9.15 \text{ kip}$$

$$F_{\max} = \mu N = 0.577(9.15) = 5.28 \text{ kip}$$

$$\text{F.S.}_{\text{sliding}} = \frac{F_{\max}}{P_a} = \frac{5.28}{2.88} = 1.83$$

We sum moments about the toe:

$$\begin{aligned} M_{B_{\text{resisting}}} &= W_1(3.5) + W_2(2) + W_3(3) + W_4(5) \\ &= 1.5(3.5) + 2.25(2) + 1.8(3) + 3.6(5) = 33.15 \text{ kip ft} \\ M_{B_{\text{overturing}}} &= 11.52 \text{ kip ft} \end{aligned}$$

Using these moments, the factor of safety is

$$\text{F.S.}_{\text{overtur}} = \frac{M_{B_{\text{resisting}}}}{M_{B_{\text{overtur}}}} = \frac{33.15}{11.52} = 2.87$$

Next, we determine the line of action of the resultant

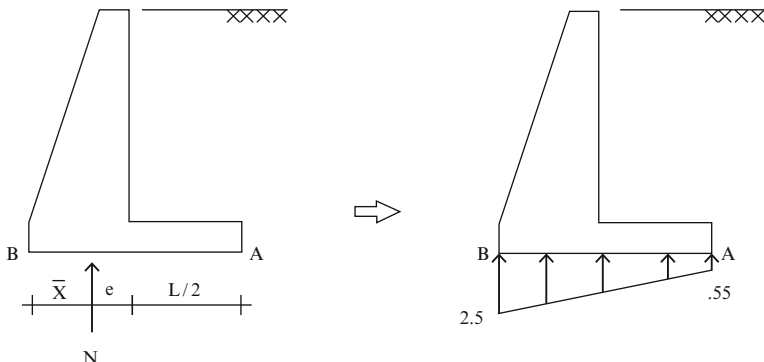
$$M_{B_{\text{total}}} = M_{B_{\text{resisting}}} - M_{B_{\text{overtur}}} = 21.63 \text{ kip ft}$$

$$\bar{x} = \frac{M_{B_{\text{total}}}}{N} = \frac{21.63}{9.15} = 2.36 \text{ ft}$$

$$e = \frac{L}{2} - \bar{x} = 3 - 2.36 = 0.64 \text{ ft} < \frac{L}{6} = 1.0 \text{ ft}$$

Lastly, we compute the pressure loading acting on the base.

$$q = \frac{N}{L} \left(1 \pm \frac{6e}{L} \right) = \frac{9.15}{6} \left(1 \pm \frac{6(0.64)}{6} \right) \Rightarrow q_1 = 2.5 \text{ kip/ft}^2, q_2 = 0.55 \text{ kip/ft}^2$$



Case “B”: For this case, we work with the free body diagram shown in Fig. E8.3e. The additional weight of soil is $W_5 = (0.120)(2)(2)(1 \text{ ft}) = 0.48 \text{ kip}$

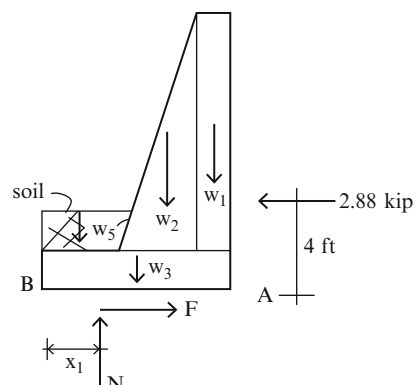


Fig. E8.3e

The calculations proceed as follows:

$$N = W_1 + W_2 + W_3 + W_5 = 1.5 + 2.25 + 1.8 + .48 = 6.03 \text{ kip}$$

$$F_{\max} = \mu N = 0.577(6.03) = 3.48 \text{ kip}$$

$$\text{F.S.}_{\text{sliding}} = \frac{F_{\max}}{P_a} = \frac{3.48}{2.88} = 1.2$$

We sum moments about the toe:

$$\begin{aligned} M_{B_{\text{resisting}}} &= W_1(5.5) + W_2(4) + W_3(3) + W_5(1) \\ &= 1.5(5.5) + 2.25(4) + 1.8(3) + 0.48(1) = 23.13 \text{ kip ft} \end{aligned}$$

$$M_{B_{\text{overturning}}} = 4(2.88) = 11.52 \text{ kip ft}$$

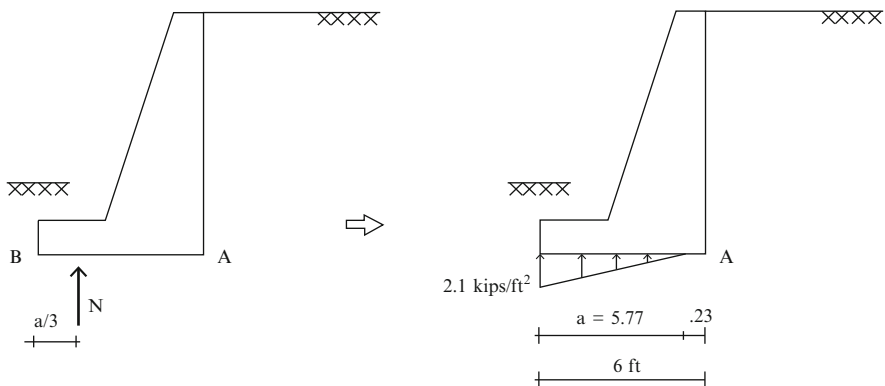
$$\text{F.S.}_{\text{overturning}} = \frac{M_{B_{\text{resisting}}}}{M_{B_{\text{overturning}}}} = \frac{23.13}{11.52} = 2.0$$

$$M_{B_{\text{total}}} = M_{B_{\text{resisting}}} - M_{B_{\text{overturning}}} = 11.61 \text{ kip ft}$$

$$\bar{x} = \frac{M_{B_{\text{total}}}}{N} = \frac{11.61}{6.03} = 1.925 \text{ ft}$$

$$e = \frac{L}{2} - \bar{x} = 3 - 1.925 = 1.07 \text{ ft} > \frac{L}{6} = 1.0 \text{ ft} \quad \therefore a = 3 \bar{x} = 5.77 \text{ ft}$$

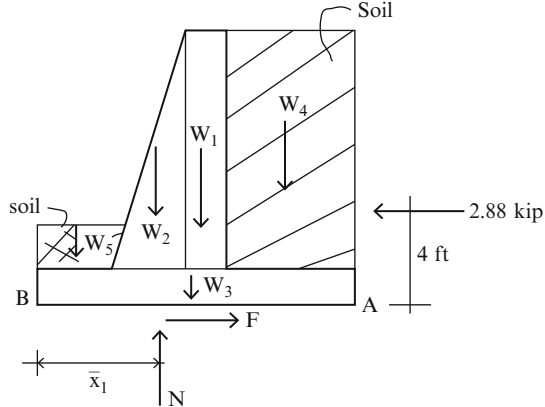
$$q_1 = \frac{2N}{a} = \frac{2(6.03)}{5.77} = 2.1 \text{ kip/ft}^2$$



Note that the line of action of the normal force is within the base but the pressure is negative at the heel.

Case “C”: We work with the free body diagram shown in Fig. E8.3f. The dimensions are defined in Fig. E8.3c. The revised value of W_3 is $W_3 = (0.15)(8)(2)(1 \text{ ft}) = 2.4 \text{ kip}$

Fig. E8.3f



Then

$$N = W_1 + W_2 + W_3 + W_4 + W_5 = 1.5 + 2.25 + 2.4 + 4.8 + 0.48 = 11.43 \text{ kip}$$

$$F_{\max} = \mu N = 0.577(11.43) = 6.6 \text{ kip}$$

$$\text{F.S.}_{\text{sliding}} = \frac{F_{\max}}{P_a} = \frac{6.6}{2.88} = 2.29$$

We sum moments about the toe:

$$\begin{aligned} M_{B_{\text{balancing}}} &= W_1(5.5) + W_2(4) + W_3(4) + W_4(7) + W_5(1) \\ &= 1.5(5.5) + 2.25(4) + 2.4(4) + 4.8(7) + .48(1) = 60.93 \text{ kip ft} \end{aligned}$$

$$\text{F.S.}_{\text{overturing}} = \frac{M_{B_{\text{resisting}}}}{M_{B_{\text{overturing}}}} = \frac{60.93}{11.52} = 5.29$$

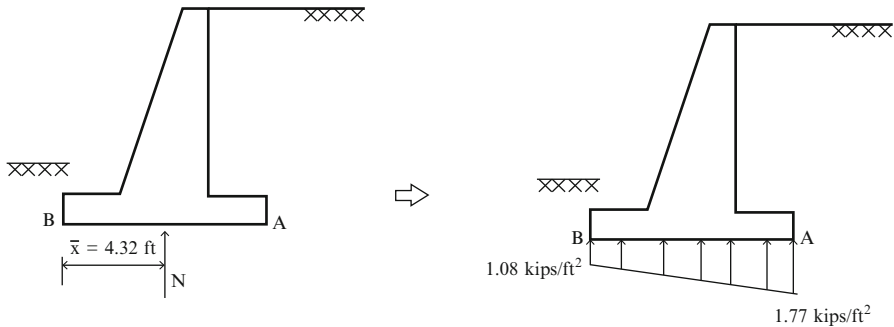
$$M_{B_{\text{total}}} = M_{B_{\text{resisting}}} - M_{B_{\text{overturing}}} = 49.41 \text{ kip ft}$$

$$\bar{x} = \frac{M_{B_{\text{total}}}}{N} = \frac{49.41}{11.43} = 4.32 \text{ ft}$$

$$e = \frac{L}{2} - \bar{x} = 4 - 4.32 = -0.32 \text{ ft}$$

$$|e| < L/6 = 1.33 \text{ ft}$$

$$\therefore q = \frac{N}{L} \left(1 \pm \frac{6e}{L} \right) = \frac{11.43}{8} \left(1 \pm \frac{6(.32)}{8} \right) \Rightarrow q_1 = 1.08 \text{ kip/ft}^2, q_2 = 1.77 \text{ kip/ft}^2$$



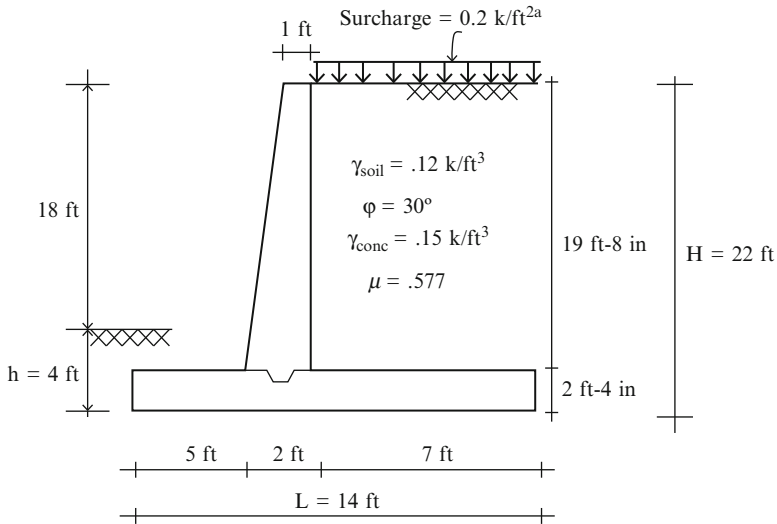
We point out that case C has the lowest peak pressure. The analysis results are summarized in the table below.

	Case A	Case B	Case C
N	9.15 kip	6.03 kip	11.43 kip
Friction	5.28 kip	3.48 kip	6.6 kip
F.S. _{sliding}	1.83	1.2	2.29
M balancing	33.15 kip ft	23.13 kip ft	60.93 kip ft
M overturning	11.52 kip ft	11.52 kip ft	11.52 kip ft
F.S. overturning	2.87	2.	5.29
\bar{x}	2.36 ft	1.925 ft	4.32 ft
e	0.64 ft < L/6 = 1	1.07 ft > L/6 = 1	0.32 ft < L/6 = 1
q ₁	2.5 kip/ft	2.1 kip/ft	1.77 kip/ft
q ₂	0.55 kip/ft	—	1.08 kip/ft

Example 8.4 Cantilever retaining wall

Given: The retaining wall and soil backfill shown in Fig. E8.4a

Determine: The factor of safety against sliding; the factor of safety against overturning; the base pressure distribution. Assume the allowable soil pressure = 4 ksf. Use the Rankine theory for soil pressure computations.

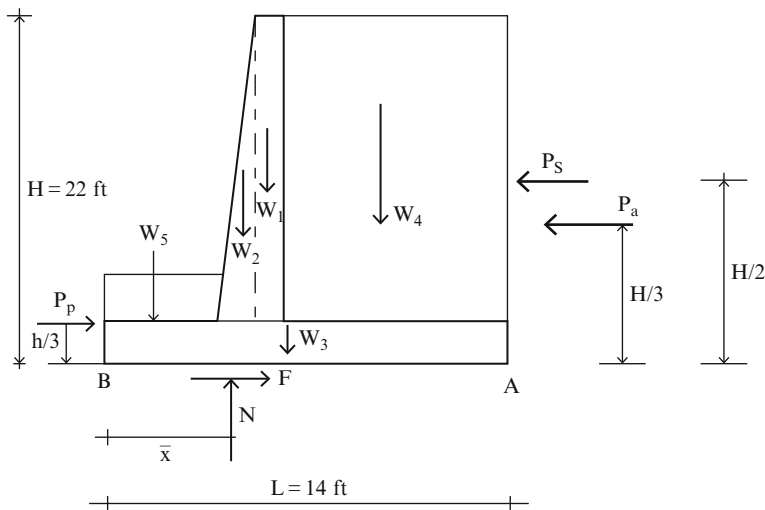
**Fig. E8.4a****Solution:**

Noting Fig. E8.4b, the soil pressure and weight forces are

$$P_a = \frac{1}{2} k_a \gamma_s H^2 = \frac{1}{2} \left(\frac{1}{3}\right) (0.12)(22)^2 = 9.68 \text{ kip}$$

$$P_p = \frac{1}{2} k_p \gamma_s H'^2 = \frac{1}{2} (3)(0.12)(4)^2 = 2.88 \text{ kip}$$

$$P_s = k_a w_s H = \left(\frac{1}{3}\right) (0.2)(22) = 1.47 \text{ kip}$$

**Fig. E8.4b**

$$W_1 = 0.15(1)(19.66) = 2.95 \text{ kip}$$

$$W_2 = 0.15(1)\left(\frac{19.66}{2}\right) = 1.47 \text{ kip}$$

$$W_3 = 0.15(2.34)(14) = 4.91 \text{ kip}$$

$$W_4 = 0.12(7)(19.66) = 16.5 \text{ kip}$$

$$W_5 = 0.12(5)(1.67) = 1.0 \text{ kip}$$

The normal and horizontal forces are

$$N = W_1 + W_2 + W_3 + W_4 + W_5 = 26.84 \text{ kip}$$

$$F_{\max} = \mu N = 0.577(26.84) = 15.5 \text{ kip}$$

$$\sum F_{\text{horizontal}} = P_a + P_s - P_p = 9.68 + 1.47 - 2.88 = 8.27 \text{ kip} \leftarrow$$

Next we compute the factors of safety.

$$\text{F.S.}_{\text{sliding}} = \frac{F_{\max}}{\sum F_{\text{horizontal}}} = \frac{15.5}{8.27} = 1.87$$

$$M_{B_{\text{overturing}}} = P_a \left(\frac{H}{3}\right) + P_s \left(\frac{H}{2}\right) = 9.68 \left(\frac{22}{3}\right) + 1.47 \left(\frac{22}{2}\right) = 87.2 \text{ kip ft}$$

$$\begin{aligned} M_{B_{\text{resisting}}} &= W_1(6.5) + W_2(5.67) + W_3(7) + W_4(10.5) + W_5(2.5) + P_p(1.33) \\ &= 2.95(6.5) + 1.47(5.67) + 4.91(7) + 16.5(10.5) + 1.0(2.5) + 2.88(1.33) \\ &= 241.5 \text{ kip ft} \end{aligned}$$

$$\text{F.S.}_{\text{overturing}} = \frac{M_{B_{\text{resisting}}}}{M_{B_{\text{overturing}}}} = \frac{241.5}{87.2} = 2.77$$

Lastly, we determine the location of the line of action of N .

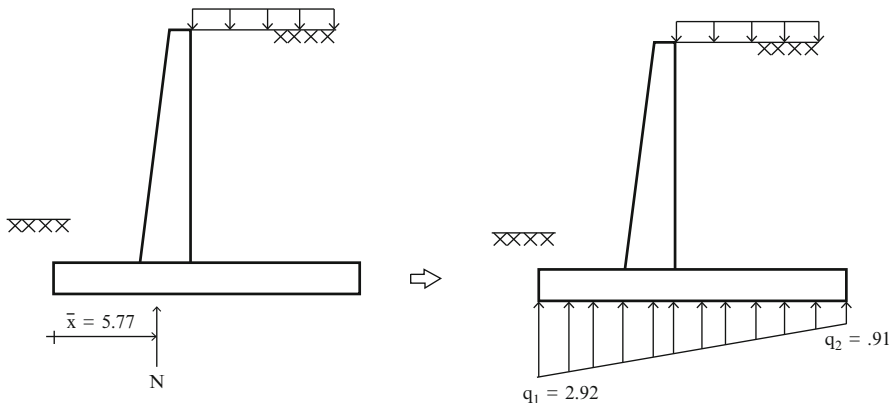
$$M_{B_{\text{total}}} = M_{B_{\text{resisting}}} - M_{B_{\text{overturing}}} = 154.8 \text{ kip ft}$$

$$\bar{x} = \frac{M_{B_{\text{total}}}}{N} = \frac{154.8}{26.84} = 5.77 \text{ ft}$$

$$e = \frac{L}{2} - \bar{x} = \frac{14}{2} - 5.77 = 1.23 \text{ ft} < \frac{L}{6} = 2.33 \text{ ft}$$

Using the above values, the peak pressures are

$$q = \frac{N}{L} \left(1 \pm \frac{6e}{L}\right) = \frac{26.84}{14} \left(1 \pm \frac{6(1.23)}{14}\right) \Rightarrow q_1 = 2.92 \text{ kip/ft}^2 \quad q_2 = 0.91 \text{ kip/ft}^2$$



Example 8.5 Retaining wall supported by concrete piles

Given: The structure shown in Fig. E8.5a. Assume all the loads acting on the wall are resisted by the axial loads in the concrete piles. Consider the pile spaced at 6 ft on center.

Use Rankine theory.

Determine: The axial loads in the piles.

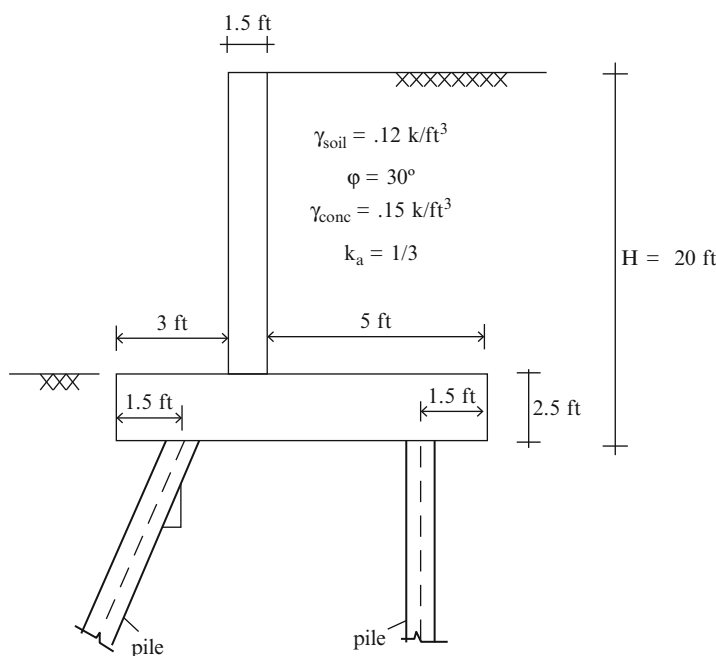


Fig. E8.5a

Solution: We consider a 6 ft segment of the wall. The free body diagram for this segment is shown in Fig. E8.5b. F_1 and F_2 denote the pile forces; P_a is the active lateral soil force; and the W term relate to various weights. We neglect the passive soil force and assume the horizontal load is carried by the inclined pile.

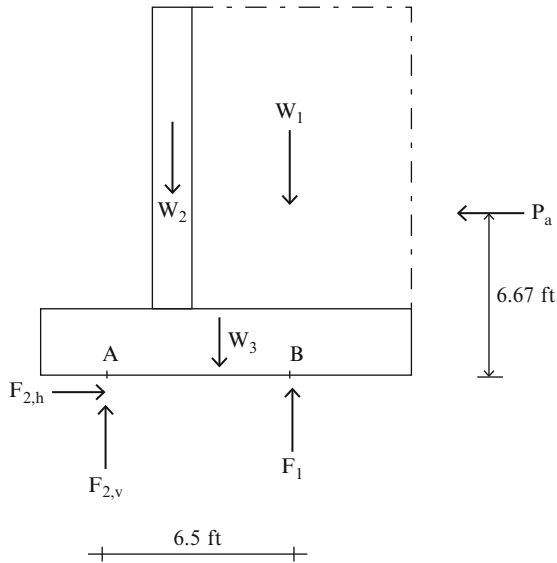
$$P_a = \frac{1}{2} \left(\frac{1}{3} \right) (0.12)(20)^2 (6) = 48 \text{ kip}$$

$$W_1 = (5)(17.5)(6)(0.12) = 63 \text{ kip}$$

$$W_2 = (1.5)(17.5)(6)(0.15) = 23.6 \text{ kip}$$

$$W_3 = (2.5)(9.5)(6)(0.15) = 21.4 \text{ kip}$$

Fig. E8.5b



By summing the moments about A , we determine F_1 :

$$\sum M_A = 0 \quad (2.25)W_2 + (3.25)W_3 + (5.5)W_1 = 6.67P + 6.5F_1 \Rightarrow F_1 = 22.92 \text{ kip}$$

Summing the vertical forces leads to

$$\sum F_y = 0 \Rightarrow F_{2,v} = 85.1 \text{ kip}$$

Similarly, the horizontal loads yields

$$\sum F_x = 0 \Rightarrow F_{2,h} = P_a = 48 \text{ kip}$$

Then, the axial force in the battered pile is

$$F_2 = \sqrt{F_h^2 + F_v^2} = 97.7$$

And the required batter is $48/85.1 = .56$

8.5 Critical Sections for Design of Cantilever Walls

The different segments of a typical cantilever retaining wall structure are shown in Fig. 8.15. The stem functions as a cantilever beam supported by the footing. Gravity and lateral loading are transmitted by the stem onto the footing which then distributes the loading onto the soil. The footing has two counteracting loadings at the heel; the loading due to the weight of the soil, and the pressure loading. The latter is usually neglected when estimating the peak negative moment in the footing. The bending moment distributions are also plotted in Fig. 8.15d. Note that for this type of structure, the bending moment distribution in the footing has both positive and negative regions. *The critical region for design is the stem-footing junction.*

Retaining wall structures are constructed using reinforced concrete. The thickness of the footing sections is governed by the shear capacity. The location and magnitude of the steel reinforcement is dictated by the sense of the bending moment distribution (i.e., positive or negative). Noting that the function of the reinforcement is to provide the tensile force required by the moment, the moment diagrams shown in Fig. 8.15d require the reinforcement patterns defined in Fig. 8.16. The actual size/number of the rebars depends on the magnitude of the moment and the particular design code used to dimension the member.

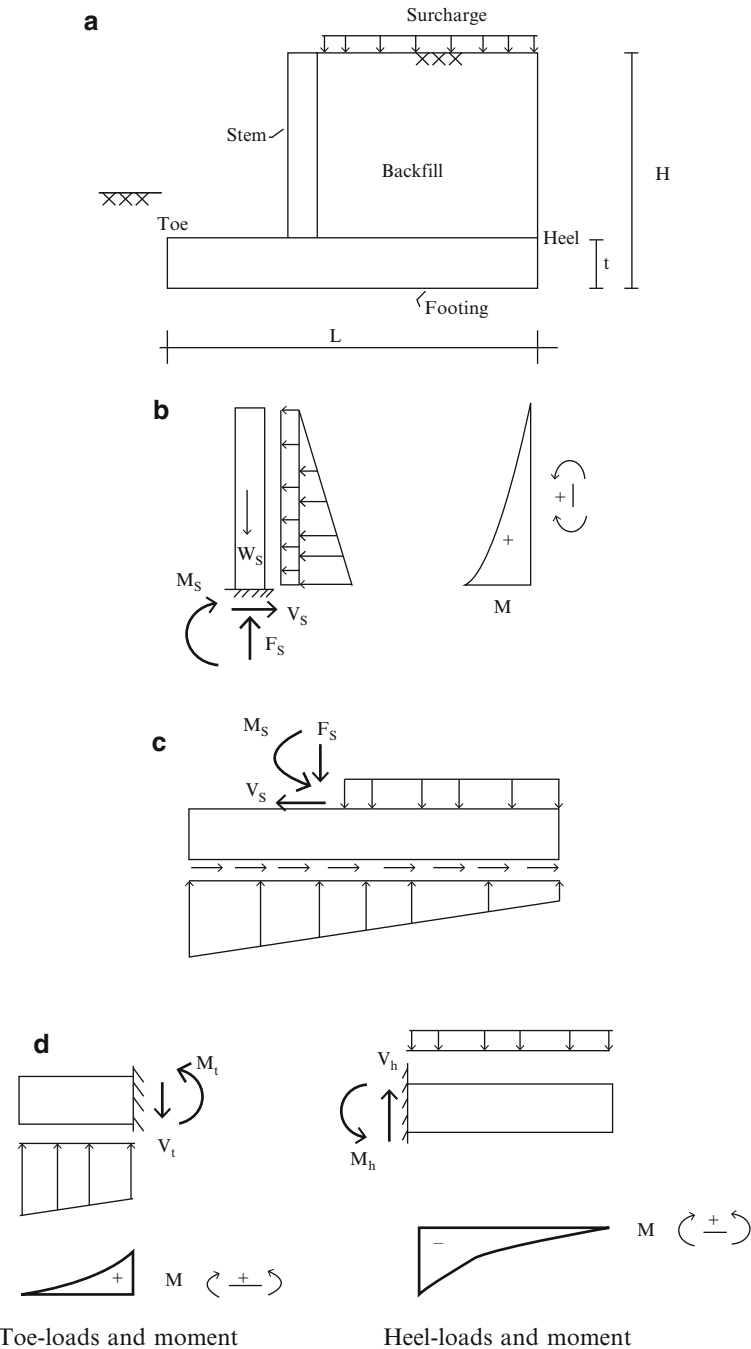


Fig. 8.15 Loadings and response pattern for cantilever Retaining Wall Structure. (a) Cantilever retaining wall components. (b) Stem—loads and bending moment. (c) Footing—loads. (d) Components of footing

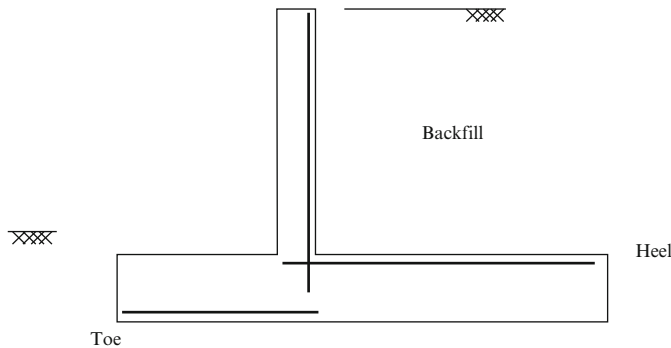


Fig. 8.16 Typical steel reinforcement patterns

Example 8.6

Given: The structure shown in Fig. E8.6a.

Determine:

- The required L_1 such that the factor of safety with respect to overturning is equal to 2.
- The tension areas in the stem, toe, and heel and show the reinforcing pattern.

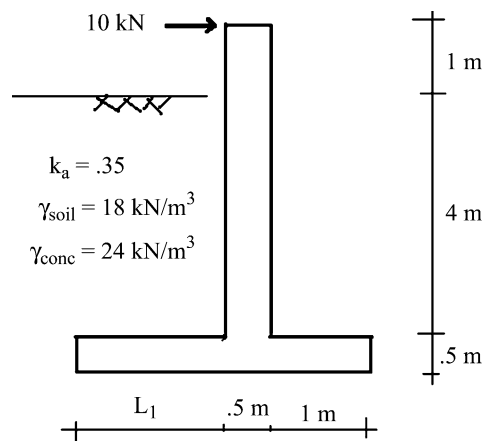
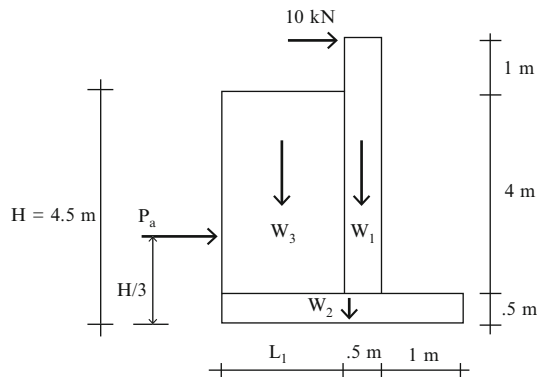


Fig. E8.6a

Solution:



$$P_a = \frac{1}{2} k_a \gamma_s H^2 = \frac{1}{2} (0.35)(18)(4.5)^2 = 63.8 \text{ kN}$$

$$W_1 = (0.5)(5)(24) = 60 \text{ kN}$$

$$W_2 = (0.5)(1.5 + L_1)(24)$$

$$W_3 = (4)(L_1)(18)$$

$$M_{B_{\text{overturning}}} = 63.8 \left(\frac{4.5}{3} \right) + 10(5.5) = 150.7$$

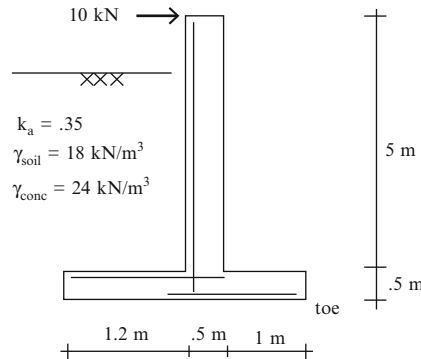
$$M_{B_{\text{resisting}}} = W_1(1.25) + W_2 \left(\frac{L_1 + 1.5}{2} \right) + W_3 \left(\frac{L_1}{2} + 1.5 \right)$$

$$\text{F.S.}_{\text{overturning}} = 2 = \frac{M_{B_{\text{resisting}}}}{M_{B_{\text{overturning}}}} = \frac{W_1(1.25) + W_2 \left(\frac{L_1 + 1.5}{2} \right) + W_3 \left(\frac{L_1}{2} + 1.5 \right)}{150.7}$$

↓

$$L_1 \text{ required} = 1.2 \text{ m}$$

Figure below shows the reinforcing for the tension areas.



8.6 Summary

8.6.1 Objectives of the Chapter

- To introduce the topic of vertical retaining wall structures used for embankments, abutments, and underground structures.
- To present a theory for establishing the lateral loading exerted by soil backfill on vertical walls.
- To develop a methodology for evaluating the stability of cantilever retaining walls when subjected to lateral loading due to backfill and surcharges.

8.6.2 Key Concepts and Facts

- The Rankine theory predicts a linear distribution of soil pressure which acts normal to a vertical face and increases with depth. The resultant force is given by

$$P_a = \frac{1}{2} \gamma H^2 k_a$$

where H is the vertical wall height, γ is the soil density, and k_a is a dimensionless coefficient that depends on the soil type and nature of the relative motion between the wall and the backfill. For active conditions,

$$k_a = \frac{1 - \sin \varphi}{1 + \sin \varphi}$$

where φ is the soil friction angle, typically $\approx 30^\circ$.

- Stability is addressed from two perspectives: Sliding and overturning. The factor of safety with respect to sliding is defined as the ratio of the peak available

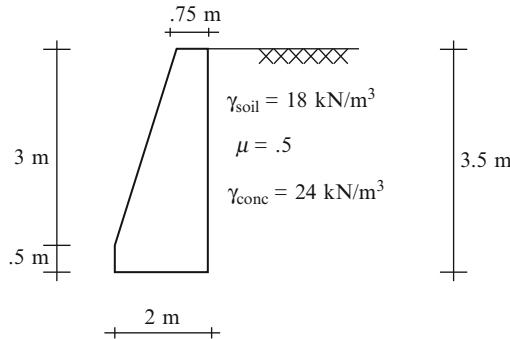
horizontal friction force to the actual friction force. The factor of safety with respect to overturning about the toe is taken as the ratio of the restoring moment to the unbalancing moment.

- One selects the dimensions of the footing, such that these factors of safety are greater than one and the resultant force due to the structural weight and the soil loads act within the middle third of the footing width.

8.7 Problems

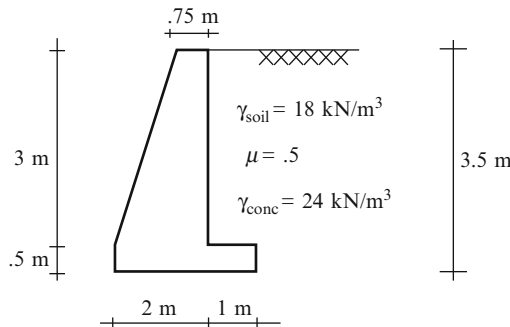
Problem 8.1

For the concrete retaining wall shown, determine the factors of safety against sliding and overturning and the base pressure distribution. Use the Rankine theory for soil pressure computations.



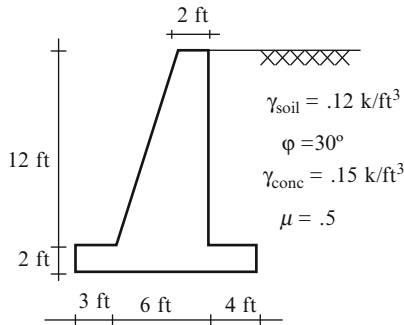
Problem 8.2

For the concrete retaining wall shown, determine the factors of safety against sliding and overturning and the base pressure distribution. Use the Rankine theory for soil pressure computations.

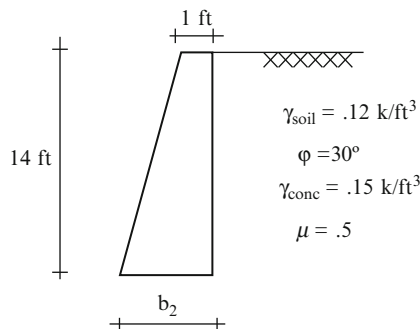


Problem 8.3

For the concrete retaining wall shown, determine the factors of safety against sliding and overturning and the base pressure distribution. Use the Rankine theory for soil pressure computations

**Problem 8.4**

For the concrete retaining wall shown, determine the required value for b_2 . Take the factors of safety for overturning and sliding to be equal to 1.75 and 1.25, respectively. Use the Rankine theory for soil pressure computations.

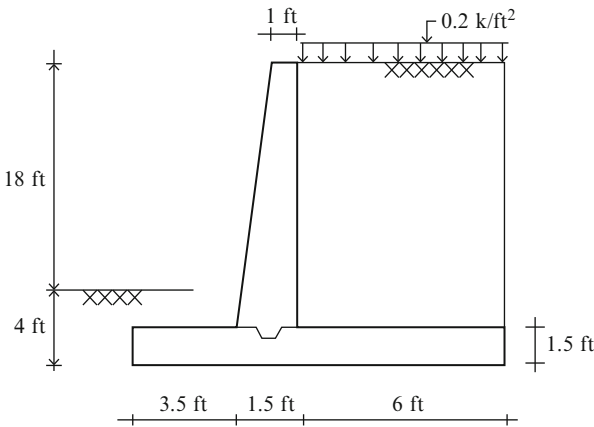
**Problem 8.5**

For the retaining wall shown, determine
 (a) The soil pressure acting on the wall
 (b) The factor of safety for overturning

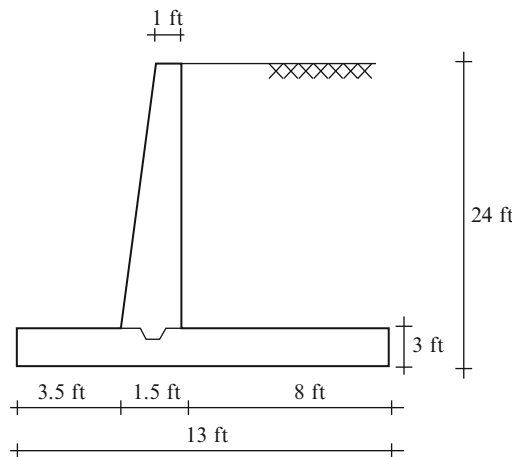
(c) The factor of safety for sliding

(d) The soil pressure distribution under the footing

Assume: $\gamma_{\text{soil}} = 0.12 \text{ kip}/\text{ft}^3$, $\gamma_{\text{concrete}} = 0.15 \text{ kip}/\text{ft}^3$, $\mu = .5$ and $\Phi = 30^\circ$.



Problem 8.6



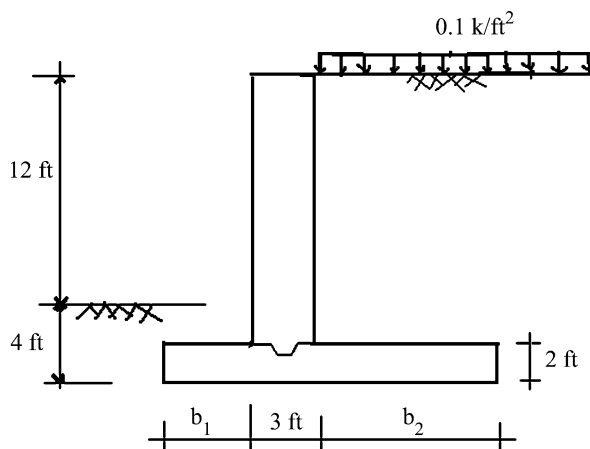
(a) Determine the factors of safety against overturning and sliding.

(b) Determine the soil pressure distribution under the footing (q_1 , q_2).

(c) Determine the moment distribution in the stem.

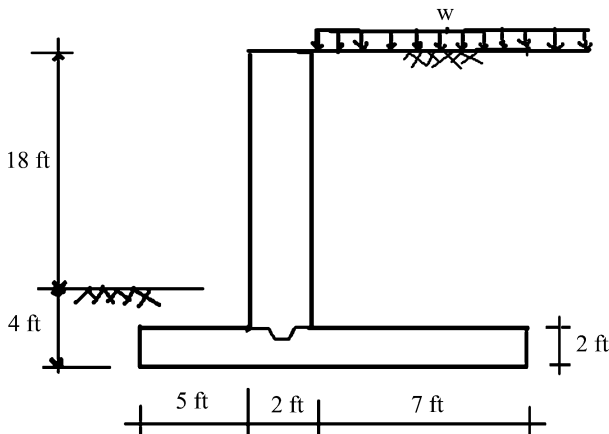
(d) Determine the bending moment distribution in the heel.

Assume: Allowable soil pressure = 5.0 ksf, $\gamma_{\text{soil}} = 0.12 \text{ kip}/\text{ft}^3$ and $\gamma_{\text{concrete}} = 0.15 \text{ kip}/\text{ft}^3$

Problem 8.7

Suggest values for b_1 and b_2 . Take the safety factors for sliding and over turning to be equal to 2.

Assume: $\gamma_{\text{soil}} = 0.12 \text{ kip/ft}^3$, $\gamma_{\text{concrete}} = 0.15 \text{ kip/ft}^3$, $\mu = .57$, and $\Phi = 30^\circ$.

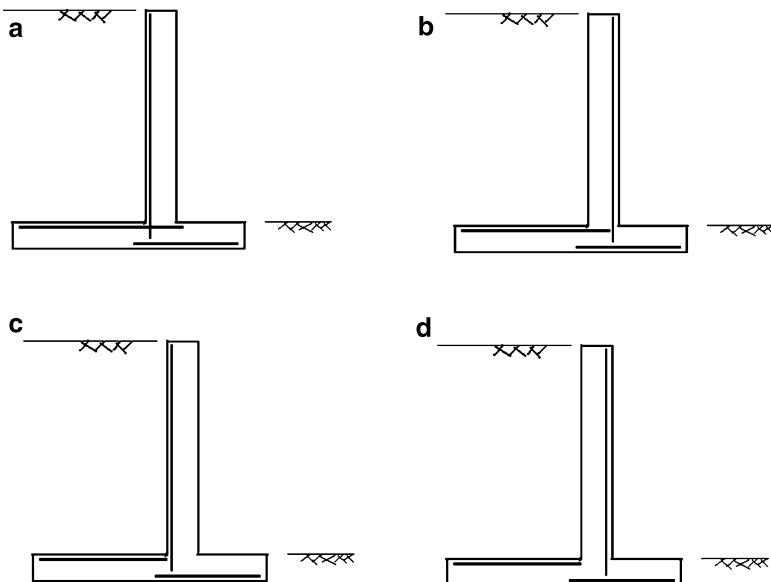
Problem 8.8

Determine the minimum value of w at which soil failure occurs (i.e., the soil pressure exceeds the allowable soil pressure).

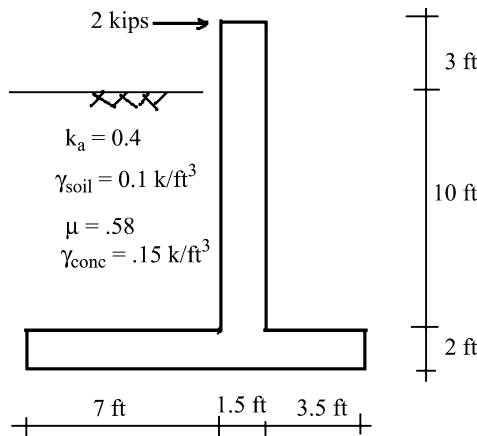
Assume: $q_{\text{allowable}} = 5 \text{ kip/ft}^2$, $\gamma_{\text{soil}} = 0.12 \text{ kip/ft}^3$, $\gamma_{\text{concrete}} = 0.15 \text{ kip/ft}^3$, $\mu = .57$ and $\Phi = 30^\circ$.

Problem 8.9

Which of the retaining walls shown below is adequately reinforced?

**Problem 8.10**

- Determine the factor of safety with respect to overturning and sliding.
- Identify the tension areas in the stem, toe, and heel and show the reinforcing pattern.
- Determine the location of the line of action of the resultant at the base of the footing



Part II

Statically Indeterminate Structures

Statically indeterminate structures are over-restrained in the sense that there are more force unknowns than available equilibrium equations. This situation arises when there are more supports than needed to prevent rigid body motion. Multi-span continuous beams and two-hinged frames are examples of this case. Indeterminacy may also result when there is an excess of members, such as a truss with multiple diagonals. Two dominant methods of analysis are used for indeterminate structures.

The traditional approach for analyzing statically indeterminate structures is based on the assumption that the structure behaves in a linear elastic manner and therefore displacement patterns corresponding to different systems of forces can be superimposed to achieve a desired displacement pattern. One replaces the displacement constraints with unknown forces, determines the deflected shapes for each unit force, and then combines and scales these shapes to obtain a final deflected shape that satisfies the constraints. Since one works with force unknowns, this approach is called the “Force Method.” It is also called the “Flexibility Method.” Engineers find the method appealing since the process of superimposing the different deflected shapes can be easily visualized and the computational details, which are suited for hand computation, provide insight on the deflection behavior.

A second method is based on solving a set of equilibrium equations expressed in terms of certain displacement measures that define the loaded configuration. It views the structure as an assemblage of members and uses a set of member end force–end displacement relations called the slope deflection equations. In general, the number of displacement unknowns is larger than the number of force unknowns, but the method is readily programmed and numerous software packages now exist. We refer to this approach as the “Displacement Method.” It is also called the “Stiffness Method” since the equations involve stiffness coefficients.

In what follows, we discuss both methods. We also describe some approximate hand calculation-based methods that are suitable for rapidly estimating the response due to gravity and lateral loads. Finally we describe the underlying theory for the Displacement Method and illustrate how to apply the method using computer software.

Overview

Up to this point we have focused on the analysis of statically determinate structures because the analysis process is fairly straightforward; only the force equilibrium equations are required to determine the member forces. However, there is another category of structures, called statically indeterminate structures, which are also employed in practice. Indeterminate structures require another set of equations, in addition to the force equilibrium equations, in order to solve for the member forces. There are two general methods for analyzing indeterminate structures, the Force (Flexibility) Method and the Displacement (Stiffness) Method. The Force Method is more suited to hand computation whereas the Displacement Method is more procedural and easily automated using a digital computer.

In this chapter, we present the underlying theory of the Force Method and illustrate its applications to a range of statically indeterminate structures including trusses, multi-span beams, arches, and frames. We revisit the analysis of these structures in the next chapter using the Displacement Method, and also in Chapter “Finite Element Displacement Method for Framed Structures,” which deals with computer-based analysis.

9.1 Introduction

The force method is a procedure for analyzing statically indeterminate structures that works with force quantities as the primary variables. It is applicable for linear elastic structures. The method is based on superimposing structural displacement profiles to satisfy a set of displacement constraints. *From a historical perspective*, the force method was the “classical” analysis tool prior to the introduction of digital-based methods. The method is qualitative in the sense that one reasons about deflected shapes and visualizes how they can be combined to satisfy the displacement constraints. We find the method very convenient for deriving analytical solutions that allow one to identify key behavior properties and to assess their

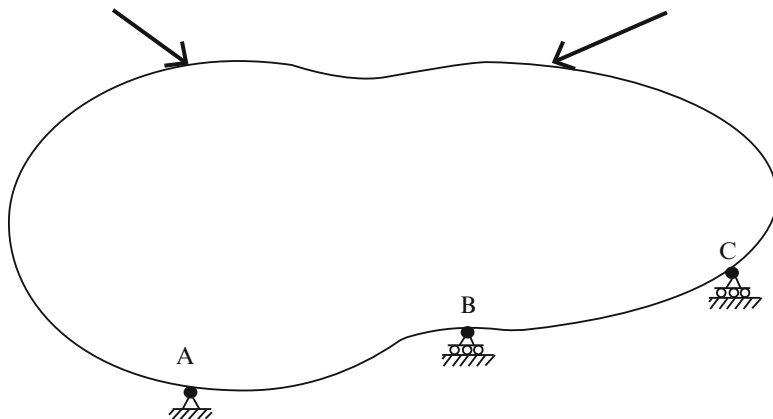


Fig. 9.1 Actual structure

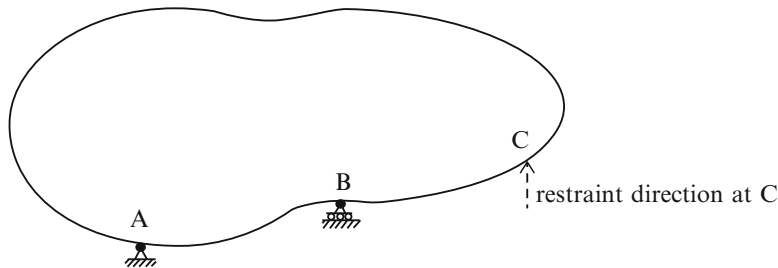


Fig. 9.2 Primary structure

influence on the structural response. The key step is establishing the displacement constraints which are referred to as the geometric compatibility equations.

Consider the structure shown in Fig. 9.1. Since there are four displacement restraints, the structure is indeterminate to the first degree, i.e., one of the restraints is not needed for stability, and the corresponding reaction force cannot be determined using only the force equilibrium equations.

The steps involved in applying the Force Method to this structure are as follows:

1. We select one of the force redundants and remove it. The resulting structure, shown in Fig. 9.2, is called the primary structure. Note that one cannot arbitrarily remove a restraint. One needs to ensure that the resulting structure is stable.
2. We apply the external loading to the primary structure and determinate the displacement at C in the direction of the restraint at C. This quantity is designated as $\Delta_{C,0}$. Figure 9.3 illustrates this notation.
3. Next, we apply a unit value of the reaction force at C to the primary structure and determine the corresponding displacement. We designate this quantity as δ_{CC} (see Fig. 9.4).

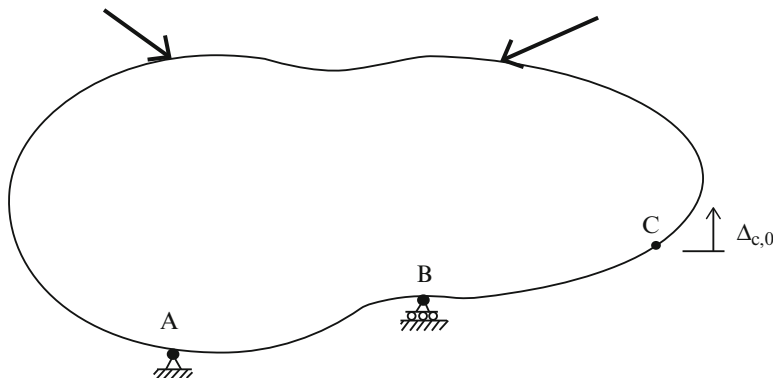


Fig. 9.3 Displacements due to the external loading

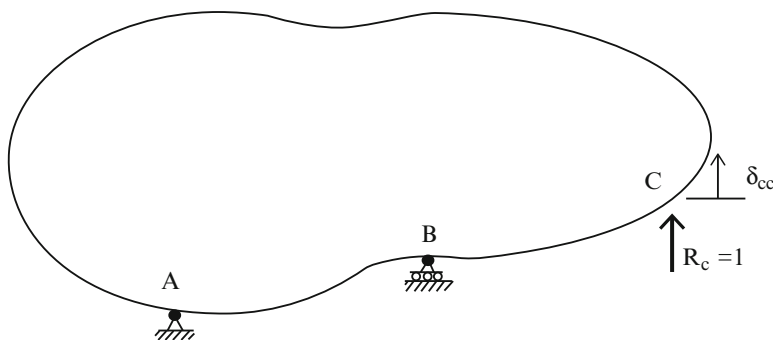


Fig. 9.4 Displacement due to unit value of R_C

4. We obtain the total displacement at C of the primary structure by superimposing the displacement profiles generated by the external loading and the reaction force at C.

$$\Delta_C|_{\text{primary structure}} = \Delta_{C,0} + \delta_{CC}R_C \quad (9.1)$$

5. The last and the key step is to require the displacement at C of the primary structure to be equal to the displacement at C of the actual structure.

$$\Delta_C|_{\text{actual}} = \Delta_C|_{\text{primary}} = \Delta_{C,0} + \delta_{CC}R_C \quad (9.2)$$

Equation (9.2) is referred to as the “geometric compatibility equation.” When this equation is satisfied, the final displacement profiles for the actual and the primary structure will be identical. It follows that the forces in the primary structure and the actual structure will also be identical.

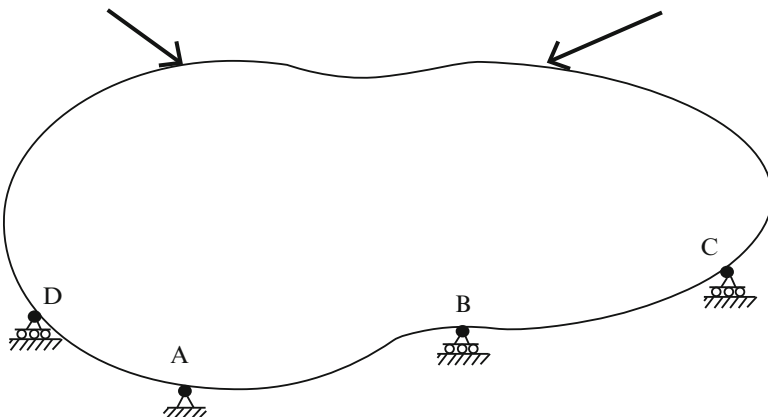


Fig. 9.5 Actual structure

1. We solve the compatibility equation for the reaction force, R_C .

$$R_C = \frac{1}{\delta_{CC}} (\Delta_C|_{\text{actual}} - \Delta_{C,0}) \quad (9.3)$$

Note that $\Delta_C|_{\text{actual}} = 0$ when the support is unyielding. When R_C is negative, the sense assumed in Fig. 9.4 needs to be reversed.

2. The last step involves computing the member forces in the actual structure. We superimpose the member forces computed using the primary structure according to the following algorithm:

$$\text{Force} = \text{Force}|_{\text{external load}} + R_C(\text{Force}|_{R_C=1}) \quad (9.4)$$

Since the primary structure is statically determinate all the material presented in Chaps. 2, 3, 4, 5, and 6 is applicable. The Force Method involves scaling and superimposing displacement profiles. The method is particularly appealing for those who have a solid understanding of structural behavior. For simple structures, one can establish the sense of the redundant force through qualitative reasoning.

Essentially the same approach is followed for structures having more than one degree of indeterminacy. For example, consider the structure shown in Fig. 9.5. There are two excess vertical restraints.

We obtain a primary structure by removing two of the vertical restraints. Note that there are multiple options for choosing the restraints to be removed. The only constraint is that the primary structure must be “stable.” Figure 9.6 shows the different choices.

Suppose we select the restraints at C and D as the redundants. We apply the external loading to the primary structure (Fig. 9.7), and determine the vertical displacements at C and D shown in Fig. 9.8.

The next step involves applying unit forces corresponding to $R_C = 1$ and $R_D = 1$ and computing the corresponding displacements at C and D. Two separate displacement analysis are required since there are two redundant reactions (Fig. 9.9).

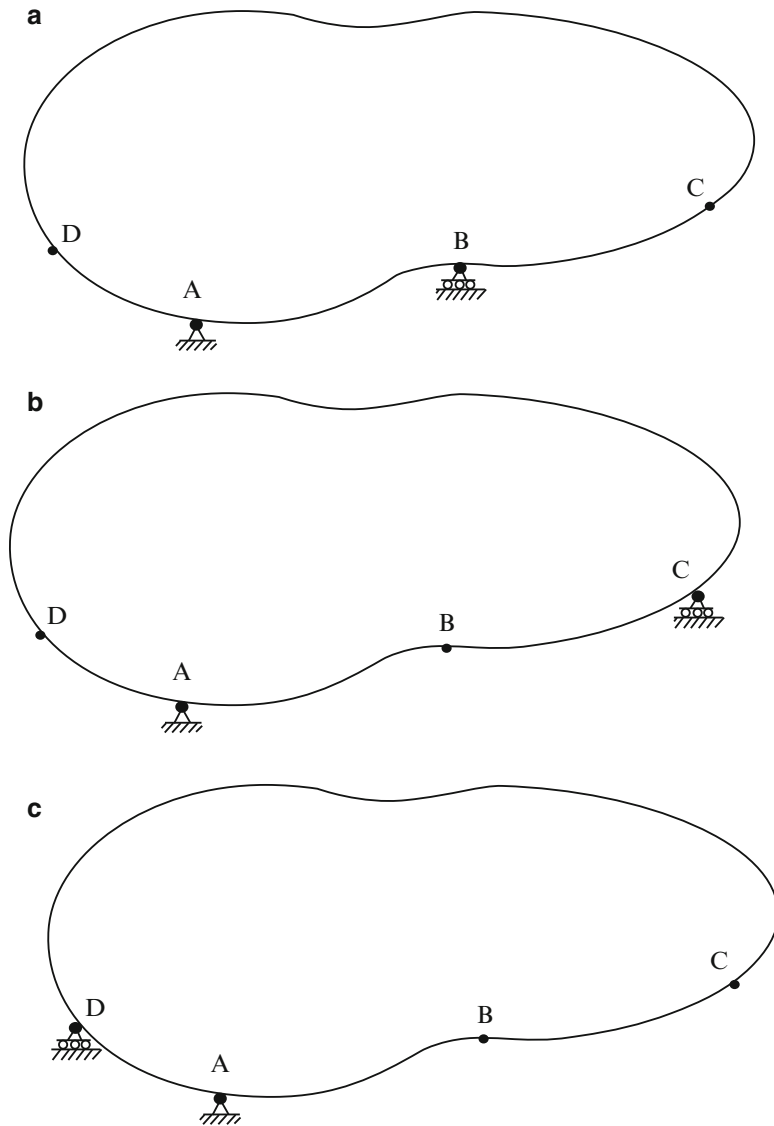
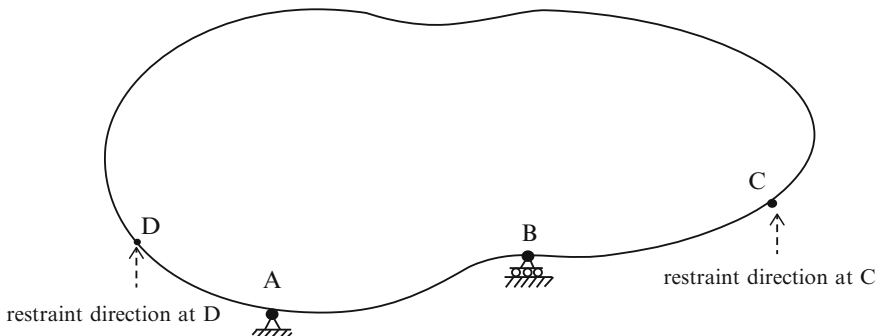
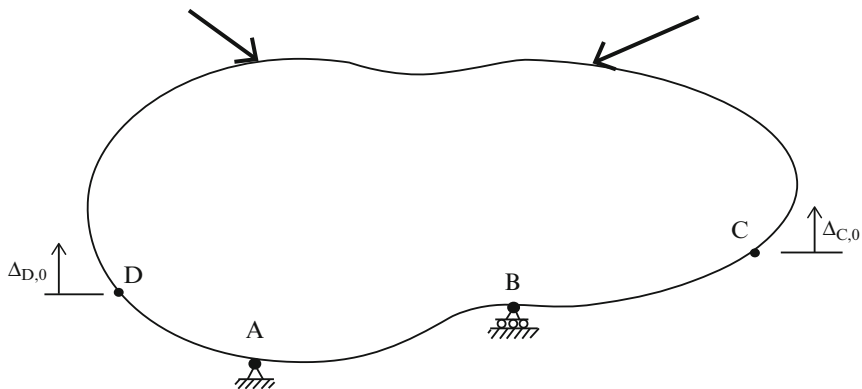


Fig. 9.6 Choices for primary structure. (a) Option 1. (b) Option 2. (c) Option 3

Combining the three displacement profiles leads to the total displacement of the primary structure.

$$\begin{aligned}\Delta_C|_{\text{primary structure}} &= \Delta_{C,0} + \delta_{CC}R_C + \delta_{CD}R_D \\ \Delta_D|_{\text{primary structure}} &= \Delta_{D,0} + \delta_{DC}R_C + \delta_{DD}R_D\end{aligned}\quad (9.5)$$

**Fig. 9.7** Primary structure**Fig. 9.8** Displacements due to external loading

The coefficients of R_C and R_D are called flexibility coefficients. It is convenient to shift over to matrix notation at this point. We define

$$\underline{\Delta}_0 = \begin{Bmatrix} \Delta_{C,0} \\ \Delta_{D,0} \end{Bmatrix} \underline{R} = \begin{Bmatrix} R_C \\ R_D \end{Bmatrix}$$

flexibility matrix $\underline{\delta} = \begin{bmatrix} \delta_{CC} & \delta_{CD} \\ \delta_{DC} & \delta_{DD} \end{bmatrix}$

(9.6)

Using this notation; the geometric compatibility equation takes the form

$$\underline{\Delta}|_{\text{actual structure}} = \underline{\Delta}_0 + \underline{\delta} \underline{R} \quad (9.7)$$

Note that $\underline{\Delta}|_{\text{actual structure}} = \underline{0}$ when the supports are unyielding. Given the choice of primary structure, the flexibility coefficients are properties of the primary structure whereas $\underline{\Delta}_0$ depends on both the external loading and the primary structure. We solve (9.7) for \underline{R} ,

$$\underline{R} = \underline{\delta}^{-1}(\underline{\Delta}|_{\text{actual structure}} - \underline{\Delta}_0) \quad (9.8)$$

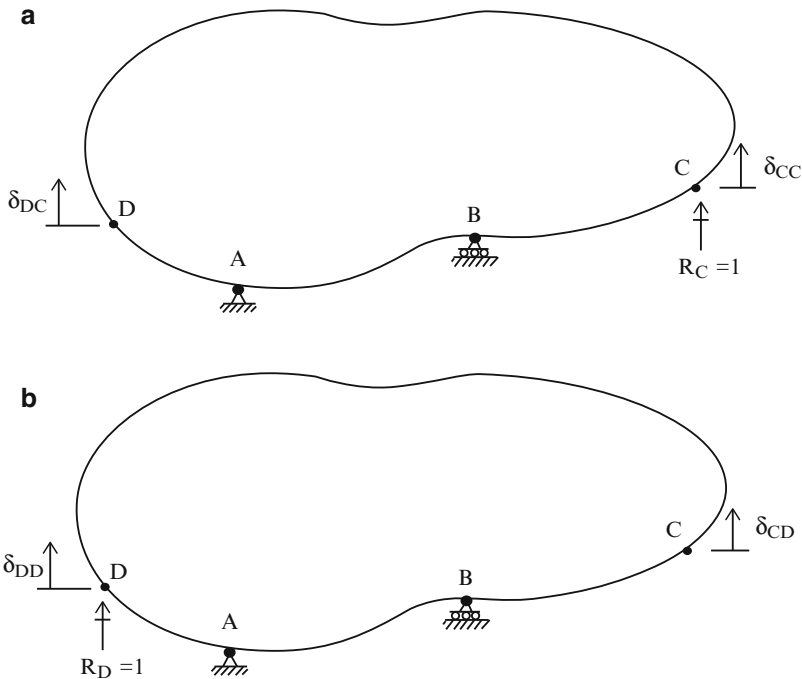


Fig. 9.9 Displacement due to unit values of the redundant. (a) $R_C = 1$. (b) $R_D = 1$

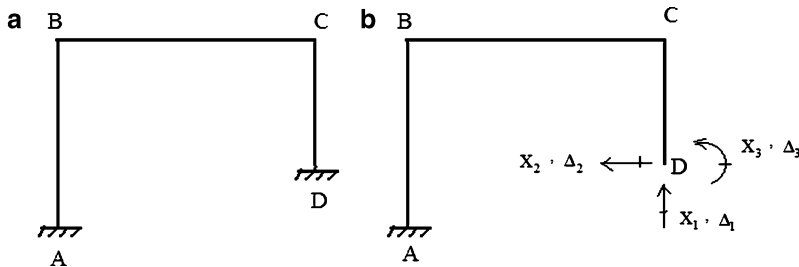


Fig. 9.10 (a) Actual structure. (b) Primary structure—redundant reactions

and then determine the member forces by superimposing the individual force states as follows:

$$\underline{F} = \underline{F}|_{\text{external load}} + (\underline{F}|_{R_C=1})R_C + (\underline{F}|_{R_D=1})R_D \quad (9.9)$$

The extension of this approach to an n th degree statically indeterminate structure just involves more computation since the individual matrices are now of order n . Since there are more redundant force quantities, we need to introduce a more systematic notation for the force and displacement quantities.

Consider the frame structure shown in Fig. 9.10a. It is indeterminate to the third degree. One choice of primary structure is shown in Fig. 9.10b. We remove the support

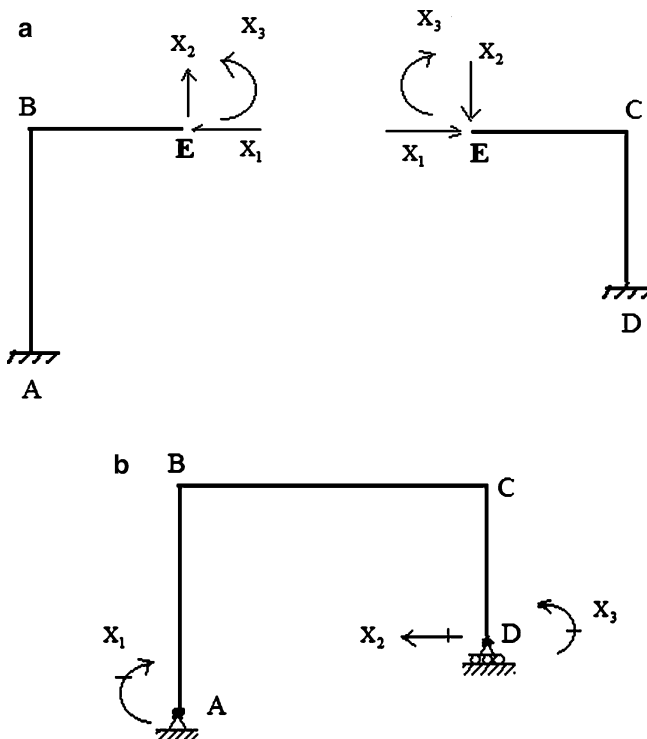


Fig. 9.11 (a) Primary structure—redundant internal forces. (b) Primary structure—redundant reactions

at D, take the reactions as the force redundants, denote the j th redundant force as X_j and the corresponding measure as Δ_j . The resulting displacements of the primary structure due to the external loading and the three force redundants are expressed as

$$\begin{aligned}\Delta_1|_{\text{primary structure}} &= \Delta_{1,0} + \delta_{11}X_1 + \delta_{12}X_2 + \delta_{13}X_3 \\ \Delta_2|_{\text{primary structure}} &= \Delta_{2,0} + \delta_{21}X_1 + \delta_{22}X_2 + \delta_{23}X_3 \\ \Delta_3|_{\text{primary structure}} &= \Delta_{3,0} + \delta_{31}X_1 + \delta_{32}X_2 + \delta_{33}X_3\end{aligned}\quad (9.10)$$

The matrix form of (9.10) is

$$\Delta|_{\text{primary structure}} = \Delta_0 + \underline{\delta} \underline{X} \quad (9.11)$$

Note that the displacement measures may be either a translation or a rotation. A major portion of the computational effort is involved with computing the flexibility coefficients using the Principle of Virtual Forces. The matrix form of the geometric compatibility equation (9.7) is generic, i.e., it is applicable for all structures. One just has to establish the appropriate form for Δ_0 and $\underline{\delta}$.

Other possible choices of primary structures are shown in Fig. 9.11. We can retain the two fixed supports, but cut the structure at an arbitrary interior point (Fig. 9.11a). The redundants are taken as the internal forces (axial, shear, and

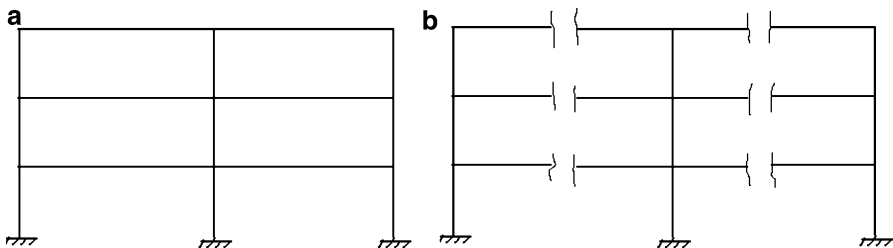


Fig. 9.12 (a) Actual structure. (b) Primary structure

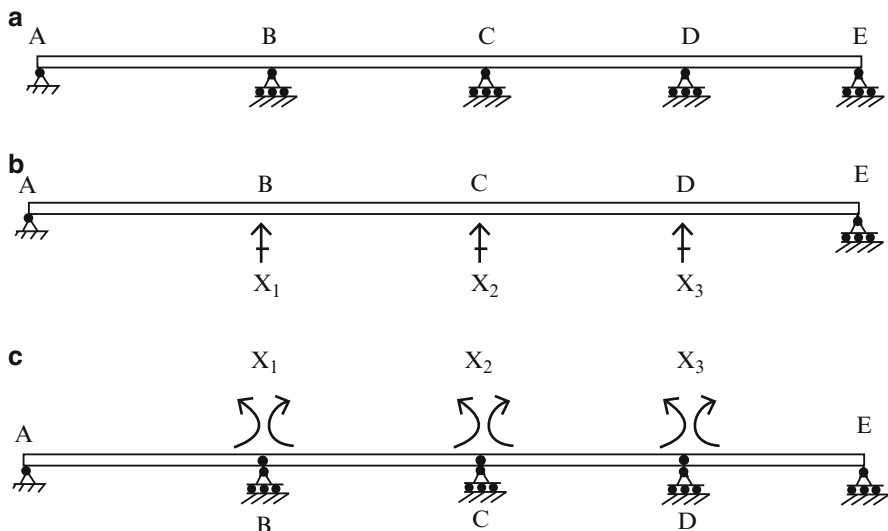


Fig. 9.13 Multi-span beam. (a) Actual structure. (b) Primary structure—redundant reactions. (c) Primary structure—redundant moments

moment) at the point. The flexibility coefficients are now interpreted as the relative displacements of the adjacent cross sections (e.g., spreading, sliding, relative rotation). Another choice involves removing excess reactions as in Fig. 9.11b.

For multi-bay multistory frames, one needs to work with internal force redundants since removing fixed supports is not sufficient to reduce the structure to a statically determinate structure. Figure 9.12 illustrates this case.

Multi-span beam-type structures are handled in a similar way when choosing a primary structure. Consider Fig. 9.13. One can either select certain excess reactions or work with bending moments at interior points. We prefer the latter choice since the computation of the corresponding flexibility coefficients is simpler due to the fact that the deflection profiles associated with the redundant moments are confined to adjacent spans.

For truss-type structures various cases arises. The truss may have more supports than needed, such as shown in Fig. 9.14a. One choice would be to remove sufficient supports such that the resulting structure is statically determinate (Fig. 9.14b).

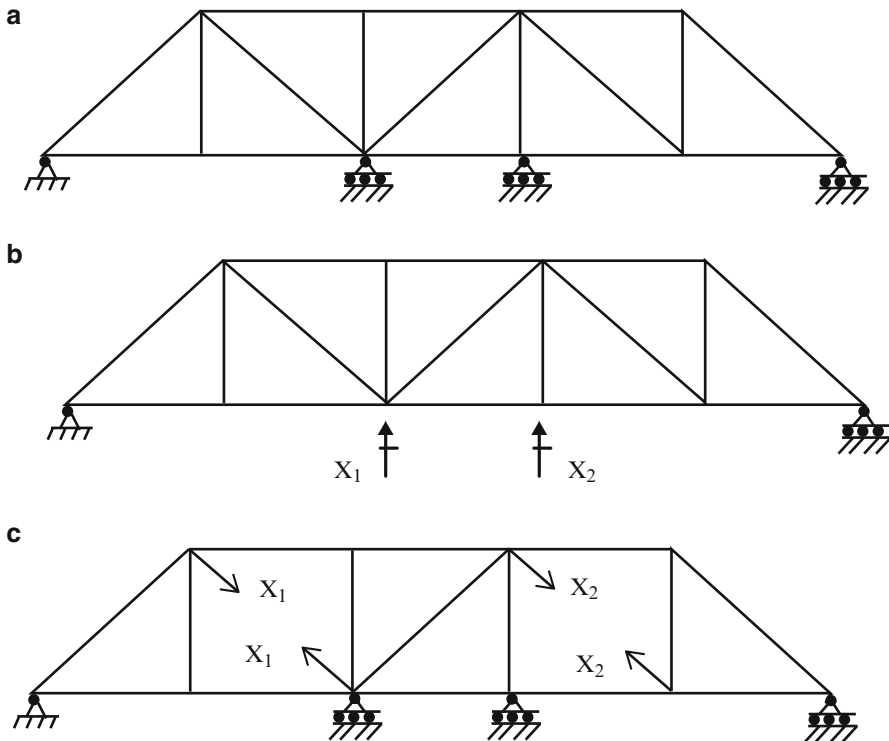


Fig. 9.14 (a) Actual structure. (b) Primary structure—redundant reactions. (c) Primary structure—redundant internal forces

We can also keep the original restraints, and remove some members, as indicated in the figure below.

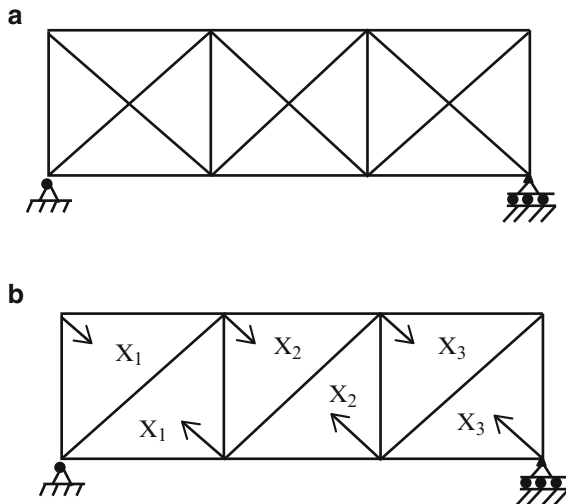
Another example is shown in Fig. 9.15a. The truss has too many members and therefore the only option is to remove some of the diagonals. Figure 9.15b illustrated one choice of redundants.

9.2 Maxwell's Law of Reciprocal Displacements

The geometric compatibility equations involve the flexibility matrix, δ . One computes the elements of δ using one of the methods described in part I, such as the Principal of Virtual Forces. Assuming there are n force redundants, δ has n^2 elements. For large n , this computation task becomes too difficult to deal with manually. However, there is a very useful relationship between the elements of δ , called “Maxwell’s Law,” which reduces the computational effort by approximately 50%. In what follows, we introduce Maxwell’s Law specialized for member systems.

We consider first a simply supported beam on unyielding supports subjected to a single concentrated unit force. Figure 9.16a defines the geometry and notation.

Fig. 9.15 (a) Actual structure. (b) Primary structure—redundant internal forces



The deflected shape due to the unit force applied at A is plotted in Fig. 9.16b. Suppose we want to determine the deflection at B due to this load applied at A. We define this quantity as δ_{BA} . Using the Principle of Virtual Forces specialized for beam bending; we apply a unit virtual force at B (see Fig. 9.16c) and evaluate the following integral:

$$\delta_{BA} = \int M_A \delta M_B \frac{dx}{EI} \quad (9.12)$$

where M_A is the moment due to the unit load applied at A, and δM_B is the moment due to the virtual unit load applied at B.

Now, suppose we want the deflection at A due to a unit load at B. The corresponding virtual force expression is

$$\delta_{AB} = \int M_B \delta M_A \frac{dx}{EI} \quad (9.13)$$

where δM_A is the virtual moment due to a unit force applied at A and M_B is the moment due to the load at B. Since we are applying unit loads, it follows that

$$\begin{aligned} M_A &= \delta M_A \\ M_B &= \delta M_B \end{aligned} \quad (9.14)$$

and we find that the expressions for δ_{AB} and δ_{BA} are identical.

$$\delta_{AB} \equiv \delta_{BA} \quad (9.15)$$

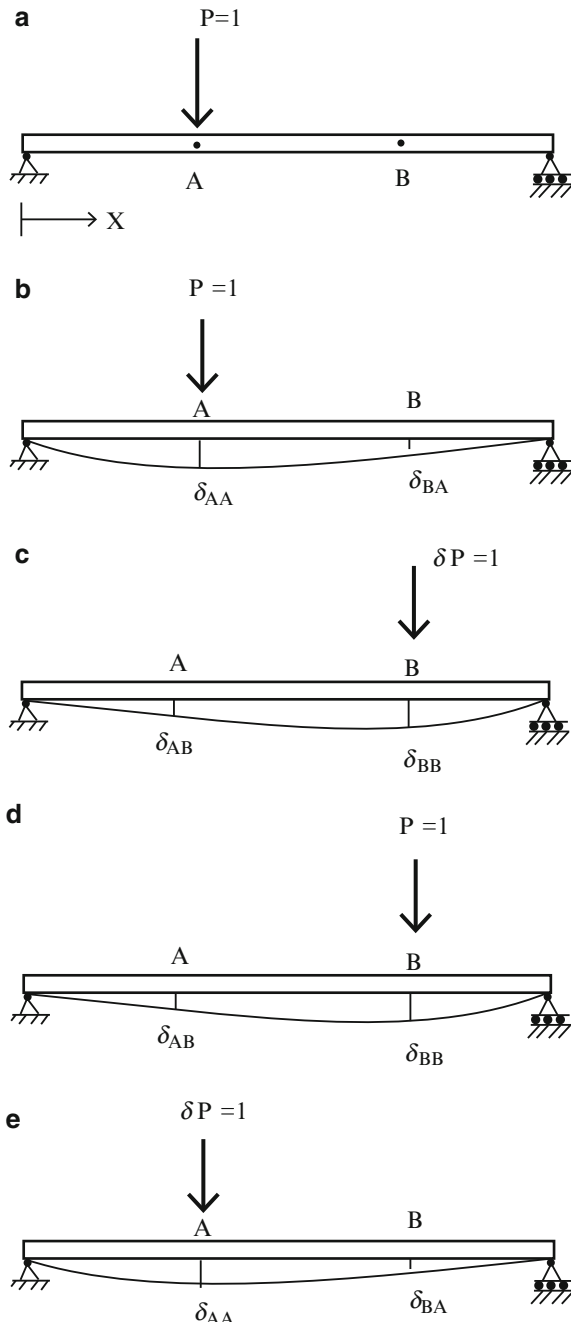


Fig. 9.16 Reciprocal loading conditions. (a) Actual structure. (b) Actual loading (M_A). (c) Virtual loading (δM_B). (d) Actual loading (M_B). (e) Virtual loading (δM_A)

This identity is called *Maxwell's Law*. It is applicable for linear elastic structures [16]. Returning back to the compatibility equations, defined by (9.7), we note that the coupling terms, δ_{ij} and δ_{ji} , are equal. We say the coefficients are symmetrical with respect to their subscripts and it follows that δ is symmetrical. Maxwell's Law leads to another result called Müller-Breslau Principle which is used to establish influence lines for indeterminate beams and frames. This topic is discussed in Chaps. 13 and 15.

9.3 Application of the Force Method to Beam-Type Structures

We apply the theory presented in the previous section to a set of beam-type structures. For completeness, we also include a discussion of some approximate techniques for analyzing partially restrained single-span beams that are also useful for analyzing frames.

Example 9.1

Given: The beam defined in Fig. E9.1a. Assume $I = 120(10)^6 \text{ mm}^4$, $L = 6 \text{ m}$, $w = 30 \text{ kN/m}$, $v_B = 40 \text{ mm}$, and $E = 200 \text{ GPa}$

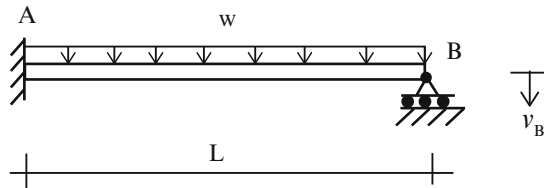


Fig. E9.1a

Determine: The reactions for the following cases:

- (i) $w, \Delta_B|_{\text{actual}} = 0$
- (ii) $W = 0, \Delta_B|_{\text{actual}} = -v_B$
- (iii) $w, \Delta_B|_{\text{actual}} = -v_B$

Solution: The beam is indeterminate to the first degree. We work with the primary structure shown below (Fig. E9.1b).

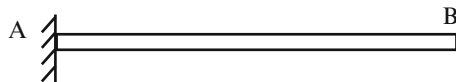


Fig. E9.1b Primary structure

Applying the external loading and the unit load results in the following deflected shapes (Figs. E9.1c and E9.1d):

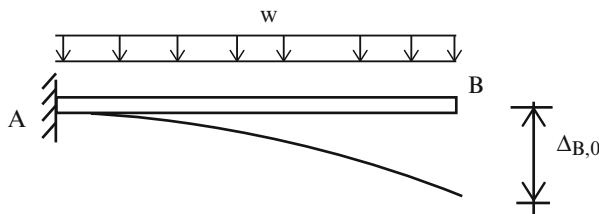


Fig. E9.1c Displacements due to external loading

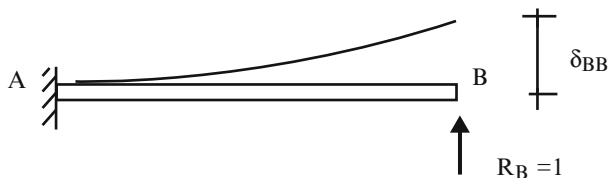


Fig. E9.1d Displacement due to the unit values of R_B

The deflection terms are given in Table 3.1.

$$\Delta_{B,0} = -\frac{wL^4}{8EI}$$

$$\delta_{BB} = \frac{L^3}{3EI}$$

Then

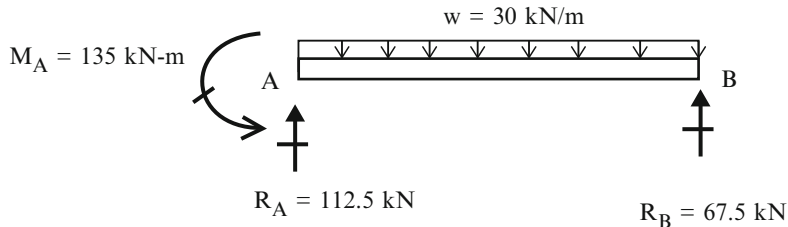
$$\begin{aligned} + \uparrow \quad \Delta_B|_{\text{actual}} &= \Delta_{B,0} + \delta_{BB}R_B \\ &\downarrow \\ \Delta_B|_{\text{actual}} &= -\frac{wL^4}{8EI} + \frac{L^3}{3EI}R_B \quad \therefore \quad R_B = \frac{\Delta_B|_{\text{actual}} + (wL^4/8EI)}{(L^3/3EI)} \end{aligned}$$

Case (i): For $\Delta_B|_{\text{actual}} = 0$ $R_B = ((wL^4/8EI)/(L^3/3EI)) = \frac{3}{8}wL = \frac{3}{8}(30)(6) = 67.5 \text{ kN} \uparrow$

Knowing the value of R_B , we determine the remaining reactions by using the static equilibrium equations.

$$\sum F_y = 0 \quad R_A = \frac{5}{8}wL = \frac{5}{8}(30)(6) = 112.5 \text{ kN} \uparrow$$

$$\sum M_{@A} = 0 \quad M_A = \frac{wL^2}{8} = 135 \text{ kN m} \quad \text{counter-clockwise}$$



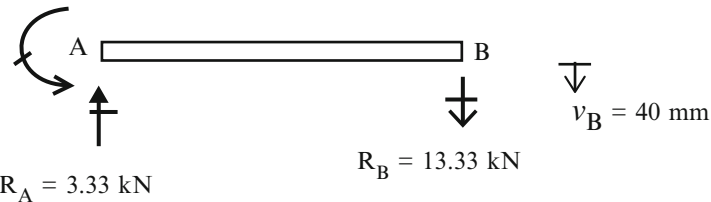
Case (ii): For $w = 0$, $\Delta_B|_{\text{actual}} = -v_B$

$$\begin{aligned} R_B &= \frac{(-v_B)}{(L^3/3EI)} = -\frac{3EI}{L^3} v_B \\ &= -\frac{3(200)(10)^6 120(10)^{-6}}{(6)^3} (0.040) = -13.33 \text{ kN} \quad \therefore R_B = 13.33 \text{ kN} \downarrow \end{aligned}$$

The reactions are

$$\begin{aligned} \sum F_y &= 0 \quad R_A = \frac{3EI}{L^3} v_B = 13.3 \text{ kN} \uparrow \\ \sum M_{@A} &= 0 \quad M_A = \frac{3EI}{L^2} v_B = 80 \text{ kN m} \quad \text{counter-clockwise} \end{aligned}$$

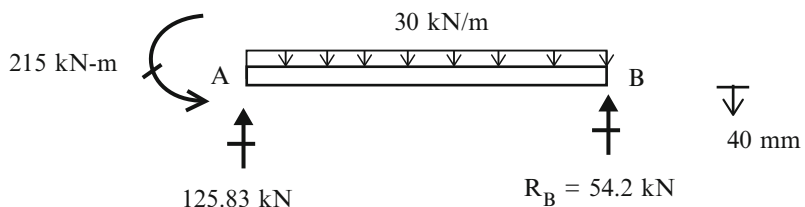
$$M_A = 80 \text{ kN-m}$$



Case (iii): For $w \neq 0$ and $\Delta_B|_{\text{actual}} = -v_B$

$$R_B = \frac{-v_B + (wL^4/8EI)}{(L^3/3EI)} = +\frac{3}{8}wL - \frac{3EI}{L^3} v_B = 67.5 - 13.33 = 54.2 \text{ kN} \uparrow$$

The reactions are



Note that since the structure is linear, one can superimpose the solutions for cases (i) and (ii).

Example 9.2

Given: The beam and loading defined in Fig. E9.2a. Assume $I = 400 \text{ in}^4$, $L = 54 \text{ ft}$, $w = 2.1 \text{ kip/ft}$, $\delta_A = 2.4 \text{ in.}$, and $E = 29,000 \text{ ksi}$.

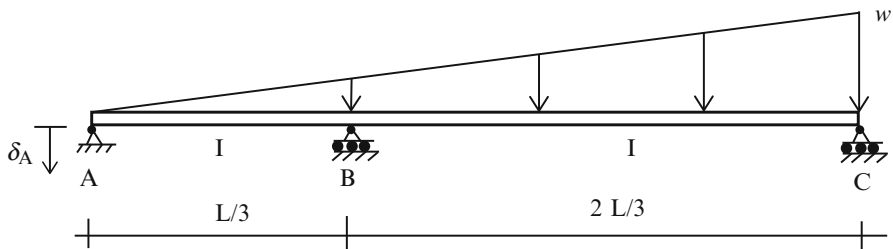


Fig. E9.2a

Determine: The reactions due to

- (i) The distributed load shown
- (ii) The support settlement at A

Solution: The beam is indeterminate to the first degree. We take the vertical reaction at B as the force unknown, and compute the deflected shapes due to w and $R_B = 1$ applied to the primary structure (Figs. E9.2b and E9.2c).

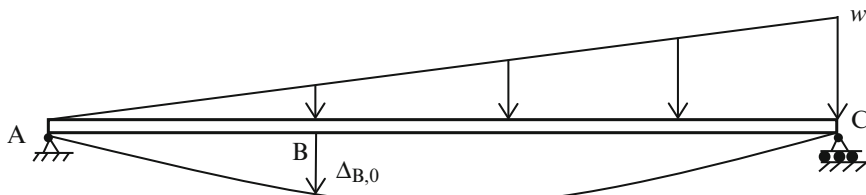


Fig. E9.2b Deflected shape due to w

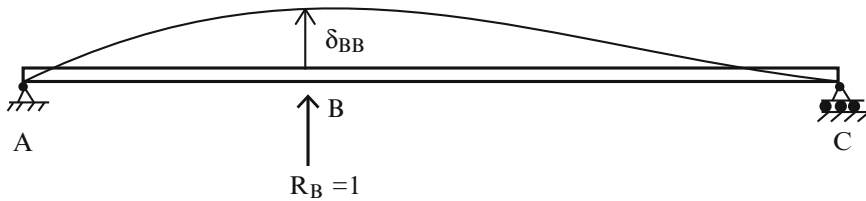


Fig. E9.2c Deflected shape due to unit value of R_B

Case (i): The distributed load shown

$$\begin{aligned} + \uparrow \quad \Delta_B|_{\text{actual}} &= \Delta_{B,0} + \delta_{BB}R_B \\ \Downarrow \\ \Delta_{B,0} + \delta_{BB}R_B &= 0 \quad \therefore \quad R_B = -\frac{\Delta_{B,0}}{\delta_{BB}} \end{aligned}$$

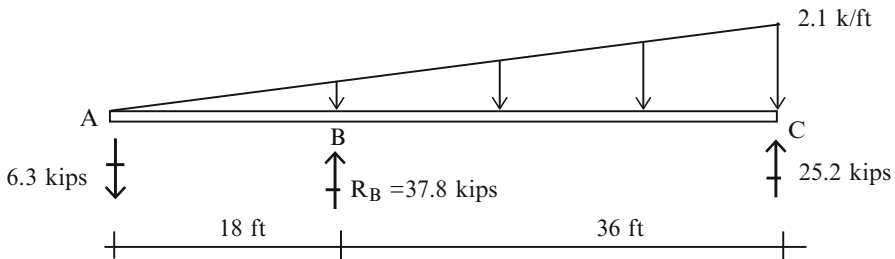
The deflection terms are given in Table 3.1.

$$\Delta_{B,0} = -\frac{4wL^4}{729EI}$$

$$\delta_{BB} = \frac{4L^3}{243EI}$$

$$\text{Then } R_B = -\frac{\Delta_{B,0}}{\delta_{BB}} = \frac{(4wL^4/729EI)}{(4L^3/243EI)} = \frac{wL}{3} = 37.8 \text{ kip} \uparrow$$

Knowing the value of R_B , we determine the remaining reactions by using the static equilibrium equations.



Case (ii): The support settlement at A (Fig. E9.2d)

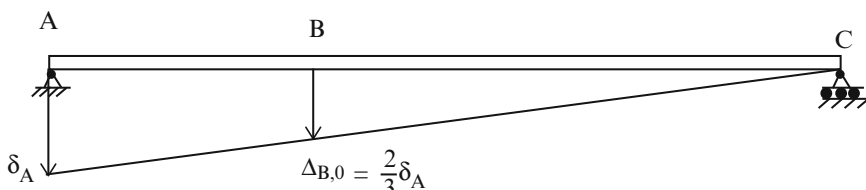


Fig. E9.2d Displacement due to support settlement at A

$$+ \uparrow \quad \Delta_B|_{\text{actual}} = \Delta_{B,0} + \delta_{BB} R_B$$

where

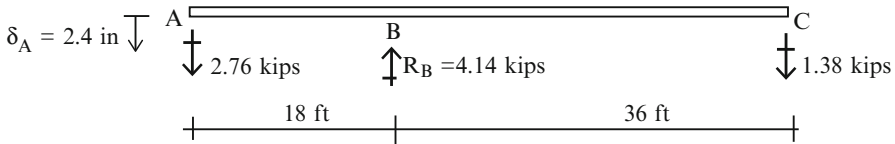
$$\delta_{BB} = \frac{4L^4}{243EI} = \frac{4(54)^3(12)^3}{243(29,000)(400)} 0.386 \text{ in.}$$

$$\Delta_{B,0} = \frac{2}{3} \delta_A = -1.6 \text{ in.}$$

Therefore

$$R_B = -\frac{\Delta_{B,0}}{\delta_{BB}} = -\frac{(-1.6)}{0.386} = 4.14 \text{ kip } \uparrow$$

We determine the remaining reactions using the static equilibrium equations.



Example 9.3

Given: The three-span beam defined in Fig. E9.3a. Assume EI constant, $L = 9 \text{ m}$, $w = 20 \text{ kN}$.

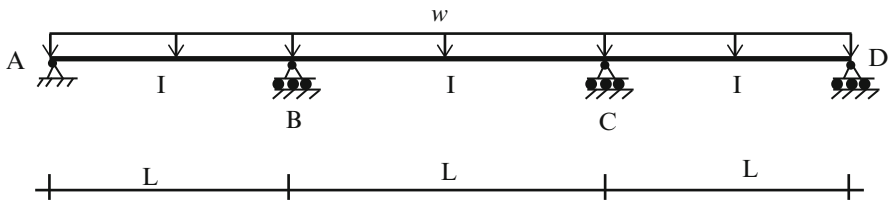


Fig. E9.3a

Determine: The reactions

Solution: The beam is indeterminate to the second degree. We remove the supports at B and C, take the vertical reactions at B and C as the force redundants and compute the deflected shapes due to w , $X_1 = 1$ and $X_2 = 1$ applied to the primary structure (Figs. E9.3b-d).

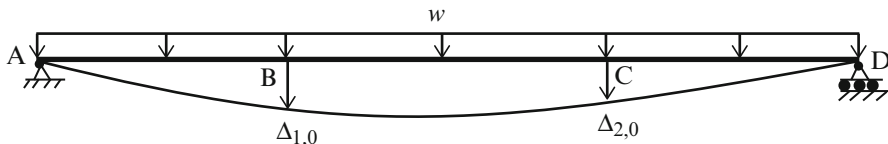


Fig. E9.3b Deflected shape due to external loading

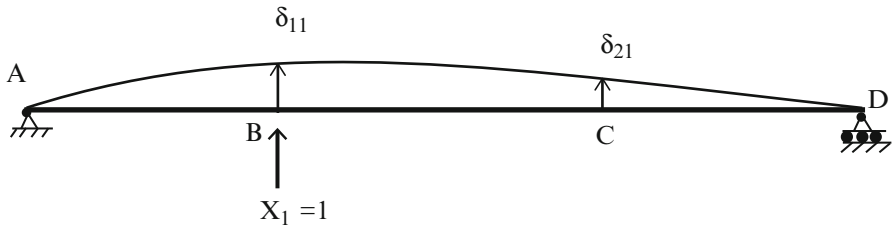


Fig. E9.3c Deflected shape due to \$X_1 = 1\$

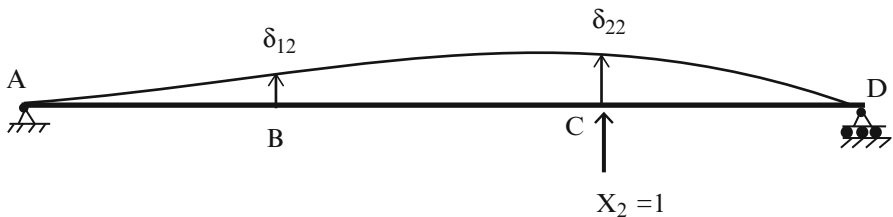


Fig. E9.3d Deflected shape due to \$X_2 = 1\$

The displacements of the primary structure due to the external loading and the two force redundants are expressed as:

$$\Delta_{1,0} + \delta_{11}X_1 + \delta_{12}X_2 = 0$$

$$\Delta_{2,0} + \delta_{21}X_1 + \delta_{22}X_2 = 0$$

Because of symmetry:

$$\Delta_{1,0} = \Delta_{2,0} = \frac{11wL^4}{12EI}$$

$$\delta_{11} = \delta_{22} = \frac{4L^3}{9EI}$$

$$\delta_{21} = \delta_{12} = \frac{7L^3}{18EI}$$

Note that the above deflection terms are given in Table 3.1.

Therefore

$$\begin{aligned} X_1 = X_2 &= \frac{\Delta_{1,0}}{\delta_{11} + \delta_{12}} = \frac{(11wL^4/12EI)}{(4L^3/9EI) + (7L^3/18EI)} = 1.1wL = 1.1(20)(9) \\ &= 198 \text{ kN} \end{aligned}$$

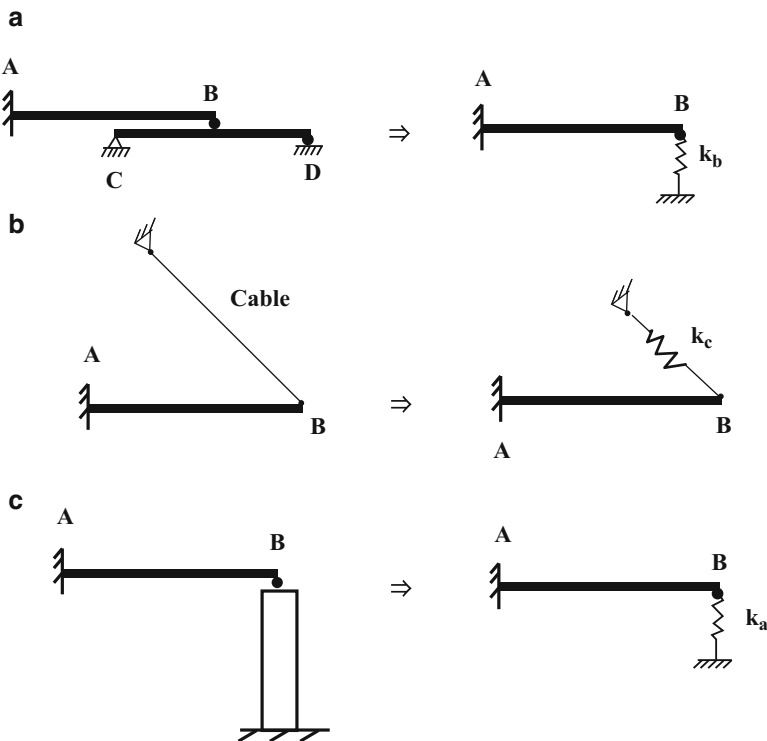
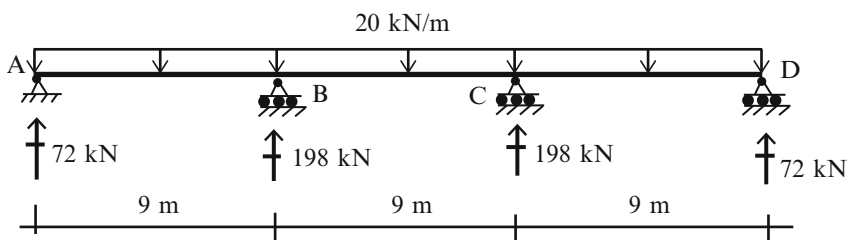


Fig. 9.17 Beam on flexible supports. (a) Beam. (b) Cable. (c) Column

Then, we determine the remaining reactions

$$\sum F_Y = 0 \quad R_A = R_D = 0.4wL = 72 \text{ kN} \uparrow$$



9.3.1 Beam with Yielding Supports

We consider next the case where a beam is supported by another member, such as another beam or a cable. Examples are shown in Fig. 9.17. When the beam is loaded, reactions are developed, and the supporting members deform.

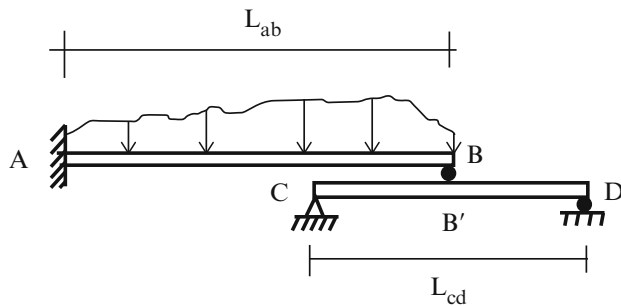
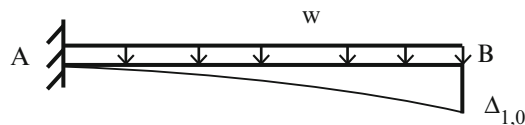


Fig. 9.18 Beam supported by another beam

Assuming linear elastic behavior, the supporting members behave as linear elastic restraints, and can be modeled as equivalent spring elements, as indicated in Fig. 9.17.

We consider here the case where a vertical restraint is provided by another beam. Figure 9.18 illustrates this case. Point B is supported by beam CD which is parallel to beam AB. In this case, point B deflects when the load is applied to beam AB. One strategy is to work with a primary structure that includes both beams such as shown in Fig. 9.19. The force redundant is now a pair of self-equilibrating forces acting at B, and the corresponding displacement measure is the relative displacement apart between the upper and lower contact points, designated as B and B'.

When the loading is uniform,



$$\Delta_{1,0} = \frac{wL^4}{8EI} \downarrow$$

The total displacement corresponding to \$X_1 = 1\$ is the sum of two terms,

$$\begin{aligned}\delta_{11} &= \delta_{11}|_{AB} + \delta_{11}|_{CD} \\ &= \frac{L^3}{3EI} + \delta_{11}|_{CD}\end{aligned}$$

Beam CD functions as a restraint on the movement of beam AB. The downward movement of B' is resisted by the bending action of beam CD. Assuming linear

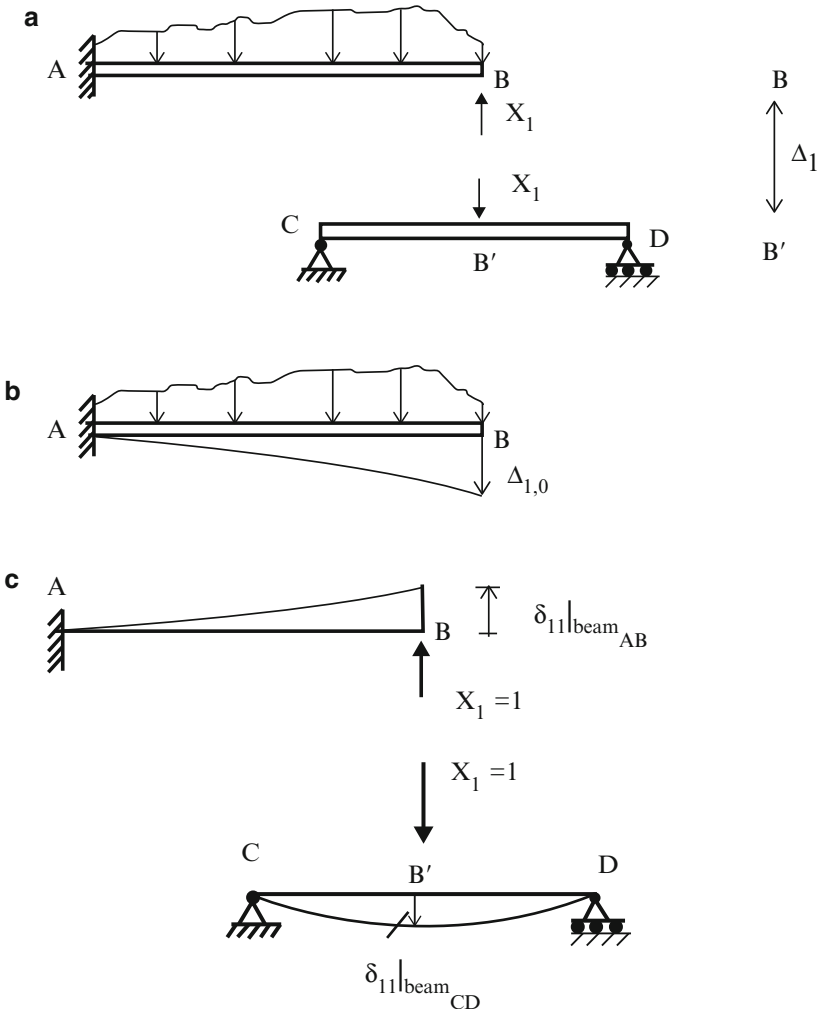


Fig. 9.19 Choice of force redundant and displacement profiles. (a) Primary structure—force redundant system. (b) Deflection due to external loading. (c) Deflection due to redundant force at B

elastic behavior, this restraint can be modeled as a linear spring of stiffness k . One chooses the magnitude of k such that the spring deflection due to the load P is the same as the beam deflection.

Then, it follows from Fig. 9.20 that

$$\delta_{11|CD} = \frac{1}{k_{CD}} \quad (9.16)$$

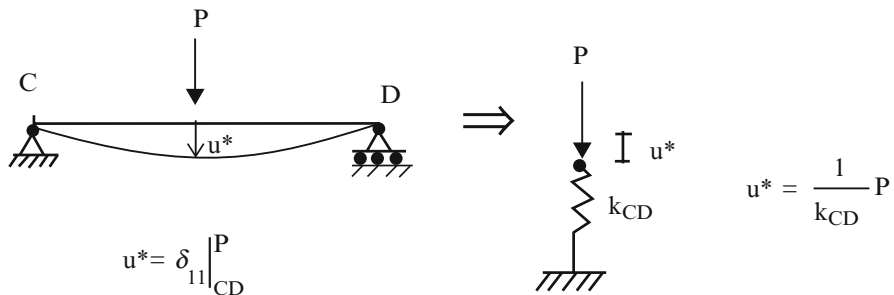


Fig. 9.20 Equivalent spring

Assuming the two beams are rigidly connected at B, the net relative displacement must be zero.

$$\Delta_1 = \Delta_{1,0} + X_1 \left(\frac{1}{k_{CD}} + \frac{L^3}{3EI} \right) = 0 \quad (9.17)$$

Solving (9.17) for X_1 leads to

$$X_1 = \left\{ \frac{-1}{(L^3/3EI) + (1/k_{CD})} \right\} \Delta_{1,0} \quad (9.18)$$

Note that the value of X_1 depends on the stiffness of beam CD. Taking $k_{CD} = \infty$ corresponds to assuming a rigid support, i.e., a roller support. When $k_{CD} = 0$, $X_1 = 0$. It follows that the bounds on X_1 are

$$0 < X_1 < \frac{3EI}{L^3} \quad (9.19)$$

Another type of elastic restraint is produced by a cable. Figure 9.21 illustrates this case. We replace the cable with its equivalent stiffness, $k_c = \frac{A_c E_c}{h}$ and work with the primary structure shown in Fig. 9.21b.

Using the results derived above, and noting that $\Delta_1 = 0$, the geometric compatibility equation is

$$\Delta_1 = \Delta_{1,0} + (\delta_{11}|_{AB} + \delta_{11}|_{BC}) X_1 = 0$$

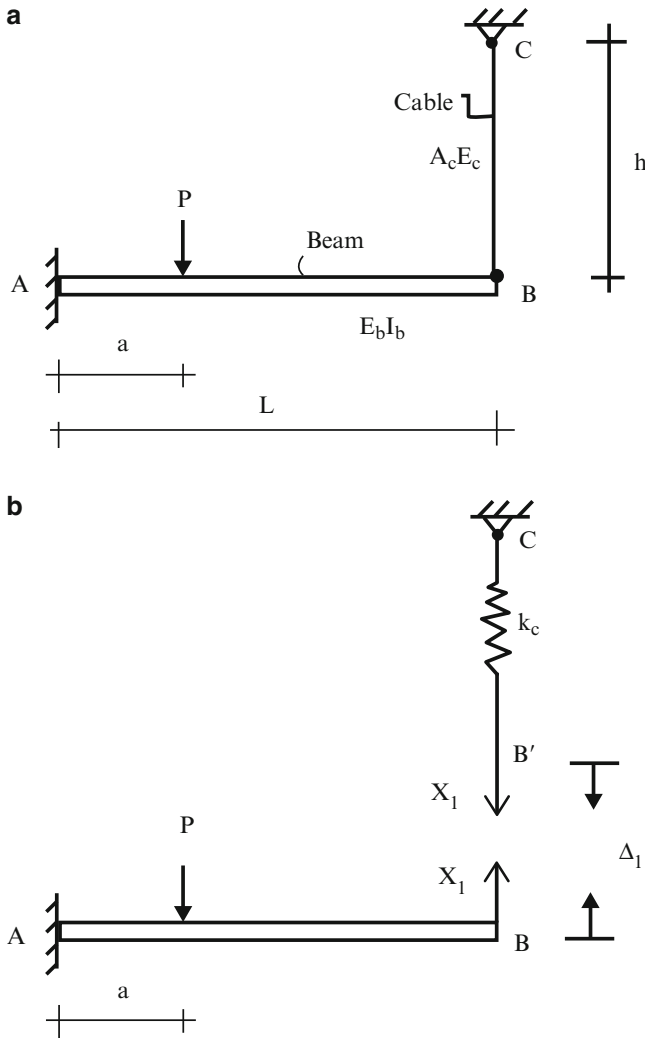
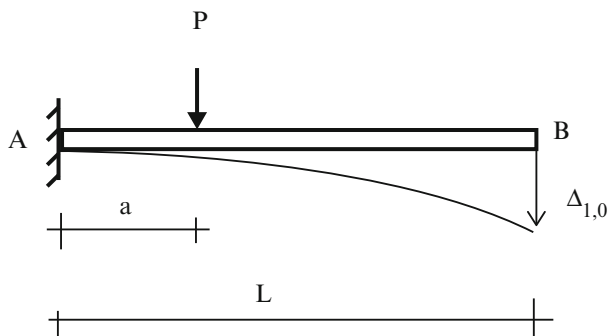


Fig. 9.21 (a) Actual structure. (b) Primary structure—force redundant system

For the external concentrated loading,



$$\Delta_{1,0} = \frac{P}{EI} \left(\frac{a^2 L}{2} - \frac{a^3}{3} \right)$$

Substituting for the various flexibility terms leads to

$$X_1 = \left[\frac{-1}{(L^3/3E_b I_b) + (1/k_c)} \right] \Delta_{1,0} \quad (9.20)$$

If $\frac{1}{k_c}$ is small with respect to $\frac{L^3}{3E_b I_b}$, the cable acts like a rigid support, i.e., X_1 approaches the value for a rigid support. When $\frac{1}{k_c}$ is large with respect to $\frac{L^3}{3E_b I_b}$, the cable is flexible and provides essentially no resistance, i.e., $X_1 \Rightarrow 0$. The ratio of cable to beam flexibilities is a key parameter for the behavior of this system.

Cable-stayed schemes are composed of beams supported with inclined cables. Figure 9.22a shows the case where there is just one cable. We follow essentially the same approach as described earlier except that now the cable is inclined. We take the cable force as the redundant and work with the structure defined in Fig. 9.22b.

Note that Δ_1 is the relative movement together of points B and B' along the inclined direction. Up to this point, we have been working with vertical displacements. Now we need to project these movements on an inclined direction.

We start with the displacement profile shown in Fig. 9.22c. The vertical deflection is v_{B0} . Projecting on the direction of the cable leads to

$$\Delta_{1,0} = -\sin\theta v_{B0} = -\sin\theta \left\{ \frac{P}{E_B I_B} \left(\frac{a^2 L_B}{2} - \frac{a^3}{6} \right) \right\} \quad (9.21)$$

Next, we treat the case where $X_1 = 1$ shown in Fig. 9.22d. The total movement consists of the elongation of the cable and the displacement of the beam.

$$\delta_{11} = \delta_{11}|_{BC} + \delta_{11}|_{AB}$$

The elongation of the cable is

$$\delta_{11}|_{BC} = \frac{L_c}{A_c E_c} = \frac{1}{k_c}$$

The beam displacement follows from Fig. 9.22e.

$$\delta_{11}|_{AB} = v_{B,1} \sin\theta = \sin\theta \left\{ \frac{\sin\theta L_B^3}{3E_B I_B} \right\} = (\sin\theta)^2 \left(\frac{L_B^3}{3E_B I_B} \right)$$

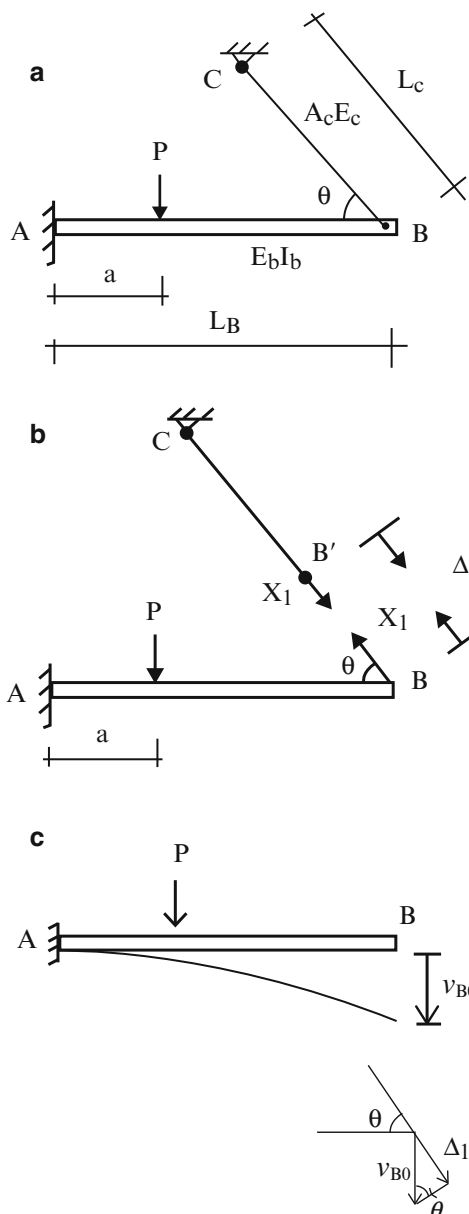
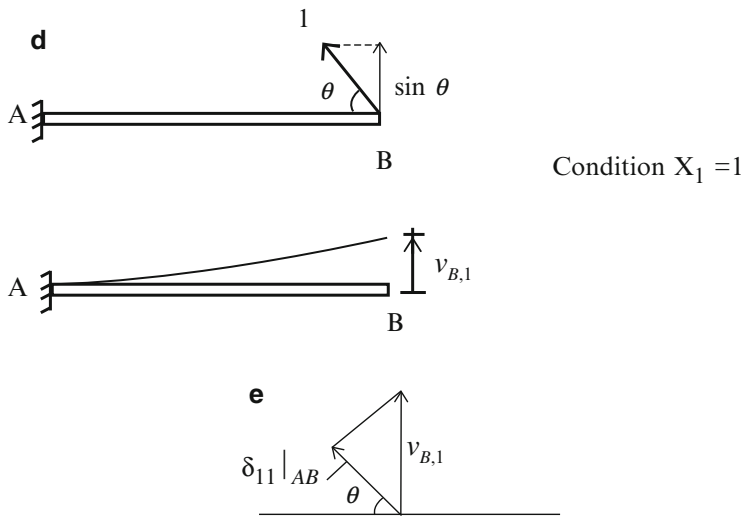


Fig. 9.22 (a) Cable stayed scheme. (b) Force redundant. (c) Deflection due to applied load. (d) Deflection due to $X_1 = 1$. (e) Displacement components

**Fig. 9.22** (continued)

Requiring $\Delta_1 = 0$ leads to

$$X_1 = \frac{1}{(\sin\theta)^2(L_B^3/3E_BI_B)+(1/k_C)} \left[\frac{P\sin\theta}{E_BI_B} \left(\frac{a^2L_B}{2} - \frac{a^3}{6} \right) \right] \quad (9.22)$$

Finally, we express X_1 in terms of the value of the vertical reaction corresponding to a rigid support at B.

$$X_1 = \frac{\sin\theta}{(\sin\theta)^2 + 3(E_BI_B/L_B^3)(L_C/E_CAC)} R|_{\text{rigid support at B}} \quad (9.23)$$

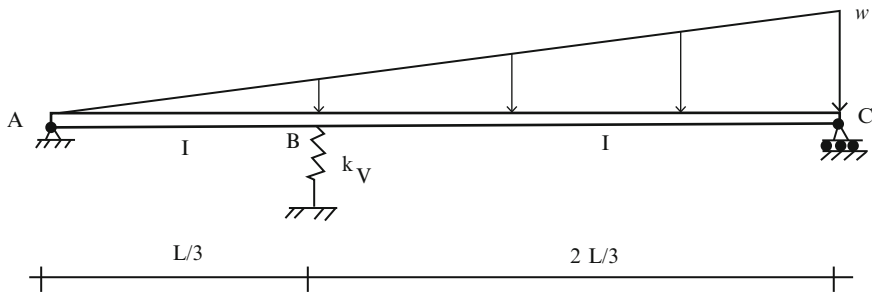
There are two geometric parameters, θ , and the ratio of I_B/L_B^3 to A_C/L_C . Note that X_1 varies with the angle θ . When cables are used to stiffen beams, such as for cable-stayed bridges, the optimum cable angle is approximately 45° . The effective stiffness provided by the cable degrades rapidly with decreasing θ .

Example 9.4

Given: The structure defined in Fig. E9.4a.

Assume $I = 400 \text{ in.}^4$, $L = 54 \text{ ft}$, $w = 2.1 \text{ kip}/\text{ft}$, $k_v = 25 \text{ kip/in.}$, and $E = 29,000 \text{ ksi}$.

Determine: The reactions, the axial force in the spring, and the displacement at B.

**Fig. E9.4a**

Solution: The structure is indeterminate to the first degree. We take the axial force in the spring at B as the force unknown.

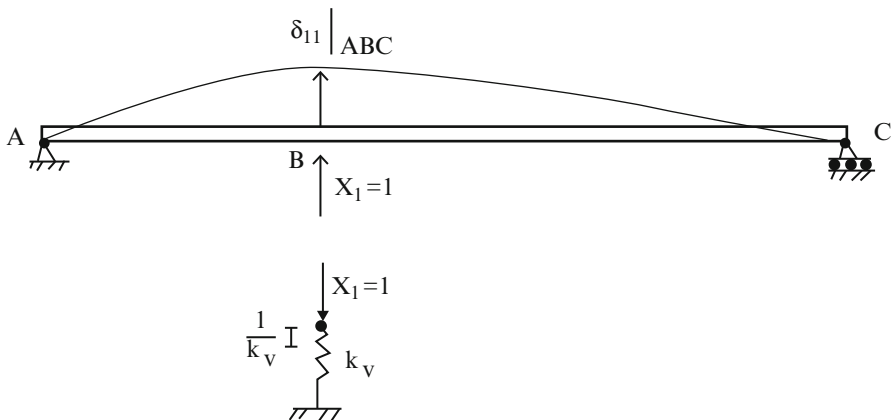
The geometric compatibility equation is

$$\Delta_{1,0} + \left(\delta_{11}|_{ABC} + \frac{1}{k_v} \right) X_1 = 0$$

The deflection terms are given in Table 3.1 (Figs. E9.4b, c).

$$\Delta_{1,0} = -\frac{4wL^4}{729EI} = 14.6 \text{ in.}$$

$$\delta_{11}|_{ABC} = \frac{4L^3}{243EI} = 0.386 \text{ in.}$$

**Fig. E9.4b** Deflected shape due to $X_1 = 1$

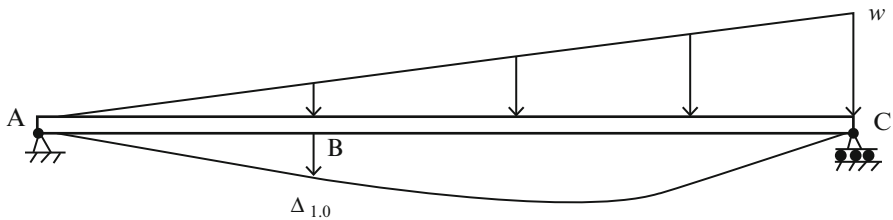
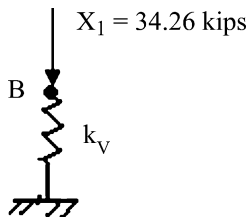


Fig. E9.4c Deflected shape due to external loading

Solving for X_1 , leads be:

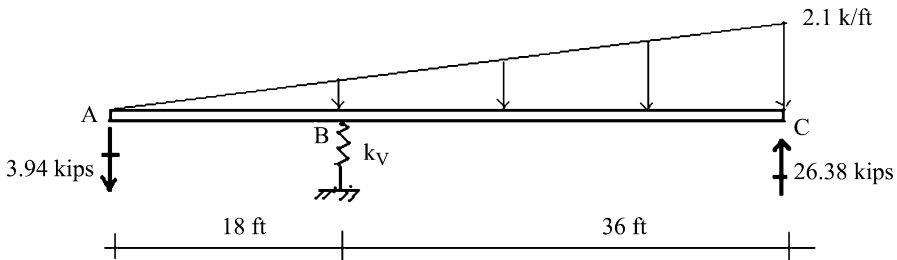
$$X_1 = \frac{\Delta_{1,0}}{\delta_{11|ABC} + (1/k_v)} = \frac{14.6}{0.386 + (1/25)} = 34.26 \text{ kip } \uparrow$$



The displacement at B is

$$v_B = \frac{X_1}{k_v} = \frac{34.26}{25} = 1.37 \text{ in. } \downarrow$$

Next, we determine the remaining reactions by using the static equilibrium equations.



Example 9.5

Given: The structure defined in Fig. E9.5a. Assume $I = 200(10)^6 \text{ mm}^4$, $L = 18 \text{ m}$, $P = 45 \text{ kN}$, $A_c = 1,300 \text{ mm}^2$, and $E = 200 \text{ GPa}$.

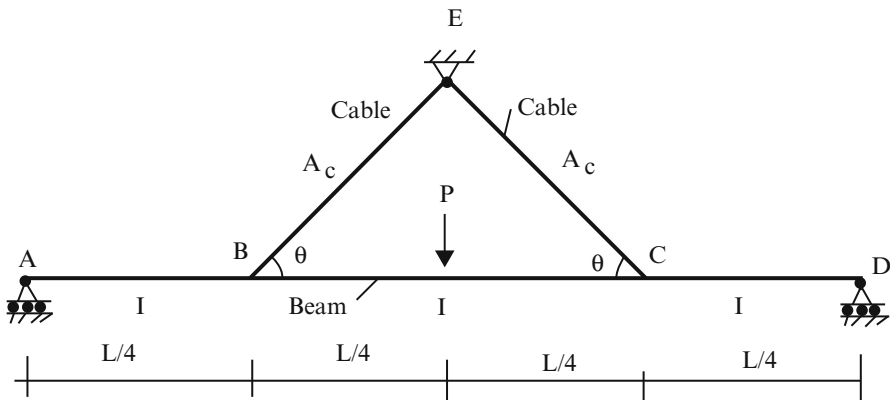


Fig. E9.5a

Determine: The forces in the cables, the reactions, and the vertical displacement at the intersection of the cable and the beam.

- (a) $\theta = 45^\circ$
- (b) $\theta = 30^\circ$

Solution: The structure is indeterminate to the second degree. We take the cable forces as the force redundants and work with the structure defined below (Fig. E9.5b).

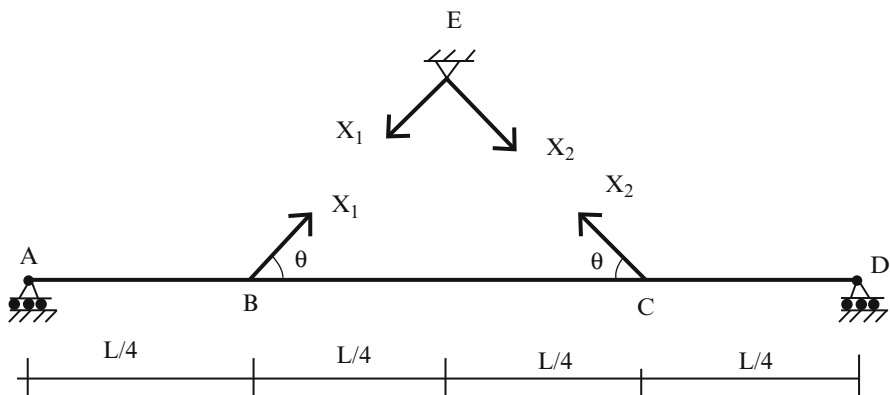


Fig. E9.5b Primary structure

Next, we compute the deflected shapes due to external loading P , $X_1 = 1$ and $X_2 = 1$ applied to the primary structure (Figs. E9.5c–e).

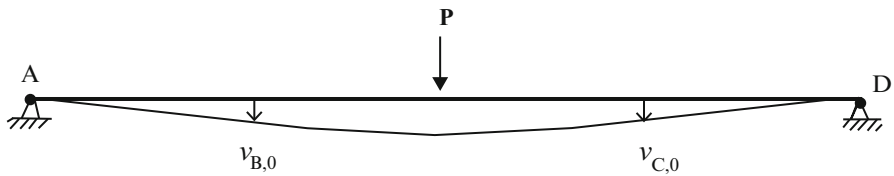


Fig. E9.5c External loading P

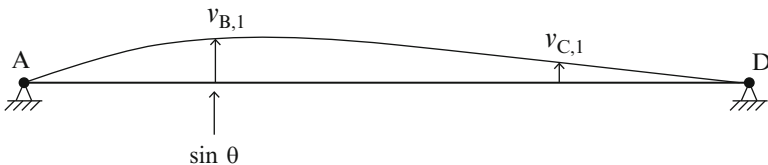


Fig. E9.5d $X_1 = 1$

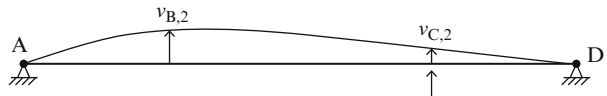


Fig. E9.5e $X_2 = 1$

The displacements of the primary structure due to the external loading and the two force redundants are expressed as

$$\Delta_{1,0} + \delta_{11}X_1 + \delta_{12}X_2 = 0$$

$$\Delta_{2,0} + \delta_{21}X_1 + \delta_{22}X_2 = 0$$

where

$$\delta_{11} = \delta_{11}|_{\text{Beam}} + \delta_{11}|_{\text{cable}}$$

$$\delta_{22} = \delta_{22}|_{\text{Beam}} + \delta_{22}|_{\text{cable}}$$

$$\delta_{12} = \delta_{12}|_{\text{Beam}}$$

$$\delta_{21} = \delta_{21}|_{\text{Beam}}$$

also

$$\Delta_{1,0} = v_{B,0} \sin \theta$$

$$\Delta_{2,0} = v_{C,0} \sin \theta$$

$$\delta_{11}|_{\text{Beam}} = v_{B,1} \sin \theta$$

$$\delta_{21}|_{\text{Beam}} = v_{C,1} \sin \theta$$

$$\delta_{21}|_{\text{Beam}} = v_{B,2} \sin \theta$$

$$\delta_{22}|_{\text{Beam}} = v_{C,2} \sin \theta$$

Because of symmetry:

$$\delta_{11}|_{\text{Beam}} = \delta_{22}|_{\text{Beam}} = v_{B,1} \sin \theta = \frac{3 \sin \theta^2 L^3}{256EI}$$

$$\delta_{12}|_{\text{Beam}} = \delta_{21}|_{\text{Beam}} = v_{B,2} \sin \theta = \frac{7 \sin \theta^2 L^3}{768EI}$$

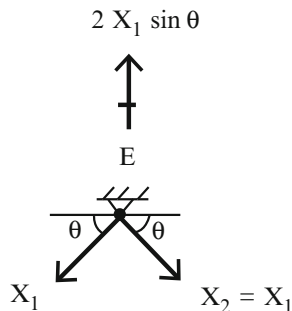
$$\Delta_{1,0} = \Delta_{2,0} = v_{B,0} \sin \theta = \frac{11 \sin \theta P L^3}{768EI}$$

$$\delta_{11}|_{\text{Cable}} = \delta_{22}|_{\text{Cable}} = \frac{L_C}{A_C E} = \frac{L}{4 \cos \theta A_C E}$$

$$X_1 = X_2$$

Lastly, the redundant forces are

$$X_1 = X_2 = \frac{\Delta_{1,0}}{(\delta_{11}|_{\text{Beam}} + \delta_{11}|_{\text{cable}}) + \delta_{12}|_{\text{Beam}}}$$

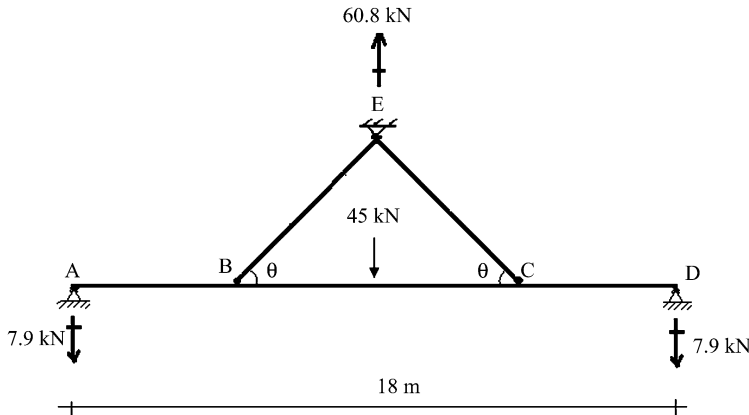


(a) For $\theta = 45^\circ$

$$X_1 = X_2 = \frac{\Delta_{1,0}}{(\delta_{11}|_{\text{Beam}} + \delta_{11}|_{\text{cable}}) + \delta_{12}|_{\text{Beam}}} = 43 \text{ kN}$$

$$\therefore 2X_1 \sin \theta = 2(43) \sin 45 = 60.8$$

The remaining reactions are determined using the static equilibrium equations.

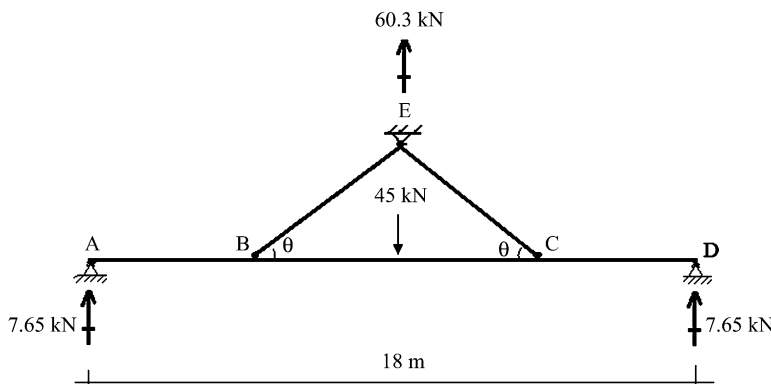


(b) For $\theta = 30^\circ$

$$X_1 = X_2 = \frac{\Delta_{1,0}}{(\delta_{11}|_{\text{Beam}} + \delta_{11}|_{\text{cable}}) + \delta_{12}|_{\text{Beam}}} = 60.3 \text{ kN}$$

$$\therefore 2X_1 \sin \theta = 2(60.3) \sin 30 = 60.3$$

The remaining reactions are



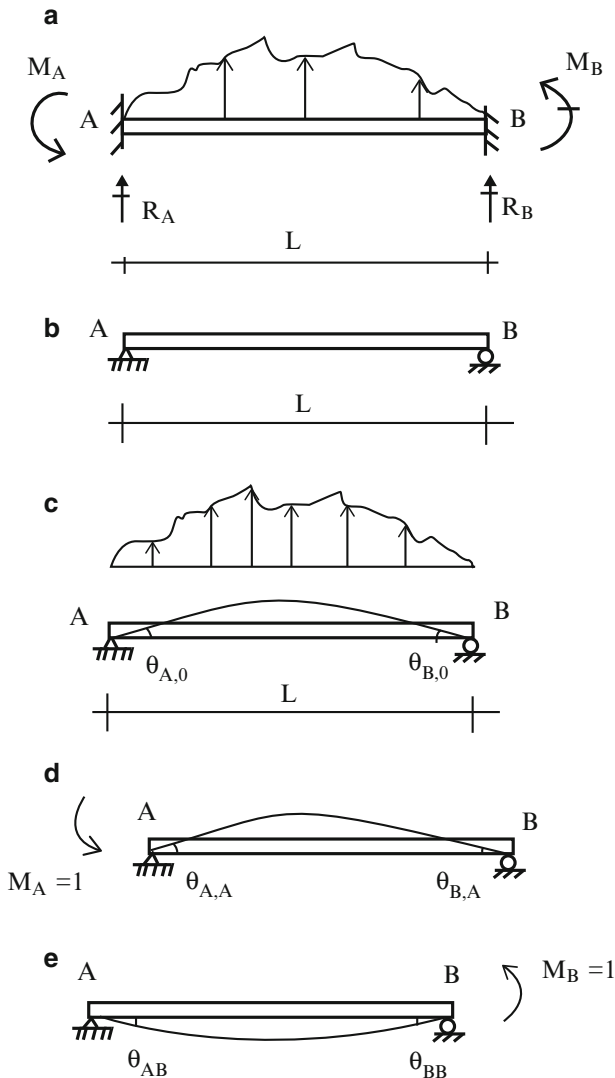


Fig. 9.23 Beam with full end restraint. (b) Primary structure. (c) External loading—displacement profile. (d) Displacement profile for $M_A = 1$. (e) Displacement profile for $M_B = 1$

9.3.2 Fixed-Ended Beams

We treat next the beam shown in Fig. 9.23a. The structure is fully restrained at each end and therefore is indeterminate to the second degree. We take as force redundants the counter clockwise end moments at each end. The corresponding displacement measures are the counterclockwise end rotations, θ_A and θ_B .

We write the general form of the compatibility equations as (we use θ instead of Δ to denote the displacement measures and M instead of X for the force measures):

$$\begin{aligned}\theta_A &= \theta_{A,0} + M_A \theta_{AA} + M_B \theta_{AB} \\ \theta_B &= \theta_{B,0} + M_A \theta_{BA} + M_B \theta_{BB}\end{aligned}\quad (9.24)$$

where $\theta_{A,0}$ and $\theta_{B,0}$ depend on the nature of the applied loading, and the other flexibility coefficients are

$$\theta_{AA} = \frac{L}{3EI}$$

$$\theta_{BB} = \frac{L}{3EI}$$

$$\theta_{AB} = \theta_{BA} = -\frac{L}{6EI}$$

We solve (9.24) for M_A and M_B

$$\begin{aligned}M_A &= \frac{2EI}{L} \{2(\theta_A - \theta_{A,0}) + (\theta_B - \theta_{B,0})\} \\ M_B &= \frac{2EI}{L} \{2(\theta_B - \theta_{B,0}) + (\theta_A - \theta_{A,0})\}\end{aligned}\quad (9.25)$$

When the ends are fixed, $\theta_A = \theta_B = 0$, and the corresponding values of M_A and M_B are called the fixed end moments. They are usually denoted as M_A^F and M_B^F

$$\begin{aligned}M_A^F &= -\frac{2EI}{L} \{2\theta_{A,0} + \theta_{B,0}\} \\ M_B^F &= -\frac{2EI}{L} \{2\theta_{B,0} + \theta_{A,0}\}\end{aligned}\quad (9.26)$$

Introducing this notation in (9.25), the expressions for the end moments reduces to

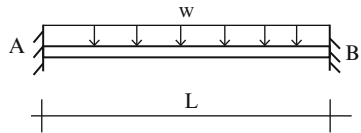
$$\begin{aligned}M_A &= \frac{2EI}{L} \{2\theta_A + \theta_B\} + M_A^F \\ M_B &= \frac{2EI}{L} \{2\theta_B + \theta_A\} + M_B^F\end{aligned}\quad (9.27)$$

We will utilize these equations in Chap. 10.

Example 9.6 Fixed end moments for uniformly distributed loading

Given: The uniform distributed loading applied to a fixed end beam (Fig. E9.6a).

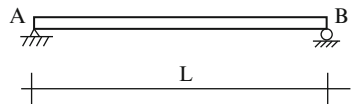
Fig. E9.6a



Determine: The fixed end moments.

Solution: We take the end moments at A and B as force redundant (Fig. E9.6b).

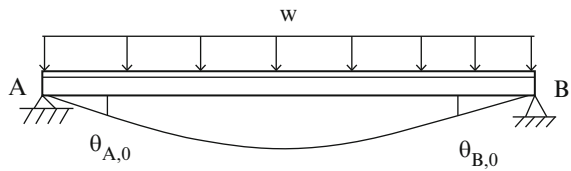
Fig. E9.6b Primary structure



Noting Table 3.1, the rotations due to the applied load are (Fig. E9.6c)

$$EI\theta_{A,0} = -\frac{wL^3}{24} \quad EI\theta_{B,0} = \frac{wL^3}{24}$$

Fig. E9.6c Deformation
of primary structure due
to applied load



Substituting their values in (9.26) leads to

$$M_A^F = -\frac{2EI}{L} \{2\theta_{A,0} + \theta_{B,0}\} = \frac{wL^2}{6} - \frac{wL^2}{12} = \frac{wL^2}{12}$$

$$M_B^F = -\frac{2EI}{L} \{2\theta_{B,0} + \theta_{A,0}\} = -\frac{wL^2}{6} + \frac{wL^2}{12} = -\frac{wL^2}{12}$$

$$M_A^F = \frac{wL^2}{12} \quad M_B^F = \frac{wL^2}{12}$$

The shear and moment diagrams are plotted in Fig. E9.6d.

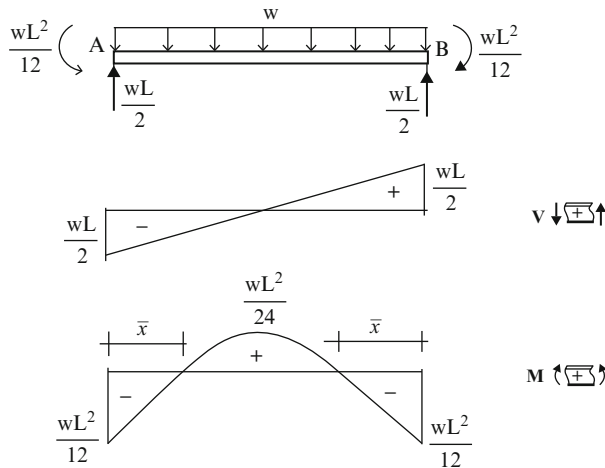


Fig. E9.6d

Note that the peak positive moment for the simply supported case is $+(wL^2/8)$. Points of inflection are located symmetrically at

$$\bar{x} = \frac{L}{2} \left(1 - \frac{1}{\sqrt{3}} \right) \approx 0.21L$$

This solution applies for full fixity. When the member is part of a frame, the restraint is provided by the adjacent members, and the end moments will generally be less than the fully fixed value.

Example 9.7 Fixed end moment—single concentrated force

Given: A single concentrated force applied at an arbitrary point $x = a$ on the fixed end beam shown in Fig. E9.7a.

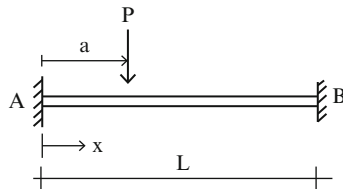


Fig. E9.7a

Determine: The fixed end moments.

Solution: We work with the primary structure defined in Fig. E9.7b.

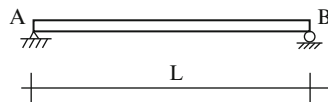


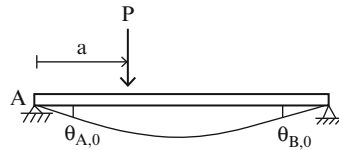
Fig. E9.7b Primary structure

Using the results listed in Table 3.1, the rotations are given by (Fig. E9.7c)

$$EI\theta_{A,0} = -\frac{Pa(L-a)(2L-a)}{6L}$$

$$EI\theta_{B,0} = \frac{Pa(L+a)}{6L}$$

Fig. E9.7c Deformation of primary structure due to external loading

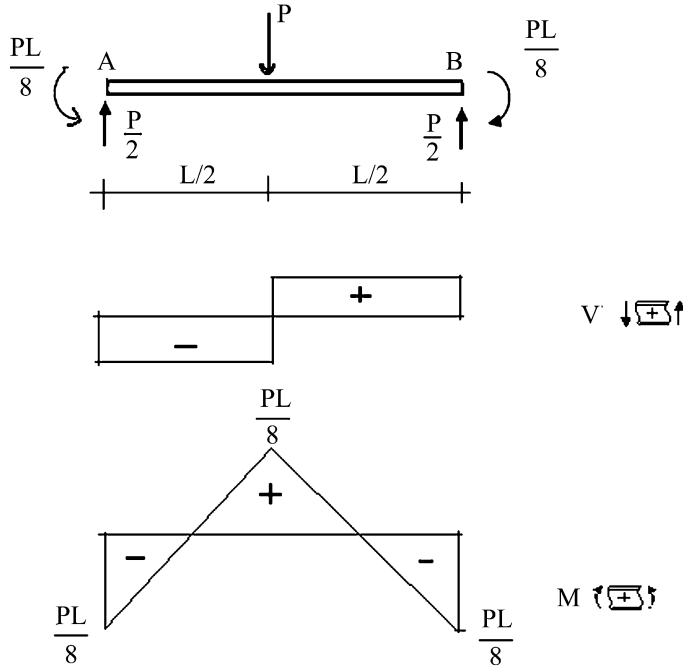


Substituting into (9.26) leads to

$$M_A^F = \frac{Pa(L-a)^2}{L^2}$$

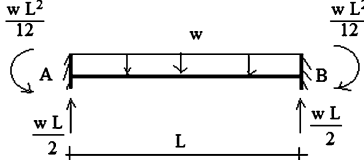
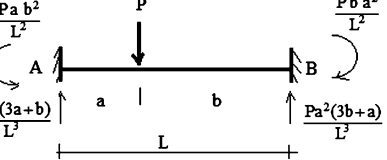
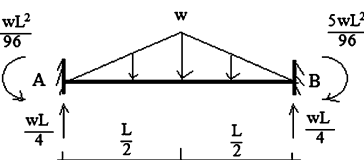
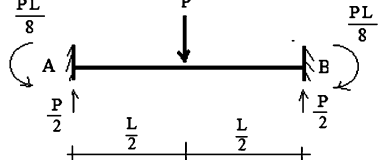
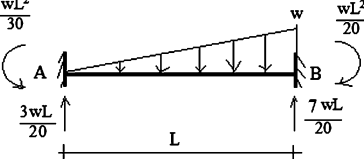
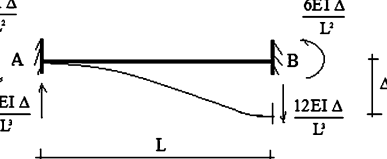
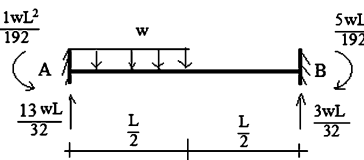
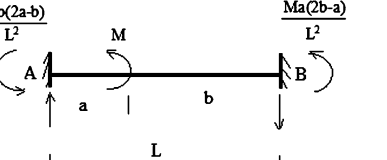
$$M_B^F = -\frac{P(L-a)a^2}{L^2}$$

The critical location for maximum fixed end moment is $a = L/2$; the corresponding maximum values are $M_A^F = -M_B^F = \frac{PL}{8}$. The shear and moment diagrams are plotted below.



Note that there is a 50% reduction in peak moment due to end fixity.

Table 9.1 Fixed end actions for fully fixed

Results for various loadings and end conditions are summarized in Tables 9.1 and 9.2.

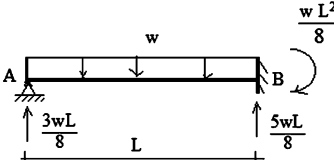
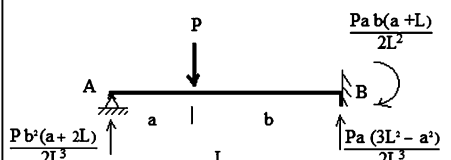
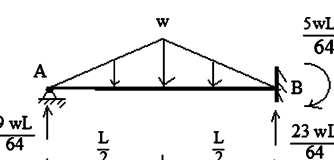
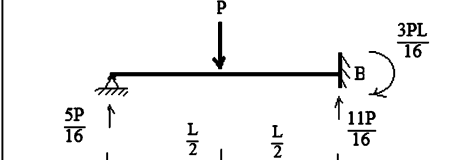
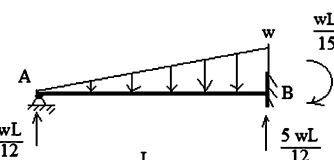
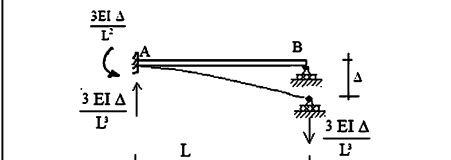
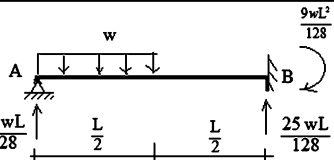
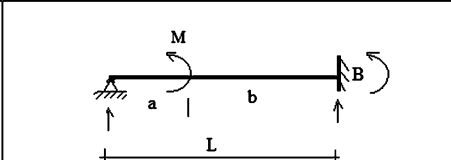
9.3.3 Analytical Solutions for Multi-span Beams

Consider the two-span beam shown in Fig. 9.24a. We allow for different lengths and different moments of inertia for the spans. Our objective here is to determine analytically how the maximum positive and negative moments vary as the load moves across the total span. We choose the negative moment at B as the redundant. The corresponding primary structure is shown in Fig. 9.24b. Here, $\Delta\theta_B$ is the relative rotation together of adjacent cross sections at B.

The geometric compatibility equation involves the relative rotation at B.

$$\Delta\theta_B = \Delta\theta_{B,0} + \delta\theta_{BB}M_B = 0$$

Table 9.2 Fixed end actions for partially fixed

The various rotation terms are given in Table 3.1. Note that the $\delta\theta_{BB}$ term is independent of the applied loading.

$$\delta\theta_{BB} = \frac{1}{3E} \left(\frac{L_1}{I_1} + \frac{L_2}{I_2} \right)$$

When the loading is on span AB (see Table 3.1),

$$\Delta\theta_{B,0} = -\frac{P}{6EI_1L_1} a(a^2 - L_1^2)$$

Then

$$M_B = \frac{-\Delta\theta_{B,0}}{\delta\theta_{BB}} = \left\{ \frac{(L_1/I_1)}{(L_1/I_1) + (L_2/I_2)} \right\} \frac{1}{2} Pa \left(1 - \frac{a^2}{L_1^2} \right) \quad (9.28)$$

Given the value of M_B , we can determine the reactions by using the static equilibrium equations.

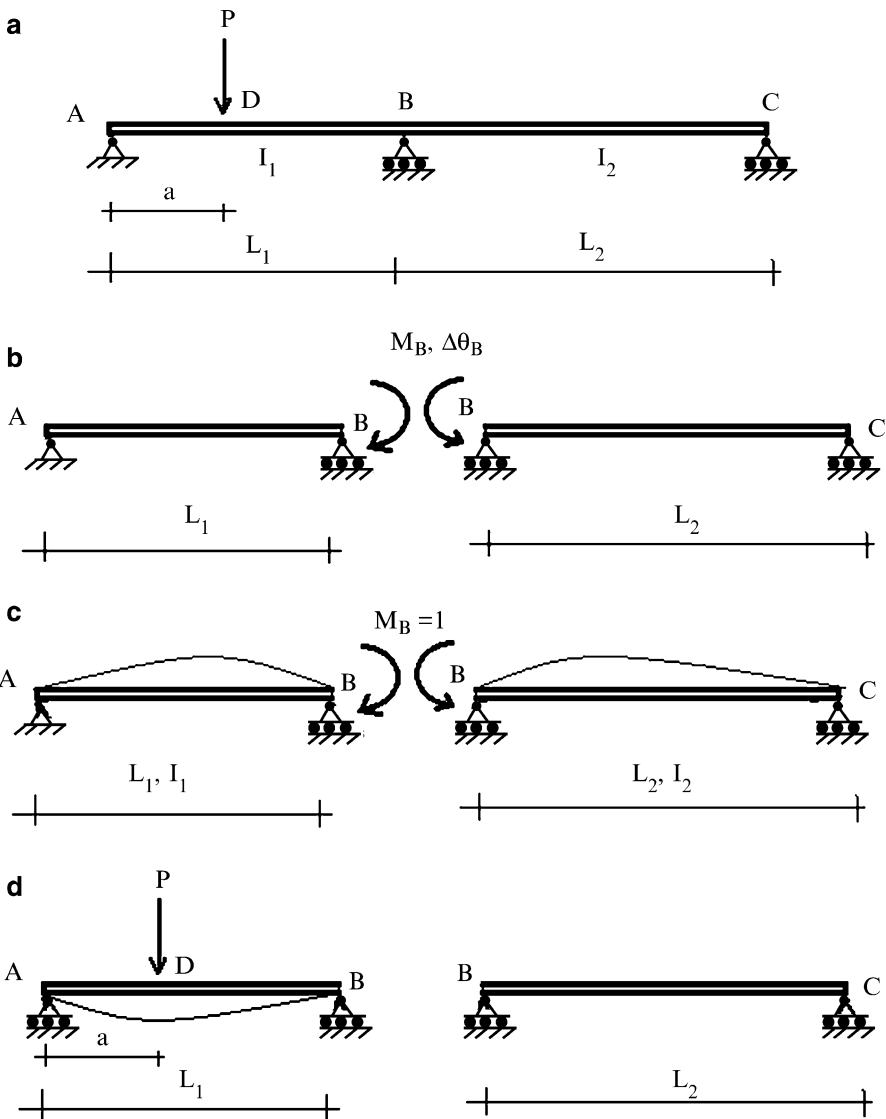


Fig. 9.24 (a) Actual structure—notation for a two-span beam. (b) Primary structure—redundant moment. (c) Displacement due to a unit value of the redundant moment. (d) Rotation due to external loading

Noting (9.28), the peak moments are given by:

$$\begin{aligned} \text{Negative moment } M_B &= -\frac{PL_1}{2}f \frac{a}{L_1} \left(1 - \frac{a^2}{L_1^2}\right) \\ \text{Positive moment } M_D &= PL_1 \left(\frac{a}{L_1}\right) \left\{ \left(1 - \frac{a}{L_1}\right) - \frac{f}{2} \frac{a^2}{L_1^2} \left(1 - \frac{a^2}{L_1^2}\right) \right\} \end{aligned} \quad (9.29)$$

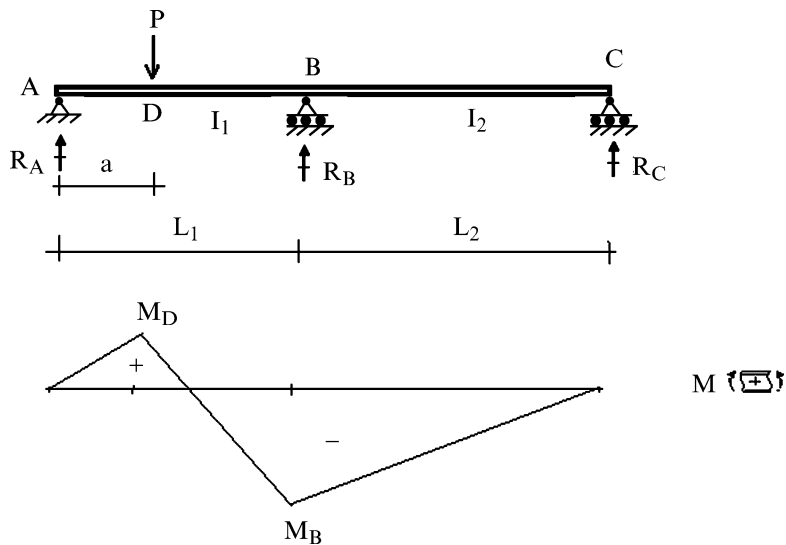


Fig. 9.25 Bending moment distribution for load on span AB

where

$$f = \frac{1}{1 + (I_1/L_1)(L_2/I_2)}$$

We define the ratio of \$I\$ to \$L\$ as the “relative stiffness” for a span and denote this parameter by \$r\$.

$$r_i = \left. \frac{I}{L} \right|_{\text{span } i} \quad (9.30)$$

With this notation, \$f\$ takes the form

$$f = \frac{1}{1 + (r_1/r_2)}$$

The typical bending moment diagram is plotted in Fig. 9.25.

When the load is on span BC, one just has to use a different expression for \$\Delta\theta_{B,0}\$. Redefining the location of P as shown in Fig. 9.26a, the solution takes the following form:

$$\Delta\theta_{B,0} = -\frac{Pb \left(1 - \frac{b}{L_2}\right) \left(2 - \frac{b}{L_2}\right)}{6EI_2}$$

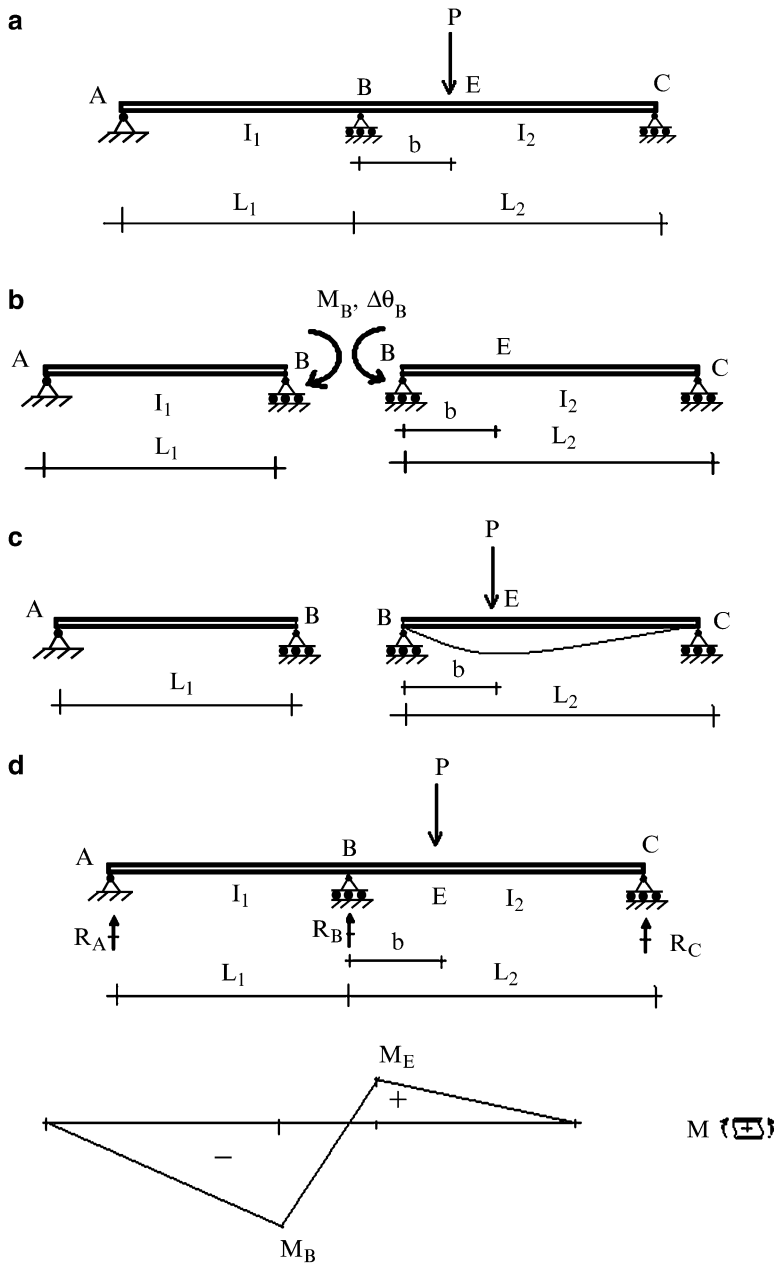


Fig. 9.26 (a) Actual structure—loading on span BC. (b) Primary structure—redundant moment. (c) Rotation due to external loading. (d) Bending moment distribution for load on span BC

Then

$$M_B = \frac{-\Delta\theta_{B,0}}{\delta\theta_{BB}} = \frac{1}{(1 + (r_2/r_1))} \left(\frac{1}{2} PL_2 \right) \frac{b}{L_2} \left(1 - \frac{b}{L_2} \right) \left(2 - \frac{b}{L_2} \right) \quad (9.31)$$

Given M_B , one can construct the moment diagram. It is similar to Fig. 9.25, but rotated 180°.

Example 9.8

Given: The two-span beam shown in Figs. E9.8a, b.

Determine: The variation of the bending moment at B with relative stiffness of the adjacent spans ($r_1/r_2=0.1, 1, \text{ and } 10$).

Fig. E9.8a

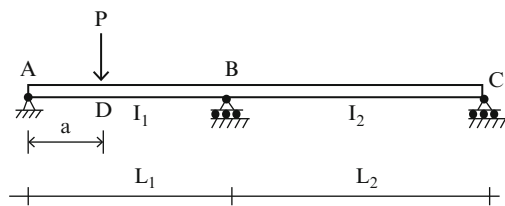
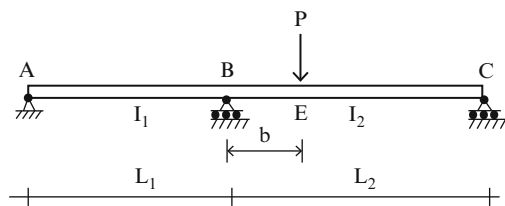
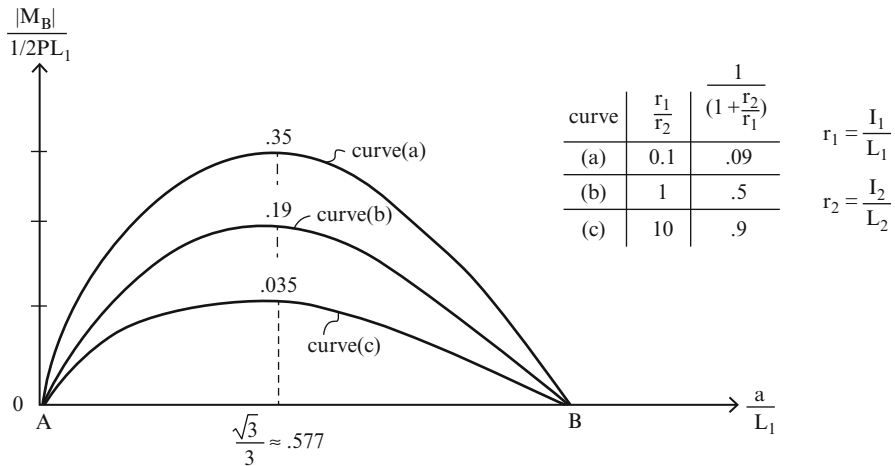
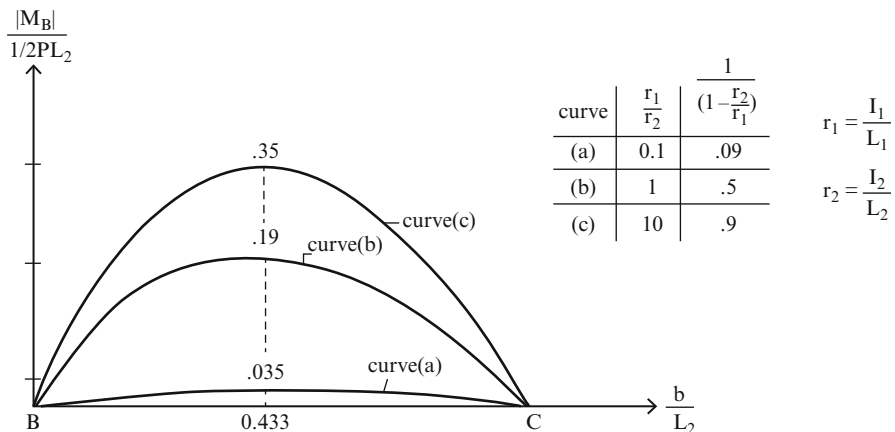


Fig. E9.8b

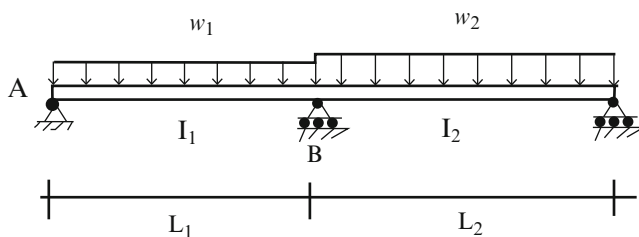


Solution: We determine the variation of the moment at B for a range of relative stiffness ratios covering the spectrum from one span being very flexible to one span being very rigid with respect to the other span using (9.29) and (9.31). Results for the individual spans are plotted in Figs. E9.8c, d.

**Fig. E9.8c** Load on the left span (9.29)**Fig. E9.8d** Load on the right span (9.31)

Example 9.9 Two-span continuous beam—uniform loading

Given: The two-span beam shown in Fig. E9.9a.

**Fig. E9.9a**

Determine: The bending moment at support B.

Solution: We take the negative moment at the interior support as the force redundant. The solution process is similar to that followed for the case of a concentrated load. One determines the relative rotations at B, and then enforces continuity at B (Fig. E9.9b).

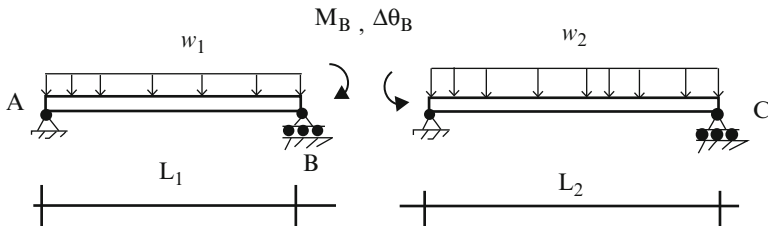


Fig. E9.9b

The various terms are (see Table 3.1)

$$\Delta\theta_{B,0} = -\frac{w_1 L_1^3}{24EI_1} - \frac{w_2 L_2^3}{24EI_2}$$

$$\delta\theta_{BB} = \frac{L_1}{3EI_1} + \frac{L_2}{3EI_2}$$

Requiring the relative rotation at B equal to zero leads to

$$M_B = \frac{-\Delta\theta_{B,0}}{\delta\theta_{BB}} = \frac{w_1 L_1^2}{8} \frac{1 + (w_2/w_1)(L_2/L_1)^2(r_1/r_2)}{1 + (r_1/r_2)}$$

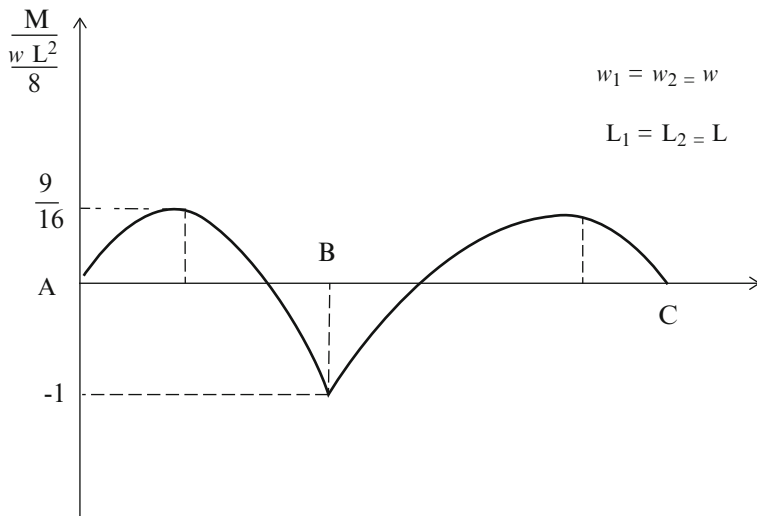
where

$$r_1 = \frac{I_1}{L_1}, \quad r_2 = \frac{I_2}{L_2}$$

Suppose the loading and span lengths are equal. In this case,

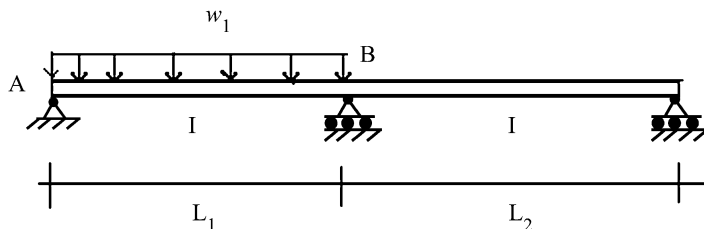
$$M_B = \frac{wL^2}{8}$$

for all combinations of I_1 and I_2 . The moment diagram is plotted below (Fig. E9.9c).

**Fig. E9.9c**

Another interesting case is where $w_2 = 0$ and $I_1 = I_2$. The solution depends on the ratio of span lengths.

$$M_B = \frac{w_1 L_1^2}{8} \frac{1}{1 + (L_2/L_1)}$$

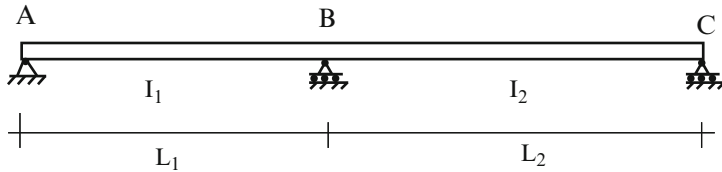


Suppose $L_2 = L_1$ and $I_1 = I_2$, then

$$M_B = \frac{1}{2} \left(\frac{w_1 L_1}{8} \right)^2$$

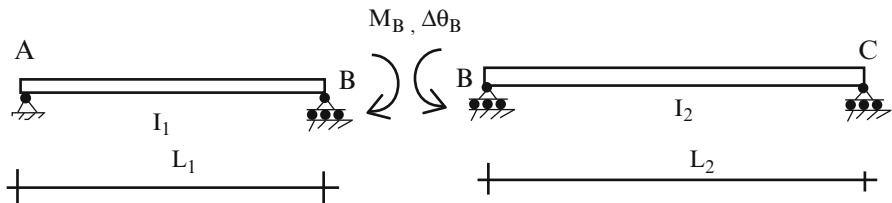
Example 9.10 Two-span continuous beam with support settlement

Given: The two-span beam shown in Fig. E9.10a. The supports at B or A experience a vertical displacement downward due to settlement of the soil under the support.

**Fig. E9.10a**

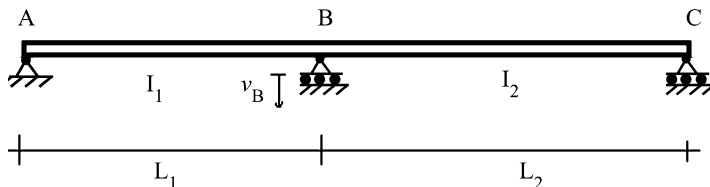
Determine: The bending moment at B.

Solution: We work with the primary structure shown in Fig. E9.10b.

**Fig. E9.10b** Primary structure—redundant moment

If the support at B moves downward an amount v_B , the relative rotation of the section at B is

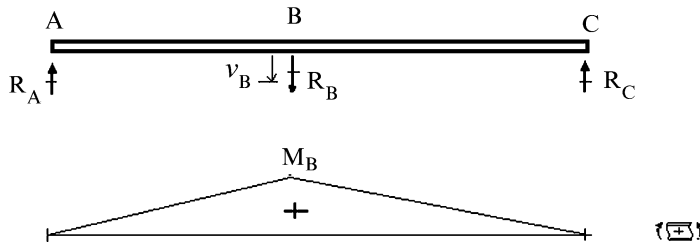
$$\Delta\theta_{B,0} = \frac{v_B}{L_1} + \frac{v_B}{L_2}$$



Compatibility requires the moment at B to be equal to

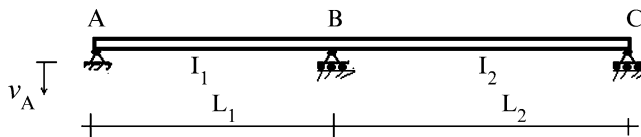
$$M_B = \frac{-\Delta\theta_{B,0}}{\delta\theta_{BB}} = -\frac{v_B((1/L_1)+(1/L_2))}{(1/3E)((L_1/I_1)+(L_2/I_2))}$$

The minus sign indicates that the bending moment is of opposite sense to that assumed in Fig. E9.10b.

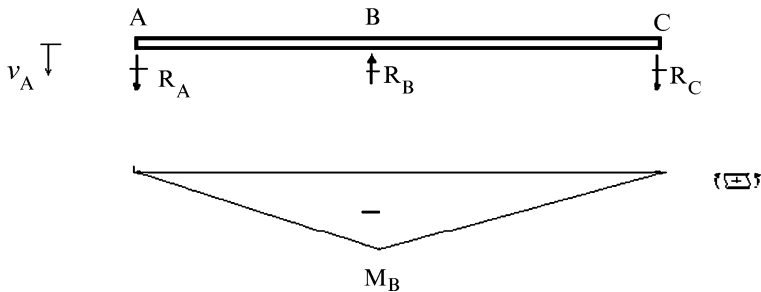


When the properties are the same for both spans ($I_1 = I_2$ and $L_1 = L_2$), M_B reduces to $M_B = \frac{3EI_1}{L_1^2} v_B$.

When the support at A moves downward an amount v_A , the behavior is reversed.



In this case, $\Delta\theta_{B,0} = -v_A/L_1$, and $M_B = \frac{v_A/L_1}{(1/3E)((L_1/I_1)+(L_2/I_2))}$



When the properties are the same for both spans ($I_1 = I_2$ and $L_1 = L_2$), M_B reduces to $M_B = \frac{3EI}{2L_1^2} v_A$.

9.4 Application to Arch-Type Structures

Chapter 6 introduced the topic of Arch structures. The discussion was concerned with how the geometry of arch structures is defined and how to formulate the equilibrium equations for statically determinate arches. Various examples were presented to illustrate how arch structures carry transverse loading by a combination of both axial and bending action. This feature makes them more efficient than beam structures for long-span applications.

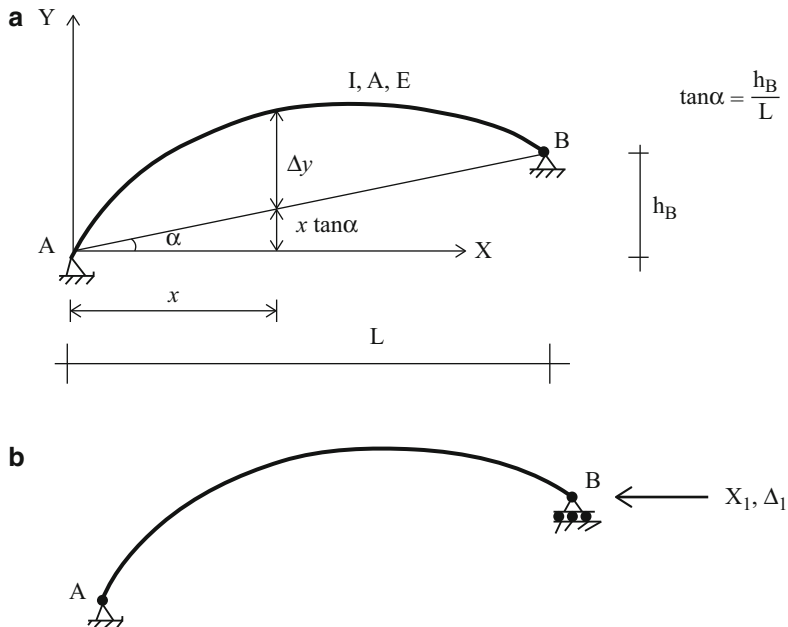


Fig. 9.27 (a) Actual structure—geometry. (b) Primary structure— redundant reaction

In what follows we extend the analytical formulation to statically indeterminate arches. We base our analysis procedure on the force method and use the principle of virtual forces to compute displacement measures. One of our objectives here is to develop a strategy for finding the geometry for which there is minimal bending moment in the arch due to a particular loading.

We consider the two-hinged arch shown in Fig. 9.27a. This structure is indeterminate to the first degree. We take the horizontal reaction at the right support as the force redundant, and use the Principle of Virtual Forces described in Sect. 6.5 to determine $\Delta_{1,0}$ the horizontal displacement due to loading, and δ_{11} , the horizontal displacement due to a unit value of X_1 .

The general expressions for these displacement measures follow from (6.9)

$$\begin{aligned}\Delta_{1,0} &= \int_s \left\{ \frac{F_0}{AE} \delta F + \frac{V_0(x)}{GA_s} \delta V + \frac{M_0(x)}{EI} \delta M \right\} ds \\ \delta_{11} &= \int_s \left\{ \frac{(\delta F)^2}{AE} + \frac{(\delta V)^2}{GA_s} + \frac{(\delta M)^2}{EI} \right\} ds\end{aligned}\quad (9.32)$$

We usually neglect the shear deformation term. Whether one can also neglect the axial deformation term depends on the arch geometry. For completeness, we will

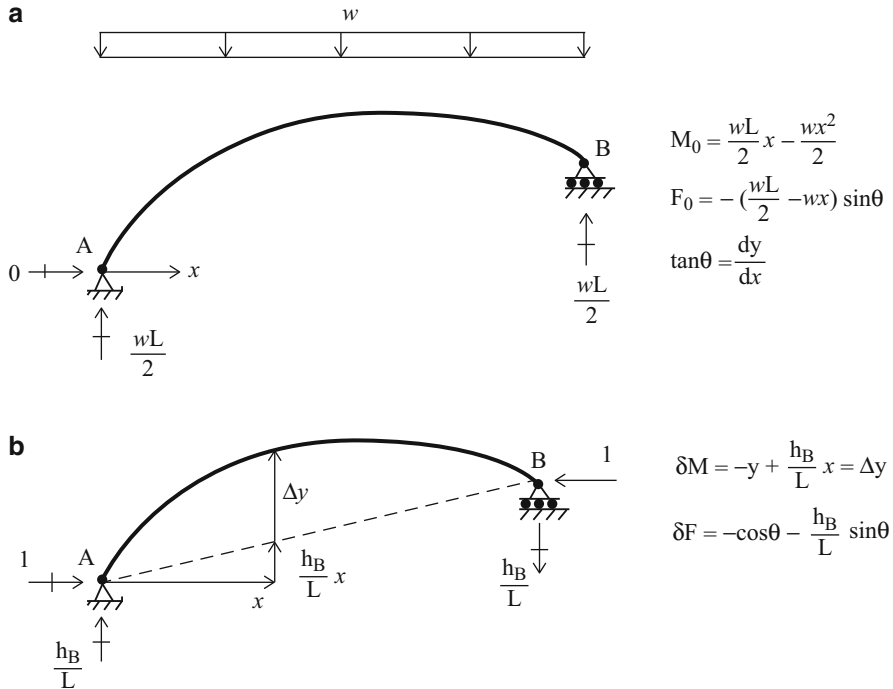


Fig. 9.28 (a) Force due to applied loading (F_0, M_0). (b) Force due to $X_1 = 1$ ($\delta F, \delta M$)

retain this term. The two internal forces systems are summarized below. We assume the applied load is uniform per projected length (Fig. 9.28).

Substituting for the force terms leads to the following expressions for the displacement measures:

$$\Delta_{1,0} = \int_0^L \left\{ \frac{1}{AE\cos\theta} \left(\frac{wL}{2} - wx \right) \sin\theta (\cos\theta + \tan\alpha \sin\theta) - \left(\frac{wL}{2}x - \frac{wx^2}{2} \right) \frac{\Delta y}{EI\cos\theta} \right\} dx$$

$$\delta_{11} = \int_0^L \left\{ \frac{(\cos\theta + \tan\alpha \sin\theta)^2}{AE\cos\theta} + \frac{(\Delta y)^2}{EI\cos\theta} \right\} dx \quad (9.33)$$

Geometric compatibility requires

$$X_1 = -\frac{\Delta_{1,0}}{\delta_{11}} \quad (9.34)$$

One can use either symbolic integration or numerical integration to evaluate the flexibility coefficients. We prefer to use the numerical integration scheme described in Sect. 3.6.6.

The solution simplifies considerably when axial deformation is neglected with respect to bending deformation. One sets $A = \infty$ in (9.33). This leads to

$$\begin{aligned}\Delta_{1,0} &= - \int_0^L \left(\frac{wL}{2}x - \frac{wx^2}{2} \right) \frac{\Delta y}{EI\cos\theta} dx = - \int_0^L \frac{M_0 \Delta y}{EI\cos\theta} dx \\ \delta_{11} &= + \int_0^L \frac{(\Delta y)^2}{EI\cos\theta} dx\end{aligned}\tag{9.35}$$

Suppose Δy is chosen such that

$$\Delta y = \beta \left[\frac{wL}{2}x - \frac{wx^2}{2} \right] \equiv \beta M_0\tag{9.36}$$

Then,

$$\Delta_{1,0} = - \frac{1}{\beta} \delta_{11}$$

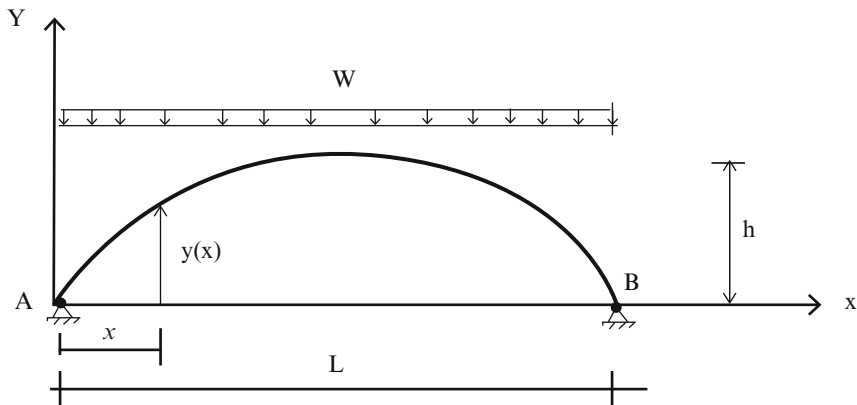
and it follows that

$$\begin{aligned}X_1 &= \frac{1}{\beta} \\ M &= M_0 + X_1 \delta M = M_0 + \left(\frac{1}{\beta} \right) (-\beta M_0) = 0\end{aligned}\tag{9.37}$$

With this choice of geometry, the arch carries the exterior load by axial action only; there is no bending. *Note that this result is based on the assumption that axial deformation is negligible.* In general, there will be a small amount of bending when h is not small with respect to L , i.e., when the arch is “deep.” *One cannot neglect axial deformation for a shallow arch.*

Example 9.11 Parabolic arch with uniform vertical loading

Given: The two-hinged parabolic arch defined in Fig. E9.11a.

**Fig. E9.11a**

Determine: The bending moment distribution.

Solution: The centriodal axis for the arch is defined by

$$y = 4h \left[\frac{x}{L} - \left(\frac{x}{L} \right)^2 \right]$$

The bending moment in the primary structure due to the uniform loading per unit x is

$$M_0 = \frac{wL}{2}x - \frac{wx^2}{2} = \frac{wL^2}{2} \left[\frac{x}{L} - \left(\frac{x}{L} \right)^2 \right]$$

We note that the expressions for y and M_0 are similar in form. One is a scaled version of the other.

$$M_0 = \frac{wL^2}{2} \frac{1}{4h} y = \frac{wL^2}{8h} y$$

Then, noticing (9.36),

$$\beta = \frac{8h}{wL^2}$$

and $X_1 = \frac{wL^2}{8h}$

The total moment is the sum of M_0 and the moment due to X_1 .

$$M = M_0 - y X_1 = \frac{wL^2}{8h} y - \frac{wL^2}{8h} y = 0$$

We see that there is no bending for this loading and geometry. We should have anticipated this result since a uniformly loaded cable assumes a parabolic shape. By definition, a cable has no bending rigidity and therefore no moment. We can consider an arch as an inverted cable. It follows that a two-hinged uniformly loaded parabolic arch behaves like an inverted cable.

Example 9.12 Approximate solutions

Given: The two-hinged arch and the loading defined in Fig. E9.12a. The integral expression for X_1 is given by 9.3.4. Noting (9.35), the solution equals to

$$X_1 \approx \frac{+\int \Delta y \frac{M_0}{EI} ds}{\int (\Delta y)^2 \frac{ds}{EI}}$$

This result applies when there is no support movement.

Determine: An approximate expression for X_1 . Assume the cross section of the arch is deeper at the abutment than at the crown, and the following approximation is used to define I ,

$$I = \frac{I_0}{\cos \theta}$$

where I_0 is the cross-sectional inertia at the crown.

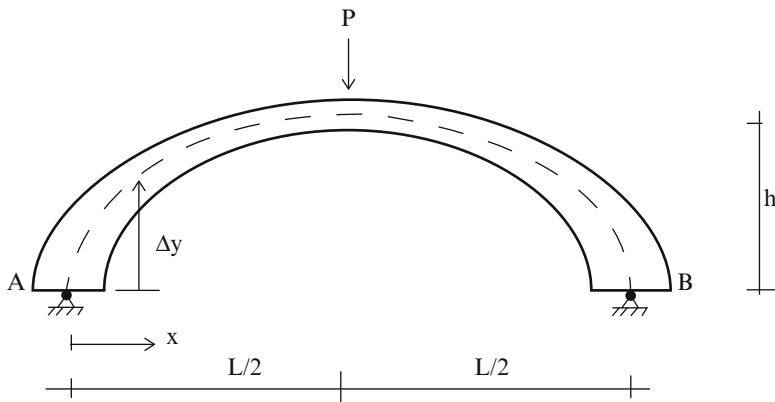


Fig. E9.12a Variable depth arch

Solution: Substituting for I and $ds = \frac{dx}{\cos \theta}$ the integrals simplify to

$$X_1 = \frac{+(1/EI_0) \int \Delta y M_0 dx}{(1/EI_0) \int (\Delta y)^2 dx}$$

and now one can easily determine analytical solutions.

Suppose a concentrated force, P , is applied at mid-span. The corresponding terms for a symmetrical parabolic arch are:

$$\begin{aligned}\Delta y &= \frac{4h}{L} \left(x - \frac{x^2}{L} \right) \\ \frac{1}{EI_0} \int \Delta y M_0 dx &\Rightarrow \frac{5}{48} \frac{PhL^2}{EI_0} \\ \frac{1}{EI_0} \int (\Delta y)^2 dx &= \frac{8}{15} \frac{h^2 L}{EI_0} \\ X_1 &= \frac{75}{384} P \left(\frac{L}{h} \right)\end{aligned}$$

Note that the bending moment is *not* zero in this case.

Example 9.13

Given: The two-hinged arch and the loading defined in Fig. E9.13a.

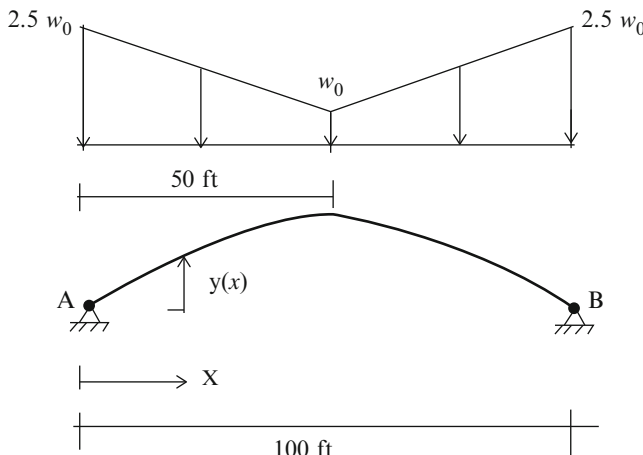


Fig. E9.13a

Determine: The particular shape of the arch which corresponds to negligible bending.

Solution: This two-hinged arch is indeterminate to the first degree. We take the horizontal reaction at the right support as the force redundant (Fig. E9.13b).

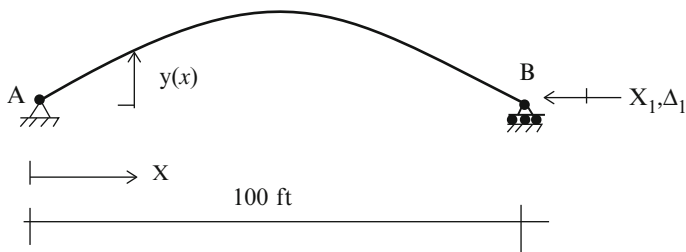


Fig. E9.13b Primary structure—redundant reaction

The applied loading is given by (Fig. E9.13c)

$$w(x) = w_0 \left\{ 2.5 - \frac{1.5}{50}x \right\} \quad 0 < x \leq 50$$

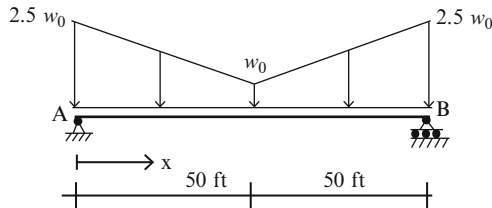


Fig. E9.13c

The corresponding shear and moment in the simply supported beam spanning AB are

$$\begin{aligned} \frac{dV}{dx} = w(x) &\Rightarrow V = w_0 \left\{ 2.5x - \frac{1.5}{100}x^2 \right\} + C_1 \\ \frac{dM}{dx} = -V &\Rightarrow M = -w_0 \left\{ \frac{2.5}{2}x^2 - \frac{1.5}{300}x^3 \right\} + C_1x + C_2 \end{aligned}$$

Enforcing the boundary conditions,

$$M(0) = 0$$

$$M(100) = 0$$

leads to

$$C_2 = 0$$

$$C_1 = w_0 \left\{ 1.25(100) - \frac{1.5(100)^2}{300} \right\} = 75w_0$$

Finally, the expression for M reduces to

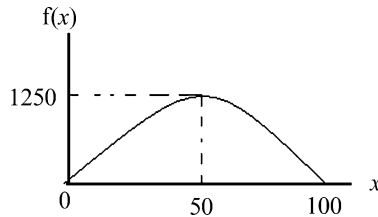
$$M = w_0 \{75x - 1.25x^2 + 0.005x^3\} \quad 0 < x \leq 50$$

follows (9.36) and (9.37).

The desired shape is

$$y(x) = \frac{M(x)}{X_1} = \frac{w_0}{X_1} \{75x - 1.25x^2 + 0.005x^3\} = \frac{w_0}{X_1} f(x)$$

The function $f(x)$ is plotted below. Note that the shape is symmetrical.



When the abutments are inadequate to resist the horizontal thrust, different strategies are employed to resist the thrust. One choice is to insert a tension tie connecting the two supports, as illustrated in Fig. 9.29a. Another choice is to connect a set of arches in series until a suitable anchorage is reached (see Fig. 9.29b). The latter scheme is commonly used for river crossings.

We take the tension in the tie as the force redundant for the tied arch. The corresponding primary structure is shown in Fig. 9.30. We just have to add the extension of the tie member to the deflection δ_{11} . The extended form for δ_{11} is

$$\rightarrow\leftarrow \quad \delta_{11} = \int y^2 \frac{ds}{EI} + \frac{L}{A_t E} \quad (9.38)$$

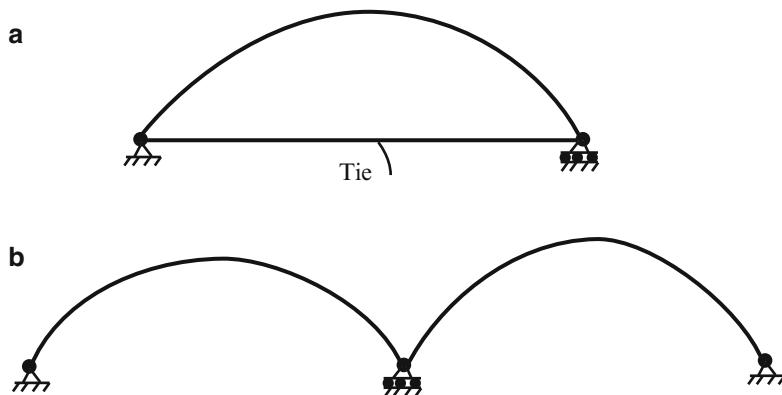


Fig. 9.29 (a) Single tie arch. (b) Multiple connected arches

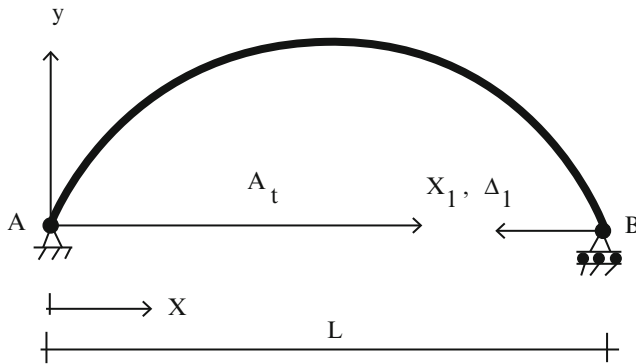


Fig. 9.30 Choice of redundant

The expression for Δ_{1,0} does not change. Then, the tension in the tie is given by:

$$X_1 = \frac{-\Delta_{1,0}}{\delta_{11}} = \frac{\int y(M_0 ds/EI)}{\int y^2(ds/EI) + (L/A_t E)} \quad (9.39)$$

Note that the horizontal reaction is reduced by inserting a tie member. However, now there is bending in the arch.

Example 9.14

Given: A parabolic arch with a tension tie connecting the supports. The arch is loaded with a uniformly distributed load per horizontal projection. Consider I to be defined as $\frac{I_0}{\cos\theta}$.

Determine: The horizontal thrust and the bending moment at mid-span (Fig. E9.14a).

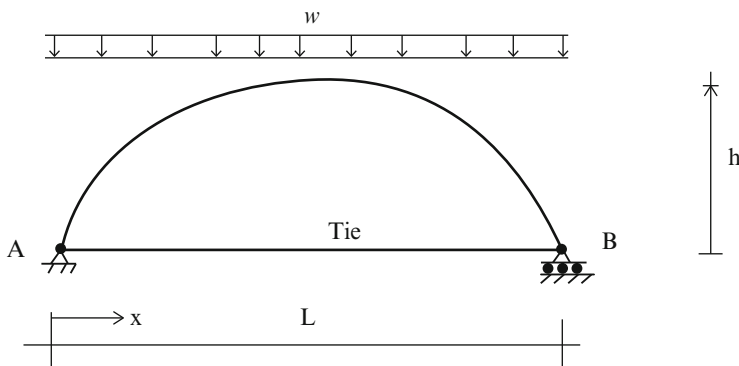


Fig. E9.14a

Solution: We note the results generated in Example 9.12 which correspond to taking $I = \frac{I_0}{\cos\theta}$.

$$\begin{aligned}\Delta_{1,0} &= - \int yM_0 \frac{ds}{EI} = - \frac{1}{EI_0} \int_0^L yM_0 dx \\ &= - \frac{1}{EI_0} \left(\frac{wL^2}{8h} \right) \int_0^L y^2 dx \\ &= - \frac{1}{EI_0} \left(\frac{8}{15} h^2 L \right) \left(\frac{wL^2}{8h} \right) = - \frac{whL^3}{15EI_0} \\ \delta_{11} &= \frac{L}{AE} + \frac{8}{15} \frac{h^2 L}{EI_0}\end{aligned}$$

The tension in the tie is

$$X_1 = \frac{-\Delta_{1,0}}{\delta_{11}} = \frac{wL^2}{8h} \frac{1}{(1 + (15/8)(I_0/Ah^2))}$$

Using this value, we determine the moment at mid-span.

$$\begin{aligned}M\left(\frac{L}{2}\right) &= M_0 - hX_1 \\ &= \frac{wL^2}{8} \left\{ 1 - \frac{1}{(1 + (15/8)(I_0/Ah^2))} \right\} \\ M\left(\frac{L}{2}\right) &= \frac{wL^2}{8} \left\{ \frac{(15/8)(I_0/Ah^2)}{(1 + (15/8)(I_0/Ah^2))} \right\} = \frac{wL^2}{8} \left\{ \frac{1}{(1 + (8/15)(Ah^2/I_0))} \right\}\end{aligned}$$

Note that the effect of the tension tie is to introduce bending in the arch.

9.5 Application to Frame-Type Structures

Chapter 4 dealt with statically determinate frames. We focused mainly on three-hinge frames since this type of structure provides an efficient solution for enclosing a space. In this section, we analyze indeterminate framed with the Force Method. In the next Chapter, we apply the Displacement Method. The analytical results generated provide the basis for comparing the structural response of determinate vs. indeterminate frames under typical loadings.

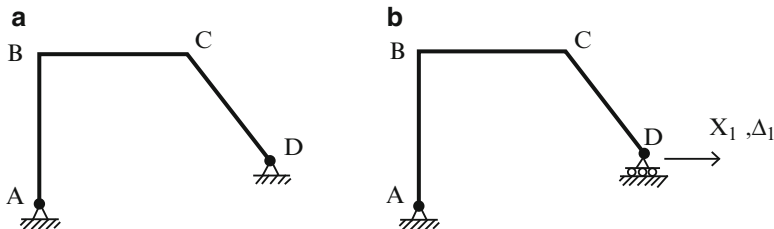


Fig. 9.31 (a) Actual structure. (b) Primary structure—redundant reaction

9.5.1 General Approach

We consider the arbitrary-shaped single bay frame structure shown in Fig. 9.31. The structure is indeterminate to the first degree. We select the horizontal reaction at the right support as the force redundant. The corresponding compatibility equation is

$$\Delta_{1,0} + \delta_{11}X_1 = \Delta_1$$

where Δ_1 is the horizontal support movement at D.

We compute the flexibility coefficients with the Principle of the Virtual Forces described in Sect. 4.6. The corresponding form for a plane frame specialized for negligible transverse deformation is given by (4.8)

$$d\delta P = \sum_{\text{members}} \int_s \left\{ \frac{M}{EI} \delta M + \frac{F}{AE} \delta F \right\} ds$$

Axial deformation is small for typical non-shallow frames, and therefore is usually neglected. The δ_{11} term is the horizontal displacement due to a horizontal unit load at D. This term depends on the geometry and member properties, not on the external loads, and therefore has to be computed only once. The $\Delta_{1,0}$ term is the horizontal displacement due to the external loading, and needs to be evaluated for each loading. Different loading conditions are treated by determining the corresponding values of $\Delta_{1,0}$. Given these displacement terms, one determines X_1 with

$$X_1 = -\frac{\Delta_{1,0}}{\delta_{11}}$$

Consider the frame shown in Fig. 9.32. Now there are three force redundant and three geometric compatibility conditions represented by the matrix equations,

$$\Delta_{1,0} + \delta X = \Delta_1$$

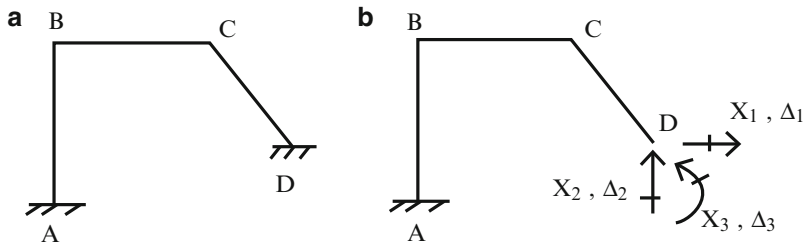


Fig. 9.32 (a) Actual structure. (b) Primary structure—redundant reactions

The flexibility matrix δ is independent of the loading, i.e., it is a property of the primary structure. Most of the computations effort is involved with computing δ and $\Delta_{1,0}$ numerically. The integration can be tedious. Sometimes numerical integration is used. However, one still has to generate the moment and axial force diagrams numerically.

If the structure is symmetrical, one can reduce the computational effort by working with simplified structural models and decomposing the loading into symmetrical and anti-symmetrical components. It is very useful for estimating in a qualitative sense, the structural response. We discussed this strategy in Chap. 3.

In what follows, we list results for different types of frames. Our primary objective is to show how these structures respond to typical loadings. We use moment diagrams and displacement profiles as the measure of the response.

9.5.2 Portal Frames

We consider the frame shown in Fig. 9.33a. We select the horizontal reaction at B as the force redundant.

The corresponding flexibility coefficient, δ_{11} , is determined with the Principle of Virtual Forces (see Chap. 4).

$$\delta_{11} = \frac{h_1^3}{3EI_1} + \frac{h_2^3}{3EI_3} + \frac{L}{3EI_2} \{ h_1^2 - h_2^2 + 3h_1h_2 \} \quad (9.40)$$

This coefficient applies for all loading. Considering the arbitrary gravity loading shown in Fig. 9.34, the expression for the displacement, $\Delta_{1,0}$, is determined in a similar way.

$$\Delta_{1,0} = -\frac{1}{EI_2} \left\{ h_1 P(L-a) \left[\frac{a^2}{2L} - \frac{L-a}{2} \right] + P \frac{h_2 - h_1}{L} \left[\left(1 - \frac{a}{L}\right) \frac{a^3}{3} - \frac{L^3}{3} - \frac{a^3}{6} + \frac{aL^2}{2} \right] \right\} \quad (9.41)$$

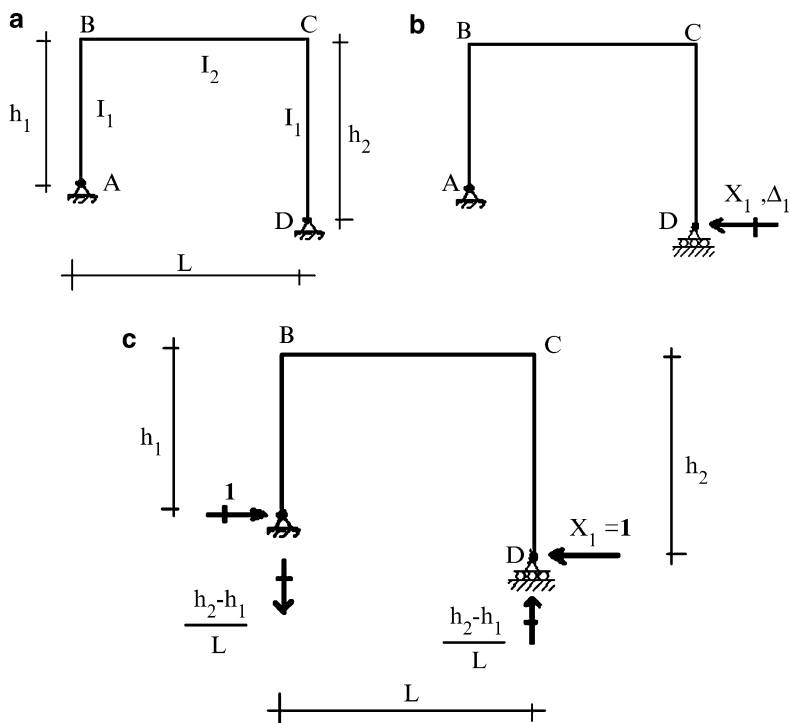


Fig. 9.33 Portal Frame. (a) Geometry. (b) Redundant. (c) Reactions due to $X_1 = 1$

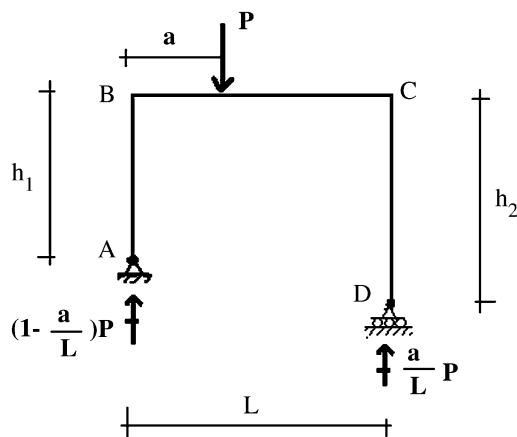


Fig. 9.34 Reactions—gravity loading

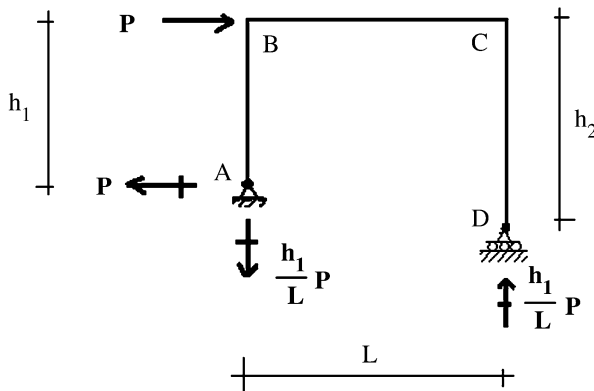


Fig. 9.35 Reactions—lateral loading

Lastly, we consider the lateral loading shown in Fig. 9.35. The displacement term due to loading is

$$\Delta_{1,0} = -\frac{1}{EI_1} \left\{ \frac{Ph_1^3}{3} \right\} + \frac{1}{EI_2} \left\{ \frac{Ph_1 L}{3} \left(\frac{h_2}{2} + h_1 \right) \right\} \quad (9.42)$$

When $h_2 = h_1 = h$ and $I_2 = I_1 = I$ these expressions simplify to

$$\begin{aligned} \delta_{11} &= \frac{2h^3}{3EI} + \frac{L}{EI}(h^2) \\ \Delta_{1,0}|_{\text{gravity}} &= -\frac{Ph}{2EI}(a)(L-a) \\ \Delta_{1,0}|_{\text{lateral}} &= -\frac{Ph^3}{3EI} - \frac{Ph^2L}{2EI} \end{aligned} \quad (9.43)$$

The corresponding bending moment diagrams for these two loading cases are shown in Fig. 9.36.

Gravity loading:

$$M_1 = hX_1$$

$$M_2 = a \left(1 - \frac{a}{L} \right) P - M_1$$

$$X_1 = \frac{PL(a/L)(1-(a/L))}{2h} \frac{1+(2/3)(h/L)}$$

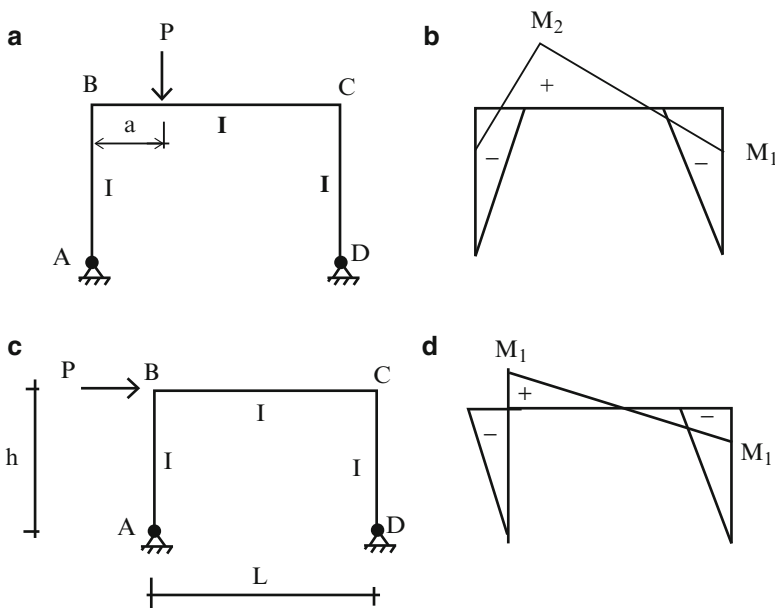


Fig. 9.36 (a) Gravity loading—two-hinge frame. (b) Moment diagram. (c) Lateral loading. (d) Moment diagram

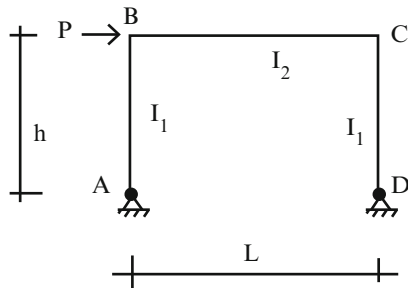


Fig. 9.37 Geometry of two-hinge portal frame

Lateral loading:

$$M_1 = hX_1$$

$$X_1 = \frac{P}{2}$$

9.5.2.1 Lateral-Loading Symmetrical Portal Frame

We consider first the two-hinged symmetrical frame shown in Fig. 9.37. This structure is indeterminate to the first degree. We decompose the loading into

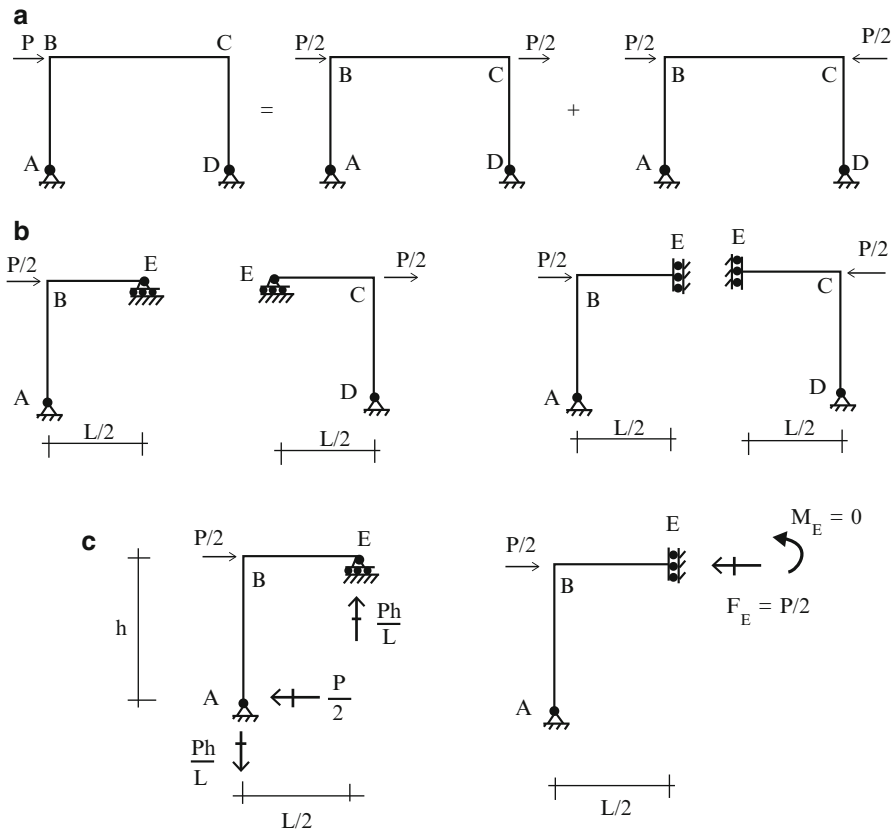


Fig. 9.38 Structural models. (a) Decomposition into anti-symmetrical and symmetrical loadings. (b) Symmetric and anti-symmetrical models. (c) Free body diagrams of anti-symmetric and symmetrical segments

symmetrical and anti-symmetrical components and generate the corresponding symmetrical and anti-symmetrical structural modes using the material presented in Sect. 3.7. These results are shown in Fig. 9.38b. Point E is at mid-span. The anti-symmetrical model is statically determinate since the bending moment at mid-span must equal zero for anti-symmetrical behavior (Fig. 9.38c).

The symmetrical loading introduces no bending in the structure, only axial force in member BE. The bending moment distribution due to the anti-symmetrical component is plotted in Fig. 9.39.

9.5.2.2 Gravity-Loading Symmetrical Portal Frame

We consider next the case of gravity loading applied to a two-hinged portal frame. Figure 9.40a defines the loading and geometry. Again, we decompose the loading and treat separately the two loading cases shown in Fig. 9.40b.

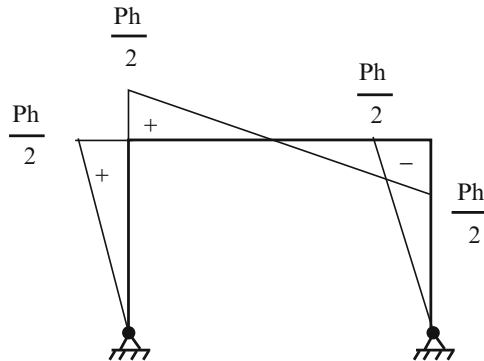


Fig. 9.39 Bending moment distribution due to the anti-symmetrical lateral loading

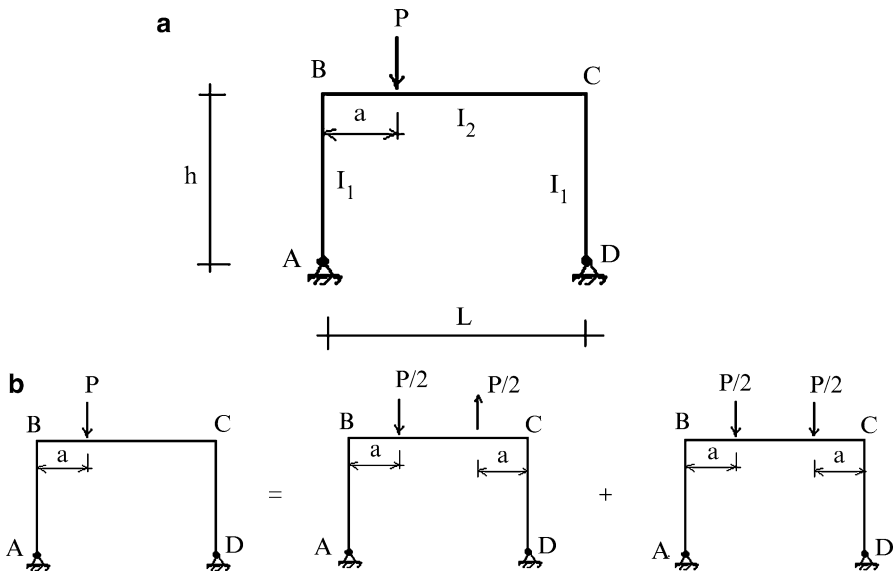


Fig. 9.40 (a) Two-hinge frame under gravity loading. (b) Decomposition of loading into symmetrical and anti-symmetrical components

Geometry and Loading

The anti-symmetrical model is statically determinate. Figure 9.41 shows the model, the corresponding free body diagram and the bending moment distribution.

The symmetrical model is statically indeterminate to one degree. We take the horizontal reaction at the right support as the force redundant, and work with the primary structure shown in Fig. 9.42.

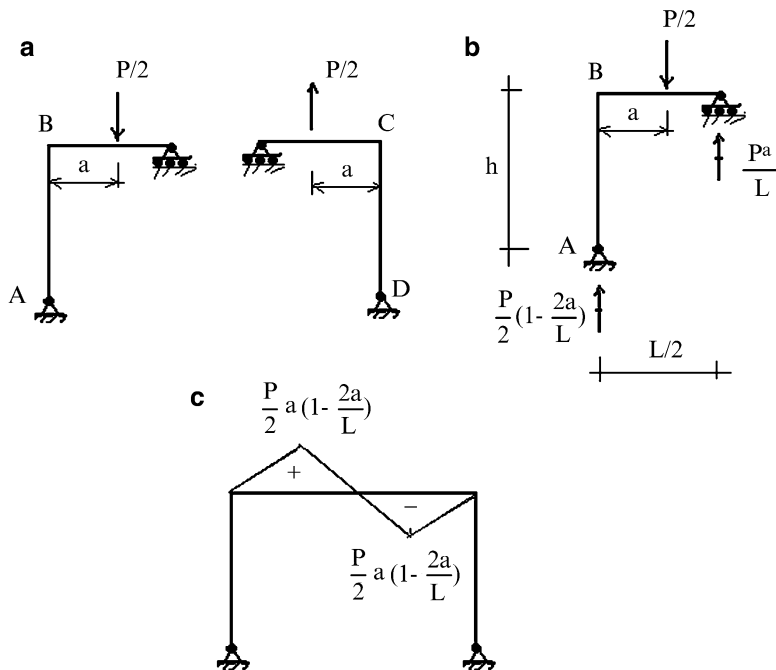


Fig. 9.41 (a) Anti-symmetrical model. (b) Free body diagram—anti-symmetrical segment. (c) Bending moment distribution—anti-symmetrical loading

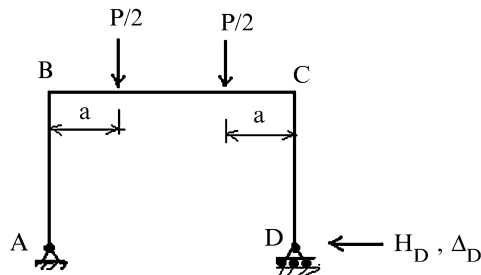


Fig. 9.42 Primary structure for two-hinge frame—symmetrical loading case

Assuming unyielding supports, the compatibility equation has the following form

$$\Delta_D = \Delta_{D,0} + \delta_{DD} H_D = 0$$

where $\Delta_{D,0}$ and δ_{DD} are the horizontal displacements at D due to the applied loading and a unit value of H_D . We use the Principle of Virtual Forces specialized for only bending deformation to evaluate these terms. The corresponding expressions are

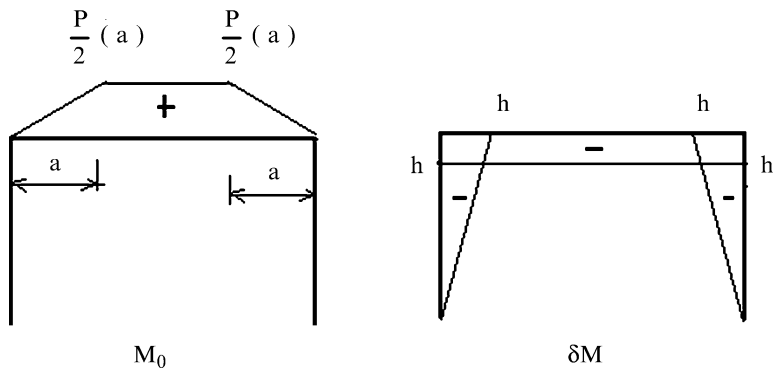


Fig. 9.43 Bending moment distributions—symmetrical loading—primary structure

$$\Delta_{D,0} = \int_S M_0 \delta M \frac{dS}{EI}$$

$$\delta_{DD} = \int_S (\delta M)^2 \frac{dS}{EI} \quad (9.44)$$

where M_0 is the moment due to the applied loading and δM is the moment due to a unit value of H_D . These moment distributions are plotted in Fig. 9.43.

Evaluating the integrals leads to:

$$\Delta_{B,0} = -\frac{P}{2} \frac{ha}{EI_2} (L-a) \quad (9.45)$$

$$\delta_{BB} = \frac{2h^3}{3EI_1} + \frac{h^2L}{EI_2}$$

Finally, the horizontal reaction at support D is

$$H_D = P \frac{a(L-a)}{2hL} \left[\frac{1}{1 + (2/3)(r_g/r_c)} \right] \quad (9.46)$$

where

$$r_c = \frac{I_1}{h} \quad r_g = \frac{I_2}{L} \quad (9.47)$$

are the relative stiffness factors for the column and girder members.

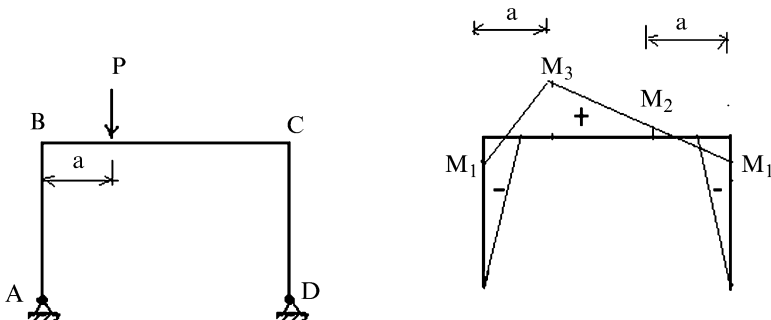


Fig. 9.44 Final bending moment distribution

Combining the results for the symmetrical and anti-symmetrical loadings results in the net bending moment distribution plotted in Fig. 9.44. The peak moments are defined by (9.48).

$$\begin{aligned} M_1 &= -\frac{Pa}{2} \left(1 - \frac{a}{L}\right) \frac{1}{1 + (2/3)(r_g/r_c)} \\ M_2 &= +\frac{Pa}{2} \left[\frac{(a/L) + (2/3)(r_g/r_c)}{1 + (2/3)(r_g/r_c)} \right] - \frac{Pa}{2} \left(1 - \frac{2a}{L}\right) \\ M_3 &= +\frac{Pa}{2} \left[\frac{(a/L) + (2/3)(r_g/r_c)}{1 + (2/3)(r_g/r_c)} \right] + \frac{Pa}{2} \left(1 - \frac{2a}{L}\right) \end{aligned} \quad (9.48)$$

Example 9.15 Two-hinge symmetrical frame—uniform gravity load

Given: The frame and loading defined in Fig. E9.15a.

Determine: The bending moment distribution.

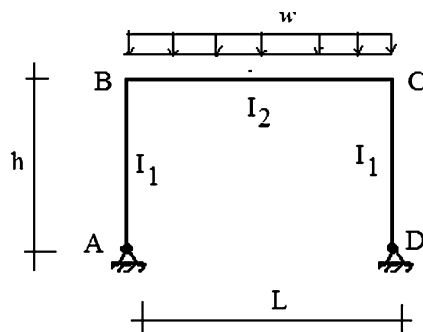
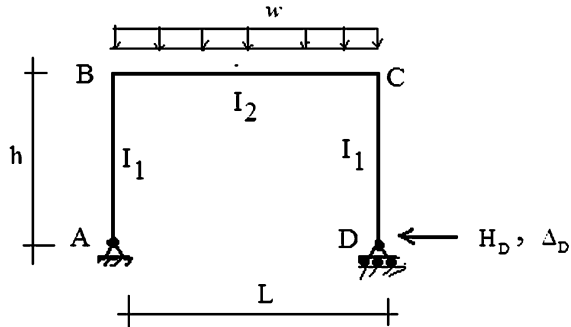


Fig. E9.15a

Fig. E9.15b

Solution: We work with the primary structure shown in Fig. E9.15b. We only need to determine the $\Delta_{D,0}$ term corresponding to the uniform loading since the δ_{DD} term is independent of the applied loading. The solution for H_D is

$$H_D = \frac{wL^2}{12h} \frac{1}{1 + (2/3)(r_g/r_c)}$$

where

$$r_g = \frac{I_2}{L}$$

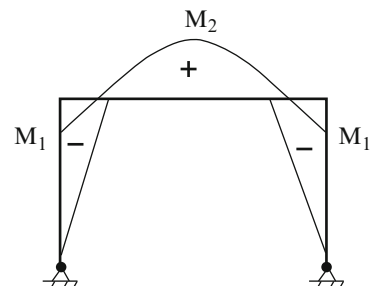
$$r_c = \frac{I_1}{h}$$

Figure E9.15c shows the bending moment distribution. The peak values are

$$M_1 = \frac{wL^2}{12} \frac{1}{1 + (2/3)(r_g/r_c)}$$

$$M_2 = \frac{wL^2}{8} \left[1 - \frac{2}{3} \frac{1}{1 + (2/3)(r_g/r_c)} \right]$$

When members AB and CD are very stiff, $r_c \rightarrow \infty$ and $H_D \rightarrow wL^2/12h$. In this case, the moment at B approaches $wL^2/12$ which is the fixed end moment for member BC.

**Fig. E9.15c** Bending moment distribution

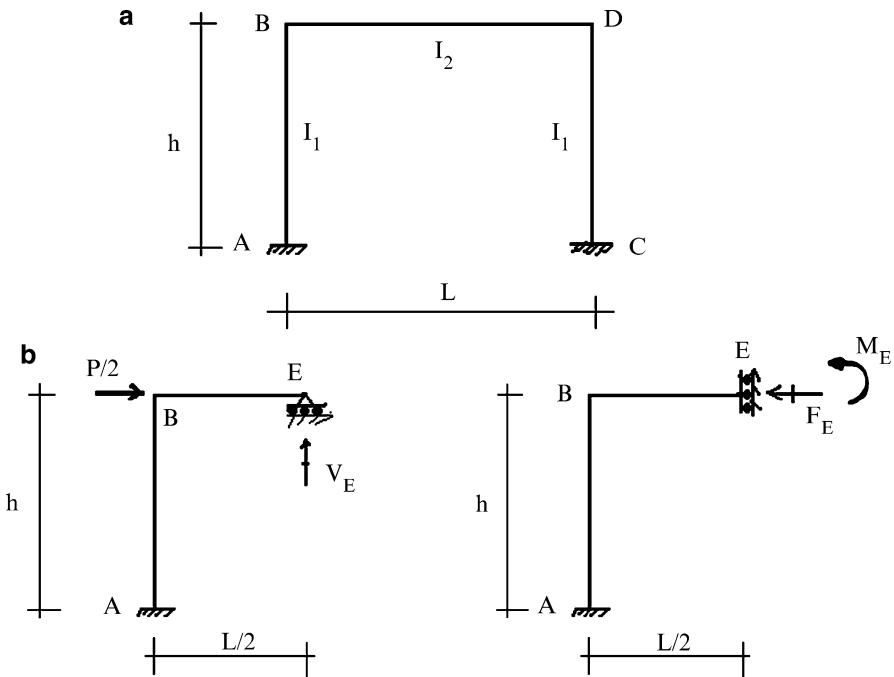


Fig. 9.45 (a) Geometry. (b) Symmetrical and anti-symmetrical primary structures

9.5.2.3 Symmetrical Portal Frames with Fixed Supports

We consider the symmetrical frame shown in Fig. 9.45. Because the structure is symmetrical, we consider the loading to consist of symmetrical and anti-symmetrical components. The structure is indeterminate to the second degree for symmetrical loading and to the first degree for anti-symmetrical loading (there is zero moment at mid-span which is equivalent to a hinge at that point). Figure 9.45b defines the primary structures corresponding to these two loading cases.

Evaluating the various displacement terms for the anti-symmetrical loading, one obtains:

$$\Delta_{E,0} = -\frac{PLh^2}{8EI_1}$$

$$\delta_{EE} = \frac{L^3}{24EI_2} + \frac{L^2h}{4EI_1}$$

$$V_E = \frac{-\Delta_{E,0}}{\delta_{EE}} = \left(\frac{Ph}{2L}\right) \frac{1}{(1 + (1/6)(L/I_2)(I_1/h))}$$

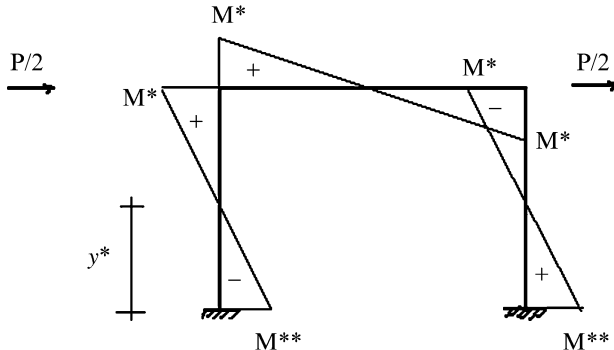


Fig. 9.46 Bending moment distribution—anti-symmetric loading

The moment diagrams are plotted in Fig. 9.46. The peak values are

$$\begin{aligned} M^* &= \pm \frac{Ph}{4} \frac{1}{1 + (1/6)(r_c/r_g)} \\ M^{**} &= \pm \frac{Ph}{2} \left[-1 + \frac{1}{2} \frac{1}{(1 + (1/6)(r_c/r_g))} \right] \\ r_c &= \frac{I_1}{h} \quad r_g = \frac{I_2}{L} \end{aligned} \quad (9.49)$$

There are inflection points located in the columns at y^* units up from the base where

$$y^* = h \left[1 - \frac{1}{2} \frac{1}{1 + (1/6)(r_c/r_g)} \right] \quad (9.50)$$

When the girder is very stiff relative to the column, $r_c/r_g \rightarrow 0$ and $y^* \rightarrow h/2$. A reasonable approximation for y^* for typical column and girder properties is $\approx 0.6h$.

Figure 9.47 shows the corresponding bending moment distribution for the two-hinged portal frame. We note that the peak positive moment is reduced approximately 50% when the supports are fixed.

We consider next the case where the girder is uniformly loaded. We skip the intermediate details and just list the end moments for member AB and the moment at mid-span (Fig. 9.48).

$$\begin{aligned} M_{BA} &= -\frac{wL^2}{12} \frac{1}{1 + (1/2)(r_g/r_c)} \\ M_{AB} &= \frac{1}{2} M_{BA} \\ M_E &= \frac{wL^2}{8} \left[1 - \frac{2}{3} \frac{1}{1 + (1/2)(r_g/r_c)} \right] \end{aligned} \quad (9.51)$$

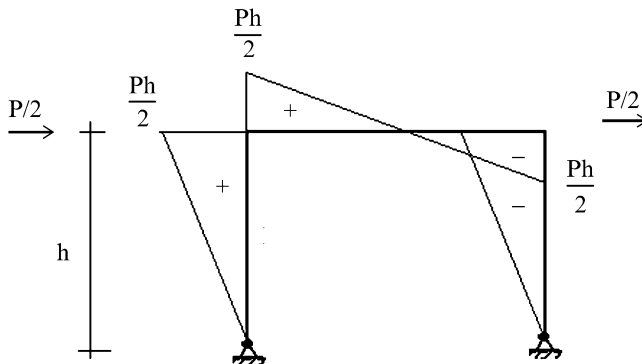


Fig. 9.47 Moment distribution for two-hinged frame

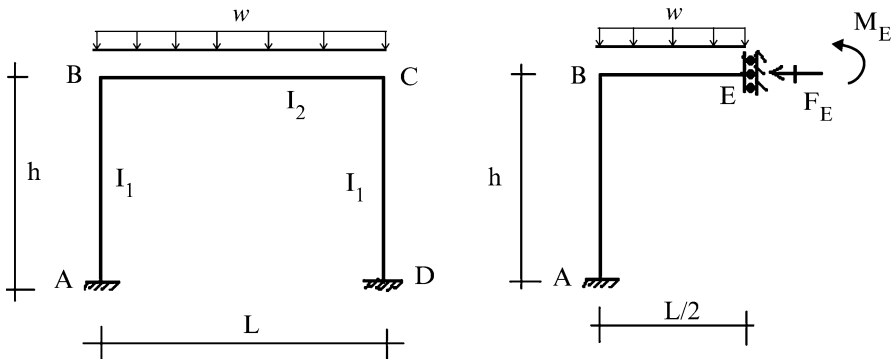


Fig. 9.48

The bending moment distribution is plotted in Fig. 9.49. The solution for the two-hinged case is shown in Fig. 9.50. These results show that the bending moment distribution is relatively insensitive to end fixity of the base.

$$M^+ = M_E$$

$$M^- = M_{BA} \frac{1 + (1/2)(r_g/r_c)}{1 + (2/3)(r_g/r_c)} = -\frac{wL^2}{12} \frac{1}{1 + (2/3)(r_g/r_c)} \quad (9.52)$$

9.5.3 Pitched Roof Frames

We consider next a class of portal frames where the roof is pitched, as shown in Fig. 9.51a. We choose to work with the primary structure defined in Fig. 9.51b.

Fig. 9.49 Bending moment distribution—symmetrical loading—fixed supports

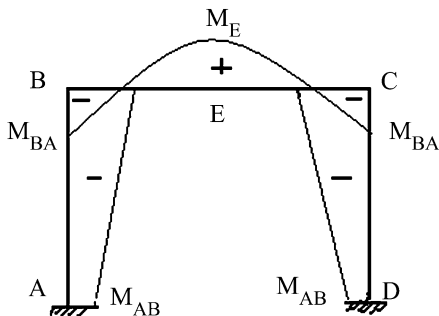
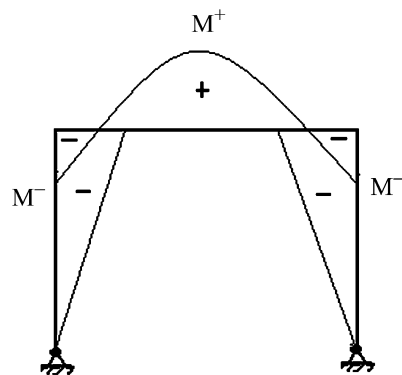


Fig. 9.50 Bending moment distribution—symmetrical loading—hinged supports



We suppose the structure is subjected to a uniform load per horizontal projection on members BC and CD. The bending moment distribution in the primary structure due to the applied loading, M_0 , is parabolic with a peak value at C (Fig. 9.52). Taking $H_E = 1$ leads to the bending moment distribution shown in Fig. 9.53. It is composed of linear segments.

Assuming the supports are unyielding, the flexibility coefficients are

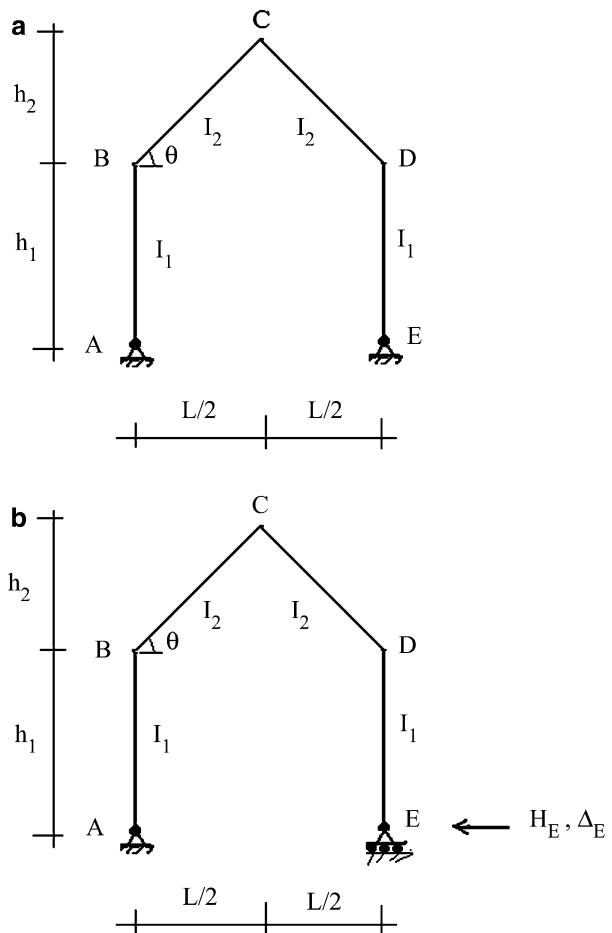
$$\Delta_{E,0} = -\frac{wL^3}{12 \cos \theta} \left\{ h_1 + \frac{5}{8} h_2 \right\} \frac{1}{EI_2}$$

$$\delta_{EE} = \frac{2}{3} \frac{h_1^3}{EI_1} + \frac{L}{EI_2 \cos \theta} \left\{ h_1^2 + h_1 h_2 + \frac{h_2^2}{3} \right\} \quad (9.53)$$

We define the relative stiffness factors as

$$r_1 = \frac{I_1}{h_1} \quad r_2* = \frac{I_2}{L*} \quad (9.54)$$

Fig. 9.51 (a) Pitched roof frame—definition sketch.
 (b) Primary structure—
 redundant reaction



where L^* is the length of the inclined roof members BC and CD.

$$L^* = \frac{L}{2\cos\theta} \quad (9.55)$$

Using this notation, the expression for the horizontal reaction at E takes the form

$$H_E = \frac{wL^2}{12h_1} \frac{1 + (5/8)(h_2/h_1)}{(1/3)(r_2*/r_1) + 1 + (h_2/h_1) + (1/3)(h_2/h_1)^2} \quad (9.56)$$

The total bending moment distribution is plotted in Fig. 9.54. Equation (9.57) contains the expressions for the peak values.

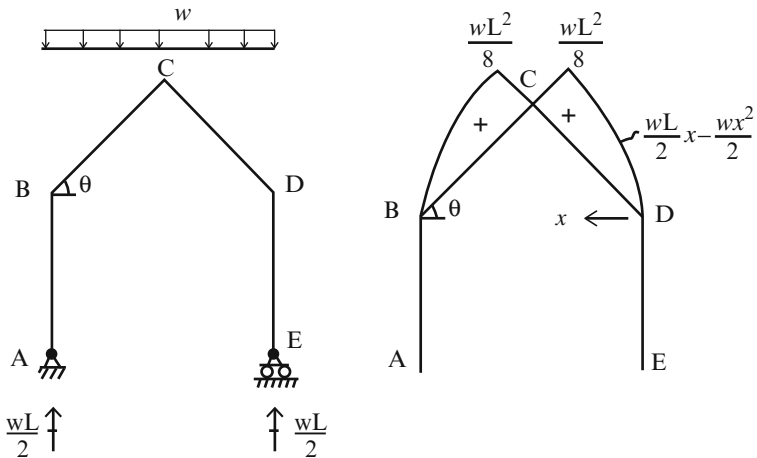


Fig. 9.52 Bending moment distribution for applied loading, M_0

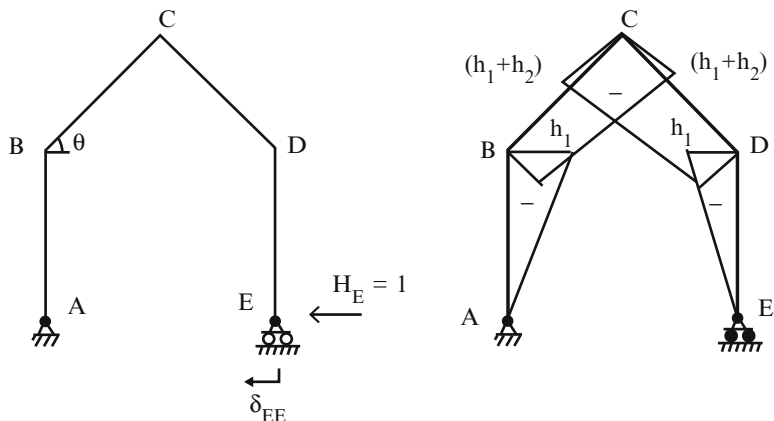


Fig. 9.53 Bending moment distribution for $H_E = 1$

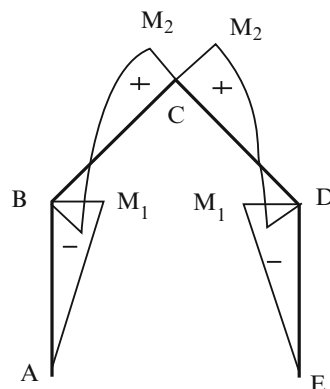


Fig. 9.54 Distribution of total bending moments

$$\begin{aligned} M_1 &= -\frac{wL^2}{12} a_1 \\ M_2 &= +\frac{wL^2}{8} a_2 \end{aligned} \quad (9.57)$$

where

$$\begin{aligned} a_1 &= \frac{1 + (5/8)(h_2/h_1)}{(1/3)(r_2^*/r_1) + 1 + (h_2/h_1) + (1/3)(h_2/h_1)^2} \\ a_2 &= 1 - \frac{2}{3} \left(1 + \frac{h_2}{h_1} \right) a_1 \end{aligned} \quad (9.58)$$

These values depend on the ratio of heights h_2/h_1 and relative stiffness, r_2^*/r_1 . One sets $h_2 = 0$ and $r_2^* = 2r_2$ to obtain the corresponding two-hinged portal frame solution. For convenience, we list here the relevant solution for the three-hinge case, with the notation modified to be consistent with the notation used in this section. The corresponding moment distributions are shown in Fig. 9.55.

The peak negative and positive moments are

$$\begin{aligned} M_1 &= \frac{wL^2}{8} \frac{h_1}{(h_1 + h_2)} \\ M_2 &= \frac{wL^2}{8} \left\{ \frac{1}{4} - \frac{1}{2} \frac{h_1}{h_1 + h_2} + \frac{1}{4} \left(\frac{h_1}{h_1 + h_2} \right)^2 \right\} \end{aligned} \quad (9.59)$$

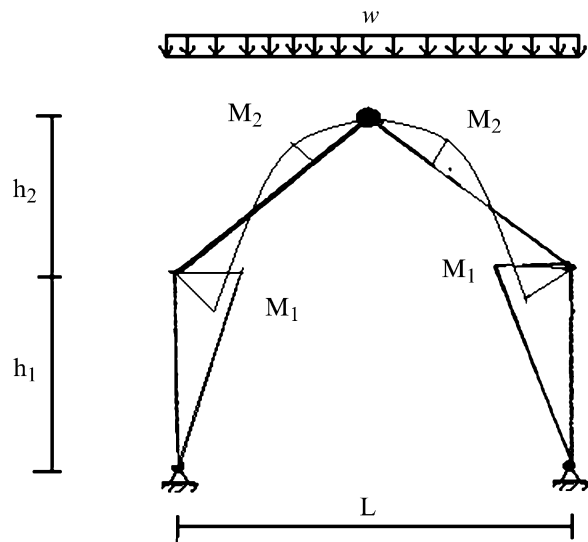


Fig. 9.55 Three-hinge solution

In order to compare the solutions, we assume $r_2^* = r_1$, and $h_2 = h_1$ in the definition equations for the peak moments. The resulting peak values are

Three-hinge case (9.59):

$$M_1 = -\frac{wL^2}{8} \left(\frac{1}{2}\right)$$

$$M_2 = +\frac{wL^2}{8} \left(\frac{1}{16}\right)$$

Two-hinge case (9.57):

$$M_1 = -\frac{wL^2}{8} \left(\frac{13}{32}\right) = -\frac{wL^2}{8} (0.406)$$

$$M_2 = +\frac{wL^2}{8} \left(\frac{3}{16}\right)$$

We see that the peak negative moment is reduced by approximately 20% when the structure is reduced to a two-hinged frame. However, the positive moment is increased by a factor of 3.

9.6 Indeterminate Trusses

Examples of indeterminate truss structures are shown in Fig. 9.56. One can choose a primary structure by taking either reactions or member forces or a combination as the force redundants. When working with member forces, one visualizes the member as being cut and works with the relative displacement of the adjacent faces. Continuity requires that the net relative displacement is zero.

We illustrate the Force Method procedure for the three member truss shown in Fig. 9.57a. The truss is indeterminate to the first degree. The force in member BC is taken as the force redundant and Δ is the relative displacement together at the end sections. Two deflection computation are required, one due to the external loads and the other due to $X = 1$. We use the Principle of Virtual Forces discussed in Sect. 2.3.4 for these computations. Results are summarized below

$$\begin{aligned} \Delta_{1,0} &= \sum F_0 \delta F \frac{L}{AE} \\ &= -\frac{1}{2\sin\theta} \left(\frac{P_y}{2\sin\theta} + \frac{P_x}{2\cos\theta} \right) \frac{L_1}{A_1 E} + \left(-\frac{1}{2\sin\theta} \right) \left(\frac{P_y}{2\sin\theta} - \frac{P_x}{2\cos\theta} \right) \frac{L_1}{A_1 E} \\ &= -\frac{P_y}{2\sin^2\theta} \frac{L_1}{A_1 E} \end{aligned}$$

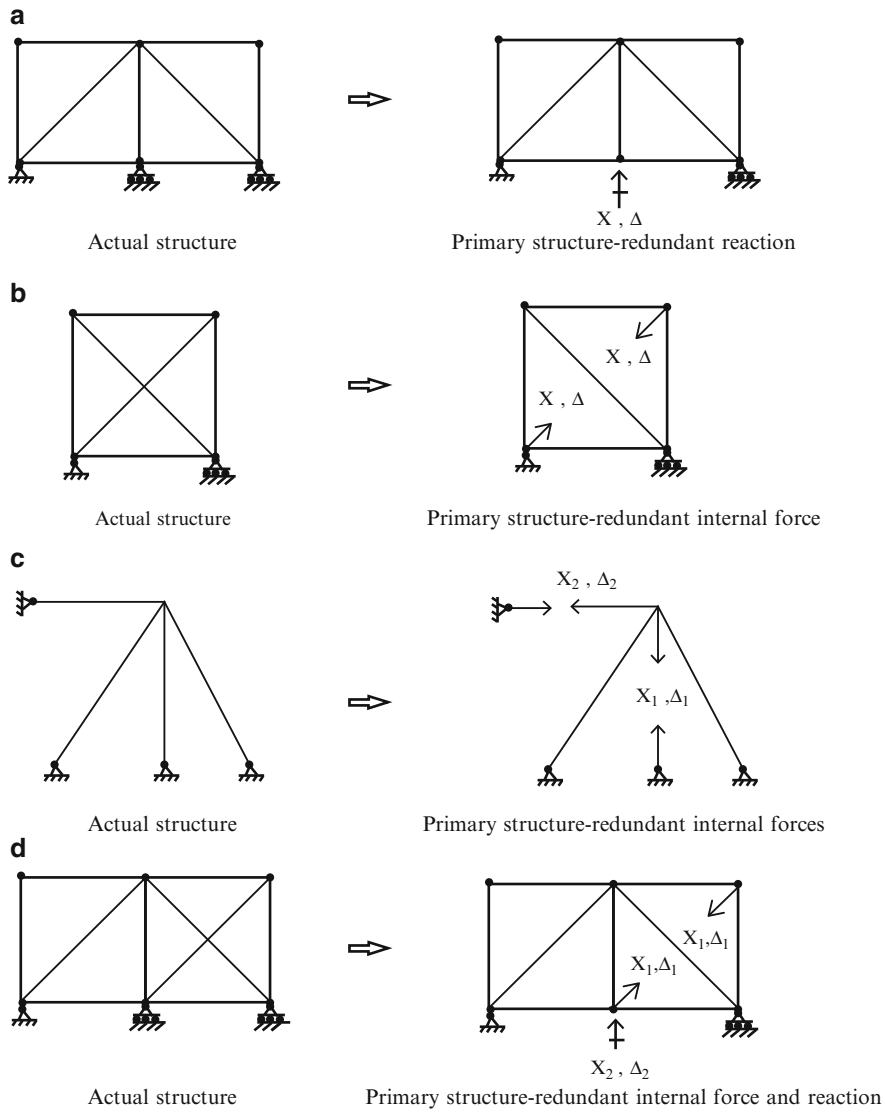


Fig. 9.56 Examples of statically indeterminate trusses

$$\begin{aligned}\delta_{11} &= \sum (\delta F)^2 \frac{L}{AE} \\ &= \frac{1}{4\sin^2\theta A_1 E} \frac{L_1}{A_1 E} + \frac{L_1 \sin\theta}{A_2 E} + \frac{1}{4\sin^2\theta A_1 E} \frac{L_1}{A_1 E} = \frac{1}{2\sin^2\theta A_1 E} \frac{L_1}{A_1 E} + \frac{L_1 \sin\theta}{A_2 E}\end{aligned}$$

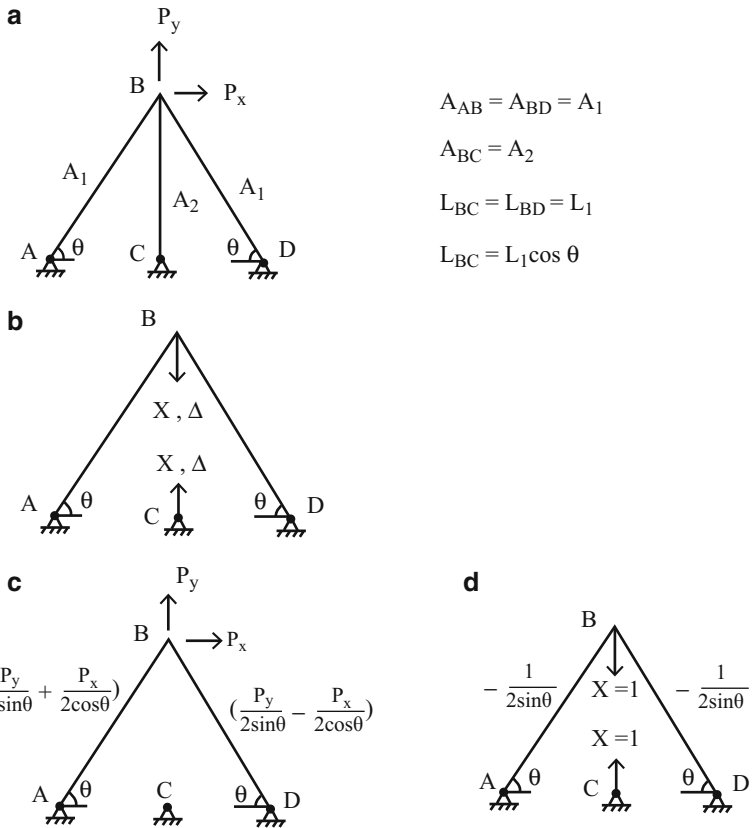


Fig. 9.57 (a) Three member truss. (b) Primary structure—redundant internal force. (c) F_0 . (d) δF ($X = 1$)

Enforcing compatibility leads to

$$\begin{aligned}
 F_{BC} = X &= -\frac{\Delta_{1,0}}{\delta_{11}} = \frac{(P_y/2\sin^2\theta)(L_1/A_1E)}{(1/2\sin^2\theta)(L_1/A_1E) + (L_1\sin\theta/A_2E)} \\
 &= P_y \frac{(A_2/\sin\theta)}{(A_2/\sin\theta) + 2A_1\sin^2\theta}
 \end{aligned} \tag{9.60}$$

Lastly, the remaining forces are determined by superimposing the individual solutions.

$$F = F_0 + \delta F X$$

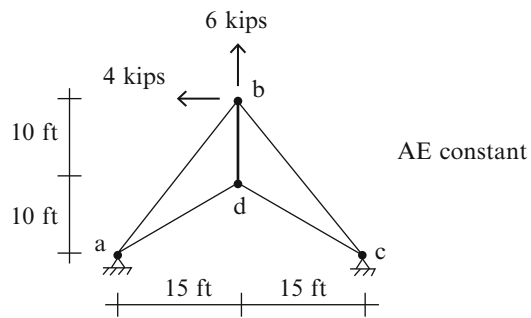
$$\begin{aligned}
 F_{AB} &= \frac{P_x}{2\cos\theta} + P_y \left\{ \frac{A_1\sin\theta}{(A_2/\sin\theta) + 2A_1\sin^2\theta} \right\} \\
 F_{DB} &= -\frac{P_x}{2\cos\theta} + P_y \left\{ \frac{A_1\sin\theta}{(A_2/\sin\theta) + 2A_1\sin^2\theta} \right\}
 \end{aligned} \tag{9.61}$$

As expected for indeterminate structures, the internal force distribution depends on the relative stiffness of the members. When A_2 is very large in comparison to A_1 , P_y is essentially carried by member BC. Conversely, if A_2 is small in comparison to A_1 , member BC carries essentially none of P_y .

Example 9.16

Given: The indeterminate truss shown in Fig. E9.16a. Assume AE is constant, $A = 2 \text{ in.}^2$, and $E = 29,000 \text{ ksi}$.

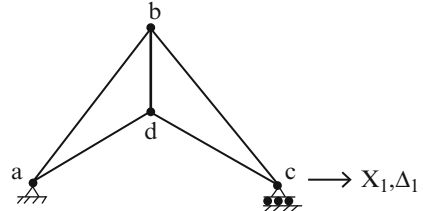
Fig. E9.16a



Determine: The member forces.

Solution: The truss is externally indeterminate to the first degree. The horizontal component of the reaction at C is taken as the force redundant (Fig. E9.16b).

Fig. E9.16b Primary structure—redundant reaction



We apply the geometric compatibility equation to this truss,

$$\Delta_{1,0} + \delta_{11}X_1 = 0$$

where

$$\Delta_{1,0} = \sum F_0 \delta F \frac{L}{AE}$$

$$\delta_{11} = \sum (\delta F)^2 \frac{L}{AE}$$

The corresponding forces are listed below (Figs. E9.16c, d).

Fig. E9.16c F_0

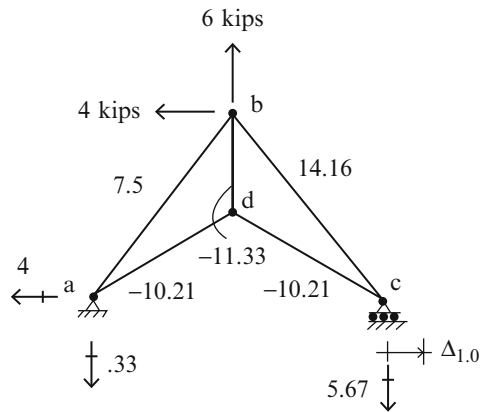
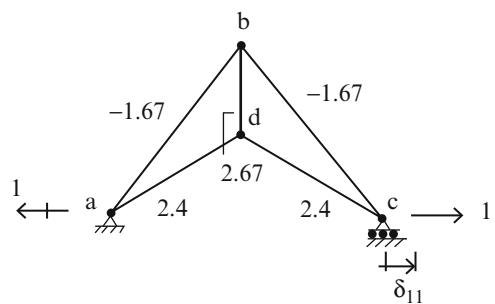


Fig. E9.16d δF ($x_1 = 1$)



Member	L (in.)	A (in. ²)	$\frac{L}{A}$	F_0	δF	$(\delta F)^2 \frac{L}{AE}$	$F_0 \delta F \frac{L}{AE}$
ab	300	2	150	7.5	-1.67	418.3/E	-1,878.7/E
bc	300	2	150	14.16	-1.67	418.3/E	-3,547/E
cd	216.3	2	108.2	-10.21	2.4	625.1/E	-2,656
da	216.3	2	108.2	-10.21	2.4	625.1/E	-2,656
bd	120	2	60	-11.33	2.67	422.7/E	-1,815/E
\sum						2,509.5/E	-12,552.7/E

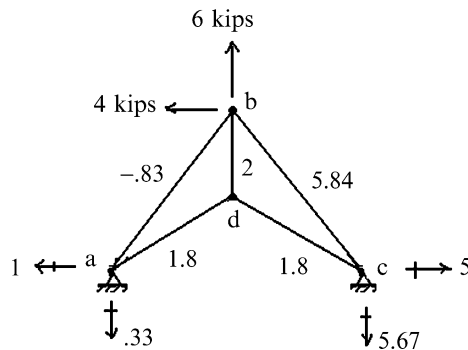
Inserting this data in the compatibility equation leads to

$$X_1 = -\frac{\Delta_{1,0}}{\delta_{11}} = \frac{1,2552.7}{2,509.5} = 5 \rightarrow$$

Then, the forces are determined by superimposing the individual solutions

$$F = F_0 + \delta F X_1$$

The final member forces and the reactions are listed below:



Example 9.17

Given: The indeterminate truss shown in Fig. E9.17a.

Determine: The member forces. Assume AE is constant, $A = 200 \text{ mm}^2$, and $E = 200 \text{ GPa}$.

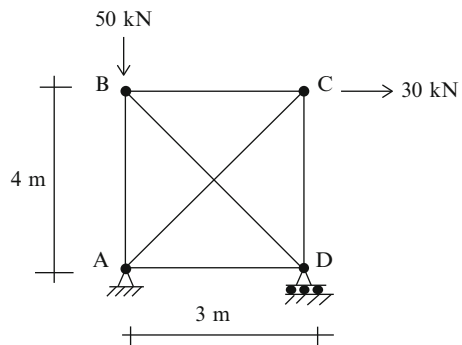
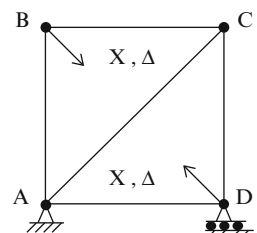


Fig. E9.17a

Solution: The truss is internally indeterminate to the first degree. The force in member BD is taken as the force redundant (Fig. E9.17b).

Fig. E9.17b Primary structure—internal force redundant



We apply the geometric compatibility equation to this truss,

$$\Delta_{1,0} + \delta_{11}X_1 = 0$$

where

$$\Delta_{1,0} = \sum F_0 \delta F \frac{L}{AE}$$

$$\delta_{11} = \sum (\delta F)^2 \frac{L}{AE}$$

The corresponding forces are listed below (Figs. E9.17c, d).

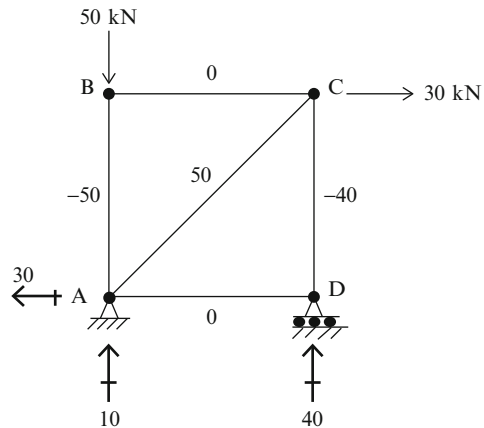


Fig. E9.17c F_0

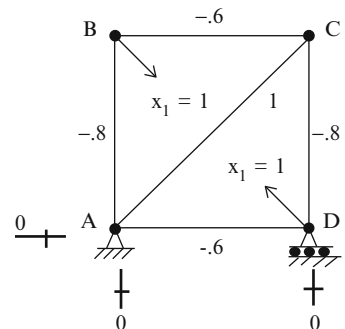


Fig. E9.17d δF ($x_1 = 1$)

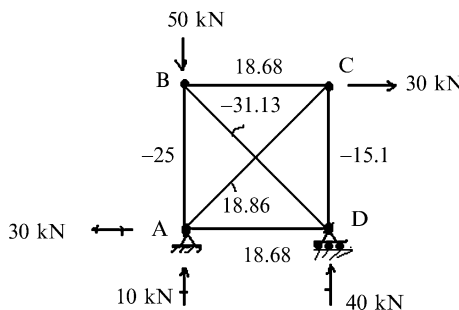
Member	L (mm)	A (mm^2)	$\frac{L}{A}$	F_0	δF	$(\delta F)^2(L/AE)$	$F_0 \delta F (L/AE)$
AB	4,000	200	20	-50	-0.8	12.8	800
BC	3,000	200	15	0	-0.6	5.4	0
CD	4,000	200	20	-40	-0.8	12.8	640
DA	3,000	200	15	0	-0.6	5.4	0
BD	5,000	200	25	0	1	25	0
AC	5,000	200	25	50	1	25	1,250
					\sum	$86.4/E$	$2,690/E$

Enforcing comparability leads to

$$X_1 = F_{BD} = -\frac{\Delta_{1,0}}{\delta_{11}} = -\frac{2,690}{86.4} = -31.13$$

$$\therefore F_{BD} = 31.13 \text{ kN compression}$$

The final member forces and the reactions are listed below.



9.7 Summary

9.7.1 Objectives

- The primary objective of this chapter is to present the Force Method, a procedure for analyzing statically indeterminate structures that works with force quantities as the unknown variables.
- Another objective is to use the Force Method to develop analytical solutions which are useful for identifying the key parameters that control the response and for conducting parameter sensitivity studies.

9.7.2 Key Factors and Concepts

- The force method is restricted to linear elastic behavior.
- The first step is to reduce the structure to a statically determinate structure by either removing a sufficient number of redundant restraints or inserting force releases at internal points. The resulting determinate structure is called the primary structure.
- Next one applies the external loading to the primary structure and determines the resulting displacements at the points where the restraints were removed.
- For each redundant force, the displacements produced by a unit force acting on the primary structure are evaluated.
- Lastly, the redundant forces are scaled such that the total displacement at each constraint point is equal to the actual displacement. This requirement is expressed as

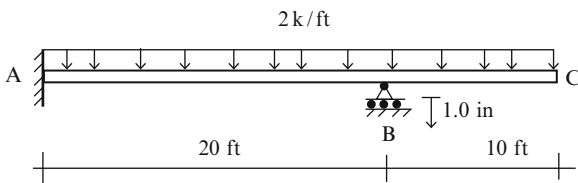
$$\Delta|_{\text{actual}} = \Delta|_{\text{loading}} + \sum_{\text{redundant forces}} (\delta_{\text{unitforce}})F$$

where the various terms are displacements at the constraint points. One establishes a separate equation for each constraint point. Note that all calculations are carried out on the primary structure.

9.8 Problems

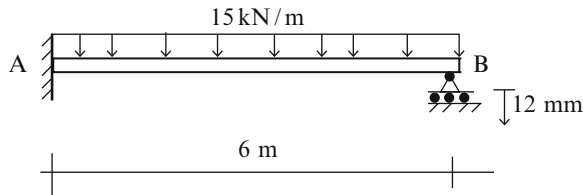
Problem 9.1

Determine the vertical reaction at B. Take $E = 29,000$ ksi and $I = 200$ in.⁴



Problem 9.2

Determine the vertical reaction at B. Take $E = 200 \text{ GPa}$ and $I = 80(10)^6 \text{ mm}^4$.

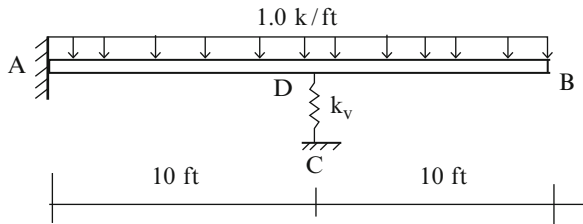
**Problem 9.3**

Determine the force in spring CD.

$$k_v = 60 \text{ kip/in.}$$

$$E = 29,000 \text{ ksi}$$

$$I = 200 \text{ in.}^4$$

**Problem 9.4**

Given the following properties and loadings, determine the reactions.

$$P = 40 \text{ kN}$$

$$w = 20 \text{ kN/m}$$

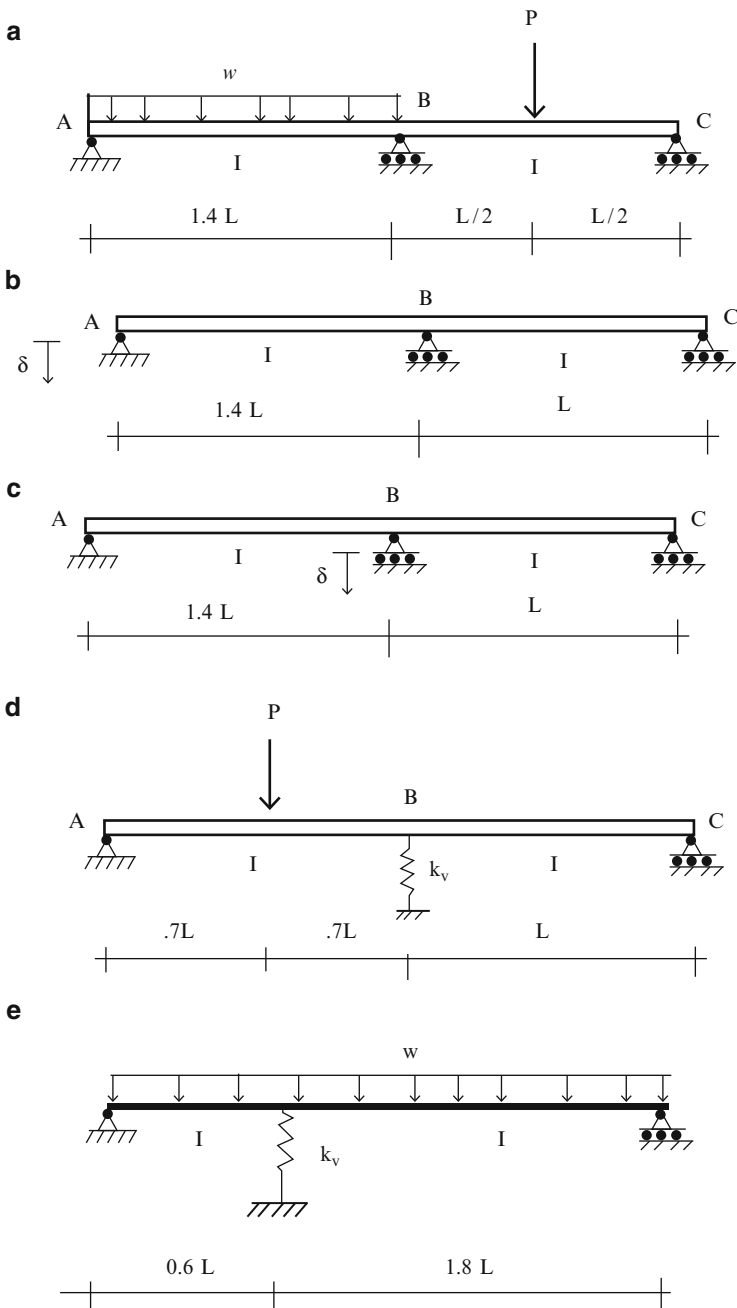
$$L = 5 \text{ m}$$

$$E = 200 \text{ GPa}$$

$$I = 170(10)^6 \text{ mm}^4$$

$$k_v = 40 \text{ kN/mm}$$

$$\delta = 20 \text{ mm}$$



Problem 9.5

Use the force method to determine the reaction at B caused by:

1. The distributed load shown
2. The support settlement at B

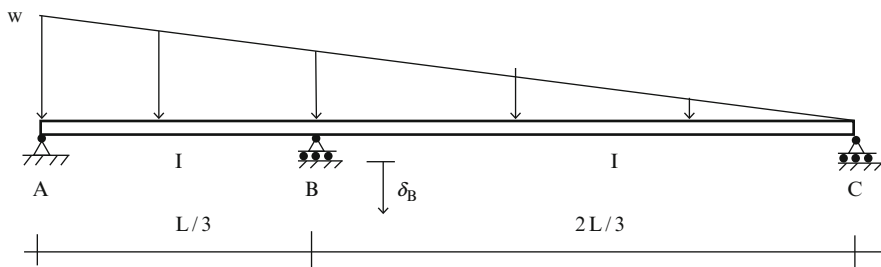
$$I = 400 \text{ in.}^4$$

$$L = 54 \text{ ft}$$

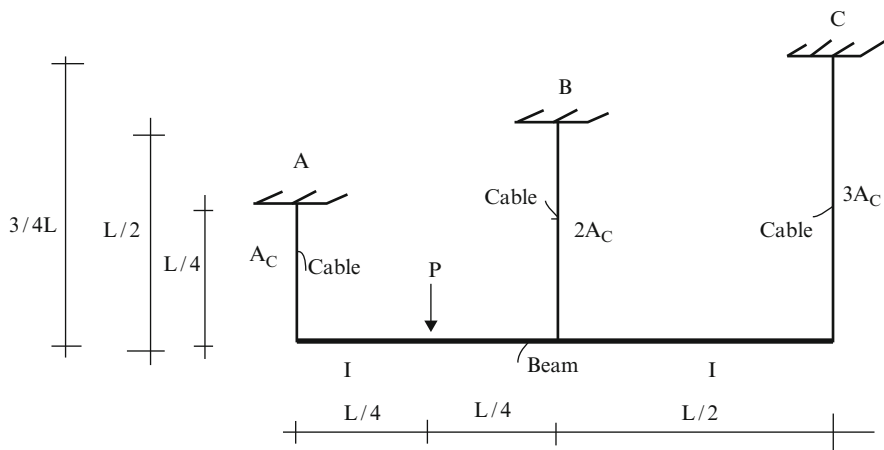
$$w = 2.1 \text{ kip/ft}$$

$$\delta_B = 1.2 \text{ in. } \downarrow$$

$$E = 29,000 \text{ ksi}$$

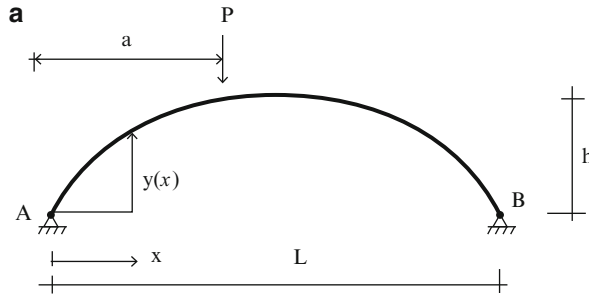
**Problem 9.6**

Use the force method to determine the forces in the cables. Assume beam is rigid. $A_C = 1,200 \text{ mm}^2$, $L = 9 \text{ m}$, $P = 40 \text{ kN}$, and $E = 200 \text{ GPa}$.



Problem 9.7

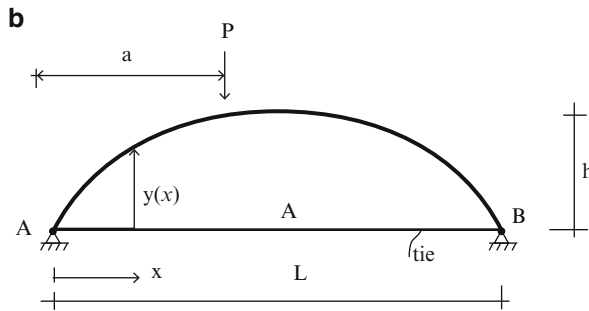
Consider the parabolic arch shown below. Assume the arch is non-shallow, i.e., h/L is order of $(1/2)$.



$$y = 4h \left(\frac{x}{L} - \left(\frac{x}{L} \right)^2 \right)$$

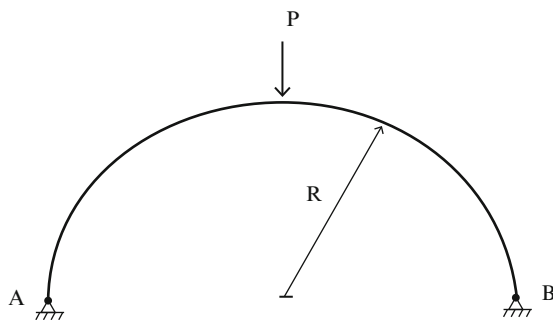
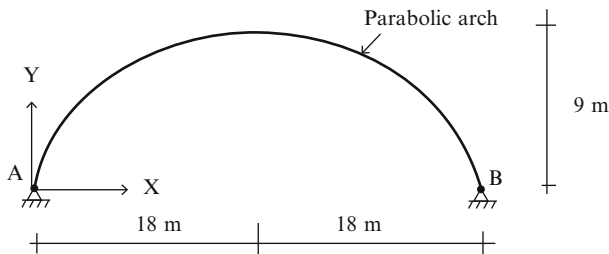
$$I = \frac{I_o}{\cos \theta}$$

- (a) Determine the horizontal reaction at B due to the concentrated load.
- (b) Utilize the results of part (a) to obtain an analytical expression for the horizontal reaction due to a distributed loading, $w(x)$.
- (c) Specialize (b) for a uniform loading, $w(x) = w_0$.
- (d) Suppose the horizontal support at B is replaced by a member extending from A to B. Repeat part (a).



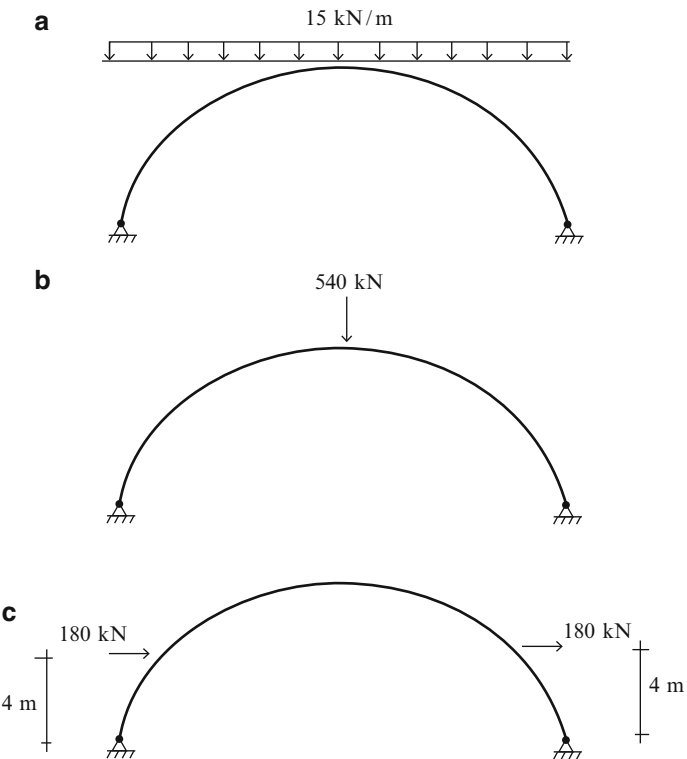
Problem 9.8

Consider the semicircular arch shown below. Determine the distribution of the axial and shear forces and the bending moment. The cross-section properties are constant.

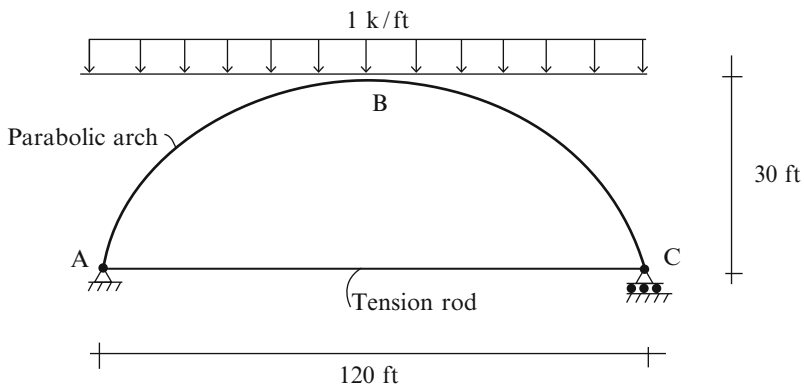
**Problem 9.9**

Use a Computer software system to determine the bending moment distribution and deflected shape produced by the following loadings.

Take $A = 20,000 \text{ mm}^2$, $I = 400(10)^6 \text{ mm}^4$ and $E = 200 \text{ GPa}$



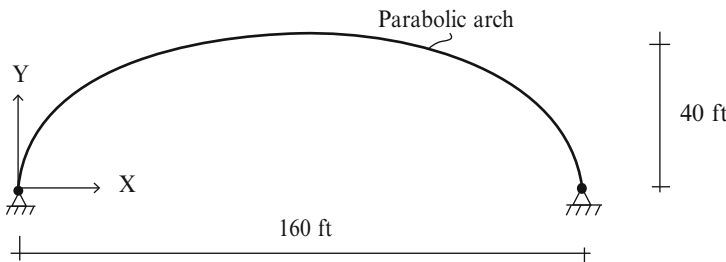
Problem 9.10



$$A = 30 \text{ in.}^2 \quad I = 1,000 \text{ in.}^4 \quad E = 29,000 \text{ ksi}$$

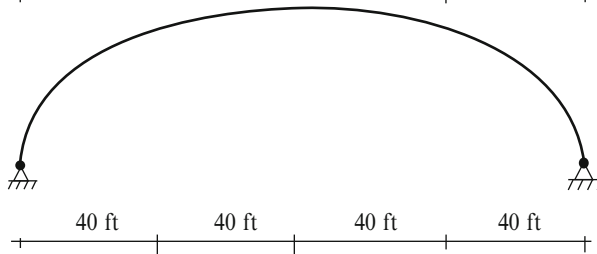
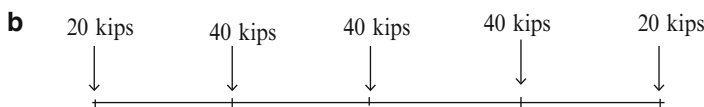
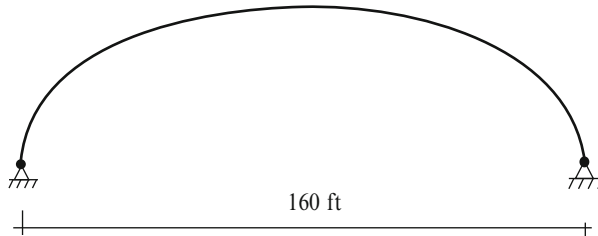
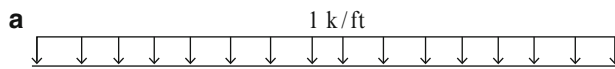
Use a Computer software system to determine the maximum bending moment and the axial force in member ABC. Consider the following values for the area of the tension rod AC: 4, 8, and 16 in.²

Problem 9.11

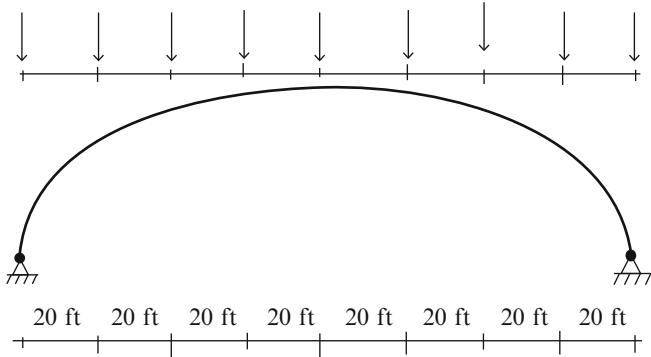


$$A = 40 \text{ in.}^2 \quad I = 1,200 \text{ in.}^4 \quad E = 29,000 \text{ ksi}$$

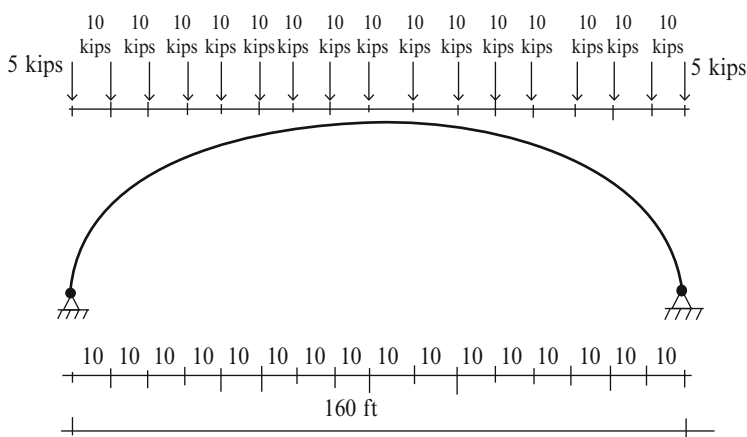
Use a Computer software system to compare the bending moment distributions generated by the following loadings:



c 10 kips 20 kips 10 kips

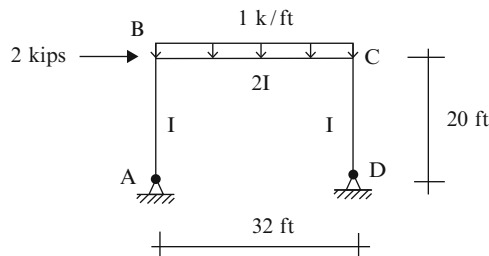


d



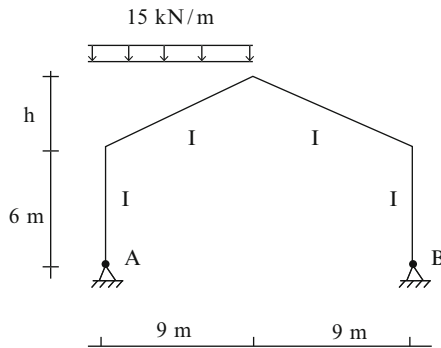
Problem 9.12

Determine the horizontal reaction at support D.

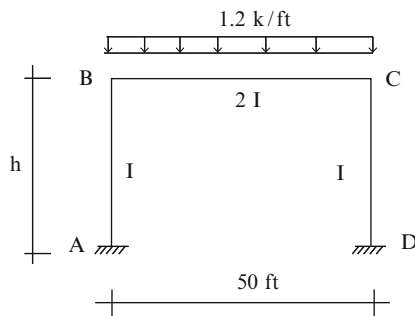


Problem 9.13

Determine the peak positive and negative moments as a function of h . Consider $h = 2, 4, 6 \text{ m}$.

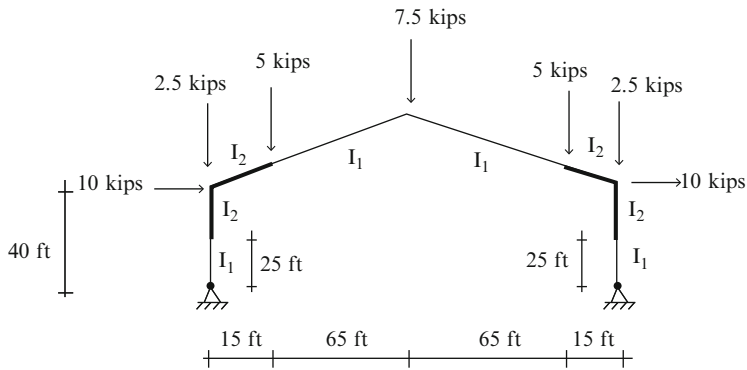
**Problem 9.14**

Determine the peak positive and negative moments as a function of h . Consider $h = 10, 20, 30 \text{ ft}$.



Problem 9.15

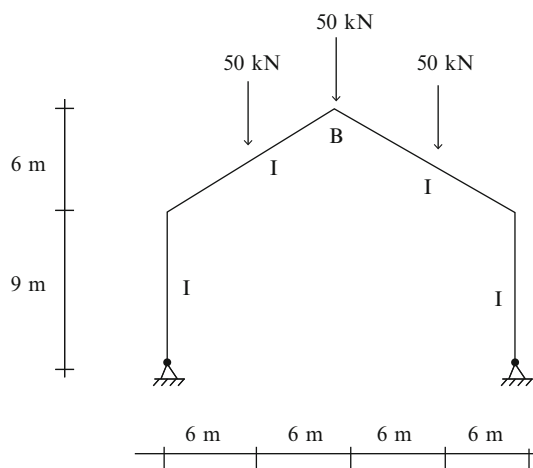
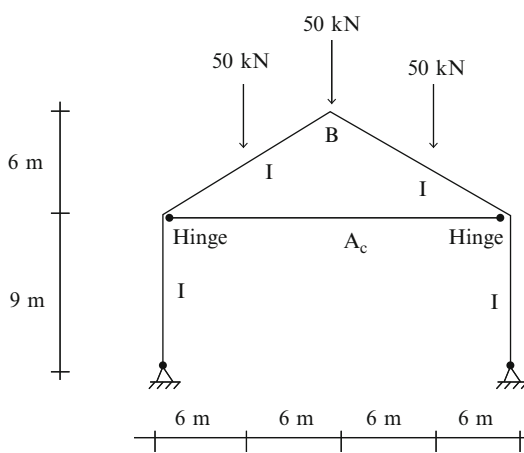
Using a Computer software system, determine the bending moment distribution and deflected shape due to the loading shown.



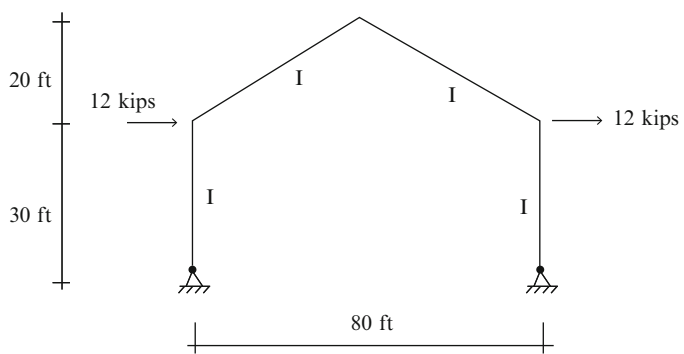
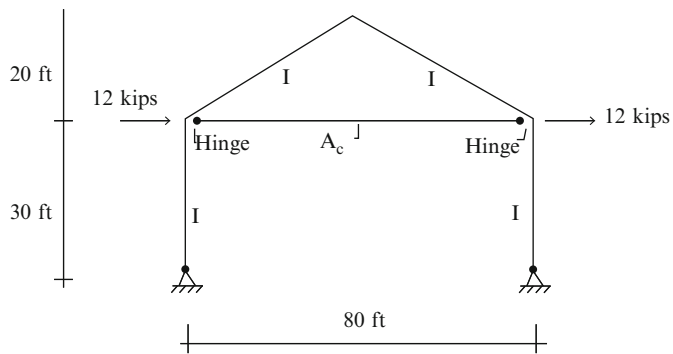
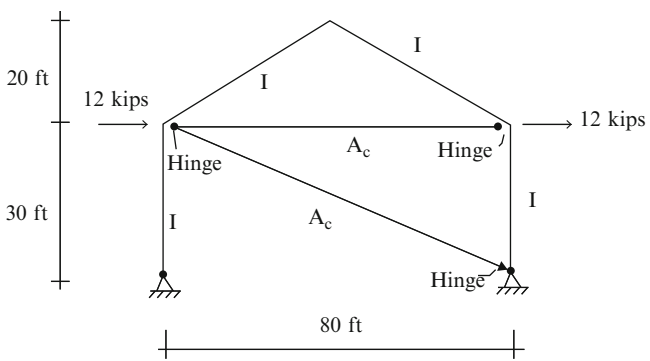
Take $I_1 = 1,000 \text{ in.}^4$, $I_2 = 2,000 \text{ in.}^4$, $E = 29,000 \text{ ksi}$ and $A = 20 \text{ in.}^2$ all members.

Problem 9.16

Compare the bending moment distributions and the vertical displacement at B for the structures defined below. Take $E = 200 \text{ GPa}$, $I = 400(10)^6 \text{ mm}^4$, $A = 100,000 \text{ mm}^2$ and $A_c = 1,200, 2,400, 4,800 \text{ mm}^2$. Use a Computer software system.

a**b****Problem 9.17**

Is there any difference in behavior for the structures shown below? Answer the question without resorting to calculations.

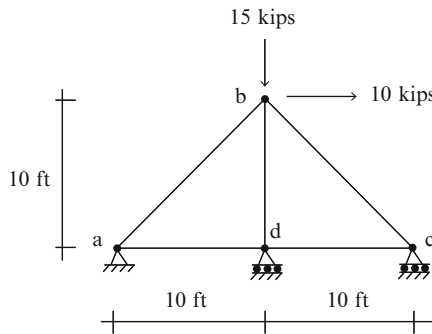
a**b****c**

Problem 9.18

Determine the reactions and the member forces for the truss shown.

$$E = 29,000 \text{ ksi}$$

$$A = 1 \text{ in.}^2 \text{ all members}$$

**Problem 9.19**

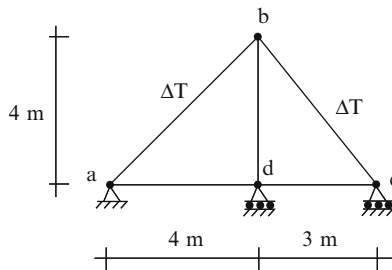
Determine the reactions and the member forces for the truss shown. Assume the vertical reaction at d as the force redundant.

$$E = 200 \text{ GPa}$$

$$A = 660 \text{ mm}^2 \text{ all members}$$

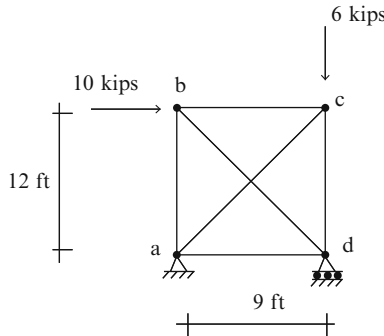
$$\alpha = 12 \times 10^{-6}/^\circ\text{C}$$

$$\Delta T = 10^\circ\text{C}$$

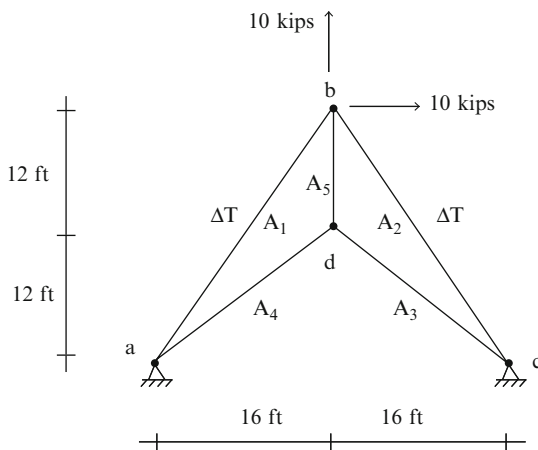


Problem 9.20

Determine the forces in the members. $E = 29,000$ ksi and $A = 1$ in. 2 all members.

**Problem 9.21**

Determine the member forces of the truss shown. Assume the horizontal reaction at c as the force redundant.



$$A_1 = A_2 = A_3 = A_4 = 10 \text{ in.}^2$$

$$A_5 = 5 \text{ in.}^2$$

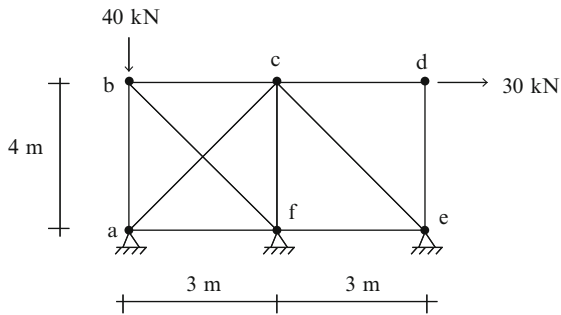
$$\alpha = 6.5 \times 10^{-6}/{}^\circ\text{F}$$

$$\Delta T = 60^\circ\text{F}$$

$$E = 29,000 \text{ ksi}$$

Problem 9.22

Determine the member forces for the truss shown. Assume $A = 1,000 \text{ mm}^2$ and $E = 200 \text{ GPa}$ for all the members. Assume the force in member ac and the reaction at support f as force redundants.



Overview

The previous chapter dealt with the Force Method, one of two procedures for analyzing statically indeterminate structures. In this chapter, we describe the second procedure, referred to as the Displacement Method. This method works with equilibrium equations expressed in terms of variables that correspond to displacement measures that define the position of a structure, such as translations and rotations of certain points on the structure. We start by briefly introducing the method specialized for frame-type structures and then apply it to truss, beam, and frame structures. Our focus in this chapter is on deriving analytical solutions and using these solutions to explain structural behavior trends. Later in Chap. 12, we describe how the method can be transformed to a computer-based analysis procedure.

10.1 Introduction

The Displacement Method works with equilibrium equations expressed in terms of displacement measures. For truss and frame-type structures, which are composed of members connected at node points, the translations and rotations of the nodes are taken as the displacement measures. For example, the plane truss shown in Fig. 10.1a has two unknown displacements (u_2, v_2). The available equilibrium equations are the two force equilibrium equations for node 2.

Planar beam-type structures have three displacement measures per node, the transverse displacements and the cross-section rotation. The corresponding equations are the shear, and moment equilibrium equations for each node. For example, the planar beam shown in Fig. 10.1b has five unknown displacements ($\theta_1, \theta_2, \theta_3, \theta_4, v_4$).

Plane frame-type structures have three displacement measure per nodes: two translations and one rotation. One works with the force and moment equilibrium equations for each unrestrained node. In general, the number of node

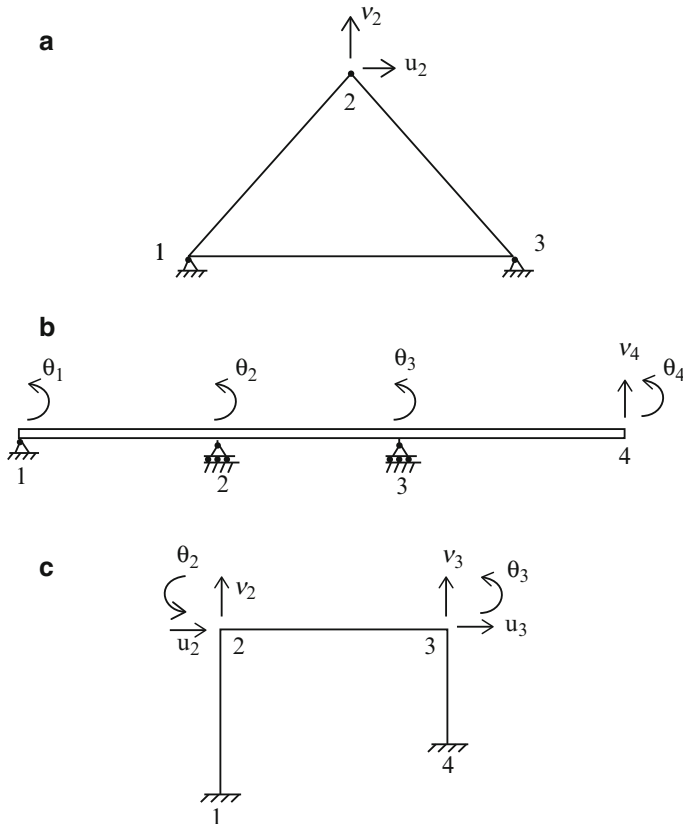


Fig. 10.1 (a) Plane truss. (b) Planar beam. (c) Plane frame

equilibrium equations will always be equal to the number of displacements. For example the plane frame shown in Fig. 10.1c has six unknown displacements ($u_2, v_2, \theta_2, u_3, v_3, \theta_3$).

The approach followed to generate equations involves the following steps:

1. Firstly, we decompose the structure into nodes and members. Note that the forces applied by a member to the node at its end are equal in magnitude but oppose in sense to the forces acting on the end of the member. The latter are called end actions.
2. Secondly, we relate the end actions for a member to the displacement measures for the nodes at the ends of the member. We carry out this procedure for each member.
3. Thirdly, we establish the force equilibrium equations for each node. This step involves summing the applied external loads and the end actions for those members which are incident on the node.
4. Fourthly, we substitute for the member end actions expressed in terms of the nodal displacements. This leads to a set of equilibrium equations relating the applied external loads and the nodal displacements.

5. Lastly, we introduce the prescribed values of nodal displacements corresponding to the supports in the equilibrium equations. The total number of unknowns is now reduced by the number of prescribed displacements. We solve this reduced set of equations for the nodal displacements and then use these values to determine the member end actions.

The solution procedure is systematic and is applicable for both statically determinate and statically indeterminate structures. Applications of the method to various types of structure are described in the following sections.

10.2 Displacement Method Applied to a Plane Truss

Consider the truss shown in Fig. 10.2. We suppose nodes 2, 3, and 4 are unyielding. We analyzed this structure with the Force Method in Sect. 9.6. We include it here to provide a comparison between the two approaches. There are two displacement measures, the horizontal and vertical translations for node 1. The structure is statically indeterminate to the first degree, so it is a trade-off whether one uses the Force Method or the Displacement Method.

The first step is to develop the equations relating the member forces and the nodal displacements. We start by expressing the change in length, e , of each member in terms of the displacements for node 1. This analysis is purely geometrical and involves projecting the nodal displacements on the initial direction of the member.

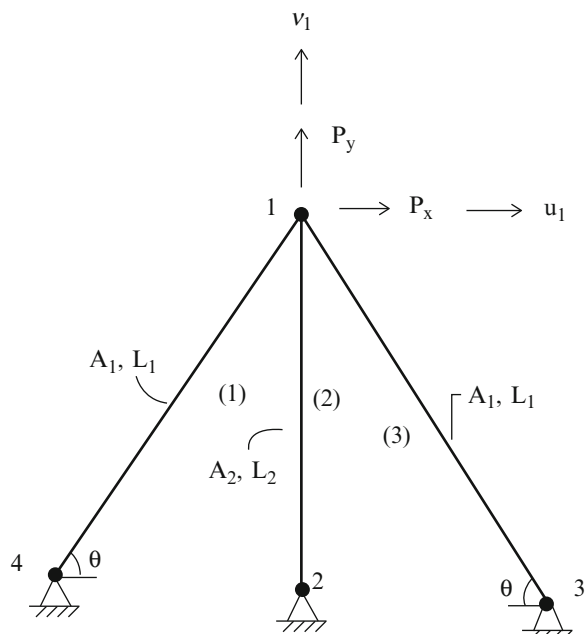


Fig. 10.2 Truss geometry and loading

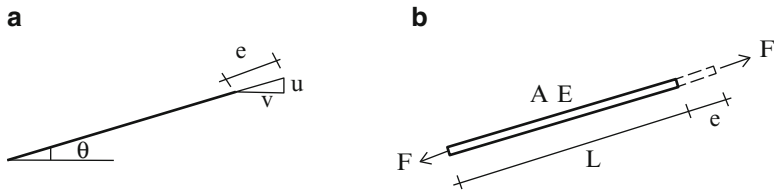


Fig. 10.3 Extension and force quantities—Axial loaded member

We define an extension as positive when the length is increased. Noting Fig. 10.3a, the extensions of members (1), (2), and (3) due to nodal displacements are given by:

$$\begin{aligned} e_{(1)} &= u_1 \cos \theta + v_1 \sin \theta \\ e_{(2)} &= v_1 \\ e_{(3)} &= -u_1 \cos \theta + v_1 \sin \theta \end{aligned} \quad (10.1)$$

Next, we express the member force in terms of the corresponding extension using the stress-strain relation for the material. Noting Fig. 10.3b, the generic equations are:

$$\begin{aligned} \varepsilon_{\text{total}} &= \varepsilon_0 + \frac{1}{E} \sigma = \frac{e}{L} \\ \sigma &= \frac{F}{A} \end{aligned}$$

where ε_0 is the initial strain due to temperature change and fabrication error. Then,

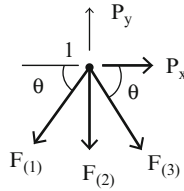
$$\begin{aligned} F &= \frac{AE}{L} e - AE\varepsilon_0 \\ &= \frac{AE}{L} e + F^F \end{aligned} \quad (10.2)$$

where F^F is the magnitude of the member force due to initial strain.

Substituting for the extensions leads to the desired expressions relating the member forces and the corresponding nodal displacements.

$$\begin{aligned} F_{(1)} &= \frac{A_1 E}{L_1} \cos \theta u_1 + \frac{A_1 E}{L_1} \sin \theta v_1 + F_{(1)}^F \\ F_{(2)} &= \frac{A_2 E}{L_2} v_1 = \frac{A_2 E}{L_1 \sin \theta} v_1 + F_{(2)}^F \\ F_{(3)} &= -\frac{A_1 E}{L_1} \cos \theta u_1 + \frac{A_1 E}{L_1} \sin \theta v_1 + F_{(3)}^F \end{aligned} \quad (10.3)$$

We generate the force-equilibrium equations for node 1 using the free body diagram show below.



$$\begin{aligned}\sum F_x &= 0 \rightarrow P_x = \cos \theta(F_{(1)} - F_{(3)}) \\ \sum F_y &= 0 \uparrow P_y = \sin \theta(F_{(1)} + F_{(3)}) + F_{(2)}\end{aligned}\quad (10.4)$$

Substituting for the member forces, one obtains a set of uncoupled equations for u_1 and v_1 .

$$\begin{aligned}P_x &= \left\{ \frac{2A_1E}{L_1} \cos^2 \theta \right\} u_1 + \cos \theta(F_{(1)}^F - F_{(3)}^F) \\ P_y &= \left\{ \frac{A_2E}{L_1 \sin \theta} + \frac{2A_1E}{L_1} \sin^2 \theta \right\} v_1 + \sin \theta(F_{(1)}^F + F_{(3)}^F) + F_{(2)}^F\end{aligned}\quad (10.5)$$

One solves these equations for u_1 and v_1 , and then determines the member forces using (10.3). The resulting expressions are:

$$\begin{aligned}F_{(1)} &= \frac{P_x^*}{2 \cos \theta} + P_y \left\{ \frac{A_1 \sin \theta}{A_2 / \sin \theta + 2A_1 \sin^2 \theta} \right\} + F_{(1)}^F \\ F_{(2)} &= P_y \left\{ \frac{A_2 / \sin \theta}{A_2 / \sin \theta + 2A_1 \sin^2 \theta} \right\} + F_{(2)}^F \\ F_{(3)} &= -\frac{P_x^*}{2 \cos \theta} + P_y \left\{ \frac{A_1 \sin \theta}{A_2 / \sin \theta + 2A_1 \sin^2 \theta} \right\} + F_{(3)}^F\end{aligned}\quad (10.6)$$

where

$$\begin{aligned}P_x^* &= P_x - \cos \theta(F_{(1)}^F - F_{(3)}^F) \\ P_y^* &= P_y - \sin \theta(F_{(1)}^F + F_{(3)}^F) + F_{(2)}^F\end{aligned}$$

For this example, it may seem like more effort is required to apply the displacement method vs. the force method. However, the displacement method generates the complete solution, i.e., both the member forces and the nodal displacements. A separate computation is required to compute the displacements when using the Force method.

10.3 Member Equations for Frame-Type Structures

The members in frame-type structures are subjected to both bending and axial action. The key equations for bending behavior of a member are the equations which relate the shear forces and moments acting on the ends of a member to the deflection and rotation of each end. These equations play a very important role in the analysis of statically indeterminate beams and frames and also provide the basis for the matrix formulation of the displacement method for structural frames. In what follows, we develop these equations using the force method.

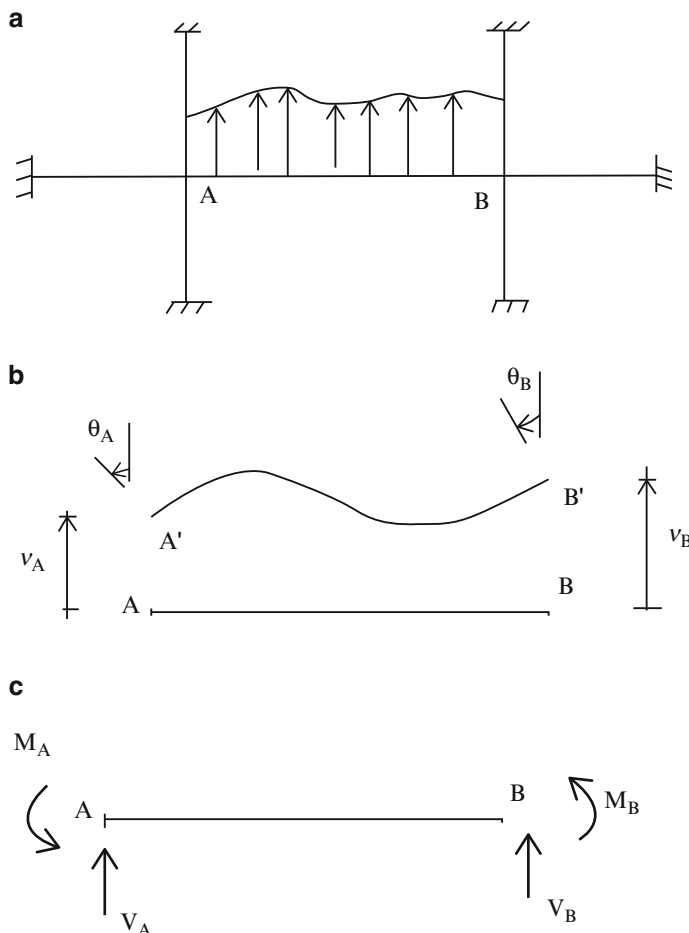
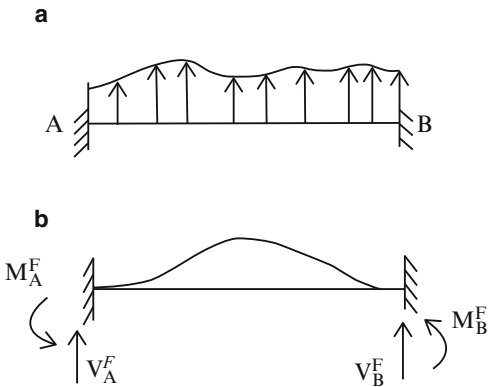
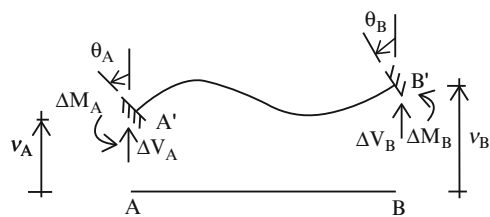


Fig. 10.4 Member deformation and end actions. (a) Initial geometry. (b) Deformed configuration for member AB. (c) Notation for end shear and moment

Fig. 10.5 Fixed end Actions.

(a) Initial. (b) Deformed

**Fig. 10.6** Response to nodal displacements

We consider the structure shown in Fig. 10.4a. We focus specifically on member AB. Both of its ends are rigidly attached to nodes. When the structure is loaded, the nodes displace and the member bends as illustrated in Fig. 10.4b. This motion produces a shear force and moment at each end. The positive sense of these quantities is defined in Figs. 10.4b, c.

We refer to the shear and moment acting at the ends as *end actions*. Our objective here is to relate the end actions (V_B, M_B, V_A, M_A) and the end displacements ($v_B, \theta_B, v_A, \theta_A$). Our approach is based on treating the external loading and end actions as separate loadings and superimposing their responses. We proceed as follows:

Step 1

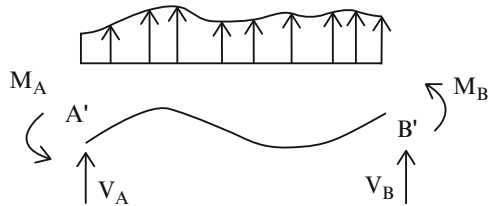
Firstly, we assume the nodes at A and B are fixed and apply the external loading to member AB. This leads to a set of end actions that we call *fixed end actions*. This step is illustrated in Fig. 10.5.

Step 2

Next, we allow the nodes to displace. This causes additional bending of the member AB resulting in additional end actions ($\Delta V_B, \Delta M_B, \Delta V_A, \Delta M_A$). Figure 10.6 illustrates this notation.

Step 3

Superimposing the results obtained in these two steps leads to the final state shown in Fig. 10.7.

Fig. 10.7 Final state

$$M_B = M_B^F + \Delta M_B$$

$$M_A = M_A^F + \Delta M_A$$

$$V_B = V_B^F + \Delta V_B$$

$$V_A = V_A^F + \Delta V_A$$

We determine the fixed end actions corresponding to the first step using the force method. Details are described in Chap. 9. Fixed end actions for various loading cases are listed in Table 9.1.

For the second step, we visualize the process as consisting of two substeps. First, we displace node B holding A fixed. Then, we displace node A, holding B fixed. Combining these cases result in the response shown in Fig. 10.8c. Superposition is valid since the behavior is linear.

These two cases are similar and can be analyzed using the same procedure. We consider first case (a) shown in Fig. 10.8a. We analyze this case by considering AB to be a cantilever beam fixed at A and subjected to unknown forces, $\Delta V_B^{(1)}$ and $\Delta M_B^{(1)}$ at B (see Fig. 10.9a).

The displacements at B are (see Table 3.1):

$$\begin{aligned} v_B &= \frac{\Delta V_B^{(1)} L^3}{3EI} + \frac{\Delta M_B^{(1)} L^2}{2EI} \\ \theta_B &= \frac{\Delta V_B^{(1)} L^2}{2EI} + \frac{\Delta M_B^{(1)} L}{EI} \end{aligned} \quad (10.7)$$

We determine $\Delta V_B^{(1)}$ and $\Delta M_B^{(1)}$ by requiring these displacements to be equal to the actual nodal displacements v_B and θ_B . Solving for $\Delta V_B^{(1)}$ and $\Delta M_B^{(1)}$ leads to

$$\begin{aligned} \Delta V_B^{(1)} &= \frac{12EI}{L^3} v_B - \frac{6EI}{L^2} \theta_B \\ \Delta M_B^{(1)} &= \frac{4EI}{L} \theta_B - \frac{6EI}{L} v_B \end{aligned} \quad (10.8)$$

The corresponding end actions at A are determined using the equilibrium conditions for the member.

$$\sum F_y = 0 \Rightarrow \Delta V_B^{(1)} + \Delta V_A^{(1)} = 0$$

$$\sum M = 0 \text{ at A} \Rightarrow \Delta M_B^{(1)} + \Delta M_A^{(1)} + L \Delta V_B^{(1)} = 0$$

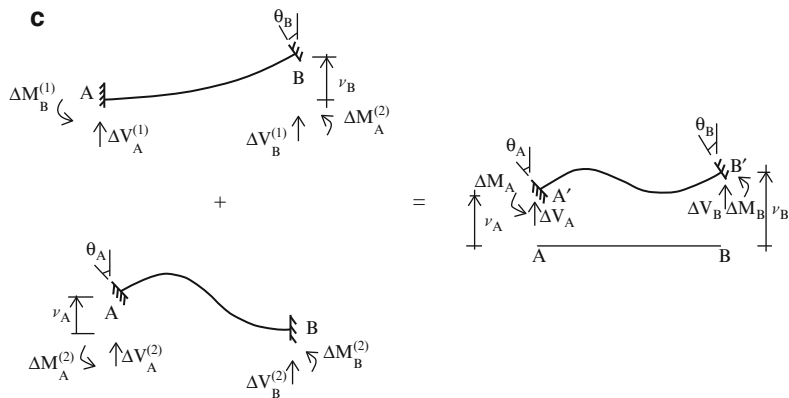
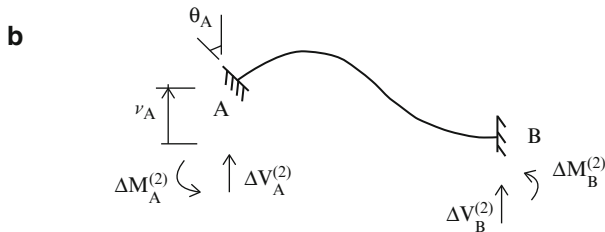
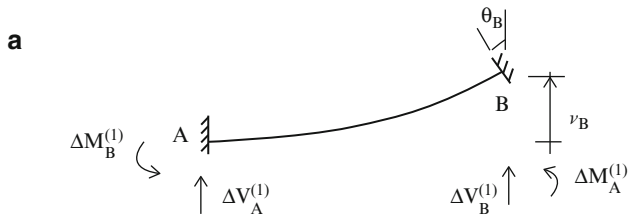


Fig. 10.8 Superposition of nodal motions. (a) Support A fixed. (b) Support B fixed. (c) Superimposed motions

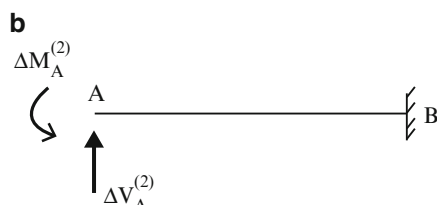
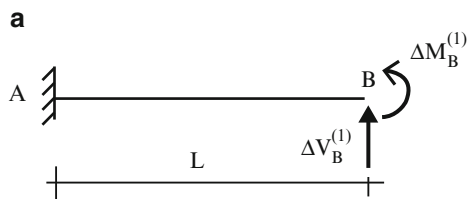


Fig. 10.9 (a) Support A fixed. (b) Support B fixed

Then

$$\begin{aligned}\Delta V_A^{(1)} &= -\frac{12EI}{L^3}v_B + \frac{6EI}{L^2}\theta_B \\ \Delta M_A^{(1)} &= -\frac{6EI}{L^2}v_B + \frac{2EI}{L}\theta_B\end{aligned}\quad (10.9)$$

Equation (10.8) and (10.9) define the end actions due to the displacement of node B with A fixed.

Case (b) of Fig. 10.8 is treated in a similar way (see Fig. 10.9b). One works with a cantilever fixed at B and solves for $\Delta V_A^{(2)}$ and $\Delta M_A^{(2)}$. The result is

$$\begin{aligned}\Delta V_A^{(2)} &= \frac{12EI}{L^3}v_A + \frac{6EI}{L^2}\theta_A \\ \Delta M_A^{(2)} &= \frac{6EI}{L^2}v_A + \frac{4EI}{L}\theta_A\end{aligned}\quad (10.10)$$

The end actions at B follow from the equilibrium conditions for the member.

$$\begin{aligned}\Delta V_B^{(2)} &= -\frac{12EI}{L^3}v_A - \frac{6EI}{L^2}\theta_A \\ \Delta M_B^{(2)} &= \frac{6EI}{L^2}v_A + \frac{4EI}{L}\theta_A\end{aligned}\quad (10.11)$$

Equations (10.10) and (10.11) define the end actions due to the displacement of node A with B fixed.

The complete solution is generated by superimposing the results for these two loading conditions and the fixed end actions.

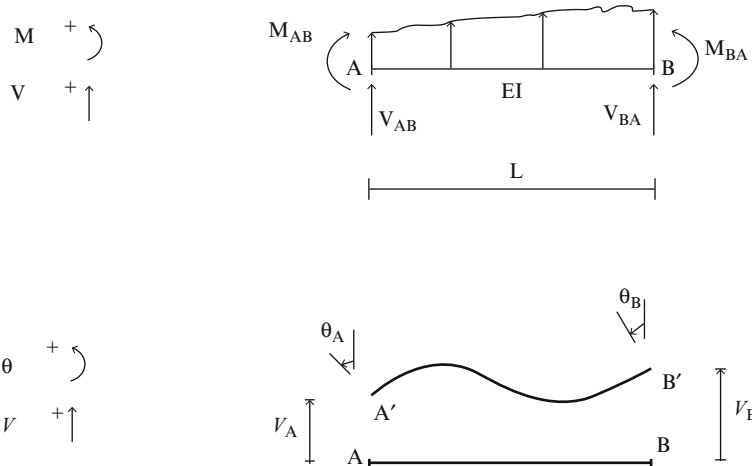
$$\begin{aligned}V_B &= \Delta V_B^{(1)} + \Delta V_B^{(2)} + V_B^F = -\frac{6EI}{L^2}(\theta_B + \theta_A) + \frac{12EI}{L^3}(v_B - v_A) + V_B^F \\ M_B &= \Delta M_B^{(1)} + \Delta M_B^{(2)} + M_B^F = +\frac{2EI}{L}(2\theta_B + \theta_A) - \frac{6EI}{L^2}(v_B - v_A) + M_B^F \\ V_A &= \Delta V_A^{(1)} + \Delta V_A^{(2)} + V_A^F = +\frac{6EI}{L^2}(\theta_B + \theta_A) - \frac{12EI}{L^3}(v_B - v_A) + V_A^F \\ M_A &= \Delta M_A^{(1)} + \Delta M_A^{(2)} + M_A^F = +\frac{2EI}{L}(\theta_B + 2\theta_A) - \frac{6EI}{L^2}(v_B - v_A) + M_A^F\end{aligned}$$

We rearrange these equations according to moment and shear quantities. The final form is written as

$$\begin{aligned}M_{AB} &= \frac{2EI}{L} \left\{ 2\theta_A + \theta_B - 3 \left(\frac{v_B - v_A}{L} \right) \right\} + M_{AB}^F \\ M_{BA} &= \frac{2EI}{L} \left\{ \theta_A + 2\theta_B - 3 \left(\frac{v_B - v_A}{L} \right) \right\} + M_{BA}^F\end{aligned}\quad (10.12a)$$

and

$$\begin{aligned} V_{AB} &= +\frac{6EI}{L^2} \left\{ \theta_A + \theta_B - 2\left(\frac{v_B - v_A}{L}\right) \right\} + V_{AB}^F \\ V_{BA} &= -\frac{6EI}{L^2} \left\{ \theta_A + \theta_B - 2\left(\frac{v_B - v_A}{L}\right) \right\} + V_{BA}^F \end{aligned} \quad (10.12b)$$



Equations (10.12) are referred to as the *slope-deflection equations*. They are based on the sign conventions and notation defined above.

10.4 The Displacement Method Applied to Beam Structures

In what follows, we first describe how the slope-deflection equations are employed to analyze horizontal beam structures, starting with two span beams and then moving on to multi-span beams and frames. The displacement measures for beams are taken as the nodal rotations; the transverse displacements are assumed to be specified.

10.4.1 Two Span Beams

We consider the two span beam shown in Fig. 10.10a. One starts by subdividing the beam into two beam segments and three nodes, as indicated in Fig. 10.10b. There are only two rotations unknowns; the rotations at nodes A and B.

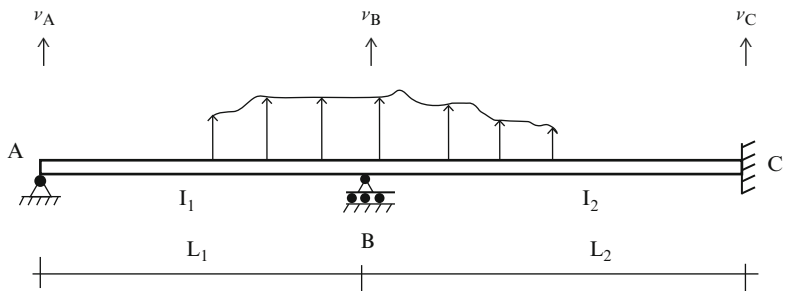
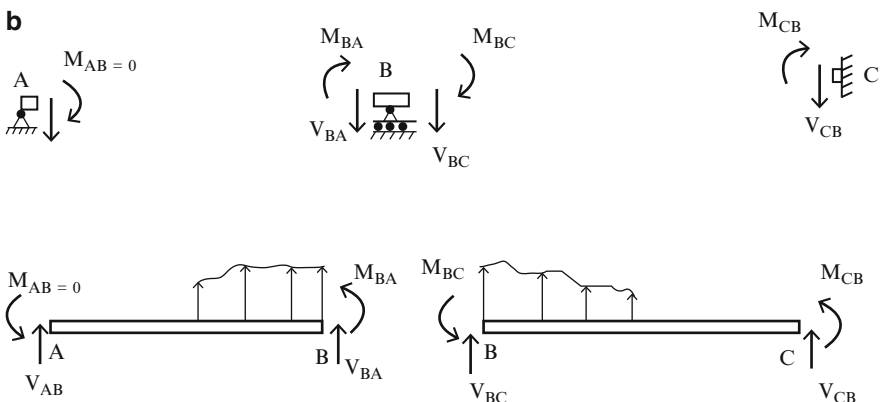
a**b**

Fig. 10.10 Decomposition of two span beam into beam segments and nodes. (a) Beam geometry and loading. (b) Segments and nodes

We enforce moment equilibrium at the nodes. The corresponding equations are:

$$M_{AB} = 0$$

$$M_{BA} + M_{BC} = 0 \quad (10.13)$$

Next we apply the slope-deflection equations (10.12a) to members AB and BC.

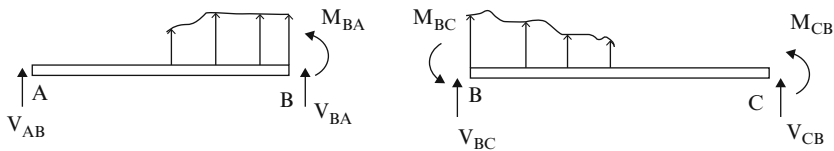
$$\begin{aligned} M_{AB} &= \frac{2EI_1}{L_1} \left\{ 2\theta_A + \theta_B - 3 \left(\frac{v_B - v_A}{L_1} \right) \right\} + M_{AB}^F \\ M_{BA} &= \frac{2EI_1}{L_1} \left\{ 2\theta_B + \theta_A - 3 \left(\frac{v_B - v_A}{L_1} \right) \right\} + M_{BA}^F \\ M_{BC} &= \frac{2EI_2}{L_2} \left\{ 2\theta_B - 3 \left(\frac{v_C - v_B}{L_2} \right) \right\} + M_{BC}^F \\ M_{CB} &= \frac{2EI_2}{L_2} \left\{ \theta_B - 3 \left(\frac{v_C - v_B}{L_2} \right) \right\} + M_{CB}^F \end{aligned} \quad (10.14)$$

Substituting for the end moments in the nodal moment equilibrium equations yields

$$\frac{4EI_1}{L_1}\theta_A + \frac{2EI_1}{L_1}\theta_B = \frac{6EI_1}{L_1} \left(\frac{v_B - v_A}{L_1} \right) - M_{AB}^F \quad (10.15)$$

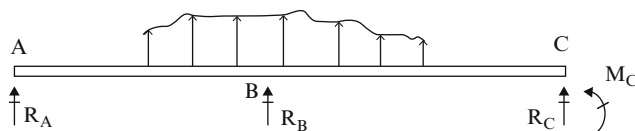
$$\frac{2EI_1}{L_1}\theta_A + \left(\frac{4EI_1}{L_1} + \frac{4EI_2}{L_2} \right)\theta_B = \frac{6EI_1}{L_1} \left(\frac{v_B - v_A}{L_1} \right) + \frac{6EI_2}{L_2} \left(\frac{v_C - v_B}{L_2} \right) - (M_{BA}^F + M_{BC}^F)$$

Once the loading, support motion and member properties are specified, one can solve for θ_B and θ_A . Substituting for the θ s in (10.14) leads to the end moments. Lastly, we calculate the end shears. Since the end moments are known, we can determine the end shear forces using either the static equilibrium equations for the members AB and BC or by using (10.12b).



Free body diagram

$$\begin{aligned} V_{AB} &= \frac{6EI_1}{L_1^2}(\theta_A + \theta_B) - \frac{12EI_1}{L_1^2} \left(\frac{v_B - v_A}{L_1} \right) + V_{AB}^F \\ V_{BA} &= -\frac{6EI_1}{L_1^2}(\theta_B + \theta_A) + \frac{12EI_1}{L_1^2} \left(\frac{v_B - v_A}{L_1} \right) + V_{BA}^F \\ V_{BC} &= \frac{6EI_2}{L_2^2}(\theta_B) - \frac{12EI_2}{L_2^2} \left(\frac{v_C - v_B}{L_2} \right) + V_{BC}^F \\ V_{CB} &= -\frac{6EI_2}{L_2^2}(\theta_B) + \frac{12EI_2}{L_2^2} \left(\frac{v_C - v_B}{L_2} \right) + V_{CB}^F \end{aligned} \quad (10.16)$$



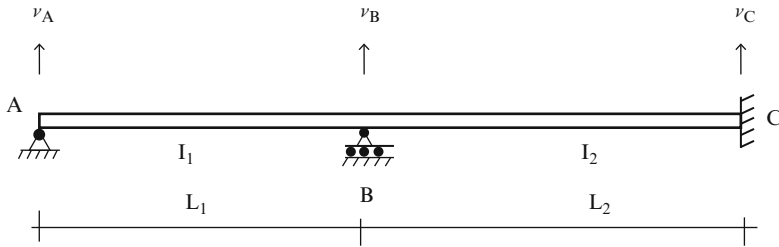


Fig. 10.11 Beam geometry and support settlements

The reactions are related to the end actions by

$$\begin{aligned} R_A &= V_{AB} \\ M_A &= M_{AB} = 0 \\ R_B &= V_{BA} + V_{BC} \\ R_C &= V_{CB} \\ M_C &= M_{CB} \end{aligned}$$

Suppose the only external action on the above two span beam is prescribed support settlements \$v_A\$, \$v_B\$, and \$v_C\$ as shown in Fig. 10.11. We compute the corresponding chord rotation terms and include these terms in the slope-deflection equations. The chord rotations are

$$\begin{aligned} \rho_{AB} &= \frac{v_B - v_A}{L_1} \\ \rho_{BC} &= \frac{v_C - v_B}{L_2} \end{aligned} \tag{10.17}$$

Noting (10.14), the chord rotation terms introduce additional end moments for each member connected to the support which experiences the settlement. The corresponding expressions for the end moments due to this support settlement are

$$\begin{aligned} M_{AB} &= \frac{2EI_1}{L_1} \{2\theta_A + \theta_B - 3\rho_{AB}\} \\ M_{BA} &= \frac{2EI_1}{L_1} \{2\theta_B + \theta_A - 3\rho_{AB}\} \\ M_{BC} &= \frac{2EI_2}{L_2} \{2\theta_B + \theta_C - 3\rho_{BC}\} \\ M_{CB} &= \frac{2EI_2}{L_2} \{2\theta_C + \theta_B - 3\rho_{BC}\} \end{aligned} \tag{10.18}$$

Substituting for the moments in the nodal moment equilibrium equations

$$M_{AB} = 0$$

$$M_{BA} + M_{BC} = 0$$

And noting that $\theta_C = 0$ results in the following equations relating the nodal rotations

$$\begin{aligned} 2\theta_A + \theta_B &= 3\rho_{AB} \\ \frac{2EI_1}{L_1}\{2\theta_B + \theta_A\} + \frac{2EI_2}{L_2}\{2\theta_B\} &= \frac{6EI_1}{L_1}\rho_{AB} + \frac{6EI_2}{L_2}\rho_{BC} \end{aligned} \quad (10.19)$$

Note that the solution depends on the ratio of EI to L for each span. One specifies ρ for each member, solves (10.19) for the θ s, and then evaluates the end actions.

Example 10.1

Given: The two span beam defined in Fig. E10.1a. Assume the supports are unyielding. Take $E = 29,000$ ksi, $I = 428$ in.⁴ and $L = 20$ ft.

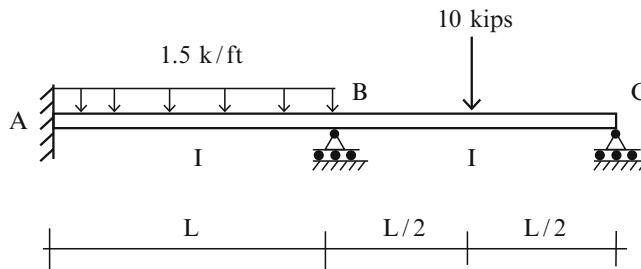
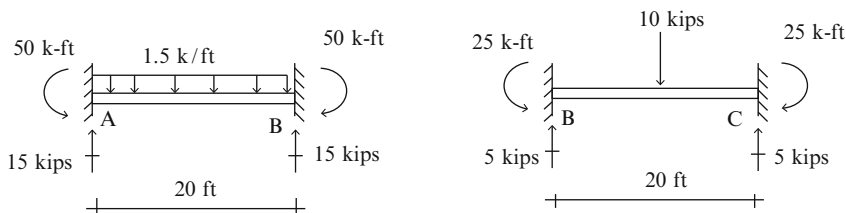


Fig. E10.1a

Determine: The end actions and the shear and moment diagrams due to the applied loading.

Solution: First we compute the fixed end actions by using Table 9.1.



$$\begin{aligned}
 M_{AB}^F &= \frac{1.5(20)^2}{12} = 50 \text{ kip ft} & V_{AB}^F &= \frac{1.5(20)}{2} = 15 \text{ kip} \\
 M_{BA}^F &= -50 \text{ kip ft} & V_{AB}^F &= \frac{1.5(20)}{2} = 15 \text{ kip} \\
 M_{BC}^F &= \frac{10(20)}{8} = 25 \text{ kip ft} & V_{BC}^F &= \frac{10}{2} = 5 \text{ kip} \\
 M_{CB}^F &= -25 \text{ kip ft} & V_{CB}^F &= \frac{10}{2} = 5 \text{ kip}
 \end{aligned}$$

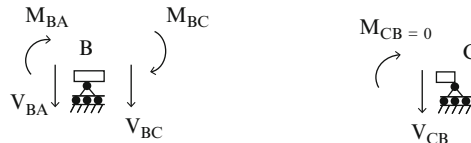
We define the relative member stiffness for each member as

$$k_{\text{member AB}} = k_{\text{member BC}} = \frac{EI}{L} = k_1 = \frac{29,000(428)}{20} \frac{1}{(12)^2} = 4,310 \text{ kip ft}$$

Next, we generate the expressions for the end moments using the slope-deflection equations (10.12) and noting that $\theta_A = 0$ and the supports are unyielding ($v_A = v_B = v_C = 0$).

$$\begin{aligned}
 M_{AB} &= 2k_1(\theta_B) + 50 \\
 M_{BA} &= 2k_1(2\theta_B) - 50 \\
 M_{BC} &= 2k_1(2\theta_B + \theta_C) + 25 \\
 M_{CB} &= 2k_1(\theta_B + 2\theta_C) - 25
 \end{aligned}$$

Enforcing moment equilibrium at nodes B and C



$$\begin{aligned}
 M_{BA} + M_{BC} &= 0 \\
 M_{CB} &= 0
 \end{aligned}$$

leads to

$$\begin{aligned}
 2k_1\theta_B + 4k_1\theta_C &= 25 \\
 8k_1\theta_B + 2k_1\theta_C &= 25 \\
 \downarrow \\
 k_1\theta_B &= 1.786 \\
 k_1\theta_C &= 5.357 \\
 \downarrow \\
 \theta_B &= 0.0004 \text{ rad} \quad \text{counter clockwise} \\
 \theta_C &= 0.0012 \text{ rad} \quad \text{counter clockwise}
 \end{aligned}$$

These rotations produce the following end moments

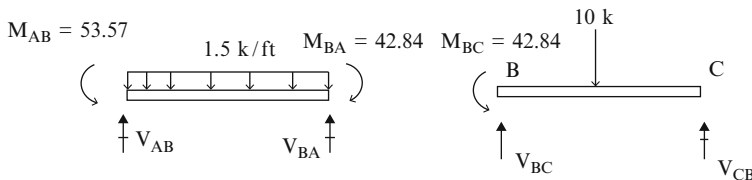
$$M_{AB} = 53.57 \text{ kip ft}$$

$$M_{BA} = -42.84 \text{ kip ft}$$

$$M_{BC} = +42.84 \text{ kip ft}$$

$$M_{CB} = 0$$

Since the end moments are known, we can determine the end shear forces using either the static equilibrium equations for the members or by using (10.12b).



Noting (10.12b), we find

$$V_{AB} = \frac{6}{L}(k_1\theta_B) + V_{AB}^F = \frac{6}{20}(1.786) + 15 = 15.53 \text{ kip}$$

$$V_{AB} = -\frac{6}{L}(k_1\theta_B) + V_{AB}^F = -\frac{6}{20}(1.786) + 15 = 14.47 \text{ kip}$$

$$V_{BC} = \frac{6}{L}(k_1\theta_B + k_1\theta_C) + V_{BC}^F = \frac{6}{20}(1.786 + 5.357) + 5 = 7.14 \text{ kip}$$

$$V_{AB} = -\frac{6}{L}(k_1\theta_B + k_1\theta_C) + V_{CB}^F = -\frac{6}{20}(1.786 + 5.357) + 5 = 2.86 \text{ kip}$$

The reactions are:

$$R_A = V_{AB} = 15.53 \text{ kip } \uparrow$$

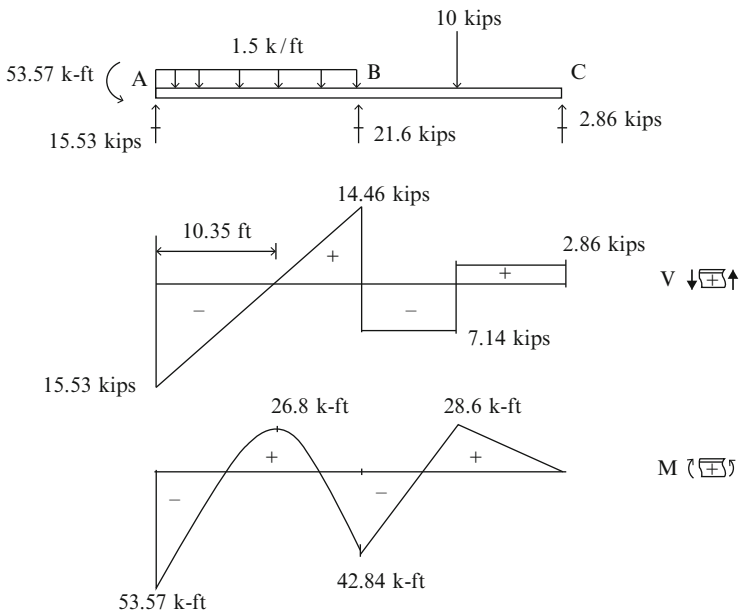
$$M_A = M_{AB} = 53.57 \text{ kip ft}$$

$$R_B = V_{BA} + V_{BC} = 21.6 \text{ kip } \uparrow$$

$$R_C = V_{CB} = 2.86 \text{ kip } \uparrow$$

$$M_C = M_{CB} = 0$$

Lastly, the shear and moment diagrams are plotted below.



Example 10.2 Two span symmetrical beam—settlement of the supports

Given: The symmetrical beam shown in Fig. E10.2a. Assume EI is constant. Take $L = 6 \text{ m}$, $I = 180(10)^6 \text{ mm}^4$, $E = 200 \text{ kN/mm}^2$.

Case (i) the middle support settles an amount $v_B = 40 \text{ mm}$.

Case (ii) the left support settles an amount $v_A = 40 \text{ mm}$.

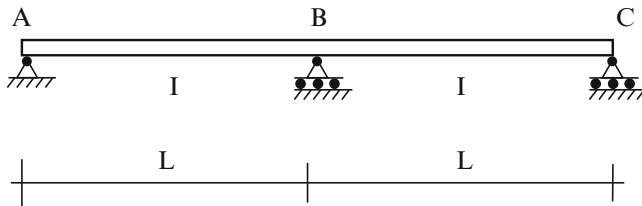


Fig. E10.2a

Determine: The end actions, the shear and bending moment diagrams.

Solution:

Case (i): Support settlement at B (Fig. E10.2b)

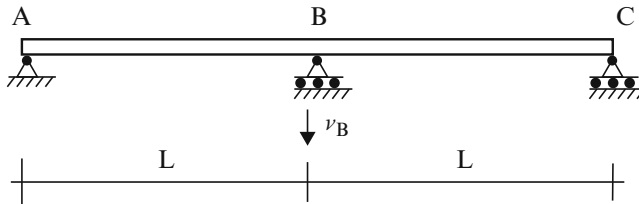


Fig. E10.2b Settlement at B

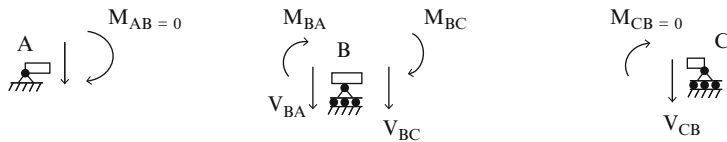
Noting (10.17) the chord rotations due to settlement at B are:

$$\begin{aligned}\rho_{AB} &= \frac{v_B - v_A}{L} = -\frac{v_B}{L} \\ \rho_{BC} &= \frac{v_C - v_B}{L} = +\frac{v_B}{L}\end{aligned}$$

Substituting for ρ_{AB} and ρ_{BC} the corresponding slope-deflection equations (10.12) take the form

$$\begin{aligned}M_{AB} &= \frac{2EI}{L}(2\theta_A + \theta_B) - \frac{6EI}{L}\rho_{AB} \\ M_{BA} &= \frac{2EI}{L}(2\theta_B + \theta_A) - \frac{6EI}{L}\rho_{AB} \\ M_{BC} &= \frac{2EI}{L}(2\theta_B + \theta_C) - \frac{6EI}{L}\rho_{BC} \\ M_{CB} &= \frac{2EI}{L}(2\theta_C + \theta_B) - \frac{6EI}{L}\rho_{BC}\end{aligned}$$

We enforce moment equilibrium at nodes A, B, and C.



The corresponding equations are:

$$\begin{aligned}M_{AB} = 0 &\Rightarrow 2\theta_A + \theta_B = -3\frac{v_B}{L} \\ M_{AB} + M_{BC} = 0 &\Rightarrow \theta_A + 4\theta_B + \theta_C = 0 \\ M_{CB} = 0 &\Rightarrow 2\theta_C + \theta_B = 3\frac{v_B}{L}\end{aligned}$$

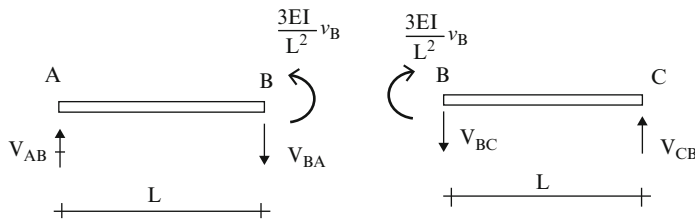
Solving for the θ s leads to

$$\begin{aligned}\theta_B &= 0 \\ \theta_A &= -\frac{3}{2} \frac{v_B}{L} \\ \theta_C &= +\frac{3}{2} \frac{v_B}{L}\end{aligned}$$

The corresponding end moments are:

$$\begin{aligned}M_{BA} &= \frac{2EI}{L} \left(-\frac{3}{2} \frac{v_B}{L} \right) - \frac{6EI}{L} \left(-\frac{v_B}{L} \right) = +\frac{3EI}{L^2} v_B = \frac{3(200)(180)10^6}{(6,000)^2} (40) \\ &= 120,000 \text{ kN mm} = 120 \text{ kN m} \\ M_{BC} &= \frac{2EI}{L} \left(\frac{3}{2} \frac{v_B}{L} \right) - \frac{6EI}{L} \left(\frac{v_B}{L} \right) = -\frac{3EI}{L^2} v_B = -120 \text{ kN m}\end{aligned}$$

Next, we determine the end shear forces using the static equilibrium equations for the members.



$$V_{AB} = V_{CB} = +\frac{3EI}{L^3} v_B = \frac{3(200)(180)10^6}{(6,000)^3} (40) = 20 \text{ kN} \uparrow$$

$$V_{BA} = V_{BC} = -\frac{3EI}{L^3} v_B = 20 \text{ kN} \downarrow$$

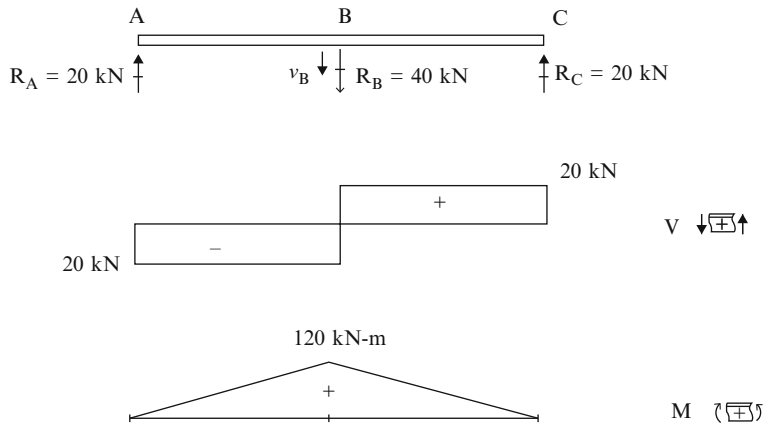
The corresponding reactions are:

$$R_A = V_{AB} = 20 \text{ kN} \uparrow$$

$$R_B = V_{BA} + V_{BC} = 40 \text{ kN} \downarrow$$

$$R_C = V_{CB} = 20 \text{ kN} \uparrow$$

One should expect that $\theta_B = 0$ because of symmetry. The shear and moment diagrams are plotted below.



Case (ii): Support settlement at A (Fig. E10.2c)

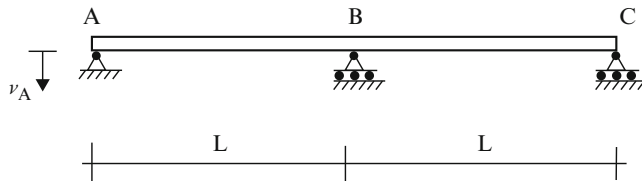


Fig. E10.2c Settlement at A

Settlement at A produces chord rotation in member AB only. The chord rotation for member AB due to settlement of node A is $\rho_{AB} = v_A/L$. Substituting for ρ_{AB} , the corresponding slope-deflection equations (10.12) take the form

$$\begin{aligned} M_{AB} &= \frac{2EI}{L}(2\theta_A + \theta_B) - \frac{6EI}{L}\rho_{AB} \\ M_{BA} &= \frac{2EI}{L}(2\theta_B + \theta_A) - \frac{6EI}{L}\rho_{AB} \\ M_{BC} &= \frac{2EI}{L}(2\theta_B + \theta_C) \\ M_{CB} &= \frac{2EI}{L}(2\theta_C + \theta_B) \end{aligned}$$

Setting $M_{AB} = M_{CB} = 0$ and $M_{AB} + M_{BC} = 0$ leads to

$$\begin{aligned}2\theta_A + \theta_B &= 3\rho_{AB} \\2\theta_C + \theta_B &= 0 \\4\theta_B + \theta_A + \theta_C &= 3\rho_{AB}\end{aligned}$$

Solving for the θ s leads to

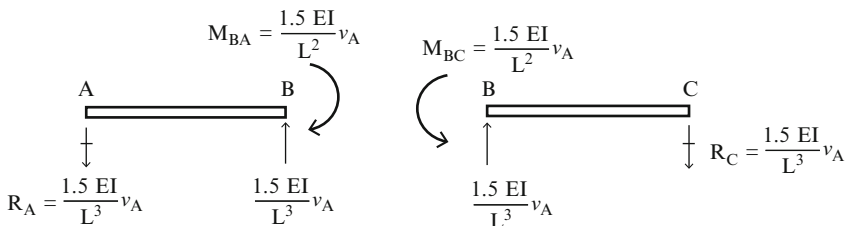
$$\begin{aligned}\theta_A &= \frac{5}{4}\rho_{AB} \\\theta_B &= \frac{1}{2}\rho_{AB} \\\theta_C &= -\frac{1}{4}\rho_{AB}\end{aligned}$$

Finally, the bending moment at B due to support settlement at A is:

$$\begin{aligned}M_{BA} &= \frac{2EI}{L} \left(\frac{v_A}{L} + \frac{5}{4} \frac{v_A}{L} \right) - \frac{6EIv_A}{L^2} = -\frac{1.5EI}{L^2}v_A = -\frac{1.5(200)(180)10^6}{(6,000)^2}(40) \\&= -60,000 \text{ kN mm} = -60 \text{ kN m}\end{aligned}\quad (40)$$

$$M_{BC} = -M_{BA} = 60 \text{ kN m} \quad \text{counterclockwise}$$

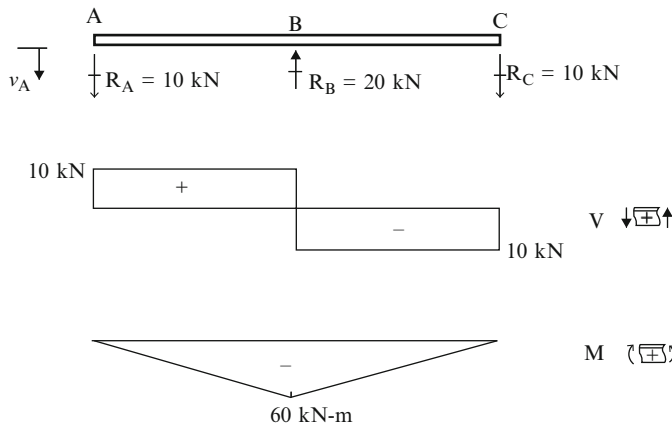
Next, we determine the end shear forces using the static equilibrium equations for the members.



Then,

$$\begin{aligned}R_A = R_C &= -\frac{1.5EI}{L^3}v_A = -\frac{1.5(200)(180)10^6}{(6,000)^3}(40) = -10 \text{ kN} \\R_B &= \frac{1.5EI}{L^3}v_A + \frac{1.5EI}{L^3}v_A = +20 \text{ kN}\end{aligned}$$

The shear and moment diagrams are plotted below.



Example 10.3 Two span beam with overhang

Given: The beam shown in Fig. E10.3a. Assume EI is constant.

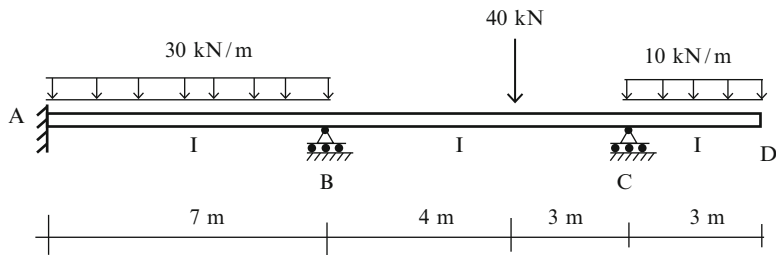
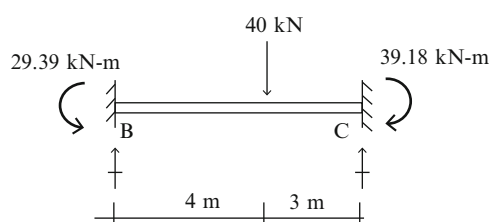
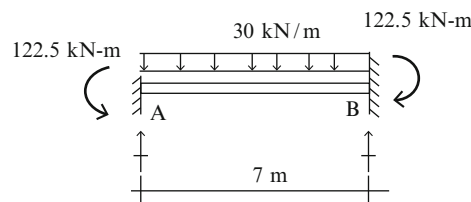


Fig. E10.3a

Determine: The end actions and the shear and moment diagrams.

Solution: First we compute the fixed end moments by using Table 9.1.



$$M_{AB}^F = +\frac{30(7)^2}{12} = +122.5 \text{ kN m}$$

$$M_{BA}^F = -122.5 \text{ kN m}$$

$$M_{BC}^F = \frac{40(4)(3)^2}{(7)^2} = +29.39 \text{ kN m}$$

$$M_{CB}^F = -\frac{40(4)^2(3)}{(7)^2} = -39.18 \text{ kN m}$$

We define the relative member stiffness for each member as

$$k_{\text{member AB}} = k_{\text{member BC}} = \frac{EI}{L} = k_1$$

Noting that $\theta_A = 0$ and the supports are unyielding ($v_A = v_B = v_C = 0$), the corresponding slope-deflection equations (10.12) take the form

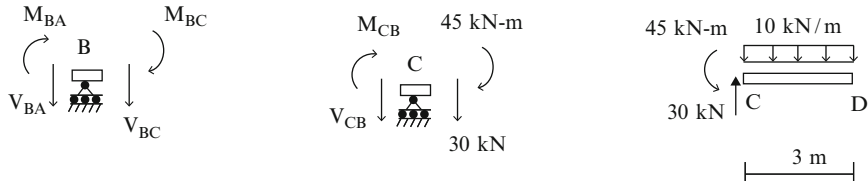
$$M_{AB} = 2k_1(\theta_B) + 122.5$$

$$M_{BA} = 2k_1(2\theta_B) - 122.5$$

$$M_{BC} = 2k_1(2\theta_B + \theta_C) + 29.39$$

$$M_{CB} = 2k_1(2\theta_C + \theta_B) - 39.18$$

We enforce moment equilibrium at the nodes B and C.



The corresponding equations are:

$$\begin{aligned} M_{BA} + M_{BC} &= 0 \quad \Rightarrow \quad 2k_1\theta_C + 6k_1\theta_B = 93.11 \\ M_{CB} + 45 &= 0 \quad \Rightarrow \quad 4k_1\theta_C + 2k_1\theta_B = -5.82 \end{aligned}$$

Following these equations leads to

$$k_1\theta_B = 13.71$$

$$k_1\theta_C = -8.31$$

The corresponding end moments are:

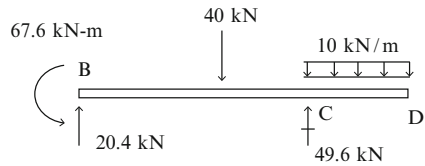
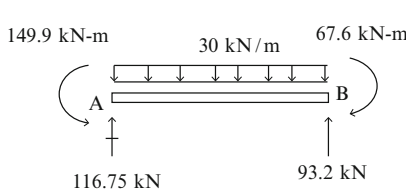
$$M_{AB} = +149.9 \text{ kN m}$$

$$M_{BA} = -67.6 \text{ kN m}$$

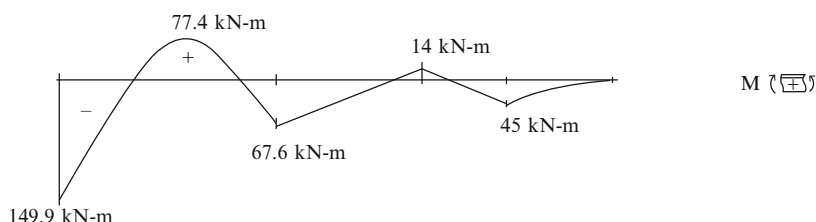
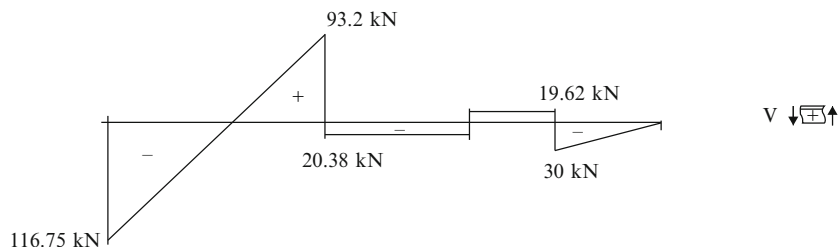
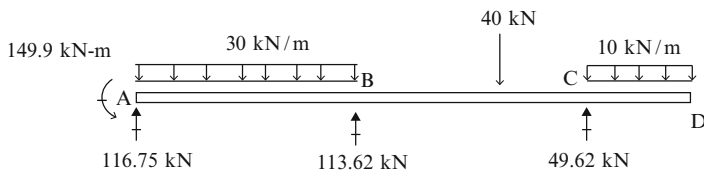
$$M_{BC} = +67.6 \text{ kN m}$$

$$M_{CB} = -45 \text{ kN m}$$

Next, we determine the end shear forces using the static equilibrium equations for the members.



The shear and moment diagrams are plotted below.



In what follows, we modify the slope-deflection equations for the end members of a multi-span continuous beam when they have either a pin or roller support. Consider the three span beam shown in Fig. 10.12a. There are three beam segments

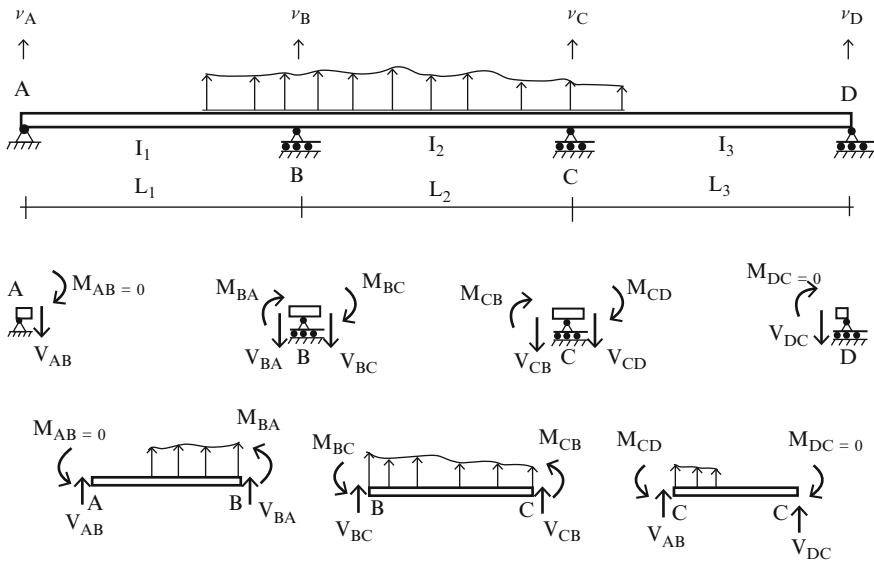


Fig. 10.12 Three span beam

and four nodes. Since the end nodes have zero moment, we can simplify the slope-deflection equations for the end segments by eliminating the end rotations. We did this in the previous examples, as part of the solution process. Now, we formalize the process and modify the slope-deflection equations before setting up the nodal moment equilibrium equations for the interior nodes.

Consider member AB. The end moment of A is zero, and we use this fact to express θ_A in terms of θ_B . Starting with the expression for M_{AB} ,

$$M_{AB} = \frac{2EI_1}{L_1} \left(2\theta_A + \theta_B - 3 \frac{v_B - v_A}{L_1} \right) + M_{AB}^F = 0$$

and solving for θ_A leads to

$$\theta_A = -\frac{1}{2}\theta_B + \frac{3}{2}\rho_{AB} - \frac{L_1}{4EI_1}M_{AB}^F$$

Then, we substitute for θ_A in the expression M_{BA} ,

$$M_{BA} = \frac{2EI_1}{L_1} \left(2\theta_B + \theta_A - 3 \frac{v_B - v_A}{L_1} \right) + M_{BA}^F$$

and obtain the following form,

$$M_{BA_{\text{modified}}} = \frac{3EI_1}{L_1} \left(\theta_B - \frac{v_B - v_A}{L} \right) + \left(M_{BA}^F - \frac{1}{2} M_{AB}^F \right) \quad (10.20)$$

Note that the presence of a pin or roller at A *reduces* the rotational stiffness at B from $4EI/L$ to $3EI/L$. Substituting for θ_A in the expression V_{AB} and V_{BA} leads to the following expressions,

$$\begin{aligned} V_{AB_{\text{modified}}} &= +\frac{6EI}{L^2} \left\{ \frac{1}{2} \theta_B - \frac{1}{2} \left(\frac{v_B - v_A}{L} \right) \right\} + V_{AB}^F \\ V_{BA_{\text{modified}}} &= -\frac{6EI}{L^2} \left\{ \frac{1}{2} \theta_B - \frac{1}{2} \left(\frac{v_B - v_A}{L} \right) \right\} + V_{BA}^F \end{aligned}$$

For member BC we use the general unchanged form

$$\begin{aligned} M_{BC} &= \frac{2EI_2}{L_2} \left(2\theta_B + \theta_C - 3 \frac{v_C - v_B}{L_2} \right) + M_{BC}^F \\ M_{CB} &= \frac{2EI_2}{L_2} \left(2\theta_C + \theta_B - 3 \frac{v_C - v_B}{L_2} \right) + M_{CB}^F \end{aligned}$$

The modified form for member CD is

$$\begin{aligned} M_{DC} &= 0 \\ M_{CD} &= \frac{3EI_3}{L_3} \left(\theta_C - \frac{v_D - v_C}{L_3} \right) + \left(M_{CD}^F - \frac{1}{2} M_{DC}^F \right) \end{aligned}$$

Nodal moment equilibrium equations

Now, we return back to Fig. 10.12. If we use the modified form of the moment expressions for members AB and CD, we *do not* have to enforce moment equilibrium at nodes A and D since we have already employed this condition to modify the equations. Therefore, we need only to consider nodes B and C. Summing moments at these nodes,

$$M_{BA} + M_{BC} = 0$$

$$M_{CB} + M_{CD} = 0$$

and substituting for the end moments expressed in terms of θ_B and θ_C leads to

$$\begin{aligned} \theta_B \left\{ \frac{3EI_1}{L_1} + \frac{4EI_2}{L_2} \right\} + \theta_C \left\{ \frac{2EI_2}{L_2} \right\} - \left\{ \frac{6EI_2}{L_2} \left(\frac{v_C - v_B}{L_2} \right) + \frac{3EI_1}{L_1} \left(\frac{v_B - v_A}{L_1} \right) \right\} + \left\{ M_{BC}^F + \left(M_{BA}^F - \frac{1}{2} M_{AB}^F \right) \right\} &= 0 \\ \theta_B \left\{ \frac{2EI_2}{L_2} \right\} + \theta_C \left\{ \frac{4EI_2}{L_2} + \frac{3EI_3}{L_3} \right\} - \left\{ \frac{6EI_2}{L_2} \left(\frac{v_C - v_B}{L_2} \right) + \frac{3EI_3}{L_3} \left(\frac{v_D - v_C}{L_3} \right) \right\} + \left\{ \left(M_{CD}^F - \frac{1}{2} M_{DC}^F \right) + M_{CB}^F \right\} &= 0 \end{aligned} \quad (10.21)$$

Given the nodal fixed end moments due to the loading and the chord rotations due to support settlement, one can solve the above simultaneous equations for

θ_B and θ_C , and determine the end moments by back substitution. Note that the solution depends on the relative magnitudes of the ratio, I/L , for each member.

In what follows, we list the modified slope-deflection equations for an end member AB or CD with a pin or roller support at either the A or D ends (see Fig. 10.12).

End member AB (exterior pin or roller at A end):

$$\begin{aligned} M_{AB} &= 0 \\ M_{BA_{\text{modified}}} &= \frac{3EI}{L} \left\{ \theta_B - \left(\frac{v_B - v_A}{L} \right) \right\} + \left(M_{BA}^F - \frac{1}{2} M_{AB}^F \right) \\ V_{AB_{\text{modified}}} &= \frac{3EI}{L^2} \left\{ \theta_B - \left(\frac{v_B - v_A}{L} \right) \right\} + V_{AB}^F - \frac{3}{2} \frac{M_{AB}^F}{L} \\ V_{BA_{\text{modified}}} &= \frac{3EI}{L^2} \left\{ \theta_B - \left(\frac{v_B - v_A}{L} \right) \right\} + V_{BA}^F + \frac{3}{2} \frac{M_{AB}^F}{L} \end{aligned} \quad (10.22a)$$

End member CD (exterior pin or roller at D end):

$$\begin{aligned} M_{DC} &= 0 \\ M_{CD_{\text{modified}}} &= \frac{3EI}{L} \left\{ \theta_C - \left(\frac{v_D - v_C}{L} \right) \right\} + \left(M_{CD}^F - \frac{1}{2} M_{DC}^F \right) \\ V_{CD_{\text{modified}}} &= \frac{3EI}{L^2} \left\{ \theta_C - \left(\frac{v_D - v_C}{L} \right) \right\} + V_{CD}^F + \frac{3}{2} \frac{M_{DC}^F}{L} \\ V_{DC_{\text{modified}}} &= -\frac{3EI}{L^2} \left\{ \theta_C - \left(\frac{v_D - v_C}{L} \right) \right\} + V_{DC}^F - \frac{3}{2} \frac{M_{DC}^F}{L} \end{aligned} \quad (10.22b)$$

Equations (10.22) are referred to as the *modified slope-deflection equations*.

Example 10.4 Two span beam with moment releases at both end

Given: The two span beam shown in Fig. E10.4a. Assume EI is constant.

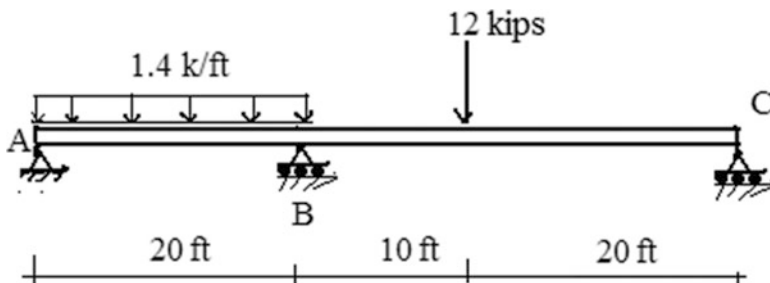


Fig. E10.4a

Determine: The end actions and the shear and moment diagrams.

Solution: The fixed end moments are (see Table 9.1):

$$M_{AB}^F = \frac{1.4(20)^2}{12} = 46.67 \text{ kip ft}$$

$$M_{BA}^F = -46.67 \text{ k ft}$$

$$M_{BC}^F = \frac{12(10)(20)^2}{(30)^2} = 53.33 \text{ kip ft}$$

$$M_{CB}^F = -\frac{12(20)(10)^2}{(30)^2} = -26.67 \text{ kip ft}$$

We define the relative member stiffness for each member as

$$k_{\text{member BC}} = \frac{EI}{L_{BC}} = k_1$$

$$k_{\text{member AB}} = \frac{EI}{L_{AB}} = 1.5 k_1$$

Next, we generate the expressions for the end moments using the modified slope-deflection equations (10.22).

$$M_{AB} = 0$$

$$M_{BA} = M_{BA_{\text{modified}}} = 3(1.5k_1)(\theta_B) + \left(M_{BA}^F - \frac{1}{2}M_{AB}^F \right) = 3(1.5k_1)(\theta_B) \\ + \left\{ -46.67 - \frac{1}{2}(46.67) \right\} = 4.5k_1 \theta_B - 70$$

$$M_{BC} = M_{BC_{\text{modified}}} = 3(k_1)(\theta_B) + \left(M_{BC}^F - \frac{1}{2}M_{CB}^F \right) = 3(k_1)(\theta_B) \\ + \left\{ +53.33 - \frac{1}{2}(-26.67) \right\} = 3k_1 \theta_B + 66.66$$

$$M_{CB} = 0$$

The moment equilibrium equation for node B expands to

$$M_{BA} + M_{BC} = 0$$

↓

$$7.5 k_1 \theta_B - 3.34 = 0$$

↓

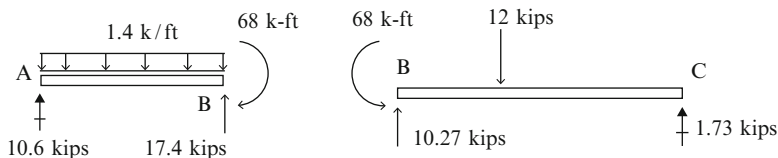
$$k_1 \theta_B = 0.4453$$

Finally, the bending moment at B is

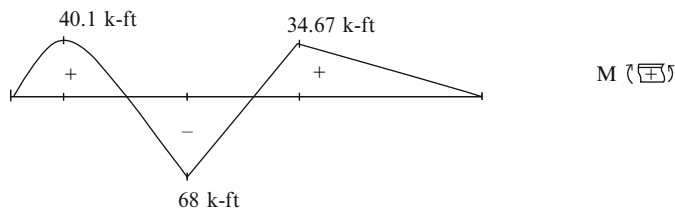
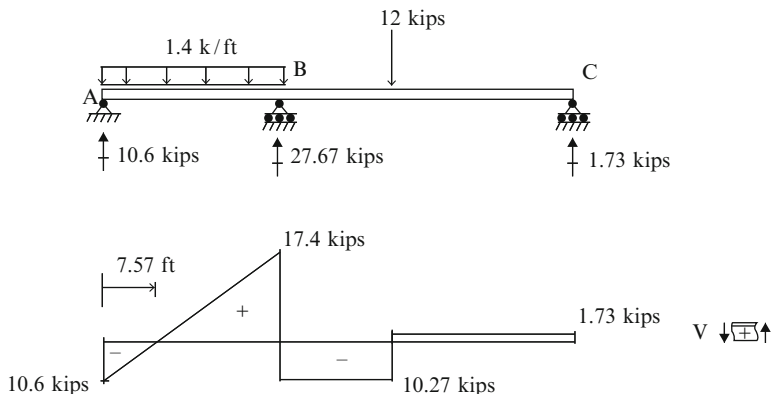
$$M_{BA} = -68 \text{ kip ft}$$

$$M_{BC} = -M_{BA} = 68 \text{ kip ft}$$

Noting the free body diagrams shown below, we find the remaining end actions.

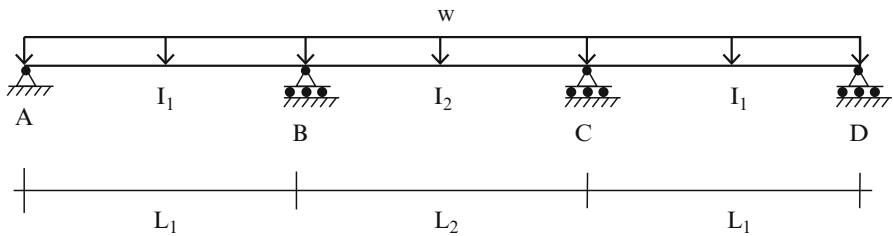


The shear and moment diagrams are plotted below.



Example 10.5 Three span beam

Given: The three span beam shown in Figs. E10.5a–c.

**Fig. E10.5a** Uniform load

Determine: The end moments and draw the moment diagram for

Case (i): uniform load w . No support settlement.

Case (ii): No loading. Support settlement at A. Consider I and L are constants.

Case (iii): No loading. Support settlement at B. Consider I and L are constants.

Solution:

Case (i): Uniform loading

The supports are unyielding. Therefore $v_A = v_B = v_C = 0$. The fixed end moments due to the uniform loading are (see Table 9.1)

$$\begin{aligned} M_{AB}^F &= +\frac{wL_1^2}{12} & M_{BA}^F &= -\frac{wL_1^2}{12} \\ M_{BC}^F &= +\frac{wL_2^2}{12} & M_{CB}^F &= -\frac{wL_2^2}{12} \\ M_{CD}^F &= +\frac{wL_1^2}{12} & M_{DC}^F &= -\frac{wL_1^2}{12} \end{aligned}$$

We use (10.22) for members AB and CD and (10.12) for member BC.

$$M_{AB} = 0$$

$$M_{BA} = M_{BA_{\text{modified}}} = \frac{3EI_1}{L_1} \theta_B + \left(M_{BA}^F - \frac{1}{2} M_{AB}^F \right) = \frac{3EI_1}{L_1} \theta_B - \frac{wL_1^2}{8}$$

$$M_{BC} = \frac{2EI_2}{L_2} \{2\theta_B + \theta_C\} + M_{BC}^F = \frac{2EI_2}{L_2} \{2\theta_B + \theta_C\} + \frac{wL_2^2}{12}$$

$$M_{CB} = \frac{2EI_2}{L_2} \{\theta_B + 2\theta_C\} + M_{CB}^F = \frac{2EI_2}{L_2} \{\theta_B + 2\theta_C\} - \frac{wL_2^2}{12}$$

$$M_{CD} = M_{CD_{\text{modified}}} = \frac{3EI_1}{L_1} \theta_C + \left(M_{CD}^F - \frac{1}{2} M_{DC}^F \right) = \frac{3EI_1}{L_1} \theta_C + \frac{wL_1^2}{8}$$

$$M_{DC} = 0$$

The nodal moment equilibrium equations are

$$M_{BA} + M_{BC} = 0$$

$$M_{CB} + M_{CD} = 0$$

Substituting for the end moments, the above equilibrium equations expand to

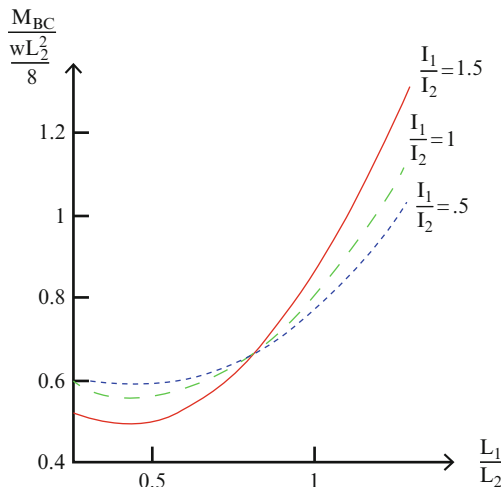
$$\begin{aligned}\theta_B \left\{ \frac{3EI_1}{L_1} + \frac{4EI_2}{L_2} \right\} + \theta_C \left\{ \frac{2EI_2}{L_2} \right\} &= -\frac{wL_2^2}{12} + \frac{wL_1^2}{8} \\ \theta_B \left\{ \frac{2EI_2}{L_2} \right\} + \theta_C \left\{ \frac{4EI_2}{L_2} + \frac{3EI_1}{L_1} \right\} &= -\frac{wL_1^2}{8} + \frac{wL_2^2}{12} \\ \Downarrow \\ \frac{EI_2}{L_2} \theta_B &= \frac{wL_2^2}{12} \left\{ \frac{-1 + \frac{3}{2}(L_1/L_2)^2}{2 + 3(I_1/I_2)(L_2/L_1)} \right\} \\ \theta_C &= -\theta_B\end{aligned}$$

The corresponding moments are

$$M_{BC} = \frac{wL_2^2}{8} \left\{ \frac{(L_1/L_2)^2 + (I_1/I_2)(L_2/L_1)}{1 + 3/2(I_1/I_2)(L_2/L_1)} \right\}$$

$$M_{CB} = -M_{BC}$$

We note that the moments are a function of (I_1/I_2) and (L_1/L_2) . The sensitivity of M_{BC} to the ratio (L_1/L_2) is plotted below for various values of (I_1/I_2) .



When I and L are constants for all the spans, the solution is

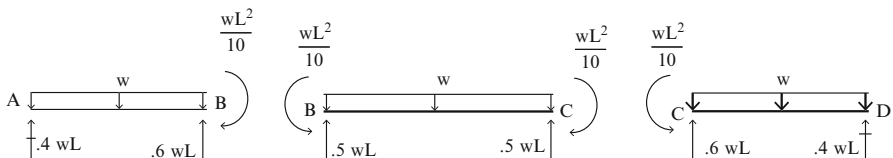
$$\begin{aligned}\theta_B &= \frac{wL^3}{24EI} \\ \theta_C &= -\frac{wL^3}{24EI}\end{aligned}$$

and

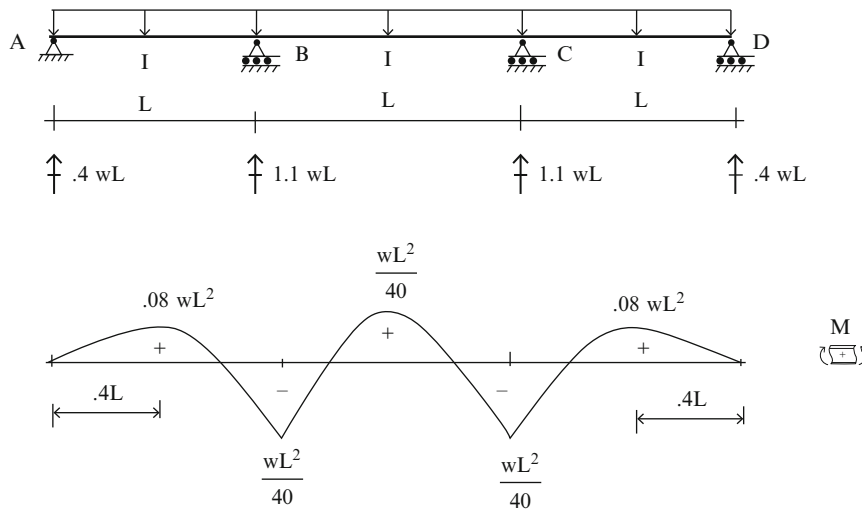
$$M_{BA} = M_{CB} = -\frac{wL^2}{10}$$

$$M_{BC} = M_{CD} = \frac{wL^2}{10}$$

We determine the end shear forces using the static equilibrium equations for the members.



The moment diagram is plotted below.



Case (ii): Support settlement at A, no loading, I and L are constants

The chord rotations are

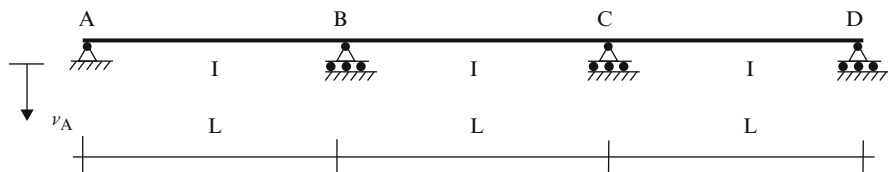


Fig. E10.5b Settlement at A

$$\rho_{AB} = +\frac{v_A}{L}$$

$$\rho_{BC} = \rho_{CD} = 0$$

Specializing (10.22) for members AB and CD and (10.12) for member BC for I and L constant, and the above notation results in

$$M_{BA \text{ modified}} = \frac{3EI}{L} \left\{ \theta_B + \frac{v_A}{L} \right\}$$

$$M_{BC} = \frac{2EI}{L} \{ 2\theta_B + \theta_C \}$$

$$M_{CB} = \frac{2EI}{L} \{ \theta_B + 2\theta_C \}$$

$$M_{CD \text{ modified}} = \frac{3EI}{L} \{ \theta_C \}$$

The nodal moment equilibrium equations are

$$M_{BA} + M_{BC} = 0 \quad \Rightarrow \quad 7\theta_B + 2\theta_C = \frac{3v_A}{L}$$

$$M_{CB} + M_{CD} = 0 \quad \Rightarrow \quad 2\theta_B + 7\theta_C = 0$$

The solution is

$$\theta_B = \frac{7v_A}{15L}$$

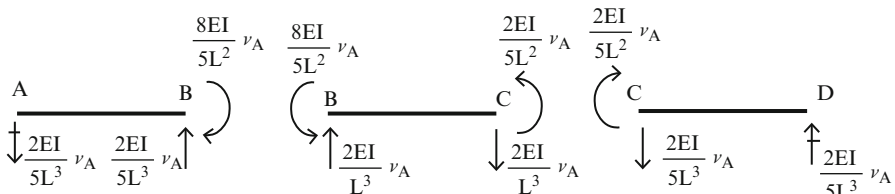
$$\theta_C = -\frac{2v_A}{15L}$$

and the corresponding moments are

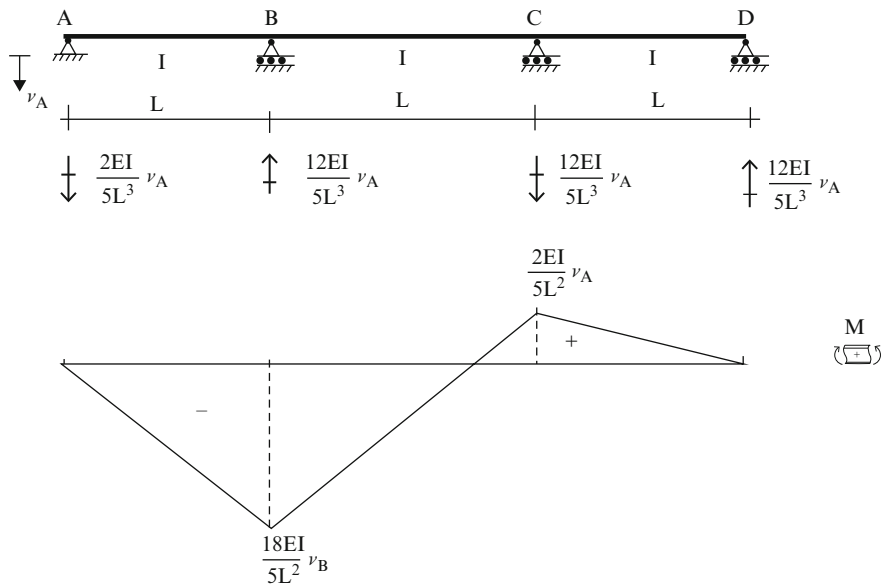
$$M_{BA} = -\frac{8EI}{5L^2} v_A$$

$$M_{CD} = \frac{2EI}{5L^2} v_A$$

We determine the end shear forces using the static equilibrium equations for the members.



The moment diagram is plotted below.



Case (iii): Support settlement at B, no loading, I and L are constants

The chord rotations are

$$\rho_{AB} = -\frac{v_B}{L}$$

$$\rho_{BC} = +\frac{v_B}{L}$$

$$\rho_{CD} = 0$$

Specializing (10.22) for members AB and CD and (10.12) for member BC for I

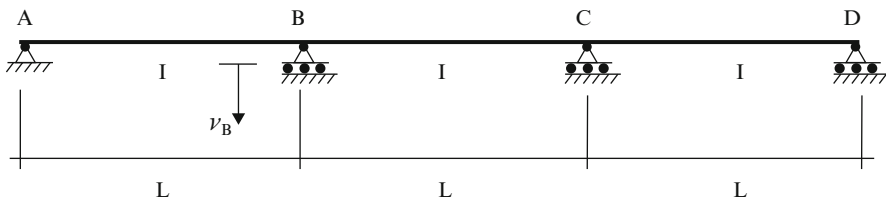


Fig. E10.5c Settlement at B

and L constant, and the above notation results in

$$M_{BA \text{ modified}} = \frac{3EI}{L} \left\{ \theta_B + \left(\frac{v_B}{L} \right) \right\}$$

$$M_{BC} = \frac{2EI}{L} \left\{ 2\theta_B + \theta_C - 3 \frac{v_B}{L} \right\}$$

$$M_{CB} = \frac{2EI}{L} \left\{ \theta_B + 2\theta_C - 3 \frac{v_B}{L} \right\}$$

$$M_{CD \text{ modified}} = \frac{3EI}{L} \{ \theta_C \}$$

The nodal moment equilibrium equations are

$$\begin{aligned} M_{BA} + M_{BC} &= 0 & 7\theta_B + 2\theta_C &= 0 \\ M_{CB} + M_{CD} &= 0 & \Rightarrow & \\ & & 2\theta_B + 7\theta_C &= \frac{6v_B}{L} \end{aligned}$$

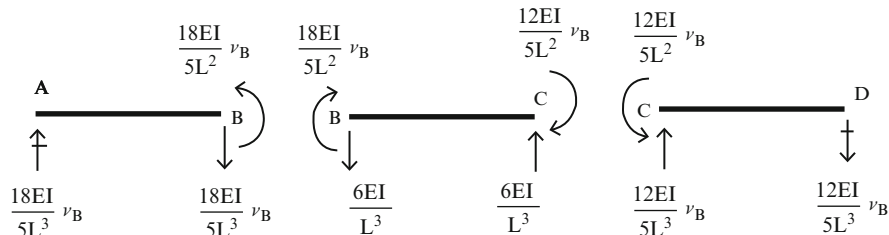
The solution is

$$\begin{aligned} \theta_B &= \frac{v_B}{5L} \\ \theta_C &= \frac{4v_B}{5L} \end{aligned}$$

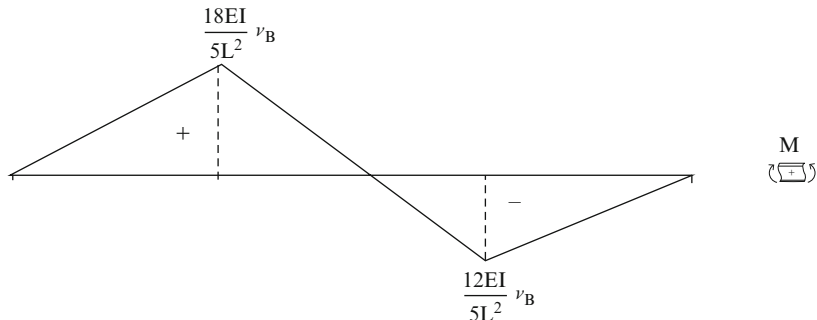
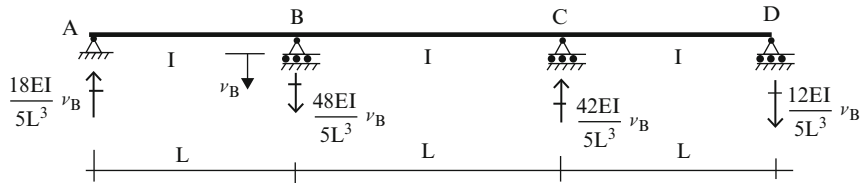
and the corresponding moments are

$$\begin{aligned} M_{BA} &= \frac{18EI}{5L^2} v_B \\ M_{CD} &= \frac{12EI}{5L^2} v_B \end{aligned}$$

We determine the end shear forces using the static equilibrium equations for the members.



Noting the free body diagrams, we find the reactions. The moment diagram is plotted below.



Example 10.6 Uniformly loaded three span symmetrical beam—fixed ends

Given: The three span symmetrical fixed end beam defined in Fig. E10.6a. This model is representative of an integral bridge with very stiff abutments at the ends of the beam.

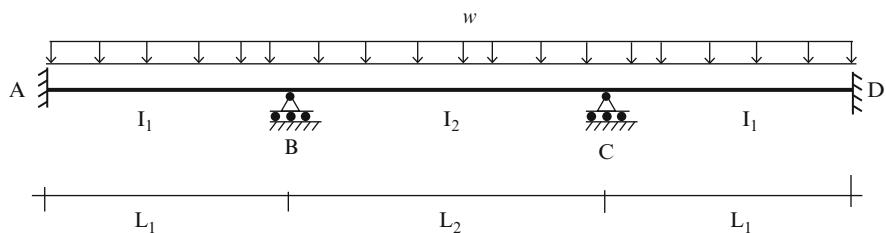


Fig. E10.6a

Determine: The end moments.

Solution: The slope-deflection equations for unyielding supports, $\theta_A = \theta_D = 0$ and symmetry $\theta_B = -\theta_C$ are

$$M_{AB} = -M_{DC} = \frac{2EI_1}{L_1}(\theta_B) + M_{AB}^F$$

$$M_{BA} = \frac{2EI_1}{L_1}(2\theta_B) + M_{BA}^F$$

$$M_{BC} = -M_{CB} = \frac{2EI_2}{L_2}(\theta_B) + M_{BC}^F$$

Where

$$M_{AB}^F = M_{CD}^F = +\frac{wL_1^2}{12}$$

$$M_{BA}^F = M_{DC}^F - \frac{wL_1^2}{12}$$

$$M_{BC}^F = +\frac{wL_2^2}{12}$$

$$M_{CB}^F = -\frac{wL_2^2}{12}$$

Summing end moments at node B

$$\begin{aligned} M_{BA} + M_{BC} &= 0 \\ \Downarrow \\ \theta_B \left\{ \frac{4EI_1}{L_1} + \frac{2EI_2}{L_2} \right\} &= -(M_{BA}^F + M_{BC}^F) \end{aligned}$$

and solving for θ_B leads to

$$\theta_B = -\theta_C = \frac{((wL_1^2/12) - (wL_2^2/12))}{((4EI_1/L_1) + (2EI_2/L_2))}$$

Suppose I and L are constants. The end rotations corresponding to this case are

$$\theta_B = \theta_C = 0$$

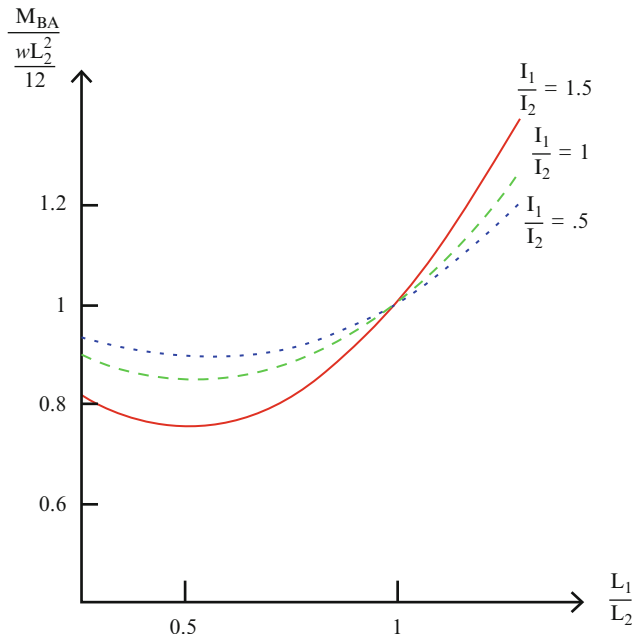
It follows that the end moments are equal to the fixed end moments.

$$\begin{aligned} M_{AB} &= \frac{wL^2}{12} \\ M_{BA} = -M_{BC} &= -\frac{wL^2}{12} \end{aligned}$$

The general solution for the moment at B follows by substituting for θ_B in either the expression for M_{BA} or M_{BC} . After some algebraic manipulation, the expression for M_{BA} reduces to

$$M_{BA} = \frac{wL_2^2}{12} \frac{\{(L_1/L_2)^2 + 2(I_1/I_2)(L_2/L_1)\}}{(1 + 2(I_1/I_2)(L_2/L_1))}$$

We note that the moments are a function of (I_1/I_2) and (L_1/L_2) . The sensitivity of M_{BA} to the ratio (L_1/L_2) is plotted below for various values of (I_1/I_2) .



10.5 The Displacement Method Applied to Rigid Frames

The essential difference between the analysis of beams and frames is the choice of the nodal displacements. The nodal variables for a beam are taken as the rotations. When there is support movement, we prescribe the nodal translation and compute the corresponding fixed end moments. In this way, the equilibrium equations always involve only rotation variables. Rigid frames are considered to be an assemblage of members rigidly connected at nodes. Since frame structures are formed by joining members at an arbitrary angle the members rotate as well as bend. When this occurs, we need to include the chord rotation terms in the slope-deflection equations, and work with both translation and rotation variables. Using these relations, we generate a set of equations relating the nodal translations and rotations by enforcing equilibrium for the nodes. The approach is relatively straightforward when there are no many displacement variables. However, for complex structures involving many displacement unknowns, one would usually employ a computer program which automates the generation and solution of the equilibrium equations.

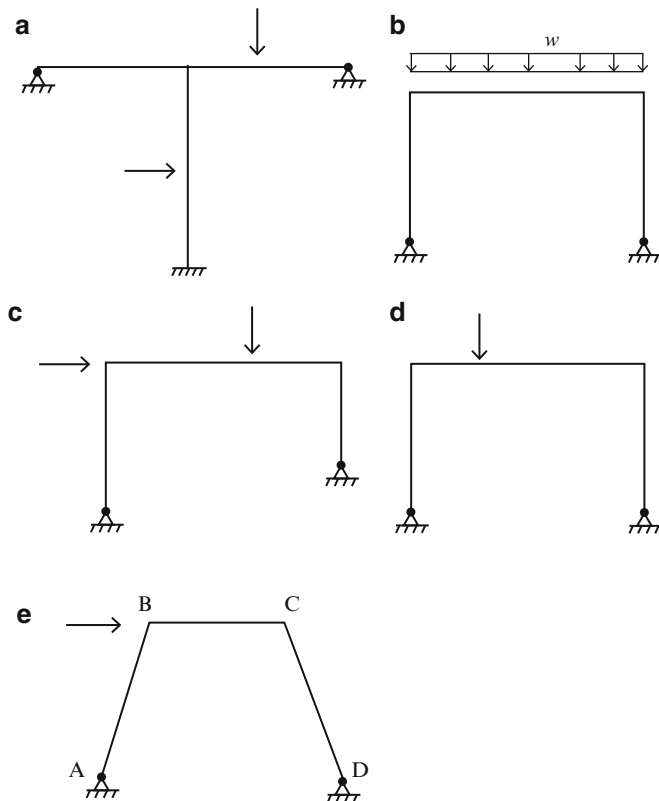


Fig. 10.13 Examples of sidesway

The term, “sideway” is used to denote the case where some of the members in a structure experience chord rotation resulting in “sway” of the structure. Whether sideway occur depends on how the members are arranged and also depends on the loading applied. For example, consider the frame shown in Fig. 10.13a. Sideway is not possible because of the horizontal restraint. The frame shown in Fig. 10.13b is symmetrical and also loaded symmetrically. Because of symmetry, there will be no sway. The frame shown in Fig. 10.13c will experience sideway. The symmetrical frame shown in Fig. 10.13d will experience sideway because of the unsymmetrical loading. All three members will experience chord rotation for the frame shown in Fig. 10.13e.

When starting an analysis, one first determines whether sideway will occur in order to identify the nature of the displacement variables. The remaining steps are relatively straight forward. One establishes the free body diagram for each node and enforces the equilibrium equations. The essential difference is that now one needs to consider force equilibrium as well as moment equilibrium. We illustrate the analysis process with the following example.

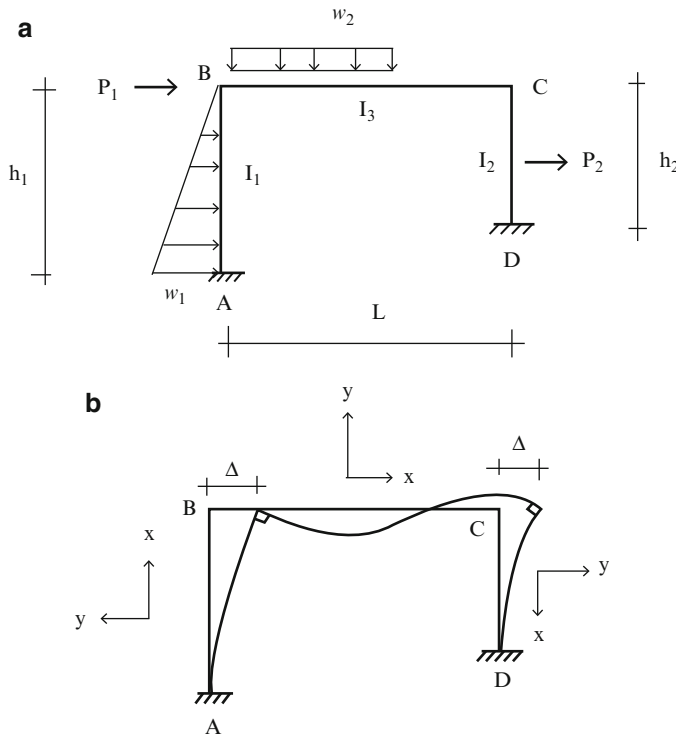


Fig. 10.14 (a) Loading. (b) Deflected shape

Consider the frame shown in Fig. 10.14. Under the action of the applied loading, nodes B and C will displace horizontally an amount Δ . Both members AB and CD will have chord rotation. There are three displacement unknowns θ_B , θ_C , and Δ . In general we neglect the axial deformation. The free body diagrams for the members and nodes are shown in Fig. 10.15. We take the positive sense of the members to be from A \rightarrow B, B \rightarrow C, and C \rightarrow D. Note that this fixes the sense of the shear forces. The end moments are always positive when counterclockwise.

Moment equilibrium for nodes B and C requires

$$\begin{aligned}\sum M_B &= 0 \Rightarrow M_{BA} + M_{BC} = 0 \\ \sum M_C &= 0 \Rightarrow M_{CB} + M_{CD} = 0\end{aligned}\tag{10.23a}$$

We also need to satisfy horizontal force equilibrium for the entire frame.

$$\sum F_x = 0 \rightarrow + \Rightarrow -V_{AB} + V_{CD} + \sum F_x = 0\tag{10.23b}$$

where $\sum F_x = P_1 + P_2 + \frac{1}{2}w_1h_1$

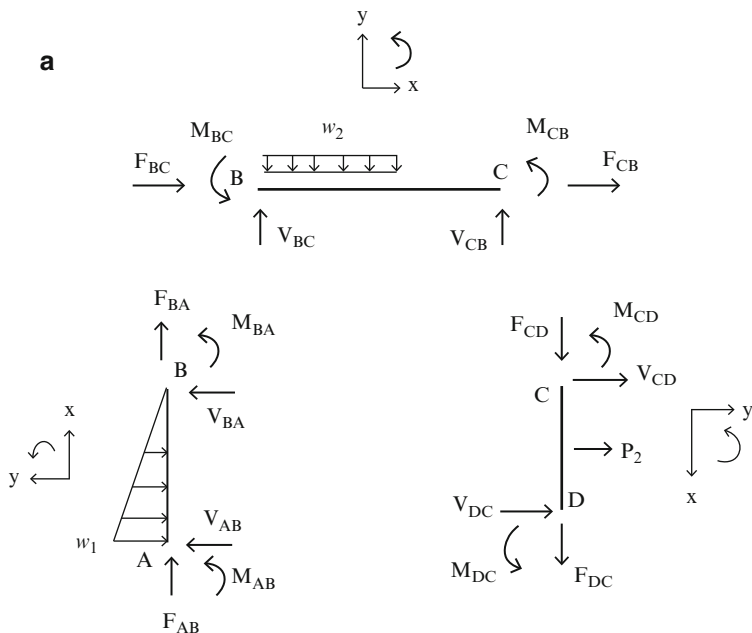
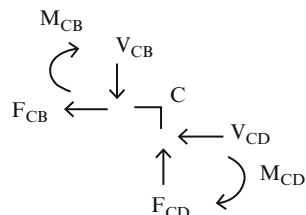
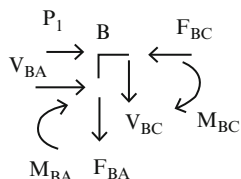
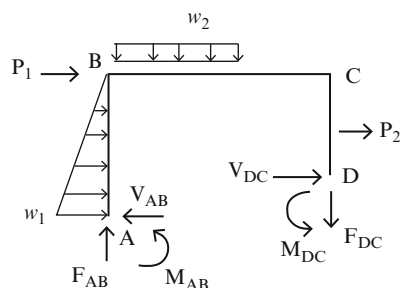
**b**

Fig. 10.15 Free body diagrams for members and nodes of the frame. (a) Members. (b) nodes



The latter equation is associated with sideway.

Noting that $\theta_A = \theta_D = 0$, $v_A = v_D = 0$, $v_B = -\Delta$, and $v_C = +\Delta$ the slope-deflection equations (10.12) simplify to

$$\begin{aligned}
 M_{AB} &= \frac{2EI_1}{h_1} \left\{ \theta_B - 3 \left(\frac{-\Delta}{h_1} \right) \right\} + M_{AB}^F \\
 M_{BA} &= \frac{2EI_1}{h_1} \left\{ 2\theta_B - 3 \left(\frac{-\Delta}{h_1} \right) \right\} + M_{BA}^F \\
 M_{BC} &= \frac{2EI_3}{L} \{ 2\theta_B + \theta_C \} + M_{BC}^F \\
 M_{CB} &= \frac{2EI_3}{L} \{ 2\theta_C + \theta_B \} + M_{CB}^F \\
 M_{CD} &= \frac{2EI_2}{h_2} \left\{ 2\theta_C - 3 \left(\frac{-\Delta}{h_2} \right) \right\} + M_{CD}^F \\
 M_{DC} &= \frac{2EI_2}{h_2} \left\{ \theta_C - 3 \left(\frac{-\Delta}{h_2} \right) \right\} + M_{DC}^F \\
 V_{AB} &= \frac{6EI_1}{h_1^2} \left\{ \theta_B + 2 \frac{\Delta}{h_1} \right\} + V_{AB}^F \\
 V_{DC} &= -\frac{6EI_2}{h_2^2} \left\{ \theta_C + 2 \frac{\Delta}{h_2} \right\} + V_{DC}^F
 \end{aligned} \tag{10.24}$$

Substituting for the end moments and shear forces, in (10.23) leads to

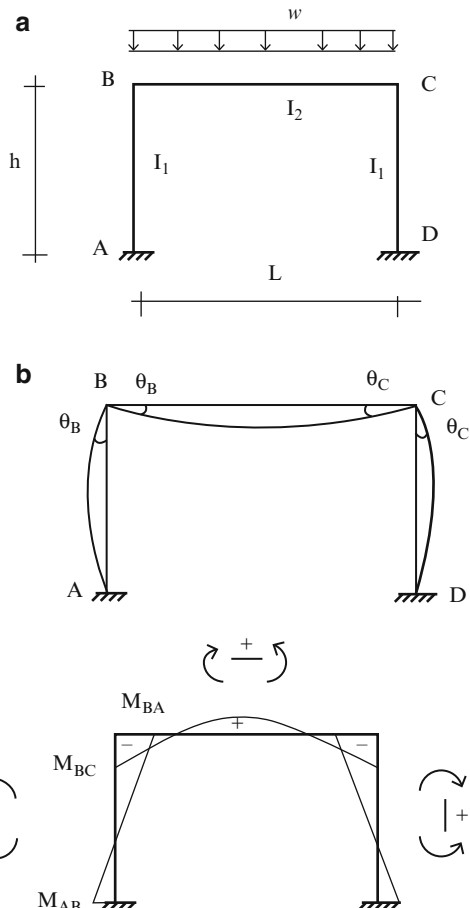
$$\begin{aligned}
 \left(\frac{4EI_1}{h_1} + \frac{4EI_3}{L} \right) \theta_B + \frac{2EI_3}{L} \theta_C + \frac{6EI_1}{h_1} \left(\frac{\Delta}{h_1} \right) + (M_{BC}^F + M_{BA}^F) &= 0 \\
 \frac{2EI_3}{L} \theta_B + \left(\frac{4EI_3}{L} + \frac{4EI_2}{h_2} \right) \theta_C + \frac{6EI_2}{h_2} \left(\frac{\Delta}{h_2} \right) + (M_{CD}^F + M_{CB}^F) &= 0 \\
 -\frac{6EI_1}{h_1} \theta_B - \frac{6EI_2}{h_2} \theta_C + \left(-\frac{12EI_1}{h_1^2} - \frac{12EI_2}{h_2^2} \right) \Delta - V_{AB}^F + V_{DC}^F + \sum F_x &= 0
 \end{aligned} \tag{10.25}$$

Once the loading and properties are specified, one can solve (10.25) for θ_B , θ_C , and Δ . The end actions are then evaluated with (10.24).

10.5.1 Portal Frames: Symmetrical Loading

Consider the symmetrical frame defined in Fig. 10.16. When the loading is also symmetrical, nodes B and C do not displace laterally, and therefore there is no chord rotation for members AB and CD. Also, the rotations at B and C are equal in magnitude but opposite in sense ($\theta_B = -\theta_C$). With these simplifications, the expressions for the end moments reduce to

Fig. 10.16 Portal frame—symmetrical loading. (a) Loading. (b) Deflected shape. (c) Moment diagram



$$\begin{aligned}
 M_{BC} &= \frac{2EI_2}{L}(\theta_B) + M_{BC}^F \\
 M_{BA} &= \frac{2EI_1}{h}(2\theta_B) \\
 M_{AB} &= \frac{1}{2}M_{BA}
 \end{aligned} \tag{10.26}$$

Moment equilibrium for node B requires

$$M_{BC} + M_{BA} = 0 \tag{10.27}$$

Substituting for the moments, the equilibrium equation expands to

$$2EI_B \left\{ 2 \frac{I_1}{h} + \frac{I_2}{L} \right\} = -M_{BC}^F$$

We solve for θ_B and then evaluate M_{BA} .

$$M_{BA} = \frac{-1}{1 + (I_2/L)/2(I_1/h)} M_{BC}^F \quad (10.28)$$

The bending moment diagram is plotted in Fig. 10.16c.

10.5.2 Portal Frames Anti-symmetrical Loading

Lateral loading produces anti-symmetrical behavior, as indicated in Fig. 10.17, and chord rotation for members AB and CD. In this case, the nodal rotations at B and C are equal in both magnitude and sense ($\theta_B = \theta_C$). The chord rotation is related to the lateral displacement of B by

$$\rho_{AB} = -\frac{v_B}{h} \quad (10.29)$$

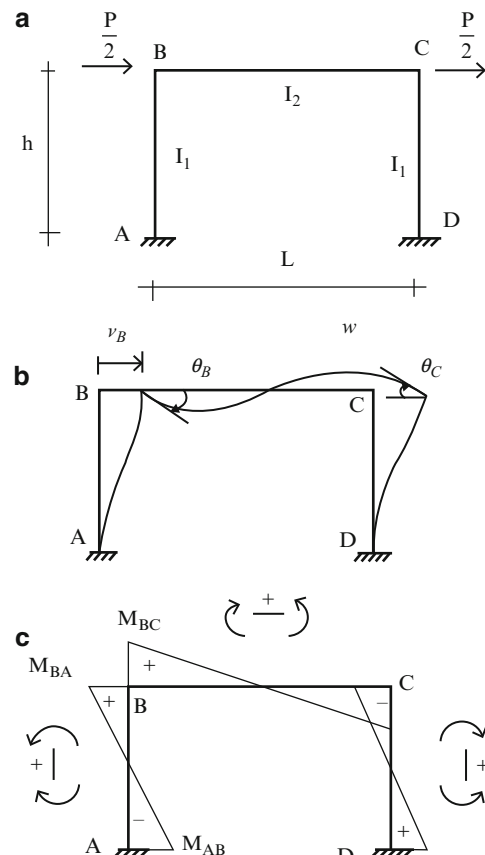


Fig. 10.17 Portal frame—anti-symmetric loading.
(a) Loading. (b) Deflected shape. (c) Moment diagram

Note that the chord rotation sign convention for the slope-deflection equations (10.12) is positive when counterclockwise. Therefore for this choice of the sense of v_B , the chord rotation for AB is negative. The corresponding expressions for the end moments are

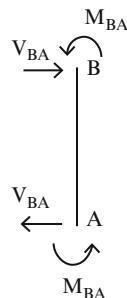
$$\begin{aligned} M_{BC} &= 2E \frac{I_2}{L} (3\theta_B) \\ M_{BA} &= 2E \frac{I_1}{h} \left(2\theta_B + \frac{3v_B}{h} \right) \\ M_{AB} &= 2E \frac{I_1}{h} \left(\theta_B + \frac{3v_B}{h} \right) \end{aligned} \quad (10.30)$$

Equilibrium requires

$$\begin{aligned} M_{BC} + M_{BA} &= 0 \\ -V_{AB} + \frac{P}{2} &= 0 \end{aligned} \quad (10.31)$$

We determine the end shear with the moment equilibrium equation for member AB.

$$\begin{aligned} V_{AB} &= \frac{M_{BA} + M_{AB}}{h} \\ &= \frac{2EI_1}{h^2} \left(3\theta_B + 6 \frac{v_B}{h} \right) \end{aligned} \quad (10.32)$$



Substituting for the moments and shear in (10.31) leads to two equations in two unknowns, θ_B and v_B . The solution has the following form

$$\begin{aligned} \theta_B &= \frac{-h^2 P}{4EI_1} \frac{1}{1 + 6(I_2/L)/(I_1/h)} \\ v_B &= \frac{h^3 P}{24EI_1} \left(\frac{1 + \frac{2}{3}((I_1/h)/(I_2/L))}{1 + (I_1/h)/6(I_2/L)} \right) \end{aligned} \quad (10.33)$$

We evaluate M_{BA} and M_{AB} using (10.30).

$$M_{BA} = \frac{Ph}{4} \frac{1}{1 + \frac{1}{6}(I_1/h)/(I_2/L)} \quad (10.34)$$

$$M_{AB} = \frac{Ph}{4} \frac{1 + 1/3(I_1/h)/(I_2/L)}{1 + 1/6(I_1/h)/(I_2/L)}$$

A typical moment diagram is shown in Fig. 10.17c. Note the sign convention for bending moment.

When the girder is very stiff with respect to the column, $I_2/L \gg I_1/h$ the solution approaches

$$\theta_B \rightarrow 0$$

$$v_B \rightarrow \frac{h^3 P}{24EI_1}$$

$$M_{BA} \rightarrow \frac{Ph}{4}$$

$$M_{AB} \rightarrow \frac{Ph}{4} \quad (10.35)$$

Example 10.7 Frame with no sideway

Given: The frame defined in Fig. E10.7a.

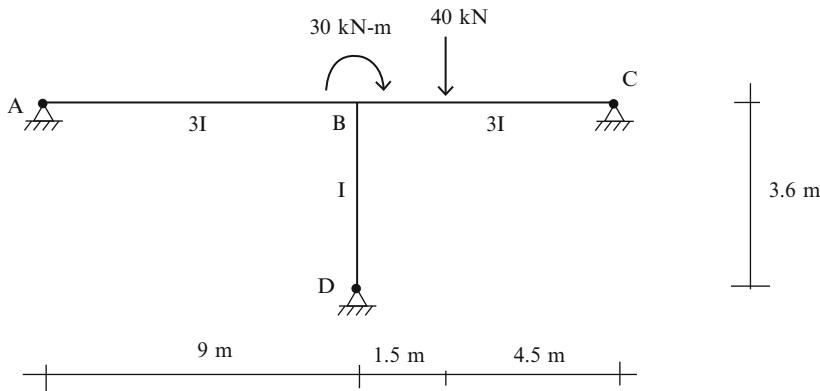


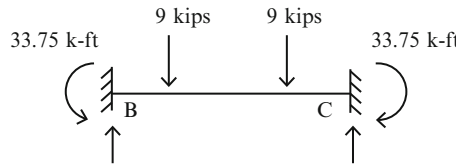
Fig. E10.7a

Determine: The end actions.

Solution: The fixed end moments are (see Table 9.1)

$$M_{BC}^F = \frac{40(1.5)(4.5)^2}{(6)^2} = 33.75 \text{ kN m}$$

$$M_{CB}^F = \frac{40(4.5)(1.5)^2}{(6)^2} = -11.25 \text{ kN m}$$



The modified slope-deflection equations (10.22) which account for moment releases at A, C, D are

$$M_{AB} = M_{DB} = M_{CB} = 0$$

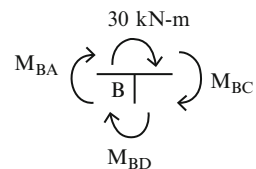
$$M_{BA} = M_{BA_{\text{modified}}} = 3 \frac{E(3I)}{9} (\theta_B) = EI\theta_B$$

$$M_{BD} = M_{BD_{\text{modified}}} = 3 \frac{E(I)}{3.6} (\theta_B) = (0.83)EI\theta_B$$

$$M_{BC} = M_{BC_{\text{modified}}} = 3 \frac{E(3I)}{6} (\theta_B) + \left\{ M_{BC}^F - \frac{1}{2}M_{CB}^F \right\} = (1.5)EI\theta_B + 39.375$$

Moment equilibrium for node B requires (Fig. E10.7b)

Fig. E10.7b



$$M_{BA} + M_{BC} + M_{BD} + 30 = 0$$

⇓

$$EI\theta_B + (0.83)EI\theta_B + (1.5)EI\theta_B + 39.375 + 30 = 0$$

⇓

$$EI\theta_B = -20.83$$

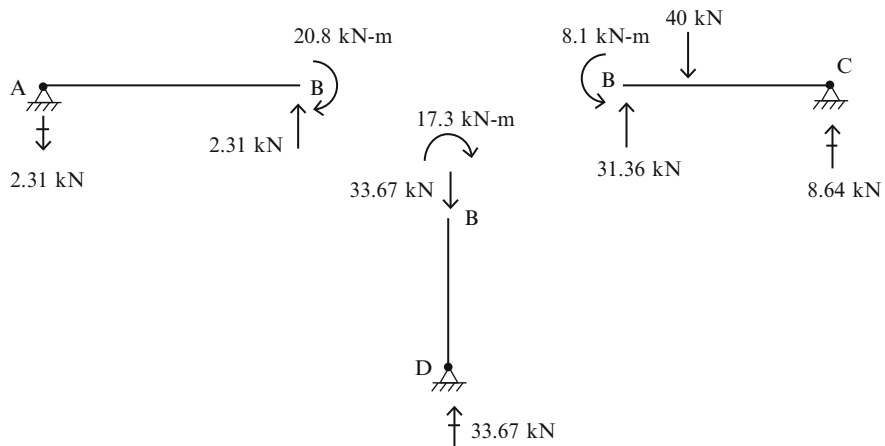
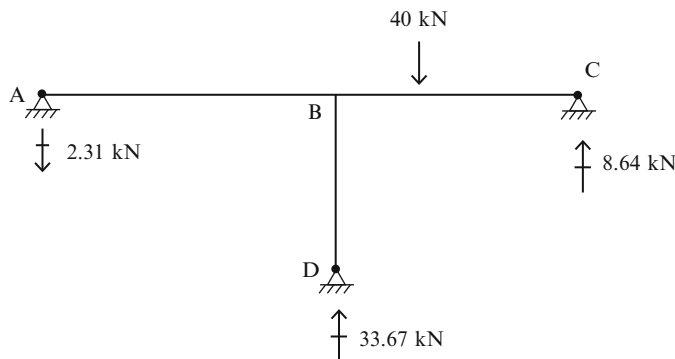
The final bending moments at B are

$$M_{BA} = -20.8 \Rightarrow M_{BA} = 20.8 \text{ kN m clockwise}$$

$$M_{BD} = -17.3 \Rightarrow M_{BD} = 17.3 \text{ kN m clockwise}$$

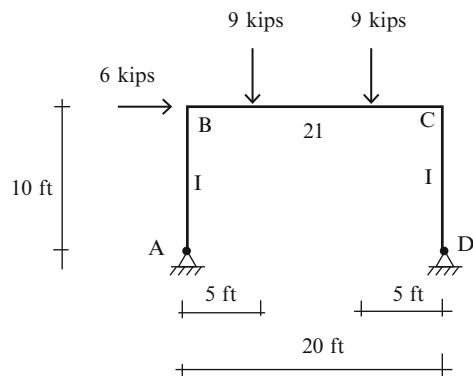
$$M_{BC} = 8.1 \Rightarrow M_{BC} = 8.1 \text{ kN m counterclockwise}$$

Noting the free body diagrams below, we find the remaining end actions (Figs. E10.7c, d).

**Fig. E10.7c** Free body diagrams**Fig. E10.7d** Reactions

Example 10.8 Frame with sideway

Given: The frame defined in Fig. E10.8a.

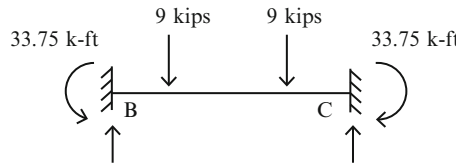
**Fig. E10.8a**

Determine: The end actions.

Solution: The fixed end moments are (see Table 9.1)

$$M_{BC}^F = \frac{9(5)(15)^2}{20^2} + \frac{9(15)(5)^2}{20^2} = 33.75 \text{ kip ft}$$

$$M_{CB}^F = -M_{BC}^F = -33.75 \text{ kip ft}$$



The chord rotations follow from the sketch below (Fig. E10.8b):

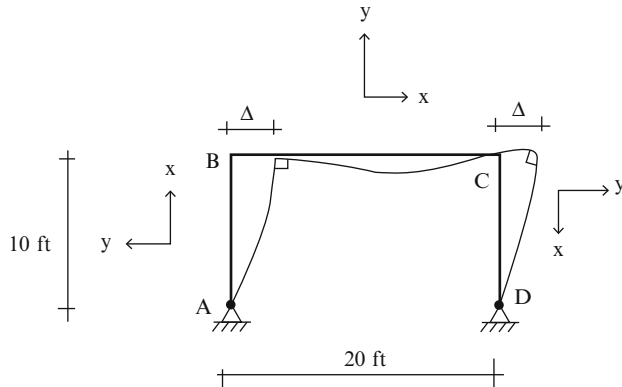


Fig. E10.8b

$$\rho_{AB} = \rho_{CD} = -\frac{\Delta}{10}$$

$$\rho_{BC} = 0$$

Substituting for the chord rotations in the slope-deflection equations [(10.12) and (10.22)] results in (Figs. E10.8c, d)

$$M_{AB} = M_{DC} = 0$$

$$M_{BA} = M_{BA_{\text{modified}}} = \frac{3E(I)}{10} \left\{ \theta_B + \frac{\Delta}{10} \right\} = 0.3EI\theta_B + 0.03EI\Delta$$

$$M_{BC} = \frac{2E(2I)}{20} \{2\theta_B + \theta_C\} + 33.75 = 0.4EI\theta_B + 0.2EI\theta_C + 33.75$$

$$M_{CB} = \frac{2E(2I)}{20} \{\theta_B + 2\theta_C\} - 33.75 = 0.2EI\theta_B + 0.4EI\theta_C - 33.75$$

$$M_{CD} = M_{CD_{\text{modified}}} = \frac{3E(I)}{10} \left\{ \theta_C + \frac{\Delta}{10} \right\} = 0.3EI\theta_C + 0.03EI\Delta$$

Also

$$V_{AB} = \frac{M_{BA}}{10}$$

$$V_{DC} = -\frac{M_{CD}}{10}$$

The end actions are listed in Fig. E10.8c.

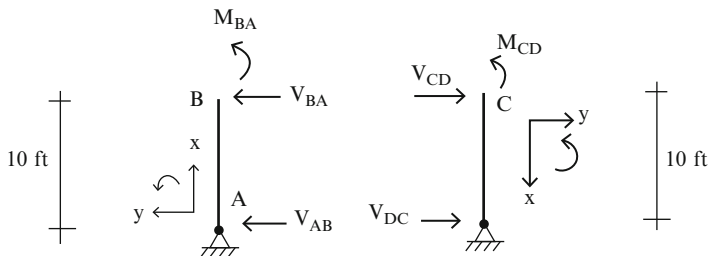


Fig. E10.8c

Enforcing equilibrium at nodes B and C yields two equations,

$$M_{BC} + M_{BA} = 0 \rightarrow 0.7EI\theta_B + 0.2EI\theta_C + 0.03EI\Delta + 33.75 = 0$$

$$M_{CB} + M_{CD} = 0 \rightarrow 0.2EI\theta_B + 0.7EI\theta_C + 0.03EI\Delta - 33.75 = 0$$

Summing horizontal forces for the entire frame leads to an additional equation,

$$\begin{aligned} \sum F_x = 0 &\rightarrow -V_{AB} + V_{DC} + 6 = 0 \\ &\downarrow \\ &-0.3EI\theta_B - 0.3EI\theta_C - 0.06EI + 60 = 0 \end{aligned}$$

Solving these three equations, one obtains

$$\begin{cases} EI\theta_B = -117.5 \\ EI\theta_C = 17.5 \\ EI\Delta = 1,500 \end{cases}$$

and then

$$\left\{ \begin{array}{lll} M_{BA} = +9.75 & M_{BA} = 9.75 \text{ kip ft} & \text{counterclockwise} \\ M_{BC} = -9.75 & M_{BC} = 9.75 \text{ kip ft} & \text{clockwise} \\ M_{CB} = -50.25 & M_{CB} = 50.25 \text{ kip ft} & \text{clockwise} \\ M_{CD} = +50.25 & M_{CD} = 50.25 \text{ kip ft} & \text{counterclockwise} \\ V_{AB} = .975 & V_{AB} = .975 \text{ kip} & \leftarrow \\ V_{DC} = -5.25 & V_{DC} = 5.25 \text{ kip} & \leftarrow \end{array} \right.$$

Noting the free body diagrams below, we find the remaining end actions (Figs. E10.8d, e).

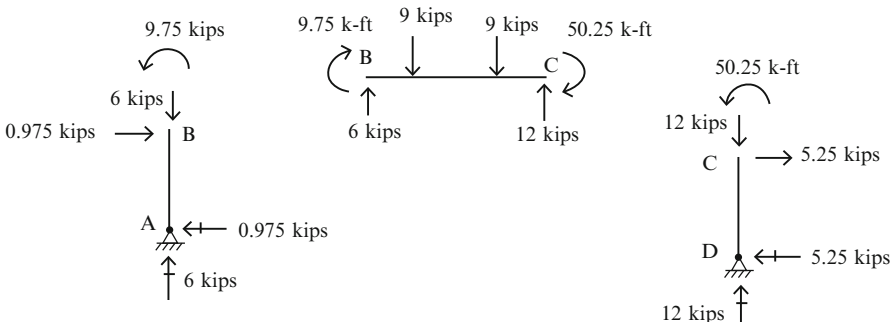


Fig. E10.8d Free body diagrams

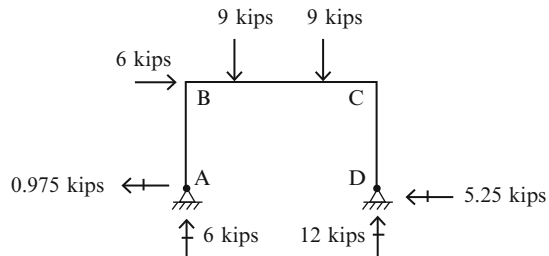


Fig. E10.8e Reactions

10.6 The Moment Distribution Solution Procedure for Multi-span Beams

10.6.1 Introduction

In the previous sections, we developed an analysis procedure for multi-span beams that is based on using the slope-deflection equations to establish a set of simultaneous equations relating the nodal rotations. These equations are equivalent to the nodal moment equilibrium equations. We generated the solution by solving these equations for the rotations and then, using these values, we determined the end moments and end shears. The solution procedure is relatively straightforward from

a mathematical perspective, but it is difficult to gain some physical insight as to how the structure is responding during the solution process. This is typical of mathematical procedures which involve mainly number crunching and are ideally suited for computer-based solution schemes.

The Moment Distribution Method is a solution procedure developed by Structural Engineers to solve the nodal moment equilibrium equations. The method was originally introduced by Hardy Cross [21] and has proven to be an efficient hand-based computational scheme for beam- and frame-type structures. Its primary appeal is its computational simplicity.

The solution is generated in an iterative manner. Each iteration cycle involves only two simple computations. Another attractive feature is the fact that one does not have to formulate the nodal equilibrium equations expressed in terms of the nodal displacements. The method works directly with the end moments. This feature allows one to assess convergence by comparing successive values of the moments as the iteration progresses. In what follows, we illustrate the method with a series of beam-type examples. Later, we extend the method to frame-type structures.

Consider the two span beam shown in Fig. 10.18. Supports A and C are fixed, and we assume that there is no settlement at B.

We assume initially that there is no rotation at B. Noting Fig. 10.19; the net unbalanced clockwise nodal moment at B is equal to the sum of the fixed end moments for the members incident on node B.

$$+ \curvearrowleft M_{\text{net}} = + \sum M_B^F = + M_{BA}^F + M_{BC}^F$$

This unbalanced moment will cause node B to rotate until equilibrium is restored. Using the slope-deflection equations, we note that the increment in the end moment for a member which is incident on B due to a counterclockwise rotation at B is proportional to the relative stiffness I/L for the member.

$$\begin{aligned} \Delta M, \theta_B + \curvearrowleft & \Delta M_{BA} = \frac{4EI_1}{L_1} \theta_B \\ & \Delta M_{BC} = \frac{4EI_2}{L_2} \theta_B \end{aligned} \quad (10.36)$$

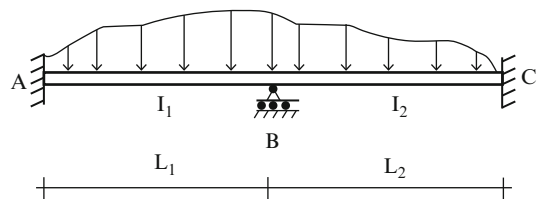


Fig. 10.18 Two span beam with fixed ends

Fig. 10.19 Nodal moments

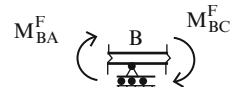
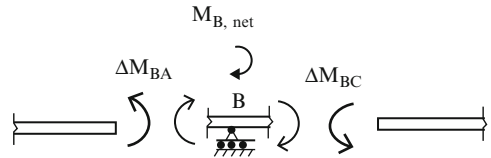


Fig. 10.20 Moment equilibrium for node B



The moments acting on the node are of opposite sense, i.e., clockwise, from Newton's law. The equilibrium state for the node is shown in Fig. 10.20.

Equilibrium requires the moment sum to vanish.

$$\Delta M_{BA} + \Delta M_{BC} + M_{B,\text{net}} = 0$$

Substituting for the moment increments yields an equation for θ_B

$$\begin{aligned} \left(\frac{4EI_1}{L_1} + \frac{4EI_2}{L_2} \right) \theta_B &= -M_{B,\text{net}} \\ \Downarrow \\ \theta_B &= \frac{1}{((4EI_1/L_1) + (4EI_2/L_2))} (-M_{B,\text{net}}) \end{aligned} \quad (10.37)$$

Lastly, we use this value of θ_B to evaluate the incremental end moments.

$$\begin{aligned} \Delta M_{BA} &= \frac{(4EI_1/L_1)}{((4EI_1/L_1) + (4EI_2/L_2))} (-M_{B,\text{net}}) \\ \Delta M_{BC} &= \frac{(4EI_2/L_2)}{((4EI_1/L_1) + (4EI_2/L_2))} (-M_{B,\text{net}}) \end{aligned} \quad (10.38)$$

The form of the solution suggests that we define a dimensionless factor, DF, for each member as follows

$$\begin{aligned} DF_{BA} &= \frac{I_1/L_1}{(I_1/L_1) + (I_2/L_2)} \\ DF_{BC} &= \frac{I_2/L_2}{(I_1/L_1) + (I_2/L_2)} \end{aligned} \quad (10.39)$$

Note that $DF_{BA} + DF_{BC} = 1.0$. With this notation, the expressions for the incremental end moments reduce to

$$\begin{aligned} \Delta M_{BA} &= -DF_{BA}(M_{B,\text{net}}) \\ \Delta M_{BC} &= -DF_{BC}(M_{B,\text{net}}) \end{aligned} \quad (10.40)$$

One distributes the unbalanced fixed end moment to the members incident on the node according to their distribution factors which depend on their relative stiffness.

The nodal rotation at B produces end moments at A and C. Again, noting the slope-deflection equations, these incremental moments are related to θ_B by

$$\Delta M_{AB} = \frac{2EI_1}{L_1} \theta_B = \frac{2EI_1/L_1}{\{(4EI_1/L_1) + (4EI_2/L_2)\}} (-M_{B,net}) = -\frac{1}{2} DF_{BA}(M_{B,net}) \quad (10.41)$$

$$\Delta M_{CB} = \frac{2EI_2}{L_2} \theta_B = \frac{2EI_2/L_2}{\{(4EI_1/L_1) + (4EI_2/L_2)\}} (-M_{B,net}) = -\frac{1}{2} DF_{BC}(M_{B,net})$$

Comparing (10.41) with (10.40), we observe that the incremental moments at the far end are $\frac{1}{2}$ the magnitude at the distributed moments at the near end.

$$\Delta M_{AB} = \frac{1}{2} \Delta M_{BA} \quad (10.42)$$

$$\Delta M_{CB} = \frac{1}{2} \Delta M_{BC}$$

We summarize the moment distribution procedure for this example. The steps are:

1. Determine the distribution factors at each free node (only node B in this case).
2. Determine the fixed end moments due to the applied loading and chord rotation for the beam segments.
3. Sum the fixed end moments at node B. This sum is equal to the unbalanced moment at node B.
4. Distribute the unbalanced nodal moment to the members incident on node B.
5. Distribute one half of the incremental end moment to the other end of each member incident on node B.

Executing these steps is equivalent to formulating and solving the nodal moment equilibrium equations at node B. Moment Distribution avoids the operation of setting up and solving the equations. It reduces the effort to a series of simple computations.

Example 10.9 Moment distribution method applied to a two span beam

Given: The two span beams shown in Fig. E10.9a.

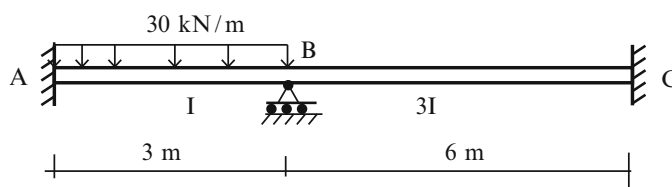


Fig. E10.9a

Determine: The end moments using moment distribution.

Solution: The fixed end moments and the distribution factors for node B are listed below.

$$M_{AB}^F = 30 \frac{(3)^2}{12} = 22.5 \text{ kN m} \quad M_{BC}^F = 0$$

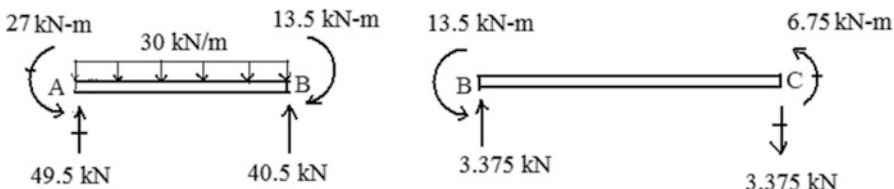
$$M_{BA}^F = -22.5 \text{ kN m} \quad M_{CB}^F = 0$$

At joint B $\left\{ \begin{array}{l} \sum I = \frac{l}{3} + \frac{3l}{6} = \frac{5l}{6} \\ DF_{BA} = \frac{l/3}{5l/6} = 0.4 \quad DF_{BC} = \frac{3l/6}{5l/6} = 0.6 \end{array} \right.$

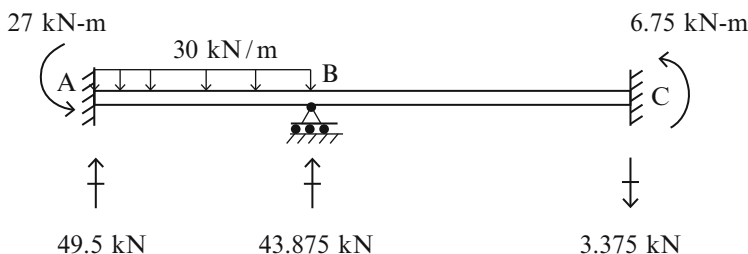
It is convenient to list the end moments and distribution factors on a sketch superimposed on the multi-span beam. A typical sketch is shown below. We distribute the 22.5 kN m unbalanced moment at B and carry over the moments to A and C. After one distribution, moment equilibrium at B is restored.

	A	B	C
DF's	1	0.4 0.6	1
FEM's	22.5	-22.5 0	0
	4.5 ←	9 13.5 →	6.75
ΣM	27	-13.5 13.5	6.75

Since the end moments are known, one can determine the end shear forces using the static equilibrium equations for the member.



Lastly, the reactions are listed below.



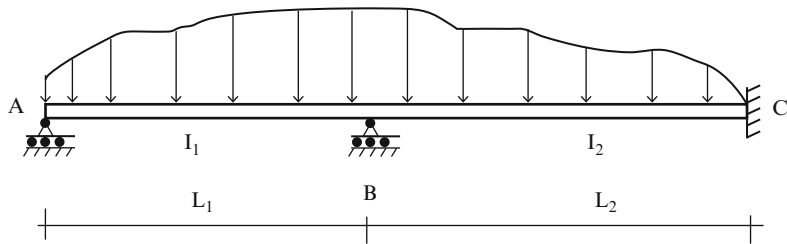


Fig. 10.21 Two span beam with a moment release at a support

10.6.2 Incorporation of Moment Releases at Supports

We consider next the case where an end member has a moment release, as shown in Fig. 10.21. We work with the modified slope-deflection equation for member AB developed in Sect. 10.3. The end moments are given by (10.22) which is listed below for convenience.

$$M_{BA,\text{modified}} = \frac{3EI_1}{L_1} \theta_B + \left\{ M_{BA}^F - \frac{1}{2} M_{AB}^F \right\} = \frac{3EI_1}{L_1} \theta_B + M_{BA,\text{modified}}^F$$

$$M_{AB} = 0$$

Then, the increment in moment for member BA due to a rotation at B is

$$\Delta M_{BA} = 4E \left(\frac{3}{4} \frac{I_1}{L_1} \right) \theta_B \quad (10.43)$$

$$\Delta M_{AB} = 0$$

We use a *reduced relative rigidity factor* $(3/4)I_1/L_1$, when computing the distribution factor for node B. Also, we use a *modified fixed end moment* (see Table 9.2). There is *no* carryover moment to A. The remaining steps are the same as for the case which A is fixed.

Example 10.10 Two span beam with a moment release at one end

Given: The beam shown in Fig. E10.10a.

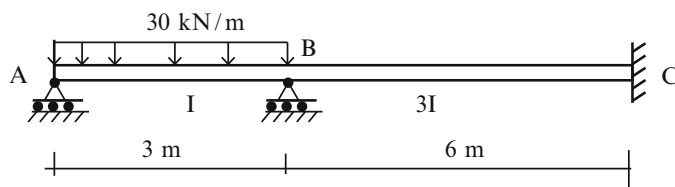
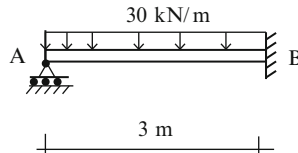


Fig. E10.10a

Determine: The end actions.

Solution: Since member AB has a moment release, we work with the modified slope-deflection equation for member AB. The computational details are listed below.

The modified fixed end moments (see Table 9.2):



$$M_{BA_{\text{modified}}}^F = M_{BA}^F - \frac{1}{2}M_{AB}^F = -\frac{30(3)^2}{8} = -33.75 \text{ kN m}$$

$$M_{AB}^F = 0$$

The modified distribution factors for node B:

$$\sum_{\text{joint B}} \frac{I}{L} = \frac{3}{4} \left(\frac{I}{3} \right) + \left(\frac{3I}{6} \right) = \frac{3I}{4}$$

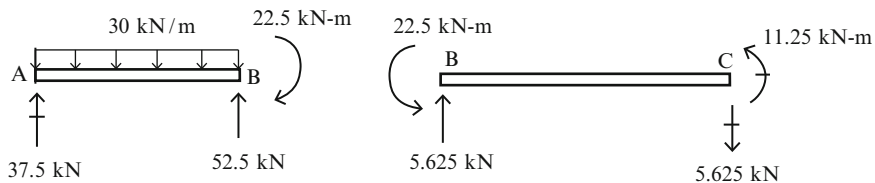
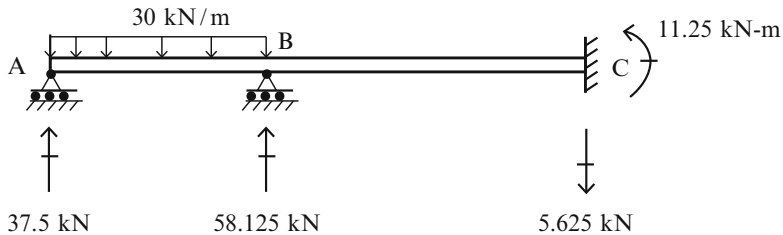
$$DF_{BA} = \frac{(3/4)(I/3)}{(3I/4)} = \frac{1}{3}$$

$$DF_{BC} = 1 - DF_{BA} = \frac{2}{3}$$

The distribution details are listed below.

	A	B	C
DF's	0	$\boxed{1/3}$ $\boxed{2/3}$	1
FEM's	0	-33.75	0
		11.25	11.25
ΣM	0	-22.5	22.5
			11.25

Noting the free body diagrams below, we find the remaining end actions (Figs. E10.10b, c).

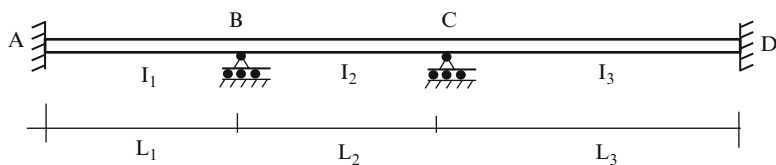
**Fig. E10.10b** Free body diagrams**Fig. E10.10c** Reactions

10.6.3 Moment Distribution for Multiple Free Nodes

The previous examples have involved only a single free node. We now extend the method for multiple free nodes. The overall approach is the same. We just have to incorporate an *iterative* procedure for successively balancing the nodal moments.

Consider the three span beam shown in Fig. 10.22. We assume nodes B and C are fixed, determine the fixed end moments for the members, and compute the unbalanced nodal moments at nodes B and C. If these moments are not equal to zero, the nodes will rotate until equilibrium is restored. Allowing a node, such as B, to rotate produces incremental end moments in members AB and BC equal to

$$\begin{aligned}\Delta M_{BA} &= \frac{4EI_1}{L_1} \theta_B & \Delta M_{AB} &= \frac{1}{2} \Delta M_{BA} \\ \Delta M_{BC} &= \frac{4EI_2}{L_2} \theta_B & \Delta M_{CB} &= \frac{1}{2} \Delta M_{BC}\end{aligned}\quad (10.44)$$

**Fig. 10.22**

Similarly, a rotation at node C produces incremental end moments in segment BC and CD.

$$\begin{aligned}\Delta M_{CB} &= \frac{4EI_2}{L_2} \theta_C & \Delta M_{BC} &= \frac{1}{2} \Delta M_{CB} \\ \Delta M_{CD} &= \frac{4EI_3}{L_3} \theta_C & \Delta M_{DC} &= \frac{1}{2} \Delta M_{CD}\end{aligned}\quad (10.45)$$

The distribution and carryover process is the same as described previously. One evaluates the distribution factors using (10.39) and takes the carryover factor as $\frac{1}{2}$. Since there is more than one node, we start with the node having the *largest unbalanced moment*, distribute this moment, and carry over the distributed moment to the adjacent nodes. This operation changes the magnitudes of the remaining unbalanced moments. We then select the node with the “largest” new unbalanced moment and execute a moment distribution and carry over at this node. The solution process proceeds by successively eliminating residual nodal moments at various nodes throughout the structure. At any step, we can assess the convergence of the iteration by examining the nodal moment residuals. Usually, only a few cycles of distribution and carry over are sufficient to obtain reasonably accurate results.

Example 10.11 Moment Distribution method applied to a three span beam

Given: The three span beam defined in Fig. E10.11a.

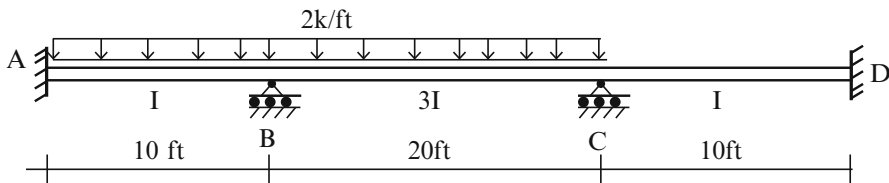


Fig. E10.11a

Determine: The end actions.

Solution: The sequence of nodal moment balancing is at the following nodes: C, B, C, B, C. We stop when the unbalanced nodal moment is approximately less than 0.5 kip ft.

The computations and distribution details are listed below.

$$\begin{aligned}M_{AB}^F &= 2 \frac{(10)^2}{12} = 16.67 \text{ kip ft} & M_{BA}^F &= -16.67 \text{ kip ft} \\ M_{BC}^F &= 2 \frac{(20)^2}{12} = 66.67 \text{ kip ft} & M_{CB}^F &= -66.67 \text{ kip ft} \\ M_{CD}^F &= M_{DC}^F = 0\end{aligned}$$

$$\text{At joint B or C} \left\{ \begin{array}{l} \sum_{\text{modified}} \frac{L}{L} = \frac{L}{10} + \frac{3L}{20} = \frac{5L}{20} \\ \text{DF}_{BA} = \text{DF}_{CD} = \frac{L/10}{5L/20} = 0.4 \\ \text{DF}_{CB} = \text{DF}_{BC} = 1 - 0.4 = 0.6 \end{array} \right.$$

$$\text{DF}_{DC} = \text{DF}_{AB} = 1$$

	A	B	C	D
DF's	[1]	[.4 .6]	[.6 .4]	[1]
FEM's	16.67	-16.67	66.67	-66.67
		20 ← → -42	40. ← → -21.	26.67 → 13.33
		6.3 ← → -12.6	8.4 ← → 4.2	
		-1.26 ← → -2.52	-1.89 ← → .37	
		.56 ← → 1.13	.75 ← → .37	
		-.22 ← → -.34		
ΣM	1.4	-47.4	+47.4	-35.8 +35.8 17.9

Noting the free body diagrams below, we find the remaining end actions (Figs. E10.11b, c).

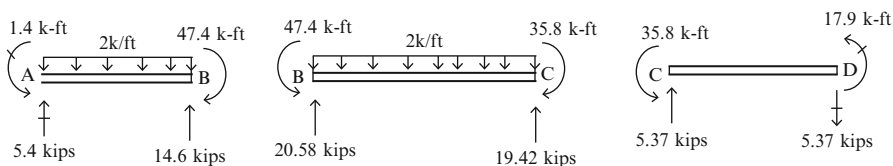


Fig. E10.11b Free body diagrams

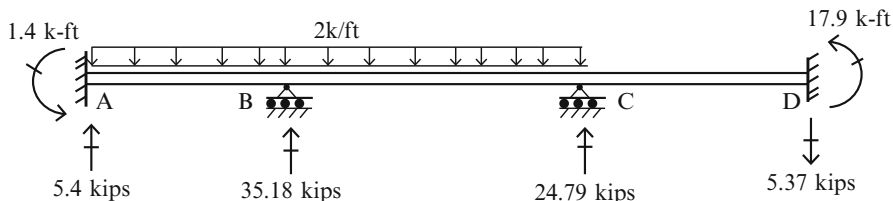


Fig. E10.11c Reactions

Example 10.12 Example 10.11 with moment releases at the end supports

Given: A three span beam with moment releases at its end supports (Figs. E10.12a–c).

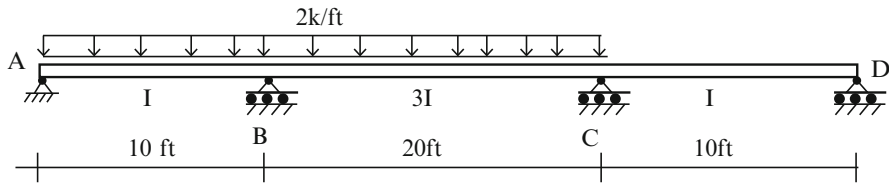


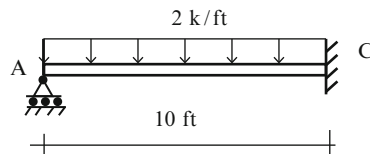
Fig. E10.12a

Determine: The end actions.

Solution: We rework Example 10.11 with moment releases at A and D. We use reduced relative rigidities for members AB and CD, and a modified fixed end moment for AB. There is no carryover from B to A or from C to D. Details are listed below.

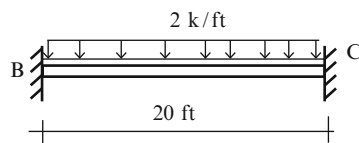
$$M_{BA_{\text{modified}}}^F = M_{BA}^F - \frac{1}{2}M_{AB}^F = -\frac{2(10)^2}{8} = -25 \text{ kip ft}$$

$$M_{AB_{\text{modified}}}^F = 0$$



$$M_{BC}^F = \frac{2(20)^2}{12} = 66.67 \text{ kip ft}$$

$$M_{CB}^F = -66.67 \text{ kip ft}$$



$$M_{CD}^F = M_{DC}^F = 0$$

$$\text{At joints B or C} \left\{ \begin{array}{l} \sum_{\text{modified}} \frac{L}{L} = \frac{3}{4} \left(\frac{I}{10} \right) + \left(\frac{3I}{20} \right) = \frac{9I}{40} \\ \text{DF}_{BA_{\text{modified}}} = \text{DF}_{CD_{\text{modified}}} = \frac{3I/40}{9I/40} = \frac{1}{3} \\ \text{DF}_{CB} = \text{DF}_{BC} = 1 - \frac{1}{3} = \frac{2}{3} \end{array} \right.$$

$$\text{DF}_{DC} = \text{DF}_{AB} = 0$$

The distribution details and end actions are listed below.

	A	B	C	D
DF's	0	1/3 2/3	2/3 1/3	0
FEM's	0	-25. 66.67	-66.67 0	0
		22.22 ← 44.44 22.22		
	-21.29	-42.59 → -21.3		
		7.1 ← 14.2 7.1		
	-2.36	-4.74 → -2.37		
		.79 ← 1.56 .79		
	-.26	-.52 → -.26		
		.17 .09		
ΣM	0	-48.9 +48.9	-30.2 +30.2	0

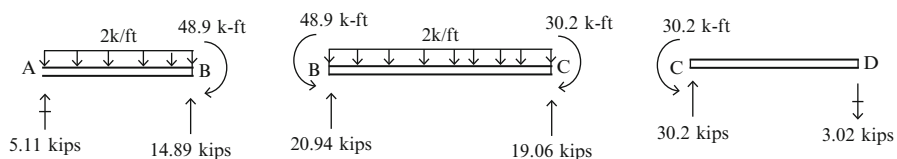


Fig. E10.12b Free body diagrams

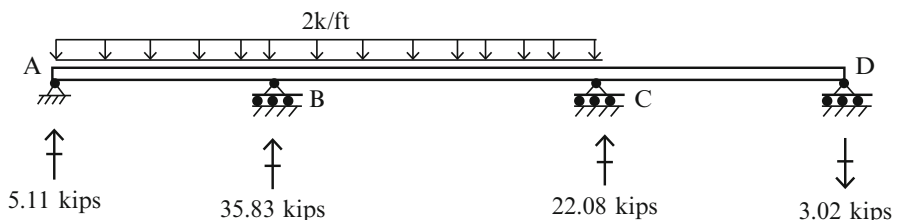


Fig. E10.12c Reactions

10.7 Moment Distribution: Frame Structures

10.7.1 Frames: No Sideway

Sideway does not occur if there is a lateral restraint. Frames with no sideway are treated in a similar way as beams. The following examples illustrate the process.

Example 10.13 Moment distribution method for a frame with no sideway

Given: The frame shown in Fig. E10.13a.

Determine: The end actions.

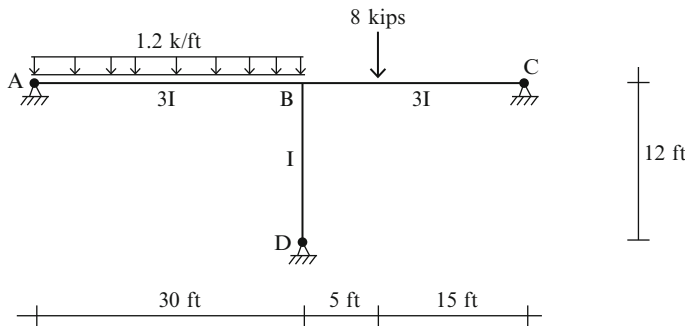
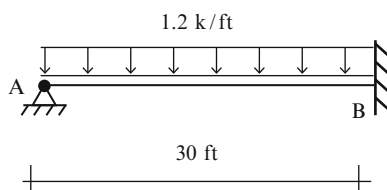


Fig. E10.13a

Solution: The distribution details and the fixed end moments and end actions are listed below.

$$M_{BA_{\text{modified}}}^F = M_{BA}^F - \frac{1}{2}M_{AB}^F = -\frac{1.2(30)^2}{8} = -135 \text{ kip ft}$$

$$M_{AB_{\text{modified}}}^F = 0$$



$$M_{BC_{\text{modified}}}^F = M_{BC}^F - \frac{1}{2}M_{CB}^F = +\frac{21PL}{128} = 26.25 \text{ kip ft}$$

$$M_{CB_{\text{modified}}}^F = 0$$

$$\sum_{\text{modified}} \frac{I}{L} = \frac{3}{4} \left(\frac{3I}{30} + \frac{3I}{20} + \frac{I}{12} \right) = \frac{I}{4}$$

$$\text{DF}_{BA_{\text{modified}}} = \frac{3/4(3I/30)}{I/4} = 0.3$$

$$\text{DF}_{BC_{\text{modified}}} = \frac{3/4(3I/20)}{I/4} = 0.45$$

$$\text{DF}_{BD_{\text{modified}}} = \frac{3/4(I/12)}{I/4} = 0.25$$

At Joint B

The distribution details are listed below (Fig. E10.13b).

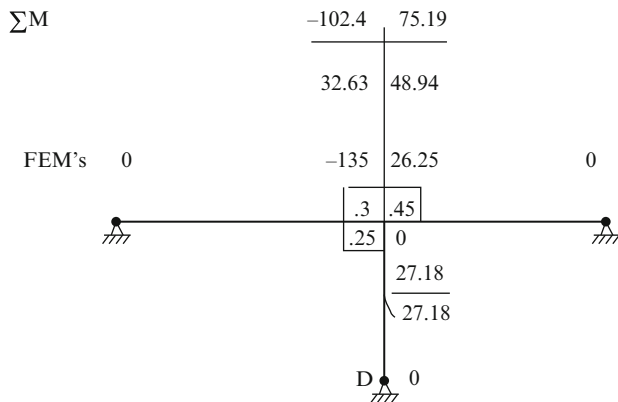
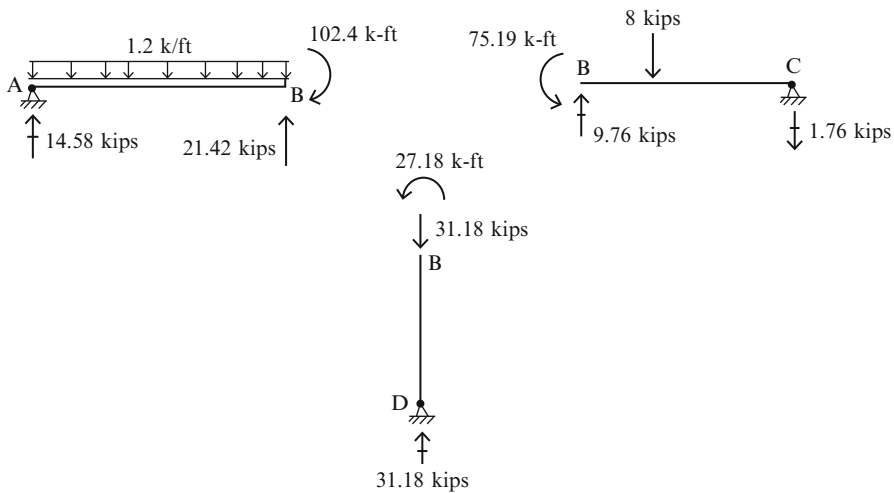


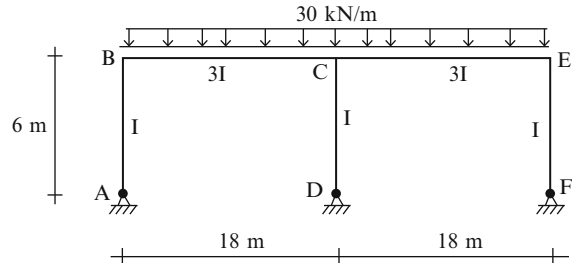
Fig. E10.13b

Noting the free body diagrams below, we find the remaining end actions (Fig. E10.13c).

**Fig. E10.13c** End actions

Example 10.14 Symmetrical two-bay portal frame—symmetrical loading

Given: The two-bay frame defined in Fig. E10.14a.

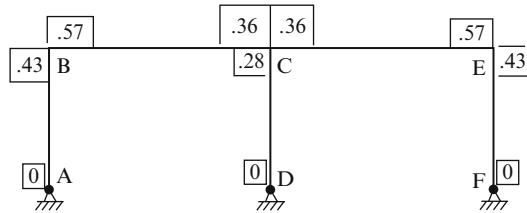
**Fig. E10.14a**

Determine: The bending moment distribution and end actions using moment distribution.

Solution: We use reduced rigidity factors for the column members and *no* carry-over to the hinged ends at nodes A, D, F (Fig. E10.14b).

$$\left\{ \begin{array}{l} \sum \frac{I}{L} = \left(\frac{I}{6}\right)\frac{3}{4} + \left(\frac{3I}{18}\right) \\ DF_{BA_{\text{modified}}} = DF_{EF_{\text{modified}}} = \frac{(I/6)3/4}{(I/6)3/4 + (3I/18)} = 0.43 \\ DF_{BC} = DF_{EC} = 1 - 0.43 = 0.57 \end{array} \right.$$

$$\left\{ \begin{array}{l} \sum \frac{I}{L} = \left(\frac{I}{6}\right) \frac{3}{4} + \frac{3I}{18} + \frac{3I}{18} = \frac{11}{24} I \\ \text{At node C} \quad DF_{CD_{\text{modified}}} = \frac{(I/6)3/4}{(11/24)I} = \frac{3}{11} = 0.28 \\ DF_{CB} = DF_{CE} = \frac{1 - 0.28}{2} = 0.36 \end{array} \right.$$

**Fig. E10.14b** Distribution factors

The fixed end moments are

$$M_{BC}^F = -M_{CB}^F = M_{CE}^F = -M_{EC}^F = +\frac{30(18)^2}{12} = +810 \text{ kN m}$$

The moment distribution sequence is listed in Fig. E10.14c. Note that there is never any redistribution at node C because of symmetry (Fig. E10.14d).

ΣM	-348.3	348.3	-1040.85	1040.85	-348.3	348.3
FEM's	-348.3	-461.7	-230.85	230.85	461.7	348.3
0	0	810	-810	810	-810	0
	B	C	0	E	F	0
	A	D	0			

Fig. E10.14c

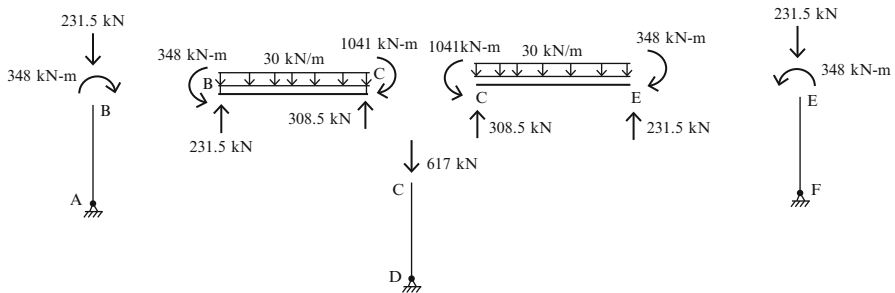


Fig. E10.14d Free body diagram

The final bending moment distributions are plotted in Fig. E10.14e.

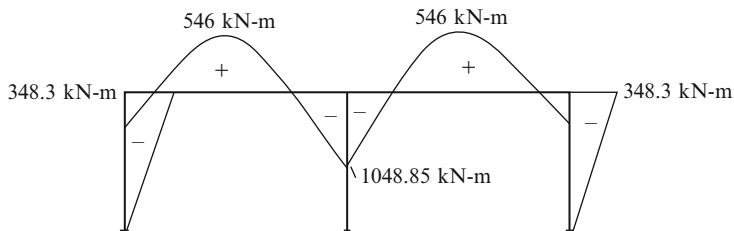


Fig. E10.14e

Example 10.15 Two-bay portal frame—support settlement

Given: The frame shown in Fig. E10.15a. Consider Support D experiences a downward settlement of $\delta = 1$ in.

Determine: The end moments. Take $E = 29,000$ ksi and $I = 2,000$ in.⁴

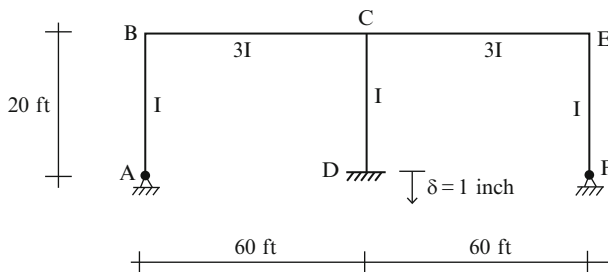
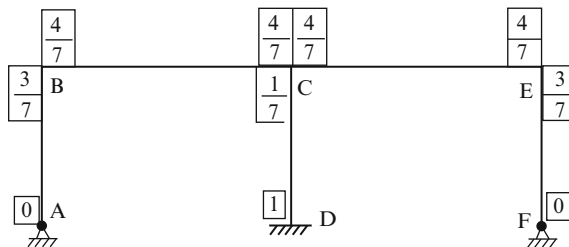


Fig. E10.15a

Solution: We use reduced factors for the column members AB and EF and no carryover to the hinged ends. The distribution factors are listed on the following sketch (Fig. E10.15b).

$$\begin{cases}
 \sum \frac{I}{L} = \left(\frac{I}{20}\right) \frac{3}{4} + \left(\frac{3I}{60}\right) = \frac{7I}{80} \\
 \text{At node B or E} \quad DF_{BA_{\text{modified}}} = DF_{EF_{\text{modified}}} = \frac{(I/20)3/4}{7I/80} = \frac{3}{7} \\
 DF_{BC} = DF_{EC} = 1 - \frac{3}{7} = \frac{4}{7} \\
 \\
 \sum \frac{I}{L} = \frac{I}{20} + \frac{3I}{20} + \frac{3I}{20} = \frac{7I}{20} \\
 \text{At node C} \quad DF_{CD} = \frac{I/20}{7I/20} = \frac{1}{7} \\
 DF_{CB} = DF_{CE} = \frac{1 - (1/7)}{2} = \frac{3}{7}
 \end{cases}$$

Fig. E10.15b Distribution factors

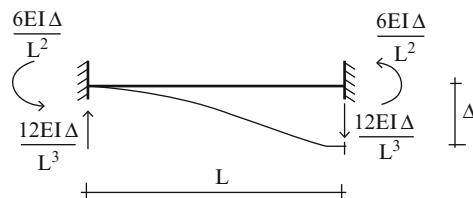


Settlement at D produces chord rotation in member BC and CE. The corresponding rotations for a 1 in. settlement are

$$\rho_{BC} = -\frac{\delta}{L}$$

$$\rho_{CE} = +\frac{\delta}{L}$$

These rotations produce the following fixed end moments (see Table 9.1),



$$M_{BC}^F = M_{CB}^F = \left\{ \frac{6E(3I)\delta}{L^2} = +\frac{18EI\delta}{L^2} \right\} = \frac{6(29,000)(6,000)(1)}{(60)^2} \frac{1}{(12)^3} = 167.8 \text{ kip ft}$$

$$M_{CE}^F = M_{EC}^F = -\frac{6E(3I)\delta}{L^2} = -\frac{18EI\delta}{L^2} = -167.8 \text{ kip ft}$$

These moments are distributed at nodes B and E. Note that no unbalanced moment occurs at node C (Fig. E10.15c).

ΣM	0	-71.9	71.9		119.8	-119.8		-71.9	71.9	0
		-71.9	-95.9	→	-47.95	47.95	←	95.9	71.9	
FEM's	0	0	167.8		167.8	-167.8		-167.8	0	0

Fig. E10.15c

The final bending moment distributions are plotted in Fig. E10.15d.

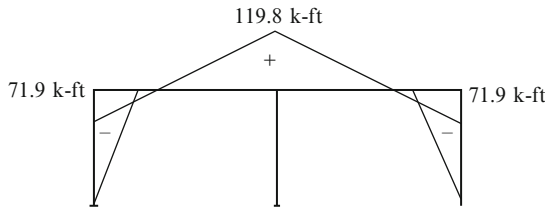


Fig. E10.15d

Example 10.16 Two-bay portal frame—temperature increase

Given: The frame shown in Fig. E10.16a. Consider member BC and CE to experience a temperature increase of ΔT .

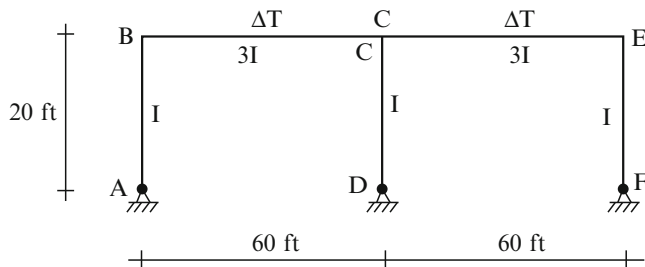


Fig. E10.16a

Determine: The end moments.

Solution: The top members will expand, causing members AB and EF to rotate. Member CD will not rotate because of symmetry. Noting Fig. E10.16b, the rotations are

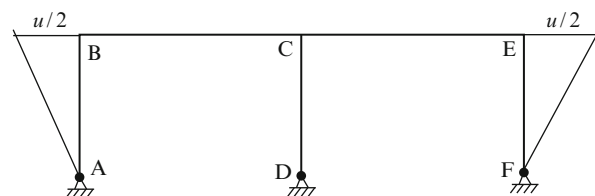
$$\rho_{AB} = \frac{u/2}{L_{AB}}$$

$$\rho_{EF} = -\frac{u/2}{L_{EF}}$$

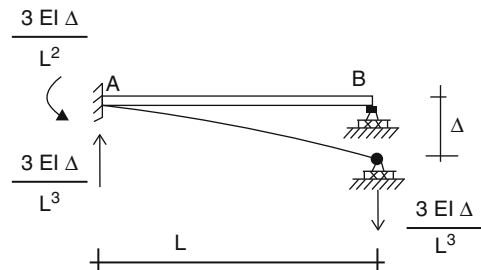
Assuming a uniform temperature increase over the total span, u is equal to

$$u = (\alpha \Delta T) \sum L = 120 \alpha \Delta T$$

Fig. E10.16b



Noting Table 9.2, the fixed end actions corresponding to the case where there is a hinge at one end are



$$M_{BA}^F = -\frac{3EI}{L_{AB}} \rho_{AB} = -\frac{3EIu}{20(12)(40)} = -\frac{EIu}{3,200} = -\frac{3}{80} EI \alpha \Delta T$$

$$M_{EF}^F = +\frac{3}{80} EI \alpha \Delta T$$

We assume the material is steel ($E = 3 \times 10^4$ ksi, $\alpha = 6.6 \times 10^{-6}/{}^\circ\text{F}$), $\Delta T = 120 {}^\circ\text{F}$, and $I = 2,000$ in.⁴

The corresponding fixed end moments are

$$M_{BA}^F = -1,782 \text{ kip in.} = -148.5 \text{ kip ft}$$

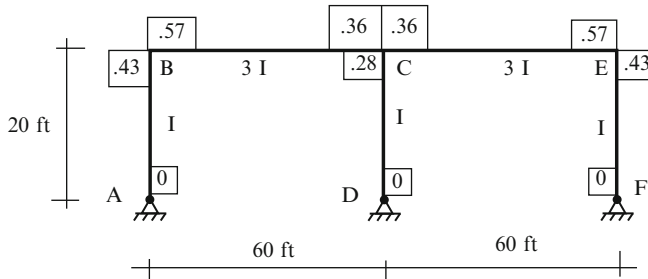
$$M_{EF}^F = +1,782 \text{ kip in.} = +148.5 \text{ kip ft}$$

The distribution factors are

$$\left\{ \begin{array}{l} \sum \frac{I}{L} = \left(\frac{I}{20}\right) \frac{3}{4} + \left(\frac{3I}{60}\right) = \frac{7I}{80} \\ \text{At node B or E} \quad DF_{BA_{\text{modified}}} = DF_{EF_{\text{modified}}} = \frac{(I/20)\frac{3}{4}}{(7I/80)} = 0.43 \\ DF_{BC} = DF_{EC} = 1 - 0.43 = 0.57 \end{array} \right.$$

$$\left\{ \begin{array}{l} \sum \frac{I}{L} = \left(\frac{I}{20}\right) \frac{3}{4} + \frac{3I}{60} + \frac{3I}{60} = \frac{11I}{80} \\ \text{At node C} \quad DF_{CD_{\text{modified}}} = \frac{(I/20)\frac{3}{4}}{11I/80} = 0.28 \\ DF_{CB} = DF_{CE} = \frac{1 - 0.28}{2} = 0.36 \end{array} \right.$$

The distribution factors are listed on the following sketch.



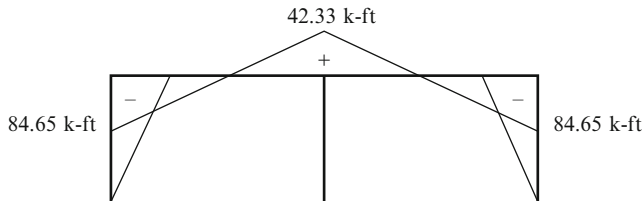
The distribution details are listed below.

ΣM	0	-84.65	84.65		42.33	-42.33		-84.65	84.65	0
FEM's	0	63.85	84.65	→	42.33	-42.33	←	-84.65	-63.85	0
	-148.5	0	0		0	0		0	148.5	0

B C E

A D F

The final bending moment distributions are plotted in the following Figure.



10.7.2 Frames with Sideway

Given a frame structure, one needs to identify whether there will be chord rotation due to lateral displacement. If sideway is possible, we introduce “holding” forces applied at certain nodes to prevent this motion and carry out a conventional moment distribution based on distribution and carryover factors. Once the fixed end moments are distributed, we can determine the member shear forces, and using these values, establish the magnitude of the holding forces. This computation is illustrated in Fig. 10.23. There is one degree of sidesway, and we restrain node B. The corresponding lateral force is H . Note that we generally neglect axial deformation for framed structures so fixing B also fixes C.

The next step involves introducing an arbitrary amount of the lateral displacement that we had restrained in Step 1, computing the chord rotations and corresponding fixed end moments, applying the holding force again, and then distributing the fixed end moments using the conventional distribution procedure. The holding force produced by this operation is illustrated in Fig. 10.24. *One combines the two solutions such that the resulting sideway force is zero.*

$$\text{Final solution} = \text{case I} + \left(\frac{H_1}{H_2} \right) \text{case II} \quad (10.46)$$

The fixed end moments due to the chord rotation produced by the horizontal displacement, Δ , are (see Table 9.1)

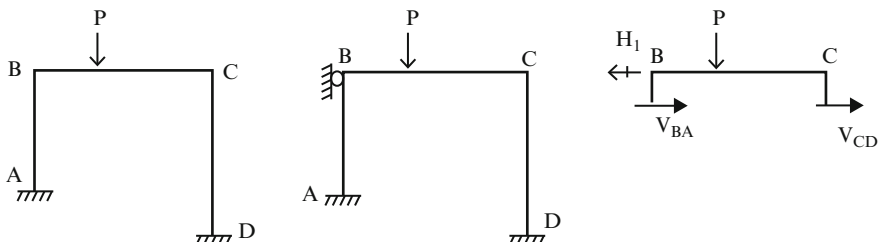
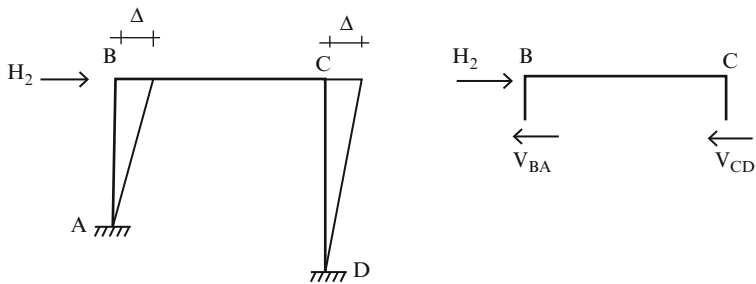


Fig. 10.23 Sideway restraining forces—case I

**Fig. 10.24** Sideway introduced—case II

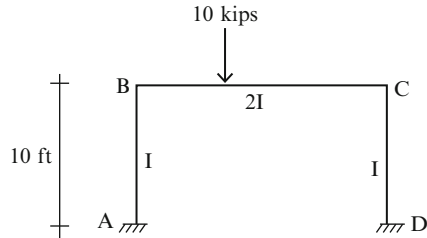
$$M_{BA}^F = M_{AB}^F = \pm \frac{6EI_{AB}}{L_{AB}^2} \Delta = \pm \frac{6EI_{AB}}{L_{AB}} \rho_{AB}$$

$$M_{DC}^F = M_{CD}^F = \pm \frac{6EI_{CD}}{L_{CD}^2} \Delta = \pm \frac{6EI_{CD}}{L_{CD}} \rho_{CD}$$

where moment quantities are counterclockwise when positive. Following this approach, one works only with chord rotation quantities and converts these measures into equivalent fixed end moments. The standard definition equations for the distribution and carryover factors are employed to distribute the moments.

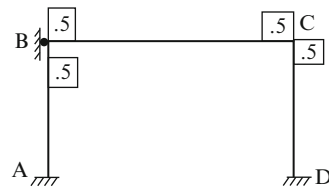
Example 10.17 Portal bent—sideway analysis

Given: The portal frame defined in Fig. E10.17a.

**Fig. E10.17a**

Determine: The end actions.

Solution: Since the loading is not symmetrical, there will be lateral motion (sideway). We restrain node B as indicated in Fig. E10.17b. The distribution factors are also indicated in the sketch.

Fig. E10.17b

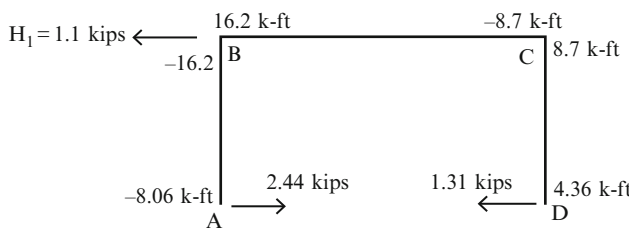
We compute the fixed end moments due to the 10 kip load.

$$M_{BC}^F = \frac{10(5)(15)^2}{20^2} = +28.13 \text{ kip ft}$$

$$M_{CB}^F = -\frac{10(15)(5)^2}{20^2} = -9.38 \text{ kip ft}$$

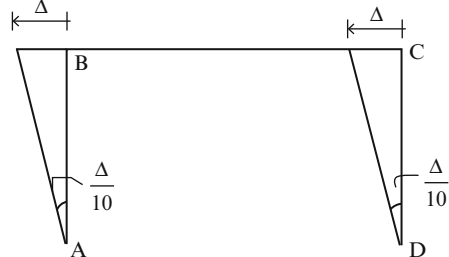
Details of the moment distribution and the end moments for case I are listed below (Fig. E10.17c). The holding force is determined by summing the shear forces in the columns and is equal to 1.1 kip.

ΣM	-8.06	-16.23	16.25	-8.73	8.71	4.36
		.12	-.12			
			.25	← .51	.51 → .25	
		-1.03 ←	-2.05	-2.05 → -1.03		
			4.10 ←	8.20	8.20 → +4.10	
		-7.03 ←	-14.06	-14.06 → -7.03		
FEM's	0	0	28.13	-9.38	0	0
	A	B	C		D	

**Fig. E10.17c** Case I—end moments and column shear

Next, we introduce a lateral displacement to the left equal to Δ . Figure E10.17d shows this operation.

Fig. E10.17d Case II—
sideway introduced



The chord rotations and corresponding fixed end moments are

$$M_{\text{BA}}^{\text{F}} = M_{\text{AB}}^{\text{F}} = M_{\text{DC}}^{\text{F}} = M_{\text{CD}}^{\text{F}} = -\frac{6EI\Delta}{h^2}$$

Since we are interested only in relative moments, we take $EI \Delta/h^2 = 1$. Details of the moment distribution and the end moments for case II are listed below (Fig. E10.17e).

.07	\leftarrow	<u>.14</u>	<u>.14</u>	\rightarrow	<u>-.03</u>	<u>-.03</u>
			<u>-.28</u>	\leftarrow	<u>-.56</u>	<u>-.56</u> \rightarrow <u>-.28</u>
1.13	\leftarrow	<u>2.25</u>	<u>2.25</u>	\rightarrow	<u>1.13</u>	
			<u>1.5</u>	\leftarrow	<u>+3.0</u>	<u>+3.0</u> \rightarrow <u>1.5</u>
FEM's -6.0		-6.0	0		0	-6.0 -6.0
A		B		C		D

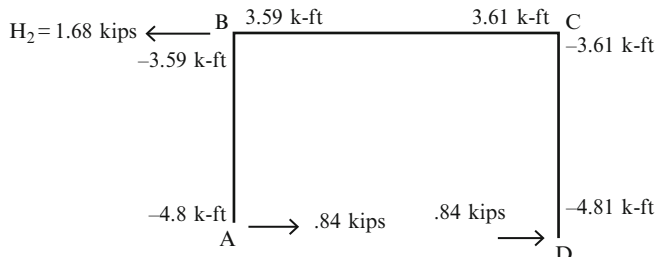


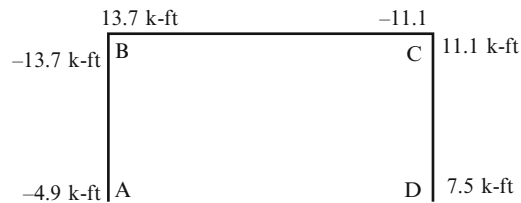
Fig. E10.17e Case II—end moments and column shear

We scale this solution by $H_1/H_2 = -1.1/1.68$ and then combine these scaled results with the results for case I.

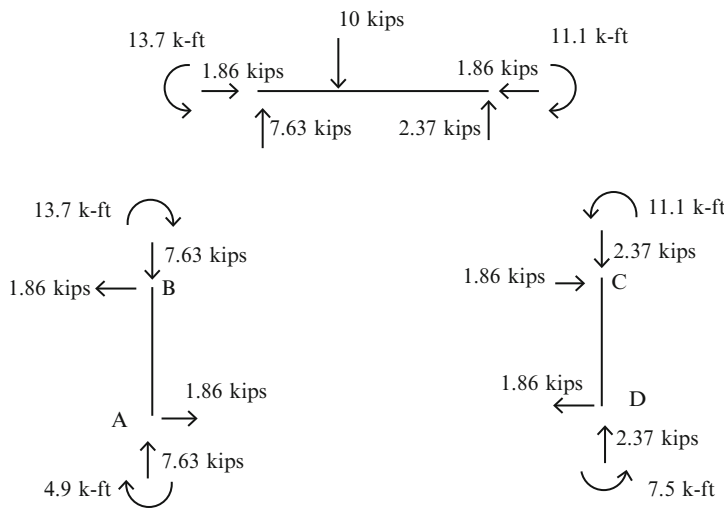
Final end moments = end moments case I + end moments case II (H_1/H_2)

The final moments are summarized in Fig. E10.17f followed by free body diagrams.

Fig. E10.17f Final end moments



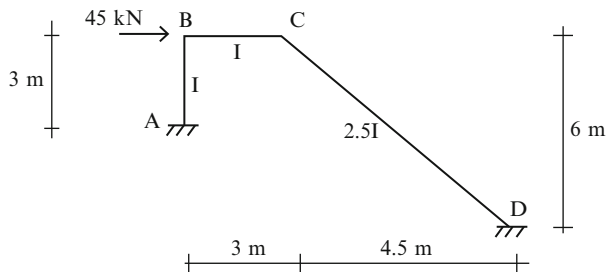
Using these moments, we find the axial and shear forces.



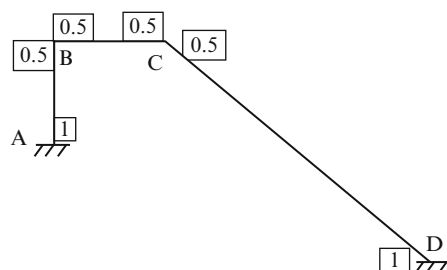
Example 10.18 Frame with inclined legs

Given: The frame shown in Fig. E10.18a.

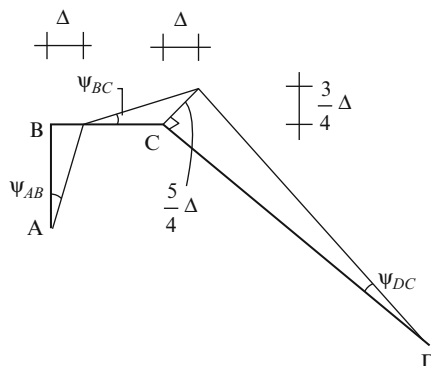
Determine: The end actions.

Fig. E10.18a

Solution: The distribution factors are listed in the sketch below (Fig. E10.18b).

Fig. E10.18b

There are no fixed end moments due to member loads. However, we need to carry out a sideway analysis (case II). We introduce a horizontal displacement at B and compute the corresponding rotation angles.



The rotation of members BC and CD are determined by requiring the horizontal displacement of node C to be equal to Δ . The angles follow from the above sketch

$$\psi_{AB} = \frac{\Delta}{3}$$

$$\psi_{BC} = \frac{3/4\Delta}{3} = \frac{\Delta}{4}$$

$$\psi_{DC} = \frac{5/4\Delta}{7.5} = \frac{\Delta}{6}$$

Finally, the chord rotations are (note: positive sense is counterclockwise)

$$\rho_{AB} = -\frac{\Delta}{3}$$

$$\rho_{BC} = +\frac{\Delta}{4}$$

$$\rho_{DC} = -\frac{\Delta}{6}$$

Using these values, we compute the fixed end moments due to chord rotation.

$$M_{AB}^F = M_{BA}^F = -\frac{6(EI)}{(3)^2} \left(-\frac{1}{3} \Delta \right) = +\frac{2}{3}(EI \Delta)$$

$$M_{BC}^F = M_{CB}^F = -\frac{6(EI)}{(3)^2} \left(+\frac{1}{4} \Delta \right) = -\frac{1}{2}(EI \Delta)$$

$$M_{CD}^F = M_{DC}^F = -\frac{6(2.5EI)}{(7.5)^2} \left(-\frac{1}{6} \Delta \right) = +\frac{1}{3}(EI \Delta)$$

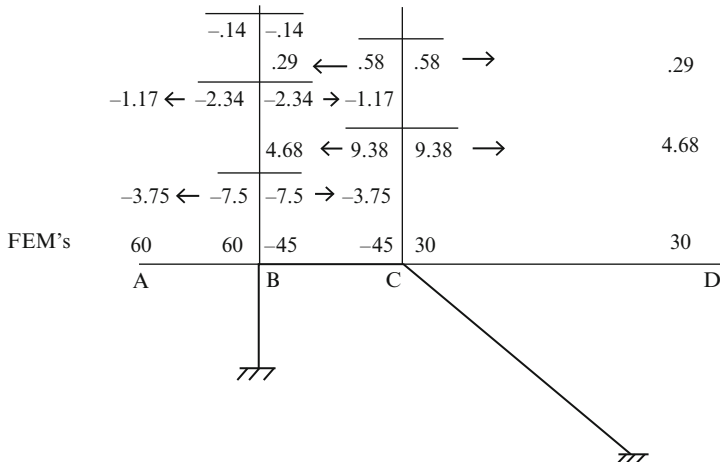
Since we need only relative moments, we take $EI \Delta = 90$
Then

$$M_{AB}^F = M_{BA}^F = +60 \text{ kN m}$$

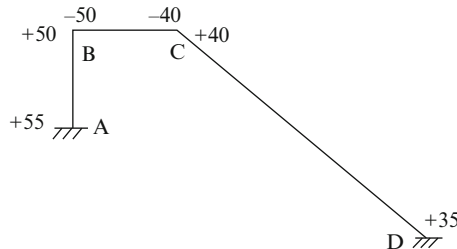
$$M_{CB}^F = M_{BC}^F = -45 \text{ kN m}$$

$$M_{DC}^F = M_{CD}^F = +30 \text{ kN m}$$

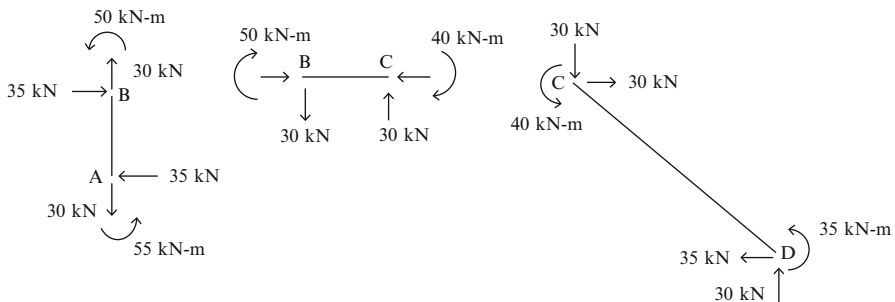
Next, we distribute the moments as shown below



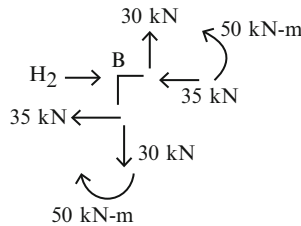
The end moments values are



Using these moments, we find the axial and shear forces.



Note that one needs the axial force in member BC in order to determine H_2 .
Summing horizontal force components at B leads to H_2 .



Therefore

$$H_2 = 35 + 35 = 70 \text{ kN}$$

Given that the actual horizontal force is 45 kN, we scale the sideway moments by $H_1/H_2 = 45/70 = 9/14$.

$$\text{Final end moments} = \text{end moments case II} \left(\frac{H_1}{H_2} \right)$$

The final end moments (kN m) are listed below (Fig. E10.18c).

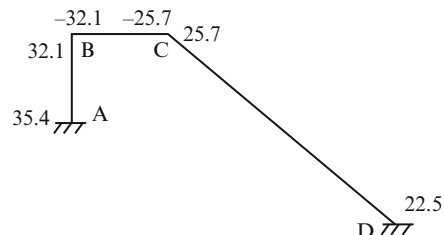
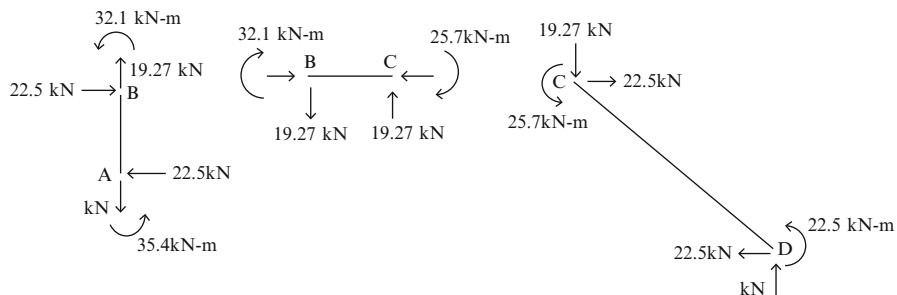


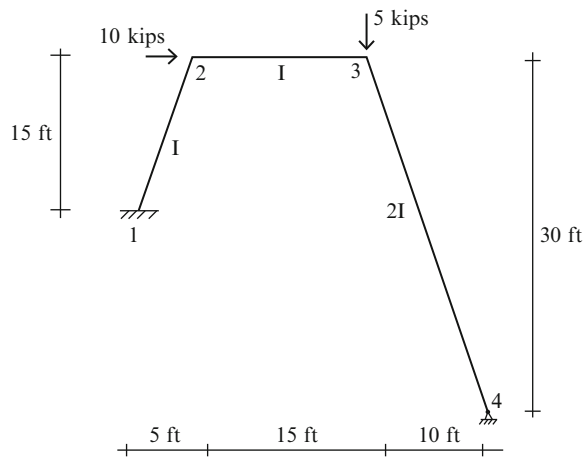
Fig. E10.18c Final moments

Using these moments, we find the axial and shear forces.



Example 10.19 Computer-based analysis—frame with inclined legs.

Fig. E10.19a



Given: The frame shown in Fig. E10.19a.

Determine: The displacement components at nodes 2 and 3, the bending moment distribution, and the reactions. Consider a range of values for I ($I = 100, 200, \text{ and } 400 \text{ in.}^4$) (Figs. E10.19b–d). Take $A = 20 \text{ in.}^2$. Use computer software.

Solution: The computer generated deflection profiles and the reactions and moment diagram are listed below (Figs. E10.19e, f). Hand computation is not feasible for this task.

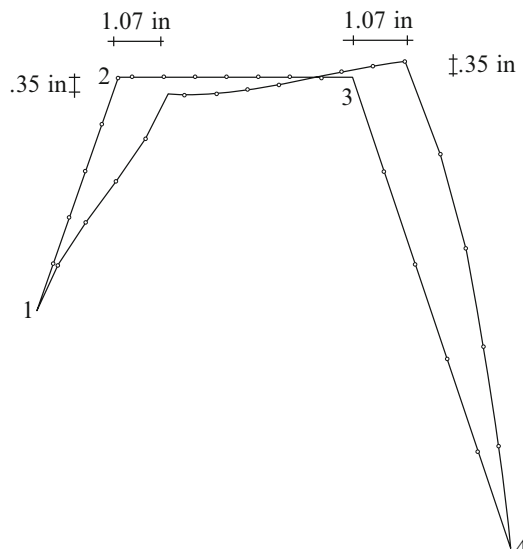


Fig. E10.19b Deflection profile— $I = 100 \text{ in.}^4$

Fig. E10.19c Deflection profile— $I = 200 \text{ in.}^4$

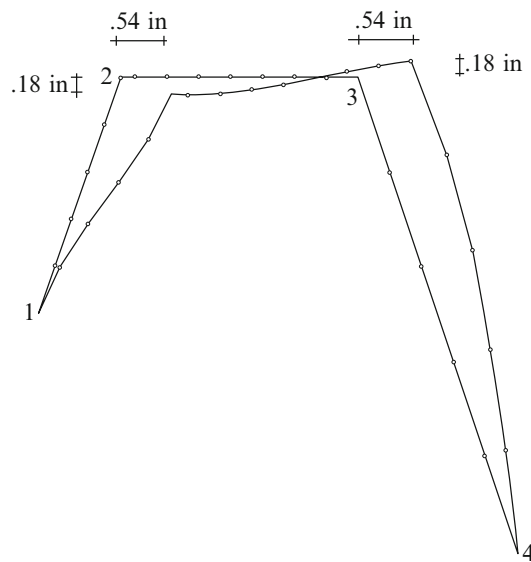
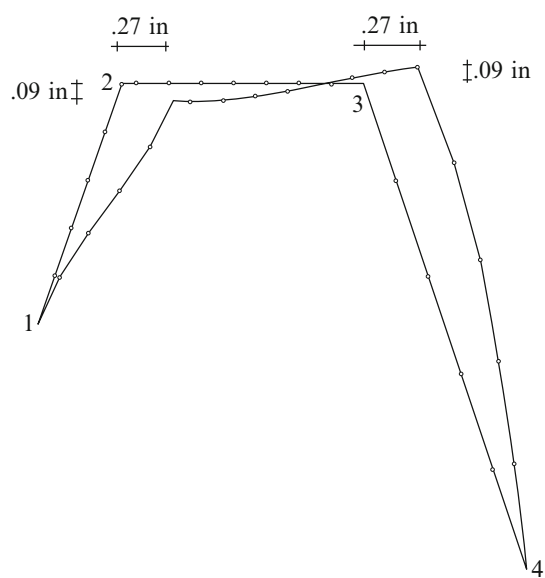


Fig. E10.19d Deflection Profile— $I = 400 \text{ in.}^4$



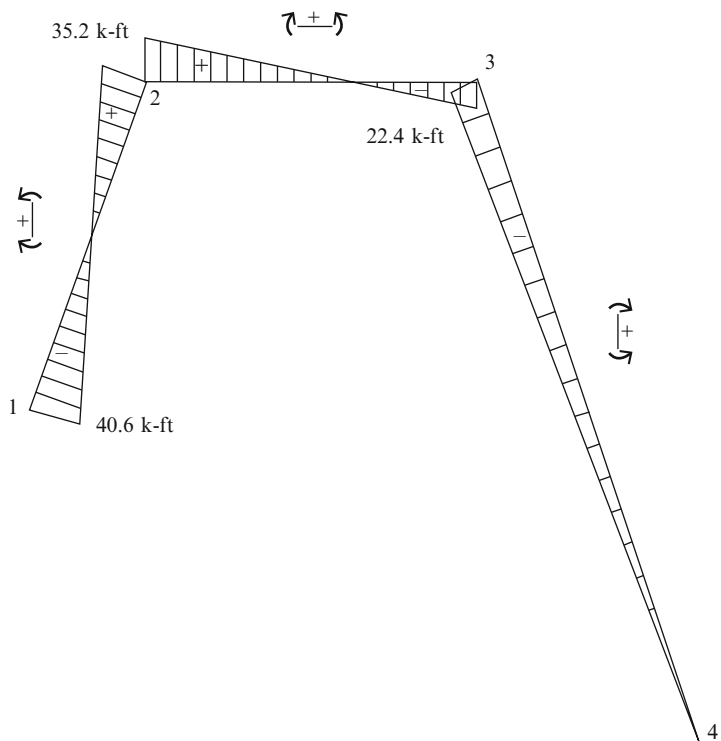


Fig. E10.19e Moment diagram

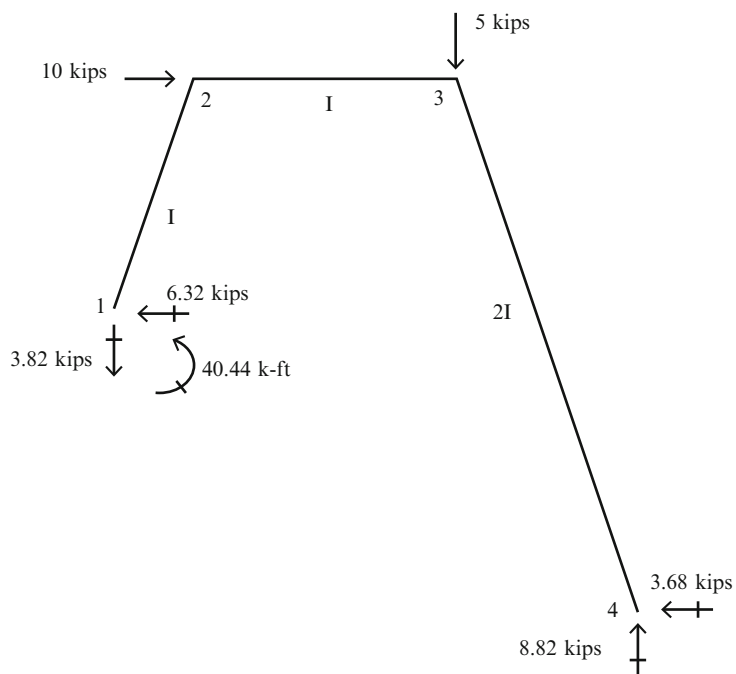


Fig. E10.19f Reactions

Note that the member forces are *invariant* since the relative stiffness of the members is the same. Also, the displacement varies linearly with I .

10.8 Plane Frames: Out of Plane Loading

We discussed this case briefly in Chap. 4, when we dealt with statically determinate plane frame structures loaded normal to the plane such as highway signs. We extend the analysis methodology here to deal with statically indeterminate cases. Our strategy is based on the displacement method, i.e., we use generalized slope-deflection equations for the members and enforce equilibrium at the nodes. This approach is more convenient than the force method and has the additional advantage that it can be readily adopted for digital computation.

10.8.1 Slope-Deflection Equations: Out of Plane Loading

Consider the prismatic member shown in Fig. 10.25a. We assume that the member is loaded in the $X-Z$ plane (note that all the previous discussions have assumed the loading is in the $X-Y$ plane). The relevant displacement measures for this loading are the rotation θ_x , the rotation θ_y , and the transverse displacement v_z . Figure 10.25b defines the positive sense for these quantities and the corresponding end actions at B .

Following the procedure described in Sect. 10.3, one can establish the equations relating the end actions at B to the end displacements at B . Their form is

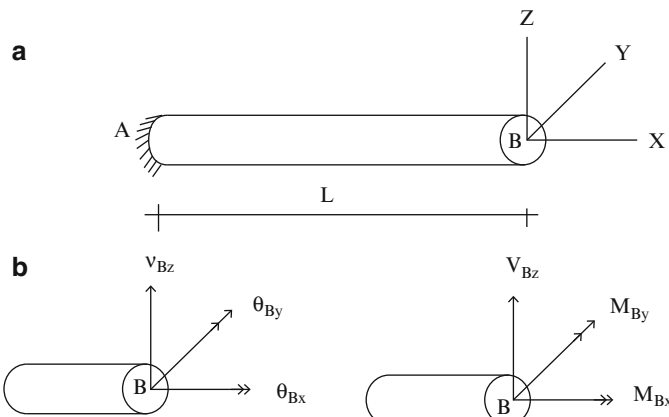


Fig. 10.25

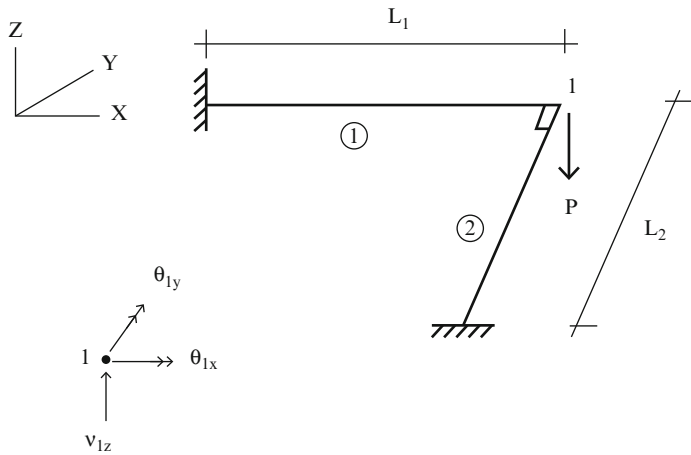


Fig. 10.26 Plane grid

$$\begin{aligned}
 M_{Bx} &= \frac{GJ}{L} \theta_{Bx} \\
 M_{By} &= \frac{4EI_y}{L} \theta_{By} + \frac{6EI_y}{L^2} v_{Bz} \\
 V_{Bz} &= \frac{12EI_y}{L^3} v_{Bz} + \frac{6EI_y}{L^2} \theta_{By}
 \end{aligned} \tag{10.47}$$

where GJ is the torsional rigidity for the cross-section, and I_y is the second moment of area with respect to y -axis.

$$I_y = \int_A z^2 dA \tag{10.48}$$

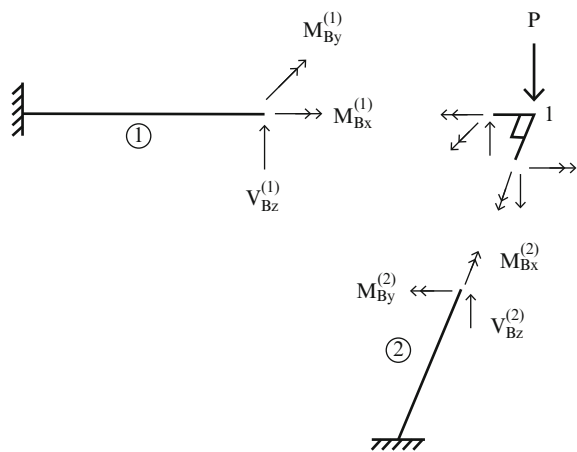
The remaining steps are essentially the same as for the planar case. One isolates the members and nodes, and enforces equilibrium at the nodes. In what follows, we illustrate the steps involved.

Consider the structure shown in Fig. 10.26. We suppose the supports are rigid. There are three unknown nodal displacement measures, θ_x , θ_y , and v_z at node 1.

Free body diagrams for the members' incident on node 1 are shown below. Requiring equilibrium at node 1 leads to the following equations (Fig. 10.27):

$$\begin{aligned}
 V_{Bz}^{(1)} + V_{Bz}^{(2)} + P &= 0 \\
 -M_{Bx}^{(1)} + M_{By}^{(2)} &= 0 \\
 M_{By}^{(1)} + M_{Bx}^{(2)} &= 0
 \end{aligned} \tag{10.49}$$

Fig. 10.27 Free body diagrams



Noting the relationship between the variables,

$$\begin{aligned}
 \theta_{Bx}^{(1)} &= \theta_{1x} \\
 \theta_{Bx}^{(2)} &= -\theta_{1y} \\
 \theta_{By}^{(1)} &= \theta_{1y} \\
 \theta_{By}^{(2)} &= -\theta_{1x} \\
 v_{Bz}^{(1)} &= v_{Bz}^{(2)} = v_{1z}
 \end{aligned} \tag{10.50}$$

the member equations take the following form,

$$\begin{aligned}
 M_{Bx}^{(1)} &= \frac{GJ_1}{L_1} \theta_{1x} \\
 M_{By}^{(1)} &= \frac{4EI_1}{L_1} \theta_{1y} + \frac{6EI_1}{L_1^2} v_{1z} \\
 V_{Bz}^{(1)} &= \frac{12EI_1}{L_1^3} v_{1z} + \frac{6EI_1}{L_1^2} \theta_{1y}
 \end{aligned} \tag{10.51}$$

and

$$\begin{aligned}
 M_{Bx}^{(2)} &= \frac{GJ_2}{L_2} \theta_{1y} \\
 M_{By}^{(2)} &= \frac{4EI_2}{L_2} (-\theta_{1x}) + \frac{6EI_2}{L_2^2} v_{1z} \\
 V_{Bz}^{(2)} &= \frac{12EI_2}{L_2^3} v_{1z} + \frac{6EI_2}{L_2^2} (-\theta_{1x})
 \end{aligned}$$

Lastly, we substitute for the end actions in the equilibrium equations leading to

$$\begin{aligned} \left[\frac{GJ_1}{L_1} + \frac{4EI_2}{L_2} \right] \theta_{1x} - \frac{6EI_2}{L_2^2} v_{1z} &= 0 \\ \left[\frac{GJ_2}{L_2} + \frac{4EI_1}{L_1} \right] \theta_{1y} + \frac{6EI_1}{L_1^2} v_{1z} &= 0 \\ 12E \left[\frac{I_1}{L_1^3} + \frac{I_2}{L_2^3} \right] v_{1z} + \frac{6EI_1}{L_1^2} \theta_{1y} - \frac{6EI_2}{L_2^2} \theta_{1x} + P &= 0 \end{aligned} \quad (10.52)$$

The solution is

$$\begin{aligned} \theta_{1x} &= \frac{6EI_2/L_2^2}{GJ_1/L_1 + 4EI_2/L_2} v_{1z} \\ \theta_{1y} &= \frac{-6EI_1/L_1^2}{GJ_2/L_2 + 4EI_1/L_1} v_{1z} \\ \left\{ -12E \left[\frac{I_1}{L_1^3} + \frac{I_2}{L_2^3} \right] + \frac{[6EI_1/L_1^2]^2}{GJ_2/L_2 + 4EI_1/L_1} + \frac{[6EI_2/L_2^2]^2}{GJ_1/L_1 + 4EI_2/L_2} \right\} v_{1z} &= +P \end{aligned} \quad (10.53)$$

When the member properties are equal,

$$\begin{aligned} I_1 &= I_2 \\ L_1 &= L_2 \\ J_1 &= J_2 \end{aligned}$$

and the solution reduces to

$$\begin{aligned} \theta_{1y} &= -\theta_{1x} \\ \text{end shear forces } V_{Bz}^{(1)} &= V_{Bz}^{(2)} = \frac{P}{2} \end{aligned} \quad (10.54)$$

Note that even for this case, the vertical displacement depends on both I and J . In practice, we usually use a computer-based scheme to analyze grid-type structures.

Example 10.20 Grid structure

Given: The grid structure defined in Fig. E10.20a. The members are rigidly connected at all the nodes. Assume the members are steel and the cross-sectional properties are constants. $I = 100 \text{ in.}^4$, $J = 160 \text{ in.}^4$.

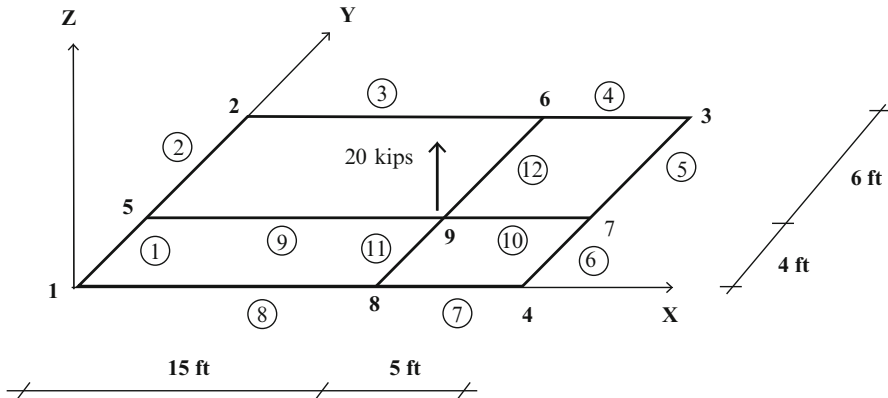
The nodal displacement restraints are as follows:

Node 1: x, y, z translation

Node 2: z translation

Node 3: z translation

Node 4: y, z translation

**Fig. E10.20a**

Determine: The deflection and member end forces at node 9. Use computer software.

Solution: The computer output data for this structure is

$$\text{Joint 9} \begin{cases} w = 0.189 \text{ in.} \\ \theta_x = 0.00051 \text{ rad} \\ \theta_y = 0.00192 \text{ rad} \end{cases}$$

Member forces at node 9

$$\text{Member (9)} \begin{cases} V_Z = 1.31 \text{ kip} \\ M_x = 0.025 \text{ kip ft} \\ M_y = 14.5 \text{ kip ft} \end{cases}$$

$$\text{Member (10)} \begin{cases} V_Z = 5.2 \text{ kip} \\ M_x = 0.55 \text{ kip ft} \\ M_y = -16.6 \text{ kip ft} \end{cases}$$

$$\text{Member (11)} \begin{cases} V_Z = 8.2 \text{ kip} \\ M_x = 0.86 \text{ kip ft} \\ M_y = 27 \text{ kip ft} \end{cases}$$

$$\text{Member (12)} \begin{cases} V_Z = 5.3 \text{ kip} \\ M_x = 1.2 \text{ kip ft} \\ M_y = -26.2 \text{ kip ft} \end{cases}$$

One checks the results by noting that the sum of the end shears at node 9 must equal the applied load of 20 kip.

10.9 Summary

10.9.1 Objectives

- To describe the Displacement Method of analysis specialized for frame-type structures.
- To develop the slope-deflection equations for planar bending of beams
- To illustrate how to apply the Displacement Method for beams and rigid frame systems using the slope-deflection equations.
- To formulate the Moment Distribution procedure and demonstrate its application to indeterminate beams and rigid frames.

10.9.2 Key Factors and Concepts

- The Displacement Method works with nodal Force Equilibrium Equations expressed in terms of displacements
- The Slope-Deflection Equations relate the end shears and moments to the end translations and rotations. Their general form for planar bending of a prismatic member AB is

$$\begin{aligned} M_{AB} &= \frac{2EI}{L} \{2\theta_A + \theta_B\} + \frac{6EI}{L} \left(\frac{v_A - v_B}{L} \right) + M_{AB}^F \\ M_{BA} &= \frac{2EI}{L} \{2\theta_B + \theta_A\} + \frac{6EI}{L} \left(\frac{v_A - v_B}{L} \right) + M_{BA}^F \\ V_{AB} &= \frac{6EI}{L^2} (\theta_A + \theta_B) + \frac{12EI}{L^3} (v_A - v_B) + V_{AB}^F \\ V_{BA} &= -\frac{6EI}{L^2} (\theta_B + \theta_A) - \frac{12EI}{L^3} (v_A - v_B) + V_{BA}^F \end{aligned}$$

- Moment Distribution is a numerical procedure for distributing the unbalanced nodal moments into the adjacent members based on relative stiffness. If one continues the process until the moment residuals are reduced to zero, one would obtain the exact solution. Normally, the process is terminated when the residuals are relatively small.
- The Slope-Deflection Equations provide the basis for the Computer-Based Analysis Procedure described in Chap. 12.

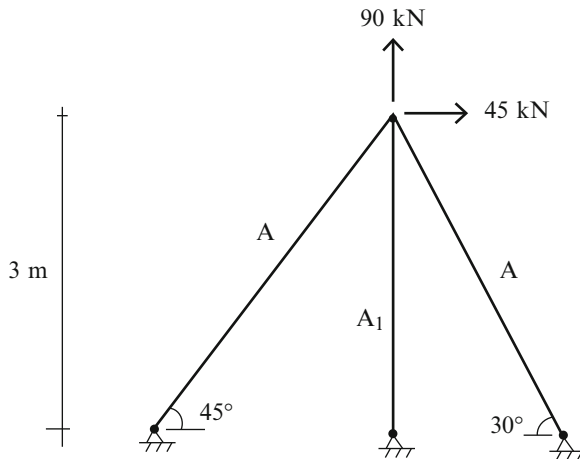
10.10 Problems

Problem 10.1

Determine the displacements and member forces for the truss shown. Consider the following values for the areas:

- (a) $A_1 = \frac{1}{2}A$
- (b) $A_1 = 2A$
- (c) Check your results with computer-based analysis.

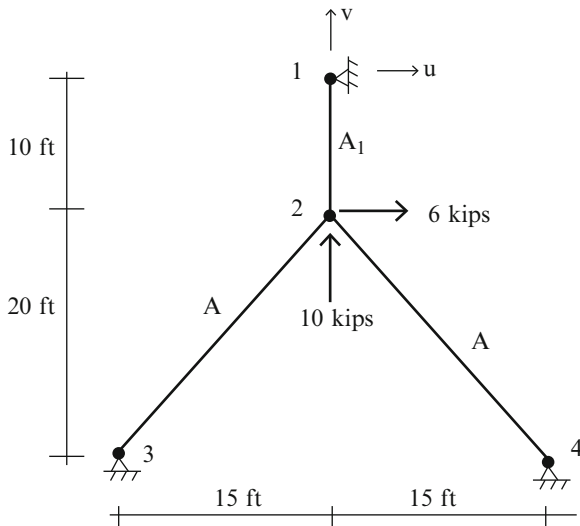
Take $E = 200$ GPa and $A = 2,000 \text{ mm}^2$



Problem 10.2

For the truss shown below, determine the member forces for:

- (a) The loading shown
- (b) Support #1 moves as follows: $u = \frac{1}{8}$ in. \rightarrow and $v = \frac{1}{2}$ in. \uparrow

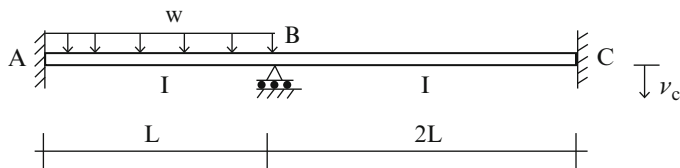


Take $A = 0.1 \text{ in.}^2$, $A_1 = 0.4 \text{ in.}^2$, and $E = 29,000 \text{ ksi}$.

For the following beams and frames defined in Problems 10.3–10.18, determine the member end moments using the slope-deflection equations.

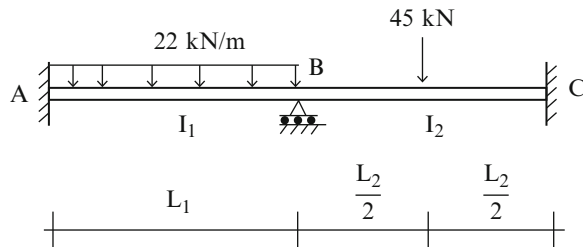
Problem 10.3

Assume $E = 29,000 \text{ ksi}$, $I = 200 \text{ in.}^4$, $L = 30 \text{ ft}$, $v_c = 0.6 \text{ in. } \downarrow$, and $w = 1.2 \text{ kip/ft}$.



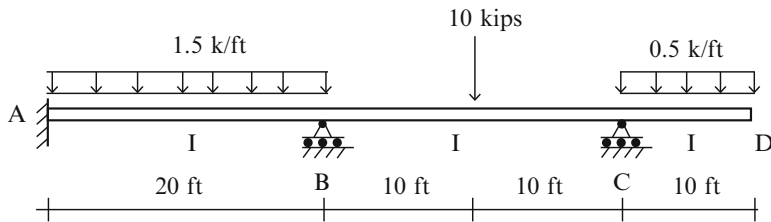
Problem 10.4

- (a) $I_1 = I_2$ and $L_1 = L_2$
- (b) $I_1 = 2I_2$ and $L_1 = L_2$
- (c) $I_1 = 2I_2$ and $L_1 = 2L_2$



Assume $E = 200 \text{ GPa}$, $I_2 = 80(10)^6 \text{ mm}^4$, and $L_2 = 6 \text{ m}$.

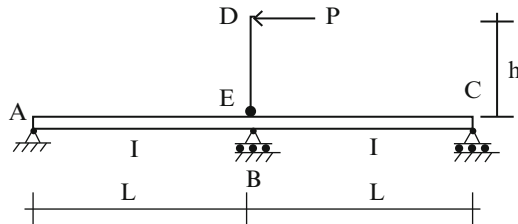
Problem 10.5



$E = 29,000 \text{ ksi}$ and $I = 300 \text{ in.}^4$

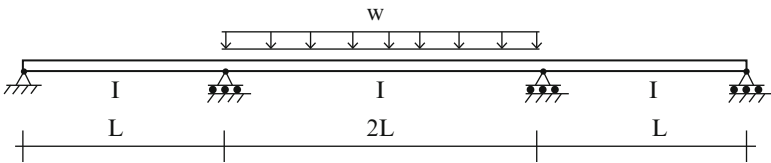
Problem 10.6

Assume $E = 200 \text{ GPa}$, $I = 80(10)^6 \text{ mm}^4$, $P = 45 \text{ kN}$, $h = 3 \text{ m}$ and $L = 9 \text{ m}$.



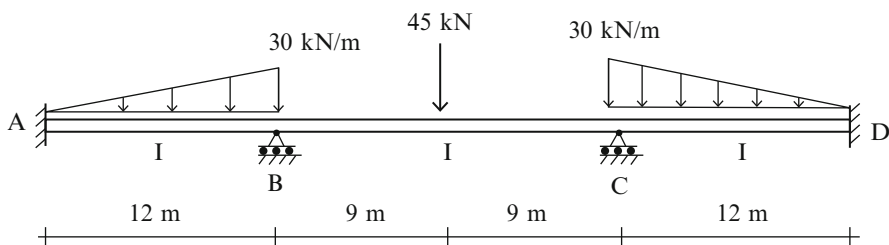
Problem 10.7

Assume $E=29,000 \text{ ksi}$, $I = 200 \text{ in.}^4$, $L = 18 \text{ ft}$, and $w = 1.2 \text{ kip/ft}$.



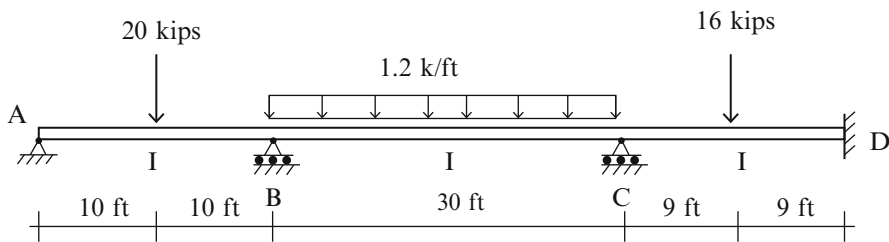
Problem 10.8

Assume $E = 200 \text{ GPa}$ and $I = 80(10)^6 \text{ mm}^4$.



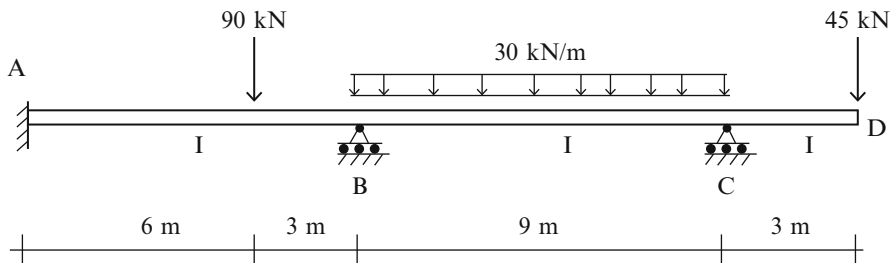
Problem 10.9

Assume $E = 29,000 \text{ ksi}$ and $I = 400 \text{ in.}^4$

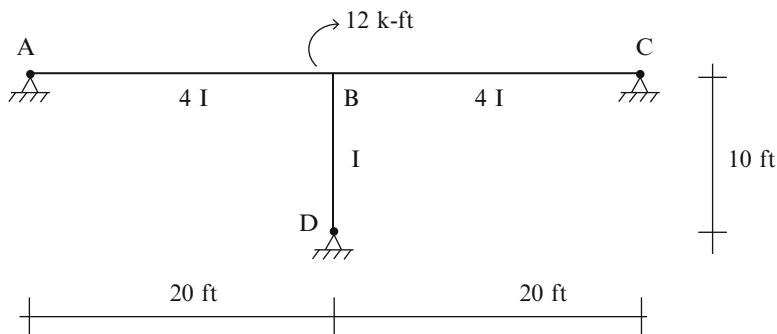


Problem 10.10

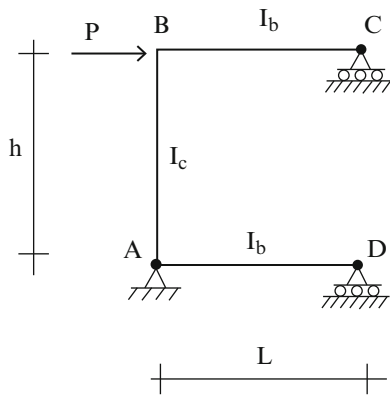
Assume $E = 200 \text{ GPa}$ and $I = 100(10)^6 \text{ mm}^4$.

**Problem 10.11**

Assume $E = 29,000 \text{ ksi}$ and $I = 100 \text{ in.}^4$.

**Problem 10.12**

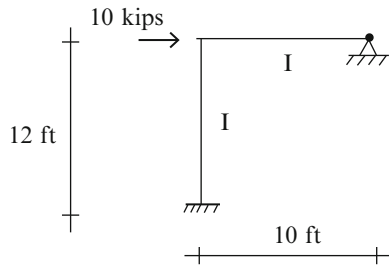
- (a) $I_b = I_c$
- (b) $I_b = 1.5I_c$



Assume $E = 200 \text{ GPa}$, $I_c = 120(10)^6 \text{ mm}^4$, $L = 8 \text{ m}$, $h = 4 \text{ m}$, and $P = 50 \text{ kN}$.

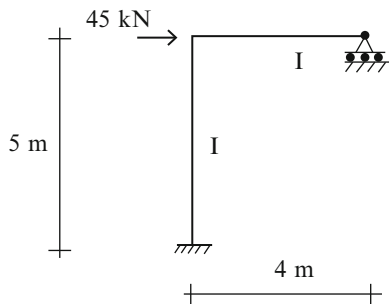
Problem 10.13

Assume $E = 29,000 \text{ ksi}$ and $I = 200 \text{ in.}^4$



Problem 10.14

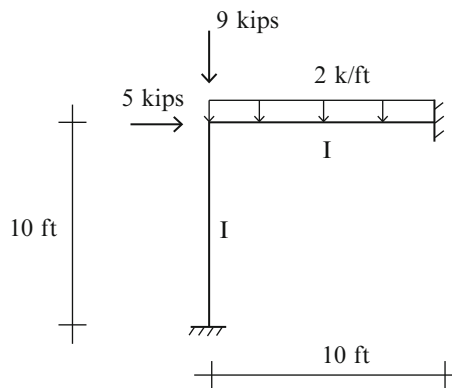
Assume $E = 200 \text{ GPa}$ and $I = 80(10)^6 \text{ mm}^4$.



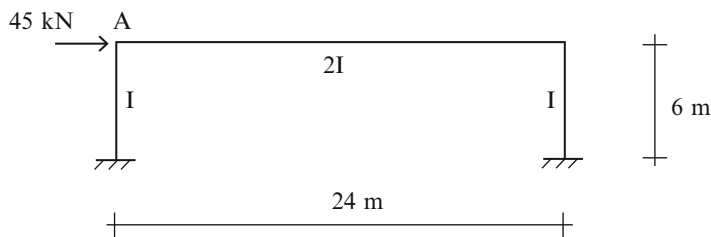
Problem 10.15

$$I = 600 \text{ in.}^4$$

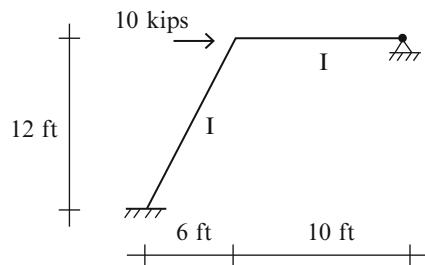
$$E = 29,000 \text{ kip/in.}^2$$

**Problem 10.16**

Assume $E = 200 \text{ GPa}$ and $I = 120(10)^6 \text{ mm}^4$.

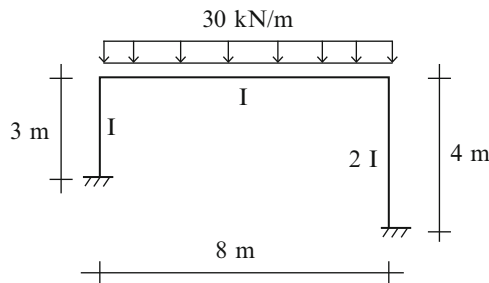
**Problem 10.17**

Assume $E = 29,000 \text{ ksi}$ and $I = 200 \text{ in.}^4$.

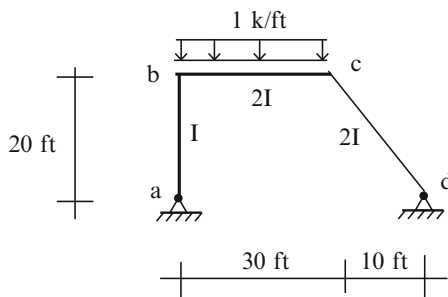


Problem 10.18

Assume $E = 200 \text{ GPa}$ and $I = 80(10)^6 \text{ mm}^4$.

**Problem 10.19**

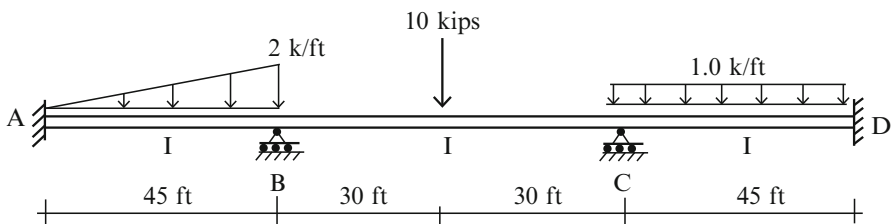
Assume $E = 29,000 \text{ ksi}$ and $I = 200 \text{ in.}^4$



For the following beams and frames defined in Problems 10.20–10.34, determine the member end moments using moment distribution.

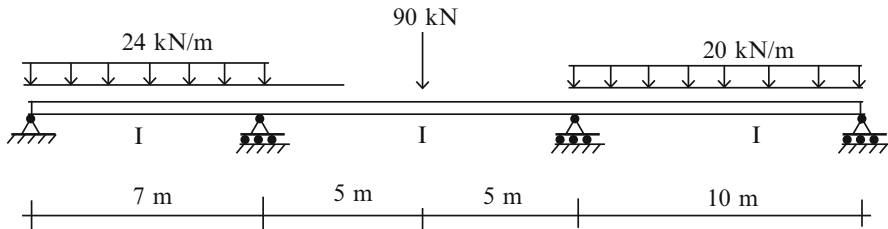
Problem 10.20

- (a) The loading shown
- (b) A support settlement of .5 in. downward at joint B in addition to the loading
- (c) Check your results with computer-based analysis

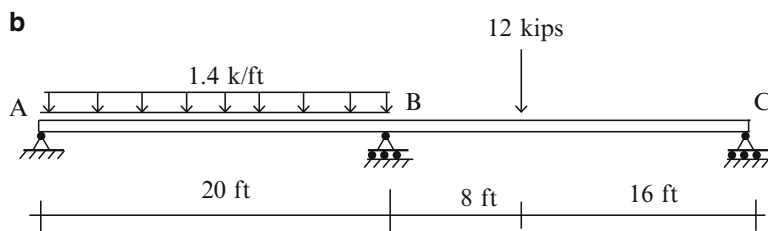
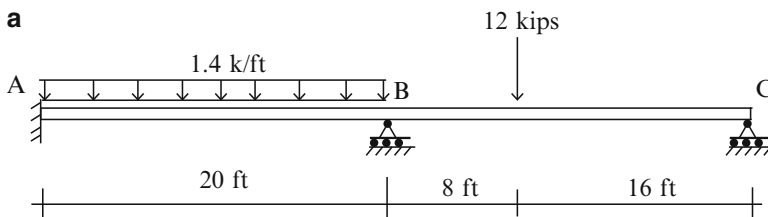


Problem 10.21

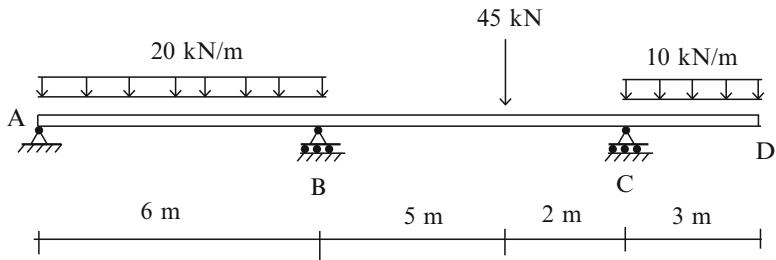
Compute the end moments and reactions. Draw the shear and moment diagrams. Check your results with computer analysis. Assume $E = 200 \text{ GPa}$ and $I = 75(10)^6 \text{ mm}^4$.

**Problem 10.22**

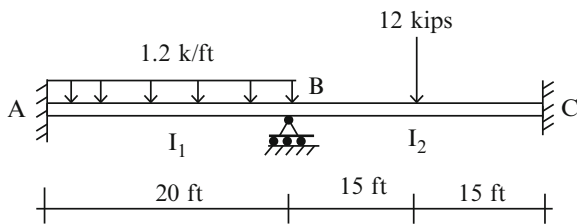
Determine the bending moments and the reactions for the following cases. Assume EI is constant

**Problem 10.23**

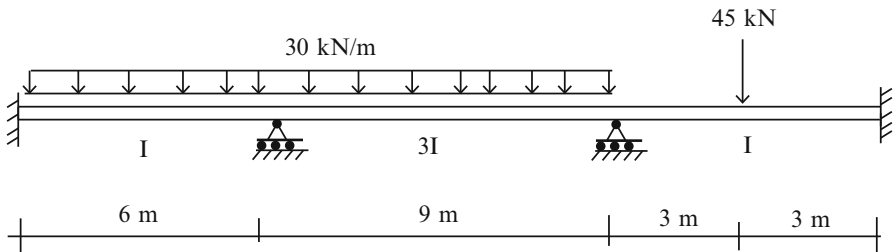
Determine the bending moment distribution for the beam shown below. Assume EI is constant.

**Problem 10.24**

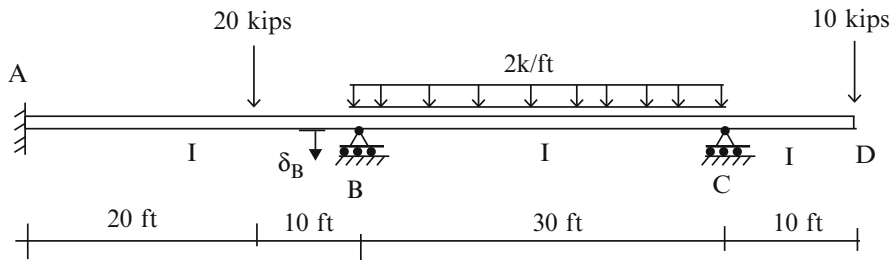
Determine the bending moment distribution. Assume $I_1 = 1.4I_2$.

**Problem 10.25**

Determine the bending moment distribution.

**Problem 10.26**

Solve for the bending moments. $\delta_B = 0.4 \text{ in.}$, $E = 29,000 \text{ ksi}$, and $I = 240 \text{ in.}^4$.

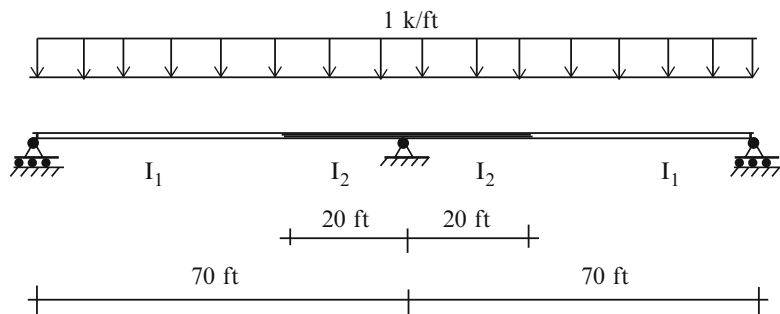
**Problem 10.27**

Determine the bending moment distribution and the deflected shape. $E = 29,000 \text{ ksi}$

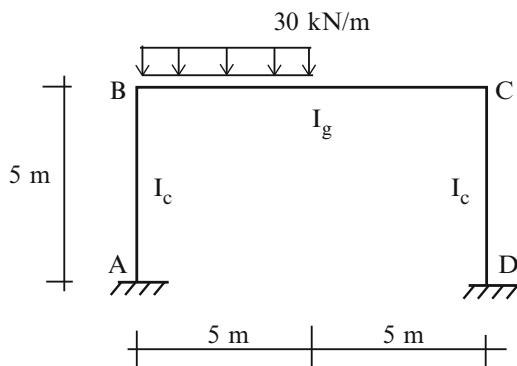
(a) Take $I_1 = I_2 = 1,000 \text{ in.}^4$

(b) Take $I_2 = 1.5I_1$. Use computer analysis.

Discuss the difference in behavior between case(a) and (b).

**Problem 10.28**

Determine the axial, shear, and bending moment distributions. Take $I_g = 2I_c$



Problem 10.29

Determine the member forces and the reactions.

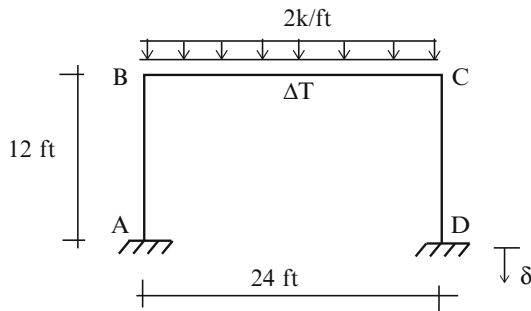
- Consider only the uniform load shown
- Consider only the support settlement of joint D ($\delta = 0.5$ in. \downarrow)
- Consider only the temperature increase of $\Delta T = 80^\circ\text{F}$ for member BC.

$$E = 29,000 \text{ ksi}$$

$$I_{AB} = I_{CD} = 100 \text{ in.}^4$$

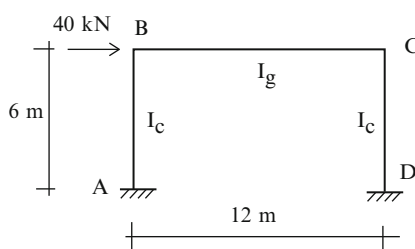
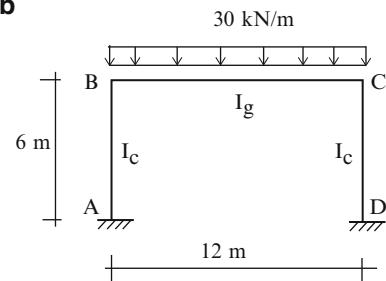
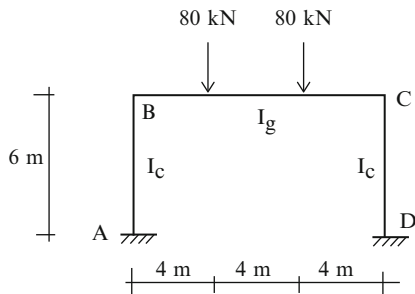
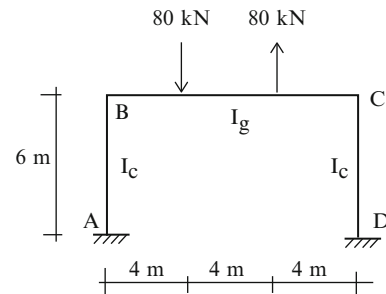
$$I_{BC} = 400 \text{ in.}^4$$

$$\alpha = 6.5 \times 10^{-6}/^\circ\text{F}$$



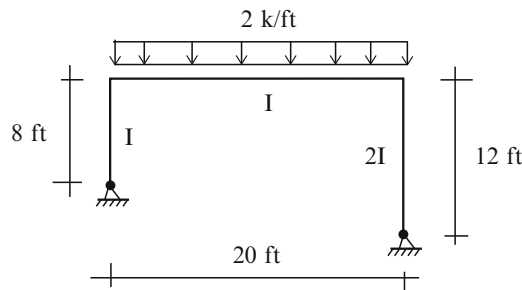
Problem 10.30

Determine the bending moment distribution for the following loadings. Take $I_g = 5I_c$.

a**b****c****d**

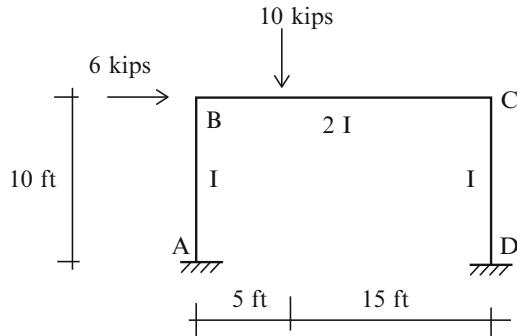
Problem 10.31

Solve for the bending moments.



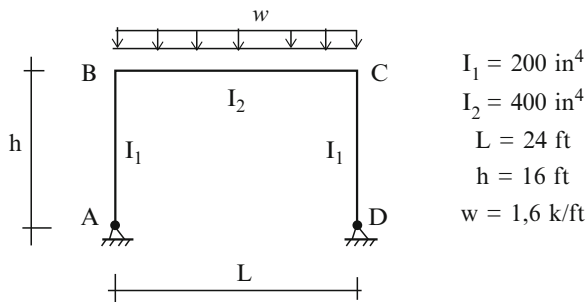
Problem 10.32

Determine the bending moment distribution.



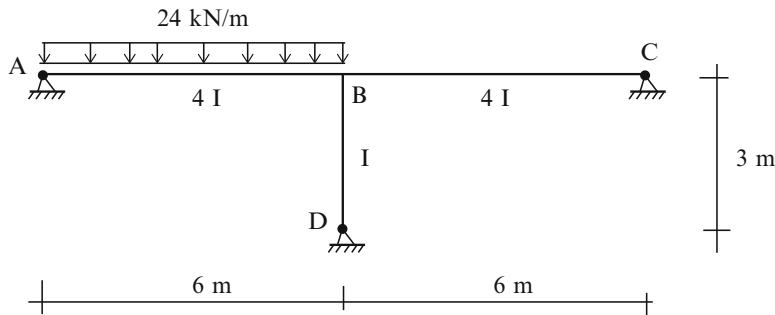
Problem 10.33

Solve for the bending moments.



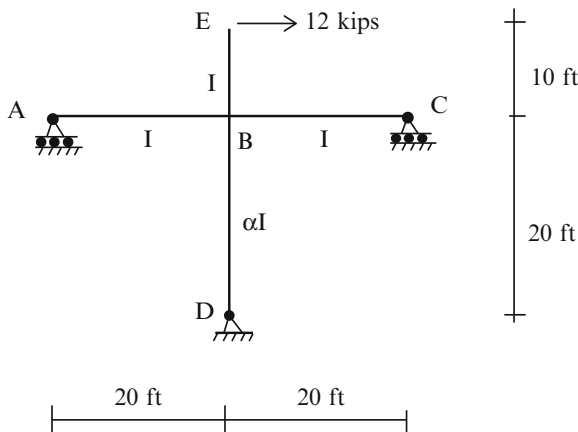
Problem 10.34

For the frame shown, determine the end moments and the reactions. Assume $E = 200 \text{ GPa}$ and $I = 40(10)^6 \text{ mm}^4$.

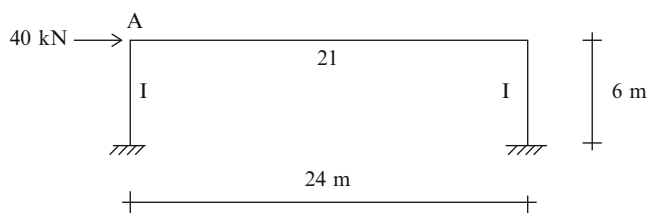
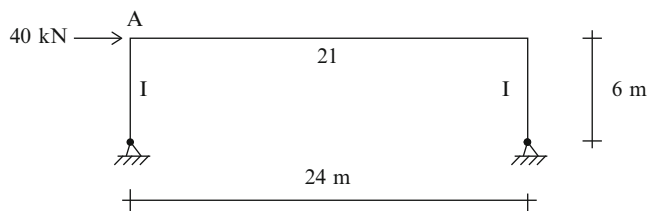
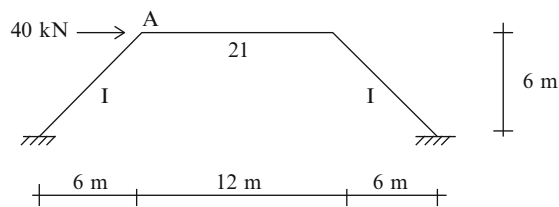
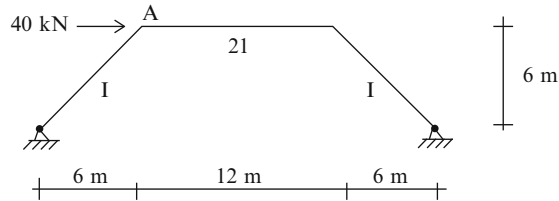


Problem 10.35

Determine analytic expression for the rotation and end moments at B. Take $I = 1,000 \text{ in.}^4$, $A = 20 \text{ in.}^2$ for all members, and $\alpha = 1.0, 2.0, 5.0$. Is there a upper limit for the end moment, M_{BD} ?

**Problem 10.36**

Compare the end moments and horizontal displacement at A for the rigid frames shown below. Check your results for parts (c) and (d) with a computer-based analysis. Take $E = 200 \text{ GPa}$ and $I = 120(10)^6 \text{ mm}^4$. $A = 10,000 \text{ mm}^2$ for all members.

a**b****c****d**

Approximate Methods for Estimating Forces in Statically Indeterminate Structures

11

Overview

In this chapter, we describe some approximate methods for estimating the forces in indeterminate structures. We start with multi-span beams subjected to gravity loading. Next, we treat rigid frame structures under gravity loading. Then, we consider rigid frame structures under lateral loading. For this case, we distinguish between short and tall buildings. For short buildings, we first describe the portal method, an empirical procedure, for estimating the shear forces in the columns, and then present an approximate stiffness approach which is more exact but less convenient to apply. For tall buildings, we model them as beams and use beam theory to estimate the forces in the columns. With all the approximate methods, our goal is to use simple hand calculation-based methods to estimate the forces which are needed for preliminary design and also for checking computer-based analysis methods.

11.1 Introduction

The internal forces in a statically indeterminate structure depend on the member cross-sectional properties. We demonstrated this dependency with the examples presented in the previous two chapters. However, in order to design a structure, one needs the internal forces. Therefore, when starting the design process, it is necessary to estimate a sufficient number of force quantities so that the structure is reduced to a statically determinate structure for which the distribution of internal forces is independent of the material properties. For bending type structures, such as multi-span beams and frames, the approximations are usually introduced by assuming moment releases at certain locations. The choice of the release locations is based on an understanding of the behavior of the structure for the particular loading under consideration. For indeterminate trusses, we assume the magnitude of certain forces. A typical case for a truss would be when there are two diagonals in a bay. We usually assume the transverse shear is divided equally between the two diagonals.

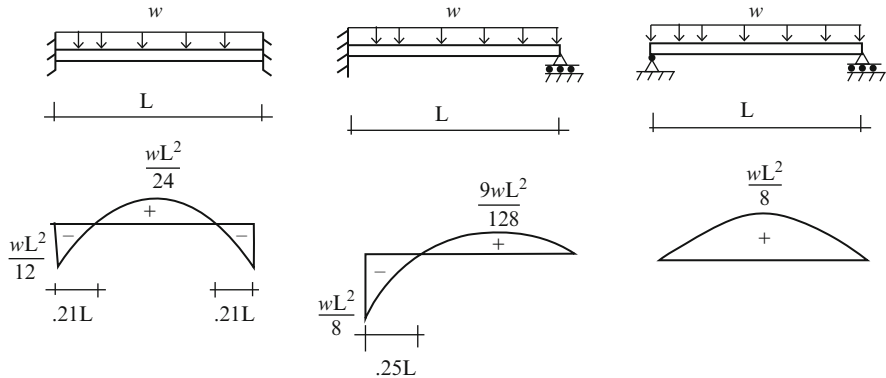


Fig. 11.1 Moment diagrams for single-span beams

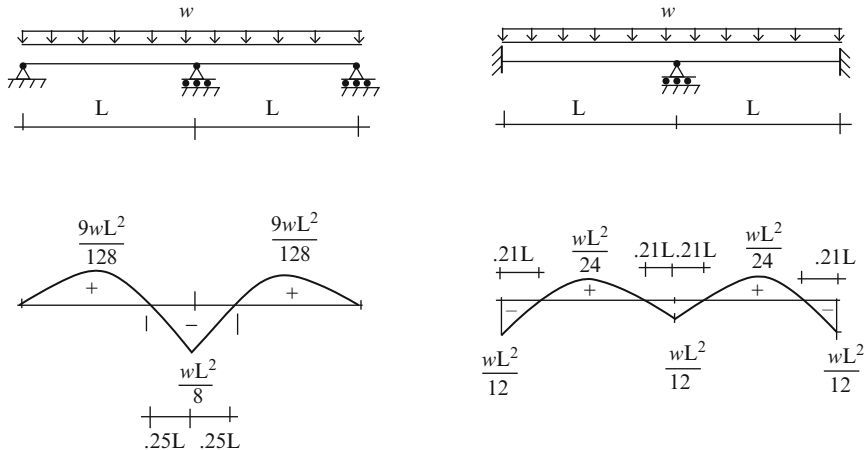


Fig. 11.2 Moment diagrams for two-span beams

11.2 Multi-span Beams: Gravity Loading

11.2.1 Basic Data-Moment Diagrams

Figures 11.1, 11.2, and 11.3 shows moment diagrams due to a uniform distributed loading for a range of beam geometries and support conditions. These results are presented in Chaps. 9 and 10. They provide the basis for assuming the location of moment releases (points of zero moment) for different combinations of span lengths and loading distributions. We utilize this information to develop various strategies for generating approximate solutions for multi-span beams.

11.2.2 Quantitative Reasoning Based on Relative Stiffness

Consider the multi-span beam shown in Fig. 11.4. Our objective is to estimate the peak positive and negative moments in span BC. As a first step, we estimate the end

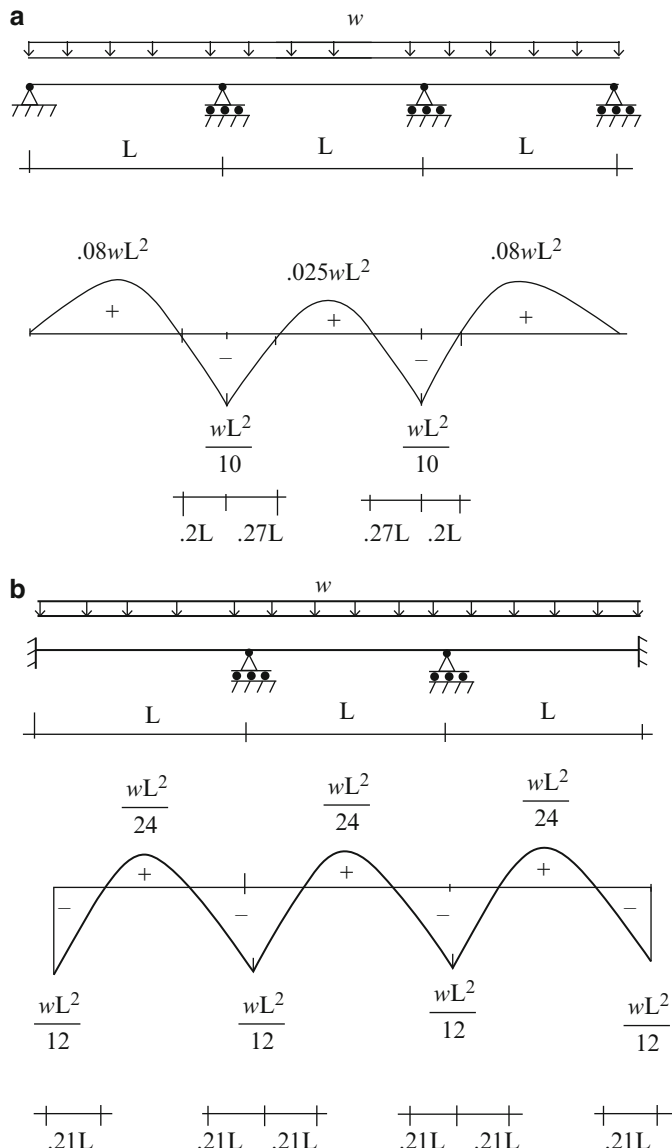
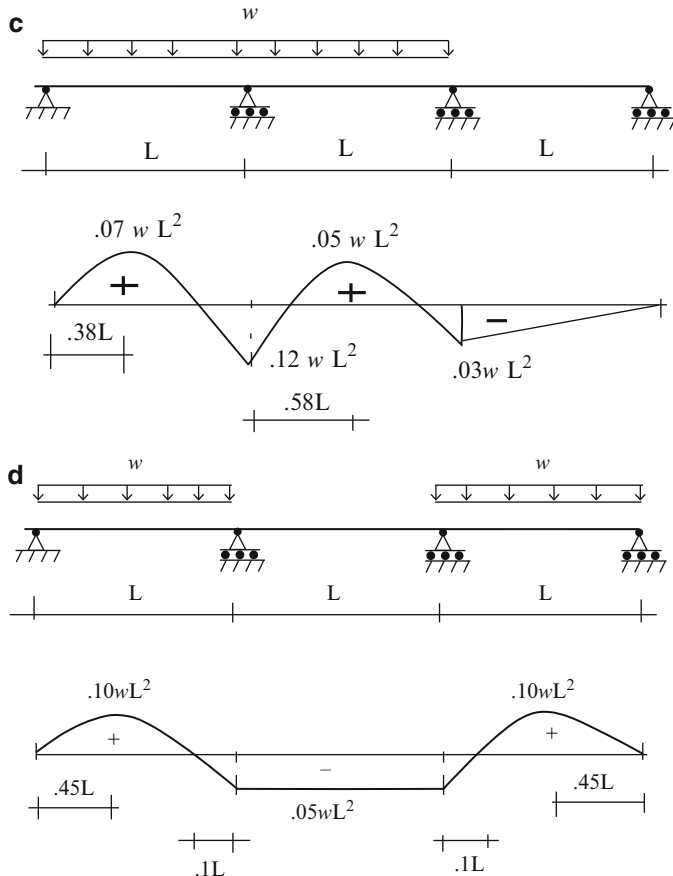
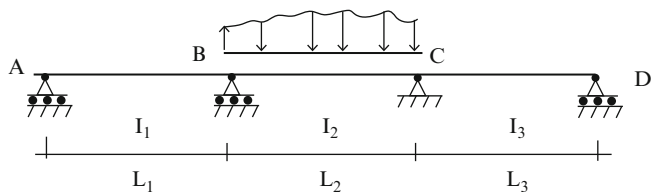


Fig. 11.3 Moment diagrams for three-span beams. (a) Simply supported. (b) Fixed at each end. (c) Partial loading. (d) Partial loading symmetrical

**Fig. 11.3** (continued)**Fig. 11.4** Multi-span beam

moments for this span using the member distribution factors which are related to the relative stiffness factors for the members. We consider node B. The distribution factors for members BA and BC are as follows (see Sect. 10.6):

$$DF_{BA} = \frac{I_1/L_1}{((I_1/L_1) + (I_2/L_2))} \quad (11.1)$$

$$DF_{BC} = \frac{I_2/L_2}{((I_1/L_1) + (I_2/L_2))}$$

Note that when I is constant for all spans, the relative stiffness parameters reduce to the inverse of the span length. Given the initial unbalanced moment at B, we distribute it according to

$$\begin{aligned}\Delta M_{BA} &= -DF_{BA}(FEM|_B) \\ \Delta M_{BC} &= -DF_{BC}(FEM|_B)\end{aligned} \quad (11.2)$$

We consider no carry over movement to the other ends.

If I_1/L_1 is small in comparison to I_2/L_2 , then DF_{BA} will be small in comparison to DF_{BC}

It follows that only a small portion of the unbalanced nodal moment at node B will be distributed to member BA. The opposite case is where I_1/L_1 is large in comparison to I_2/L_2 . Now DF_{BC} is small vs. DF_{BA} . Essentially all of the unbalanced nodal moment is distributed to member BA. The final end moment in member BC is close to its initial value (the initial fixed end moment) since there is relatively little distribution.

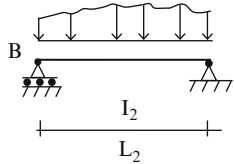
When I is constant for all the spans, the relative stiffness parameters reduce to the inverse of the span lengths. In this case, one compares the ratio of adjacent span lengths. The limiting cases for extreme values of these ratios are listed in Fig. 11.5.

11.3 Multistory Rigid Frames: Gravity Loading

Gravity type loading is usually the dominant loading for multistory frames. It consists of both dead and live loading. Consider the frame shown in Fig. 11.6. We suppose the loading is a uniform gravity load, w . Our objective here is to determine the positive and negative moments in beam AB.

a

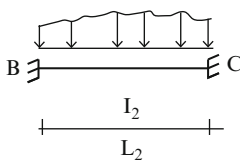
$$\frac{I_1}{L_1} \ll \frac{I_2}{L_2}$$

If $I_1 = I_2 = I$ and $L_2 \ll L_1$ 

$$\frac{I_3}{L_3} \ll \frac{I_2}{L_2}$$

If $I_2 = I_3 = I$ and $L_2 \ll L_3$ **b**

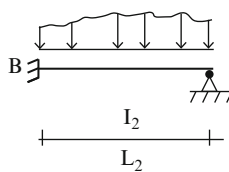
$$\frac{I_1}{L_1} \gg \frac{I_2}{L_2}$$

If $I_1 = I_2 = I$ and $L_2 \gg L_1$ 

$$\frac{I_3}{L_3} \gg \frac{I_2}{L_2}$$

If $I_2 = I_3 = I$ and $L_2 \gg L_3$ **c**

$$\frac{I_1}{L_1} \gg \frac{I_2}{L_2}$$

If $I_1 = I_2 = I$ and $L_2 \gg L_1$ 

$$\frac{I_3}{L_3} \ll \frac{I_2}{L_2}$$

If $I_2 = I_3 = I$ and $L_2 \ll L_3$

Fig. 11.5 Summary of approximate models for extreme values of L_1/L_2 and L_3/L_2 . (a) Hinged model. (b) Clamped end model. (c) Clamped/hinged model

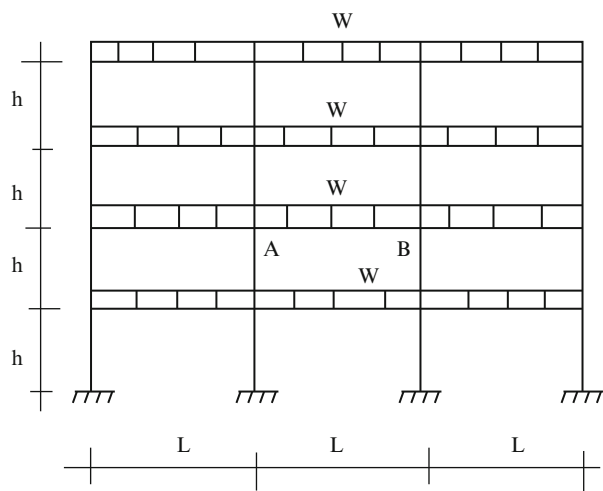


Fig. 11.6 Multistory frame—gravity loading

One can estimate moments at the ends and at the center by assuming moment releases in the beams. Assuming moment releases at $0.1L$ leads to

$$M_{\text{center}}^+ = \frac{w(0.8L)^2}{8} = 0.08wL^2$$

$$M_A = M_B = w \frac{(0.1L)^2}{2} + w(0.4L)(0.1L) = 0.045wL^2$$

11.4 Multistory Rigid Frames: Lateral Loading

Consider the rigid frame shown in Fig. 11.7a. Under a lateral loading, the frame develops inflection points (points where the bending moment is equal to zero) in the columns and beams. Most of the approximate methods published in the literature are based on the assumption that the inflection points occur at mid-height of the columns and mid-span of the beams, as indicated in Fig. 11.7c. This assumption,

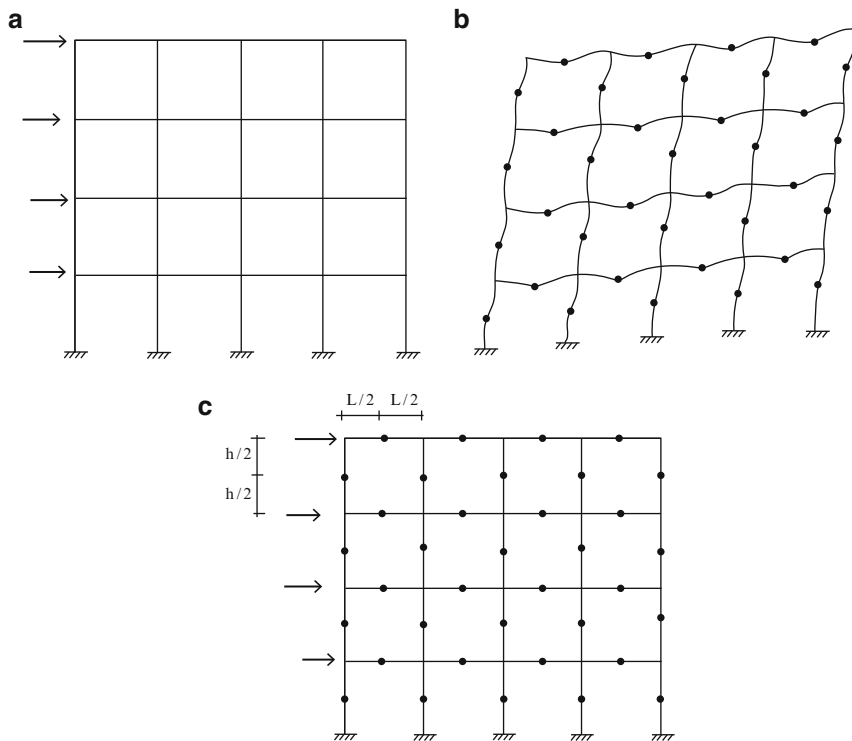


Fig. 11.7 Multistory rigid frame. (a) Initial position. (b) Deflected Position. (c) Assumed location of inflection points

coupled with an assumption concerning how the column axial and shear forces are distributed within a story, is sufficient to allow us to compute estimates for the end moments, the axial forces, and the shear forces in the columns.

In this section, we present two different approaches for estimating the forces in the columns. The first approach estimates the column shears in a story, and is applicable mainly for *low-rise rigid frames*. The second approach estimates the axial forces in the columns. Because of the nature of the underlying assumptions, the latter procedure is appropriate only for *tall, narrow rigid frames*. Both procedures are derived using the idealized model of the structure shown in Fig. 11.7c, i.e., with inflection points at mid-height of the columns and mid-span of the beams.

11.4.1 Portal Method

The Portal Method is an empirical procedure for estimating the forces in low-rise rigid frames subjected to lateral loads. In addition to assuming inflection points in the columns and beams, *the shear in the exterior columns is assumed to be one-half the shear in the interior columns*, which is taken to be equal for all the interior columns. We use this method to generate the first estimate of the member forces. Of particular interest are the end moments in the columns.

Example 11.1 Application of the Portal method

Given: The rigid frame shown in Fig. E11.1a.

Determine: The axial force, shear force, and bending moment in the beams and columns using the Portal method.

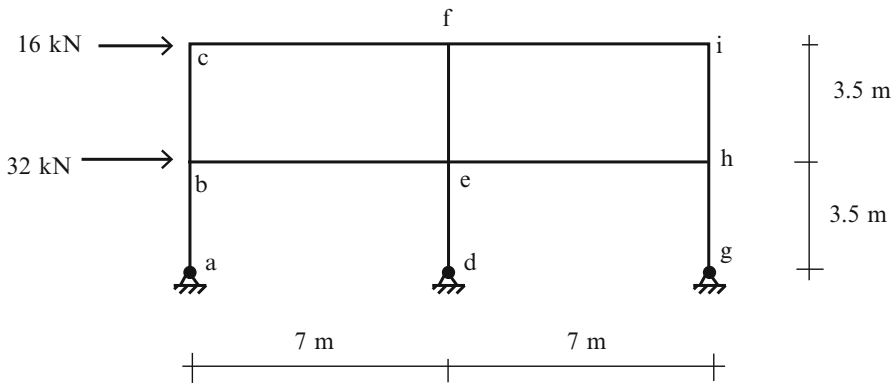


Fig. E11.1a

Solution: The Portal method assumes the exterior column shear, V_E , is equal to one-half the interior column shear force V_I , which is taken to be equal for all the interior columns.

$$V_E = \frac{1}{2} V_I$$

Summing the column shear forces for this structure leads to an expression for the total story shear.

$$\begin{aligned} V_T &= 2V_E + V_I \\ &= 2V_I \end{aligned}$$

Then,

$$\begin{aligned} V_I &= \frac{1}{2} V_T \\ V_E &= \frac{1}{2} V_I = \frac{1}{4} V_T \end{aligned}$$

We range over the stories and generate the column shear for each story. The calculations are summarized below.

Story	V_T (kN)	V_I (kN)	V_E (kN)
Top	16	8	4
Bottom	48	24	12

Given the column shear forces, one can determine the column end moments using the assumption that there are inflection points at certain locations in the columns. For this structure, since the base is pinned, the inflection points for the first story are at the base. The inflection points for the second story are taken at mid-height. The free body diagrams for the various segments are shown below along with the final results. Once the column end moments are known, we can determine the end moments and shear forces in the beams and lastly, the axial forces in the columns using equilibrium equations (Figs. E11.1b-h).

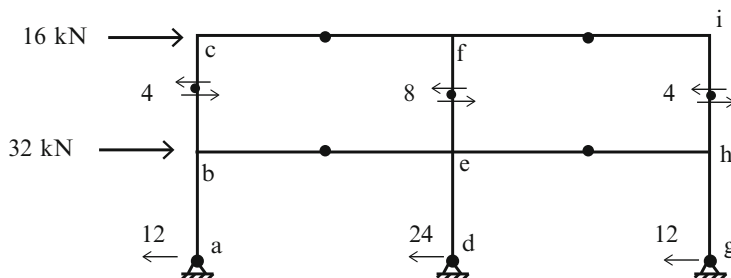
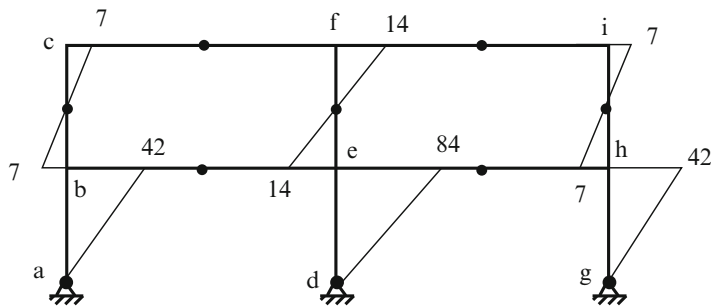
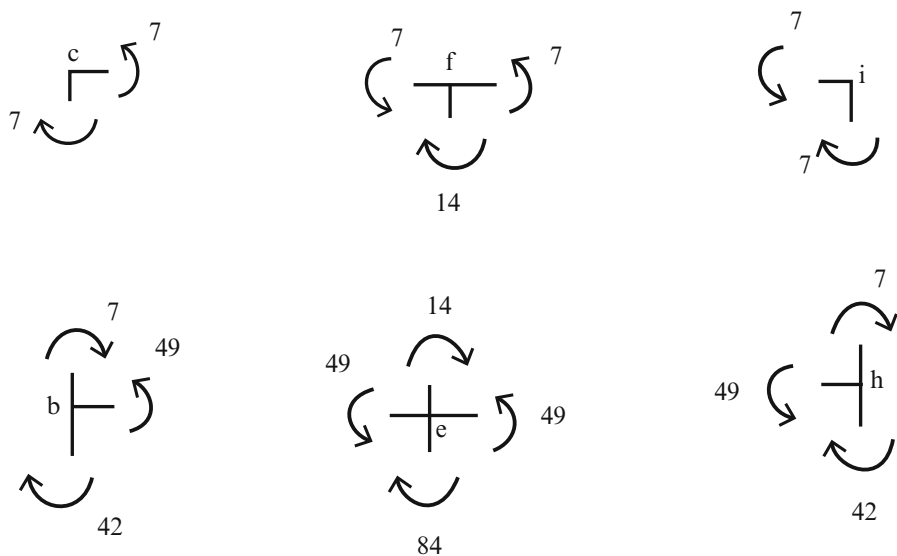
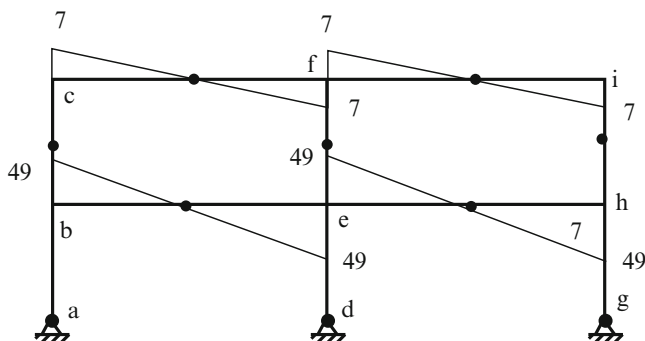


Fig. E11.1b Shear distribution for the columns (kN)

**Fig. E11.1c** Bending moment distribution for the columns (kN m)**Fig. E11.1d** Moments at the joints (kN m)**Fig. E11.1e** Bending moment distribution for the beams (kN m)

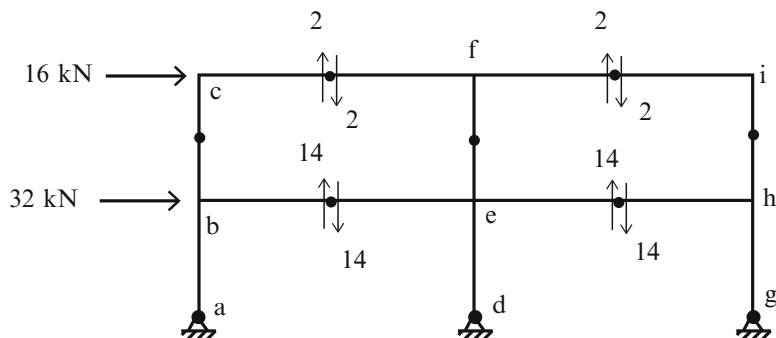


Fig. E11.1f Shear distribution for the beams (kN)

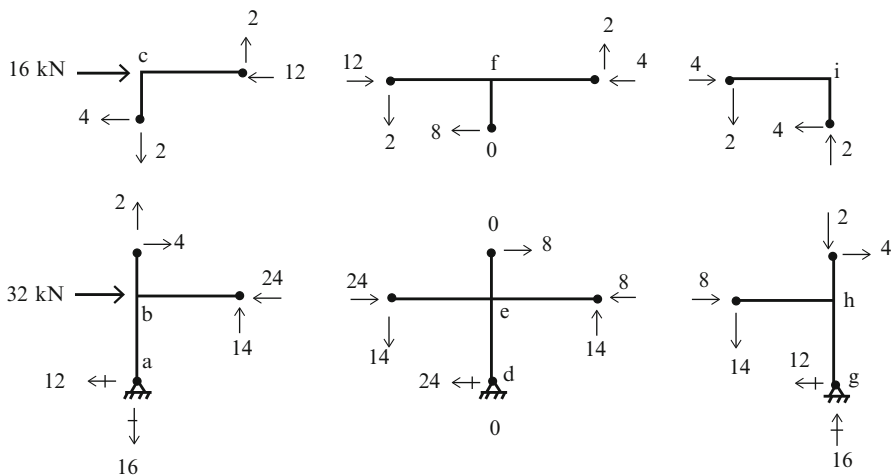


Fig. E11.1g Axial and shear forces (kN)

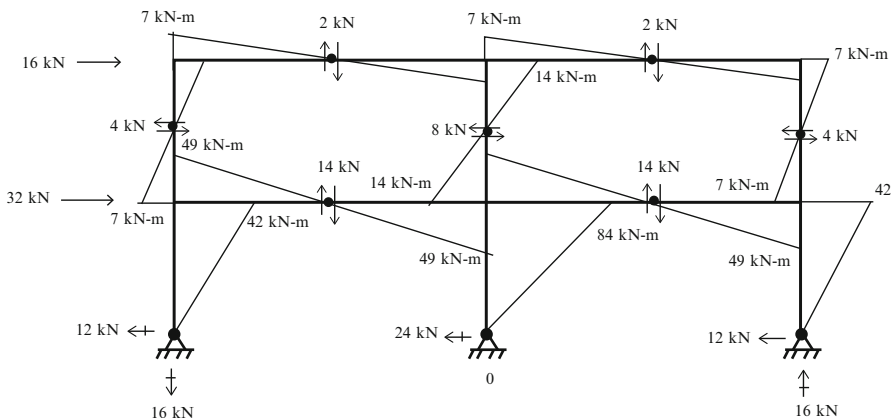


Fig. E11.1h Reactions, shear forces and moment distributions

Example 11.2 Application of the Portal method

Given: The rigid frame shown in Fig. E11.2a.

Determine: The reactions and the bending moments in the beams and columns using the Portal method.

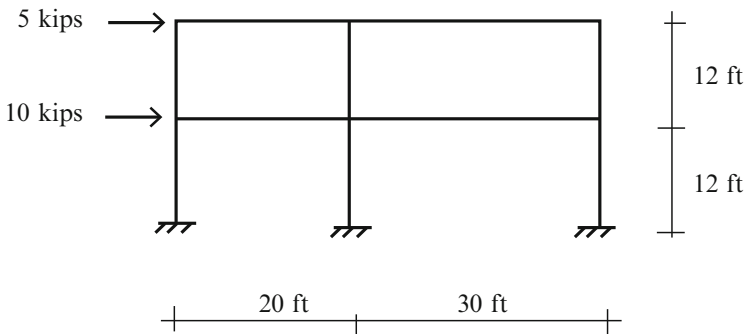


Fig. E11.2a

Solution: The Portal method assumes the exterior column shear, V_E , is equal to one-half the interior column shear force V_I . The calculations are summarized in the table below. Note that, since the base is fixed, we assume inflection points at mid-height for the first story (Figs. E11.2b-h).

Story	V_T (kip)	V_I (kip)	V_E (kip)
Top	5	2.5	1.25
Bottom	15	7.5	3.75

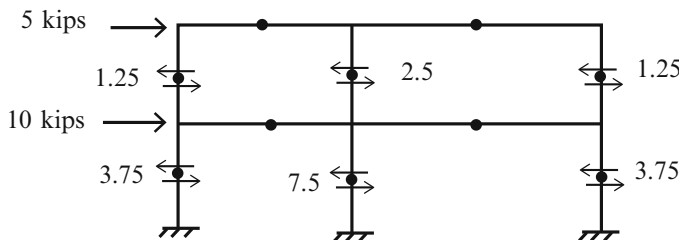
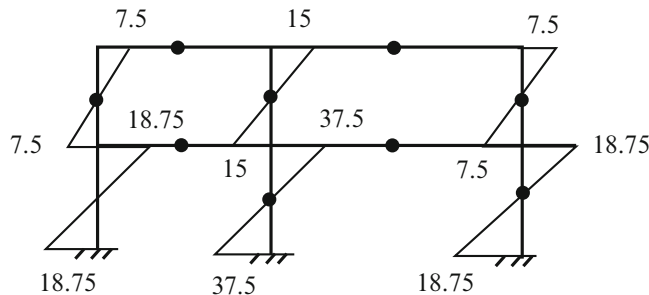
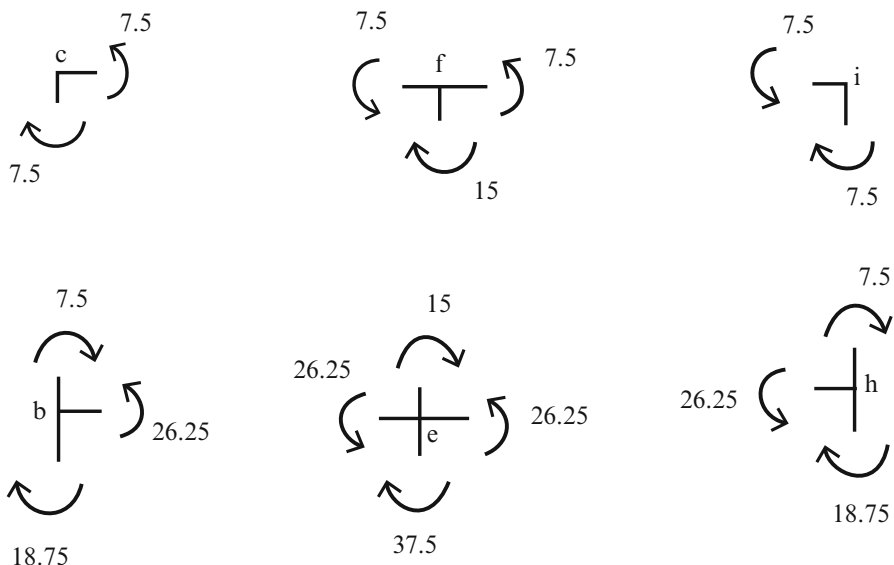
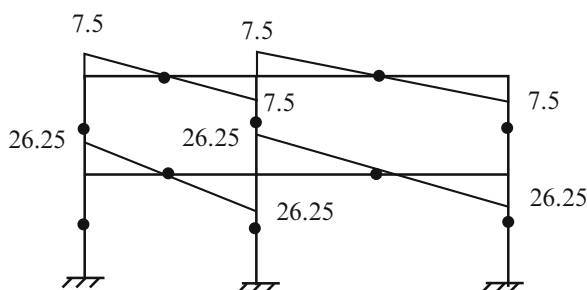


Fig. E11.2b Shear distribution for the columns (kip)

**Fig. E11.2c** Bending moment distribution for the columns (kip ft)**Fig. E11.2d** Moments at the joints (kip ft)**Fig. E11.2e** Bending moment distribution for the beams (kip ft)

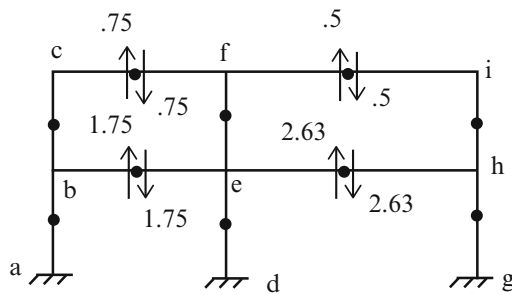


Fig. E11.2f Shear distribution for the beams (kip)

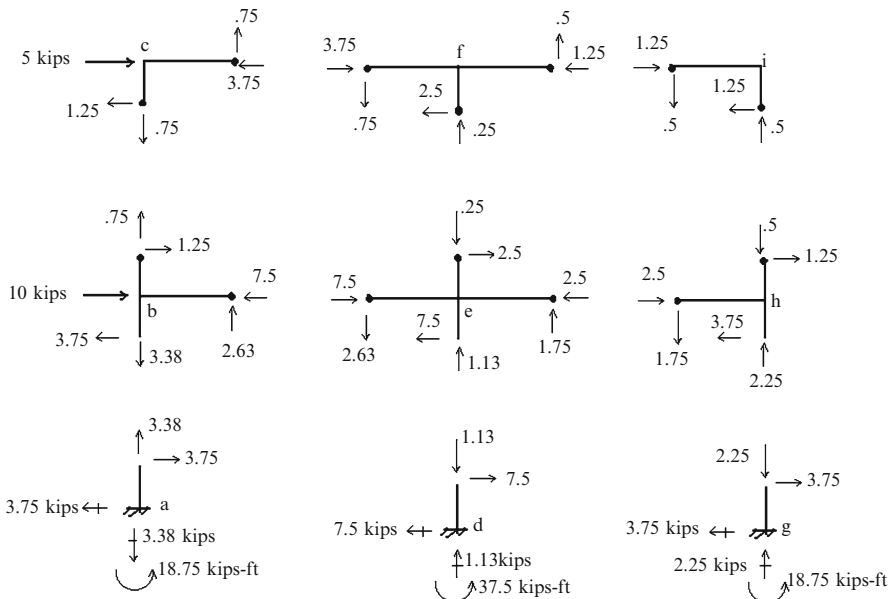


Fig. E11.2g Axial and shear forces (kip)

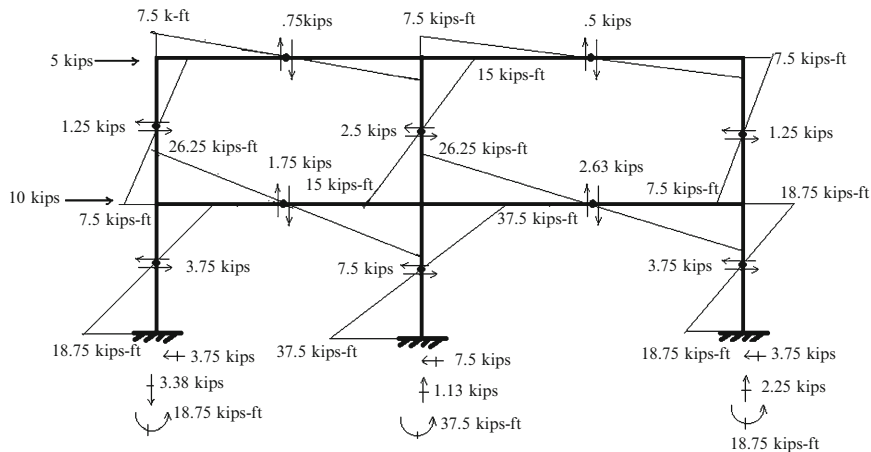


Fig. E11.2h Reactions, shear forces and moment distribution

11.4.2 Shear Stiffness Method: Low-Rise Rigid Frames

The idealized model is defined in Fig. 11.8. We consider a segment bounded by floor $i + 1$ and floor i . For convenience, we assume I_b and L are *constant* in a story. We allow for different values of I for the exterior and interior columns. We define V_T as the sum of the lateral loads acting on floor $i + 1$, and all the floors above floor $i + 1$. This quantity represents the *total transverse shear* for the story. Next, we define Δu as the differential lateral displacement between floor i and floor $i + 1$. We assume the floor beams are *rigid* with respect to axial deformation so that all points on the floor experience the same lateral displacement, Δu . Lastly, we assume the floors do not move in the vertical direction, and insert rollers as indicated in Fig. 11.9. Our objective in this section is to establish an expression for the column shear forces in a story as a function of the total transverse shear for the story.

We visualize the model to consist of the sub-elements shown in Fig. 11.9b. Each sub-element experiences the same Δu . The resistance force ΔP_i for sub-element i depends on the stiffness of the element.

$$\Delta P_i = k_i \Delta u \equiv V_i \quad (11.3)$$

Then, summing the forces over the number of sub-elements leads to

$$V_T = \sum V_i = \left(\sum k_i \right) \Delta u = k_T \Delta u \quad (11.4)$$

Noting (11.3) and (11.4), the shear carried by sub-element i is given by

$$V_i = \Delta P_i = \left(\frac{k_i}{\sum k_i} \right) V_T = \left(\frac{k_i}{k_T} \right) V_T \quad (11.5)$$

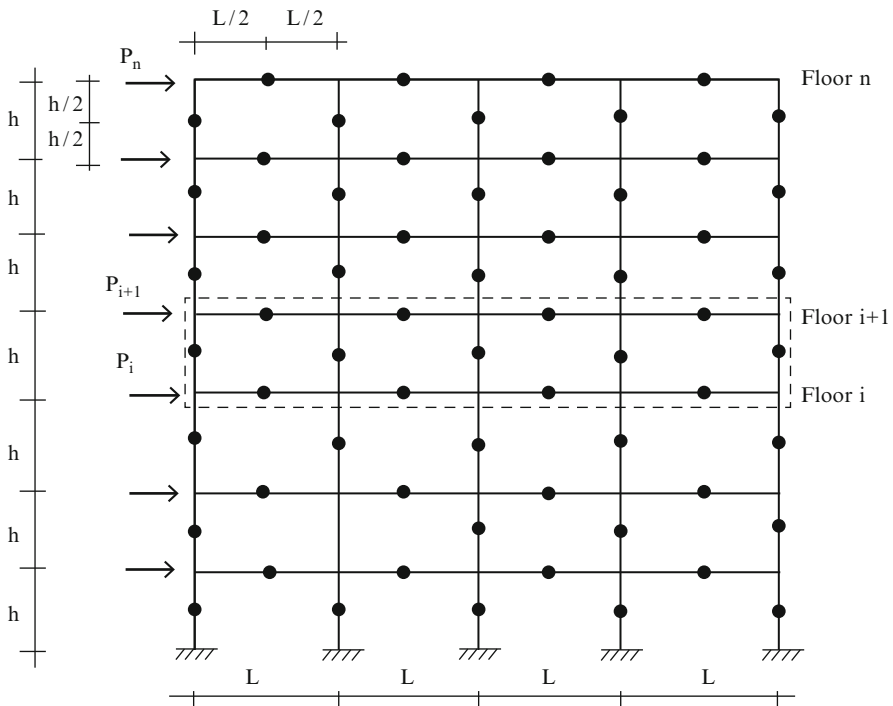


Fig. 11.8 Low-rise frame

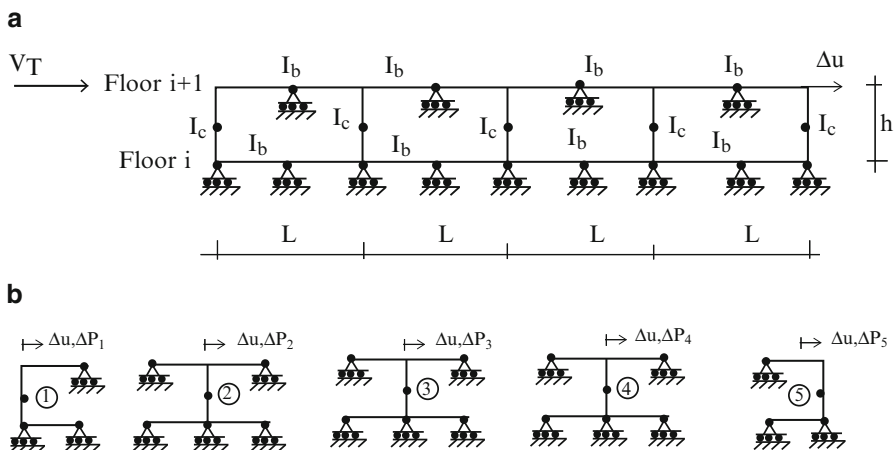


Fig. 11.9 (a) Idealized model for a story in a low-rise frame. (b) Sub-elements of the idealized model—low-rise frame

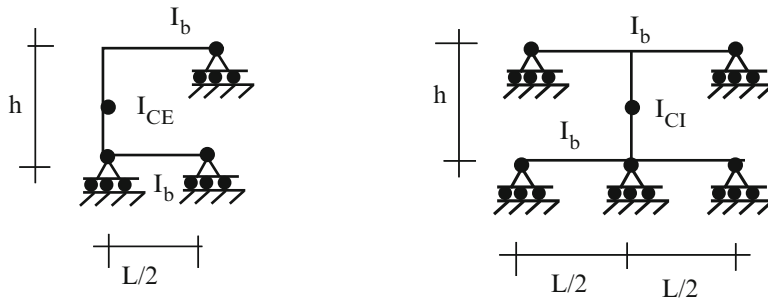


Fig. 11.10 Typical sub-elements. (a) Exterior. (b) Interior

Table 11.1 Stiffness ratios: Upper stories

$(I_{CI}/h)/(I_b/L)$	$\frac{k_E}{k_I}$	$\frac{I_{CE}}{I_{CI}} = 1/2$	$\frac{I_{CE}}{I_{CI}} = 1$
0	0.5	1	
0.25	0.45	0.9	
0.5	0.417	0.83	
1.0	0.375	0.75	
1.5	0.35	0.7	
2.0	0.33	0.67	

According to (11.5), the shear in a column depends on the ratio of the shear stiffness of the corresponding sub-element to the total story shear stiffness.

Using the slope-deflection equations presented in Sect. 10.3, one can derive the following expressions for the sub-element shear stiffness factors (Fig. 11.10):

Exterior Element—upper story

$$k_E = \frac{12EI_{CE}}{h^3} \left\{ \frac{1}{1 + (I_{CE}/h)/(I_b/L)} \right\} = \frac{12EI_{CE}}{h^3} f_E \quad (11.6)$$

Interior Element—upper story

$$k_I = \frac{12EI_{CI}}{h^3} \left\{ \frac{1}{1 + (1/2)((I_{CI}/h)/(I_b/L))} \right\} = \frac{12EI_{CI}}{h^3} f_I \quad (11.7)$$

where the dimensionless factor, $(I_c/h)/(I_b/L)$, accounts for the flexibility of the beam.

Values of k_E/k_I for a range of values of $(I_{CI}/h)/(I_b/L)$ and I_{CE}/I_{CI} are tabulated below (Table 11.1).

Noting (11.5) we observe that the ratio of the shear in the exterior column to the shear in the interior column is given by

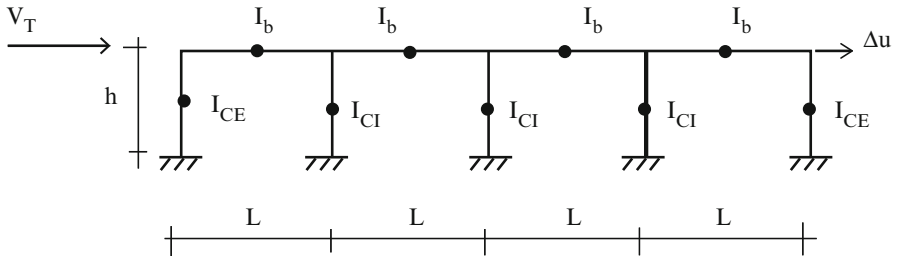


Fig. 11.11 Transverse shear model for bottom story—fixed support

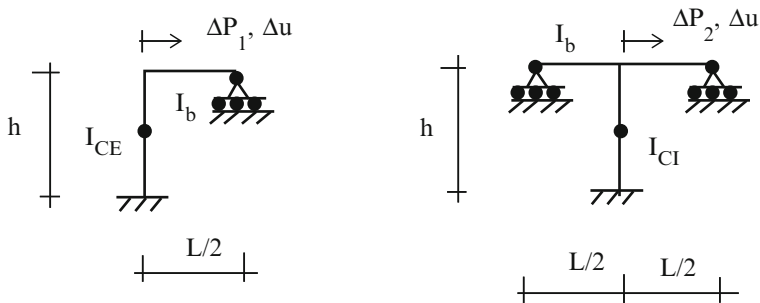


Fig. 11.12 Typical sub-elements for base story—fixed support. (a) Exterior. (b) Interior

$$\frac{V|_{E-\text{col}}}{V|_{I-\text{col}}} = \frac{k_E}{k_I} \quad (11.8)$$

The derivation listed above applies for the upper stories, and needs to be modified for the bottom story. Figure 11.11 shows the idealized model used to estimate the story stiffness for the case where the base is fixed. The sub-elements are illustrated in Fig. 11.12 and the corresponding story stiffness factors are defined by (11.9) and (11.10).

Exterior Element—Base Story (Fixed support)

$$k_{BE} = \frac{12EI_{CE}}{h^3} \left\{ \frac{1 + \frac{1}{6} \left(\frac{I_{CE}/h}{I_b/L} \right)}{1 + \frac{2}{3} \left(\frac{I_{CE}/h}{I_b/L} \right)} \right\} = \frac{12EI_{CE}}{h^3} f_{BE} \quad (11.9)$$

Interior Element—Base Story (Fixed support)

$$k_{BI} = \frac{12EI_{CI}}{h^3} \left\{ \frac{1 + \frac{1}{12} \left(\frac{I_{CI}/h}{I_b/L} \right)}{1 + \frac{1}{3} \left(\frac{I_{CI}/h}{I_b/L} \right)} \right\} = \frac{12EI_{CI}}{h^3} f_{BI} \quad (11.10)$$

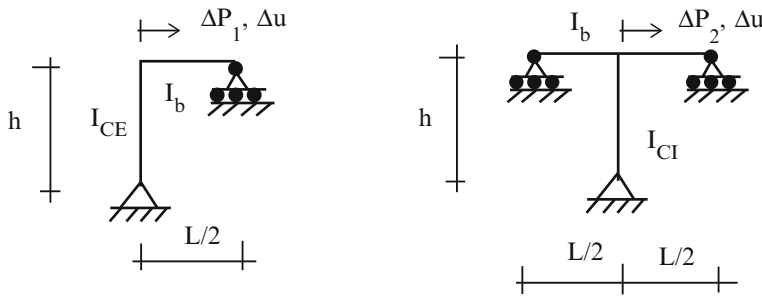


Fig. 11.13 Typical sub-elements for base story—hinged support. (a) Exterior. (b) Interior

When the base is hinged, we use the expressions listed in (11.11) and (11.12). In this case, we do not assume an inflection point at mid-height of the first story (Fig. 11.13).

Exterior Element—Base Story (Hinged support)

$$k_{BE} = \frac{3EI_{CE}}{h^3} \left\{ \frac{1}{1 + (1/2)((I_{CE}/h)/(I_b/L))} \right\} = \frac{3EI_{CE}}{h^3} f_{BE} \quad (11.11)$$

Interior Element—Base Story (Hinged support)

$$k_{BI} = \frac{3EI_{CI}}{h^3} \left\{ \frac{1}{1 + (1/4)((I_{CI}/h)/(I_b/L))} \right\} = \frac{3EI_{CI}}{h^3} f_{BI} \quad (11.12)$$

The base shears are related by

$$V|_{E-\text{col}} = V|_{I-\text{col}} \frac{k_{BE}}{k_{BI}} \quad (11.13)$$

Values of k_{BE}/k_{BI} for a range of $(I_{CI}/h)/(I_b/L)$ for both hinged and fixed supports are listed in the Table 11.2.

Table 11.2 Stiffness ratios: Lowest story

$(I_{CI}/h)/(I_b/L)$	Hinged support		Fixed support	
	$\frac{k_E}{k_I}$	$I_{CE} = 1/2 I_{CI}$	$\frac{k_E}{k_I}$	$I_{CE} = 1/2 I_{CI}$
	$I_{CE} = I_{CI}$		$I_{CE} = I_{CI}$	$I_{CE} = I_{CI}$
0	0.5	1	0.5	1
0.25	0.472	0.944	0.472	0.948
0.5	0.45	0.9	0.455	0.91
1.0	0.417	0.833	0.431	0.862
1.5	0.393	0.783	0.471	0.833
2.0	0.375	0.75	0.408	0.816

Example 11.3 Approximate analysis based on the shear stiffness method

Given: The frame shown in Fig. E11.3a.

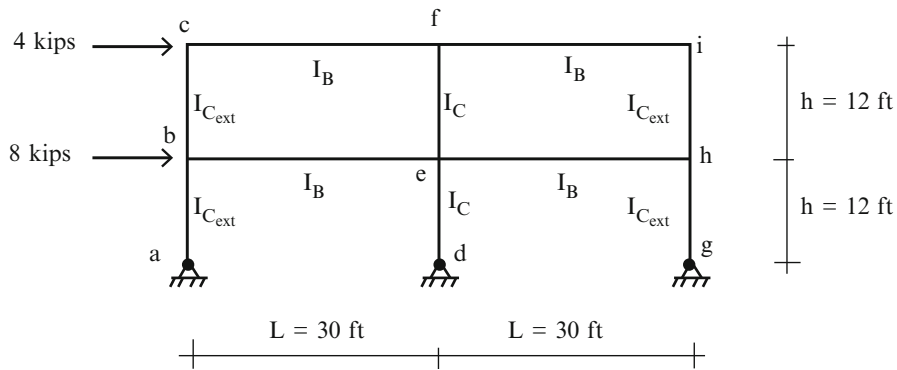


Fig. E11.3a

Determine: The column shear forces using the shear stiffness model and the member properties defined as cases A, B, C, and D.

$$\text{Case A: } I_{C_{ext}} = \frac{1}{2}I_C \text{ and } I_B = 4I_C \Rightarrow \frac{I_{C_{ext}}/h}{I_B/L} = \frac{I_C/h}{I_B/L} = 0.31$$

$$\text{Case B: } I_{C_{ext}} = I_C \text{ and } I_B = 4I_C \Rightarrow \frac{I_{C_{ext}}/h}{I_B/L} = \frac{I_C/h}{I_B/L} = 0.625$$

$$\text{Case C: } I_{C_{ext}} = \frac{1}{2}I_C \text{ and } I_B = 2I_C \Rightarrow \frac{I_{C_{ext}}/h}{I_B/L} = 0.625 \frac{I_C/h}{I_B/L} = 1.25$$

$$\text{Case D: } I_{C_{ext}} = I_C \text{ and } I_B = 2I_C \Rightarrow \frac{I_{C_{ext}}/h}{I_B/L} = \frac{I_C/h}{I_B/L} = 1.25$$

Solution: Using (11.6), (11.7), and (11.9), (11.10) the sub-element stiffnesses are

Case A	Case B	Case C	Case D
<i>Top story</i>			
$f_E = 0.762$	$f_E = 0.615$	$f_E = 0.444$	$f_E = 0.615$
$f_I = 0.762$	$f_I = 0.762$	$f_I = 0.615$	$f_I = 0.615$
$\frac{k_E}{k_I} = 0.5$	$\frac{k_E}{k_I} = 0.808$	$\frac{k_E}{k_I} = 0.722$	$\frac{k_E}{k_I} = 0.5$
<i>Bottom story</i>			
$f_{BE} = 0.865$	$f_{BE} = 0.762$	$f_{BE} = 0.615$	$f_{BE} = 0.762$
$f_{BI} = 0.865$	$f_{BI} = 0.865$	$f_{BI} = 0.762$	$f_{BI} = 0.762$
$\frac{k_{BE}}{k_{BI}} = 0.5$	$\frac{k_{BE}}{k_{BI}} = 0.881$	$\frac{k_{BE}}{k_{BI}} = 0.808$	$\frac{k_{BE}}{k_{BI}} = 0.5$

Noting that

$$\frac{V_E}{V_I} = \frac{k_E}{k_I}$$

we express the total shear as

$$V_{\text{Total}} = 2V_E + V_I = \left[2\left(\frac{k_E}{k_I}\right) + 1 \right] V_I$$

Once I is specified for the interior and exterior columns, we can evaluate the ratio, k_E/k_I , and then V_I . The computations corresponding to Cases A, B, C, and D are summarized below. We also list the results predicted by the Portal method. Note that the Portal Method agrees exactly with the stiffness method when $I_{C_{\text{exterior}}} = \frac{1}{2}I_{C_{\text{interior}}}$ (Cases A and D).

Story	V_T (kip)	Stiffness method										Portal method	
		Case A		Case B		Case C		Case D					
		V_E (kip)	V_I (kip)	V_E (kip)	V_I (kip)	V_E (kip)	V_I (kip)	V_E (kip)	V_I (kip)	V_E (kip)	V_I (kip)		
Top	4	1	2	1.235	1.53	1.18	1.64	1	2	1	2		
Bottom	12	3	6	3.83	4.34	3.7	4.59	3	6	3	6		

11.4.3 Low-Rise Rigid Frames with Bracing

Lateral load

A rigid frame resists lateral loading through bending action of the columns. When a bracing system is combined with the frame, both of these systems participate in carrying the lateral load. From a stiffness perspective, the load is distributed according to the relative stiffness, i.e., the stiffer element carries more loads. For low-rise frames, the transverse shear stiffness is the controlling parameter. Figure 11.14 illustrates the structural scheme for a one-story structure. A similar arrangement is used for multistory structures. Of particular interest is the distribution of lateral load between the rigid frame and the brace.

The individual systems are defined in Fig. 11.15.

We assume all sub-elements experience the same lateral displacement Δu , and express the lateral loads carried by each structural system as

$$P_{\text{frame}} = k_{\text{frame}} \Delta u$$

$$P_{\text{brace}} = k_{\text{brace}} \Delta u \quad (11.14)$$

where k_{frame} , k_{brace} denote the frame and brace stiffness factors. Summing these forces, we write

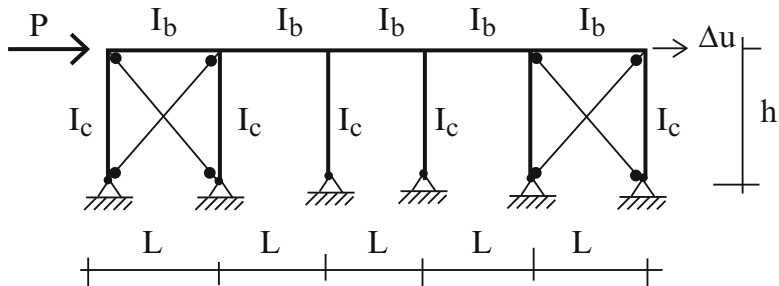


Fig. 11.14 Rigid frame with bracing

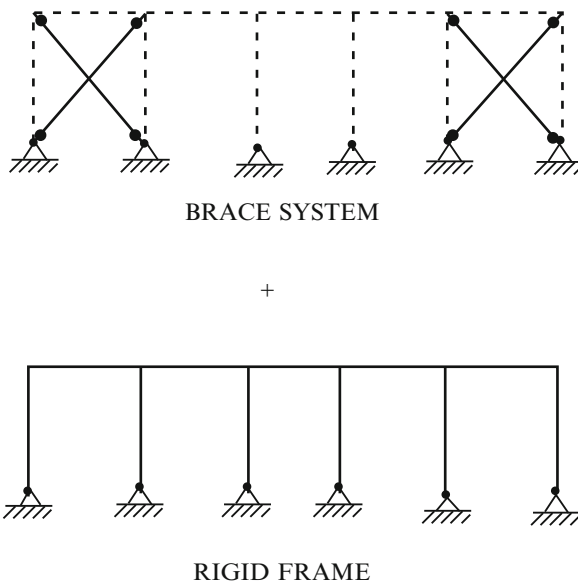


Fig. 11.15 Individual systems

$$P = P_{\text{frame}} + P_{\text{brace}} = (k_{\text{brace}} + k_{\text{frame}}) \Delta u = k_T \Delta u \quad (11.15)$$

Solving for Δu and back substituting in (11.14) results in

$$\begin{aligned} P_{\text{frame}} &= \frac{k_{\text{frame}}}{k_T} P \\ P_{\text{brace}} &= \frac{k_{\text{brace}}}{k_T} P \end{aligned} \quad (11.16)$$

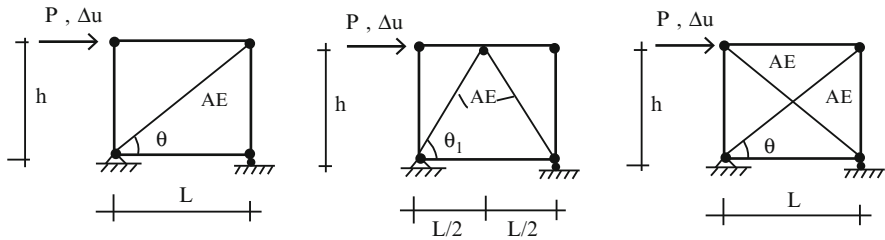


Fig. 11.16 Diagonal bracing systems. (a) Single. (b) Chevron. (c) X Brace

Also,

$$\frac{P_{\text{frame}}}{P_{\text{brace}}} = \frac{k_{\text{frame}}}{k_{\text{brace}}} \quad (11.17)$$

According to (11.16), the lateral force carried by a system depends on its relative stiffness. Increasing k_{brace} shifts load onto the bracing system.

Considering a single story, the lateral load required to introduce an inter-story lateral displacement Δu is equal to

$$P_{\text{frame}} = k_{\text{frame}} \Delta u \quad (11.18)$$

where k_{frame} is estimated by combining (11.11) and (11.12).

$$k_{\text{frame}} = \frac{3E}{h^3} \left\{ \frac{2I_{\text{CE}}}{1 + (1/2)((I_{\text{CE}}/h)/(I_b/L))} + \sum_{\text{intercol}} \frac{I_{\text{CI}}}{1 + (1/4)((I_{\text{CI}}/h)/(I_b/L))} \right\} \quad (11.19)$$

Once the member properties are known, one can evaluate k_{frame} . We need to develop a similar expression for a brace.

Typical bracing schemes are shown in Fig. 11.16. The lateral load is carried equally by the diagonal members. One determines k_{brace} using structural mechanics concepts such as deformation and equilibrium. The analytical expressions for the different schemes are

$$\begin{aligned} k_{\text{brace}(\text{single})} &= \frac{AE}{h} (\sin \theta \cos^2 \theta) \\ k_{\text{brace}(\text{chevron})} &= \frac{2AE}{h} (\sin \theta_1 \cos^2 \theta_1) \\ k_{\text{brace}(\text{xbrace})} &= \frac{2AE}{h} (\sin \theta \cos^2 \theta) \end{aligned} \quad (11.20)$$

The diagonal forces reverse when the lateral load reverses, which occurs for wind and earthquake loading.

Example 11.4 Shear force distribution

Given: The one-story frame defined in Fig. E11.4a.

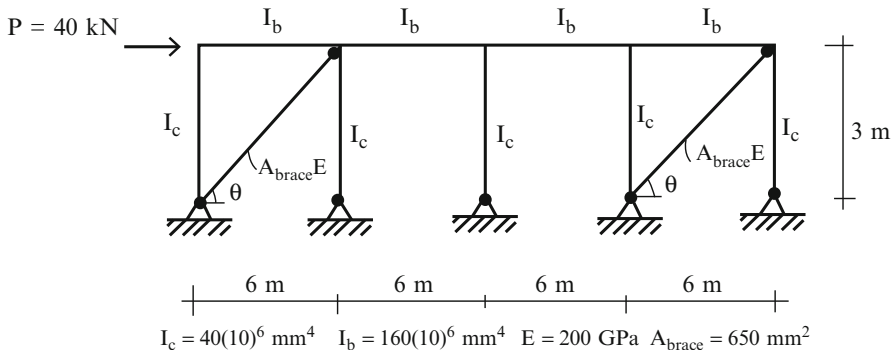


Fig. E11.4a

Determine: The column shears and the diagonal brace forces.

Solution: Using (11.19), the frame stiffness is

$$\begin{aligned} k_{\text{frame}} &= \frac{3EI_c}{h^3} \left(\frac{2}{1 + (1/2)((I_c/h)/(I_b/L))} + \frac{3}{1 + (1/4)((I_c/h)/(I_b/L))} \right) \\ &= \frac{3EI_c}{h^3} \left(\frac{8}{5} + \frac{8}{3} \right) = 12.8 \frac{EI_c}{h^3} \end{aligned}$$

The brace stiffness follows from (11.20). Note that there are two braces.

$$k_{\text{brace}} = 2 \frac{A_{\text{brace}}E}{h} (\sin \theta \cos^2 \theta) = \frac{A_{\text{brace}}E}{h} 2(0.447)(0.894)^2 = 0.714 \frac{A_{\text{brace}}E}{h}$$

Noting (11.16), the individual forces are related by

$$P_{\text{frame}} = \left(\frac{k_{\text{frame}}}{k_{\text{brace}}} \right) P_{\text{brace}} = 17.9 \left(\frac{I_c}{A_{\text{brace}}h^2} \right) P_{\text{brace}}$$

Summing the forces leads to

$$P_{\text{frame}} + P_{\text{brace}} = P \Rightarrow \left(17.9 \frac{I_c}{A_{\text{brace}}h^2} + 1 \right) P_{\text{brace}} = 40$$

Then

$$P_{\text{brace}} = \frac{40}{1 + (17.9) \left(\left(40(10)^6 \right) / \left((650)(3,000)^2 \right) \right)} = 35.6 \text{ kN}$$

$$P_{\text{frame}} = 4.36 \text{ kN}$$

The force in each diagonal brace is given by

$$F_b = \frac{P_{\text{brace}}}{2\cos\theta} = 19.9 \text{ kN}$$

We evaluate the column shear forces using the corresponding stiffness factors defined by (11.11) and (11.12).

$$k_E = \frac{3EI_c}{h^3} \left(\frac{4}{5} \right)$$

$$k_I = \frac{3EI_c}{h^3} \left(\frac{8}{9} \right)$$

$$\frac{V_E}{V_I} = \frac{k_E}{k_I} = \frac{4/5}{8/9} = \frac{9}{10}$$

$$\therefore V_E = 0.9V_I$$

Summing the shears,

$$2V_E + 3V_I = 4.36 \Rightarrow 1.8V_I + 3V_I = 4.36$$

Then

$$V_I = 0.91 \text{ kN}$$

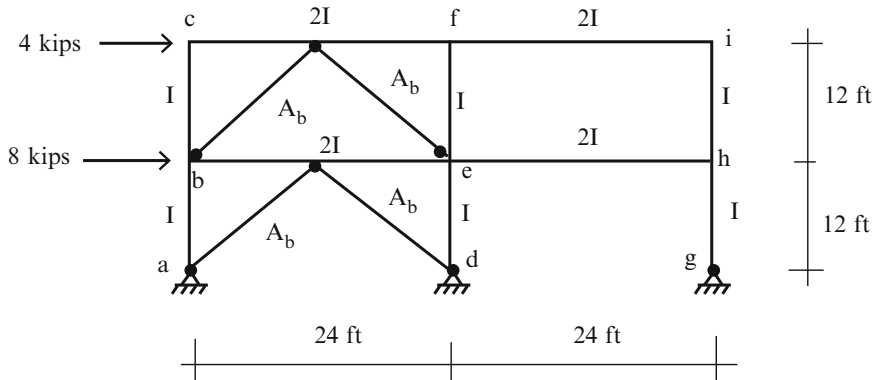
$$V_E = 0.82 \text{ kN}$$

Note that the brace carries the major portion of the story shear.

Example 11.5 Shear force distribution

Given: The braced rigid frame defined in Fig. E11.5a. $A_b = 0.8 \text{ in.}^2$, $E = 29,000 \text{ ksi}$, and $I = 150 \text{ in.}^4$.

Determine: The lateral forces carried by the frame and brace systems.

**Fig. E11.5a****Solution:**

$$P_{\text{frame}} + P_{\text{brace}} = 4 \text{ kip} \text{ Upper floor}$$

$$P_{\text{frame}} + P_{\text{brace}} = 12 \text{ kip} \text{ Lower floor}$$

*Frame:**Upper story sub-element: Equations (11.6) and (11.7)*

$$k_E = \frac{6EI_c}{h^3} \Rightarrow k_{\text{frame}} = \frac{EI_c}{h^3} (2(6) + 8) = \frac{20EI_c}{h^3} = \frac{20(29,000)150}{(12 \times 12)^3} = 29.14 \text{ k/in.}$$

$$k_I = \frac{8EI_c}{h^3}$$

Base story sub-element: Equations (11.11) and (11.12)

$$k_E = \frac{2EI_c}{h^3} \Rightarrow k_{\text{frame}} = \frac{EI_c}{h^3} (2(2) + 2.4) = \frac{6.4EI_c}{h^3} = 9.32 \text{ k/in.}$$

$$k_I = \frac{2.4EI_c}{h^3}$$

Brace:

$$k_{\text{brace}} = \frac{2EA_b}{h} \sin \theta_1 (\cos \theta_1)^2 = 0.707 \frac{EA_b}{h} = \frac{0.707(0.8)(29,000)}{12(12)} = 113.9 \text{ k/in.}$$

Shear distributions

$$P_{\text{frame}} = \left(\frac{k_{\text{frame}}}{k_{\text{brace}}} \right) P_{\text{brace}} \Rightarrow \begin{aligned} P_{\text{frame}} &= \left(\frac{29.14}{113.9} \right) P_{\text{brace}} = 0.256 P_{\text{brace}} && \text{Upper floor} \\ P_{\text{frame}} &= \left(\frac{9.32}{113.9} \right) P_{\text{brace}} = 0.082 P_{\text{brace}} && \text{Lower floor} \end{aligned}$$

Then

$$(0.256 + 1)P_{\text{brace}} = 4 \text{ kip} \Rightarrow P_{\text{brace}} = 3.18 \text{ kip} \quad \text{Upper floor}$$

$$(0.082 + 1)P_{\text{brace}} = 12 \text{ kip} \Rightarrow P_{\text{brace}} = 11.09 \text{ kip} \quad \text{Lower floor}$$

Therefore

$$P_{\text{frame}} = 0.256P_{\text{brace}} = 0.81 \text{ kip} \quad \text{Upper floor}$$

$$P_{\text{frame}} = 0.082P_{\text{brace}} = 0.91 \text{ kip} \quad \text{Lower floor}$$

Example 11.6 Shear force distribution

Given: The braced frame defined in Fig. E11.6a.

Determine: The required brace area A_b , to limit the inter-story displacement to 10 mm for each story. Assume $E = 200 \text{ GPa}$.

Solution:

$$P_{\text{brace}} = 16 \text{ Upper floor}$$

$$P_{\text{brace}} = 16 + 32 = 48 \text{ Lower floor}$$

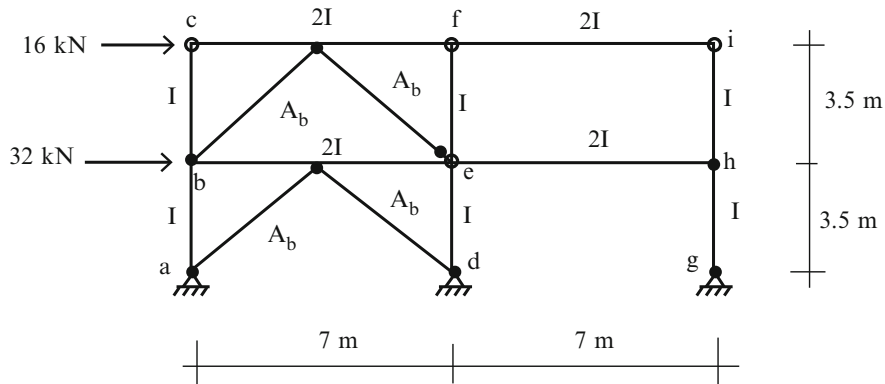
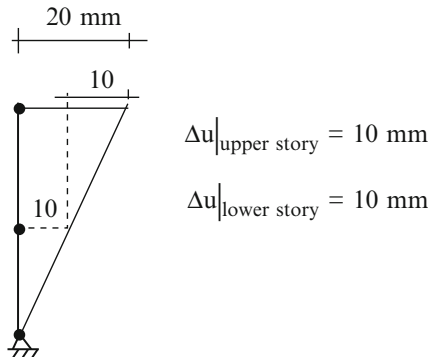


Fig. E11.6a

$$k_{\text{brace}} = \frac{2EA_b}{h} \sin \theta_1 (\cos \theta_1)^2 = 0.707 \frac{EA_b}{h}$$

$$P_{\text{brace}} = k_{\text{brace}} u$$



$$\text{Upper floor } 16 = 0.707 \frac{EA_b}{h} \Delta u_{\text{upper}} \Rightarrow A_b \geq \frac{16(3,500)}{0.707(10)(200)} = 39.6 \text{ mm}^2$$

$$\text{Lower floor } 48 = 0.707 \frac{EA_b}{h} \Delta u_{\text{lower}} \Rightarrow A_b \geq \frac{48(3,500)}{0.707(10)(200)} = 118.8 \text{ mm}^2$$

The value for the lower floor controls the design.²

$$\therefore A_{b\text{required}} = 118.8 \text{ mm}^2$$

11.5 High-Rise Rigid Frames: The Cantilever Method

The approximate procedure described above is applicable for low-rise rigid frames, which behave as “shear type” frames; i.e., the floors displace laterally but do not rotate. One determines the axial forces in the columns using the shear forces in the floor beams. High-rise frames behave more like a cantilever beam. As illustrated in Fig. 11.17b the floors rotate as rigid planes. Their behavior is similar to what is assumed for the cross section of a beam in the formulation of the bending theory of beams; they experience both a translation and a rotation. Just as for beams, the rotational component produces axial strain in the columns. The column shears and moments are found from equilibrium considerations, given the axial forces in the columns. In what follows, we describe an idealized structural model that is used to establish the distribution of column axial forces in a story. This approach is called the “Cantilever Method.”

One normally applies this method to estimate the axial forces in the columns at the base of the building, i.e., where the bending moment due to lateral loading is a maximum.

We consider the typical tall building shown in Fig. 11.19. Given the lateral load, we can determine the bending moment and transverse shear at mid-height of each story. We denote these quantities as M_{i+1} and $V_{T_{i+1}}$ (Fig. 11.18).

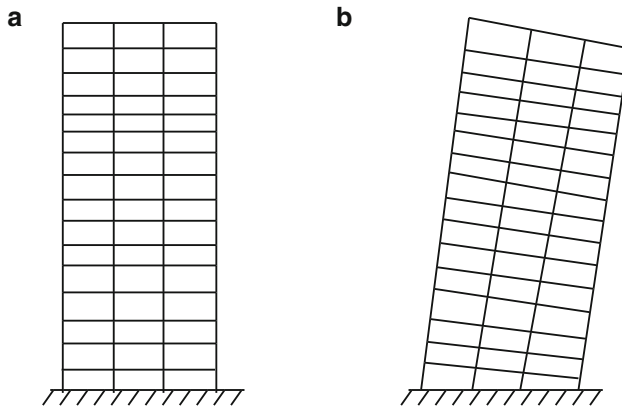


Fig. 11.17 Lateral deflections—tall building

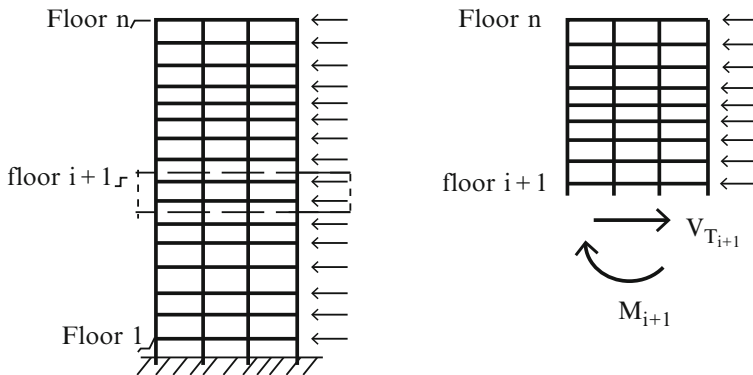


Fig. 11.18 Tall building model

Now, we isolate a segment of the building consisting of floors $i + 1$, i , and the columns connecting these floors. Figure 11.19 shows this segment. The floors are assumed to be rigid plates, and the columns are represented as axial springs. Floor $i + 1$ experiences a rotation, $\Delta\beta$, with respect to floor i due to the moment M_{i+1} .

We position a reference axis at point o and define x_i as the X coordinate for spring i . The corresponding axial stiffness is k_i . We locate the origin of the reference axis such that

$$\sum k_i x_i = 0 \quad (11.21)$$

Note that the axial stiffness is equal to the column stiffness,

Fig. 11.19 Column-beam model for a story bounded by floors i and $i + 1$

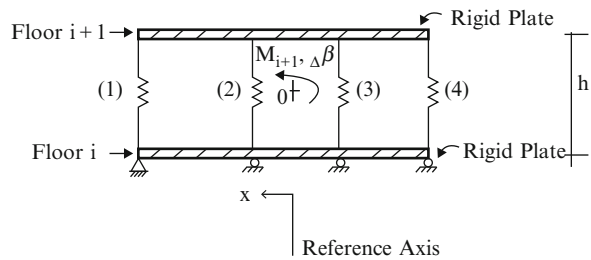
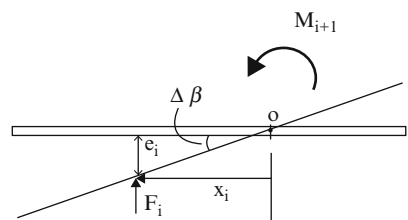


Fig. 11.20 Deformation due to relative rotation



$$k_i = \frac{A_i E}{h} \quad (11.22)$$

where A_i is the cross-sectional area and h is the column height. Then, when E is constant, (11.21) can be written as

$$\sum A_i x_i = 0 \quad (11.23)$$

In this case, one can interpret the reference axis as equivalent to the centroidal axis for the column areas in the story.

We suppose the floors rotate about O and define $\Delta\beta$ as the relative rotation between adjacent floors. The deformation introduced in spring i follows from Fig. 11.20.

$$e_i = x_i \Delta\beta$$

$$F_i = k_i e_i = k_i x_i \Delta\beta \quad (11.24)$$

Summing moments about O , and equating the result to the applied moment, M_{i+1} results in

$$M_{i+1} = \left(\sum k_i x_i^2 \right) \Delta\beta \quad (11.25)$$

Here, M_{i+1} represents the moment due to the lateral loads applied *on and above* floor $i + 1$. We solve for $\Delta\beta$ and then back substitute in the expression for F_i . The result is

$$F_i = k_i x_i \frac{M_{i+1}}{\left(\sum k_i x_i^2\right)} = x_i A_i \left(\frac{E}{h \sum k_i x_i^2} \right) M_{i+1} \quad (11.26)$$

We see that the column force distribution is proportional to the distance from the reference axis and the relative column cross-sectional area. One does not need to specify the actual areas, only the ratio of areas.

One should note that this result is based on the assumption that the *floor acts as a rigid plate*. Stiff belt type trusses are frequently incorporated at particular floors throughout the height so that the high-rise frame behaves consistent with this hypothesis.

Example 11.7 Approximate analysis based on the cantilever method

Given: The symmetrical 42-story plane frame shown in Fig. E11.7a. Assume the building is supported on two caissons located at the edges of the base. Consider the base to be rigid.

Determine: The axial forces in the caissons.

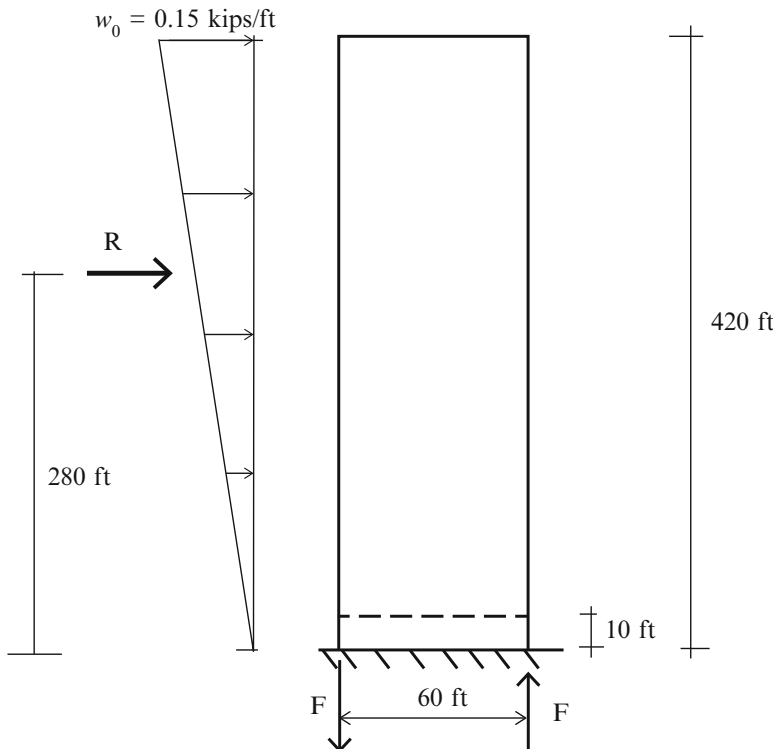


Fig. E11.7a

Solution: The Moment at the base is given by

$$R = \frac{w_0 H}{2} = 210 w_0$$

$$M = \frac{2H}{3} R = 58,800 \quad w_0 = 8,820 \text{ kip ft}$$

This moment is resisted by the pair of caisson forces which are equivalent to a couple.

$$60F = 8,820$$

$$F = 147 \text{ kip}$$

Example 11.8 Approximate analysis based on the cantilever method

Given: The symmetrical plane frame shown in Fig. E11.8a.

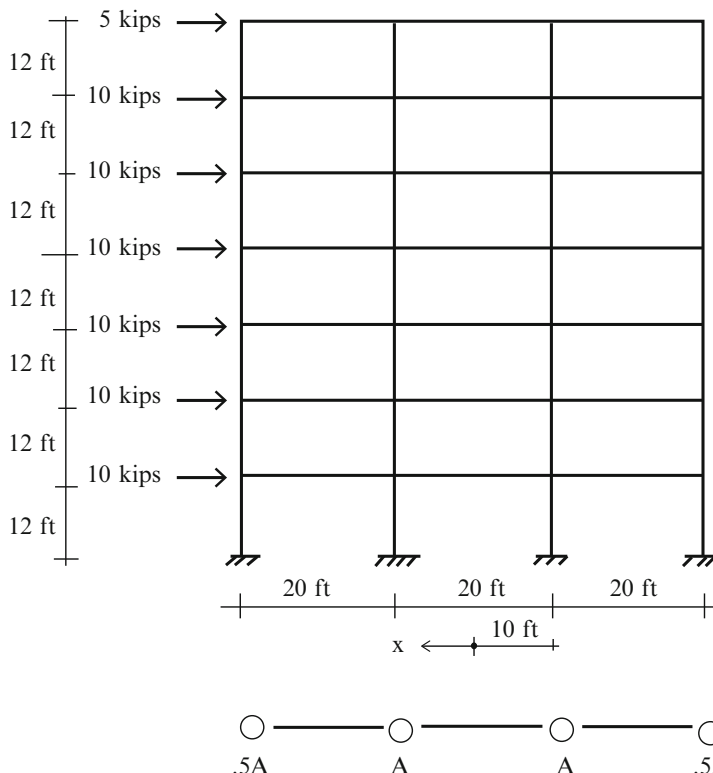


Fig. E11.8a

Determine: The column axial forces in the bottom story for the distribution of column areas shown.

Solution: The rotational stiffness for the story is:

$$K_x = \sum k_i x_i^2 = \frac{E}{h} \sum A_i x_i^2 = 1,100 \left(\frac{EA}{h} \right)$$

The bending moment at mid-height of the first story is 1,100 kip ft. Then, substituting for M_{i+1} and K_x in (11.26) leads to the axial forces in the columns (Fig. E11.8b),

$$F_2 = (10) \frac{AE}{h} \left(\frac{2,550}{1,100(AE/h)} \right) = 23.2 \text{ kip}$$

$$F_1 = (30) \frac{2AE}{h} \left(\frac{2,550}{1,100(AE/h)} \right) = 34.8 \text{ kip}$$

$$F_3 = -F_2 = -23.2 \text{ kip}$$

$$F_4 = -F_1 = -34.8 \text{ kip}$$

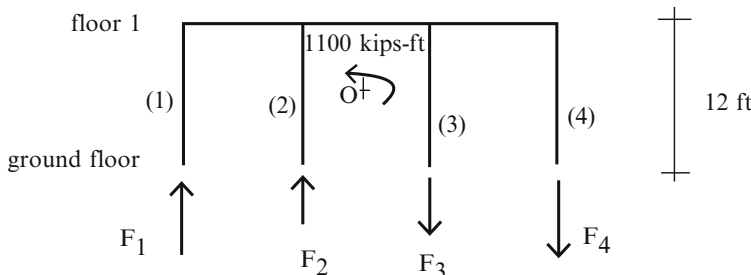


Fig. E11.8b

This computation is repeated for successive stories. Once all the column axial forces are known, one can compute the column shears by assuming inflection points at the midpoints of the columns and beams and applying static equilibrium conditions. The procedure is similar to that followed in Example 11.2.

11.6 Summary

11.6.1 Objectives of the Chapter

Our goals in this chapter are

- To describe some approximate methods for estimating the bending moment distribution in multi-span beams and multi-bay frames subjected to gravity loading.
- To present approximate methods for analyzing multistory rigid frames subjected to lateral loading.

11.6.2 Key Concepts

- Reasoning in a qualitative sense about the behavior using the concept of relative stiffness provides the basis for a method to estimate the bending moment distribution in multi-span beams.
- Two methods are described for analyzing low-rise rigid frame structures.
- The Portal method.

The Portal method assumes the shear forces in the interior columns are equal to a common value, and the shears in the exterior columns are equal to $\frac{1}{2}$ this value. This is an empirical-based procedure.

- The shear stiffness method.

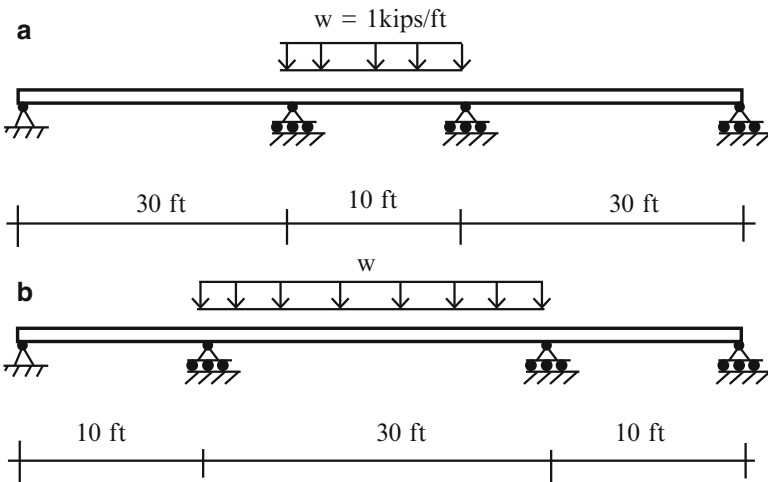
The shear stiffness method uses simplified structural models to estimate the shear forces in the columns given the total shear force for a story. This procedure predicts that the shear force in a particular column is proportional to the relative stiffness. It follows that a stiff column attracts more load than a flexible column.

- High-rise rigid frames are modeled as equivalent cantilever beams. The floor slabs are considered rigid and the bending rigidity is generated through the axial action of the columns. One starts with the bending moment at the midpoint between a set of floors, and determines the axial forces in the columns. According to this method, the axial force depends on the axial rigidity of the column and the distance from the centroidal axis.

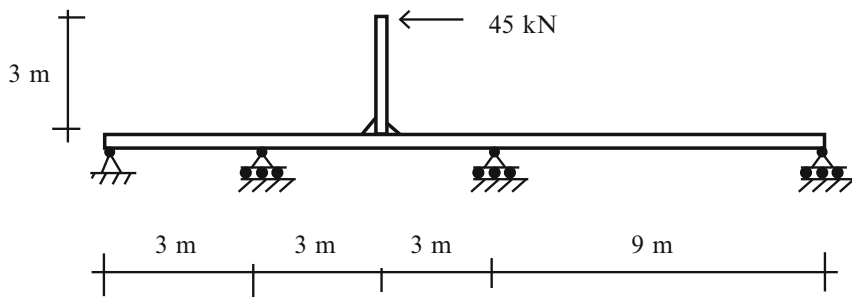
11.7 Problems

Problem 11.1

Estimate the bending moment distribution for the cases listed below. Use qualitative reasoning based on relative stiffness. Assume I constant.

**Problem 11.2**

Estimate the bending moment distribution. Use qualitative reasoning based on relative stiffness. Assume I as constant.

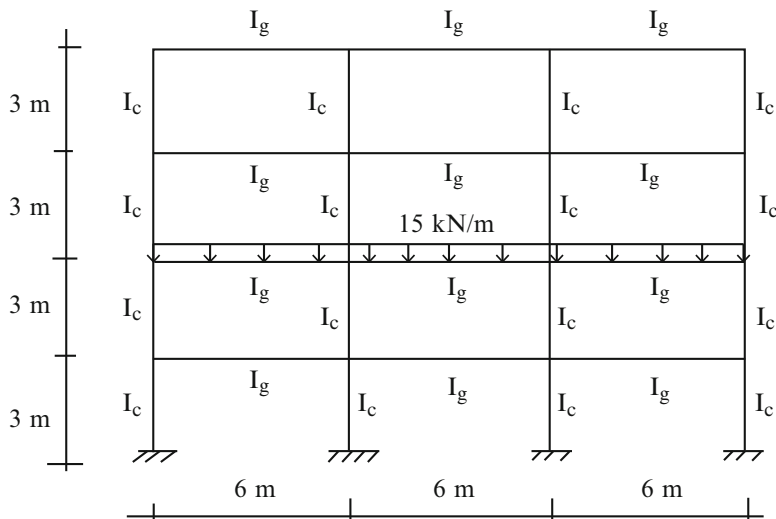
**Problem 11.3**

Solve Problem 11.1 cases (a) and (b) using moment distribution. Compare the approximate and exact results.

Problem 11.4

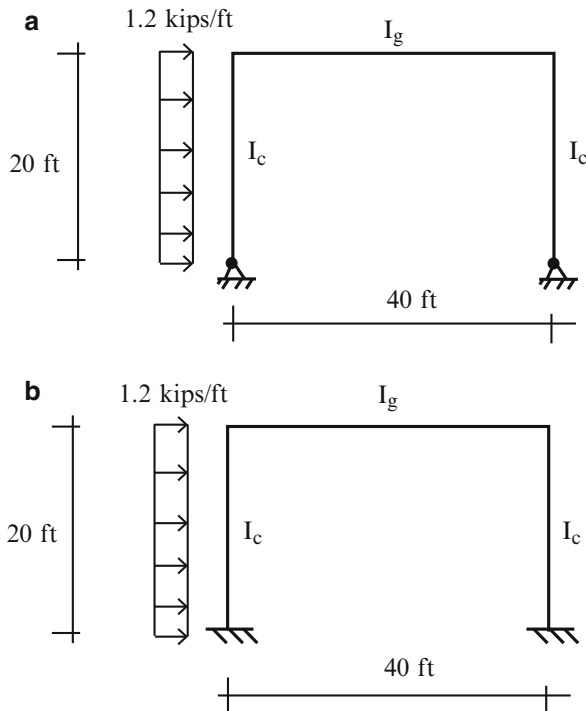
Consider the multistory steel frame shown below. Determine the maximum positive and negative moments in the beams using the following approaches:

1. Assume inflection points at $0.1L$ from each end of the beams.
2. Use a computer software system. Assume $I_g = 2I_c$



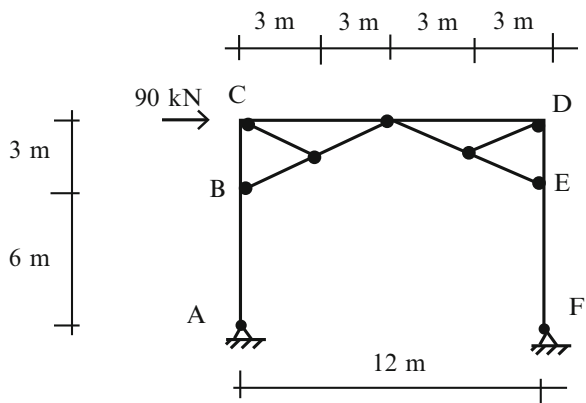
Problem 11.5

Estimate the axial force, shear force, and bending moment distributions. Assume $I_g = 2I_c$



Problem 11.6

Members AC and FD are continuous. Estimate the bending moment distribution in AC and FD, and the axial forces in the pin-ended members. Compare your results with results generated with a computer software system.



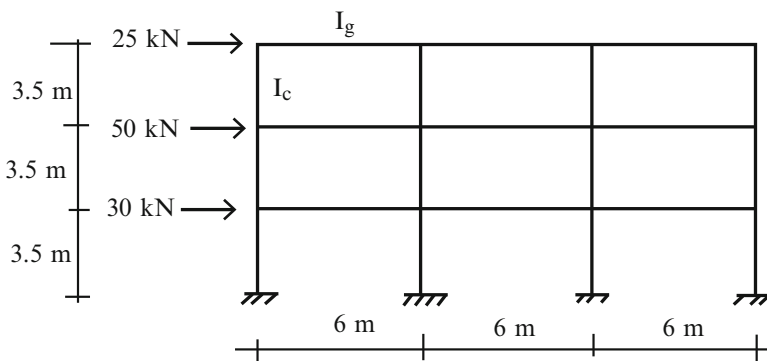
Problem 11.7

Repeat problem 11.6 assuming fixed supports at A and F.

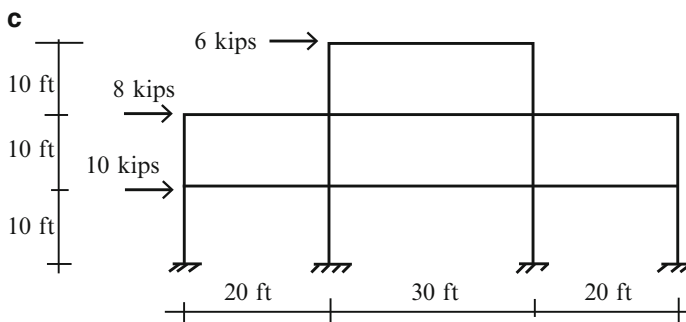
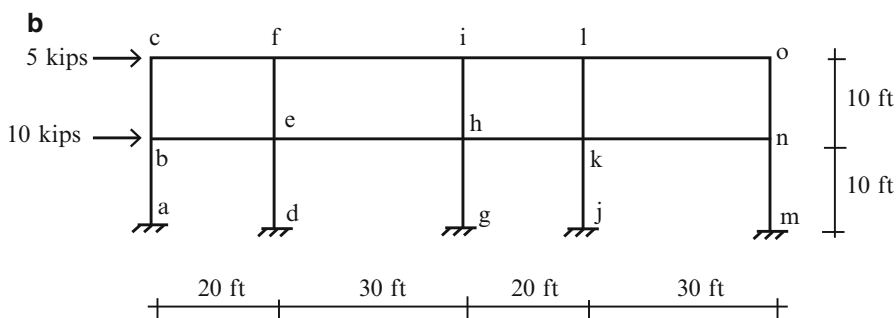
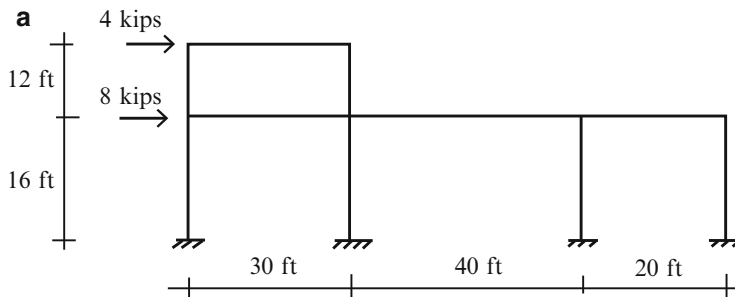
Problem 11.8

Consider the steel frame shown below. Assume $I_g = 3I_c$ for all the members. Determine the moment at each end of each member using

- (a) The Portal method.
- (b) The shear stiffness method.

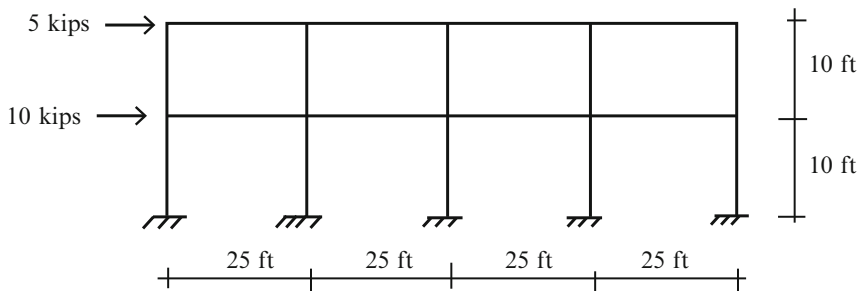
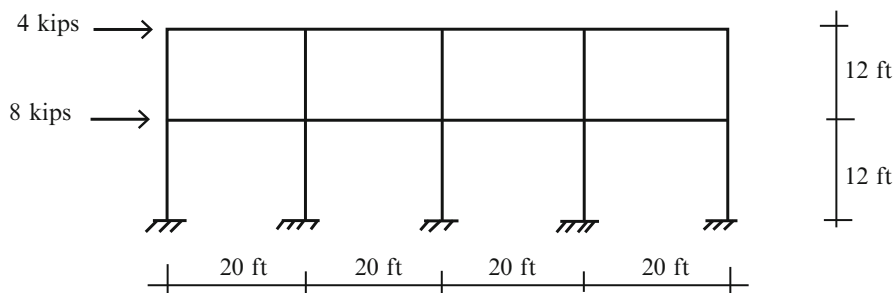
**Problem 11.9**

For the steel frames shown, estimate the axial force, shear force, and moments for all of the members using the Portal method. Compare your results with results generated with a computer software system. Take $I_c = 480 \text{ in.}^4$ for all the columns and $I_b = 600 \text{ in.}^4$ for all the beams.

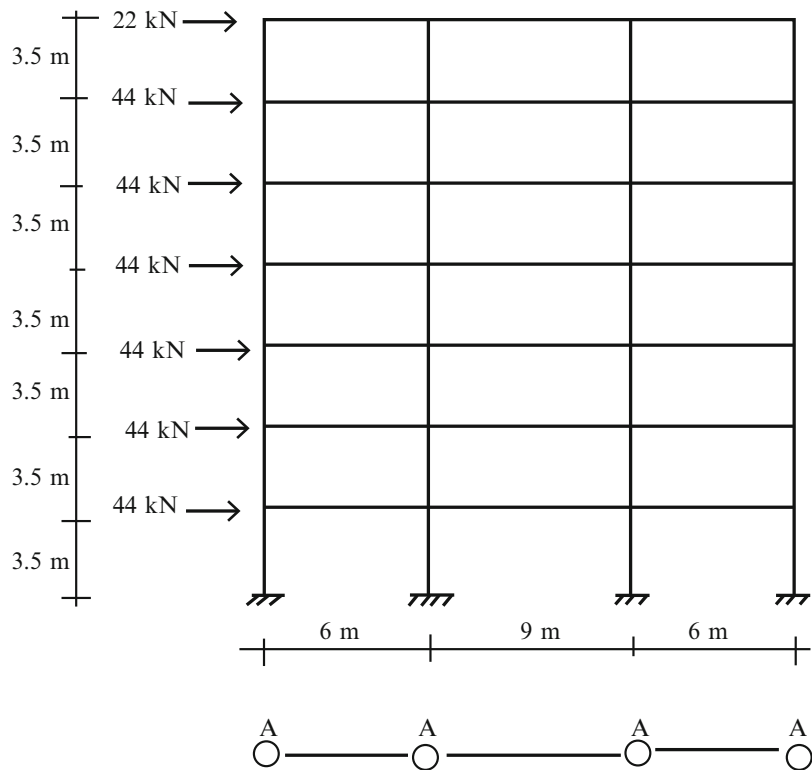


Problem 11.10

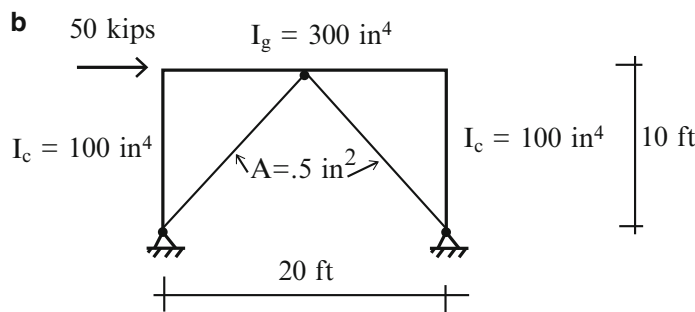
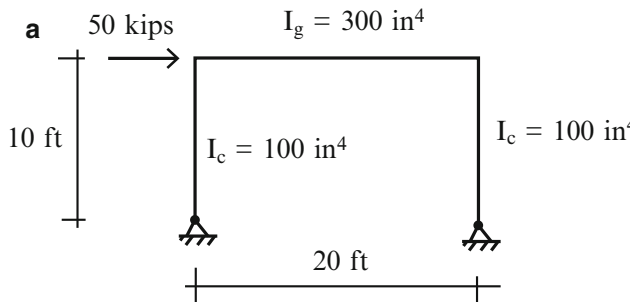
For the steel frames shown, estimate the axial force, shear force, and moments for all of the members. Take $I_c = 480 \text{ in.}^4$ for all the columns and $I_b = 600 \text{ in.}^4$ for all the beams. Use the Stiffness method.

a**b****Problem 11.11**

Estimate the column axial forces in the bottom story for the distribution of column areas shown.

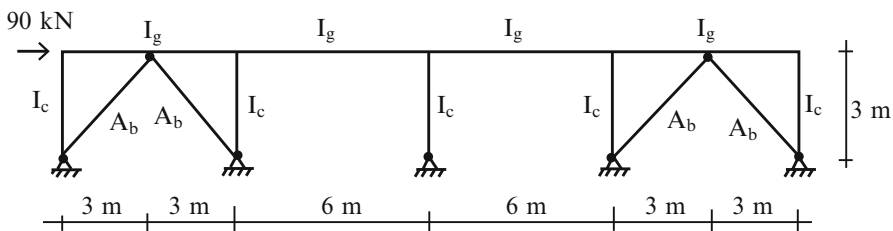
**Problem 11.12**

Estimate the column shears for cases (a) and (b). Compare your results with computer-based solutions.



Problem 11.13

Consider the rigid steel frame with bracing shown below. Estimate the column shears and brace forces. Take $I_c = 40(10)^6 \text{ mm}^4$, $I_g = 120(10)^6 \text{ mm}^4$, $A_b = 650 \text{ mm}^2$, $E = 200 \text{ GPa}$. Compare your results with a computer-based solution.



Overview

In this chapter we revisit the Displacement Method for structures such as trusses, beams, and frames which are composed of member type elements. *Our objective is to identify the basic steps involved in applying the Displacement Method that can be represented as computer procedures.* We utilize matrix notation since it is the natural language of computation, and systematically reformulate the different steps as a sequence of matrix operations. This reformulation is referred to as the Finite Element Displacement Method. It is relatively straight forward to convert these matrix operations into computer code once one selects a computer language.

12.1 Introduction

In Chaps. 9 and 10 we described two methods for analyzing indeterminate structures, namely the Force and Displacement Methods. The examples that we presented were deliberately kept simple to minimize the computational effort since our objective was to demonstrate “how” the methods are applied rather than the computational details. However, one can appreciate that as a structure becomes more complex, the computational effort becomes the limiting issue for hand computation. Therefore, it is necessary to resort to computer-based procedures in order to execute the various phases of the analysis process. One needs to be familiar with commercial computer-based analysis codes since the extensive use of digital computers in structural analysis and design has revolutionized the practice of structural engineering over the past 40 years.

12.2 Key Steps of the Finite Element Displacement Method for Member Systems

Chapter 10 discussed the methodology of the Displacement Method and presented examples of beam and frame structures analyzed by this method. We summarize here the key steps involved in applying the Displacement Method to member type structures. In later sections, we re-examine each step and represent the set of actions as a set of matrix operations.

Step #1: Formulate the member end force–end displacement equations

Using beam theory, we express the forces acting on the ends of a member in terms of the displacement measures for the ends. These equations are referred to as member end action–end displacement equations. Their derivation is contained in Sect. 10.2. A subset of these equations are called the slope-deflection equations. In the derivation, the force and displacement quantities are referred to a local reference frame associated with the orientation of the member.

Step #2: Select a global reference frame and transform member variables

We select a common reference frame and refer both the nodal and member force and displacement quantities to this common frame. This step involves shifting back and forth from member frames to the global frame and allows one to deal with structures having arbitrary geometries.

Step #3: Establish the nodal force equilibrium equations

We enforce force equilibrium at each node. This step involves summing the end actions for those members which are incident on the node. Then, using the member equations, we substitute for the end actions in terms of the nodal displacements that correspond to the end displacements for the member. This operation leads to a set of linear algebraic equations which relate the external forces applied to the nodes and the nodal displacements. The coefficient matrix for this set is called the “System Stiffness Matrix.”

Step #4: Introduce displacement constraints

Supports at nodes introduce constraints on certain nodal displacements. For example, if a node is fully fixed, all the displacement measures associated with the node are equal to zero. Introducing displacement constraints reduces the total number of displacement variables, and one works with a “reduced” set of equilibrium equations. Depending on the structure, a certain number of supports are required to prevent initial instability.

Step #5: Solve the nodal equilibrium equations

We solve the nodal force equilibrium equations for the nodal displacements. When the number of unknown displacements is large this step is not feasible without a digital computer.

Step #6: Determine member end actions

We substitute the values of the nodal displacements obtained from the solution of the nodal equilibrium equations into the member force–displacement relations and solve for the member end forces.

Step #7: Check on nodal force equilibrium

The last step involves substituting for the member end forces in the nodal force equilibrium equations to check that the external nodal forces are equilibrated by the member forces. This step provides information on the reactions; it also provides a check on statics. Static discrepancy is generally related to the computational accuracy associated with solving the nodal equilibrium equations. Most computers now use double precision representation and numerical accuracy is usually not a problem.

12.3 Matrix Formulation of the Member Equations: Planar Behavior

In what follows, we present the member equations for the two-dimensional case where bending occurs in the x - y plane. Figure 12.1 shows the end actions and end displacements *referred to the local member frame*. We use a subscript l to denote quantities referred to the local frame. The x axis coincides with the centroidal axis for the member, and the y and z axes are the principal inertia directions for the cross section. Subscripts B and A denote the positive and negative ends of the member. It is convenient to represent the set of end forces and end displacements as matrices defined as follows:

- End Displacements

$$\mathbf{U}_{\ell B} = \begin{Bmatrix} u_{\ell B} \\ v_{\ell B} \\ \theta_B \end{Bmatrix} \quad \mathbf{U}_{\ell A} = \begin{Bmatrix} u_{\ell A} \\ v_{\ell A} \\ \theta_A \end{Bmatrix} \quad (12.1)$$

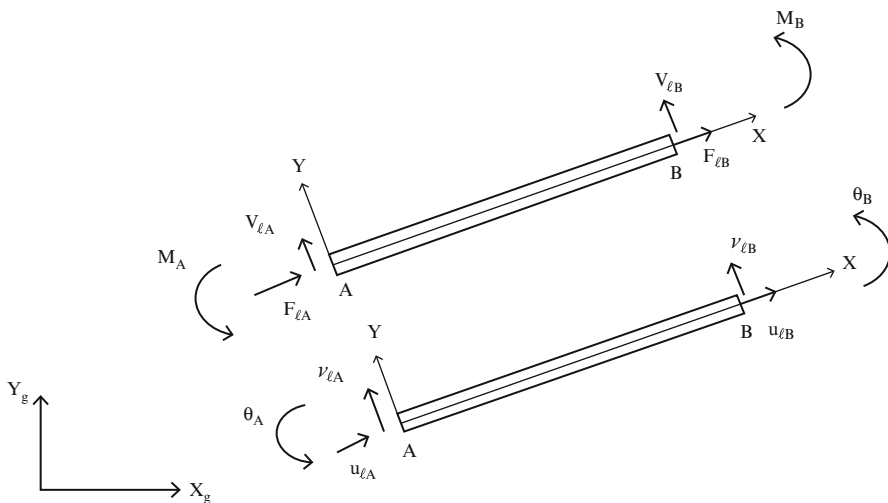


Fig. 12.1 End forces and displacements—local member frame—planar behavior

- End Forces

$$\mathbf{P}_{\ell B} = \begin{Bmatrix} F_{\ell B} \\ V_{\ell B} \\ M_B \end{Bmatrix} \quad \mathbf{P}_{\ell A} = \begin{Bmatrix} F_{\ell A} \\ V_{\ell A} \\ M_A \end{Bmatrix} \quad (12.2)$$

Note that the positive sense for moment and rotation is taken as counter-clockwise, i.e., from X toward Y .

We derived the complete set of equations relating the end forces and end displacements in Chap. 10 and used a subset of these equations (10.12) to analyze bending of beams and frames. That analysis was approximate in the sense that the axial deformation of the members was neglected. Consequently, the axial forces had to be determined from the force equilibrium conditions. In what follows, we remove this assumption. The resulting analysis is now applicable for both truss and frame type structures. The formulation is now more involved since there are now more unknowns, but this is not a problem when a computer is used to solve the equations. The complete set of planar equations for the end actions at B are:

$$\begin{aligned} F_{\ell B} &= \frac{AE}{L}(u_{\ell B} - u_{\ell A}) + F_{\ell B}^F \\ V_{\ell B} &= -\frac{6EI}{L^2}(\theta_B + \theta_A) + \frac{12EI}{L^3}(v_{\ell B} - v_{\ell A}) + V_{\ell B}^F \\ M_B &= \frac{2EI}{L}(2\theta_B + \theta_A) - \frac{6EI}{L^2}(v_{\ell B} - v_{\ell A}) + M_B^F \end{aligned} \quad (12.3)$$

where $F_{\ell B}^F$, $V_{\ell B}^F$, M_B^F are the fixed end actions generated by the loading applied to the member with the ends fixed. Using the global equilibrium equations for the member, one obtains a similar set of equations for the end actions at A.

$$\begin{aligned} F_{\ell A} &= \frac{AE}{L}(-u_{\ell B} + u_{\ell A}) + F_{\ell A}^F \\ V_{\ell A} &= \frac{6EI}{L^2}(\theta_B + \theta_A) + \frac{12EI}{L^3}(v_{\ell A} - v_{\ell B}) + V_{\ell A}^F \\ M_A &= \frac{2EI}{L}(2\theta_A + \theta_B) - \frac{6EI}{L^2}(v_{\ell B} - v_{\ell A}) + M_A^F \end{aligned} \quad (12.4)$$

Both sets of equations (12.3) and (12.4) are restricted to prismatic members, i.e., members with constant cross-sectional properties.

We introduce the matrix notation defined by (12.1) and (12.2), and express the end action equations as

$$\begin{aligned} \mathbf{P}_{\ell B} &= \mathbf{k}_{\ell BB}\mathbf{U}_{\ell B} + \mathbf{k}_{\ell BA}\mathbf{U}_{\ell A} + \mathbf{P}_{\ell B}^F \\ \mathbf{P}_{\ell A} &= \mathbf{k}_{\ell AB}\mathbf{U}_{\ell B} + \mathbf{k}_{\ell AA}\mathbf{U}_{\ell A} + \mathbf{P}_{\ell A}^F \end{aligned} \quad (12.5)$$

where the expanded form of the individual stiffness and force matrices are

$$\begin{aligned}
 \mathbf{k}_{\ell BB} &= \begin{bmatrix} \frac{AE}{L} & 0 & 0 \\ 0 & \frac{12EI}{L^3} & -\frac{6EI}{L^2} \\ 0 & -\frac{6EI}{L^2} & \frac{4EI}{L} \end{bmatrix} & \mathbf{k}_{\ell BA} &= \begin{bmatrix} -\frac{AE}{L} & 0 & 0 \\ 0 & -\frac{12EI}{L^3} & -\frac{6EI}{L^2} \\ 0 & \frac{6EI}{L^2} & \frac{2EI}{L} \end{bmatrix} & \mathbf{P}_{\ell B}^F &= \left\{ \begin{array}{l} F_{\ell B}^F \\ V_{\ell B}^F \\ M_{\ell B}^F \end{array} \right\} \\
 \mathbf{k}_{\ell AA} &= \begin{bmatrix} \frac{AE}{L} & 0 & 0 \\ 0 & \frac{12EI}{L^3} & \frac{6EI}{L^2} \\ 0 & \frac{6EI}{L^2} & \frac{4EI}{L} \end{bmatrix} & \mathbf{k}_{\ell AB} &= \begin{bmatrix} -\frac{AE}{L} & 0 & 0 \\ 0 & -\frac{12EI}{L^3} & \frac{6EI}{L^2} \\ 0 & -\frac{6EI}{L^2} & \frac{2EI}{L} \end{bmatrix} & \mathbf{P}_{\ell A}^F &= \left\{ \begin{array}{l} F_{\ell A}^F \\ V_{\ell A}^F \\ M_{\ell A}^F \end{array} \right\}
 \end{aligned} \tag{12.6}$$

The matrices $\mathbf{k}_{\ell BB}$, $\mathbf{k}_{\ell AA}$, $\mathbf{k}_{\ell BA}$, $\mathbf{k}_{\ell AB}$ are called the member stiffness matrices referred to the local member frame. Note that once the end displacements $\mathbf{U}_{\ell B}$ and $\mathbf{U}_{\ell A}$ are known, one can determine the end actions $\mathbf{P}_{\ell B}$ and $\mathbf{P}_{\ell A}$. The member stiffness matrices are functions of the member properties (A, I, L) and the material property E . The fixed end actions ($\mathbf{P}_{\ell B}^F$ and $\mathbf{P}_{\ell A}^F$) depend on the external loading applied to the member.

Example 12.1 The fixed end actions

Given: The linearly loaded beam shown in Fig. E12.1.

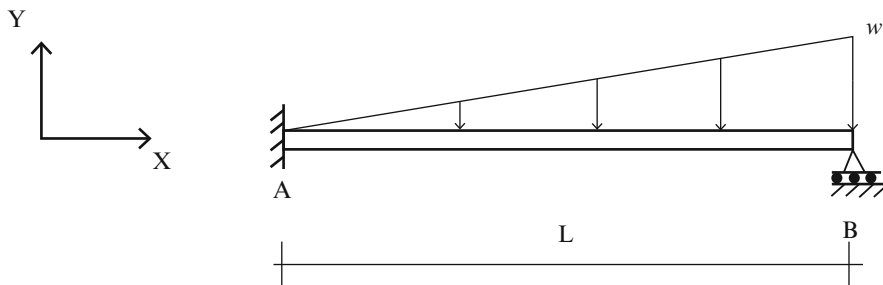


Fig. E12.1

Determine: The fixed end forces.

Solution: The fixed end forces are determined using the Force Method described in Chap. 9 (Table 9.1).

$$\mathbf{P}_{\ell B}^F = \left\{ \begin{array}{l} 0 \\ \frac{7wL}{20} \\ -\frac{wL^2}{20} \end{array} \right\} \quad \mathbf{P}_{\ell A}^F = \left\{ \begin{array}{l} 0 \\ \frac{3wL}{20} \\ \frac{wL^2}{30} \end{array} \right\}$$

12.4 Local and Global Reference Frames

Consider the structure shown in Fig. 12.2. There are five nodes and four members. We number these artifacts consecutively starting with one. The local X axis for a member is selected to coincide with the longitudinal axis, as indicated on the figure; the Y axis is taken to be 90° counter-clockwise from the X axis. The member equations presented in the previous section involve force and displacement quantities referred to the *local member frames*. Figure 12.3 illustrates the situation for node two. The end displacements are related to the nodal displacements. However, one must first select a *common reference frame* for the nodal displacements. We choose the global frame shown in Fig. 12.2. Once the local frames are specified with respect to the global frame (X_g, Y_g), one can derive the relationships between the displacement and force variables.

Consider the reference frames shown in Fig. 12.4. Starting with quantities referred to the local member frame, we project them on the global directions using trigonometric relations. One obtains

$$\begin{aligned} u &= u_l \cos \alpha - v_l \sin \alpha \\ v &= u_l \sin \alpha + v_l \cos \alpha \end{aligned} \quad (12.7)$$

Introducing matrix notation, we write $\mathbf{U} = \begin{Bmatrix} u \\ v \\ \theta \end{Bmatrix}$ and $\mathbf{U}_l = \begin{Bmatrix} u_l \\ v_l \\ \theta \end{Bmatrix}$ and express (12.7) as a matrix product.

$$\mathbf{U} = \mathbf{R}_{lg} \mathbf{U}_l \quad (12.8)$$

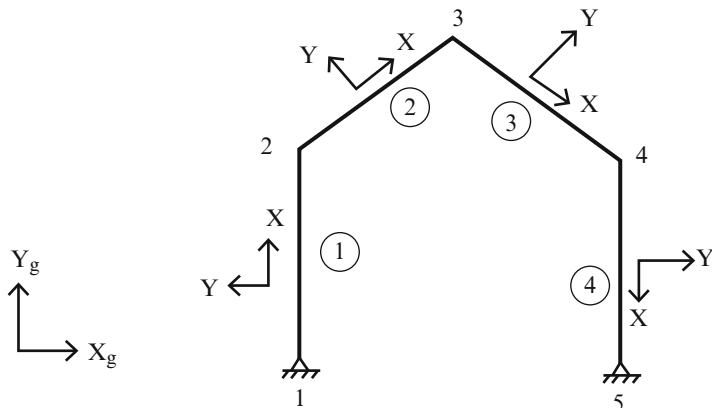


Fig. 12.2 Local and global reference frames

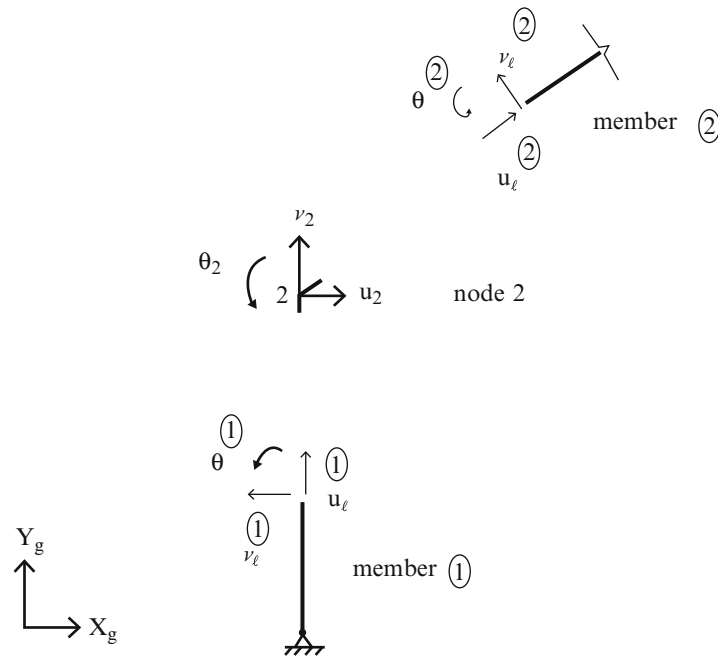


Fig. 12.3 Member and nodal frames at node 1

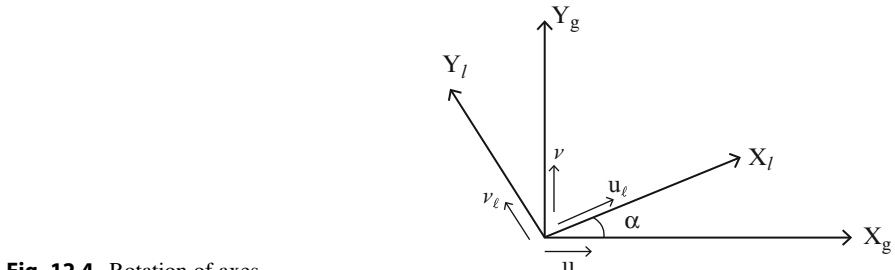


Fig. 12.4 Rotation of axes

where

$$\mathbf{R}_{lg} = \begin{bmatrix} \cos \alpha & -\sin \alpha & 0 \\ \sin \alpha & \cos \alpha & 0 \\ 0 & 0 & 1 \end{bmatrix}$$

We interpret \mathbf{R}_{lg} as a rotation transformation matrix from the local to the global frame. The transformation from the global to the local frame is expressed in a similar way,

$$\mathbf{U}_l = \mathbf{R}_{gl}\mathbf{U} \quad (12.9)$$

where \mathbf{R}_{gl} has the following form.

$$\mathbf{R}_{gl} = \begin{bmatrix} \cos\alpha & \sin\alpha & 0 \\ -\sin\alpha & \cos\alpha & 0 \\ 0 & 0 & 1 \end{bmatrix}$$

Comparing these two forms for \mathbf{R} , we observe that one is both the inverse and the transpose of the other.

$$\mathbf{R}_{gl} = (\mathbf{R}_{lg})^T = (\mathbf{R}_{lg})^{-1} \quad (12.10)$$

A matrix having this property is said to be orthogonal.

Example 12.2 Rotation Matrices

Given: The structure defined in Fig. E12.2a.

Determine: The rotation matrices for the members.

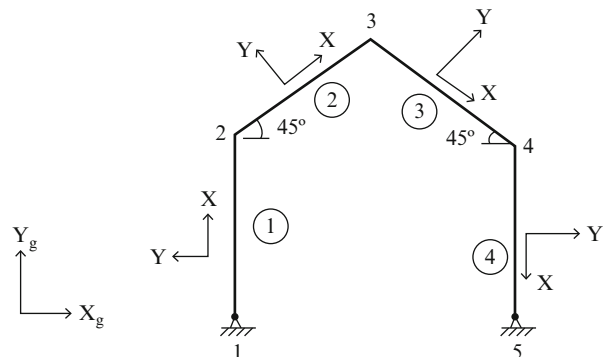


Fig. E12.2a

Solution:

Member ①	$\alpha = +90^\circ$
\mathbf{R}_{lg}	$\begin{bmatrix} 0 & -1 & 0 \\ 1 & 0 & 0 \\ 0 & 0 & 1 \end{bmatrix} \quad \mathbf{R}_{gl} = \begin{bmatrix} 0 & 1 & 0 \\ -1 & 0 & 0 \\ 0 & 0 & 1 \end{bmatrix}$
Member ②	$\alpha = +45^\circ$
\mathbf{R}_{lg}	$\begin{bmatrix} \frac{\sqrt{2}}{2} & -\frac{\sqrt{2}}{2} & 0 \\ \frac{\sqrt{2}}{2} & \frac{\sqrt{2}}{2} & 0 \\ 0 & 0 & 1 \end{bmatrix}$
Member ③	$\alpha = -45^\circ$
\mathbf{R}_{lg}	$\begin{bmatrix} \frac{\sqrt{2}}{2} & \frac{\sqrt{2}}{2} & 0 \\ -\frac{\sqrt{2}}{2} & \frac{\sqrt{2}}{2} & 0 \\ 0 & 0 & 1 \end{bmatrix}$
Member ④	$\alpha = -90^\circ$
\mathbf{R}_{lg}	$\begin{bmatrix} 0 & +1 & 0 \\ -1 & 0 & 0 \\ 0 & 0 & 1 \end{bmatrix}$

We suppose the external nodal forces are referred to the global frame. Then, we need to transform the member end forces from the member frame to the global frame. End forces transform in a similar way as displacements, i.e.

$$\mathbf{P} = \mathbf{R}_{lg}\mathbf{P}_\ell \quad (12.11)$$

Operating on the member matrix equations defined by (12.5) and noting (12.9) and (12.11), the “transformed” equations expressed in terms of quantities referred to the global frame take the following form,

$$\begin{aligned} \mathbf{P}_B &= \mathbf{k}_{BB}\mathbf{U}_B + \mathbf{k}_{BA}\mathbf{U}_A + \mathbf{P}_B^F \\ \mathbf{P}_A &= \mathbf{k}_{AB}\mathbf{U}_B + \mathbf{k}_{AA}\mathbf{U}_A + \mathbf{P}_A^F \end{aligned} \quad (12.12)$$

where the member stiffness and end action matrices referred to the global frames are defined by

$$\begin{aligned} \mathbf{k}_{BB} &= \mathbf{R}_{lg}\mathbf{k}_{\ell BB}(\mathbf{R}_{lg})^T & \mathbf{k}_{BA} &= \mathbf{R}_{lg}\mathbf{k}_{\ell BA}(\mathbf{R}_{lg})^T \\ \mathbf{k}_{AA} &= \mathbf{R}_{lg}\mathbf{k}_{\ell AA}(\mathbf{R}_{lg})^T & \mathbf{k}_{AB} &= \mathbf{R}_{lg}\mathbf{k}_{\ell AB}(\mathbf{R}_{lg})^T \\ \mathbf{P}_B^F &= \mathbf{R}_{lg}\mathbf{P}_{\ell B}^F & \mathbf{P}_A^F &= \mathbf{R}_{lg}\mathbf{P}_{\ell A}^F \end{aligned} \quad (12.13)$$

Given \mathbf{R}_{lg} , one operates, according to (12.13), on the “local” stiffness matrices given by (12.6) to obtain their global forms.

12.5 Nodal Force Equilibrium Equations

The force equilibrium equations for a node involve the end actions for those members which are incident on the node. We need to distinguish between positive and negative incidence, i.e. whether the positive or negative end of the member is incident on the node. Up to this point, we have used subscript B to denote the *positive* end, and A for the *negative* end of a member. To allow for automating the process of assembling the nodal equilibrium equations and computing the member end forces given the member end displacements, we introduce a numbering scheme for the members and the associated end nodes.

We number the members consecutively from 1 to N_m , where N_m is the total number of members. We also define

$$\begin{aligned} n_+ &= \text{node number located at the positive end of member } m \\ n_- &= \text{node number located at the negative end of member } m \end{aligned} \quad (12.14)$$

The connectivity of the members and nodes is defined by a table, which lists for each member the node numbers corresponding to the positive end and negative end. The following table is the member node incidence table for the structure defined in Fig. 12.2.

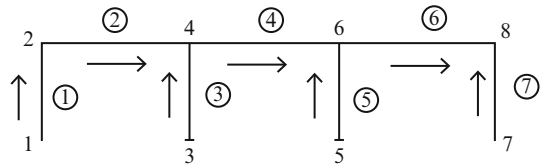
Member-node incidence table

Member m	Negative node n_-	Positive node n_+
1	4	1
2	1	2
3	2	3
4	3	5

The incidence table provides the “instructions” for assembling the nodal equations. We will illustrate this feature later.

Example 12.3 Construction of a member node incidence Table

Given: The structure shown in Fig. E12.3a.

Fig. E12.3a

Determine: The member node incidence table.

Solution: There are seven members and eight nodes. One loops over the members and lists the node numbers at the positive and negative ends of each member (the positive sense for a member is indicated with an arrow). The result is listed below.

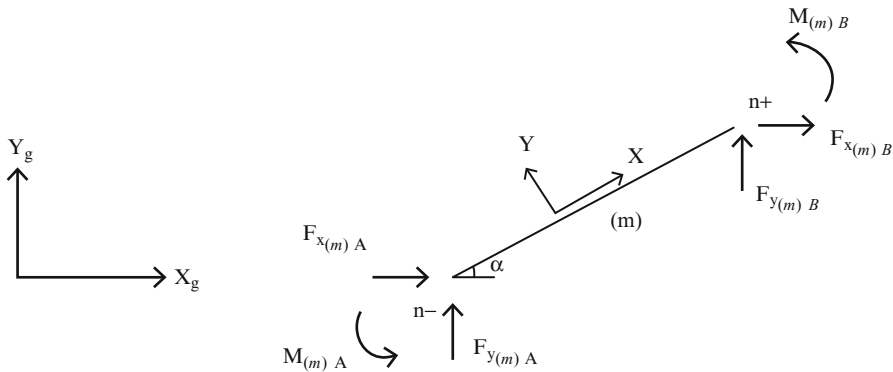
Member-node incidence table

Member m	Negative node n_-	Positive node n_+
1	1	2
2	2	4
3	3	4
4	4	6
5	5	6
6	6	8
7	7	8

Using the notation introduced above and noting (12.12), we denote the global end actions for member m with a subscript (m) .

$$\begin{aligned}\mathbf{P}_{(m)B} &= \mathbf{k}_{(m)BB} \mathbf{U}_{(m)B} + \mathbf{k}_{(m)BA} \mathbf{U}_{(m)A} + \mathbf{P}_{(m)B}^F \\ \mathbf{P}_{(m)A} &= \mathbf{k}_{(m)AB} \mathbf{U}_{(m)B} + \mathbf{k}_{(m)AA} \mathbf{U}_{(m)A} + \mathbf{P}_{(m)A}^F\end{aligned}\quad (12.15)$$

The expanded forms of the matrices in (12.15) referred to the global frame follow from (12.13). We assume member m is oriented at the angle, α (see Fig. 12.5).

**Fig. 12.5** Member end actions referred to global frame

$$\begin{aligned}
 \mathbf{k}_{(m)AA} &= \begin{bmatrix} \left(\frac{AE}{L}\cos^2\alpha + \frac{12EI}{L^3}\sin^2\alpha\right) & \left(\frac{AE}{L} - \frac{12EI}{L^3}\right)\sin\alpha \cos\alpha & -\frac{6EI}{L^2}\sin\alpha \\ \left(\frac{AE}{L} - \frac{12EI}{L^3}\right)\sin\alpha \cos\alpha & \left(\frac{AE}{L}\sin^2\alpha + \frac{12EI}{L^3}\cos^2\alpha\right) & \frac{6EI}{L^2}\cos\alpha \\ -\frac{6EI}{L^2}\sin\alpha & \frac{6EI}{L^2}\cos\alpha & \frac{4EI}{L} \end{bmatrix} \\
 \mathbf{k}_{(m)AB} &= \begin{bmatrix} -\left(\frac{AE}{L}\cos^2\alpha + \frac{12EI}{L^3}\sin^2\alpha\right) & -\left(\frac{AE}{L} - \frac{12EI}{L^3}\right)\sin\alpha \cos\alpha & -\frac{6EI}{L^2}\sin\alpha \\ -\left(\frac{AE}{L} - \frac{12EI}{L^3}\right)\sin\alpha \cos\alpha & -\left(\frac{AE}{L}\sin^2\alpha + \frac{12EI}{L^3}\cos^2\alpha\right) & \frac{6EI}{L^2}\cos\alpha \\ \frac{6EI}{L^2}\sin\alpha & -\frac{6EI}{L^2}\cos\alpha & \frac{2EI}{L} \end{bmatrix} \\
 \mathbf{k}_{(m)BA} &= \begin{bmatrix} -\left(\frac{AE}{L}\cos^2\alpha + \frac{12EI}{L^3}\sin^2\alpha\right) & -\left(\frac{AE}{L} - \frac{12EI}{L^3}\right)\sin\alpha \cos\alpha & \frac{6EI}{L^2}\sin\alpha \\ -\frac{AE}{L} - \frac{12EI}{L^3}\sin\alpha \cos\alpha & -\left(\frac{AE}{L}\sin^2\alpha + \frac{12EI}{L^3}\cos^2\alpha\right) & -\frac{6EI}{L^2}\cos\alpha \\ -\frac{6EI}{L^2}\sin\alpha & \frac{6EI}{L^2}\cos\alpha & \frac{2EI}{L} \end{bmatrix} \\
 \mathbf{k}_{(m)BB} &= \begin{bmatrix} \left(\frac{AE}{L}\cos^2\alpha + \frac{12EI}{L^3}\sin^2\alpha\right) & \left(\frac{AE}{L} - \frac{12EI}{L^3}\right)\sin\alpha \cos\alpha & \frac{6EI}{L^2}\sin\alpha \\ \left(\frac{AE}{L} - \frac{12EI}{L^3}\right)\sin\alpha \cos\alpha & \left(\frac{AE}{L}\sin^2\alpha + \frac{12EI}{L^3}\cos^2\alpha\right) & -\frac{6EI}{L^2}\cos\alpha \\ \frac{6EI}{L^2}\sin\alpha & -\frac{6EI}{L^2}\cos\alpha & \frac{4EI}{L} \end{bmatrix}
 \end{aligned} \tag{12.16}$$

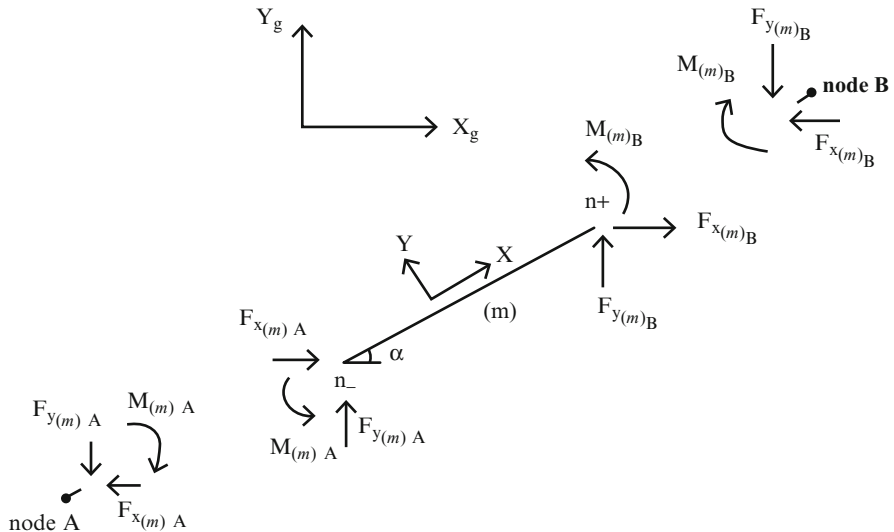


Fig. 12.6 Member reaction forces

$$\begin{aligned}
 U_{(m)B} &= \begin{Bmatrix} u_{(m)B} \\ v_{(m)B} \\ \theta_{(m)B} \end{Bmatrix} & U_{(m)A} &= \begin{Bmatrix} u_{(m)A} \\ v_{(m)A} \\ \theta_{(m)A} \end{Bmatrix} \\
 P_{(m)B} &= \begin{Bmatrix} F_{x(m)B} \\ F_{y(m)B} \\ M_{(m)B} \end{Bmatrix} & P_{(m)A} &= \begin{Bmatrix} F_{x(m)A} \\ F_{y(m)A} \\ M_{(m)A} \end{Bmatrix} \\
 P_{(m)B}^F &= \begin{Bmatrix} F_{x(m)B}^F \\ F_{y(m)B}^F \\ M_{(m)B}^F \end{Bmatrix} & P_{(m)A}^F &= \begin{Bmatrix} F_{x(m)A}^F \\ F_{y(m)A}^F \\ M_{(m)A}^F \end{Bmatrix}
 \end{aligned} \tag{12.17}$$

Note that all terms in (12.16) and (12.17) are referred to the *global reference frame*.

Figure 12.6 shows the forces (end actions) acting on member AB and the nodes located at each end. The nodal forces are \$-\mathbf{P}_{(m)A}\$ and \$-\mathbf{P}_{(m)B}\$, i.e., their sense is opposite to the actual end actions.

To generate the force equilibrium equations for a node, one sums up the applied external forces and the member reaction forces associated with the node. We express the matrix equilibrium equation for node j as

$$\mathbf{P}_{Ej} + \sum_{n_+=j} (-\mathbf{P}_{(m)B}) + \sum_{n_-=j} (-\mathbf{P}_{(m)A}) = 0 \tag{12.18}$$

where \mathbf{P}_{Ej} is the applied external force vector for node j and the Σ is for those members having one end incident on node j . Noting (12.15), we observe that the

equilibrium equation for node j involves the displacements of those nodes which are connected to node j by members. We utilize this observation later.

We generate the complete set of nodal equilibrium equations by evaluating (12.18) for all the nodes. It is convenient to work with matrices expressed in a form that is partitioned according to the “natural” size of the nodal vectors. For a planar frame, the size of the nodal vectors is 3×1 . For a plane truss, the size is 2×1 . For a horizontal beam, the size is 2×1 . We suppose there are N_n nodes. Then, there will be N_n matrix equations similar in form to (12.18). We express the total set of equations as a single matrix equation,

$$\mathbf{P}_E = \mathbf{KU} + \mathbf{P}_I \quad (12.19)$$

where the partitioned forms of the individual matrices are

$$\begin{aligned} \mathbf{U} &= \text{system displacement vector} = \begin{Bmatrix} \mathbf{U}_1 \\ \mathbf{U}_2 \\ \vdots \\ \mathbf{U}_{N_n} \end{Bmatrix} \\ \mathbf{P}_E &= \text{external nodal force vector} = \begin{Bmatrix} \mathbf{P}_{E1} \\ \mathbf{P}_{E2} \\ \vdots \\ \mathbf{P}_{EN_n} \end{Bmatrix} \\ \mathbf{P}_I &= \text{nodal force vector due to member fixed end actions} = \begin{Bmatrix} \mathbf{P}_{I1}^F \\ \mathbf{P}_{I2}^F \\ \vdots \\ \mathbf{P}_{IN_n}^F \end{Bmatrix} \\ \mathbf{K} &= \text{system stiffness matrix} = [\mathbf{K}_{ij}] i, j = 1, 2, \dots, N_n \end{aligned}$$

Note that the system stiffness matrix, \mathbf{K} , has N_n partitioned rows and columns.

We generate the partitioned forms of the system stiffness matrix and internal nodal force vector by looping over the members and noting (12.18). The information for n_+ and n_- for a given member m is provided by the member–node incidence table and leads to the following assembly algorithms for $m = 1, 2, \dots, N_m$:

For \mathbf{K} :

$$\begin{aligned} \mathbf{k}_{(m)AA} &\text{ in row } n_-, \text{ column } n_- \\ \mathbf{k}_{(m)AB} &\text{ in row } n_-, \text{ column } n_+ \\ \mathbf{k}_{(m)BA} &\text{ in row } n_+, \text{ column } n_- \\ \mathbf{k}_{(m)BB} &\text{ in row } n_+, \text{ column } n_+ \end{aligned} \quad (12.20)$$

For \mathbf{P}_I :

$$\begin{aligned} & \mathbf{P}_{(m)A}^F \text{ in row } n_- \\ & \mathbf{P}_{(m)B}^F \text{ in row } n_+ \end{aligned} \quad (12.21)$$

This assembly process is called the “Direct Stiffness Method.” It is generally employed by most commercial analysis software codes since it is relatively straightforward to implement. We can deduce from the assembly algorithm that the system stiffness matrix is square and symmetrical. The nonzero elements tend to be clustered in a band centered on the diagonal.

Example 12.4 Assembly process

Given: The plane frame shown in Fig. E12.4a.

Determine: The system stiffness and nodal force matrices.

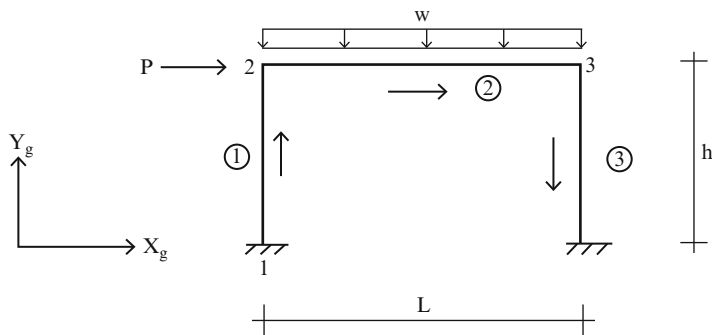


Fig. E12.4a

Solution: We first number the members and nodes as indicated in Fig. E12.4a, and then generate the member-node incidence table listed below.

Member-node incidence table

Member m	Negative node n_-	Positive node n_+
1	1	2
2	2	3
3	3	4

Using the member-node incident table we replace the member end force and displacement matrices with

$$\begin{aligned} \mathbf{U}_B &\Rightarrow \mathbf{U}_{n+} \quad \mathbf{P}_B \Rightarrow \mathbf{P}_{n+} \\ \mathbf{U}_A &\Rightarrow \mathbf{U}_{n-} \quad \mathbf{P}_A \Rightarrow \mathbf{P}_{n-} \end{aligned}$$

In (12.15) the operation is carried out for each member. The resulting expressions for the end forces expressed in terms of the nodal displacements are

$$\begin{aligned}\mathbf{P}_{(1)2} &= \mathbf{k}_{(1)BB}\mathbf{U}_2 + \mathbf{k}_{(1)BA}\mathbf{U}_1 + \mathbf{P}_{(1)B}^F \\ \mathbf{P}_{(1)1} &= \mathbf{k}_{(1)AB}\mathbf{U}_2 + \mathbf{k}_{(1)AA}\mathbf{U}_1 + \mathbf{P}_{(1)A}^F\end{aligned}$$

$$\begin{aligned}\mathbf{P}_{(2)3} &= \mathbf{k}_{(2)BB}\mathbf{U}_3 + \mathbf{k}_{(2)BA}\mathbf{U}_2 + \mathbf{P}_{(2)B}^F \\ \mathbf{P}_{(2)2} &= \mathbf{k}_{(2)AB}\mathbf{U}_3 + \mathbf{k}_{(2)AA}\mathbf{U}_2 + \mathbf{P}_{(2)A}^F\end{aligned}$$

$$\begin{aligned}\mathbf{P}_{(3)4} &= \mathbf{k}_{(3)BB}\mathbf{U}_4 + \mathbf{k}_{(3)BA}\mathbf{U}_3 + \mathbf{P}_{(3)B}^F \\ \mathbf{P}_{(3)3} &= \mathbf{k}_{(3)AB}\mathbf{U}_4 + \mathbf{k}_{(3)AA}\mathbf{U}_3 + \mathbf{P}_{(3)A}^F\end{aligned}$$

Next, we equate the external nodal force to the sum of the member forces at each node. This step leads to the nodal force equilibrium equations.

$$\begin{aligned}\mathbf{P}_{E1} &= \mathbf{P}_{(1)1} \\ \mathbf{P}_{E2} &= \mathbf{P}_{(2)2} + \mathbf{P}_{(1)2} \\ \mathbf{P}_{E3} &= \mathbf{P}_{(2)3} + \mathbf{P}_{(3)3} \\ \mathbf{P}_{E4} &= \mathbf{P}_{(3)4}\end{aligned}$$

Substituting for the end forces expressed in terms of the nodal displacements, these equations expand to

$$\begin{aligned}\mathbf{P}_{E1} &= \mathbf{k}_{(1)AA}\mathbf{U}_1 + \mathbf{k}_{(1)AB}\mathbf{U}_2 + \mathbf{P}_{(1)A}^F \\ \mathbf{P}_{E2} &= \mathbf{k}_{(1)BA}\mathbf{U}_1 + (\mathbf{k}_{(1)BB} + \mathbf{k}_{(2)AA})\mathbf{U}_2 + \mathbf{k}_{(2)AB}\mathbf{U}_3 + \mathbf{P}_{(2)A}^F + \mathbf{P}_{(1)B}^F \\ \mathbf{P}_{E3} &= \mathbf{k}_{(2)BA}\mathbf{U}_2 + (\mathbf{k}_{(2)BB} + \mathbf{k}_{(3)AA})\mathbf{U}_3 + \mathbf{k}_{(3)AB}\mathbf{U}_4 + \mathbf{P}_{(3)A}^F + \mathbf{P}_{(2)B}^F \\ \mathbf{P}_{E4} &= \mathbf{k}_{(3)BA}\mathbf{U}_3 + \mathbf{k}_{(3)BB}\mathbf{U}_4 + \mathbf{P}_{(3)B}^F\end{aligned}$$

Lastly, we write these equations as a single equation in terms of “system” matrices [see (12.19)]. The forms of the system matrices are listed below.

$$\mathbf{U} = \begin{Bmatrix} \mathbf{U}_1 \\ \mathbf{U}_2 \\ \mathbf{U}_3 \\ \mathbf{U}_4 \end{Bmatrix} \quad \mathbf{P}_E = \begin{Bmatrix} \mathbf{P}_{E1} \\ \mathbf{P}_{E2} \\ \mathbf{P}_{E3} \\ \mathbf{P}_{E4} \end{Bmatrix} \quad \mathbf{P}_I = \begin{Bmatrix} \mathbf{P}_{(1)A}^F \\ (\mathbf{P}_{(1)B}^F + \mathbf{P}_{(2)A}^F) \\ (\mathbf{P}_{(2)B}^F + \mathbf{P}_{(3)A}^F) \\ \mathbf{P}_{(3)B}^F \end{Bmatrix}$$

$$\mathbf{K} = \begin{bmatrix} \mathbf{k}_{(1)AA} & \mathbf{k}_{(1)AB} & 0 & 0 \\ \mathbf{k}_{(1)BA} & (\mathbf{k}_{(1)BB} + \mathbf{k}_{(2)AA}) & \mathbf{k}_{(2)AB} & 0 \\ 0 & \mathbf{k}_{(2)BA} & (\mathbf{k}_{(2)BB} + \mathbf{k}_{(3)AA}) & \mathbf{k}_{(3)AB} \\ 0 & 0 & \mathbf{k}_{(3)BA} & \mathbf{k}_{(3)BB} \end{bmatrix}$$

There are four nodes in this example, so the partitioned form of \mathbf{K} is 4×4 . The expanded size of \mathbf{K} for this two-dimensional plane frame will be 12×12 since there are three variables per node.

In this example, we chose to list all the equations first and then combine them in a single “system” equation. Normally, one would apply the algorithms defined by (12.20) and (12.21) and directly assemble the system matrices.

12.6 Introduction of Nodal Supports

Introducing a support at a node corresponds to prescribing the value of certain nodal displacements. For example, a hinge prevents translation in two orthogonal directions. Full fixity eliminates both translation and rotation at a node. When supports are introduced, the number of displacement unknowns is decreased by the number of displacement restraints. However, each displacement constraint produces an unknown reaction so that the “total” number of unknowns (nodal displacements and nodal reaction forces) remains constant. In order to determine the unknown displacements, we work with a reduced set of equilibrium equations. We illustrate this process with the following example.

Example 12.5 Example of fully fixed supports

Given: The structure defined in Fig. E12.5a. Suppose nodes one and four are fully fixed.

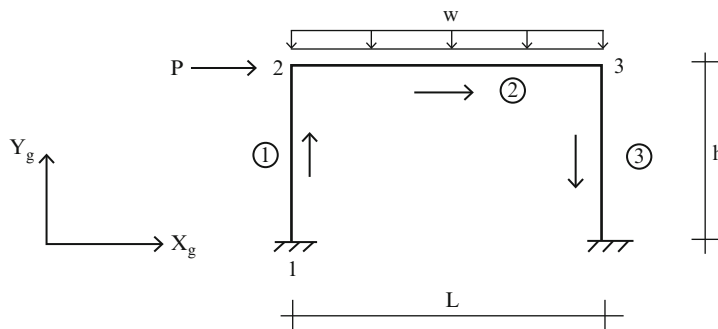


Fig. E12.5a

Determine: The reduced system matrices.

Solution: The system matrices are presented in Example 12.4. We start with the complete set of nodal force equilibrium equations generated in the previous example.

$$\mathbf{P}_{E1} = \mathbf{k}_{(1)AA}\mathbf{U}_1 + \mathbf{k}_{(1)AB}\mathbf{U}_2 + \mathbf{P}_{(1)A}^F$$

$$\mathbf{P}_{E2} = \mathbf{k}_{(1)BA}\mathbf{U}_1 + (\mathbf{k}_{(1)BB} + \mathbf{k}_{(2)AA})\mathbf{U}_2 + \mathbf{k}_{(2)AB}\mathbf{U}_3 + \mathbf{P}_{(2)A}^F + \mathbf{P}_{(1)B}^F$$

$$\mathbf{P}_{E3} = \mathbf{k}_{(2)BA}\mathbf{U}_2 + (\mathbf{k}_{(2)BB} + \mathbf{k}_{(3)AA})\mathbf{U}_3 + \mathbf{k}_{(3)AB}\mathbf{U}_4 + \mathbf{P}_{(3)A}^F + \mathbf{P}_{(2)B}^F$$

$$\mathbf{P}_{E4} = \mathbf{k}_{(3)BA}\mathbf{U}_3 + \mathbf{k}_{(3)BB}\mathbf{U}_4 + \mathbf{P}_{(3)B}^F$$

Nodes 1 and 4 are fully fixed. The external nodal forces \mathbf{P}_{E1} and \mathbf{P}_{E4} represent the reactions at these nodes. We set $\mathbf{U}_1 = \mathbf{U}_4 = 0$ and rearrange the order of the equations so that \mathbf{P}_{E1} and \mathbf{P}_{E4} are last. This step leads to two sets of equations,

$$\mathbf{P}_{E2} = (\mathbf{k}_{(1)BB} + \mathbf{k}_{(2)AA})\mathbf{U}_2 + \mathbf{k}_{(2)AB}\mathbf{U}_3 + \mathbf{P}_{(2)A}^F + \mathbf{P}_{(1)B}^F$$

$$\mathbf{P}_{E3} = \mathbf{k}_{(2)BA}\mathbf{U}_2 + (\mathbf{k}_{(2)BB} + \mathbf{k}_{(3)AA})\mathbf{U}_3 + \mathbf{P}_{(3)A}^F + \mathbf{P}_{(2)B}^F$$

and

$$\mathbf{P}_{E1} = \mathbf{k}_{(1)AB}\mathbf{U}_2 + \mathbf{P}_{(1)A}^F$$

$$\mathbf{P}_{E4} = \mathbf{k}_{(3)BA}\mathbf{U}_3 + \mathbf{P}_{(3)B}^F$$

We solve the first set for \mathbf{U}_2 and \mathbf{U}_3 . Then, we use these displacements to determine the reactions \mathbf{P}_{E1} and \mathbf{P}_{E4} with the second set of equations. Note that the total number of unknowns remains the same when displacement constraint is introduced.

12.6.1 Systematic Approach

The systematic approach for introducing displacement constraints involves rearranging the system displacement vector \mathbf{U} into two segments and also rearranging the rows and columns of \mathbf{P} and \mathbf{K} consistent with this reordering of \mathbf{U} . We write the rearranged system matrices as

$$\begin{aligned} \mathbf{K} \rightarrow \mathbf{K}' &= \begin{pmatrix} \mathbf{K}'_{11} & | & \mathbf{K}'_{12} \\ \hline \mathbf{K}'_{21} & | & \mathbf{K}'_{22} \end{pmatrix} \\ \mathbf{U} \rightarrow \left\{ \begin{array}{l} \mathbf{U}' \\ \mathbf{U}'' \end{array} \right\} & \quad \mathbf{P}_E \rightarrow \left\{ \begin{array}{l} \mathbf{P}'_E \\ \mathbf{P}''_E \end{array} \right\} \quad \mathbf{P}_I \rightarrow \left\{ \begin{array}{l} \mathbf{P}'_I \\ \mathbf{P}''_I \end{array} \right\} \end{aligned} \quad (12.23)$$

where \mathbf{U}' contains the *unknown* displacements, \mathbf{U}'' contains the *prescribed* support movements, \mathbf{P}'_E contains the *prescribed* joint loads, and \mathbf{P}''_E contains the *unknown forces* (reactions).

With this reordering, the system equation takes the following form.

$$\begin{Bmatrix} \mathbf{P}'_E \\ \mathbf{P}''_E \end{Bmatrix} = \begin{pmatrix} \mathbf{K}'_{11} & | & \mathbf{K}'_{12} \\ \mathbf{K}'_{21} & | & \mathbf{K}'_{22} \end{pmatrix} \begin{Bmatrix} \mathbf{U}' \\ \mathbf{U}'' \end{Bmatrix} + \begin{Bmatrix} \mathbf{P}'_I \\ \mathbf{P}''_I \end{Bmatrix} \quad (12.24)$$

Expanding the matrix product results in two matrix equations

$$\begin{aligned} \mathbf{P}'_E &= \mathbf{K}'_{11}\mathbf{U}' + \mathbf{K}'_{12}\mathbf{U}'' + \mathbf{P}'_I \\ \mathbf{P}''_E &= \mathbf{K}'_{21}\mathbf{U}' + \mathbf{K}'_{22}\mathbf{U}'' + \mathbf{P}''_I \end{aligned} \quad (12.25)$$

We solve the first equation for \mathbf{U}'

$$\mathbf{U}' = (\mathbf{K}'_{11})^{-1}(\mathbf{P}'_E - \mathbf{K}'_{12}\mathbf{U}'' - \mathbf{P}'_I) \quad (12.26)$$

Note that the prescribed support movements are converted to equivalent nodal forces. Given \mathbf{U}' , we use the second equation in (12.25) to determine the reaction forces. This step involves only matrix multiplication. With this approach, one can deal separately with the nodal loads, member loads, and support movements.

Expanding the right hand side of (12.26) leads to solutions due to the different loading conditions

Joint loads only: ($\mathbf{U}'' = 0$, $\mathbf{P}'_I = 0$, $\mathbf{P}''_I = 0$)

$$\begin{aligned} \mathbf{U}' &= (\mathbf{K}'_{11})^{-1}(\mathbf{P}'_E) \\ \mathbf{P}''_E &= \mathbf{K}'_{21}\mathbf{U}' \end{aligned}$$

Support settlements only: ($\mathbf{P}'_E = 0$, $\mathbf{P}'_I = 0$, $\mathbf{P}''_I = 0$)

$$\begin{aligned} \mathbf{U}' &= (\mathbf{K}'_{11})^{-1}(-\mathbf{K}'_{12}\mathbf{U}'') \\ \mathbf{P}''_E &= \mathbf{K}'_{21}\mathbf{U}' + \mathbf{K}'_{22}\mathbf{U}'' \end{aligned}$$

Member loads only: ($\mathbf{U}'' = 0$, $\mathbf{P}'_E = 0$)

$$\begin{aligned} \mathbf{U}' &= (\mathbf{K}'_{11})^{-1}(-\mathbf{P}'_I) \\ \mathbf{P}''_E &= \mathbf{K}'_{21}\mathbf{U}' + \mathbf{P}''_I \end{aligned}$$

Lastly, we determine the end member forces in the global coordinate frame and then transform them to the local frame. The operations for member m are

$$\begin{aligned}
 P_{(m)B} &= k_{(m)BB} U_{n^+} + k_{(m)BA} U_{n^-} + P_{(m)B}^F \\
 P_{(m)A} &= k_{(m)AB} U_{n^+} + k_{(m)AA} U_{n^-} + P_{(m)A}^F \\
 P_{\ell(m)_B} &= R_{g\ell} P_{(m)_B} \\
 P_{\ell(m)_A} &= R_{g\ell} P_{(m)_A}
 \end{aligned} \tag{12.27}$$

Example 12.6 Example of support movement

Given: The structure defined in Fig. E12.6a. Consider nodes 1 and 4 to experience support settlements of δ_1 and δ_4 .

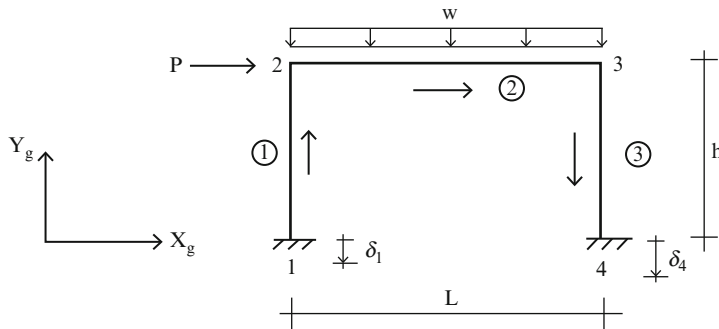


Fig. E12.6a

Determine: The rearranged system matrices

Solution: The system matrices are presented in Example 12.4. We place the displacement matrices corresponding to the partially fixed nodes in \mathbf{U}'' .

$$\mathbf{K} = \begin{bmatrix} \mathbf{k}_{(1)AA} & \mathbf{k}_{(1)AB} & 0 & 0 \\ \mathbf{k}_{(1)BA} & (\mathbf{k}_{(1)BB} + \mathbf{k}_{(2)AA}) & \mathbf{k}_{(2)AB} & 0 \\ 0 & \mathbf{k}_{(2)BA} & (\mathbf{k}_{(2)BB} + \mathbf{k}_{(3)AA}) & \mathbf{k}_{(3)AB} \\ 0 & 0 & \mathbf{k}_{(3)BA} & \mathbf{k}_{(3)BB} \end{bmatrix}$$

$$\mathbf{U}' = \left\{ \mathbf{U}_2 \atop \mathbf{U}_3 \right\} = \begin{Bmatrix} u_2 \\ v_2 \\ \theta_2 \\ u_3 \\ v_3 \\ \theta_3 \end{Bmatrix} \quad \mathbf{U}'' = \left\{ \mathbf{U}_1 \atop \mathbf{U}_4 \right\} = \begin{Bmatrix} u_1 = 0 \\ v_1 = -\delta_1 \\ \theta_1 = 0 \\ u_4 = 0 \\ v_4 = -\delta_4 \\ \theta_4 = 0 \end{Bmatrix}$$

The modified form of \mathbf{K} consistent with this reordering of \mathbf{U} is generated by moving the first partitioned row and column back to the third location. The steps are

$$\mathbf{K}' = \left[\begin{array}{ccc|cc} (\mathbf{k}_{(1)}\mathbf{BB} + \mathbf{k}_{(2)}\mathbf{AA}) & \mathbf{k}_{(2)}\mathbf{AB} & & \mathbf{k}_{(1)}\mathbf{AB} & \mathbf{0} \\ \mathbf{k}_{(2)}\mathbf{BA} & (\mathbf{k}_{(2)}\mathbf{BB} + \mathbf{k}_{(3)}\mathbf{AA}) & & \mathbf{0} & \mathbf{k}_{(3)}\mathbf{AB} \\ \hline \mathbf{k}_{(1)}\mathbf{AB} & \mathbf{0} & & \mathbf{k}_{(1)}\mathbf{AA} & \mathbf{0} \\ \mathbf{0} & \mathbf{k}_{(3)}\mathbf{BA} & & \mathbf{0} & \mathbf{k}_{(3)}\mathbf{BB} \end{array} \right]$$

Noting (12.24), the partitioned form of \mathbf{K}' is

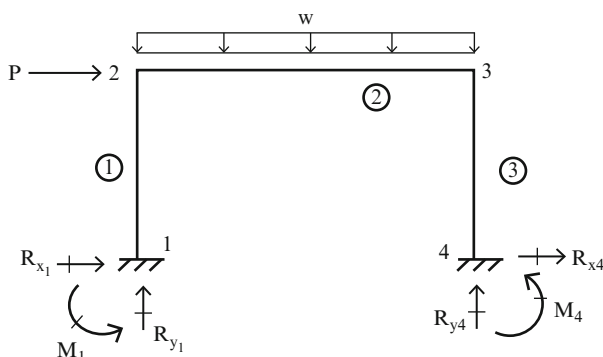
$$\mathbf{K}'_{11} = \begin{bmatrix} (\mathbf{k}_{(1)}\mathbf{BB} + \mathbf{k}_{(2)}\mathbf{AA}) & \mathbf{k}_{(2)}\mathbf{AB} \\ \mathbf{k}_{(2)}\mathbf{BA} & (\mathbf{k}_{(2)}\mathbf{BB} + \mathbf{k}_{(3)}\mathbf{AA}) \end{bmatrix} \quad \mathbf{K}'_{12} = \begin{bmatrix} \mathbf{k}_{(1)}\mathbf{BA} & \mathbf{0} \\ \mathbf{0} & \mathbf{k}_{(3)}\mathbf{BA} \end{bmatrix}$$

$$\mathbf{K}'_{21} = \begin{bmatrix} \mathbf{k}_{(1)}\mathbf{AB} & \mathbf{0} \\ \mathbf{0} & \mathbf{k}_{(3)}\mathbf{AB} \end{bmatrix} \quad \mathbf{K}'_{22} = \begin{bmatrix} \mathbf{k}_{(1)}\mathbf{AA} & \mathbf{0} \\ \mathbf{0} & \mathbf{k}_{(3)}\mathbf{BB} \end{bmatrix}$$

We perform a similar operation on the rows of \mathbf{P}_E and \mathbf{P}_I . The corresponding reordered partitioned nodal forces are:

$$\mathbf{P}'_E = \begin{Bmatrix} \mathbf{P}_{E2} \\ \mathbf{P}_{E3} \end{Bmatrix} \quad \mathbf{P}'_I = \begin{Bmatrix} (\mathbf{P}^F_{(1)B} + \mathbf{P}^F_{(2)A}) \\ (\mathbf{P}^F_{(2)B} + \mathbf{P}^F_{(3)A}) \end{Bmatrix}$$

$$\mathbf{P}''_E = \begin{Bmatrix} \mathbf{P}_{E1} \\ \mathbf{P}_{E4} \end{Bmatrix} = \begin{Bmatrix} R_{x1} \\ R_{y1} \\ M_1 \\ R_{x4} \\ R_{y4} \\ M_4 \end{Bmatrix} \quad \mathbf{P}''_I = \begin{Bmatrix} \mathbf{P}^F_{(1)A} \\ \mathbf{P}^F_{(3)B} \end{Bmatrix}$$



Throughout the chapter, matrix computations are carried out using computer software such as MATHLAB (29) or MATHCAD (30).

Example 12.7 Two member plane frame—partially fixed

Given: The frame shown in Fig. E12.7a. E , I , and A are constant for both members.

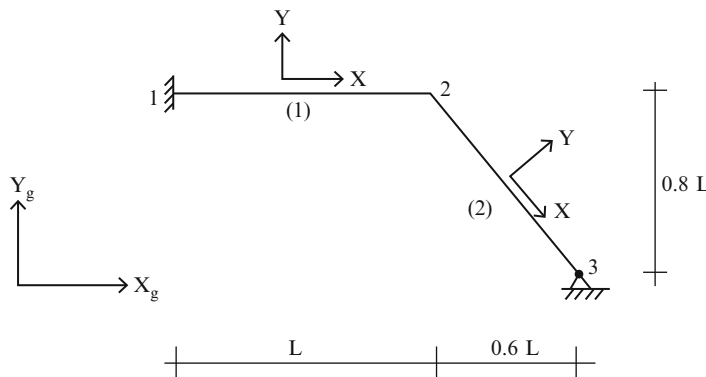


Fig. E12.7a

Determine: (a) The various matrices for the matrix displacement formulation. (b) Solve for the joint displacements, member forces and reactions due to the loading defined in Fig. E12.7b. Use the following values for the parameters: $L = 15 \text{ ft}$, $I = 170 \text{ in.}^4$, $A = 10 \text{ in.}^2$ and $E = 29,000 \text{ ksi}$.

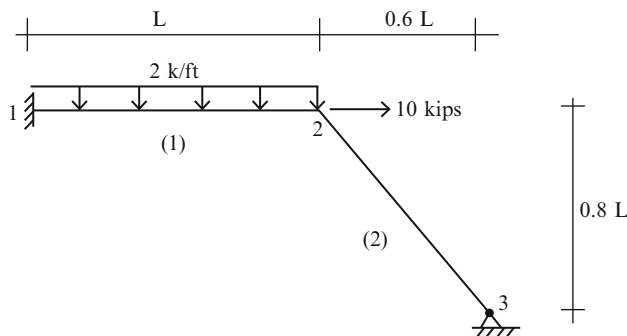


Fig. E12.7b

Solution:

We start with the geometric data. The topological and geometric information is listed below

Geometric data:

Member m	n_-	n_+	α
(1)	1	2	0
(2)	2	3	-53.13°

Member m	α	$\cos \alpha$	$\sin \alpha$	$\sin \alpha \cos \alpha$	$\cos^2 \alpha$	$\sin^2 \alpha$
(1)	0	1	0	0	1	0
(2)	-53.13°	0.6	-0.8	-0.48	0.36	0.64

Generate stiffness matrices:

The system stiffness matrix and displacement vector have the following form

$$\mathbf{K} = \begin{bmatrix} \mathbf{k}_{(1)AA} & \mathbf{k}_{(1)AB} & 0 \\ \mathbf{k}_{(1)BA} & \mathbf{k}_{(1)BB} & 0 \\ 0 & 0 & 0 \end{bmatrix} + \begin{bmatrix} 0 & 0 & 0 \\ 0 & \mathbf{k}_{(2)AA} & \mathbf{k}_{(2)AB} \\ 0 & \mathbf{k}_{(2)BA} & \mathbf{k}_{(2)BB} \end{bmatrix} = \begin{bmatrix} \mathbf{k}_{(1)AA} & \mathbf{k}_{(1)AB} & 0 \\ \mathbf{k}_{(1)BA} & (\mathbf{k}_{(1)BB} + \mathbf{k}_{(2)AA}) & \mathbf{k}_{(2)AB} \\ 0 & \mathbf{k}_{(2)BA} & \mathbf{k}_{(2)BB} \end{bmatrix}$$

$$\mathbf{U} = \begin{Bmatrix} \mathbf{U}_1 \\ \mathbf{U}_2 \\ \mathbf{U}_3 \end{Bmatrix} = \begin{Bmatrix} u_1 \\ v_1 \\ \theta_1 \\ u_2 \\ v_2 \\ \theta_2 \\ u_3 \\ v_3 \\ \theta_3 \end{Bmatrix}$$

We determine the individual member matrices using (12.16). These matrices are referred to the global reference frame.

$$\mathbf{k}_{(1)AA} = \begin{bmatrix} \frac{AE}{L} & 0 & 0 \\ 0 & \frac{12EI}{L^3} & \frac{6EI}{L^2} \\ 0 & \frac{6EI}{L^2} & \frac{4EI}{L} \end{bmatrix} \quad \mathbf{k}_{(1)AB} = \begin{bmatrix} -\frac{AE}{L} & 0 & 0 \\ 0 & -\frac{12EI}{L^3} & \frac{6EI}{L^2} \\ 0 & -\frac{6EI}{L^2} & \frac{2EI}{L} \end{bmatrix}$$

$$\mathbf{k}_{(1)BA} = \begin{bmatrix} -\frac{AE}{L} & 0 & 0 \\ 0 & -\frac{12EI}{L^3} & -\frac{6EI}{L^2} \\ 0 & \frac{6EI}{L^2} & \frac{2EI}{L} \end{bmatrix} \quad \mathbf{k}_{(1)BB} = \begin{bmatrix} \frac{AE}{L} & 0 & 0 \\ 0 & \frac{12EI}{L^3} & -\frac{6EI}{L^2} \\ 0 & -\frac{6EI}{L^2} & \frac{4EI}{L} \end{bmatrix}$$

$$\mathbf{k}_{(1)AA} = \begin{bmatrix} \left(\frac{AE}{L}0.36 + \frac{12EI}{L^3}0.64\right) & \left(\frac{AE}{L} - \frac{12EI}{L^3}\right)(-0.48) & -\frac{6EI}{L^2}(-0.8) \\ \left(\frac{AE}{L} - \frac{12EI}{L^3}\right)(-0.48) & \left(\frac{AE}{L}0.64 + \frac{12EI}{L^3}0.36\right) & \frac{6EI}{L^2}0.6 \\ -\frac{6EI}{L^2}(-0.8) & \frac{6EI}{L^2}0.6 & \frac{4EI}{L} \end{bmatrix}$$

$$\mathbf{k}_{(2)AB} = \begin{bmatrix} -\left(\frac{AE}{L}0.36 + \frac{12EI}{L^3}0.64\right) & (-0.48)\left(-\frac{AE}{L} + \frac{12EI}{L^3}\right) & -\frac{6EI}{L^2}(-0.8) \\ \left(-\frac{AE}{L} + \frac{12EI}{L^3}\right)(-0.48) & -\left(\frac{AE}{L}0.64 + \frac{12EI}{L^3}0.36\right) & \frac{6EI}{L^2}0.6 \\ \frac{6EI}{L^2}(-0.8) & -\frac{6EI}{L^2}0.6 & \frac{2EI}{L} \end{bmatrix}$$

$$\mathbf{k}_{(2)BA} = \begin{bmatrix} -\left(\frac{AE}{L}0.36 + \frac{12EI}{L^3}0.64\right) & (-0.48)\left(-\frac{AE}{L} + \frac{12EI}{L^3}\right) & \frac{6EI}{L^2}(-0.8) \\ -(-0.48)\left(\frac{AE}{L} + \frac{12EI}{L^3}\right) & -\left(\frac{AE}{L}0.64 + \frac{12EI}{L^3}0.36\right) & -\frac{6EI}{L^2}0.6 \\ -\frac{6EI}{L^2}(-0.8) & \frac{6EI}{L^2}0.6 & \frac{2EI}{L} \end{bmatrix}$$

$$\mathbf{k}_{(2)BB} = \begin{bmatrix} \left(\frac{AE}{L}0.36 + \frac{12EI}{L^3}0.64\right) & (-0.48)\left(\frac{AE}{L} - \frac{12EI}{L^3}\right) & \frac{6EI}{L^2}(-0.8) \\ \left(\frac{AE}{L} - \frac{12EI}{L^3}\right)(-0.48) & \left(\frac{AE}{L}0.64 + \frac{12EI}{L^3}0.36\right) & -\frac{6EI}{L^2}0.6 \\ \frac{6EI}{L^2}(-0.8) & -\frac{6EI}{L^2}0.6 & \frac{4EI}{L} \end{bmatrix}$$

Substituting for these matrices, the system stiffness matrix takes the following form.

$$\mathbf{K} = \begin{bmatrix} \frac{AE}{L} & 0 & 0 & -\frac{AE}{L} & 0 & 0 & 0 & 0 & 0 \\ 0 & \frac{12EI}{L^2} & \frac{6EI}{L^2} & 0 & -\frac{12EI}{L^2} & \frac{6EI}{L^2} & 0 & 0 & 0 \\ 0 & \frac{6EI}{L^2} & \frac{4EI}{L} & 0 & -\frac{6EI}{L^2} & \frac{2EI}{L} & 0 & 0 & 0 \\ -\frac{AE}{L} & 0 & 0 & \left(\frac{AE}{L}0.36 + \frac{12EI}{L^3}0.64\right) & -0.48\left(\frac{AE}{L} - \frac{12EI}{L^3}\right) & -\frac{6EI}{L^2}(-0.8) & -\left(\frac{AE}{L}0.36 + \frac{12EI}{L^3}0.64\right) & -0.48\left(-\frac{AE}{L} + \frac{12EI}{L^3}\right) & -\frac{6EI}{L^2}(-0.8) \\ 0 & -\frac{12EI}{L^3} & -\frac{6EI}{L^2} & -0.48\left(\frac{AE}{L} - \frac{12EI}{L^3}\right) & \left(\frac{AE}{L}0.64 + \frac{12EI}{L^3}1.36\right) & \frac{6EI}{L^2}(-0.4) & -0.48\left(-\frac{AE}{L} + \frac{12EI}{L^3}\right) & -\left(\frac{AE}{L}0.64 + \frac{12EI}{L^3}0.36\right) & \frac{6EI}{L^2}0.6 \\ 0 & \frac{6EI}{L^2} & \frac{2EI}{L} & -\frac{6EI}{L^2}(-0.8) & \frac{6EI}{L^2}(-0.4) & \frac{8EI}{L} & \frac{6EI}{L^2}(-0.8) & -\frac{6EI}{L^2}(0.6) & \frac{2EI}{L} \\ 0 & 0 & 0 & -\left(\frac{AE}{L}0.36 + \frac{12EI}{L^3}0.64\right) & -0.48\left(-\frac{AE}{L} + \frac{12EI}{L^3}\right) & \frac{6EI}{L^2}(-0.8) & \left(\frac{AE}{L}0.36 + \frac{12EI}{L^3}0.64\right) & -0.48\left(\frac{AE}{L} - \frac{12EI}{L^3}\right) & \frac{6EI}{L^2}(-0.8) \\ 0 & 0 & 0 & 0.48\left(\frac{AE}{L} + \frac{12EI}{L^3}\right) & -\left(\frac{AE}{L}0.64 + \frac{12EI}{L^3}0.36\right) & -\frac{6EI}{L^2}(0.6) & -0.48\left(\frac{AE}{L} - \frac{12EI}{L^3}\right) & \left(\frac{AE}{L}0.64 + \frac{12EI}{L^3}0.36\right) & -\frac{6EI}{L^2}(0.6) \\ 0 & 0 & 0 & -\frac{6EI}{L^2}(-0.8) & \frac{6EI}{L^2}(0.6) & \frac{2EI}{L} & \frac{6EI}{L^2}(-0.8) & -\frac{6EI}{L^2}(0.6) & \frac{4EI}{L} \end{bmatrix}$$

Introduce displacement constraints:

We note that node 1 is fully fixed but node 3 is partially fixed, i.e., the rotation θ_3 is unknown. We rearrange the rows and columns of \mathbf{K} , and the rows of \mathbf{U} , \mathbf{P}_E and \mathbf{P}_I . This step leads to the resulting partitioned vectors and matrices listed below.

$$\mathbf{U}' = \begin{Bmatrix} u_2 \\ v_2 \\ \theta_2 \\ \theta_3 \end{Bmatrix} \quad \mathbf{U}'' = \begin{Bmatrix} u_1 \\ v_1 \\ \theta_1 \\ u_3 \\ v_3 \end{Bmatrix}$$

$$\mathbf{K}'_{11} = \begin{bmatrix} \left(\frac{AE}{L}1.36 + \frac{12EI}{L^3}0.64\right) & (-0.48)\left(\frac{AE}{L} - \frac{12EI}{L^3}\right) & -\frac{6EI}{L^2}(-0.8) & -\frac{6EI}{L^2}(-0.8) \\ (-0.48)\left(\frac{AE}{L} - \frac{12EI}{L^3}\right) & \left(\frac{AE}{L}0.64 + \frac{12EI}{L^3}1.36\right) & \frac{6EI}{L^2}(-0.4) & \frac{6EI}{L^2}(0.6) \\ -\frac{6EI}{L^2}(-0.8) & \frac{6EI}{L^2}(-0.4) & \frac{8EI}{L} & \frac{2EI}{L} \\ -\frac{6EI}{L^2}(-0.8) & \frac{6EI}{L^2}(0.6) & \frac{2EI}{L} & \frac{4EI}{L} \end{bmatrix}$$

$$\mathbf{K}'_{12} = \begin{bmatrix} -\frac{AE}{L} 0 & 0 & -\left(\frac{AE}{L}0.36 + \frac{12EI}{L^3}0.64\right) & -0.48\left(-\frac{AE}{L} + \frac{12EI}{L^3}\right) \\ 0 & -\frac{12EI}{L^3} & -\frac{6EI}{L^2} & \left(-\frac{AE}{L} + \frac{12EI}{L^3}\right)(-0.48) \\ 0 & \frac{6EI}{L^2} & \frac{2EI}{L} & -\frac{6EI}{L^2}(-0.8) \\ 0 & 0 & 0 & \frac{6EI}{L^2}(-0.8) \end{bmatrix}$$

$$\mathbf{K}'_{21} = \begin{bmatrix} -\frac{AE}{L} & 0 & 0 & 0 \\ 0 & -\frac{12EI}{L^3} & \frac{6EI}{L^2} & 0 \\ 0 & -\frac{6EI}{L^2} & \frac{2EI}{L} & 0 \\ -\left(\frac{AE}{L}0.36 + \frac{12EI}{L^3}0.64\right) & (-0.48)\left(-\frac{AE}{L} + \frac{12EI}{L^3}\right) & \frac{6EI}{L^2}(-0.8) & \frac{6EI}{L^2}(-0.8) \\ -\left(\frac{AE}{L} + \frac{12EI}{L^3}\right)(-0.48) & -\left(\frac{AE}{L}0.64 + \frac{12EI}{L^3}0.36\right) & -\frac{6EI}{L^2}0.6 & -\frac{6EI}{L^2}0.6 \end{bmatrix}$$

$$\mathbf{K}'_{22} = \begin{bmatrix} \frac{AE}{L} & 0 & 0 & 0 & 0 \\ 0 & \frac{12EI}{L^3} & \frac{6EI}{L^2} & 0 & 0 \\ 0 & \frac{6EI}{L^2} & \frac{4EI}{L} & 0 & 0 \\ 0 & 0 & 0 & \left(\frac{AE}{L}0.36 + \frac{12EI}{L^3}0.64\right) & \left(\frac{AE}{L} - \frac{12EI}{L^3}\right)(-0.48) \\ 0 & 0 & 0 & \left(\frac{AE}{L} - \frac{12EI}{L^3}\right)(-0.48) & \left(\frac{AE}{L}0.64 + \frac{12EI}{L^3}0.36\right) \\ 0 & 0 & 0 & \frac{6EI}{L^2}(-0.8) & -\frac{6EI}{L^2}0.6 \end{bmatrix}$$

Introduce the member properties and evaluate the stiffness terms:

We evaluate the individual stiffness matrices using the following values for the parameters ($L = 15$ ft, $I = 170$ in.⁴, $A = 10$ in.², $E = 29,000$ ksi).

$$\mathbf{K}'_{11} = \begin{bmatrix} 2.198 \times 10^3 & -768.464 & 730.37 & 730.37 \\ -768.464 & 1.045 \times 10^3 & -365.185 & 547.778 \\ 730.37 & -365.185 & 2.191 \times 10^5 & 5.475 \times 10^4 \\ 730.37 & 547.778 & 5.478 \times 10^4 & 1.096 \times 10^5 \end{bmatrix}$$

$$\mathbf{K}'_{21} = \begin{bmatrix} -1.61 \times 10^3 & 0 & 0 & 0 \\ 0 & -10.14 & 913 & 0 \\ 0 & -913 & 548 \times 10^4 & 0 \\ -586.5 & -768.5 & -730.4 & -730.4 \\ 778.2 & -1.035 \times 10^3 & -547.8 & -547.8 \end{bmatrix}$$

We need the inverse of \mathbf{K}'_{11} to solve for the displacement due to a given loading. Its form is

$$(\mathbf{K}'_{11})^{-1} = \begin{bmatrix} 6.17 \times 10^{-4} & 4.574 \times 10^{-4} & 3.492 \times 10^{-7} & -6.575 \times 10^{-6} \\ 4.574 \times 10^{-4} & 1.301 \times 10^{-3} & 3.464 \times 10^{-6} & -1.128 \times 10^{-5} \\ 3.492 \times 10^{-7} & 3.464 \times 10^{-6} & 5.227 \times 10^{-6} & -2.633 \times 10^{-6} \\ -6.575 \times 10^{-6} & -1.128 \times 10^{-5} & -2.633 \times 10^{-6} & 1.054 \times 10^{-5} \end{bmatrix}$$

Specify loading:

Next, we consider the loading shown in Fig. E12.7b. The fixed end actions due to the uniform loading applied to member 1 are defined in Fig. E12.7c.

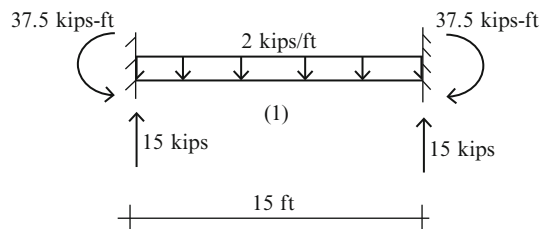


Fig. E12.7c

The system load vectors corresponding to these loads are:

$$\mathbf{P}'_E = \begin{Bmatrix} 10 \\ 0 \\ 0 \\ 0 \end{Bmatrix} \quad \mathbf{P}'_I = \begin{Bmatrix} 0 \\ 15.0 \\ -37.5(12) \\ 0 \end{Bmatrix} \quad \mathbf{P}''_I = \begin{Bmatrix} 0 \\ 15.0 \\ 37.5(12) \\ 0 \\ 0 \end{Bmatrix}$$

Determine the unknown displacements:

Finally, we determine the unknown displacements using (12.26):

$$\mathbf{U}' = (\mathbf{K}'_{11})^{-1}(\mathbf{P}'_E - \mathbf{P}'_I)$$

↓

$$\begin{Bmatrix} u_2 \\ v_2 \\ \theta_2 \\ \theta_3 \end{Bmatrix} = \begin{bmatrix} 6.17 \times 10^{-4} & 4.574 \times 10^{-4} & 3.492 \times 10^{-7} & -6.575 \times 10^{-6} \\ 4.574 \times 10^{-4} & 1.301 \times 10^{-3} & 3.464 \times 10^{-6} & -1.128 \times 10^{-5} \\ 3.492 \times 10^{-7} & 3.464 \times 10^{-6} & 5.227 \times 10^{-6} & -2.633 \times 10^{-6} \\ -6.575 \times 10^{-6} & -1.128 \times 10^{-5} & -2.633 \times 10^{-6} & 1.054 \times 10^{-5} \end{bmatrix} \times \begin{bmatrix} \begin{Bmatrix} 10 \\ 0 \\ 0 \\ 0 \end{Bmatrix} - \begin{Bmatrix} 0 \\ 15.0 \\ -(37.5 \times 12) \\ 0 \end{Bmatrix} \end{bmatrix} = \begin{Bmatrix} -5.329 \times 10^{-4} \\ -0.013 \\ 2.304 \times 10^{-3} \\ -1.081 \times 10^{-3} \end{Bmatrix}$$

$$u_2 = 0.00053 \text{ in.} \leftarrow$$

$$v_2 = 0.013 \text{ in.} \downarrow$$

$$\theta_2 = 0.002304 \text{ rad}$$

$$\theta_3 = 0.001081 \text{ rad}$$

Determine unknown forces (reactions):

Given the displacements, one determines the reactions with

$$\mathbf{P}''_E = \mathbf{K}'_{21}\mathbf{U}' + \mathbf{K}'_{22}\mathbf{U}'' + \mathbf{P}''_I \Rightarrow \begin{Bmatrix} R_{x1} \\ R_{y1} \\ M_1 \\ R_{x3} \\ R_{y3} \end{Bmatrix} = \mathbf{K}'_{21} \begin{Bmatrix} u_2 \\ v_2 \\ \theta_2 \\ \theta_3 \end{Bmatrix} + \mathbf{P}''_I$$

$$\begin{aligned}
 \left\{ \begin{array}{l} R_{x1} \\ R_{y1} \\ M_1 \\ R_{x3} \\ R_{y3} \end{array} \right\} &= \begin{bmatrix} -1.61 \times 10^3 & 0 & 0 & 0 \\ 0 & -10.14 & 913 & 0 \\ 0 & -913 & 548 \times 10^4 & 0 \\ -586.5 & -768.5 & -730.4 & -730.4 \\ 778.2 & -1.035 \times 10^3 & -547.8 & -547.8 \end{bmatrix} \\
 &\times \begin{Bmatrix} -5.329 \times 10^{-4} \\ -0.013 \\ 2.304 \times 10^{-3} \\ -1.081 \times 10^{-3} \end{Bmatrix} + \begin{Bmatrix} 0 \\ 15.0 \\ (37.5 \times 12) \\ 0 \\ 0 \end{Bmatrix} \\
 &= \begin{Bmatrix} 0.86 \text{ kip} \\ 17.24 \text{ kip} \\ 588.4 \text{ kip/in.} \\ -10.86 \text{ kip} \\ 12.76 \text{ kip} \end{Bmatrix}
 \end{aligned}$$

The reactions are listed on Fig. E12.7d

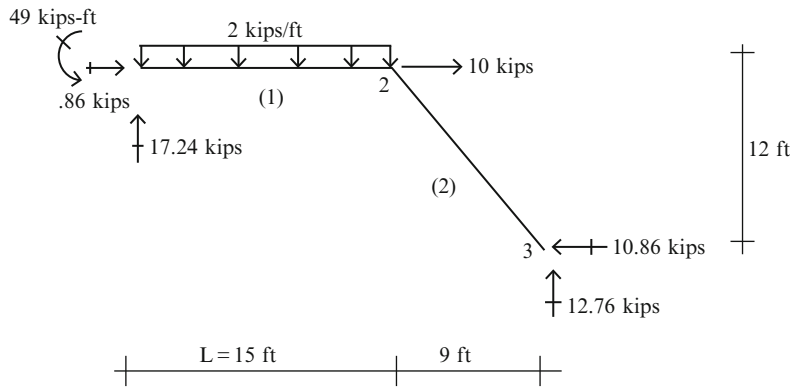


Fig. E12.7d

Determine member forces in the local coordinates:

Lastly, we determine the member end actions in the global and local coordinate system using (12.27). Applying these equations for members 1 and 2 leads to the following results:

Fixed end actions

$$\mathbf{P}_{(1)A}^F = \begin{Bmatrix} 0 \\ 15 \text{ kip} \\ 37.5(12) \text{ kip/in.} \end{Bmatrix} \quad \mathbf{P}_{(1)B}^F = \begin{Bmatrix} 0 \\ 15 \text{ kip} \\ -37.5(12) \text{ kip/in.} \end{Bmatrix} \quad \mathbf{P}_{(2)A}^F = \mathbf{P}_{(2)B}^F = 0$$

Global end actions

$$\begin{aligned} P_{(1)A} &= k_{(1)AB} \begin{Bmatrix} u_2 \\ v_2 \\ \theta_2 \end{Bmatrix} + P_{(1)A}^F = \begin{Bmatrix} 0.86 \text{ kip} \\ 17.24 \text{ kip} \\ 588.4 \text{ kip/in.} \end{Bmatrix} \\ P_{(1)B} &= k_{(1)BB} \begin{Bmatrix} u_2 \\ v_2 \\ \theta_2 \end{Bmatrix} + P_{(1)B}^F = \begin{Bmatrix} -0.86 \text{ kip} \\ 12.76 \text{ kip} \\ -183.4 \text{ kip/in.} \end{Bmatrix} \\ P_{(2)A} &= k_{(2)AB} \begin{Bmatrix} 0 \\ 0 \\ \theta_3 \end{Bmatrix} + k_{(2)AA} \begin{Bmatrix} u_2 \\ v_2 \\ \theta_2 \end{Bmatrix} = \begin{Bmatrix} 10.86 \text{ kip} \\ -12.76 \text{ kip} \\ 183.4 \text{ kip/in.} \end{Bmatrix} \\ P_{(2)B} &= k_{(2)BB} \begin{Bmatrix} 0 \\ 0 \\ \theta_3 \end{Bmatrix} + k_{(2)BA} \begin{Bmatrix} u_2 \\ v_2 \\ \theta_2 \end{Bmatrix} = \begin{Bmatrix} -10.86 \text{ kip} \\ 12.76 \text{ kip} \\ 0.0 \end{Bmatrix} \end{aligned}$$

Local end actions

$$\begin{aligned} \mathbf{P}_{\ell(1)A} &= \begin{Bmatrix} F_{(1)A} \\ V_{(1)A} \\ M_{(1)A} \end{Bmatrix} = R_{g\ell} P_{(1)A} = \begin{bmatrix} 1 & 0 & 0 \\ 0 & 1 & 0 \\ 0 & 0 & 1 \end{bmatrix} \begin{Bmatrix} 0.86 \\ 17.24 \\ 588.4 \end{Bmatrix} = \begin{Bmatrix} 0.86 \text{ kip} \\ 17.24 \text{ kip} \\ 588.4 \text{ kip/in.} \end{Bmatrix} \\ \mathbf{P}_{\ell(1)B} &= \begin{Bmatrix} F_{x(1)B} \\ V_{(1)B} \\ M_{(1)B} \end{Bmatrix} = R_{g\ell} P_{(1)A} = \begin{bmatrix} 1 & 0 & 0 \\ 0 & 1 & 0 \\ 0 & 0 & 1 \end{bmatrix} \begin{Bmatrix} -0.86 \\ 12.76 \\ -213.96 \end{Bmatrix} = \begin{Bmatrix} -0.86 \text{ kip} \\ 12.76 \text{ kip} \\ -183.4 \text{ kip/in.} \end{Bmatrix} \\ \mathbf{P}_{\ell(2)A} &= \begin{Bmatrix} F_{(2)A} \\ V_{(2)A} \\ M_{(2)A} \end{Bmatrix} = \mathbf{R}_{g\ell} \mathbf{P}_{(2)A} = \begin{bmatrix} 0.6 & -0.8 & 0 \\ 0.8 & 0.6 & 0 \\ 0 & 0 & 1 \end{bmatrix} \begin{Bmatrix} 10.86 \\ -12.76 \\ 183.4 \end{Bmatrix} = \begin{Bmatrix} 16.72 \text{ kip} \\ 1.03 \text{ kip} \\ 183.4 \text{ kip/in.} \end{Bmatrix} \\ \mathbf{P}_{\ell(2)B} &= \begin{Bmatrix} F_{(2)B} \\ V_{(2)B} \\ M_{(2)B} \end{Bmatrix} = \mathbf{R}_{g\ell} \mathbf{P}_{(2)B} = \begin{bmatrix} 0.6 & -0.8 & 0 \\ 0.8 & 0.6 & 0 \\ 0 & 0 & 1 \end{bmatrix} \begin{Bmatrix} -10.86 \\ 12.76 \\ 0.0 \end{Bmatrix} = \begin{Bmatrix} -16.72 \text{ kip} \\ -1.03 \text{ kip} \\ 0.0 \end{Bmatrix} \end{aligned}$$

The local member end actions are listed in Fig. E12.7e.

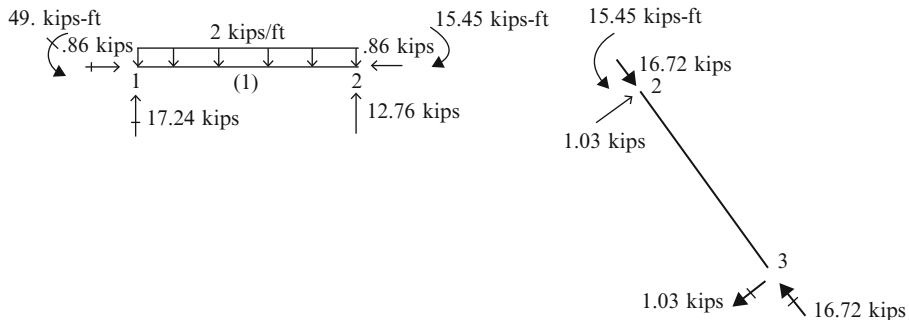


Fig. E12.7e

Example 12.8 Two member plane frame—fully fixed

Given: The frame shown in Fig. E12.8a. E , I , and A are constant for both members. Take $L = 5 \text{ m}$, $I = 70(10)^6 \text{ mm}^4$, $A = 6,500 \text{ mm}^2$, $M = 20 \text{ kN/m}$, and $E = 200 \text{ GPa}$.

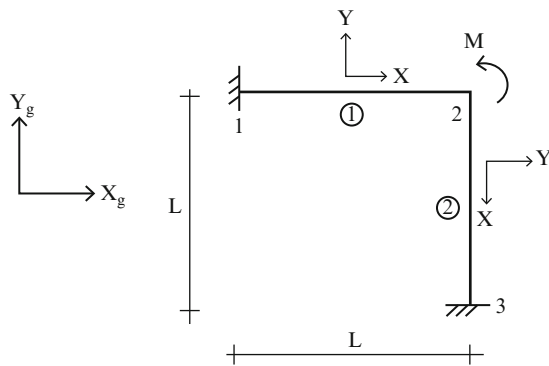


Fig. E12.8a

Determine: The reactions

Solution: We start with the geometric data. The topological and geometric information is listed below

Geometric data:

Member m	n_-	n_+	α
(1)	1	2	0
(2)	2	3	-90°

Member m	α	$\cos \alpha$	$\sin \alpha$	$\sin \alpha \cos \alpha$	$\cos^2 \alpha$	$\sin^2 \alpha$
(1)	0	1	0	0	1	0
(2)	-90°	0	-1	0	0	1

The system stiffness matrix and displacement vector have the following form

$$\begin{aligned}\mathbf{K} &= \begin{bmatrix} \mathbf{k}_{(1)AA} & \mathbf{k}_{(1)AB} & 0 \\ \mathbf{k}_{(1)BA} & \mathbf{k}_{(1)BB} & 0 \\ 0 & 0 & 0 \end{bmatrix} + \begin{bmatrix} 0 & 0 & 0 \\ 0 & \mathbf{k}_{(2)AA} & \mathbf{k}_{(2)AB} \\ 0 & \mathbf{k}_{(2)BA} & \mathbf{k}_{(2)BB} \end{bmatrix} \\ &= \begin{bmatrix} \mathbf{k}_{(1)AA} & \mathbf{k}_{(1)AB} & 0 \\ \mathbf{k}_{(1)BA} & (\mathbf{k}_{(1)BB} + \mathbf{k}_{(2)AA}) & \mathbf{k}_{(2)AB} \\ 0 & \mathbf{k}_{(2)BA} & \mathbf{k}_{(2)BB} \end{bmatrix}\end{aligned}$$

We determine the individual member matrices using (12.16). These matrices are referred to the global reference frame.

$$\mathbf{k}_{(1)AA} = \begin{bmatrix} \frac{AE}{L} & 0 & 0 \\ 0 & \frac{12EI}{L^3} & \frac{6EI}{L^2} \\ 0 & \frac{6EI}{L^2} & \frac{4EI}{L} \end{bmatrix} \quad \mathbf{k}_{(1)AB} = \begin{bmatrix} -\frac{AE}{L} & 0 & 0 \\ 0 & -\frac{12EI}{L^3} & \frac{6EI}{L^2} \\ 0 & -\frac{6EI}{L^2} & \frac{2EI}{L} \end{bmatrix}$$

$$\mathbf{k}_{(1)BA} = \begin{bmatrix} -\frac{AE}{L} & 0 & 0 \\ 0 & -\frac{12EI}{L^3} & -\frac{6EI}{L^2} \\ 0 & \frac{6EI}{L^2} & \frac{2EI}{L} \end{bmatrix} \quad \mathbf{k}_{(1)BB} = \begin{bmatrix} \frac{AE}{L} & 0 & 0 \\ 0 & \frac{12EI}{L^3} & -\frac{6EI}{L^2} \\ 0 & -\frac{6EI}{L^2} & \frac{4EI}{L} \end{bmatrix}$$

$$\mathbf{k}_{(2)AA} = \begin{bmatrix} \frac{12EI}{L^3} & 0 & \frac{6EI}{L^2} \\ 0 & \frac{AE}{L} & 0 \\ \frac{6EI}{L^2} & 0 & \frac{4EI}{L} \end{bmatrix} \quad \mathbf{k}_{(2)AB} = \begin{bmatrix} -\frac{12EI}{L^3} & 0 & \frac{6EI}{L^2} \\ 0 & -\frac{AE}{L} & 0 \\ \frac{6EI}{L^2} & 0 & \frac{2EI}{L} \end{bmatrix}$$

$$\mathbf{k}_{(2)BA} = \begin{bmatrix} -\frac{12EI}{L^3} & 0 & -\frac{6EI}{L^2} \\ 0 & -\frac{AE}{L} & 0 \\ \frac{6EI}{L^2} & 0 & \frac{2EI}{L} \end{bmatrix} \quad \mathbf{k}_{(2)BB} = \begin{bmatrix} \frac{12EI}{L^3} & 0 & \frac{6EI}{L^2} \\ 0 & \frac{AE}{L} & 0 \\ \frac{6EI}{L^2} & 0 & \frac{4EI}{L} \end{bmatrix}$$

Substituting for these matrices, the system stiffness matrix takes the following form using the following values for the parameters $L = 5 \text{ m}$, $I = 70(10)^6 \text{ mm}^4$, $A = 6,500 \text{ mm}^2$, and $E = 200 \text{ GPa}$.

$$\mathbf{K} = \begin{bmatrix} 260 & 0 & 0 & -260 & 0 & 0 & 0 & 0 & 0 \\ 0 & 1.344 & 3.36 \times 10^3 & 0 & -1.344 & 3.36 \times 10^3 & 0 & 0 & 0 \\ 0 & 3.36 \times 10^3 & 1.12 \times 10^7 & 0 & -3.36 \times 10^3 & 5.6 \times 10^6 & 0 & 0 & 0 \\ -260 & 0 & 0 & 261.344 & -1.584 \times 10^{-14} & 3.36 \times 10^3 & -1.344 & 1.584 \times 10^{-14} & 3.36 \times 10^3 \\ 0 & -1.344 & -3.36 \times 10^3 & -1.584 \times 10^{-14} & 261.344 & -3.36 \times 10^3 & 1.584 \times 10^{-14} & -260 & 2.057 \times 10^{-13} \\ 0 & 3.36 \times 10^3 & 5.6 \times 10^6 & 3.36 \times 10^3 & -3.36 \times 10^3 & 2.24 \times 10^7 & -3.36 \times 10^3 & -2.057 \times 10^{-13} & 5.6 \times 10^6 \\ 0 & 0 & 0 & -1.344 & 1.584 \times 10^{-14} & -3.36 \times 10^3 & 1.344 & -1.584 \times 10^{-14} & -3.36 \times 10^3 \\ 0 & 0 & 0 & 1.584 \times 10^{-14} & -260 & -2.057 \times 10^{-13} & -1.584 \times 10^{-14} & 260 & -2.057 \times 10^{-13} \\ 0 & 0 & 0 & 3.36 \times 10^3 & 2.057 \times 10^{-13} & 5.6 \times 10^6 & -3.36 \times 10^3 & -2.057 \times 10^{-13} & 1.12 \times 10^7 \end{bmatrix}$$

We note that nodes 1 and 3 are fully fixed. We rearrange the rows and columns of \mathbf{K} , and the rows of \mathbf{U} , \mathbf{P}_E accordingly. This step leads to the resulting partitioned vectors and matrices listed below (Fig. E12.8b).

$$\mathbf{U}' = \begin{Bmatrix} u_2 \\ v_2 \\ \theta_2 \end{Bmatrix} \quad \mathbf{U}'' = 0 \quad \mathbf{P}''_E = \begin{Bmatrix} R_{x1} \\ R_{y1} \\ M_1 \\ R_{x3} \\ R_{y3} \end{Bmatrix} \quad \mathbf{P}'_E = \begin{Bmatrix} 0 \\ 0 \\ 20(10)^3 \end{Bmatrix} \quad \mathbf{P}'_I = \mathbf{P}''_I = 0$$

$$\mathbf{K}'_{11} = \begin{pmatrix} 261 & -1.584 \times 10^{-14} & 3.36 \times 10^3 \\ -1.584 \times 10^{-14} & 261.344 & -3.36 \times 10^3 \\ 3.36 \times 10^3 & -3.36 \times 10^3 & 2.24 \times 10^7 \end{pmatrix}$$

$$\mathbf{K}'_{21} = \begin{pmatrix} -260 & 0 & 0 \\ 0 & -1.344 & 3.36 \times 10^3 \\ 0 & -3.36 \times 10^3 & 5.6 \times 10^6 \\ -1.344 & 1.584 \times 10^{-14} & -3.36 \times 10^3 \\ 1.584 \times 10^{-14} & -260 & -2.057 \times 10^{-13} \\ 3.36 \times 10^3 & 2.057 \times 10^{-13} & 5.6 \times 10^6 \end{pmatrix}$$

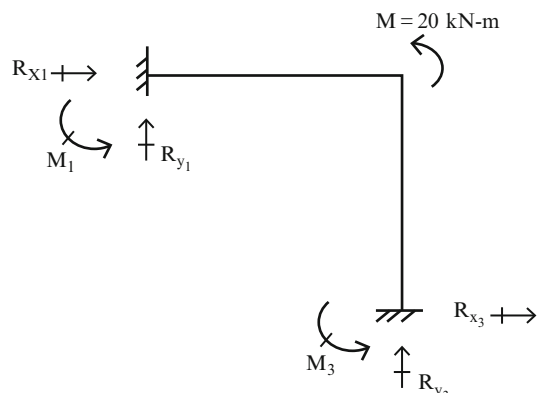


Fig. E12.8b Nodal forces

Then

$$\mathbf{K}'_{11}^{-1} = \begin{pmatrix} 3.834 \times 10^{-3} & -7.408 \times 10^{-6} & -5.762 \times 10^{-7} \\ -7.408 \times 10^{-6} & 3.834 \times 10^{-3} & 5.762 \times 10^{-7} \\ -5.762 \times 10^{-7} & 5.762 \times 10^{-7} & 4.482 \times 10^{-8} \end{pmatrix}$$

Then, we determine the unknown displacements using the following equation

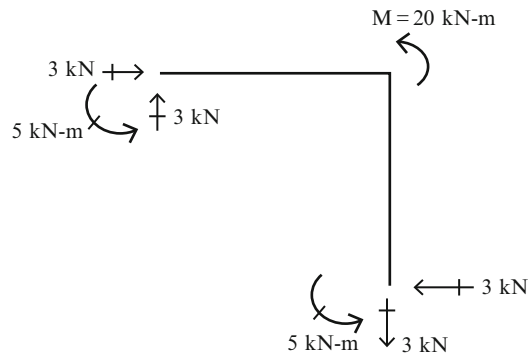
$$\mathbf{U}' = (\mathbf{K}'_{11})^{-1}(\mathbf{P}'_E)$$

Given the displacements, one determines the reactions

$$\mathbf{P}''_E = \mathbf{K}'_{21}\mathbf{U}' = \mathbf{K}'_{21}(\mathbf{K}'_{11})^{-1}(\mathbf{P}'_E) \Rightarrow \begin{Bmatrix} R_{x1} \\ R_{y1} \\ M_1 \\ R_{x3} \\ R_{y3} \end{Bmatrix} = \begin{Bmatrix} 3 \\ 3 \\ 5 \\ -3 \\ -3 \\ 5 \end{Bmatrix}$$

The results are shown on Fig. E12.8c.

Fig. E12.8c



12.7 Specialized Formulation for Beam and Truss Structures

The formulation presented in the previous sections applies for frame type structures which involve both axial and bending actions. Beams and trusses are special cases where only one type of action occurs. Trusses support loads by axial action; beams support transverse loads through bending action. It is relatively easy to specialize the general frame formulation for these limiting cases.

12.7.1 The Steps Involved for Plane Truss Structures

The member end actions for a truss member consist of only an axial force, i.e., there is no shear or moment. Also, each node of a plane truss has only two displacement unknowns; the nodal rotation occurs independent of the translation and has no effect on the member force. We take these simplifications into account by defining “reduced” member force and nodal matrices. The formulation is exactly the same as described in Sects. 12.3 through 12.6. One only has to work with modified stiffness, end action, and nodal displacement matrices.

We start with the member equations. Figure 12.7 shows the member force and displacement measures referred to the local member frame. Note that now, the member matrices are just scalar quantities.

$$\begin{aligned} \mathbf{U}_{\ell B} &= u_{\ell B} & \mathbf{U}_{\ell A} &= u_{\ell A} \\ \mathbf{P}_{\ell A} &= F_{\ell A} & \mathbf{P}_{\ell B} &= F_{\ell B} \end{aligned} \quad (12.28)$$

We consider (12.5) to be the general matrix expression for the member equations but interpret the various terms as “reduced” matrices. Their form follows by deleting the second and third row and column of the matrices listed in (12.6).

$$\begin{aligned} \mathbf{k}_{\ell BB} &= \frac{AE}{L} & \mathbf{k}_{\ell BA} &= -\frac{AE}{L} \\ \mathbf{k}_{\ell BA} &= -\frac{AE}{L} & \mathbf{k}_{\ell AA} &= \frac{AE}{L} \\ \mathbf{P}_{\ell B}^F &= F_{\ell B}^F & \mathbf{P}_{\ell A}^F &= F_{\ell A}^F \end{aligned} \quad (12.29)$$

We need to modify the rotation matrix in a similar way. Now, there are two nodal displacement measures and only one local displacement measure.

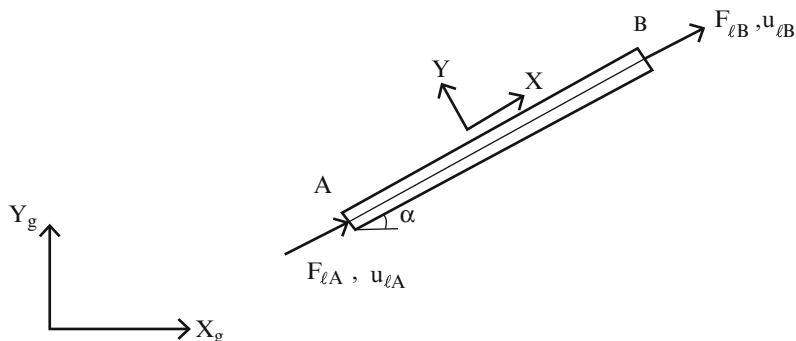


Fig. 12.7 End force and end displacement—local member truss—planar behavior

$$\mathbf{U} = \begin{Bmatrix} u \\ v \end{Bmatrix} \quad (12.30)$$

$$\mathbf{U}_\ell = u_\ell$$

Noting (12.8), we write

$$\mathbf{U} = \mathbf{R}_{\ell g} u_\ell$$

$$\mathbf{R}_{\ell g} = \begin{Bmatrix} \cos \alpha \\ \sin \alpha \end{Bmatrix} \quad (12.31)$$

We use this form for $\mathbf{R}_{\ell g}$ to transform between the local and global frames.

Given $\mathbf{R}_{\ell g}$, we generate the global form of the member matrices using (12.13). A typical term is

$$\mathbf{k} = \mathbf{R}_{\ell g} \mathbf{k}_l (\mathbf{R}_{\ell g})^T \quad (12.32)$$

where \mathbf{k}_l is defined by (12.29). Expanding (12.32) leads to

$$\mathbf{k}_{AA} = \mathbf{k}_{BB} = \mathbf{k} = \left(\frac{AE}{L} \right) \begin{bmatrix} \cos^2 \alpha & \sin \alpha \cos \alpha \\ \sin \alpha \cos \alpha & \sin^2 \alpha \end{bmatrix} \quad (12.33)$$

$$\mathbf{k}_{AB} = \mathbf{k}_{BA} = -\mathbf{k} = -\left(\frac{AE}{L} \right) \begin{bmatrix} \cos^2 \alpha & \sin \alpha \cos \alpha \\ \sin \alpha \cos \alpha & \sin^2 \alpha \end{bmatrix}$$

Noting (12.33), we observe that now \mathbf{k} is of order of (2×2) for a plane truss vs. (3×3) for a plane frame.

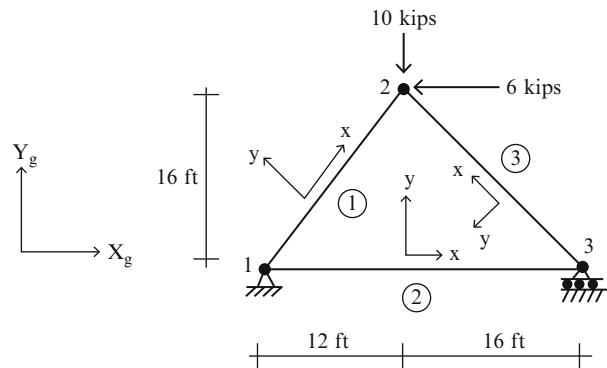
Lastly, we determine the end member forces for member m in the local frame.

$$F_{\ell_{(m)} B} = \left(\frac{AE}{L} \right)_{(m)} [\cos \alpha_{(m)} \sin \alpha_{(m)}] (\mathbf{U}_{n^+} - \mathbf{U}_{n^-}) + F_{\ell_{(m)} B}^F \quad (12.34)$$

$$F_{\ell_{(m)} A} = -\left(\frac{AE}{L} \right)_{(m)} [\cos \alpha_{(m)} \sin \alpha_{(m)}] (\mathbf{U}_{n^+} - \mathbf{U}_{n^-}) + F_{\ell_{(m)} A}^F$$

Example 12.9 Statically determine truss

Given: The truss shown in Fig. E12.9a.

Fig. E12.9a

Determine: The joint displacements, reactions, and member forces using the Displacement Method. $A_{(1)} = A_{(2)} = A_{(3)} = A = 2 \text{ in.}^2$, $\alpha = 6.5 \times 10^{-6}/^\circ\text{F}$, and $E = 29,000 \text{ ksi}$.

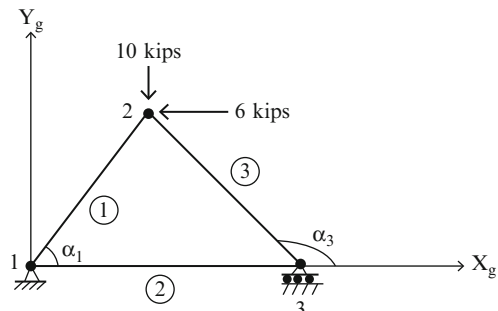
(a) Due to the loading shown

(b) Due to temperature decrease of 40°F for all members.

Solution: We start with the geometric data. The topological and geometric information is listed below

Member m	n_-	n_+	α	L (ft)	$\frac{\Delta E}{E}$ (kip/in.)
(1)	1	2	53.13	20	241.7
(2)	1	3	0	28	172.6
(3)	3	2	135	22.63	213.6

Member m	$\alpha_{(m)}$	$\sin \alpha$	$\cos \alpha$	$\sin \alpha \cos \alpha$	$\sin \alpha^2$	$\cos \alpha^2$
(1)	53.13	0.8	0.6	0.48	0.64	0.36
(2)	0	0	1	0	0	1
(3)	135	-0.707	0.707	-0.5	0.5	0.5

**Fig. E12.9b**

We determine the individual member matrices using (12.33).

$$\mathbf{k}_{(m)AA} = \mathbf{k}_{(m)BB} = \mathbf{k}_{(m)} = \left(\frac{AE}{L}\right)_{(m)} \begin{bmatrix} \cos^2\alpha_{(m)} & \sin\alpha_{(m)} \cos\alpha_{(m)} \\ \sin\alpha_{(m)} \cos\alpha_{(m)} & \sin^2\alpha_{(m)} \end{bmatrix}$$

$$\mathbf{k}_{(m)AB} = \mathbf{k}_{(m)BA} = -\mathbf{k}_{(m)} = -\left(\frac{AE}{L}\right)_{(m)} \begin{bmatrix} \cos^2\alpha_{(m)} & \sin\alpha_{(m)} \cos\alpha_{(m)} \\ \sin\alpha_{(m)} \cos\alpha_{(m)} & \sin^2\alpha_{(m)} \end{bmatrix}$$

The system stiffness matrix and displacement vector have the following form

$$\mathbf{K} = \begin{bmatrix} \mathbf{k}_{(1)AA} & \mathbf{k}_{(1)AB} & 0 \\ \mathbf{k}_{(1)BA} & \mathbf{k}_{(1)BB} & 0 \\ 0 & 0 & 0 \end{bmatrix} + \begin{bmatrix} \mathbf{k}_{(2)AA} & 0 & \mathbf{k}_{(2)AB} \\ 0 & 0 & 0 \\ \mathbf{k}_{(2)BA} & 0 & \mathbf{k}_{(2)BB} \end{bmatrix} \begin{bmatrix} 0 & 0 & 0 \\ 0 & \mathbf{k}_{(3)AA} & \mathbf{k}_{(3)AB} \\ 0 & \mathbf{k}_{(3)BA} & \mathbf{k}_{(3)BB} \end{bmatrix}$$

$$= \begin{bmatrix} (\mathbf{k}_{(1)AA} + \mathbf{k}_{(2)AA}) & \mathbf{k}_{(1)AB} & \mathbf{k}_{(2)AB} \\ \mathbf{k}_{(1)BA} & (\mathbf{k}_{(1)BB} + \mathbf{k}_{(3)AA}) & \mathbf{k}_{(3)AB} \\ \mathbf{k}_{(2)BA} & \mathbf{k}_{(3)BA} & (\mathbf{k}_{(2)BB} + \mathbf{k}_{(3)BB}) \end{bmatrix}$$

$$\mathbf{U} = \begin{Bmatrix} \mathbf{U}_1 \\ \mathbf{U}_2 \\ \mathbf{U}_3 \end{Bmatrix} = \begin{Bmatrix} u_1 \\ v_1 \\ u_2 \\ v_2 \\ u_3 \\ v_3 \end{Bmatrix}$$

By Substituting for individual matrices using (12.33), the system stiffness matrix takes the following form:

$$\mathbf{K} = \begin{pmatrix} 259.619 & 116 & -87 & -116 & -172.619 & 0 \\ 116 & 154.666 & -116 & -154.666 & 0 & 0 \\ -87 & -116 & 193.791 & 9.21 & -106.79 & 106.79 \\ -116 & -154.666 & 9.21 & 261.457 & 106.79 & -106.79 \\ -172.619 & 0 & -106.79 & -106.79 & 279.409 & -106.79 \\ 0 & 0 & 106.79 & 106.79 & -106.79 & 106.79 \end{pmatrix}$$

We note that node 1 is fully fixed but node 3 is partially fixed. We rearrange the rows and columns of \mathbf{K} , and the rows of \mathbf{U} . This step leads to the resulting partitioned vectors and matrices listed below.

$$\mathbf{U}' = \begin{Bmatrix} u_2 \\ v_2 \\ u_3 \end{Bmatrix} \quad \mathbf{U}'' = \begin{Bmatrix} u_1 \\ v_1 \\ v_3 \end{Bmatrix}$$

$$\mathbf{K}'_{11} = \begin{pmatrix} 193.791 & 9.21 & -106.79 \\ 9.21 & 261.457 & 106.79 \\ -106.79 & 106.79 & 279.409 \end{pmatrix} \quad \mathbf{K}'_{12} = \begin{pmatrix} -87 & -116 & 106.79 \\ -116 & -154.666 & -106.79 \\ 0 & 0 & -106.79 \end{pmatrix}$$

$$\mathbf{K}'_{21} = \begin{pmatrix} -87 & -116 & -172.619 \\ -116 & -154.666 & 0 \\ 106.79 & -106.79 & -106.79 \end{pmatrix} \quad \mathbf{K}'_{22} = \begin{pmatrix} 259.619 & 116 & 0 \\ 116 & 154.666 & 0 \\ 0 & 0 & 106.79 \end{pmatrix}$$

We need the inverse of \mathbf{K}'_{11} to solve for the displacement due to a given loading. Its form is

$$(\mathbf{K}'_{21})^{-1} = \begin{pmatrix} 0.007 & -0.002 & 0.003 \\ -0.002 & 0.005 & -0.002 \\ 0.003 & -0.002 & 0.006 \end{pmatrix}$$

Part (a): Loading shown in Fig. E12.9a

The system load vectors corresponding to this loading are

$$\mathbf{P}'_E = \begin{Bmatrix} -6 \\ -10 \\ 0 \end{Bmatrix} \quad \mathbf{P}'_I = \mathbf{P}''_I = 0$$

We determine the unknown displacements using

$$\mathbf{U}' = (\mathbf{K}'_{11})^{-1}(\mathbf{P}'_E) \quad \Rightarrow \quad \begin{Bmatrix} u_2 \\ v_2 \\ u_3 \end{Bmatrix} = (\mathbf{K}'_{11})^{-1}(\mathbf{P}'_E) = \begin{Bmatrix} -0.026 \\ -0.039 \\ 0.005 \end{Bmatrix}$$

Given the displacements, one determines the reactions with

$$\mathbf{P}''_E = \mathbf{K}'_{21}\mathbf{U}' \quad \Rightarrow \quad \begin{Bmatrix} R_{1x} \\ R_{1y} \\ R_{3y} \end{Bmatrix} = \mathbf{K}'_{21}\mathbf{U}' = \begin{Bmatrix} 6 \\ 9.14 \\ 0.86 \end{Bmatrix}$$

Finally we determine member forces:

$$F_{\ell_{(m)}B} = \left(\frac{AE}{L} \right)_{(m)} [\cos \alpha_{(m)} \sin \alpha_{(m)}] (\mathbf{U}_{n^+} - \mathbf{U}_{n^-}) + F_{\ell_{(m)}B}^F$$

$$F_{\ell_{(1)}B} = -11.43 \text{ kip}$$

$$F_{\ell_{(2)}B} = 0.86 \text{ kip}$$

$$F_{\ell_{(3)}B} = -1.21 \text{ kip}$$

Part (b): $\Delta T = -40^\circ$ for all members

We determine the fixed end actions caused by the temperature decrease (Figs. E12.9c and E12.9d).

$$F_l^F = EA\alpha \Delta T = (29,000)(2)(6.5 \times 10^{-6})(40) = 15.08 \text{ kip}$$

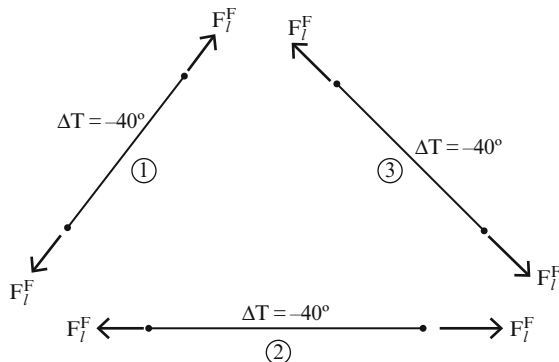


Fig. E12.9c Fixed end actions—members

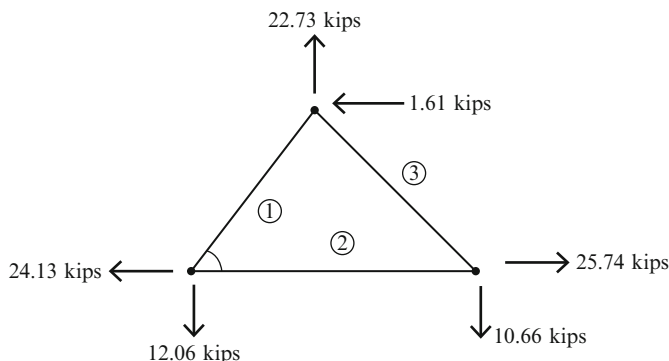


Fig. E12.9d Fixed end actions—joints

The system load vectors corresponding to these loads are

$$\mathbf{P}'_E = 0 \quad \mathbf{P}'_I = \begin{Bmatrix} -1.61 \\ 22.73 \\ 25.74 \end{Bmatrix} \quad \mathbf{P}''_I = \begin{Bmatrix} -24.13 \\ -12.06 \\ -10.66 \end{Bmatrix}$$

We determine the unknown displacements using

$$\mathbf{U}' = (\mathbf{K}'_{11})^{-1}(-\mathbf{P}'_1) \Rightarrow$$

$$\begin{Bmatrix} u_2 \\ v_2 \\ u_3 \end{Bmatrix} = (\mathbf{K}'_{11})^{-1}(-\mathbf{P}'_1) = \begin{Bmatrix} -0.037 \text{ in.} \\ -0.05 \text{ in.} \\ -0.087 \text{ in.} \end{Bmatrix} \Rightarrow \begin{Bmatrix} u_2 \\ v_2 \\ u_3 \end{Bmatrix} = \begin{Bmatrix} 0.037 \text{ in. } \leftarrow \\ 0.05 \text{ in. } \downarrow \\ 0.087 \text{ in. } \leftarrow \end{Bmatrix}$$

Given the displacements, one determines the reactions. For a determinate truss the reactions will be zero. Also the member forces will be zero.

$$\mathbf{P}''_E = \mathbf{K}'_{21}\mathbf{U}' + \mathbf{P}''_I \Rightarrow \begin{Bmatrix} R_{1x} \\ R_{1y} \\ R_{3y} \end{Bmatrix} = \mathbf{K}'_{21}\mathbf{U}' + \mathbf{P}''_I = \begin{Bmatrix} 0 \\ 0 \\ 0 \end{Bmatrix}$$

$$F_{\ell_{(m)}B} = \left(\frac{AE}{L}\right)_{(m)} [\cos \alpha_{(m)} \sin \alpha_{(m)}] (\mathbf{U}_{n^+} - \mathbf{U}_{n^-}) + F_{\ell_{(m)}B}^F$$

$$F_{\ell_{(1)}B} = F_{\ell_{(2)}B} = F_{\ell_{(3)}B} = 0$$

12.7.2 The Steps Involved for Beam Structures with Transverse Loading

The member forces for a beam member subjected to transverse loading consist only of shear and moment, i.e., there is no axial force. Also, each node of a beam has only *two displacement unknowns; the rotation and transverse displacement*. We take these simplifications into account by defining “reduced” member and nodal matrices. The procedure is similar to that followed for the trusses.

We start with the member equations. Figure 12.8 shows the member force and displacement measures. For beam structures, the local and global frames are taken to be the same. The “reduced” displacement and end action matrices are

$$\begin{aligned} \mathbf{U}_{\ell B} &= \begin{Bmatrix} v_{\ell B} \\ \theta_B \end{Bmatrix} & \mathbf{U}_{\ell A} &= \begin{Bmatrix} v_{\ell A} \\ \theta_A \end{Bmatrix} \\ \mathbf{P}_{\ell B} &= \begin{Bmatrix} V_{\ell B} \\ M_B \end{Bmatrix} & \mathbf{P}_{\ell A} &= \begin{Bmatrix} V_{\ell A} \\ M_A \end{Bmatrix} \end{aligned} \quad (12.35)$$

We obtain the “reduced” member stiffness matrices by deleting the first row and column of the matrices listed in (12.6).

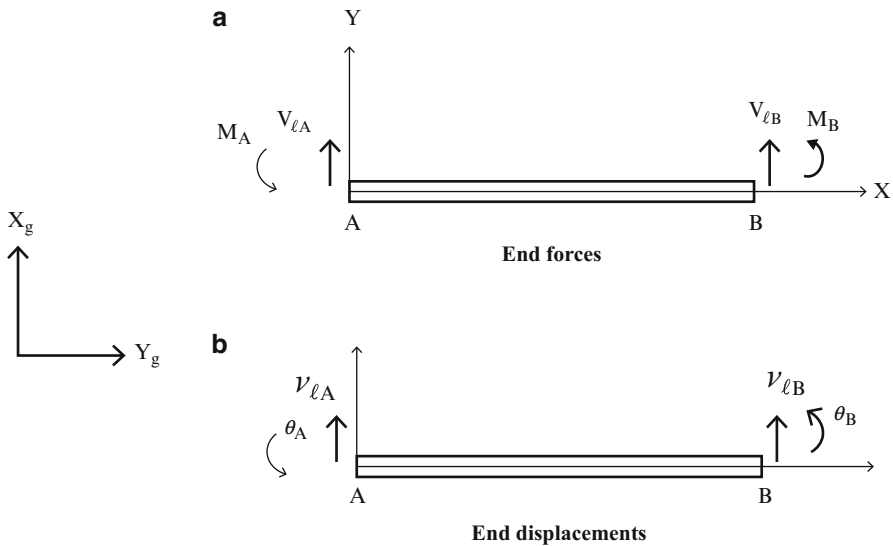


Fig. 12.8 Member end forces and displacements

$$\begin{aligned}
 \mathbf{k}_{BB} &= \begin{bmatrix} \frac{12EI}{L^3} & -\frac{6EI}{L^2} \\ -\frac{6EI}{L^2} & \frac{4EI}{L} \end{bmatrix} & \mathbf{k}_{BA} &= \begin{bmatrix} -\frac{12EI}{L^3} & -\frac{6EI}{L^2} \\ \frac{6EI}{L^2} & \frac{2EI}{L} \end{bmatrix} \\
 \mathbf{k}_{AA} &= \begin{bmatrix} \frac{12EI}{L^3} & \frac{6EI}{L^2} \\ \frac{6EI}{L^2} & \frac{4EI}{L} \end{bmatrix} & \mathbf{k}_{AB} &= \begin{bmatrix} -\frac{12EI}{L^3} & \frac{6EI}{L^2} \\ -\frac{6EI}{L^2} & \frac{2EI}{L} \end{bmatrix}
 \end{aligned} \tag{12.36}$$

The remaining steps involved in assembling the system matrices and introducing the support fixity are the *same* as described earlier for the general frame. Note that no rotation transformations are required here since the local and global frames coincide.

$$\mathbf{P}_{\ell B} = \mathbf{k}_{\ell BB} \mathbf{U}_{\ell B} + \mathbf{k}_{\ell BA} \mathbf{U}_{\ell A} + \mathbf{P}_{\ell B}^F$$

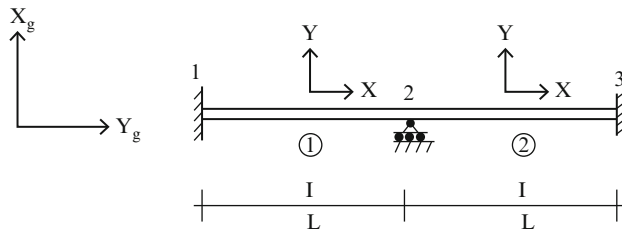
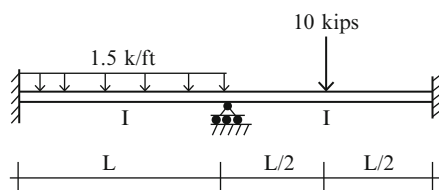
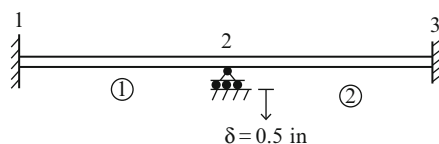
$$\mathbf{P}_{\ell A} = \mathbf{k}_{\ell AB} \mathbf{U}_{\ell B} + \mathbf{k}_{\ell AA} \mathbf{U}_{\ell A} + \mathbf{P}_{\ell A}^F$$

Example 12.10 Two-span beam

Given: The beam shown in Fig. E12.10a. The properties are taken as

$$L_{(1)} = L_{(2)} = L = 20 \text{ ft}, I_{(1)} = I_{(2)} = I = 428 \text{ in.}^4, E = 29,000 \text{ ksi}$$

Determine: The joint displacements and member forces due to (i) the loading in Fig. E12.10b, (ii) support settlement in Fig. E12.10c.

**Fig. E12.10a****Fig. E12.10b****Fig. E12.10c****Solution:**

We start with the geometric data listed below

Member	n_-	n_-
(1)	1	2
(2)	2	3

The system stiffness matrix has the following form.

$$\begin{aligned} \mathbf{K} &= \begin{bmatrix} \mathbf{k}_{(1)AA} & \mathbf{k}_{(1)AB} & 0 \\ \mathbf{k}_{(1)BA} & \mathbf{k}_{(1)BB} & 0 \\ 0 & 0 & 0 \end{bmatrix} + \begin{bmatrix} 0 & 0 & 0 \\ 0 & \mathbf{k}_{(2)AA} & \mathbf{k}_{(2)AB} \\ 0 & \mathbf{k}_{(2)BA} & \mathbf{k}_{(2)BB} \end{bmatrix} \\ &= \begin{bmatrix} \mathbf{k}_{(1)AA} & \mathbf{k}_{(1)AB} & 0 \\ \mathbf{k}_{(1)BA} & (\mathbf{k}_{(1)BB} + \mathbf{k}_{(2)AA}) & \mathbf{k}_{(2)AB} \\ 0 & \mathbf{k}_{(2)BA} & \mathbf{k}_{(2)BB} \end{bmatrix} \end{aligned}$$

The member stiffness matrices follow from (12.36). Since the lengths and cross-sectional properties are equal, the corresponding matrices are equal.

$$\mathbf{k}_{(1)BB} = \mathbf{k}_{(2)BB} = \begin{bmatrix} \frac{12EI}{L^3} & -\frac{6EI}{L^2} \\ -\frac{6EI}{L^2} & \frac{4EI}{L} \end{bmatrix} \quad \mathbf{k}_{(1)BA} = \mathbf{k}_{(2)BA} = \begin{bmatrix} -\frac{12EI}{L^3} & -\frac{6EI}{L^2} \\ \frac{6EI}{L^2} & \frac{2EI}{L} \end{bmatrix}$$

$$\mathbf{k}_{(1)AA} = \mathbf{k}_{(2)AA} = \begin{bmatrix} \frac{12EI}{L^3} & \frac{6EI}{L^2} \\ \frac{6EI}{L^2} & \frac{4EI}{L} \end{bmatrix} \quad \mathbf{k}_{(1)AB} = \mathbf{k}_{(2)AB} = \begin{bmatrix} -\frac{12EI}{L^3} & \frac{6EI}{L^2} \\ -\frac{6EI}{L^2} & \frac{2EI}{L} \end{bmatrix}$$

Substituting for the member matrices, the system matrix expand to:

$$\mathbf{K} = \begin{pmatrix} \frac{12EI}{L^3} & \frac{6EI}{L^2} & -\frac{12EI}{L^3} & \frac{6EI}{L^2} & 0 & 0 \\ \frac{6EI}{L^2} & \frac{4EI}{L} & -\frac{6EI}{L^2} & \frac{2EI}{L} & 0 & 0 \\ -\frac{12EI}{L^3} & -\frac{6EI}{L^2} & \frac{24EI}{L^3} & 0 & -\frac{12EI}{L^3} & \frac{6EI}{L^2} \\ \frac{6EI}{L^2} & \frac{2EI}{L} & 0 & \frac{8EI}{L} & -\frac{6EI}{L^2} & \frac{2EI}{L} \\ 0 & 0 & -\frac{12EI}{L^3} & -\frac{6EI}{L^2} & \frac{12EI}{L^3} & -\frac{6EI}{L^2} \\ 0 & 0 & \frac{6EI}{L^2} & \frac{2EI}{L} & -\frac{6EI}{L^2} & \frac{4EI}{L} \end{pmatrix}$$

The system nodal displacement and nodal load terms follow from (12.19).

$$\mathbf{U} = \begin{Bmatrix} v_1 \\ \theta_1 \\ v_2 \\ \theta_2 \\ v_3 \\ \theta_3 \end{Bmatrix} \quad \mathbf{P}_E = \begin{Bmatrix} R_{y1} \\ M_1 \\ R_{y2} \\ M_2 \\ R_{y3} \\ M_3 \end{Bmatrix} \quad \mathbf{P''}_I = \begin{Bmatrix} V_{(1)A}^F \\ M_{(1)A}^F \\ (V_{(1)B}^F + V_{(2)A}^F) \\ (M_{(1)B}^F + M_{(2)A}^F) \\ V_{(2)B}^F \\ M_{(2)B}^F \end{Bmatrix}$$

Nodes 1 and 3 are fully fixed and node 2 is partially fixed. The only unknown displacement is θ_2 . We rearrange the rows and columns according to the systematic approach described in Sect. 12.6.1. Noting (12.23) and (12.24), the rearranged terms are

$$\mathbf{U}' = \{\theta_2\} \quad \mathbf{U}'' = \begin{Bmatrix} v_1 \\ \theta_1 \\ v_2 \\ v_3 \\ \theta_3 \end{Bmatrix}$$

and

$$\mathbf{P}'_E = \{M_2\} \quad \mathbf{P}''_E = \begin{Bmatrix} R_{y1} \\ M_1 \\ R_{y2} \\ R_{y3} \\ M_3 \end{Bmatrix}$$

$$\mathbf{P}'_I = \left\{ (M_{(1)B}^F + M_{(2)A}^F) \right\} \quad \mathbf{P}'' = \begin{Bmatrix} V_{(1)A}^F \\ M_{(1)A}^F \\ (V_{(1)B}^F + V_{(2)A}^F) \\ V_{(2)B}^F \\ M_{(2)B}^F \end{Bmatrix}$$

$$\mathbf{K}' = \left(\begin{array}{c|ccccc} \frac{8EI}{L} & \frac{6EI}{L^2} & \frac{2EI}{L} & 0 & \frac{-6EI}{L^2} & \frac{2EI}{L} \\ \hline \frac{6EI}{L^2} & \frac{12EI}{L^3} & \frac{6EI}{L^2} & \frac{-12EI}{L^3} & 0 & 0 \\ \frac{2EI}{L} & \frac{6EI}{L^2} & \frac{4EI}{L} & \frac{-6EI}{L^2} & 0 & 0 \\ 0 & \frac{-12EI}{L^3} & \frac{-6EI}{L^2} & \frac{24EI}{L^3} & \frac{-12EI}{L^3} & \frac{6EI}{L^2} \\ \frac{-6EI}{L^2} & 0 & 0 & \frac{-12EI}{L^3} & \frac{12EI}{L^3} & \frac{6EI}{L^2} \\ \frac{2EI}{L} & 0 & 0 & \frac{6EI}{L^2} & \frac{-6EI}{L^2} & \frac{4EI}{L} \end{array} \right)$$

$$\mathbf{K}'_{11} = \left\{ \frac{8EI}{L} \right\} \quad \mathbf{K}'_{12} = \left\{ \frac{6EI}{L^2} \quad \frac{2EI}{L} \quad 0 \quad \frac{-6EI}{L^2} \quad \frac{2EI}{L} \right\}$$

$$\mathbf{K}'_{21} = \left\{ \begin{array}{l} \frac{6EI}{L^2} \\ \frac{2EI}{L} \\ 0 \\ \frac{-6EI}{L^2} \\ \frac{2EI}{L} \end{array} \right\} \quad \mathbf{K}'_{22} = \left[\begin{array}{ccccc} \frac{12EI}{L^3} & \frac{6EI}{L^2} & \frac{-12EI}{L^3} & 0 & 0 \\ \frac{6EI}{L^2} & \frac{4EI}{L} & \frac{-6EI}{L^2} & 0 & 0 \\ \frac{-12EI}{L^3} & \frac{-6EI}{L^2} & \frac{24EI}{L^3} & \frac{-12EI}{L^3} & \frac{6EI}{L^2} \\ 0 & 0 & \frac{-12EI}{L^3} & \frac{12EI}{L^3} & \frac{-6EI}{L^2} \\ 0 & 0 & \frac{6EI}{L^2} & \frac{-6EI}{L^2} & \frac{4EI}{L} \end{array} \right]$$

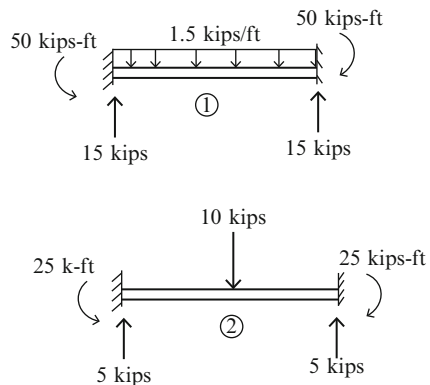
The inverse of \mathbf{K}'_{11} is

$$(\mathbf{K}'_{11})^{-1} = \frac{L}{8EI} = \frac{20(12)}{8(29,000)(428)} = 2.417(10^{-6})$$

(i) *Loading:*

We consider the loading shown in Fig. E12.10b. The fixed end actions due to the loading applied to members 1 and 2 are defined in Fig. E12.10d.

Fig. E12.10d



Substituting for the fixed end actions, the various nodal displacement and load terms reduce to

$$\mathbf{U}' = \{\theta_2\} \quad \mathbf{U}'' = 0 \text{ (No support movement)}$$

$$\mathbf{P}'_E = \{0\} \quad \mathbf{P}'_I = \{(-50 + 25)\} = \{-25\} \quad \mathbf{P}''_I = \begin{Bmatrix} 15.0 \\ 50.0 \\ (15.0 + 5.0) \\ 5.0 \\ -25.0 \end{Bmatrix}$$

The unknown displacement is determined with (12.26) specialized for this example

$$\mathbf{U}' = (\mathbf{K}'_{11})^{-1}(\mathbf{P}'_E - \mathbf{K}'_{12}\mathbf{U}'' - \mathbf{P}'_I)$$

↓

$$\mathbf{U}' = (\mathbf{K}'_{11})^{-1}(-\mathbf{P}'_I)$$

↓

$$\theta_2 = \left(\frac{L}{8EI} \right) (25.0 \text{ kip/ft}) = \frac{3.125 L}{EI} = \frac{3.125(20)(12)}{29,000(428)} = 0.0000604 \text{ rad}$$

Given the displacement, one determines the reactions with the second equation in (12.25):

$$\mathbf{P}''_E = \mathbf{K}'_{21}\mathbf{U}' + \mathbf{K}'_{22}\mathbf{U}'' + \mathbf{P}''_I$$

↓

$$\mathbf{P}''_E = \mathbf{K}'_{21}\mathbf{U}' + \mathbf{P}''_I$$

↓

$$\begin{Bmatrix} R_{y1} \\ M_{1-} \\ R_{y2} \\ R_{y3} \\ M_3 \end{Bmatrix} = \begin{Bmatrix} \frac{6EI}{L^2} \\ \frac{2EI}{L} \\ 0 \\ -\frac{6EI}{L^2} \\ \frac{2EI}{L} \end{Bmatrix} \left(\frac{3.125L}{EI} \right) + \begin{Bmatrix} 15.0 \\ 50.0 \\ 20.0 \\ 5.0 \\ -25.0 \end{Bmatrix} = \begin{Bmatrix} 15.94 \\ 56.25 \\ 20.0 \\ 4.06 \\ -18.75 \end{Bmatrix}$$

The reactions are listed on Fig. E12.10e.

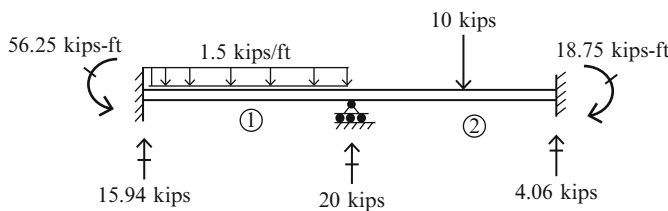


Fig. E12.10e

Lastly, we compute the member end actions.

$$\begin{aligned} \mathbf{P}_{(1)A} &= \begin{Bmatrix} V_{(1)A} \\ M_{(1)A} \end{Bmatrix} = \mathbf{k}_{(1)AB} \begin{Bmatrix} v_2 \\ \theta_2 \end{Bmatrix} + \begin{Bmatrix} V_{(1)A}^F \\ M_{(1)A}^F \end{Bmatrix} \\ &= \begin{bmatrix} -\frac{12EI}{L^3} & \frac{6EI}{L^2} \\ -\frac{6EI}{L^2} & \frac{2EI}{L} \end{bmatrix} \left\{ \frac{3.125L}{EI} \right\} + \begin{Bmatrix} 15.0 \\ 50.0 \end{Bmatrix} = \begin{Bmatrix} 15.94 \\ 56.25 \end{Bmatrix} \end{aligned}$$

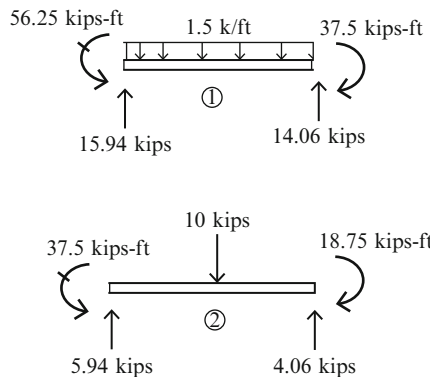
$$\begin{aligned} \mathbf{P}_{(1)B} &= \begin{Bmatrix} V_{(1)B} \\ M_{(1)B} \end{Bmatrix} = \mathbf{k}_{(1)BB} \begin{Bmatrix} v_2 \\ \theta_2 \end{Bmatrix} + \begin{Bmatrix} V_{(1)B}^F \\ M_{(1)B}^F \end{Bmatrix} \\ &= \begin{bmatrix} \frac{12EI}{L^3} & -\frac{6EI}{L^2} \\ -\frac{6EI}{L^2} & \frac{4EI}{L} \end{bmatrix} \left\{ \frac{3.125L}{EI} \right\} + \begin{Bmatrix} 15.0 \\ -50.0 \end{Bmatrix} = \begin{Bmatrix} 14.06 \\ -37.50 \end{Bmatrix} \end{aligned}$$

$$\begin{aligned}\mathbf{P}_{(2)A} &= \begin{Bmatrix} V_{(2)A} \\ M_{(2)A} \end{Bmatrix} = \mathbf{k}_{(2)AA} \begin{Bmatrix} v_2 \\ \theta_2 \end{Bmatrix} + \begin{Bmatrix} V_{(2)A}^F \\ M_{(2)A}^F \end{Bmatrix} \\ &= \begin{bmatrix} \frac{12EI}{L^3} & \frac{6EI}{L^2} \\ \frac{6EI}{L^2} & \frac{4EI}{L} \end{bmatrix} \begin{Bmatrix} 0 \\ \frac{3.125L}{EI} \end{Bmatrix} + \begin{Bmatrix} 5.0 \\ 25.0 \end{Bmatrix} = \begin{Bmatrix} 5.94 \\ 37.50 \end{Bmatrix}\end{aligned}$$

$$\begin{aligned}\mathbf{P}_{(2)B} &= \begin{Bmatrix} V_{(2)B} \\ M_{(2)B} \end{Bmatrix} = k_{(1)BA} \begin{Bmatrix} v_2 \\ \theta_2 \end{Bmatrix} + \begin{Bmatrix} V_{(2)B}^F \\ M_{(2)B}^F \end{Bmatrix} \\ &= \begin{bmatrix} -\frac{12EI}{L^3} & -\frac{6EI}{L^2} \\ \frac{6EI}{L^2} & \frac{2EI}{L} \end{bmatrix} \begin{Bmatrix} 0 \\ \frac{3.125L}{EI} \end{Bmatrix} + \begin{Bmatrix} 5.0 \\ -25.0 \end{Bmatrix} = \begin{Bmatrix} 4.06 \\ -18.75 \end{Bmatrix}\end{aligned}$$

The results are summarized on the following figure (Fig. E12.10f).

Fig. E12.10f



(ii) *Support Settlement:*

We consider a support settlement of $\delta = 0.5$ in. \downarrow at joint 2. The corresponding loading terms are

$$\mathbf{U}' = \{\theta_2\} \quad \mathbf{U}'' = \begin{Bmatrix} v_1 \\ \theta_1 \\ v_2 \\ v_3 \\ \theta_3 \end{Bmatrix} = \begin{Bmatrix} 0 \\ 0 \\ \delta \\ 0 \\ 0 \end{Bmatrix} \quad \mathbf{P}'_E = \{0\} \quad \mathbf{P}'_I = 0 \quad \mathbf{P}''_I = 0$$

Then noting (12.26),

$$\mathbf{U}' = (\mathbf{K}'_{11})^{-1}(-\mathbf{K}'_{12}\mathbf{U}'')$$

↓

$$\theta_2 = -\frac{L}{8EI} \begin{Bmatrix} \frac{6EI}{L^2} & \frac{2EI}{L} & 0 & -\frac{6EI}{L^2} & \frac{2EI}{L} \end{Bmatrix} \begin{Bmatrix} 0 \\ 0 \\ \delta \\ 0 \\ 0 \end{Bmatrix} = 0.0$$

We evaluate the reactions with (12.25). In this case $\mathbf{U}' = 0$.

$$\mathbf{P}''_E = \mathbf{K}'_{22}\mathbf{U}''$$

↓

$$\begin{Bmatrix} R_{y1} \\ M_1 \\ R_{y2} \\ R_{y3} \\ M_3 \end{Bmatrix} = \begin{bmatrix} \frac{12EI}{L^3} & \frac{6EI}{L^2} & -\frac{12EI}{L^3} & 0 & 0 \\ \frac{6EI}{L^2} & \frac{4EI}{L} & -\frac{6EI}{L^2} & 0 & 0 \\ -\frac{12EI}{L^3} & -\frac{6EI}{L^2} & \frac{24EI}{L^3} & -\frac{12EI}{L^3} & \frac{6EI}{L^2} \\ 0 & 0 & -\frac{12EI}{L^3} & \frac{12EI}{L^3} & -\frac{6EI}{L^2} \\ 0 & 0 & \frac{6EI}{L^2} & -\frac{6EI}{L^2} & \frac{4EI}{L} \end{bmatrix} \begin{Bmatrix} 0 \\ 0 \\ \delta \\ 0 \\ 0 \end{Bmatrix} = \begin{Bmatrix} -\frac{12EI}{L^3}\delta \\ -\frac{6EI}{L^2}\delta \\ \frac{24EI}{L^3}\delta \\ -\frac{12EI}{L^3}\delta \\ \frac{6EI}{L^2}\delta \end{Bmatrix}$$

Using the given properties and taking $\delta = -0.5$ in. results in the forces shown below (Figs. E12.10g and E12.10h).

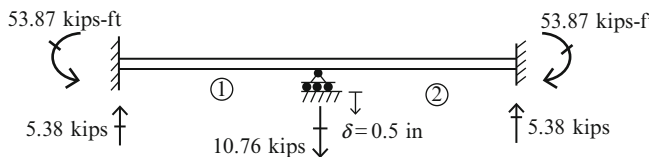


Fig. E12.10g

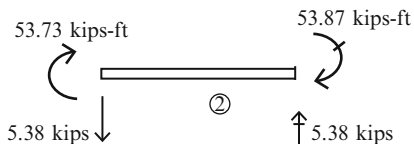
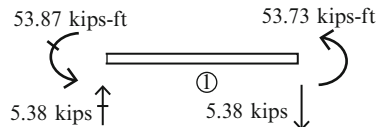


Fig. E12.10h

Example 12.11 Two-span beam with a spring support at mid-span

Given: The structure shown in Fig. E12.11a. Node 2 is supported with a spring of stiffness $k_v=200$ kip/ft. Taken $L = 20$ ft, $I = 428$ in.⁴, and $E = 29,000$ ksi.

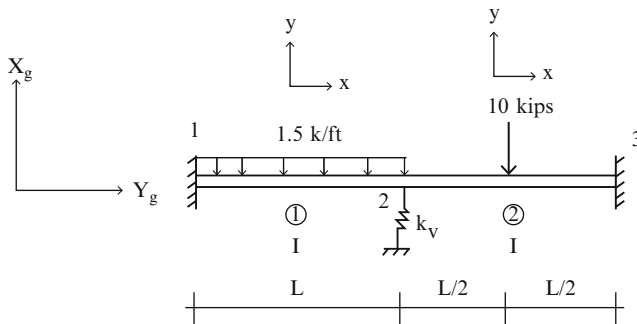


Fig. E12.11a

Determine: The displacements at node 2 and the member end forces (Fig. E12.11b)

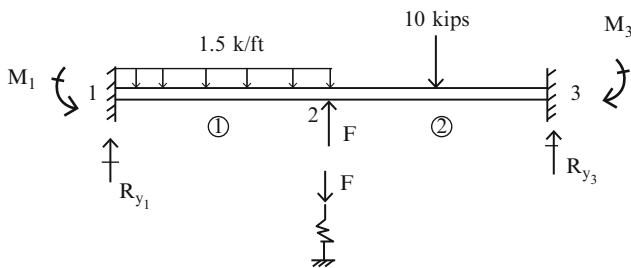


Fig. E12.11b

Solution:

Nodes 1 and 3 are fully fixed and node 2 is restrained by a linear elastic spring. The unknown displacements at node 2 are the vertical displacement v_2 and the rotation θ_2 . We arrange the rows and columns of the system matrix consistent with this support condition. The spring is introduced by adding an external nodal force at node 2 with a magnitude equal to $F = -k_v v_2$. The minus sign is needed since the spring force acts in the opposite direction to the displacement. We utilize the results for \mathbf{K} and \mathbf{P}_I contained in Example 12.10. The initial and rearranged matrices are

$$\mathbf{K} = \begin{pmatrix} \frac{12EI}{L^3} & \frac{6EI}{L^2} & -\frac{12EI}{L^3} & \frac{6EI}{L^2} & 0 & 0 \\ \frac{6EI}{L^2} & \frac{4EI}{L} & -\frac{6EI}{L^2} & \frac{2EI}{L} & 0 & 0 \\ -\frac{12EI}{L^3} & -\frac{6EI}{L^2} & \frac{24EI}{L^3} & 0 & -\frac{12EI}{L^3} & \frac{6EI}{L^2} \\ \frac{6EI}{L^2} & \frac{2EI}{L} & 0 & \frac{8EI}{L} & -\frac{6EI}{L^2} & \frac{2EI}{L} \\ 0 & 0 & -\frac{12EI}{L^3} & -\frac{6EI}{L^2} & \frac{12EI}{L^3} & -\frac{6EI}{L^2} \\ 0 & 0 & \frac{6EI}{L^2} & \frac{2EI}{L} & -\frac{6EI}{L^2} & \frac{4EI}{L} \end{pmatrix}$$

$$\mathbf{U} = \begin{Bmatrix} v_1 \\ \theta_1 \\ v_2 \\ \theta_2 \\ v_3 \\ \theta_3 \end{Bmatrix} \quad \mathbf{P}_E = \begin{Bmatrix} R_{y1} \\ M_{1-} \\ (V_{(1)B} + V_{(2)A}) \\ (M_{(1)B} + M_{(2)A}) \\ R_{y3} \\ M_3 \end{Bmatrix}$$

and

$$\mathbf{U}' = \begin{Bmatrix} v_2 \\ \theta_2 \end{Bmatrix} \quad \mathbf{U}'' = \begin{Bmatrix} v_1 \\ \theta_1 \\ v_3 \\ \theta_3 \end{Bmatrix}$$

$$\mathbf{P}'_E = \begin{Bmatrix} -k_v v_2 \\ 0 \end{Bmatrix} \quad \mathbf{P}'_I = \begin{Bmatrix} 20.0 \\ -25.0 \end{Bmatrix}$$

$$\mathbf{K}' = \begin{pmatrix} \frac{24EI}{L^3} & 0 & -\frac{12EI}{L^3} & -\frac{6EI}{L^2} & -\frac{12EI}{L^3} & \frac{6EI}{L^2} \\ 0 & \frac{8EI}{L} & \frac{6EI}{L^2} & \frac{2EI}{L} & -\frac{6EI}{L^2} & \frac{2EI}{L} \\ -\frac{12EI}{L^3} & \frac{6EI}{L^2} & \frac{12EI}{L^3} & \frac{6EI}{L^2} & 0 & 0 \\ -\frac{6EI}{L^2} & \frac{2EI}{L} & \frac{6EI}{L^2} & \frac{4EI}{L} & 0 & 0 \\ \frac{12EI}{L^3} & -\frac{6EI}{L^2} & 0 & 0 & \frac{12EI}{L^3} & -\frac{6EI}{L^2} \\ \frac{6EI}{L^2} & \frac{2EI}{L} & 0 & 0 & -\frac{6EI}{L^2} & \frac{4EI}{L} \end{pmatrix}$$

$$\mathbf{K}'_{11} = \begin{bmatrix} \frac{24EI}{L^3} & 0 \\ 0 & \frac{8EI}{L} \end{bmatrix} \quad \mathbf{K}'_{12} = \begin{bmatrix} -\frac{12EI}{6EI} & -\frac{6EI}{2EI} & -\frac{12EI}{6EI} & \frac{6EI}{2EI} \\ \frac{L^3}{L^2} & \frac{L^2}{L} & \frac{L^3}{L^2} & \frac{L^2}{L} \end{bmatrix}$$

$$\mathbf{K}'_{21} = \begin{bmatrix} -\frac{12EI}{6EI} & \frac{6EI}{2EI} \\ -\frac{L^2}{12EI} & \frac{L}{6EI} \\ \frac{L^3}{6EI} & -\frac{L^2}{2EI} \\ \frac{6EI}{L^2} & \frac{2EI}{L} \end{bmatrix} \quad \mathbf{K}'_{22} = \begin{bmatrix} \frac{12EI}{6EI} & \frac{6EI}{4EI} & 0 & 0 \\ \frac{L^3}{L^2} & \frac{L^2}{L} & 0 & 0 \\ 0 & 0 & \frac{12EI}{6EI} & -\frac{6EI}{4EI} \\ 0 & 0 & -\frac{L^3}{L^2} & \frac{4EI}{L} \end{bmatrix}$$

Assuming nodes 1 and 3 are fixed, the reduced equations are

$$\mathbf{P}'_E = \mathbf{K}'_{11}\mathbf{U}' + \mathbf{P}'_I$$

Noting the matrices listed above, this equation expands to

$$\begin{Bmatrix} -k_v v_2 \\ 0 \end{Bmatrix} = \begin{Bmatrix} 20.0 \\ -25.0 \end{Bmatrix} + \frac{EI}{L} \begin{bmatrix} \frac{24}{L^2} & 0 \\ 0 & 8 \end{bmatrix} \begin{Bmatrix} v_2 \\ \theta_2 \end{Bmatrix}$$

We transfer the term involving v_2 over to the right hand side and solve for v_2 , θ_2 .

$$\begin{bmatrix} \left(\frac{24EI}{L^3} + k_v\right) & 0 \\ 0 & \frac{8EI}{L} \end{bmatrix} \begin{Bmatrix} v_2 \\ \theta_2 \end{Bmatrix} = \begin{Bmatrix} -20.0 \\ +25.0 \end{Bmatrix}$$

When a particular nodal displacement is elastically restrained, we modify the system stiffness matrix \mathbf{K} , by adding the spring stiffness to the *diagonal entry that corresponds to the displacement*. We then rearrange the rows and columns to generate \mathbf{K}' . Continuing with computation, the displacements at node 2 are

$$(\mathbf{K}'_{11})^{-1} = \begin{bmatrix} \left(\frac{24EI}{L^3} + k_v\right) & 0 \\ 0 & \frac{8EI}{L} \end{bmatrix}^{-1} = \begin{bmatrix} \frac{1}{(24EI/L^3) + k_v} & 0 \\ 0 & \frac{L}{8EI} \end{bmatrix}$$

$$\begin{Bmatrix} v_2 \\ \theta_2 \end{Bmatrix} = (\mathbf{K}'_{11})^{-1}(-\mathbf{P}'_I) = \begin{bmatrix} \frac{1}{(24EI/L^3) + k_v} & 0 \\ 0 & \frac{L}{8EI} \end{bmatrix} \begin{Bmatrix} -20.0 \\ +25.0 \end{Bmatrix} = \begin{Bmatrix} -0.523 \text{ in.} \\ 0.000725 \text{ rad} \end{Bmatrix}$$

$$\begin{Bmatrix} v_2 \\ \theta_2 \end{Bmatrix} = (\mathbf{K}'_{11})^{-1}(-\mathbf{P}'_I) = \begin{bmatrix} \frac{1}{(24EI/L^3) + k_v} & 0 \\ 0 & \frac{L}{8EI} \end{bmatrix} \begin{Bmatrix} -20.0 \\ +25.0 \end{Bmatrix} = \begin{Bmatrix} -0.523 \text{ in.} \\ 0.000725 \text{ rad} \end{Bmatrix}$$

Lastly, the reactions are determined with

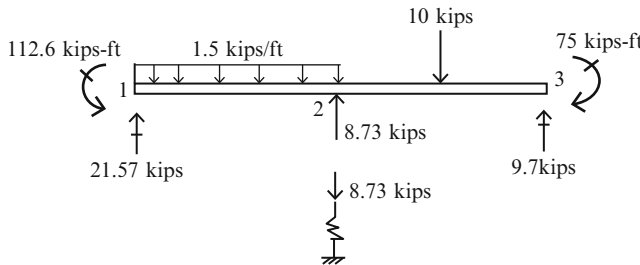
$$\mathbf{P''}_E = \mathbf{K}'_{21} \mathbf{U}' + \mathbf{P''}_I$$

↓

$$\begin{Bmatrix} R_{y1} \\ M_{1\perp} \\ R_{y3} \\ M_3 \end{Bmatrix} = \begin{bmatrix} -\frac{12EI}{L^3} & \frac{6EI}{L^2} \\ -\frac{6EI}{L^2} & \frac{2EI}{L} \\ \frac{12EI}{L^3} & -\frac{6EI}{L^2} \\ \frac{6EI}{L^2} & \frac{2EI}{L} \end{bmatrix} \begin{Bmatrix} -0.523 \\ 0.000725 \end{Bmatrix} + \begin{Bmatrix} 15.0 \\ 50.0 \\ 5.0 \\ -25.0 \end{Bmatrix} = \begin{Bmatrix} 21.57 \text{ kip} \\ 112.64 \text{ kip/ft} \\ 9.7 \text{ kip} \\ -75.13 \text{ kip/ft} \end{Bmatrix}$$

$$F = -k_v v_2 = -(200 \text{ kip/ft}) \left(\frac{1}{12} \right) (-0.5230) = 8.73 \text{ kip}$$

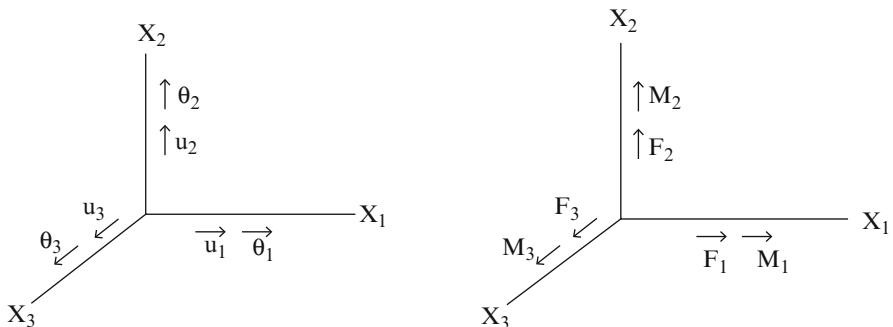
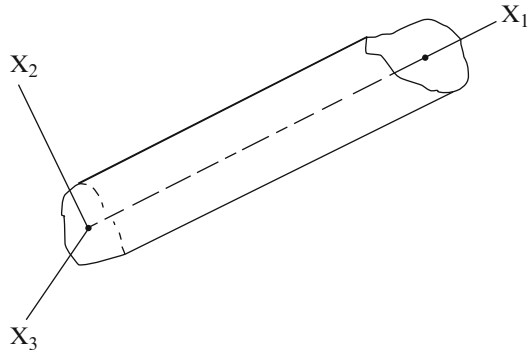
The results are listed below.



12.8 Three-Dimensional Formulation

In what follows, we extend the planar formulation in the previous sections to deal with the case where the loading is three dimensional (3D). The basic approach is the same; one just has to expand the definition of the displacement, end action, and member stiffness matrices. The three-dimensional formulation is much more detailed, and is generally executed using a digital computer.

We start by defining the local coordinate system for a prismatic member. We take the x_1 direction to coincide with the centroidal axis, and x_2 and x_3 as the principle inertia directions for the cross section. Figure 12.9 shows this notation. The inertia properties for x_2 and x_3 are defined as

Fig. 12.9 3D beam**Fig. 12.10** Coordinate systems

$$\begin{aligned} I_2 &= \int_A x_3^2 dA \\ I_3 &= \int_A x_2^2 dA \end{aligned} \quad (12.37)$$

There are 6 displacement measures for the 3D case, 3 translations and 3 rotations. We refer these quantities to the local directions and use the notation defined in Fig. 12.10a. The corresponding force measures are defined in a similar manner.

Using this notation, the 3D versions of the displacement and end action matrices are

$$\begin{aligned} \mathbf{U} &= \{u_1 \quad u_2 \quad u_3 \quad \theta_1 \quad \theta_2 \quad \theta_3\} \\ \mathbf{P} &= \{F_1 \quad F_2 \quad F_3 \quad M_1 \quad M_2 \quad M_3\} \end{aligned} \quad (12.38)$$

We express the end action displacement relations in the same form as for the planar case. Noting (12.5), we write:

$$\mathbf{P}_A = \mathbf{k}_{AB}\mathbf{U}_B + \mathbf{k}_{AA}\mathbf{U}_A + \mathbf{P}_A^F$$

$$\mathbf{P}_B = \mathbf{k}_{BB}\mathbf{U}_B + \mathbf{k}_{BA}\mathbf{U}_A + \mathbf{P}_B^F$$

where the \mathbf{k} matrices are now of order 6×6 . Their expanded forms are listed below.

$$\mathbf{k}_{AA} = \begin{bmatrix} AE & 0 & 0 & 0 & 0 & 0 \\ L & \frac{12EI_3}{L^3} & 0 & 0 & 0 & \frac{6EI_3}{L^2} \\ 0 & 0 & \frac{12EI_2}{L^3} & 0 & -\frac{6EI_2}{L^2} & 0 \\ 0 & 0 & 0 & \frac{GJ}{L} & 0 & 0 \\ 0 & 0 & -\frac{6EI_2}{L^2} & 0 & \frac{4EI_2}{L} & 0 \\ 0 & \frac{6EI_3}{L^2} & 0 & 0 & 0 & \frac{4EI_3}{L} \end{bmatrix}$$

$$\mathbf{k}_{BB} = \begin{bmatrix} AE & 0 & 0 & 0 & 0 & 0 \\ L & \frac{12EI_3}{L^3} & 0 & 0 & 0 & -\frac{6EI_3}{L^2} \\ 0 & 0 & \frac{12EI_2}{L^3} & 0 & \frac{6EI_2}{L^2} & 0 \\ 0 & 0 & 0 & \frac{GJ}{L} & 0 & 0 \\ 0 & 0 & \frac{6EI_2}{L^2} & 0 & \frac{4EI_2}{L} & 0 \\ 0 & -\frac{6EI_3}{L^2} & 0 & 0 & 0 & \frac{4EI_3}{L} \end{bmatrix}$$

$$\mathbf{k}_{BA} = \begin{bmatrix} AE & 0 & 0 & 0 & 0 & 0 \\ L & \frac{12EI_3}{L^3} & 0 & 0 & 0 & \frac{6EI_3}{L^2} \\ 0 & 0 & \frac{12EI_2}{L^3} & 0 & -\frac{6EI_2}{L^2} & 0 \\ 0 & 0 & 0 & \frac{GJ}{L} & 0 & 0 \\ 0 & 0 & \frac{6EI_2}{L^2} & 0 & -\frac{2EI_2}{L} & 0 \\ 0 & -\frac{6EI_3}{L^2} & 0 & 0 & 0 & -\frac{2EI_3}{L} \end{bmatrix}$$

$$\mathbf{k}_{AB} = \begin{bmatrix} \frac{AE}{L} & 0 & 0 & 0 & 0 & 0 \\ 0 & \frac{12EI_3}{L^3} & 0 & 0 & 0 & -\frac{6EI_3}{L^2} \\ 0 & 0 & \frac{12EI_2}{L^3} & 0 & -\frac{6EI_2}{L^2} & 0 \\ 0 & 0 & 0 & \frac{GJ}{L} & 0 & 0 \\ 0 & 0 & -\frac{6EI_2}{L^2} & 0 & \frac{2EI_2}{L} & 0 \\ 0 & -\frac{6EI_3}{L^2} & 0 & 0 & 0 & -\frac{2EI_3}{L} \end{bmatrix}$$

These matrices are transformed to the global reference frame using the following matrix

$$\begin{aligned} \mathbf{R}_{lg} &= \begin{bmatrix} \mathbf{R}' & 0 \\ 0 & \mathbf{R}' \end{bmatrix} \\ \mathbf{R}' &= \begin{bmatrix} \alpha_{11} & \alpha_{12} & \alpha_{13} \\ \alpha_{21} & \alpha_{22} & \alpha_{23} \\ \alpha_{31} & \alpha_{32} & \alpha_{33} \end{bmatrix} \\ \alpha_{ij} &= \cos(\mathbf{x}_{ig}, \mathbf{x}_{jl}) \end{aligned} \tag{12.39}$$

The operation involves the following computation

$$\mathbf{K}|_{\text{global}} = \mathbf{R}_{lg} \mathbf{k} \mathbf{R}_{lg}^T \tag{12.40}$$

The remaining steps are the same as the 2D case.

12.9 Summary

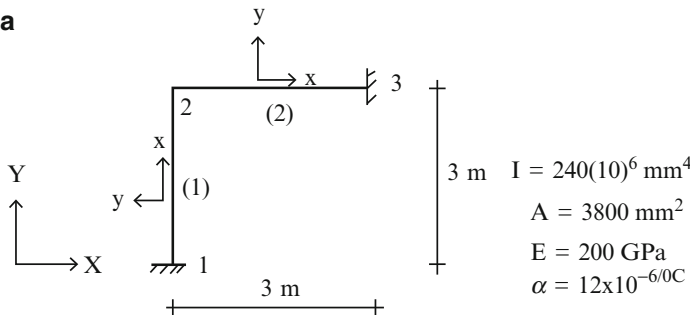
12.9.1 Objectives

- Formulate the governing equations corresponding to the various steps in the displacement method using matrix notation.
- Introduce the concept of a local reference frame for each member and a fixed global reference frame for the structure.
- Develop the matrix form of the member force–displacement relations.
- Derive expressions for the various member stiffness matrices.
- Introduce the concept of a member–node incidence table and show how it is used to assemble the system equilibrium equations.
- Develop a procedure for introducing nodal displacement restraints.
- Specialize the rigid frame formulation for trusses and multi-span beams.

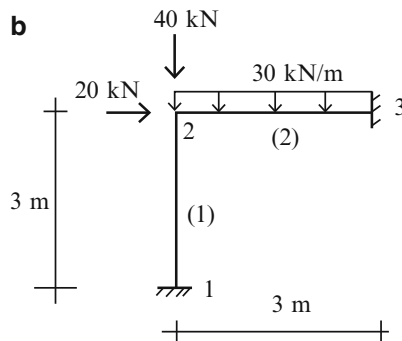
12.10 Problems

Problem 12.1

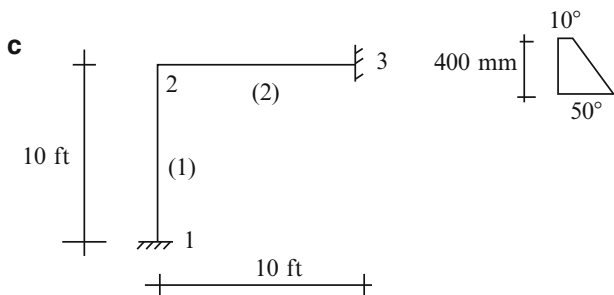
For the rigid frame shown below, use the direct stiffness method to find the joint displacements, reactions, and member forces for the following conditions.

a

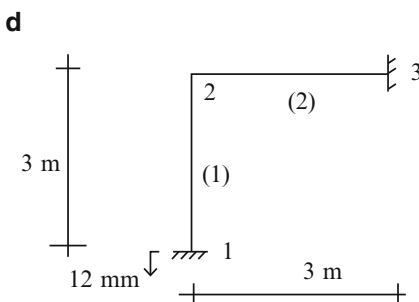
(a) The loading shown

b

(b) Member 2 experiences a uniform temperature change throughout its span. The temperature varies linearly through the depth, from 10°C at the top to 50°C at the bottom.



(c) Support 1 settles 12 mm.



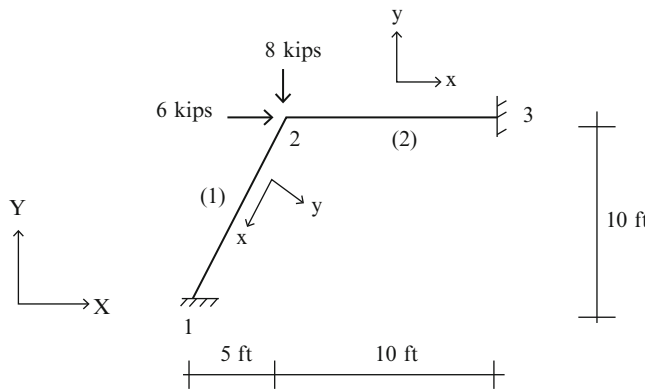
Problem 12.2

For the rigid frame shown below, use the direct stiffness method to find the joint displacements, reactions, and member forces. Take $I = 160(10)^6 \text{ mm}^4$, $A = 6500 \text{ mm}^2$, $E = 200 \text{ GPa}$

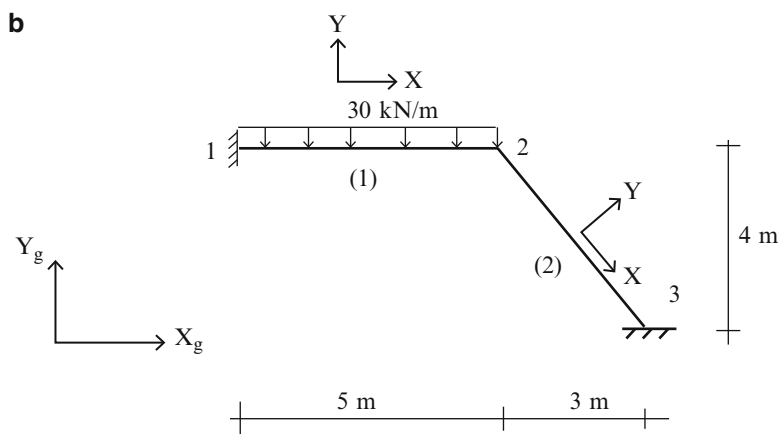
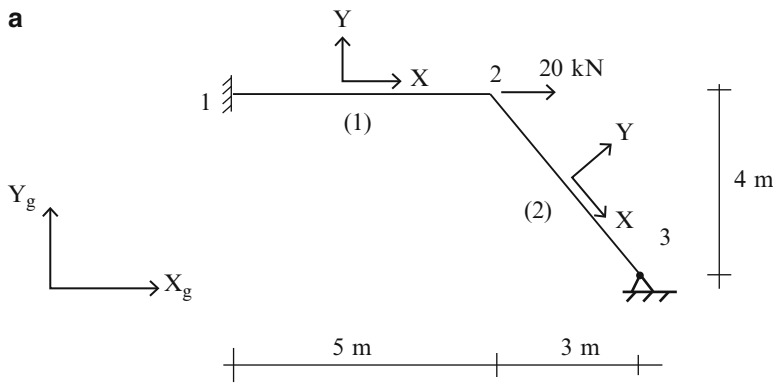
$$I = 400 \text{ in.}^4$$

$$A = 10 \text{ in.}^2$$

$$E = 29,000 \text{ kip/in.}^2$$

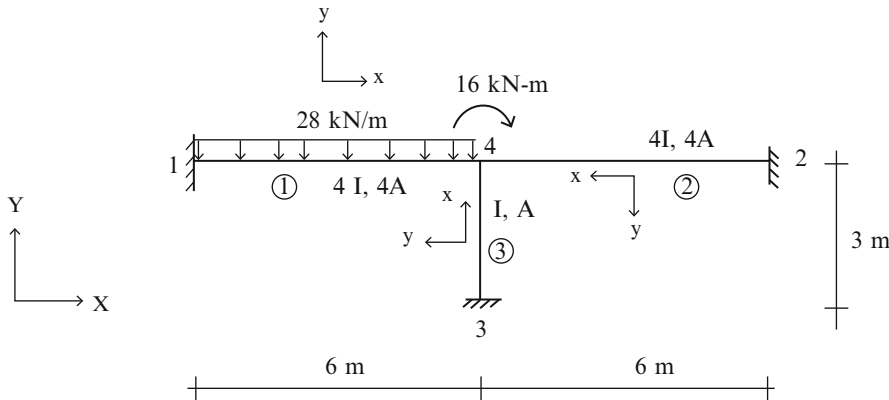
**Problem 12.3**

For the rigid frames shown below, use the direct stiffness method to find the joint displacements, reactions, and member forces.



Problem 12.4

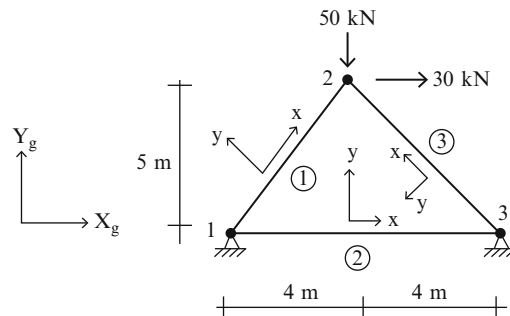
For the rigid frame shown, use partitioning to determine \mathbf{K}'_{11} , \mathbf{K}'_{21} , \mathbf{P}'_E , and \mathbf{P}'_I for the loadings shown. $I = 40(10)^6 \text{ mm}^4$, $A = 3,000 \text{ mm}^2$, and $E = 200 \text{ GPa}$.

**Problem 12.5**

For the truss shown, use the direct stiffness method to find the joint displacements, reactions, and member forces.

$$A = 1,200 \text{ mm}^2$$

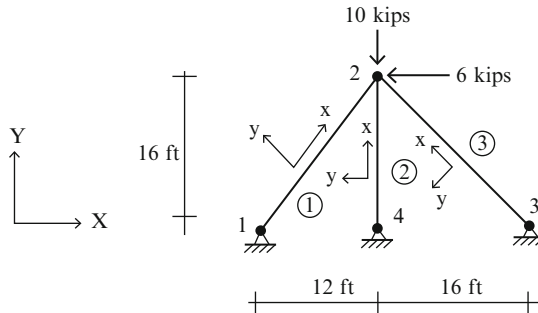
$$E = 200 \text{ GPa}$$



Problem 12.6

For the truss shown, use the direct stiffness method to find the joint displacements, reactions, and member forces for

- (a) The loading shown
- (b) A support settlement of 0.5 in. at joint 4



$$A = 2 \text{ in.}^2$$

$$E = 29,000 \text{ ksi}$$

Problem 12.7

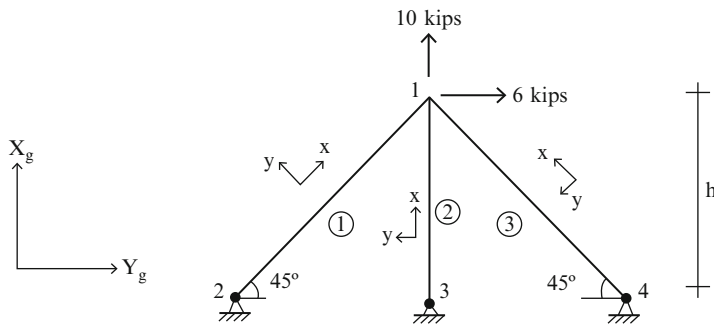
For the truss shown, use the direct stiffness method to find the joint displacements, reactions, and member forces due to (a) the loading shown, (b) a temperature decrease of 10°C for all members, (c) a support settlement of $\delta = 12 \text{ mm}$ downward at node 4.

$$A = 1,200 \text{ mm}^2$$

$$E = 200 \text{ GPa}$$

$$\alpha = 12 \times 10^{-6}/\text{C}^\circ$$

$$h = 3 \text{ m}$$

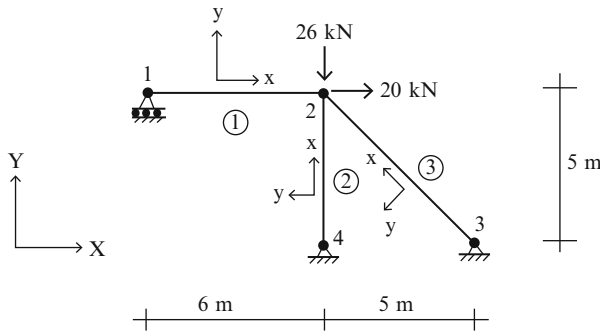


Problem 12.8

For the truss shown, determine \mathbf{K}'_{11} and \mathbf{K}'_{21} .

$$A = 2,000 \text{ mm}^2$$

$$E = 200 \text{ GPa}$$

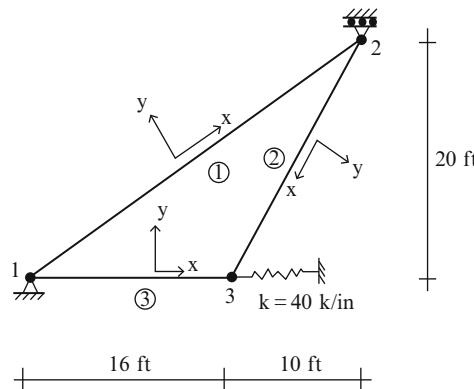


Problem 12.9

For the truss shown, determine \mathbf{K}'_{11} and \mathbf{K}'_{22} .

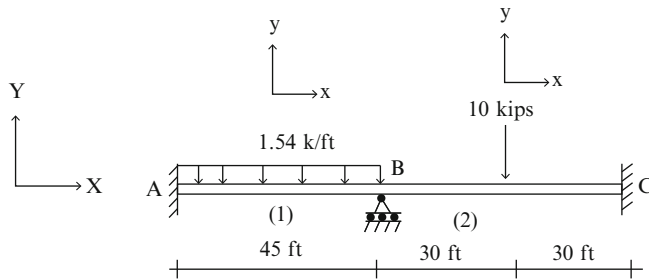
$$A = 3 \text{ in.}^2$$

$$E = 29,000 \text{ ksi}$$

**Problem 12.10**

For the beam shown, use the direct stiffness method to find the joint displacements, reactions, and member forces for the loading shown.

(1)



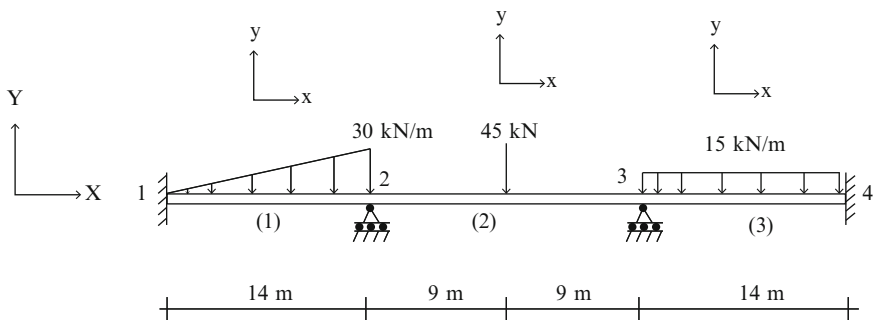
$$I = 300 \text{ in.}^4$$

$$E = 29,000 \text{ ksi}$$

Problem 12.11

For the beam shown, use the direct stiffness method to find the joint displacements, reactions, and member forces for

- (a) The loading shown
- (b) A support settlement of 12 mm at joint 2

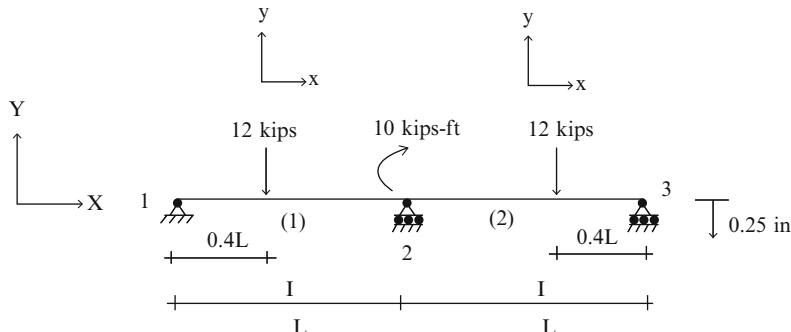


$$I = 120(10)^6 \text{ mm}^4$$

$$E = 200 \text{ GPa}$$

Problem 12.12

Given the system matrix listed below. Determine \mathbf{K}'_{11} , \mathbf{K}'_{21} , \mathbf{U}'' , \mathbf{P}'_I , \mathbf{P}''_I , \mathbf{P}'_E , and \mathbf{P}''_E for the loading and displacement constraint shown. $L = 30 \text{ ft}$, $I = 300 \text{ in.}^4$, and $E = 29,000 \text{ ksi}$.

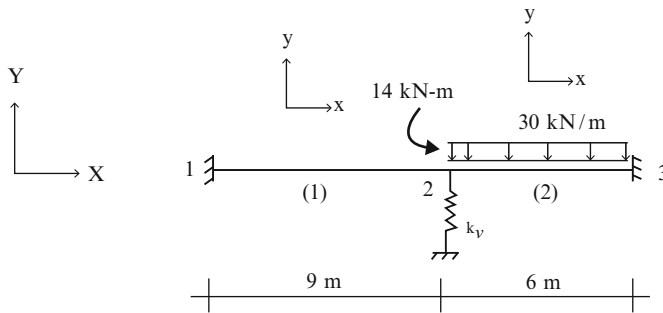


$$\mathbf{K} = \begin{pmatrix} \frac{12EI}{L^3} & \frac{6EI}{L^2} & -\frac{12EI}{L^3} & \frac{6EI}{L^2} & 0 & 0 \\ \frac{6EI}{L^2} & \frac{4EI}{L} & -\frac{6EI}{L^2} & \frac{2EI}{L} & 0 & 0 \\ -\frac{12EI}{L^3} & -\frac{6EI}{L^2} & \frac{24EI}{L^3} & 0 & -\frac{12EI}{L^3} & \frac{6EI}{L^2} \\ \frac{6EI}{L^2} & \frac{2EI}{L} & 0 & \frac{8EI}{L} & -\frac{6EI}{L^2} & \frac{2EI}{L} \\ 0 & 0 & -\frac{12EI}{L^3} & -\frac{6EI}{L^2} & \frac{12EI}{L^3} & -\frac{6EI}{L^2} \\ 0 & 0 & \frac{6EI}{L^2} & \frac{2EI}{L} & -\frac{6EI}{L^2} & \frac{4EI}{L} \end{pmatrix} \quad \mathbf{U} = \begin{pmatrix} v_1 \\ \theta_1 \\ v_2 \\ \theta_2 \\ v_3 \\ \theta_3 \end{pmatrix}$$

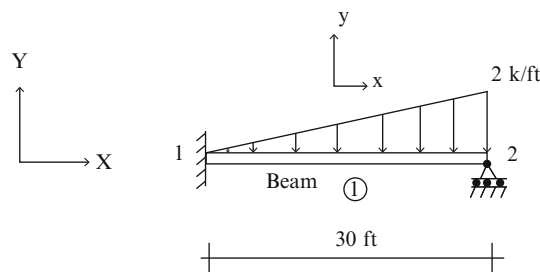
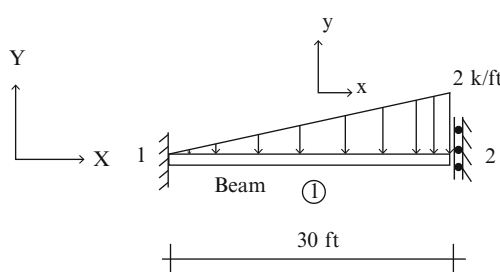
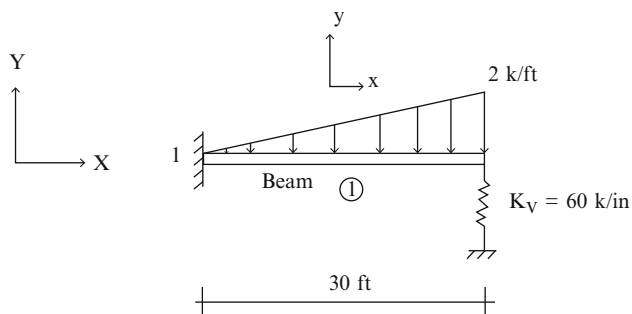
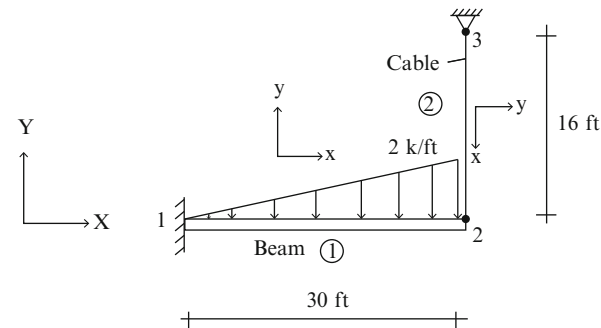
Problem 12.13

Investigate the effect of varying the spring stiffness on the behavior (moment and deflected profile) of the structure shown below. Consider a range of values of k_v .

$$I = 120(10)^6 \text{ mm}^4, E = 200 \text{ GPa} \text{ and } k_v = \begin{cases} 18 \text{ kN/mm} \\ 36 \text{ kN/mm} \\ 90 \text{ kN/mm} \end{cases}$$

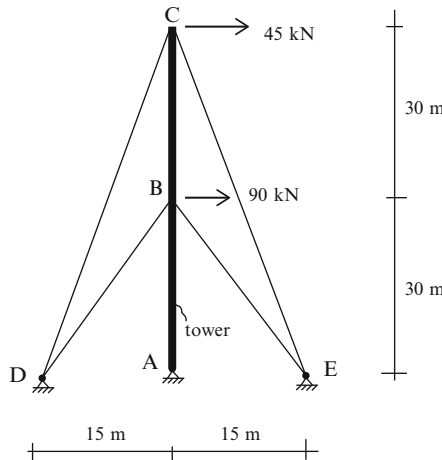
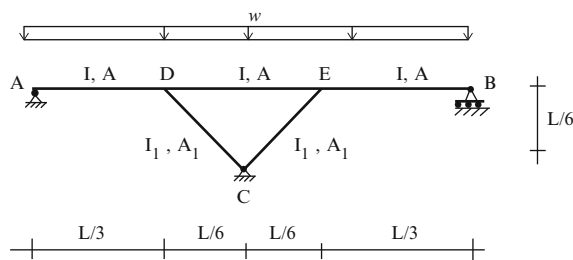
**Problem 12.14**

Determine the bending moment and deflection profiles for the following structures. Take $I = 300 \text{ in.}^4$, $A_{\text{Cable}} = 3 \text{ in.}^2$, and $E = 29,000 \text{ kip/in.}^2$.

a**b****c****d**

Problem 12.15

Consider the guyed tower defined in the sketch. The cables have an initial tension of 220 kN. Determine the horizontal displacements at B, C, the change in cable tension, and the bending moment distribution in member ABC. Treat the cables as axial elements. Develop a computer-based scheme to solve this problem. Take $I_{\text{tower}} = 200(10)^6 \text{ mm}^4$, $A_{\text{cable}} = 650 \text{ mm}^2$, $A_{\text{tower}} = 6,000 \text{ mm}^2$, and the material to be steel.

**Problem 12.16**

Consider the rigid frame shown above. Investigate how the response changes when A_1 is varied. Use computer software. Vary A_1 from 2 to 10 in.² Take $I = 600 \text{ in.}^4$, $A = 5 \text{ in.}^2$, $L = 200 \text{ ft}$, $I_1 = 300 \text{ in.}^4$, $w = 1 \text{ kip/ft}$. Material is steel.

Problem 12.17

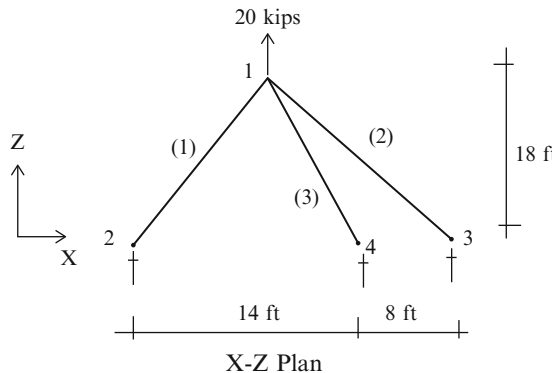
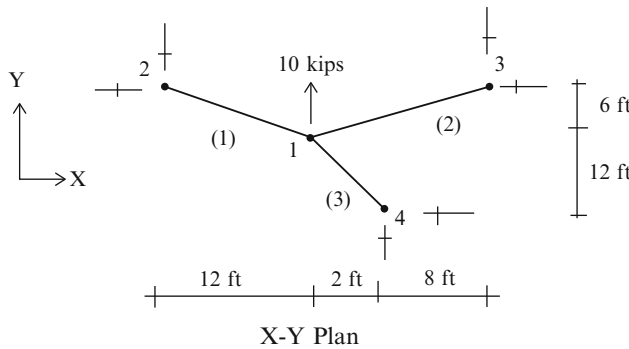
- Develop a computer code to automate the generation of the member stiffness matrices defined by (12.6). Assume A , E , I , L are given.
- Develop a computer code to carry out the operations defined by (12.13).
- Develop a computer code to carry out the operation defined by (12.20) and (12.21).

Problem 12.18

For the space truss shown, use the direct stiffness method to find displacements at joint 1.

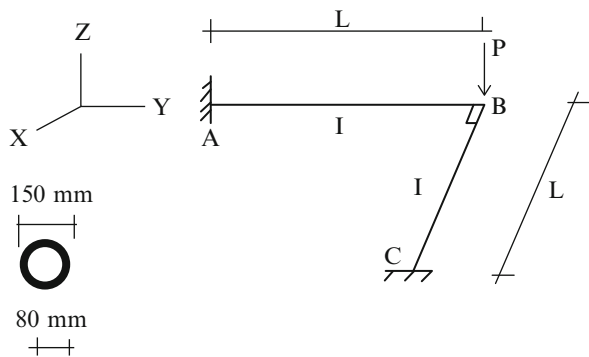
$$A = 3 \text{ in.}^2$$

$$E = 29,000 \text{ ksi}$$



Problem 12.19

For the space frame shown, use the direct stiffness method to find displacements at joint B. The load P is applied perpendicular to the plane ABC. The cross section is circular tube. Take $L = 4$ m, $P = 30$ kN, $E = 200$ GPa, and $G = 77$ GPa.



Part III

Practice of Structural Engineering

The practice of structural engineering involves identifying possible loading patterns, conceptualizing candidate structural systems, developing idealized physical models, applying the possible loading patterns to these idealized models, using analysis methods to determine the peak values of the response variables needed for design detailing, and selecting the design details using an appropriate design code. In this section we focus on selecting loading patterns, idealizing three-dimensional frame structures, and establishing the peak values of the response variables needed for design detailing. Computer-based analysis is used extensively for this phase.

Multi-span horizontal structures are discussed in the next chapter. The topics range from girder bridges to arch bridges to cable-stayed bridges. The following chapter presents a strategy for modeling three-dimensional low-rise rigid frame structures subjected to varying loads. The last chapter describes in detail the process followed to establish the critical loading patterns for multistory frames.

Overview

In this chapter, we discuss the role of analysis in the structural engineering process for multi-span horizontal structures such as bridges. Typical examples of a girder bridge, an arch bridge, and a cable-stayed bridge are shown in Fig. 13.1. Multi-span girders are actually variable depth horizontal beams. They are used extensively in medium span highway bridge systems. Arch and cable-stayed structures are efficient for spans ranging up to 1,000 m.

Chapters 9 and 10 dealt with analysis methods for indeterminate structures. We will utilize some of the analytical results presented in those chapters to estimate critical loading patterns. Most of the analysis effort required in the engineering process is related to determining the maximum values of bending moment, axial force, and shear corresponding to the typical bridge loadings. Establishing these values for indeterminate structures requires a considerable amount of computational effort. We will illustrate this computational process for the different types of bridges such as continuous girder, arch, and cable-stayed schemes using a commercial structural analysis software system.

13.1 The Engineering Process for Girders

The objective of the structural engineering process for a beam is to define the physical makeup, i.e., the location of supports, the material, the shape and dimensions of the cross-section, and special cross-section features such as steel reinforcement in the case of a reinforced concrete beam. Given the absolute maximum values of shear and moment at a particular location, the choice of material, and the general shape of the cross-section, one determines the specific cross-sectional dimensions by applying numerical procedures specified by a design code. This phase of the engineering process is called design detailing. *We focus here on that aspect of the process associated with the determination of the “maximum” values of shear and moment.*



Fig. 13.1 Bridge structures. (a) Multi-span girder bridge. (b) Arch bridge. (c) Cable stayed

In general, shear and bending moment result when an external loading is applied to a beam. Throughout the text, we have shown how one can establish the shear and moment distributions corresponding to a given loading. For statically determinate beams, the internal forces depend only on the external loading and geometry; they are independent of the cross-sectional properties. When the beam is indeterminate, such as a multi-span beam, the internal forces depend on the relative span lengths and cross-sectional properties. In this case, one needs to iterate on the geometry and properties in order to estimate the internal forces.

Now, the loading consists of two contributions: dead and live. The dead loading is fixed, i.e., its magnitude and spatial distribution are constant over time. Live loading is, by definition, time varying over the life of the structure. This variability poses a problem when we are trying to establish the maximum values of shear and moment. We need to consider a number of live load positions in order to identify the particular live load location that results in the absolute maximum values of shear and moment. One approach for multi-span beams is based on determining, for each position of the live load, the absolute maximum value throughout the span. Plots of global maxima vs. live load position are called *force envelopes*. Another approach determines the values of a force quantity at a particular point for all positions of the live load. Plots of force quantities at a particular point vs. load position are called *force influence lines*.

It is important to distinguish between influence lines and force envelopes. An influence line relates a *force quantity at a particular point to the position of the live load*, whereas a *force envelope relates the absolute maximum value of the force quantity along the span to the position of the load*. We apply both approaches to establish design values.

13.2 Influence Lines for Indeterminate Beams Using Müller-Breslau Principle

The topic of influence lines for statically determinate beams was introduced in Chap. 3. We include here a discussion of how one can generate influence lines for indeterminate beams using Müller-Breslau principle [25]. We introduce the principle using the beam structure shown in Fig. 13.2a as an example. Later, in Chap. 15, we apply it to rigid frames.

Suppose one wants the influence line for the *negative moment at A* due to a downward vertical load. According to Müller-Breslau, one works with a modified structure obtained by inserting a moment release at A and applies a negative moment at A. The resulting structure is shown in Fig. 13.2b.

The deflected shapes of the modified structure due to a unit load applied at an arbitrary point, and a unit negative moment at A, are plotted in Fig. 13.2c, d. Since the beam is continuous at A, compatibility requires the net relative rotation at A to vanish. Then

$$\begin{aligned} \theta_{Ax} + \theta_{AA}M_A &= 0 \\ \Downarrow \\ M_A &= -\frac{\theta_{Ax}}{\theta_{AA}} \end{aligned} \tag{13.1}$$

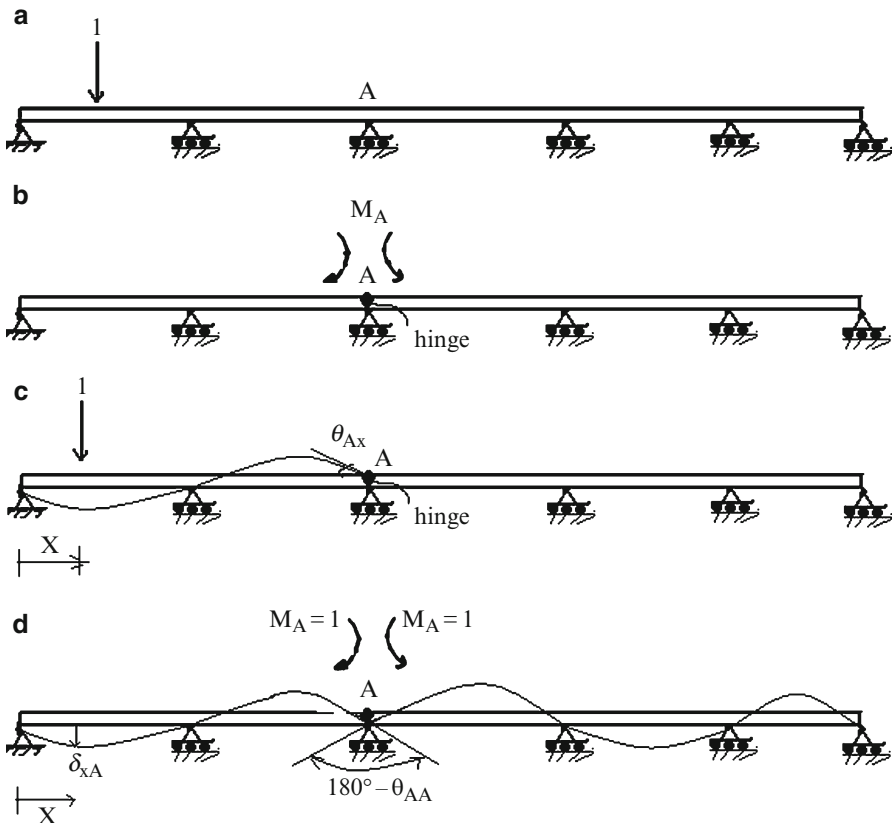


Fig. 13.2 Application of Müller-Breslau principle (a) Example structure. (b) Negative moment. (c) Deflection due to load. (d) Deflection due to moment

We note that $\theta_{AX} = \delta_{xA}$ according to Maxwell's law of reciprocal displacements (see Sect. 9.2). Then (13.1) can be written as

$$M_A = -\frac{\delta_{xA}}{\theta_{AA}} \quad (13.2)$$

Since δ_{xA} is at an arbitrary point, it follows that the deflected shape of the modified structure due to a unit value of M_A is a scaled version of the influence line for M_A . The sense of M_A is determined by comparing the direction of the displacement with the direction of the applied load. In this example, the positive direction of the load is *downward*, so the sense of M_A is the same as for the M_A applied when the *displacement is upward*. The loading zones for the positive and negative values of M_A are shown in Fig. 13.3, which is based on the conventional sign convention for moment, i.e., positive when compression on the upper fiber. Note that we applied a negative moment to generate the deflected shape.

We repeat this process to establish the influence line for the maximum positive moment at D, the center of span AC. The sequence of steps is illustrated in Fig. 13.4. Figure 13.5 defines the loading zones for positive and negative moment.

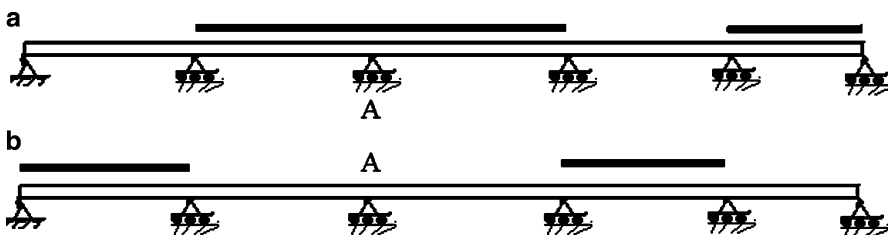


Fig. 13.3 Loading zones for moment at A. (a) Negative moment at A. (b) Positive moment at A

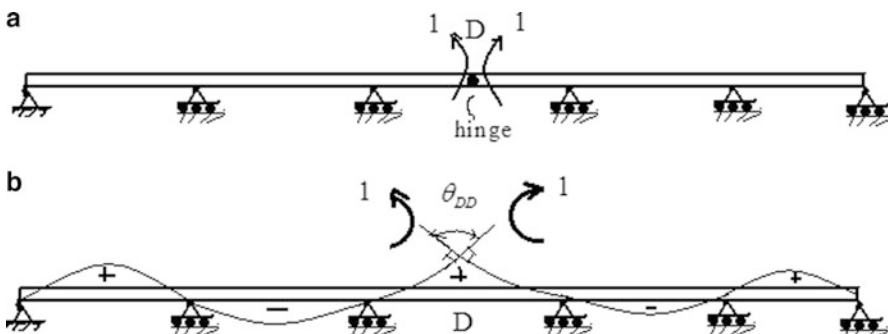


Fig. 13.4 Modified structure and deflected shape for positive moment at D

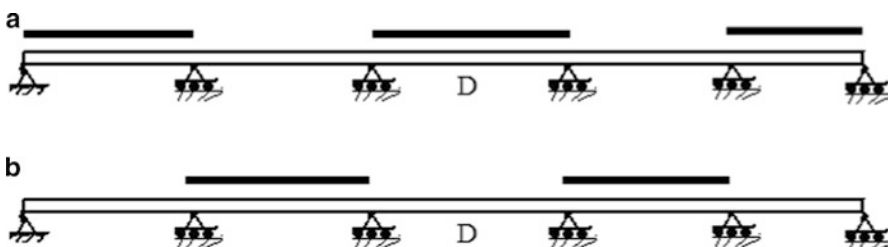


Fig. 13.5 Loading zones for Moment at D. (a) Positive value. (b) Negative value

Summarizing the discussion presented above; the process of applying Müller-Breslau principle to establish the influence line for a redundant force quantity involves the following steps.

1. Modify the actual structure by removing the restraint corresponding to the force quantity of interest.
 2. Apply a unit value of the force quantity at the release and determine the deflected shape.
 3. This deflected shape is a scaled version of the influence line. It consists of positive and negative zones for the force quantity. If the applied loading is a unit downward load, the positive zone includes those regions where the deflection is upward.
- Since it is relatively easy to sketch deflected shapes, Müller-Breslau principle allows one with minimal effort to establish the critical loading pattern for a redundant force quantity.

Example 13.1 Application of Müller-Breslau principle

Given: The four span beam shown in Fig. E13.1a.

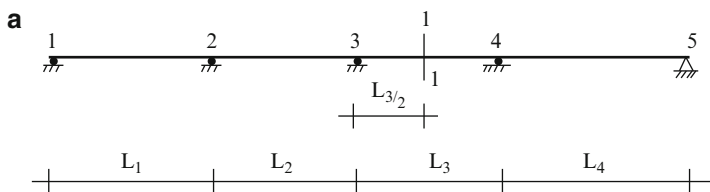


Fig. E13.1a

Determine: The influence lines for the upward vertical reaction at support 3 (R_3), the negative moment at support 3 (M_3), the positive moment at section 1-1 (M_{1-1}), and shear at section 1-1 (V_{1-1}). Also determine the critical loading patterns for a uniformly distributed load that produce the maximum values of R_3 , M_3 , M_{1-1} , and V_{1-1} .

Solution: The deflected shapes and influence lines for a unit downward load are plotted below.

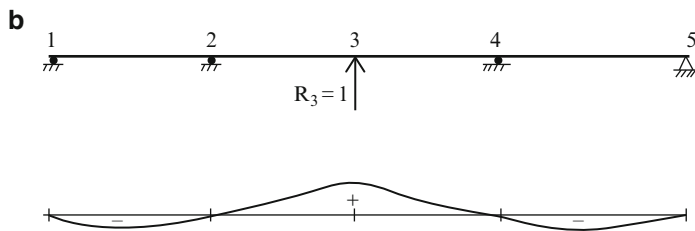


Fig. E13.1b Influence line for R_3

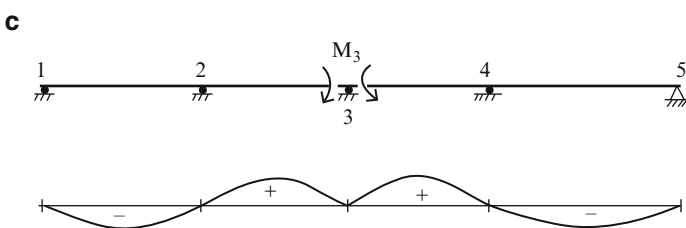


Fig. E13.1c Influence line for M_3

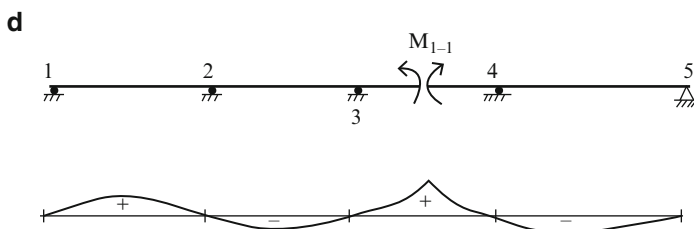
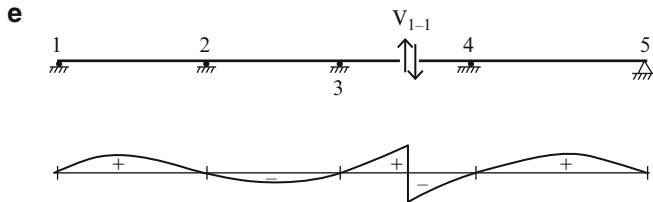
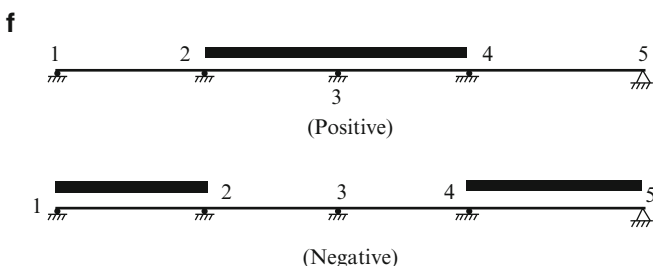
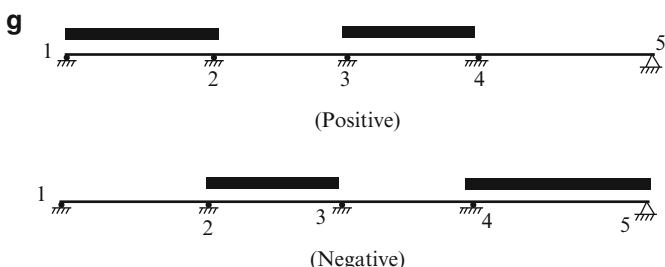
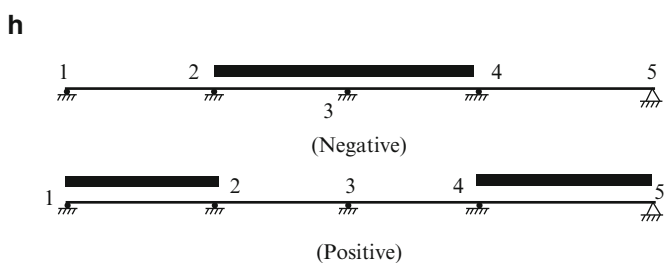


Fig. E13.1d Influence line for M_{1-1}

**Fig. E13.1e** Influence line for V_{1-1}

Loading patterns that produce the peak positive and negative values of these force parameters are shown in Figs. E13.1f–i.

**Fig. E13.1f** Loading patterns for absolute maximum R_3 **Fig. E13.1g** Loading patterns for absolute maximum M_{1-1} **Fig. E13.1h** Loading patterns for absolute maximum M_3

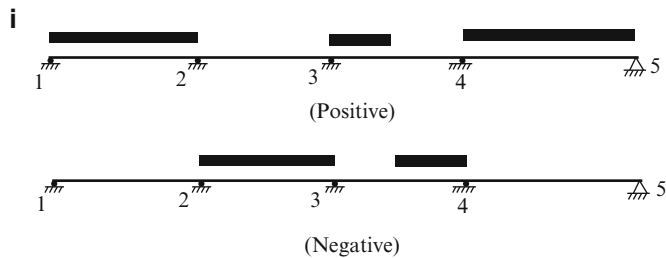


Fig. E13.1i Loading patterns for absolute maximum V_{1-1}

13.3 Engineering Issues for Multi-span Girder Bridges

13.3.1 Geometric Configurations

The superstructure of a typical highway girder bridge consists of longitudinal girders which support a concrete deck. The girders may be fabricated from either steel or concrete. The substructure is composed of piers and abutments which are founded on either shallow foundations or piles. In general, the makeup of the substructure depends on the soil conditions at the site. Bearings are employed to connect the girders to the substructure.

Bridge spans are classified as either short, medium, or long according to the total span length. Typical categories are

- Short: less than 125 ft (38 m)
- Medium: 125–400 ft (38–120 m)
- Long: over 400 ft (120 m)

Typical highway bridge structural systems are composed of continuous beams. One could replace the continuous beam with an arrangement of simply supported beams. However, this choice requires additional bearings and introduces discontinuities in the deck slab at the interior supports. The discontinuity in the deck slab creates a serious problem since it provides a pathway for moisture and leads to corrosion of the bearings at the supports. Using a continuous beam allows one to achieve continuity of the deck slab and also eliminates some bearings. It is the preferred structural scheme for new bridges. Typical span arrangements are shown in Fig. 13.6. The current trend is to use a constant girder cross-section throughout the span.

Historically, girder bridges were configured as a collection of single spans. This scheme is illustrated in Fig. 13.7a. In order to deal with longer interior spans, the cantilever scheme shown in Fig. 13.7b was introduced. Both schemes involve discontinuities in the girder/deck which provide pathways for moisture and lead to deterioration. To eliminate the interior discontinuities, the obvious option is to use a continuous girder such as shown in Fig. 13.7c. We demonstrated in Chap. 9

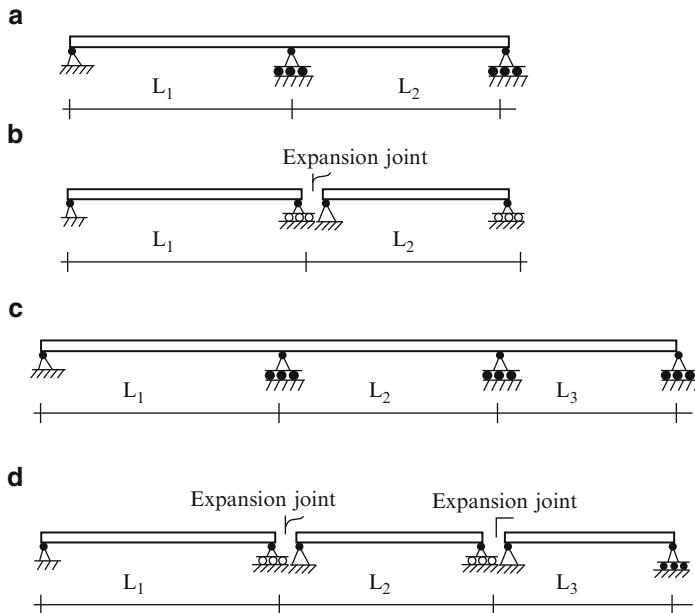


Fig. 13.6 Span arrangements for multi-span beams. (a) Two spans continuous. (b) Two spans simply supported. (c) Three spans continuous. (d) Three spans simply supported

that continuous beams are more efficient structurally, i.e., the peak internal forces are less than the corresponding forces for the simply supported case. Therefore, the required cross-section tends to be lighter.

Even when a continuous girder is used, there still remains the problem of the discontinuities at the end supports (abutments). The problem is solved by using the scheme shown in Fig. 13.8. The abutments walls are supported on flexible piles that are rigidly connected to the deck/girder system. This concept is called an “integral abutment bridge.” Since the abutment is rigidly attached to the deck/girder, a temperature change of the deck produces a longitudinal displacement of the abutment wall. In order to minimize the effect of the resulting lateral force, the abutments are supported on flexible piles and loose granular backfill is placed behind the wall. The longitudinal displacement due to temperature varies linearly with the span length, and consequently the maximum span length is limited by the seasonal temperature change.

We generate an idealized model by replacing the action of the soil and piles with equivalent springs [23]. Figure 13.9a illustrates this approach. An estimate of the effect of support stiffness is obtained using the model shown in Fig. 13.9b.

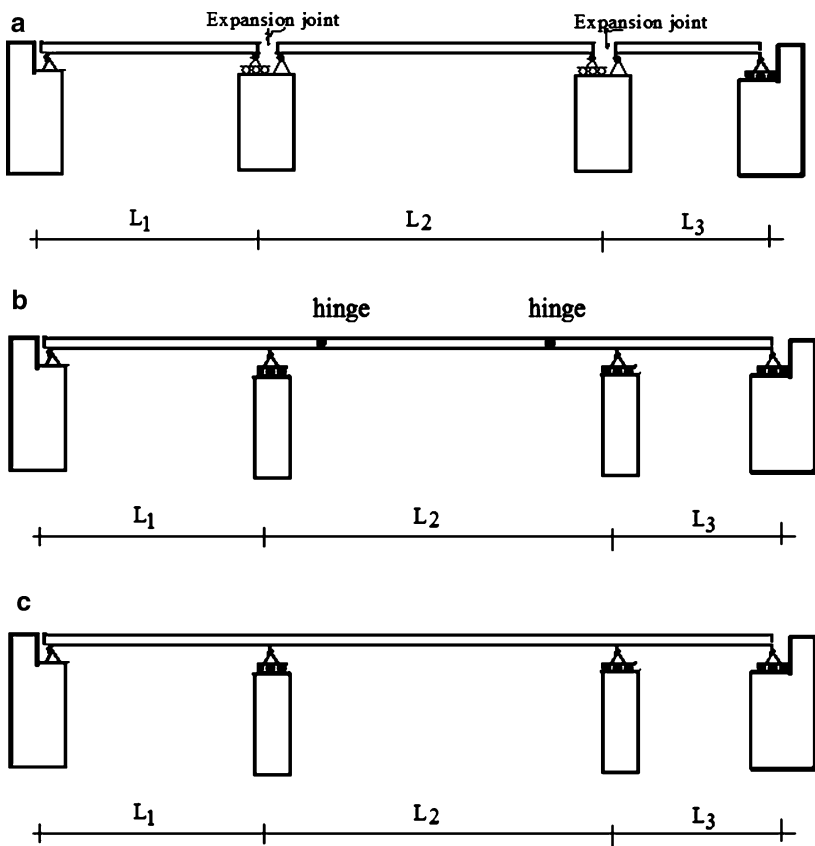


Fig. 13.7 Multi-span bridge schemes (a) Simple spans. (b) Cantilever spans. (c) Continuous spans



Fig. 13.8 (a) Three-span integral abutment bridge in Orange Massachusetts. (b) Elevation—three-span integral abutment bridge

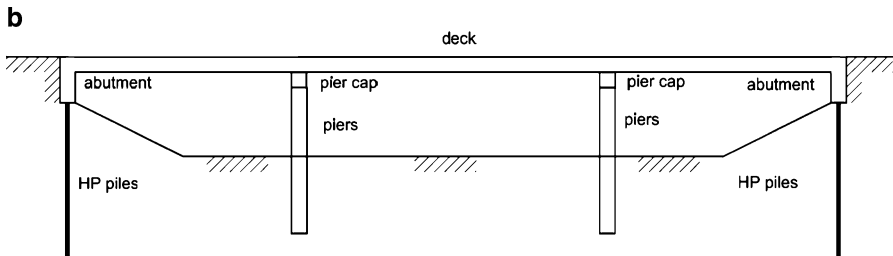


Fig. 13.8 (continued)

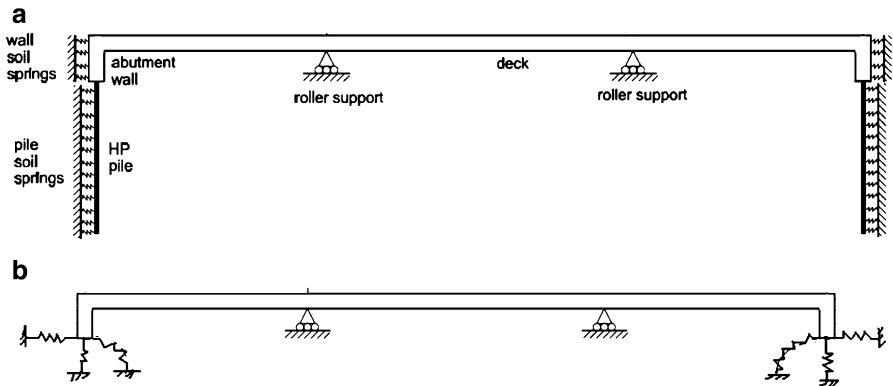


Fig. 13.9 Idealized models for an integral abutment bridge (a) Global model. (b) Simplified model

13.3.2 Choice of Span Lengths

Given some overall crossing length, one needs to decide on the number and relative magnitude of the spans to be used to achieve the crossing. We utilize here some of the analytical results for multi-span continuous beams with constant I subject to uniform loading generated in Chaps. 9 and 10. Figure 13.10 shows how the maximum moment varies with increasing number of spans. Note that there is a significant reduction in peak moment as the number of spans is increased, for a given overall length. Note also that the bending moment distribution for constant I is independent of the value of I .

In general, for constant I , the bending moment distribution depends on the ratio of the span lengths. For the symmetrical case shown in Fig. 13.11, the analytical solution for the negative moment at an interior support has the form (see Example 10.5)

$$M_{\text{max}}^{-} = g \left(\frac{L_2}{L_1} \right) \frac{w L_1^2}{8} \quad (13.3)$$

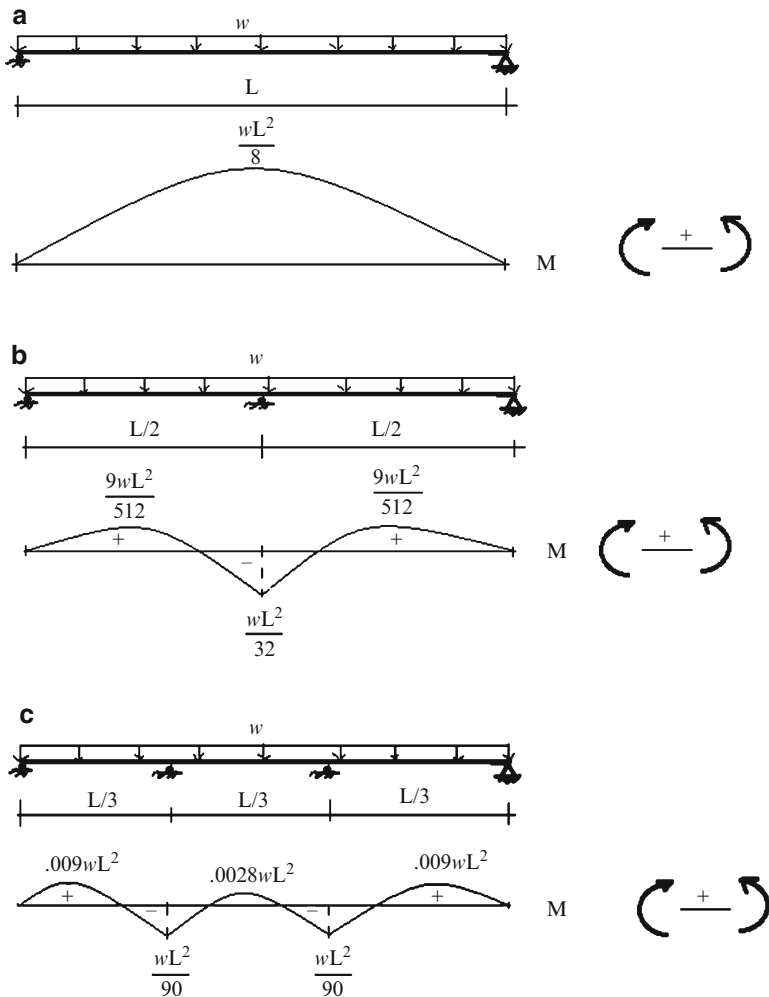


Fig. 13.10 Variation of the bending moment distribution. (a) Simply supported. (b) Two-span scheme. (c) Three-span scheme

where

$$g\left(\frac{L_2}{L_1}\right) = \frac{1 + (L_2/L_1)^2}{1 + (3/2)(L_2/L_1)}$$

We express L_1 and L_2 as

$$\begin{aligned} L_2 &= \alpha L \\ L_1 &= \frac{(1 - \alpha)}{2} L \end{aligned} \tag{13.4}$$

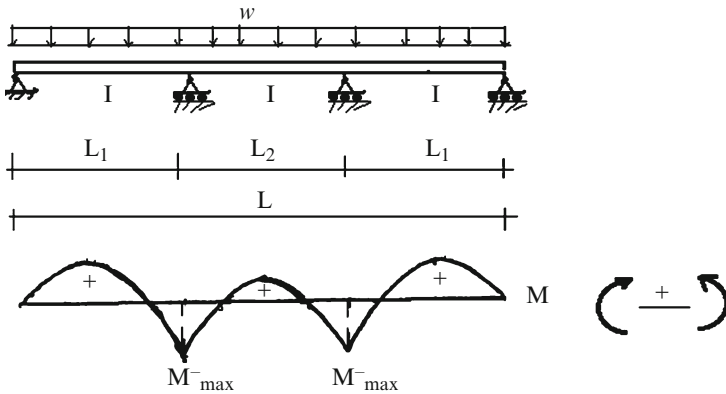


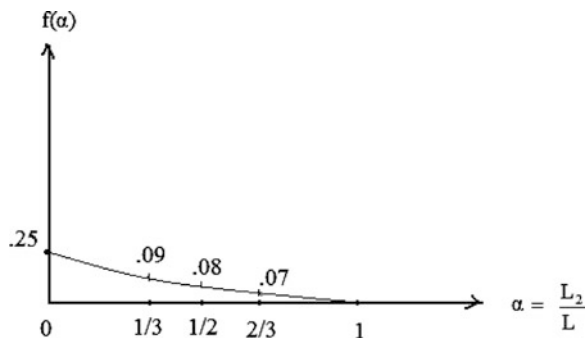
Fig. 13.11 Bending moment distribution—three-span symmetrical scheme

With this notation, (13.3) expands to

$$M^{-}_{\max} = \frac{wL^2}{8} f(\alpha) \quad (13.5)$$

$$f(\alpha) = \frac{1 - 3\alpha + 7\alpha^2 - 5\alpha^3}{4(1 + 2\alpha)}$$

The variation of f with α is plotted below.



Taking $L_2=L_1$ corresponds to $\alpha=1/3$. The more common case is where α is between $1/3$ and $1/2$. When spans L_1 and L_2 are chosen, one applies the uniformly distributed loading and determines the peak value of negative moment using (13.5).

13.3.3 Live Loads for Multi-span Highway Bridge Girders: Moment Envelopes

The live load for a highway bridge is assumed to consist of two components: a uniform loading intended to simulate small vehicles, such as cars, and a set of concentrated loads that characterize heavy vehicles, such as a truck.

13.3.3.1 Set of Concentrated Live Loads

The action of a heavy vehicle traveling across the total span is simulated by positioning a set of concentrated loads at various locations along the span. The load magnitude and axle spacing vary, depending on the code that governs the design. For each load position, we determine the bending moment at specific points along the span. When the beam is statically determinate, it is possible to develop an analytical solution for the peak moment. This approach is described in Chap. 3. However, when the beam is indeterminate, one must resort to a numerical procedure. This approach is illustrated in Fig. 13.12. In practice, one first discretizes the spans, and then positions the load at the individual discrete points. Assuming there are n discrete points, one needs to carry out n analyses. This results in n bending moment distributions. At each discrete point, we determine the maximum positive and negative values from the set of n values generated by the n analyses. Finally, we construct a plot showing the “maximum” values of moment at each discrete point. This plot allows one to readily identify the absolute “maximum” moment by scanning over the plot. Since the values at each discrete point represent the *peak values at the point for all positions of the loading*, one can interpret the plot as a “discretized” moment envelope. Working with a refined span discretization provides detailed information on the shear and moment distributions. For example, 30 separate analyses are required to generate the discrete moment envelope for the span discretization shown in Fig. 13.12c. We discuss next how one establishes the magnitudes of the concentrated loads.

13.3.3.2 Transverse Distribution of Truck Load to Stringers

Figure 13.13 shows typical slab stringer highway bridge cross-sections. The roadway is supported by a reinforced concrete slab which rests on a set of longitudinal beams, called stringers. The stringers may be either steel sections or concrete elements.

In order to determine the truck load applied to the stringer, we position the truck such that one set of wheels are directly on the stringer. Figure 13.14 illustrates this case. *Note that P is the axle load.*

We assume the slab acts as a simply supported beam spanning between the stringers. This assumption is conservative. Then the load on stringer “A” is

$$P_{A\max} = \frac{P}{2} + \frac{P}{2} \left(\frac{S-a}{S} \right) = \frac{P}{2} \left(2 - \frac{a}{S} \right)$$

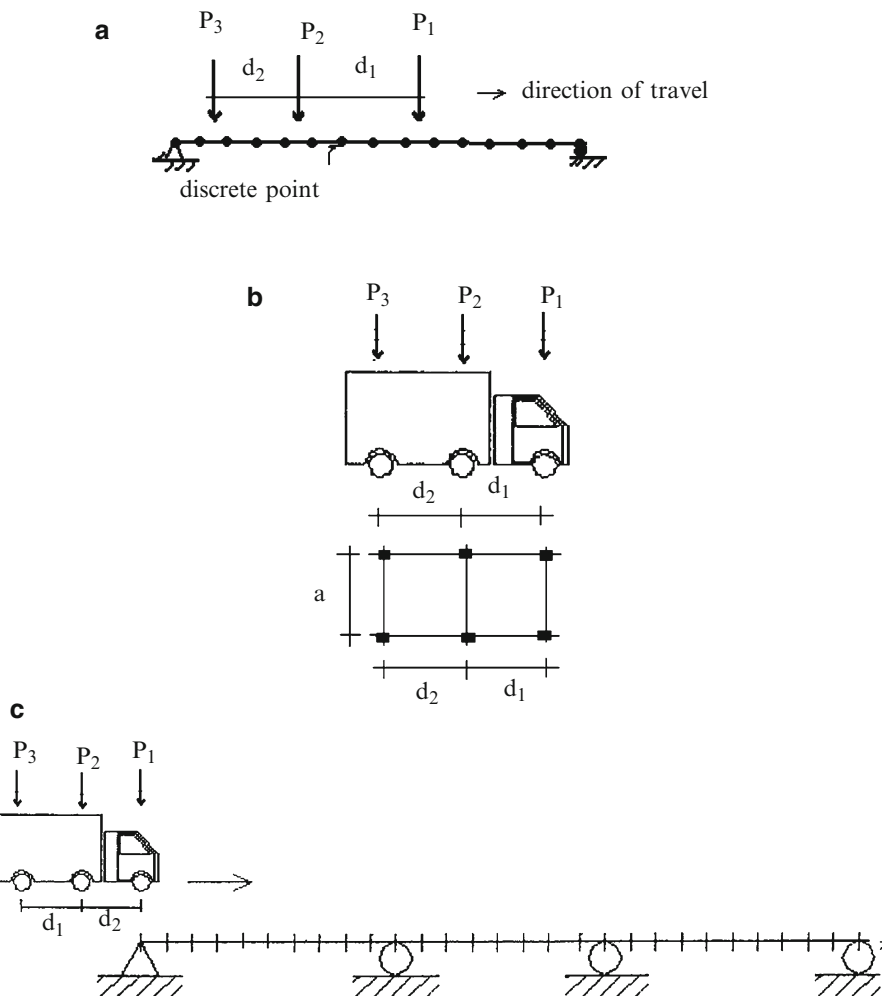
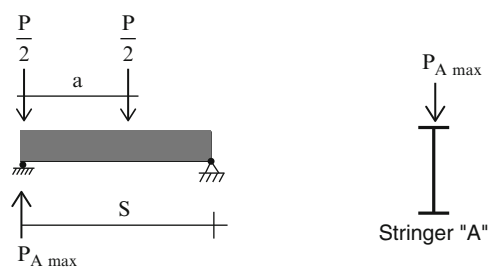


Fig. 13.12 Truck loading and span discretization. (a) Span discretization. (b) Three axle truck. (c) Multi-span discretization



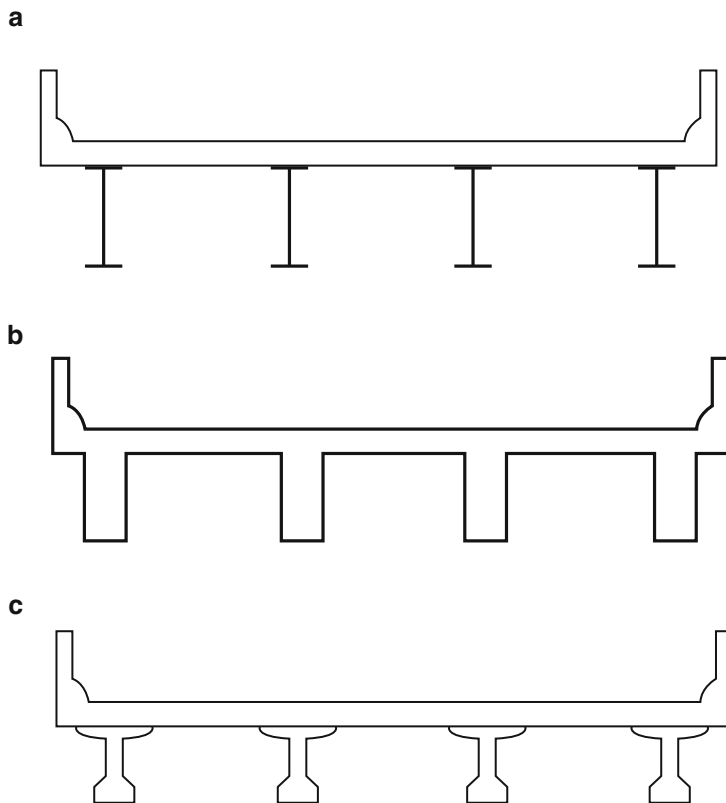


Fig. 13.13 Typical slab-stringer bridge deck cross-sections (a) Steel girders. (b) Concrete T beams. (c) Precast concrete beams

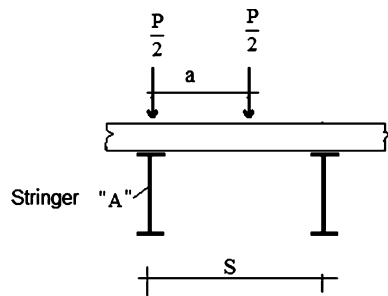


Fig. 13.14 Transverse position of vehicle wheel loads

The axle distribution factor is defined as

$$DF = \frac{1}{2} \left(2 - \frac{a}{S} \right) \quad (13.6)$$

Using this definition, the load on the stringer is represented as

$$P_{A\max} = P(DF)$$

Taking $S = 8$ ft and $a = 6$ ft, yields $P_{A\max} \approx 0.625P$

Another effect that needs to be included is impact. The loading is applied rapidly as the vehicle travels onto the bridge. A measure of the loading duration is the ratio of span length to vehicle velocity. When a loading is applied suddenly and maintained constant, the effect on the response of a structure is equivalent to the application of a static load whose magnitude is equal to twice the actual load. The concept of an impact factor is introduced to handle this effect. Intuitively one would expect this factor to be larger for short spans, i.e., to vary inversely with span length. An impact magnification factor (I) of 30 % is commonly used. With this notation, the load on the stringer is given by

$$P_{i\text{ design}} = P_i(1 + I)DF \quad (13.7)$$

where P_i is the axle load.



13.3.3.3 Uniform Live Load

Small vehicles are modeled as a uniform loading applied selectively to individual spans. The purpose of this loading is to simulate the case where a set of passenger cars is stalled in a lane on one or more spans. *One uses the influence lines for the moments at mid-span and the interior supports to establish the loading patterns for lane loads.* The loading patterns for a three-span system are listed in Fig. 13.15c, d. Loading cases 1 and 2 produce the peak positive moment at the midpoint of the interior span; cases 3 and 4 generate the peak negative moment at the interior supports.

Given the loading patterns, one generates the bending moment distribution for each loading condition and then establishes the maximum values of the positive and negative moments at the *same discrete locations* selected for the truck loading. These results define the discrete moment envelope for the structure. Four separate analyses (cases 1–4) are required to construct the discrete moment envelope corresponding to the lane loading for this three-span example.

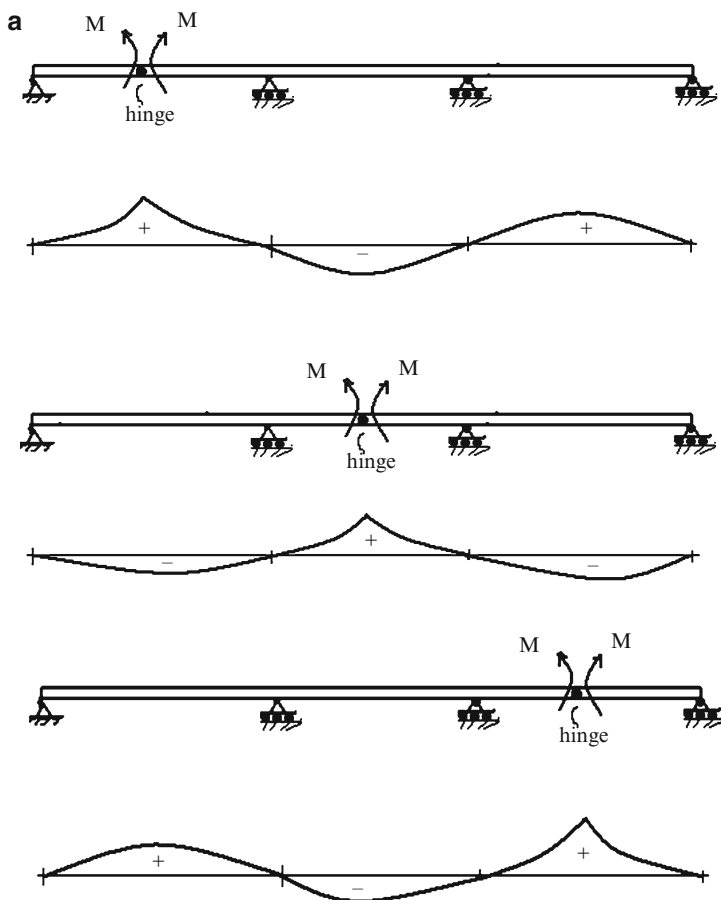
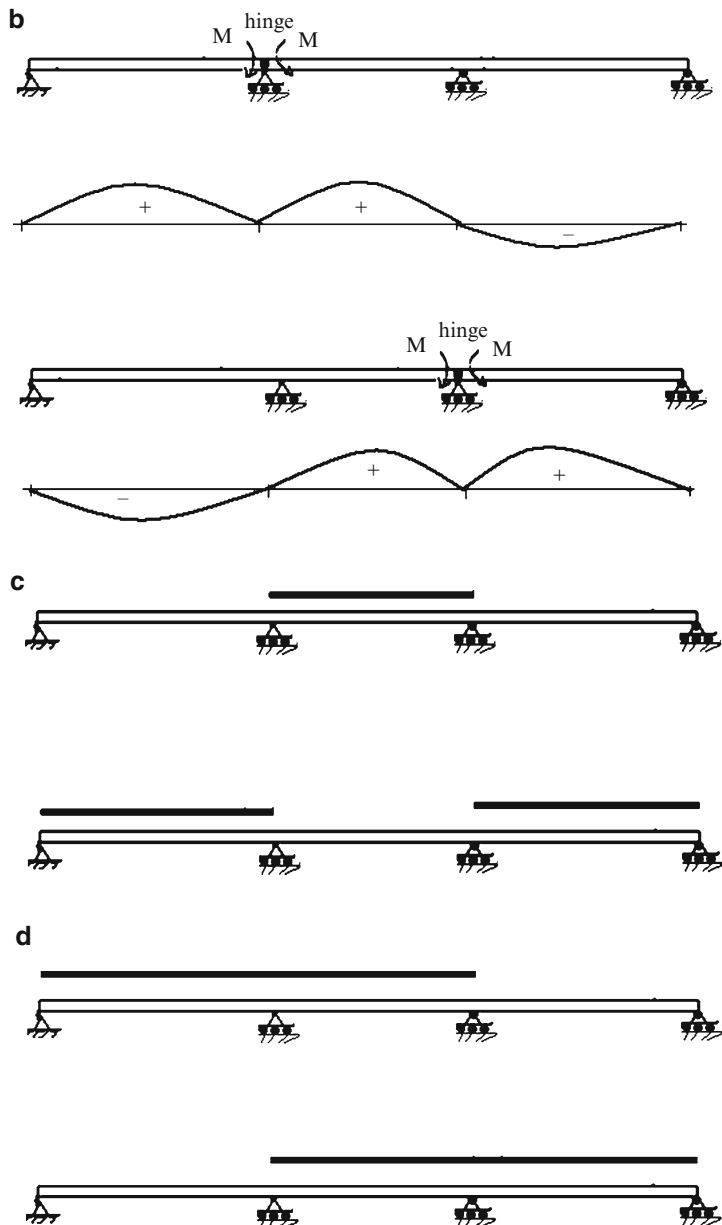


Fig. 13.15 Lane load cases—loading patterns. (a) Influence lines for positive moments at mid-spans. (b) Influence lines for negative moments at the supports. (c) Maximum positive moment at mid-spans (cases 1 and 2). (d) Max negative moments at the supports (cases 3 and 4)

13.3.4 Loading Due to Support Settlements

In addition to the gravity loading associated with the weight of the beam and vehicles, one also needs to consider the moments induced in the structure due to support settlement. This calculation is relatively straightforward. The analytical solutions for two- and three-span symmetrical beams are generated in, Examples 10.2 and 10.6. We give those results in Fig. 13.16 for convenience. Note that the peak moments are linear functions of EI .

Note that the peak moment varies as $1/L^2$. Therefore support settlement is more significant for short spans vs. long spans.

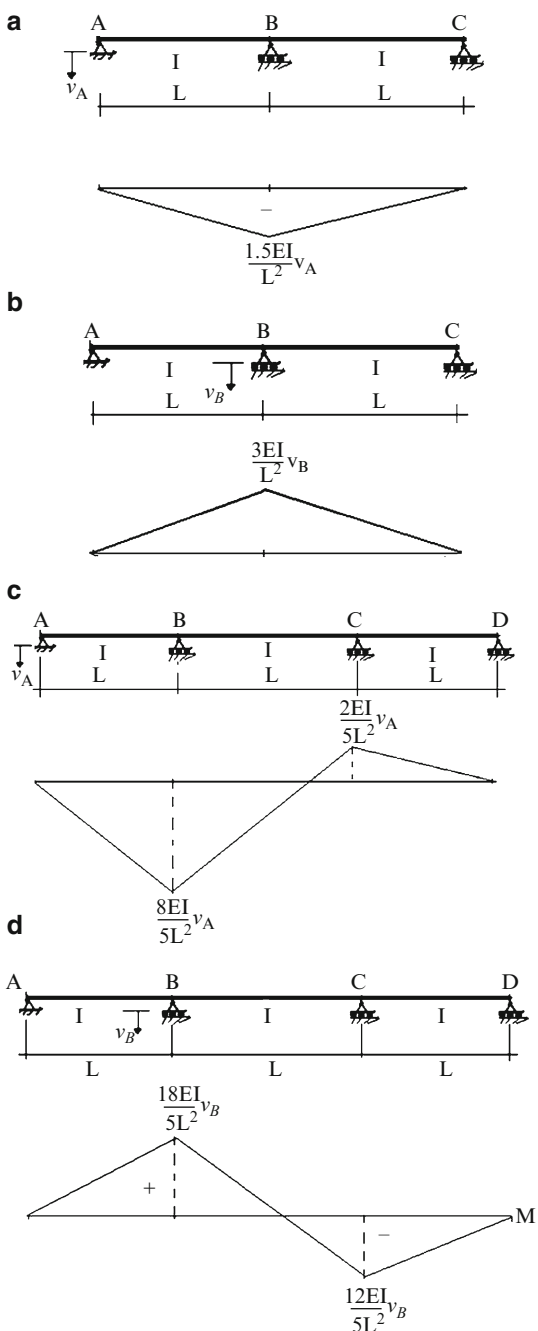
**Fig. 13.15** (continued)

Example 13.2 Effect of span length on support settlement

Given: The three-span beam shown in Fig. E13.2a. The beam properties are $E = 200 \text{ GPa}$ and $I = 9,000(10)^6 \text{ mm}^4$.

Fig. 13.16 Moments due to support settlements.

- (a) Two-span case for v_A .
- (b) Two-span case for v_B .
- (c) Three-span case for v_A .
- (d) Three-span case for v_B



Determine: The bending moment distribution due to support settlement of 25 mm at supports A and B. Consider the following cases: (a) $L = 10 \text{ m}$, (b) $L = 20 \text{ m}$

Solution: The resulting moments are plotted in Figs. E13.2b and E13.2c. These results demonstrate that the effect of support settlement is more critical for the shorter span [case (a)].

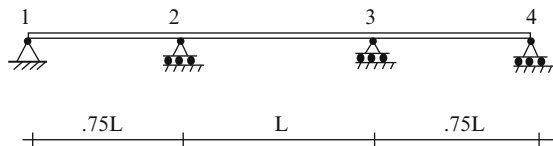


Fig. E13.2a

Case a: $L = 10 \text{ m}$

Case b: $L = 20 \text{ m}$

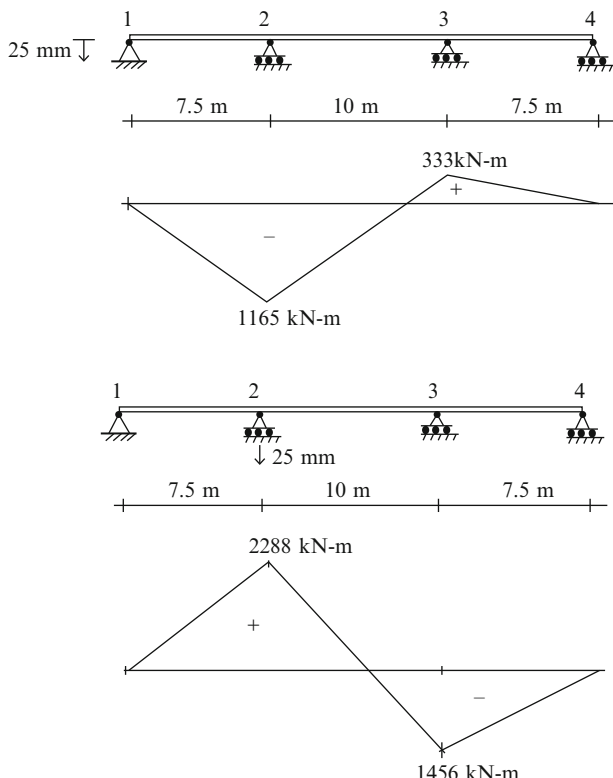


Fig. E13.2b Case a results

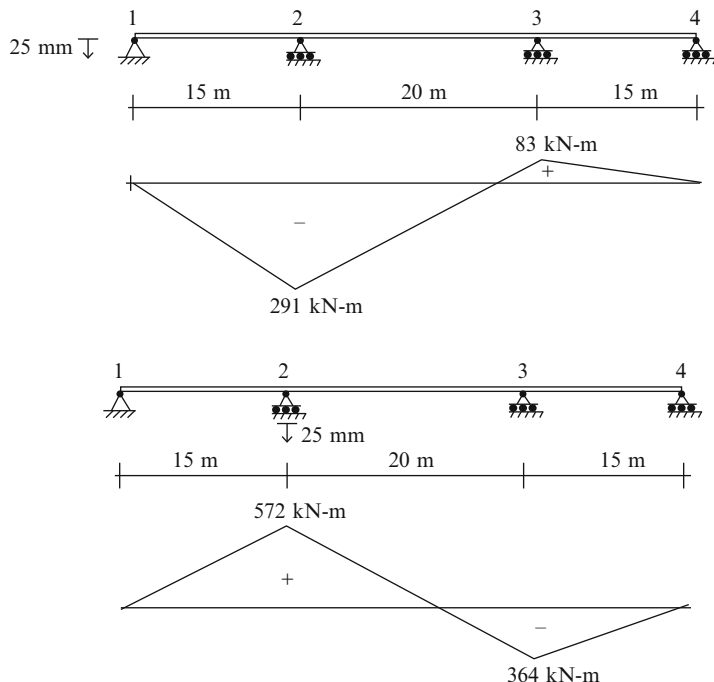


Fig. E13.2c Case b results

13.4 Case Studies

13.4.1 Case Study I: A Three-Span Continuous Girder Bridge

We illustrate the process of establishing design values using an actual bridge as a case study.

The bridge is a three-span continuous girder bridge, with spans measuring 80 ft, 110 ft, and with an overall length of 270 ft. The superstructure consists of an 8 in. thick concrete slab acting in composite with four lines of steel girders spaced at 8.67 ft on center. The girder cross-section is constant throughout the length. The deck carries two traffic lanes, continuous over the entire length of the bridge. The bearings are either hinge or roller supports. Figures 13.17 and 13.18 show

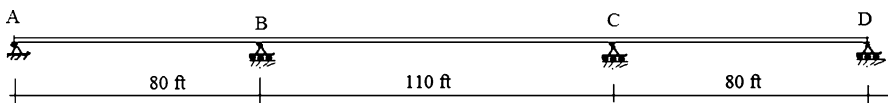


Fig. 13.17 Girder bridge system

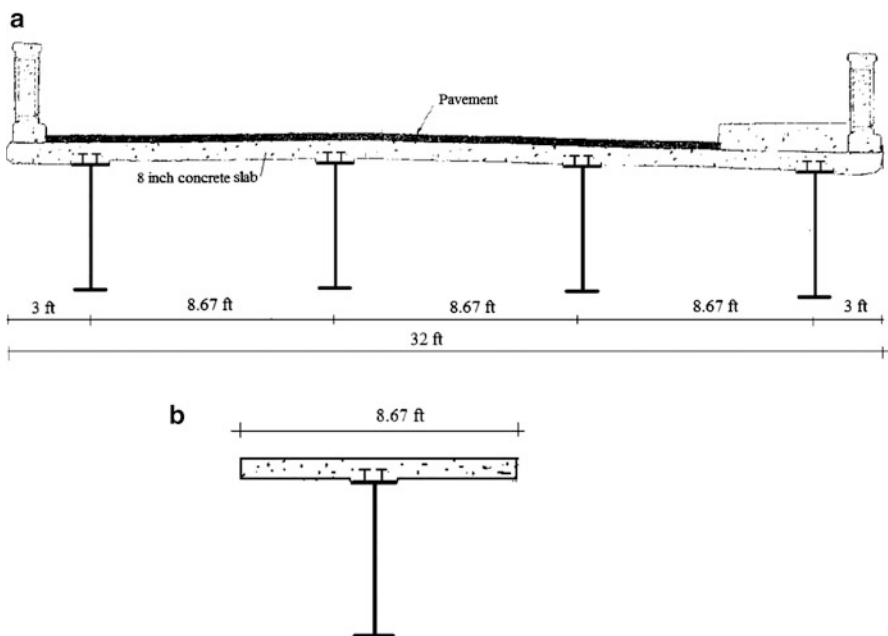


Fig. 13.18 (a) Cross-section—bridge deck. (b) Cross-section of single composite beam

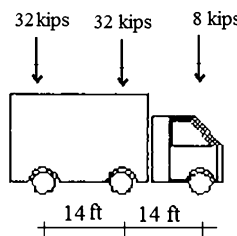


Fig. 13.19 Truck load

the makeup of the bridge system and the details of the cross-section. The bridge is modeled using an equivalent section equal to approximately one-fourth of the cross-section of the bridge (one girder plus a 8.67 ft slab). Figure 13.18b defines the model used for this analysis.

Our objectives are

1. To determine the discrete moment envelopes for truck and lane loading corresponding to a live uniform lane loading of 0.64 kip/ft and a truck loading defined in Fig. 13.19.
2. To establish the absolute peak values (positive and negative) for moment due to dead loading of 2.1 kip/ft, lane loading, and design truck loading.

Fig. 13.20 Uniform dead load pattern

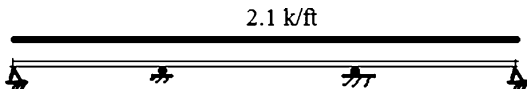
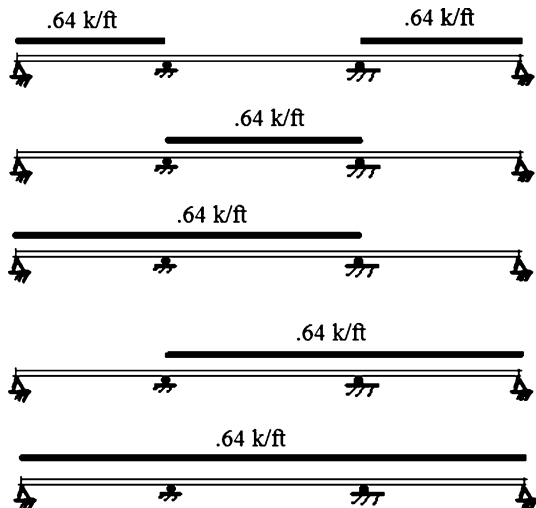


Fig. 13.21 Uniform lane load patterns for positive and negative moments



- To determine the moments due to: 1 in. settlement of support A; 1 in. settlement of support B.

Loading patterns:

The loading patterns for the uniform dead and lane loading are shown in Figs. 13.20 and 13.21.

We discretize the individual spans into ten segments, as indicated in Fig. 13.22. A computer software system is used to generate the solutions and the discrete moment envelopes. One can assume an arbitrary value for I since the moment results are independent of I .

Computer-based analysis is ideally suited for generating discrete envelopes. Certain software packages have incorporated special features that automate the process of moving the load across the span and compiling the peak positive and negative moment values at each discrete section. Both the positive and negative moment envelopes are required in order to dimension the beam cross-section.

Dead load:

The envelopes for dead load coincide with the actual moment and shear distribution shown below (Fig. 13.23).

The peak values of shear, moment, and deflection are listed below.

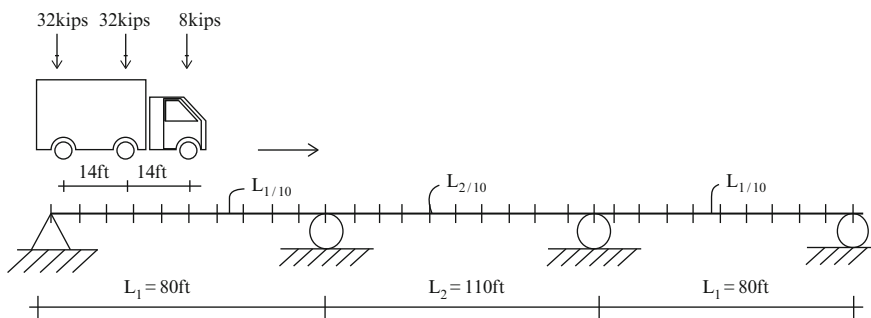
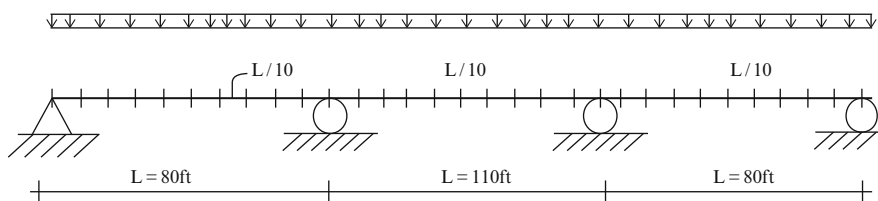
a**b**

Fig. 13.22 Span discretization for live loads. (a) Truck. (b) Lane load

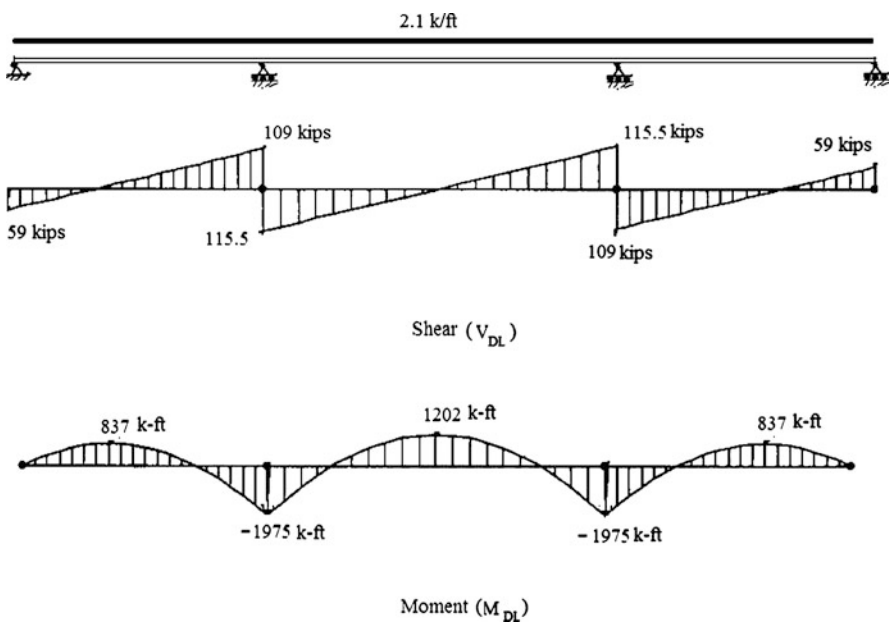


Fig. 13.23 Dead load shear and moment distributions

$$\left\{ \begin{array}{l} M_{DLmax}^- = 1,975 \text{ kip ft} \\ M_{DLmax}^+ = 1,202 \text{ kip ft} \\ V_{DLmax} = 115.5 \text{ kip} \\ \delta_{DLmax} = 1.1 \text{ in. span II} \\ \delta_{DLmax} = 1.26 \text{ in. span I or III} \end{array} \right.$$

13.4.1.1 Uniform Lane Load

The uniform load patterns defined in Fig. 13.21 are analyzed separately and the following envelopes are generated (Fig. 13.24).

13.4.1.2 Truck Loading

The truck loading defined in Fig. 13.22a is passed over the span leading to the following discrete envelopes (Fig. 13.25).

The truck loading needs to be modified to account for the distribution between adjacent stringers and impact. The final values are determined using

$$DF = \frac{1}{2} \left(2 - \frac{a}{S} \right) = \frac{1}{2} \left(2 - \frac{6}{8.67} \right) = 0.65$$

$$M_{Design, truck} = M_{LL, truck} (1 + I)DF = M_{LL, truck} 1.3(0.65) = 0.845M_{LL, truck}$$

Numerical results for the modified discrete moment envelope values at the discrete points (interval of $L/10$) are listed in Tables 13.1, 13.2, and 13.3. Note

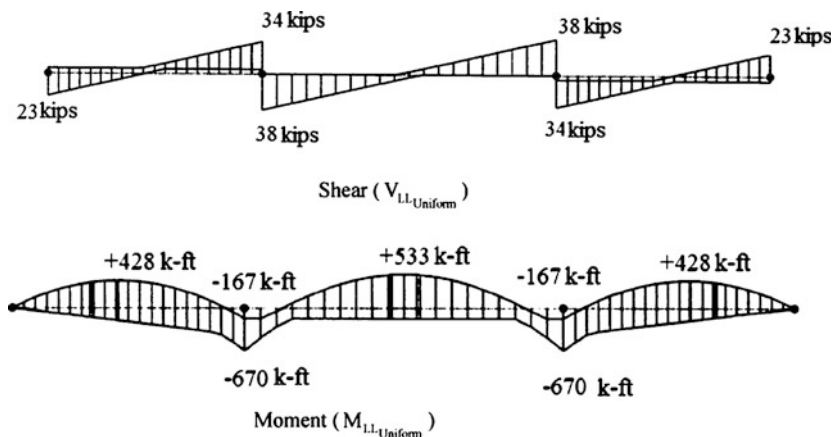


Fig. 13.24 Uniform lane load discrete envelopes

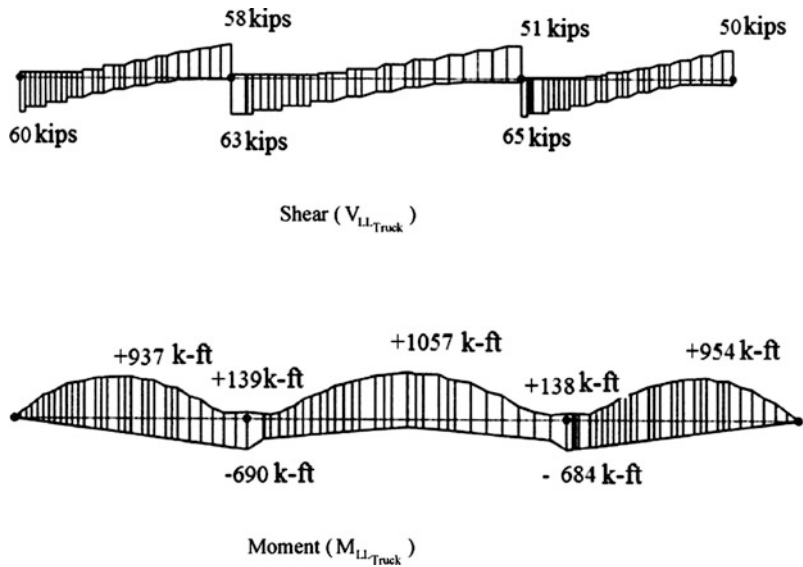


Fig. 13.25 Truck loading discrete envelopes

Table 13.1 Discrete envelope values: Span I (kip ft)

Span I					
X	M_{DL}	$M_{Design_{truck}}^+$	$M_{Design_{truck}}^-$	$M_{LL\text{ uniform}}^+$	$M_{LL\text{ uniform}}^-$
0	0	0	0	0	0
0.1L	407	344	-58	168	-43
0.2L	680	576	-117	294	-87
0.3L	819	703	-175	380	-130
0.4L	823	775	-233	425	-174
0.5L	693	792	-292	428	-217
0.6L	428	718	-350	391	-261
0.7L	29	568	-408	313	-304
0.8L	-504	357	-466	194	-348
0.9L	-1172	106	-525	34	-419
L	-1975	117	-583	-	-670

that the results for span III are similar but not identical to the results for span I. Although the structure is symmetrical, the truck loading is not symmetrical.

13.4.1.3 Support Settlement

We deal with support settlement by assuming a value for EI (in this case we take $E = 29,000$ ksi and $I = 48,110$ in.⁴). Once the actual EI is established, we scale the moment results. The corresponding moment diagrams are plotted in Fig. 13.26.

Table 13.2 Discrete envelope values: Span II (kip ft)

Span II					
X	M_{DL}	$M_{Design, truck}^+$	$M_{Design, truck}^-$	$M_{LL, uniform}^+$	$M_{LL, uniform}^-$
0	-1975	117	-583	-	-670
0.1L	-831	116	-351	-	-291
0.2L	58	430	-298	192	-167
0.3L	693	674	-247	387	-167
0.4L	1074	823	-194	495	-167
0.5L	1202	893	-144	533	-167
0.6L	107	851	-196	495	-167
0.7L	693	700	-248	378	-167
0.8L	58	454	-301	192	-167
0.9L	-831	143	-353	-	-291
L	-1975	117	-583	-	-670

Table 13.3 Discrete envelope values: Span III (kip ft)

Span III					
X	M_{DL}	$M_{Design, truck}^+$	$M_{Design, truck}^-$	$M_{LL, uniform}^+$	$M_{LL, uniform}^-$
0	-1975	167	-578	-	-670
0.1L	-1172	105	-520	34	-419
0.2L	-504	330	-462	194	-348
0.3L	29	532	-405	313	-304
0.4L	428	682	-346	391	-261
0.5L	693	777	-289	428	-217
0.6L	823	806	-232	425	-174
0.7L	819	742	-173	380	-130
0.8L	680	575	-116	294	-130
0.9L	407	334	-57	168	-43
L	0	0	0	0	0

13.4.2 Case Study II: Two-Hinged Parabolic Arch Response: Truck Loading

This study illustrates how one evaluates the behavior of a typical two-hinged arch bridge subjected to a truck loading. An example structure is shown in Fig. 13.27; the idealized model is defined in Fig. 13.28. We model the roadway as a continuous longitudinal beam supported at 10 ft intervals by axial members attached to the parabolic arch. The truck loading is transmitted through the axial elements to the arch. We generate discrete force envelopes for the arch using an analysis software system applied to the discretized model. A similar discretization strategy was employed in Chap. 6. Results for the bending moment and axial force due to the truck loading are plotted in Figs. 13.29 and 13.30. Figure 13.29 is obtained by subdividing the arch into 100 straight segments having a constant projection, Δx , of

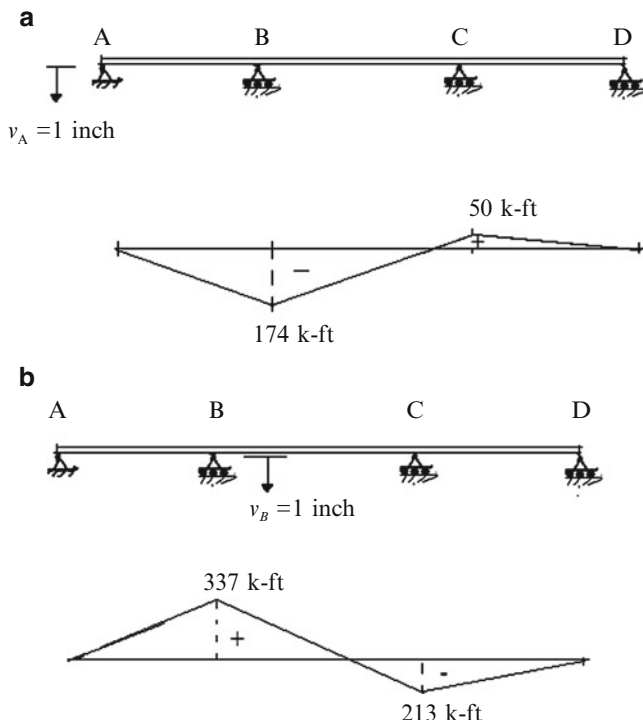


Fig. 13.26 Moment due to support settlements ($E = 29,000 \text{ ksi}$ and $I = 48,110 \text{ in.}^4$) (a) Settlement at A. (b) Settlement at B



Fig. 13.27 Two-hinged arch bridge

0.3 m. Figure 13.30 is generated by subdividing the arch into ten straight segments having a constant projection, Δx , of 3 m.

The discrete force envelope plots are useful for displaying the variation in response, e.g., the range in moment values. However, to determine the absolute extreme values, one has to scan over the data. This process leads to the following “absolute values”

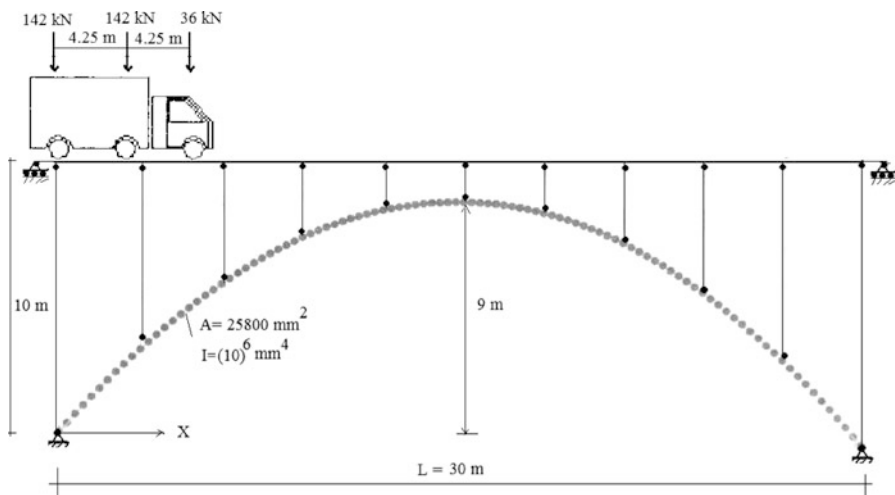


Fig. 13.28 Parabolic-arch geometry and loading-idealized model

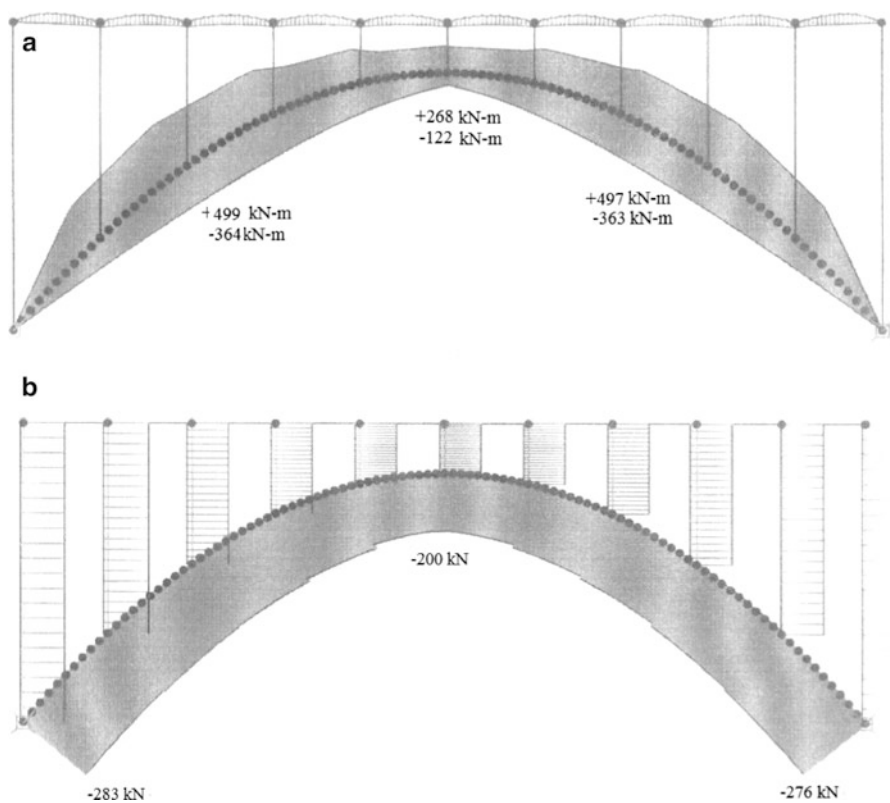


Fig. 13.29 Discrete force envelopes—Truck loading-100 straight segments. (a) Moment envelope. (b) Axial envelope

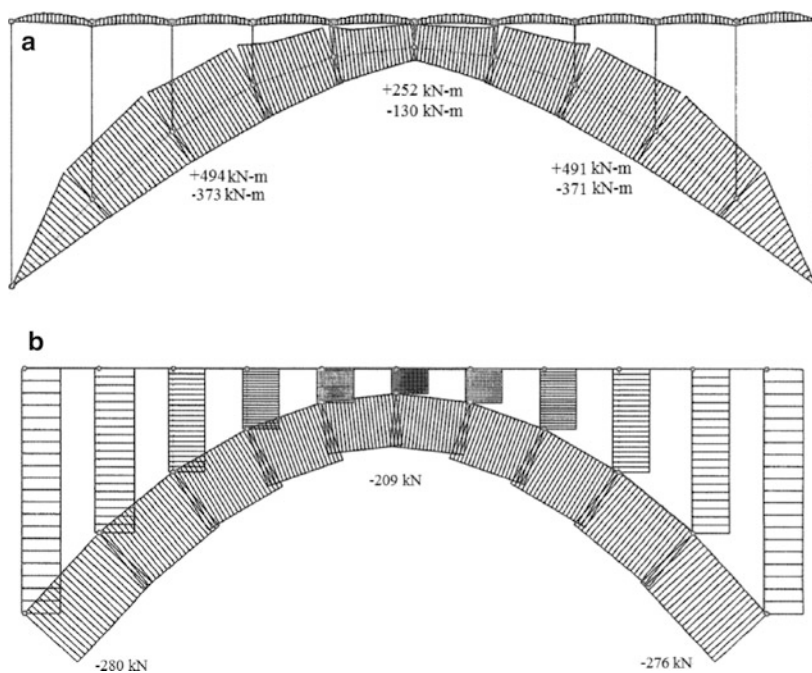


Fig. 13.30 Discrete force envelopes—Truck loading-10 straight segments. (a) Bending envelope. (b) Axial envelope

$$100 \text{ straight segment} \begin{cases} M_{\max}^+ = +499 \text{ kN m} \\ M_{\max}^- = -381 \text{ kN m} \\ P_{\max} = -283 \text{ kN} \end{cases} \quad 10 \text{ straight segment} \begin{cases} M_{\max}^+ = +494 \text{ kN m} \\ M_{\max}^- = -381 \text{ kN m} \\ P_{\max} = -280 \text{ kN} \end{cases}$$

In general, it is a good strategy to consider at least two discretizations. In this example, we observe that the ten segment model produces quite reasonable results.

13.4.3 Case Study III: Three-Span Parabolic Arch Response: Truck Loading

We consider next the three-span arch system shown in Fig. 13.31. The span lengths, discretizations, and the truck loading are the same as for case study I. It is of interest to compare the peak values of the force envelopes for the two different structural models. The discretized model consists of straight segments having a constant horizontal projection of 1 ft. A computer software package was used to generate the corresponding discrete force envelopes which are plotted in Figs. 13.32 and 13.33.

Comparing the moment envelopes for the arch and the girder, we note that arch system has lower peak moment values. However, the arch system has axial forces

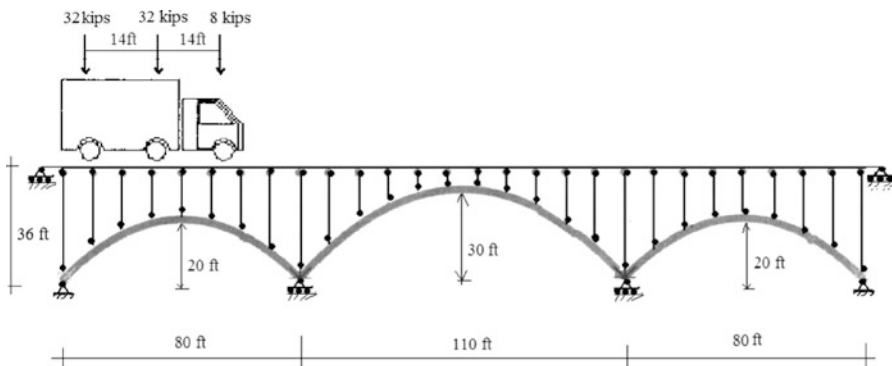


Fig. 13.31 Idealized model—three-span arch

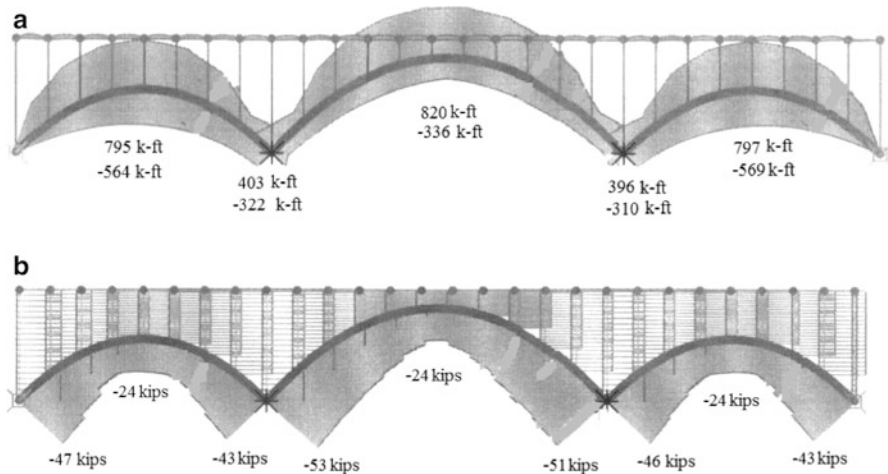


Fig. 13.32 Discrete force envelopes—three-span arch. (a) Moment envelope—three-span arch. (b) Axial envelope—three-span arch

so that the cross-section must be designed for combined bending and axial action. There are no axial forces in the girder system, just pure bending.

13.4.4 Case Study IV: Cable-Stayed Bridge

This case study concerns the cable-stayed bridge concept, a type of structure that requires some special modeling strategies and exhibits a completely different behavioral pattern than girder and arch-type structures. It has evolved as the dominant choice for long span crossings. A typical configuration is shown in Fig. 13.34. The terms “harp” and “fan” refer to the positioning of the cables on the tower. A modified fan arrangement is usually adopted to avoid congestion on the tower.

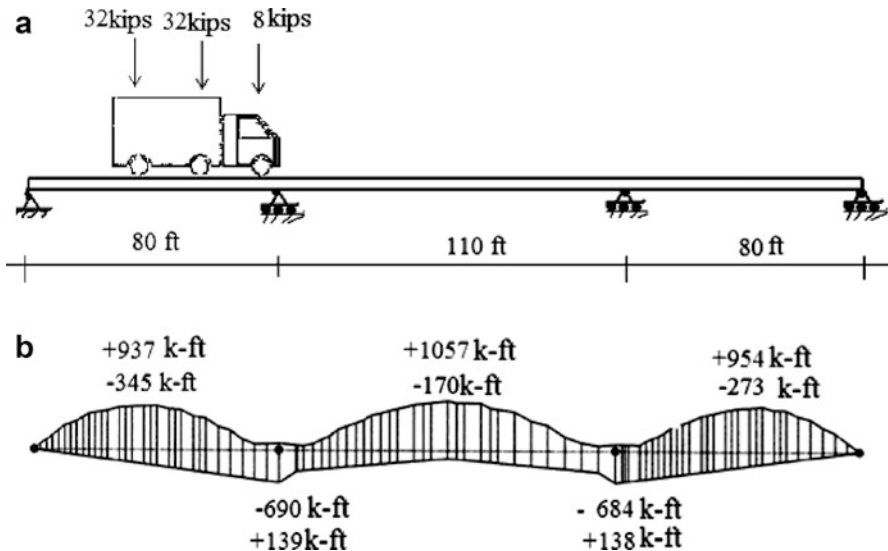


Fig. 13.33 Discrete force envelope- three-span girder. (a) Geometry and loading. (b) Moment envelope



Fig. 13.34 Typical cable-stayed scheme

Of particular interest is the load path for vertical loading applied to the girder. Without the cables, the girder carries the load by bending action throughout the total span. Since the maximum moment varies as to the square of the span length, this structural concept is not feasible for long spans. The effect of the cables is to provide a set of vertical supports to the girder, thus reducing the moment in the girder. In what follows we illustrate this effect using the idealized structure shown in Fig. 13.35

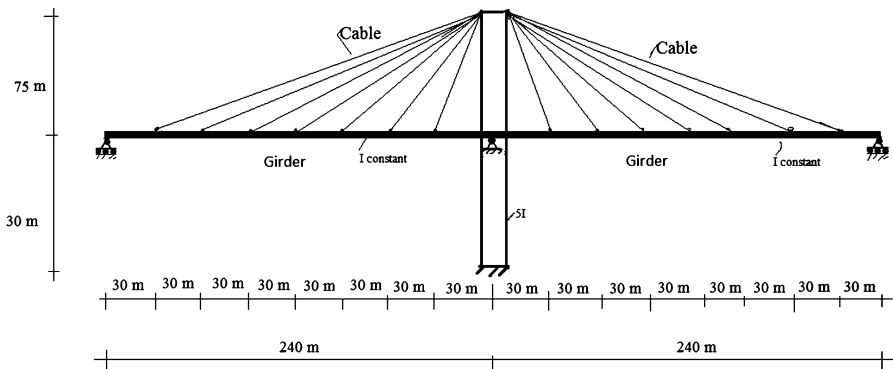
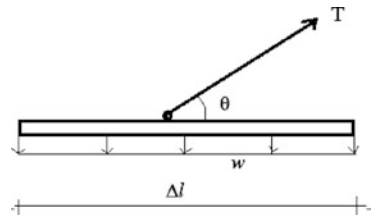


Fig. 13.35 Idealized cable-stayed scheme

Fig. 13.36 Tributary area for cable



We suppose the girder is continuous, and the cable layout is symmetrical (equally spaced on the longitudinal axis). There are seven pairs of symmetrical cables. Each cable has a different cross-sectional area. The girder is hinged at the tower, but free to expand at the two end supports. We model the cables as straight members that are hinged at their ends to the tower and the girder. In this way, they function as axial elements and transmit the gravity loading applied to the girder up to the tower. The net effect is to reduce the bending moment in the girder.

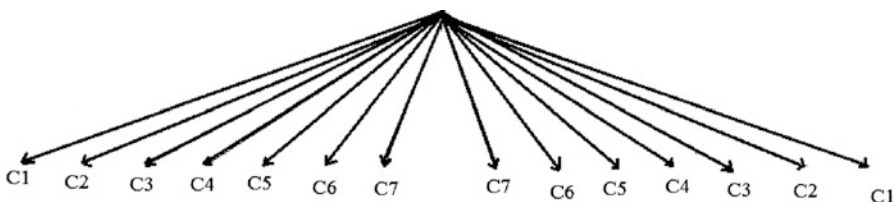
Starting with nodes at the supports and the cable-girder intersection points, one may also discretize the girder between the cable nodes to obtain more refined displacement and moment profiles. Since the structure is indeterminate, we need to specify member properties in order to execute an analysis. We estimate the cable areas by assuming an individual cable carries the tributary loading on a segment adjacent to the cable. This estimate is based on strength.

$$A_C = \frac{T}{\sigma_{\text{all}}} = \frac{w\Delta l}{\sigma_{\text{all}} \sin \theta}$$

where σ_{all} is some fraction of the yield stress and Δl is the cable spacing. This equation shows that the required area increases with decreasing θ . Therefore, one must increase the cable area as the distance from the tower increases. A lower limit on θ is usually taken as 15° (Fig. 13.36).

Taking $w = 10 \text{ kN/m}$, $\Delta l = 30 \text{ m}$, and $\sigma_{\text{all}} = 0.69 \text{ kN/mm}^2$ leads to the estimated cable areas listed below.

Cable	θ°	$\frac{1}{\sin \theta}$	$A_{\text{cable}} (\text{mm}^2)$
C1	19.6	3	1,305
C2	22.6	2.3	1,130
C3	26.5	2.2	957
C4	32	1.9	827
C5	39.8	1.6	696
C6	51.3	1.3	566
C7	68.2	1.1	480



We estimate I for the girder by assuming the bending moment diagram is similar to the distribution for a uniformly loaded multi-span beam. The peak negative moment for this case is $w(\Delta l)^2/12$. Given these estimated properties, one analyzes the structure and iterates on the properties until the design requirements are satisfied.

Figure 13.37 shows the forces and displacement profile corresponding to $I_{\text{girder}} = 420(10)^6 \text{ mm}^4$ and the following set of cable areas for cables 1–7, respectively (1,305, 1,130, 957, 827, 696, 566, and 480 mm^2). The girder cross-sectional area is taken as 120,000 mm^2 . Note that the bending moment diagram for the girder is similar to that observed for a multi-span uniformly loaded beam. We also point out that the response is sensitive to the girder cross-sectional area since there is significant compression in the girder.

An estimate of the vertical displacement based on the axial force corresponding to strength is given by

$$v = \frac{\sigma L}{E \sin \theta}$$

The displacement profile for the girder agrees with this approximation. The peak value occurs for the outermost cable which has the largest L and smallest angle.

A suggested peak value for displacement under live load is $L/800$, which for this geometry translates to 300 mm. We can decrease the deflection by increasing the areas for the outer cables. Assuming an individual cable act as a single vertical

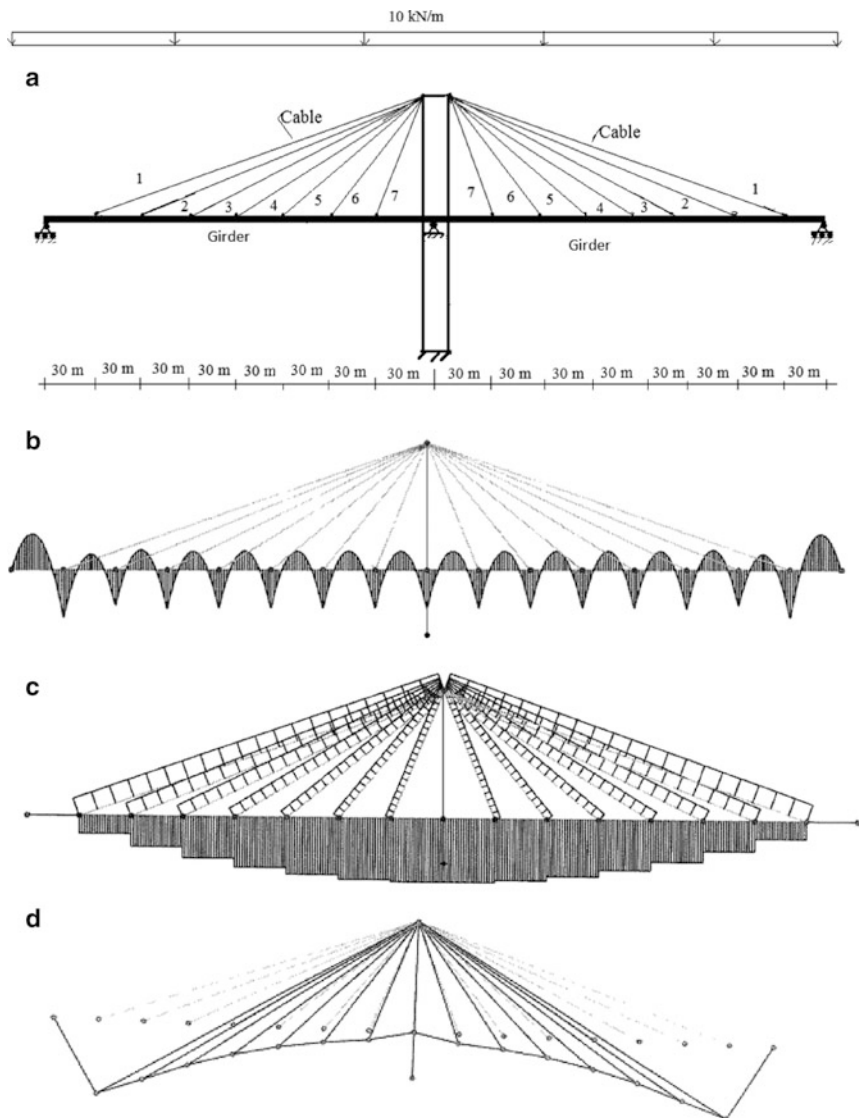


Fig. 13.37 Force and displacement profiles. (a) Geometry and loading. (b) Moment in girder. (c) Axial forces in cables and girder. (d) Displacement profile of girder

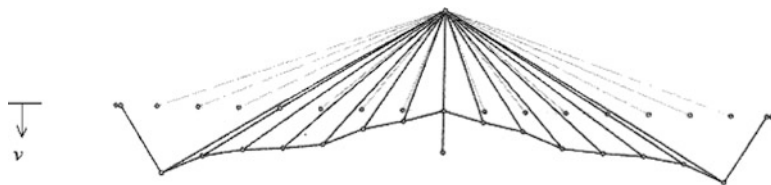


Fig. 13.38 Final displacement profile of girder

spring subjected to the loading $w(\Delta l)$, and requiring the displacement to be equal to v_{all} leads to the following estimate for the cable area

$$A_c = \frac{w(\Delta l)L_c}{v_{\text{all}}E\sin\theta}$$

where L_c is the cable length. Holding the girder properties constant, we use this approximate expression to increase the cable areas to (14,000, 11,500, 8,500, 5,000, 3,000, 3,000, 2,000 mm²) and repeat the analysis. The displacement profile of the girder for this case is plotted in Fig. 13.38 and also summarized in the table listed below. Note that the displacement is sensitive to the cable area and the angle of inclination; the cable tension is governed primarily by strength. This case study illustrates the role of computer simulation in developing the design of cable-stayed structures. One refines the design through iteration. This example also illustrates how cable-stayed structures carry the load primarily through axial action in the cables. The girder functions mainly to transmit the deck loading to the cables, i.e., the bending is localized between the cable support points.

Cable	A_{cable} (mm ²)	Tension (kN)	$v \downarrow$ (mm)	A_{cable} (mm ²)	Tension (kN)	$v \downarrow$ (mm)
C1	1,305	914	2,382	14,000	998	297
C2	1,130	810	1,864	11,500	761	217
C3	957	665	1,341	8,500	675	186
C4	827	567	940	5,000	566	176
C5	696	467	630	3,000	467	157
C6	566	387	428	3,000	386	86
C7	480	315	287	3,000	386	48

13.5 Summary

13.5.1 Objectives

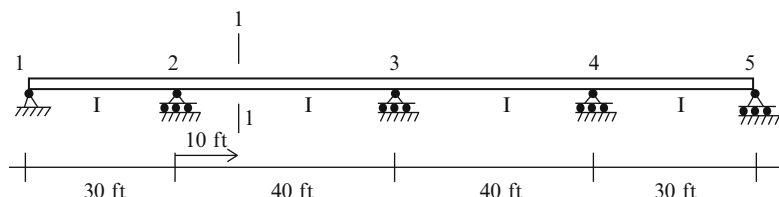
- To present Müller-Breslau principle and illustrate how it is used to establish loading patterns that produce the maximum value of a force quantity at a particular point on a structure.
- To describe a procedure for determining the load on an individual stringer due to an axle load applied to the deck of a slab-stringer bridge system.
- To describe and illustrate a computer-based procedure for generating global force envelopes for indeterminate horizontal structures subjected to a set of concentrated loads.
- To illustrate the different behavioral patterns for multi-span girder, arch and cable-stayed systems.

13.5.2 Key Facts and Concepts

- Müller-Breslau principle is used to establish influence lines for indeterminate structures. One works with a structure generated by removing the constraint provided by the force quantity. The deflected shape of the structure due to a unit value of the force quantity is a scaled version of the influence line.
- The global moment envelope for a horizontal structure is generated by applying the loading at discrete points on the longitudinal axes, tabulating the bending moment at each discrete point for all the loading cases, and selecting the largest positive and negative values .A computer-based procedure is used for this task.
- Support settlement can produce bending moments which are significant for short span bridges.

13.6 Problems

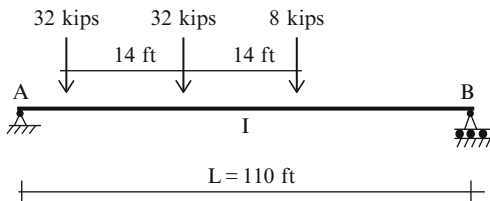
Problem 13.1



- (a) Using Müller-Breslau principle, sketch the influence lines for the vertical upward reaction at support 3 (R_3), the negative moment at support 2 (M_2), and the negative moment at section 1-1 (M_{1-1})
- (b) Use a software package to determine:
- The maximum values of R_3 , M_2 , and M_{1-1} caused by a uniformly distributed dead load of 2 kip/ft.
 - The maximum value of M_2 caused by a uniformly distributed live load of 1 kip/ft.

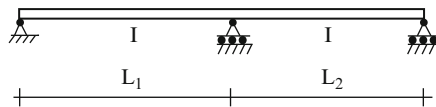
Problem 13.2

Consider the single span bridge shown below. Using the analytical procedure described in Sect. 3.10.3.2, determine the absolute maximum value of moment developed as the truck loading defined below passes over the span. Repeat the analysis using computer software.



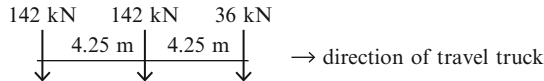
Problem 13.3

Consider the following set of span lengths. Use computer software to determine global moment envelopes for the lane and truck loadings defined below.

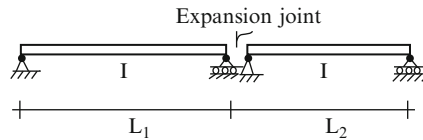


Lane load: $w = 10 \text{ kN/m}$ uniform

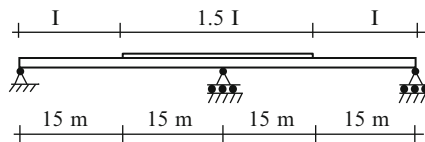
Truck load:



- $L_1 = L_2 = 30 \text{ m}$, EI is constant
- $L_1 = 15 \text{ m}$ $L_2 = 30 \text{ m}$, EI is constant
- $L_1 = L_2 = 30 \text{ m}$, EI is constant

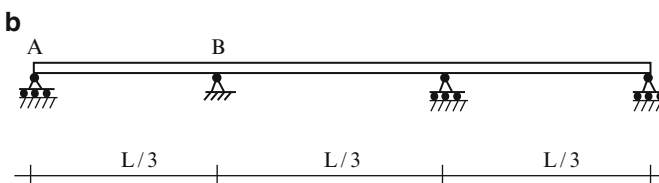
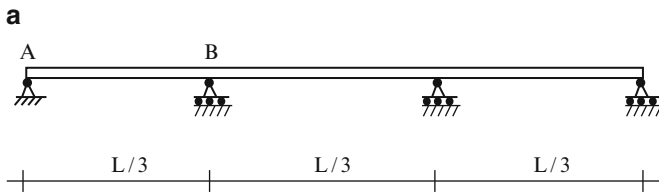


- (d) Compare the global moment envelopes for the structure shown below with the envelopes generated in part (a). Is there any effect of varying I ?



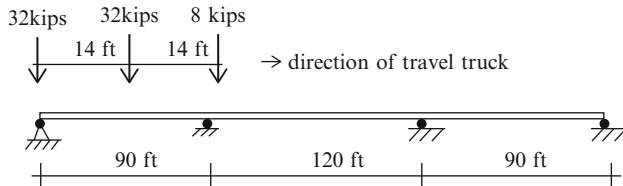
Problem 13.4

Consider the multi-span bridge shown below. Suppose the bridge is expected to experience a temperature change of ΔT over its entire length. Where would you place a hinge support: at A or at B? Determine the end movement corresponding to your choice of support location.



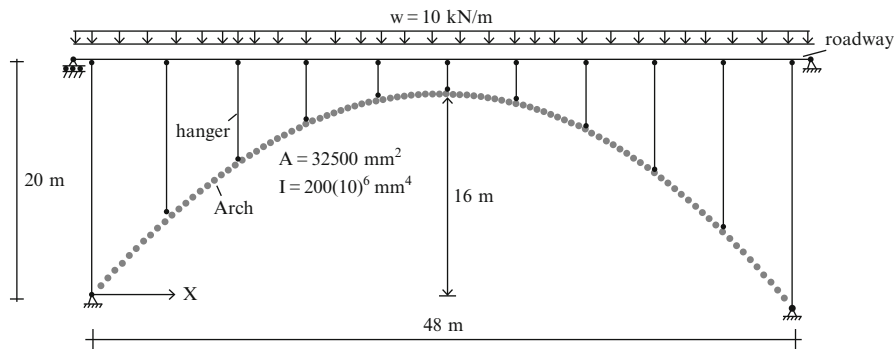
Problem 13.5

Most design codes limit the deflection due to live loading to some fraction of length, say L/α , where α is on the order of 500. Generate the global “deflection” envelope for the multi-span beam and truck loading shown below. Take $E = 29,000$ ksi and $I = 60,000$ in.⁴



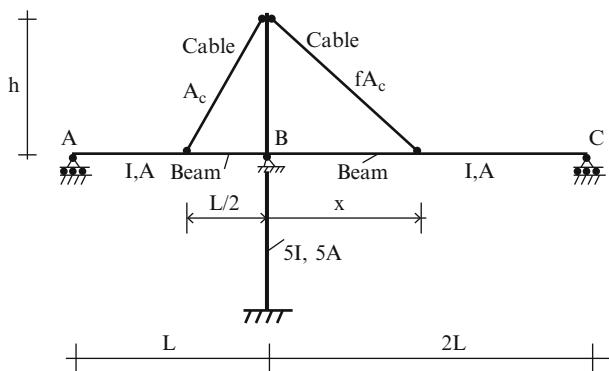
Problem 13.6

Investigate convergence of the internal forces for the parabolic arch shown as the discretization is refined. Take the interval as 2.4, 1.2, and 0.6 m.



Problem 13.7

Suppose a uniform loading is applied to span ABC. Investigate how the response changes as x varies from $L/2$ to L . Take $h = L/2$, $A = 50 \text{ in.}^2$, $A_C = 2 \text{ in.}^2$, $w = 1 \text{ kip/ft}$, $f = 1 + (2x/L)^2$.

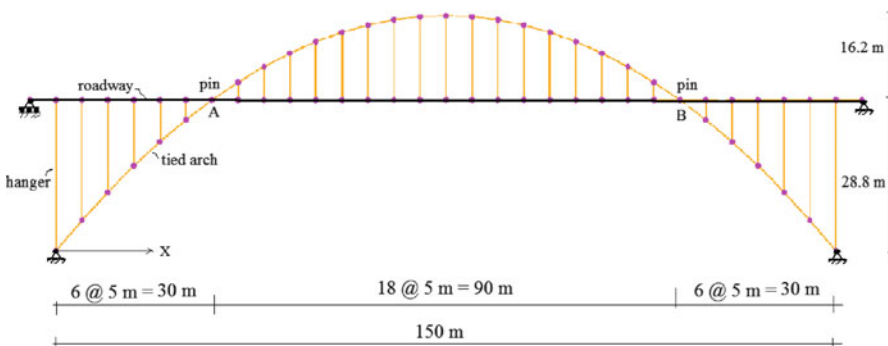


Problem 13.8

Determine the structural response (forces and displacements) of the idealized tied arch shown below under a uniformly distributed gravity load of 30 kN/m. arch

Assume $A_{\text{arch}} = 26,000 \text{ mm}^2, I_{\text{Arch}} = 160(10)^6 \text{ mm}^4, A_{\text{hanger}} = 2(10)^6 \text{ mm}^2$

Note: roadway girder and arch are pinned to together at points A and B.



An actual structure is shown below.

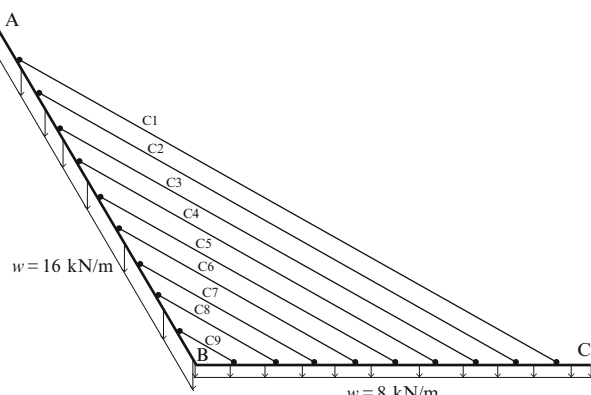
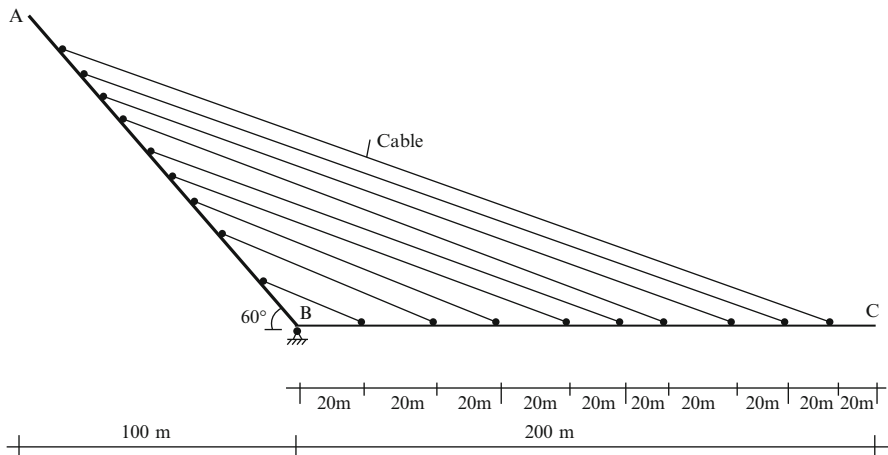


Problem 13.9

Determine the distribution of internal forces and displacements for the cable-stayed structure shown below. Member AB acts as counterweight for loading applied on member BC. The two members are connected by nine parallel equally spaced cables. Self-weight of members AB and BC is 16 and 8 kN/m, respectively. Assume $A_{\text{Cable}} = 50,000 \text{ mm}^2$ and $E = 200 \text{ GPa}$. Consider the following cases:

- $I_{AB} = I_{BC} = 40(10)^9 \text{ mm}^4$
- $I_{AB} = 4I_{BC}$ $I_{BC} = 40(10)^9 \text{ mm}^4$
- Uniform live load of 2 kN/m applied to member BC in addition to self-weight.

$$I_{AB} = 4I_{BC} \quad I_{BC} = 40(10)^9 \text{ mm}^4$$

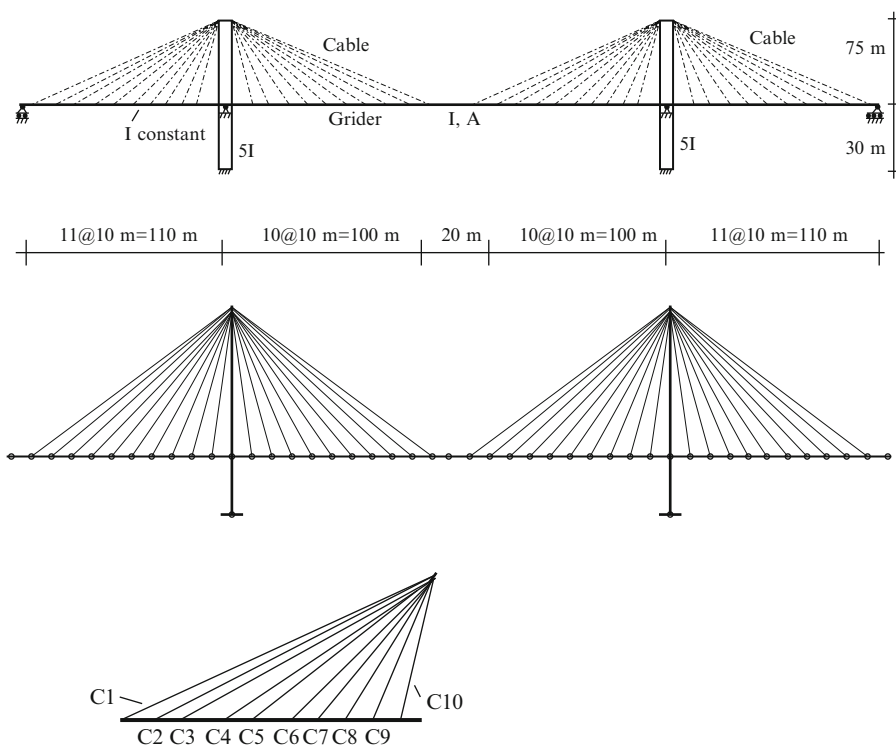


An illustration of this structural concept created by Santiago Calatrava is shown below. This bridge is located in Seville Spain.



Problem 13.10

Consider the symmetrical cable structure shown below. Determine a set of cable areas ($C_1 - C_{10}$) such that the maximum vertical displacement is less than 375 mm under a uniformly distributed live load of 10 kN/m. Assume $I_{\text{girder}} = 400(10)^6 \text{ mm}^4$, $A_{\text{girder}} = 120(10)^3 \text{ mm}^2$. Take the allowable stress as 700 MPa.



Overview

Buildings are complex physical systems. Structural Engineers deal with this complexity by creating idealized structural models that define the key structural components, the overall makeup of the building structure, and the loadings that it needs to withstand. The information provided by the idealized model allows one to apply analysis and design methods directly to the model and then extrapolate the results to the actual building.

We begin the chapter with a description of the various types of building systems and the associated structural components. In general, a building consists of plane frame structures which are interconnected by floor systems. We describe approaches for establishing the *lateral loads* due to wind and earthquake excitation. These loads are evaluated at each floor level and then distributed to the individual plane frames using the concepts of center of mass and center of twist. At this point, one has the appropriate lateral loading to analyze the plane frames. The topic of loading on building frames is discussed further in the next chapter where we also consider gravity loads acting on the floor systems.

14.1 Types of Multistory Building Systems

The majority of the activities in Structural Engineering are concerned with the design of Structural Systems for buildings. Approximately 95% of the building inventory consists of buildings having less than ten stories. Buildings of this type are classified as low-rise buildings. Figure 14.1 illustrates the typical makeup of a low-rise building. The primary structural components are beams, columns, and floor plates. Members are usually arranged in an orthogonal pattern to form a three-dimensional framework. Plate-type elements span between the beams to form the flooring system. We visualize the three-dimensional (3D) framework to be composed of plane frames which are connected by floor plates. This interpretation allows us to analyze the individual plane frames rather than the complete 3D structure.

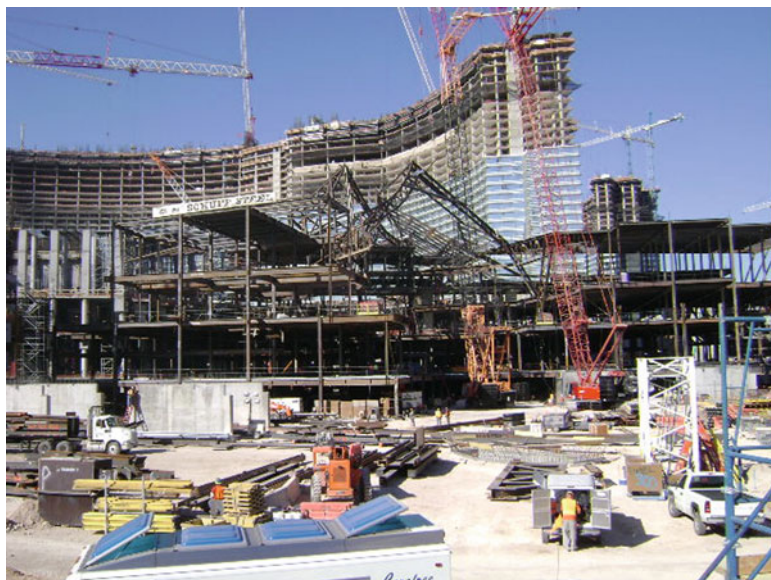


Fig. 14.1 Typical makeup of a structural system for a low-rise building

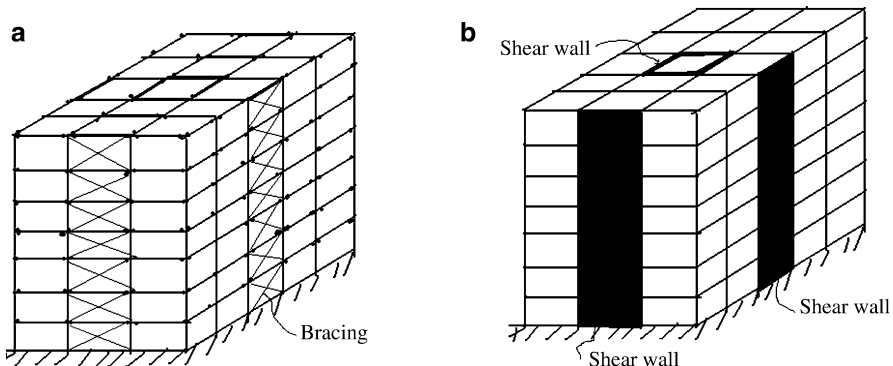


Fig. 14.2 (a) Steel braced frame with bracing. (b) Concrete frame with shear walls

Frames are designated according to how the beams and columns are interconnected at their end points. When the members are rigidly connected so that no relative rotation can occur, end moments develop under loading and the frame is said to be “rigid.” Rigid frames may employ either Steel or Concrete construction.

The opposite case is when the beams are pinned to the columns. No end moments are developed and the frame behaves similar to a truss. Some form of bracing is needed since a rectangular pinned frame is unstable under lateral load. These structures are called “braced” frames. Figure 14.2a shows a typical braced frame structure. The bracing consists of sets of diagonal elements placed within certain bays and extending over the height of the structure. This system is designed

to carry all the lateral loading. Note that at least two orthogonal bracing systems are needed to ensure stability under an arbitrary lateral loading. Braced frames are constructed using steel components.

Depending on the magnitude of the lateral loading, lateral stiffness systems may also be incorporated in rigid frames to carry a fraction of the lateral loading. For concrete rigid frames, the stiffening is achieved by incorporating shear walls located either within or on the exterior of the building and extending over the entire height. Figure 14.2b illustrates this scheme. These walls function as cantilever beams and provide additional lateral restraint. For steel rigid frames, the stiffening system may be either a concrete shear wall or a diagonal steel member scheme.

14.2 Treatment of Lateral Loading

Lateral loading may be due to either wind or earthquake acting on the building. These actions may occur in an arbitrary direction. For rectangular buildings, such as shown in Fig. 14.3, the directions are usually taken normal to the faces. One determines the component of the resultant force for each direction. Figure 14.4 illustrates this approach.

The resultant force is distributed to the individual floors and then each floor load is distributed to the nodes on the floor. This process leads to a set of nodal forces acting on the individual frames. We express the force acting at floor j of frame i as

$$P_x|_{\text{frame } i \text{ floor } j} = f_{ij} R_x \quad (14.1)$$

How one establishes f_{ij} is discussed in Sect. 14.3.

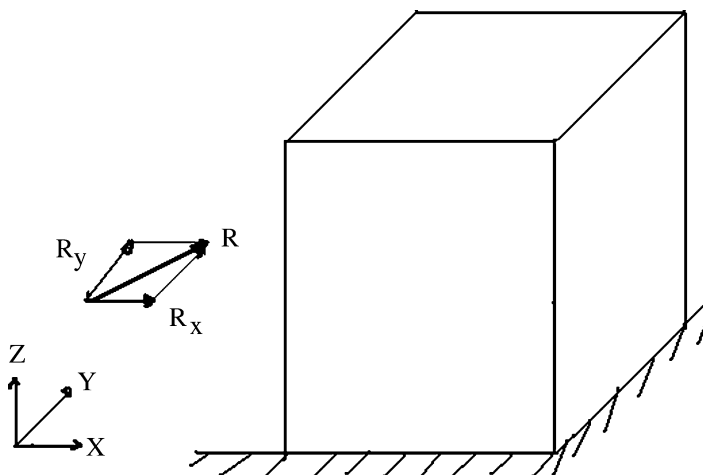


Fig. 14.3 Rectangular building

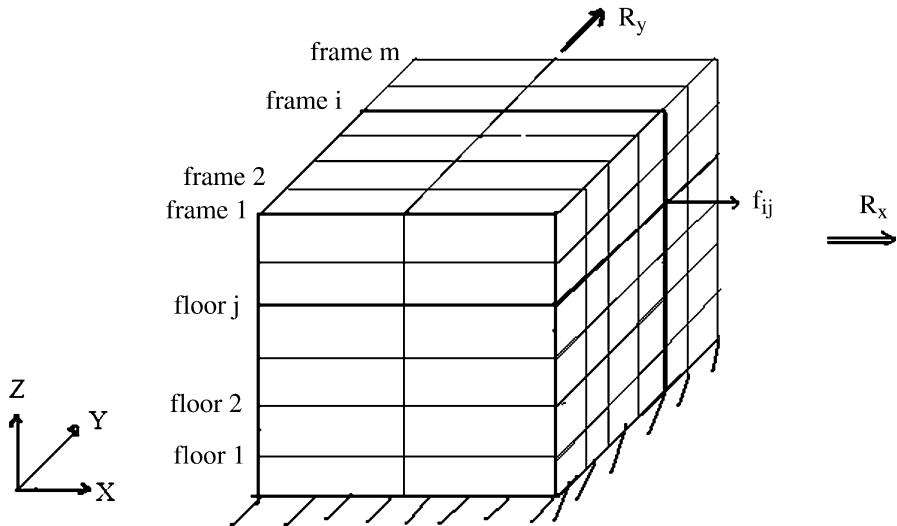


Fig. 14.4

14.2.1 Wind Loading

We suppose the wind acts in the x direction, as shown in Fig. 14.5a. The normal pressure varies in the vertical direction according to a power law (e.g., $p \sim z^{1/7}$). We approximate the distribution with a set of step functions centered at the floor levels and generate the resultant force for each floor by integrating over the tributary area associated with the floor. This process is illustrated in Fig. 14.5b, c. The individual floor forces are given by

$$P_i = p(z_i) \left[\frac{z_{i+1} - z_i}{2} + \frac{z_i - z_{i-1}}{2} \right] B = p(z_i) \left[\frac{z_{i+1} - z_{i-1}}{2} \right] B \quad (14.2)$$

$$i = 1, 2, \dots, n$$

This computation is repeated for wind acting in the Y direction. It remains to distribute the loads acting at the floor levels of the facade to nodes of the individual plane frames. The final result is a set of lateral nodal loads for each plane frame.

The underlying strategy for this approach is based on analyzing plane frames vs. a three-dimensional system. This approach works when the structural geometry is composed of parallel plane frames which produce an orthogonal pattern of columns and beams. If the structural geometry is irregular, one has to analyze the full 3D structural system. In this case, one subdivides the façade area into panels centered on the structural nodes contained in the façade area and generates the force for structural node j with

$$P_j = p(z_j) A_j \quad (14.3)$$

where A_j is the tributary area for structural node j .

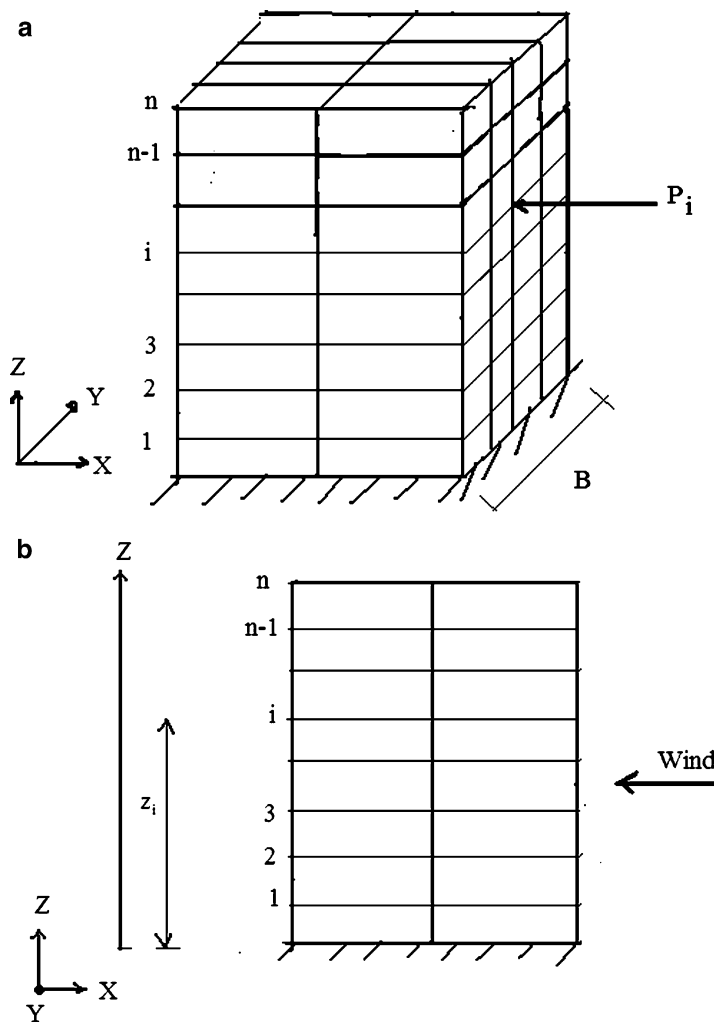


Fig. 14.5 Lateral floor forces due to wind pressure. (a) Wind in X direction. (b) Wind on $Y-Z$ face. (c) Floor loads due to wind load on $Y-Z$ face

14.2.2 Earthquake Loading

Seismic loading is generated by an earthquake passing through the site. An earthquake is the result of slippage between adjacent tectonic plates which releases energy in the form of pressure waves that produce both horizontal and vertical ground motion. For civil structures, in seismically active regions, the horizontal motion produces the most critical lateral loading since the design of civil structures is usually controlled by vertical gravity loading. Data on earthquake ground motion is continuously collected and distributed by the US Geological Survey National Earthquake Information Center [17]. Figure 14.6 contains a typical

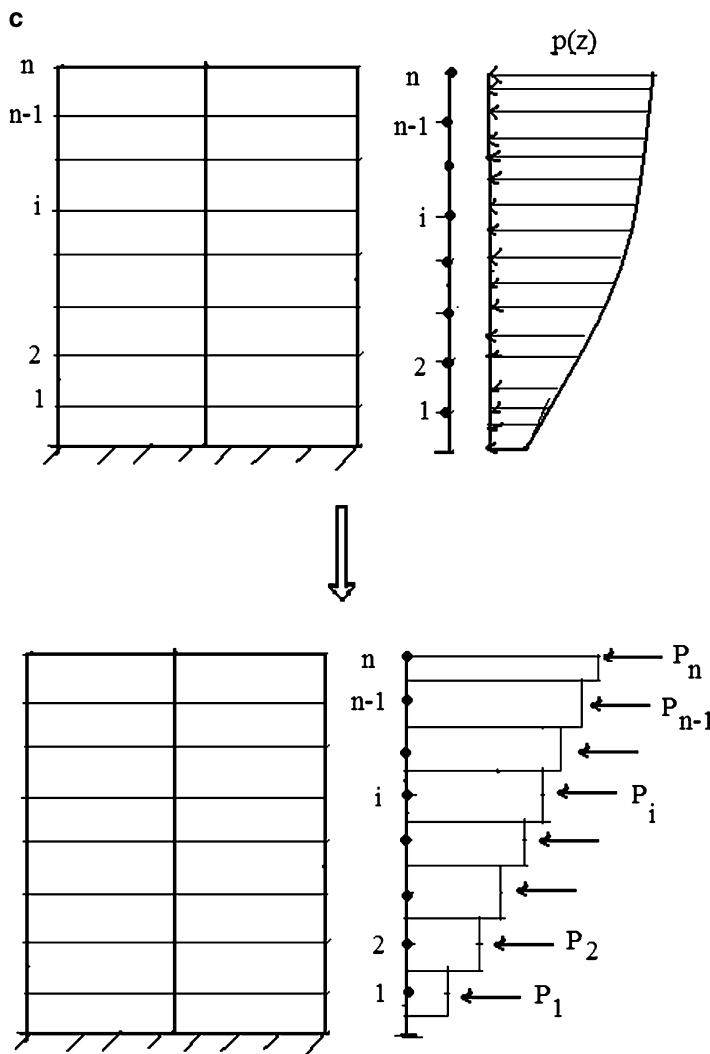


Fig. 14.5 (continued)

plot of ground acceleration vs. time for the 1994 Northridge California earthquake. The information of interest is the peak ground acceleration, denoted as pga, with respect to g , the acceleration due to gravity. In this case, the pga is equal to $0.6g$. We point out that seismic loading is cyclic, of varying amplitude, and of short duration, on the order of 20–30 s for a typical earthquake.

Seismic loading is discussed in Sect. 1.3.6. We briefly review the important features of seismic loading here and then describe how one uses this information to generate the lateral loading for a building. The lateral forces produced by the horizontal ground motion require the incorporation of lateral bracing systems. Structures located in high

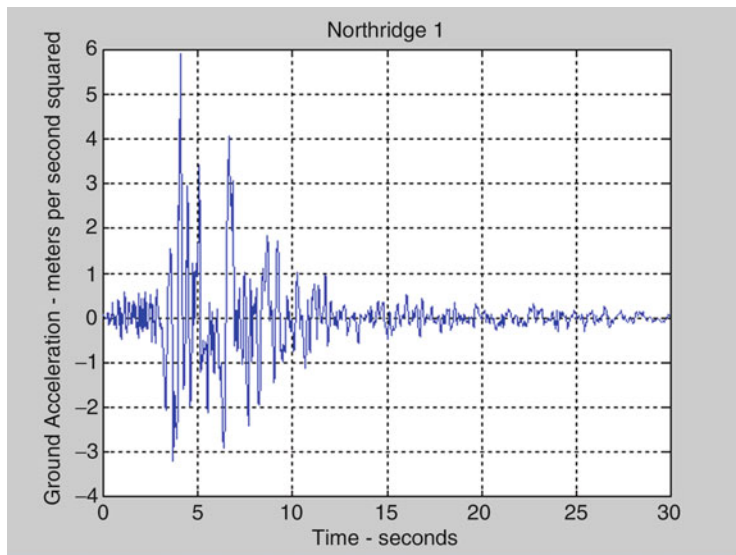
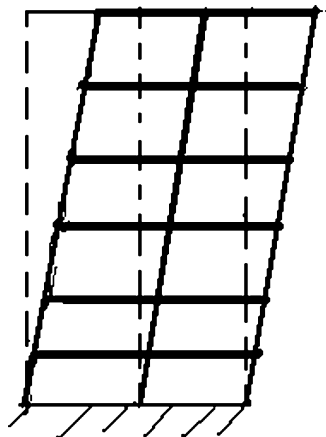


Fig. 14.6 Ground acceleration time history—Northbridge (1994) California Earthquake

Fig. 14.7 Seismic response of low-rise frames with respect to ground



seismic activity regions, such as Japan, Greece, and the Western parts of the USA, are required to meet more extreme performance standards, and the design is usually carried out by firms that specialize in Seismic design.

Figure 14.7 illustrates how a typical low-rise rigid frame building responds to horizontal ground motion. The floor slabs act like rigid plates and displace horizontally with respect to the ground due to bending of the columns. Since there are no external loads applied to the floors, *the deformation has to be due to the inertia forces associated with the floor masses*. The magnitude of these forces depends on the floor masses and the floor accelerations.

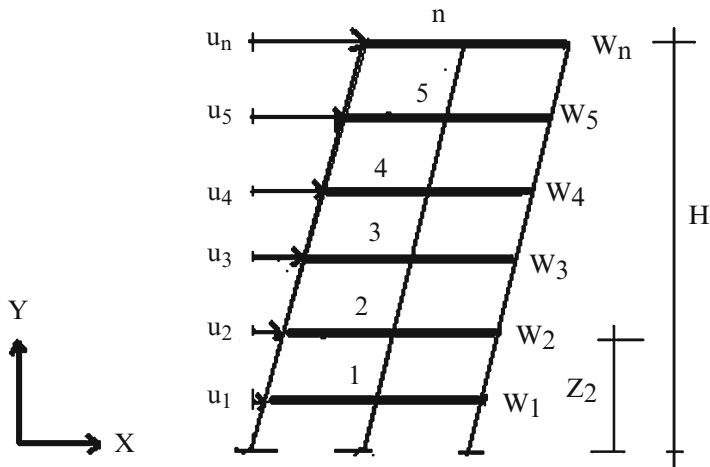


Fig. 14.8 Lateral displacement profile with respect to ground

The lateral displacement profile is assumed to be a linear function of Z as indicated in Fig. 14.8.

$$u_i(z) = u_{\text{ground}} + \frac{Z_i}{H} u(H)$$

where $u(H)$ is the relative displacement of the top floor with respect to the ground, and Z_i is the vertical coordinate of floor i . This assumption leads to the following expression for the total acceleration of a typical floor:

$$a|_{\text{floor } i} = a_g(t) + \frac{Z_i}{H} \frac{d^2 u(H)}{dt^2} \quad (14.4)$$

where $a_g(t)$ is the ground acceleration time history. Applying Newton's law, the force required to accelerate floor i , assuming it moves as a rigid body and the lateral displacement profile is linear, is

$$P|_{\text{floor } i} = \frac{W_i}{g} \left\{ a_g(t) + \frac{Z_i}{H} \frac{d^2 u(H)}{dt^2} \right\} \quad (14.5)$$

This force is provided by the shear forces in the columns adjacent to the floor.

Given an earthquake ground motion time history, one applies this floor loading to a structure and determines the structural response. The solution for the acceleration at the top floor is expressed as [26]

$$\frac{d^2 u(H)}{dt^2} = -\Gamma(a_g(t) + \theta(t)) \quad (14.6)$$

where $\theta(t)$ depends on the earthquake ground motion and the structural period; Γ is a dimensionless parameter that depends on the distribution of floor masses,

$$\Gamma = \frac{\sum_{i=1}^N m_i \frac{Z_i}{H}}{\sum_{i=1}^N m_i \left(\frac{Z_i}{H}\right)^2} = \frac{H \sum_{i=1}^N W_i Z_i}{\sum_{i=1}^N W_i (Z_i)^2} \quad (14.7)$$

Substituting for the top floor acceleration, the inertia force expands to

$$P|_{\text{floor } i} = \frac{W_i}{g} a_g(t) \left\{ 1 - \Gamma \frac{Z_i}{H} \right\} + \frac{W_i}{g} \left\{ -\Gamma \frac{Z_i}{H} \theta(t) \right\} \quad (14.8)$$

The peak values of $a_g(t)$ and $\theta(t)$ do not generally occur at the same time. Also the magnitude of Γ is of order one and the maximum value of $\theta(t)$ is usually larger than $a_{g,\max}$. Therefore, the *peak force* at floor i is approximated as:

$$P|_{\text{floor } i} \approx \frac{Z_i W_i}{H} \left\{ \Gamma \frac{S_a}{g} \right\} \quad (14.9)$$

where S_a is defined as the maximum absolute value of $\theta(t)$. In the seismic literature, S_a is called the spectral acceleration. It is *the maximum acceleration that an equivalent single degree of freedom system experiences when subjected to the earthquake*. Summing up the floor forces leads to the resultant force which is also equal to the maximum shear force at the base.

$$V|_{\text{base}} = \sum P|_{\text{floor } i} \approx \frac{\left(\sum_{i=1}^N W_i Z_i \right)^2}{\sum_{i=1}^N W_i (Z_i)^2} \frac{S_a}{g} \quad (14.10)$$

Finally, we express the force for floor i in terms of $V|_{\text{base}}$.

$$P|_{\text{floor } i} = \left(\frac{W_i Z_i}{\sum W_i Z_i} \right) V|_{\text{base}} \quad (14.11)$$

The spectral acceleration measure, S_a , depends on the ground motion time history $a_g(t)$ and the period of the structure, T .

A simple approximation for T for a low-rise building is

$$T \approx \frac{N}{10} \text{ s} \quad (14.12)$$

where N is the number of stories. Values of S_a vs. the structural period, T , have been compiled by various agencies, such as the US Geological Survey's National Earthquake Information Center [17] for a range of earthquakes, and used to construct design plots such as illustrated below in Fig. 14.9. One estimates T and determines S_a with this plot. The limiting values for the plot, such as S_{DS} and S_{D1} , depend on S_{MS} and S_{M1} which are defined for a particular site and seismic design

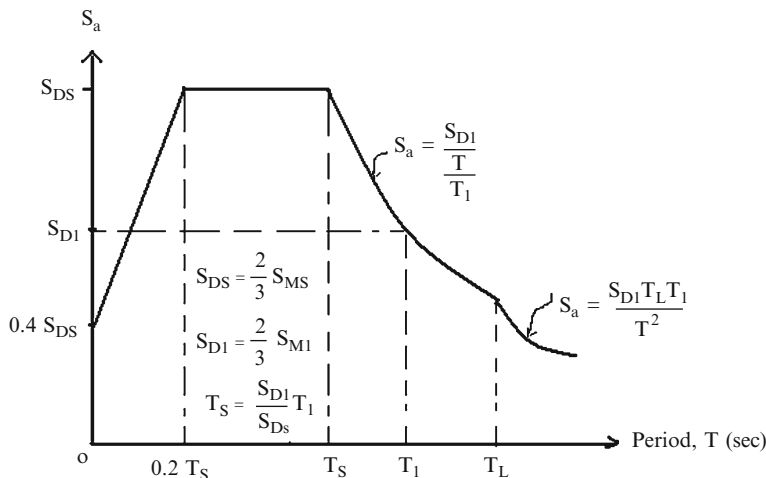


Fig. 14.9 Peak acceleration vs. structural period [8]

code [8]. Values of S_{MS} , S_{M1} , and T_L are listed on the USGS website, usgs.gov/hazards: S_{M1} is usually taken as the spectral acceleration for 5% damping and 1 s period (i.e., $T_1 = 1$ s); S_{MS} is the spectral acceleration for 5% damping and 0.2 s period and T_L is the long transition period. The worst case scenario is for the structural period to be between $0.2T_S$ and T_S . When $T \gg T_L$, the seismic load is significantly less than the load corresponding to the region $0.2T_S < T < T_S$.

Example 14.1

Given: The three story building shown in Figs. E14.1a, b. Assume the building is subjected to an earthquake in the North–South direction. Take the spectral acceleration as $S_a = 0.4g$

Determine: The base shear and earthquake forces on the individual floors.

Solution: We use (14.10). The base shear is given by

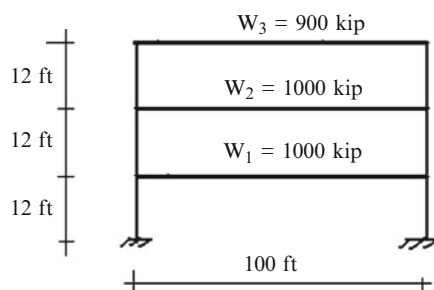


Fig. E14.1a Elevation

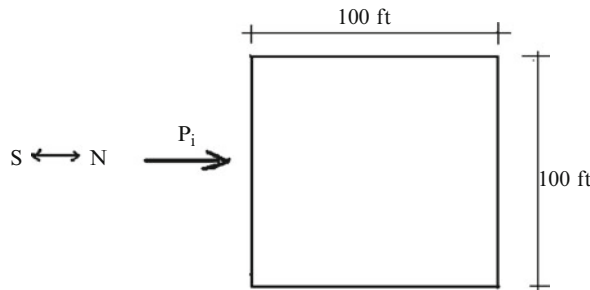


Fig. E14.1b Typical floor plan

$$V|_{\text{base}} = \frac{\left(\sum_{i=1}^3 Z_i W_i \right)^2}{\sum_{i=1}^3 W_i (Z_i)^2} \frac{S_a}{g} = \frac{\{1,000(12) + 1,000(24) + 900(36)\}^2}{\{1,000(12)^2 + 1,000(24)^2 + 900(36)^2\}} \frac{S_a}{g}$$

$$= 3,420(0.4) = 1,368 \text{ kip}$$

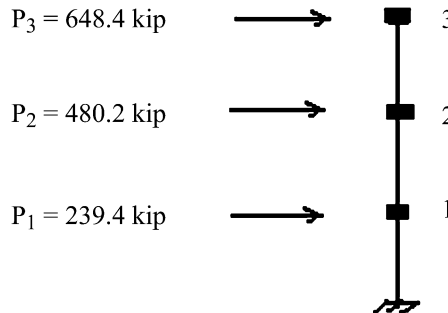
Then, applying (14.11), we obtain the individual floor loads.

$$\sum_{i=1}^3 W_i Z_i = \{(12(1,000) + 24(1,000) + 36(900)\} = 68,400$$

$$P_1 = \frac{12(1,000)}{68,400} V|_{\text{base}} = 0.175(1,368) = 239.4 \text{ kip}$$

$$P_2 = \frac{24(1,000)}{68,400} V|_{\text{base}} = 0.351(1,368) = 480.2 \text{ kip}$$

$$P_3 = \frac{36(900)}{68,400} V|_{\text{base}} = 0.474(1,368) = 648.4 \text{ kip}$$



Example 14.2

Given: The three story building shown in Figs. E14.2a, b. The floor weights are indicated. There is also an additional weight located on the top floor.

Determine: The earthquake floor forces for a North–South earthquake of intensity $S_a = 0.4g$.

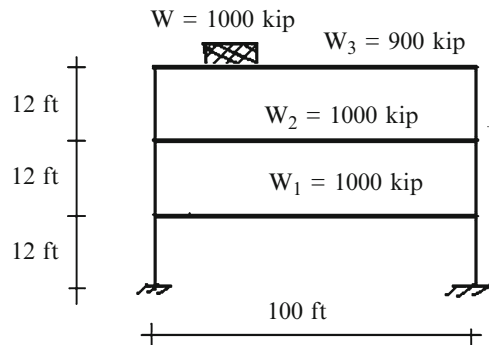


Fig. E14.2a Elevation

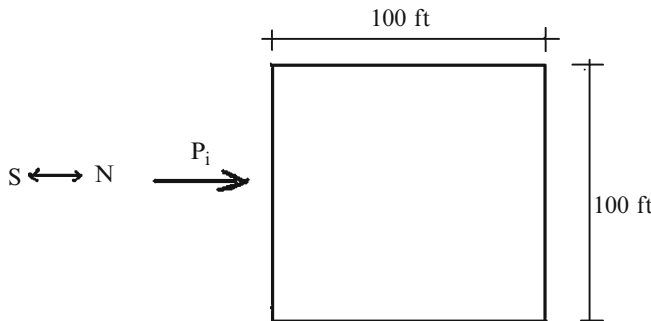


Fig. E14.2b Typical floor plan

Solution: The computations are organized in the following table.

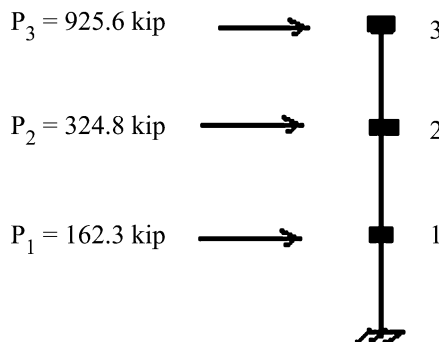
Floor	Z_i	W_i	$W_i Z_i (10^3)$	$W_i (Z_i)^3 (10^3)$
1	12	1,000	12	144
2	24	1,000	24	596
3	36	900	32.4	1050
Roof	36	1,000	36	1296
			104.4×10^3	$3,086 \times 10^3$

$$V|_{\text{base}} = (0.4) \frac{(104.4(1,000))^2}{3,086(1,000)} = 1412.7 \text{ kip}$$

$$P_1 = \frac{12,000}{104.4(1,000)} (1,412.7) = 162.3 \text{ kip}$$

$$P_2 = \frac{24(1,000)}{104.4(1,000)} (1,412.7) = 324.8 \text{ kip}$$

$$P_3 = \frac{(32.4 + 36)(1,000)}{104.4(1,000)} (1,412.7) = 925.6 \text{ kip}$$



Note that the shear in the top story is increased considerably due to the additional mass on the third floor.

14.3 Building Response Under Lateral Loads

Up to this point, we have discussed how one generates the lateral loads acting at the floor levels. These loads are resisted by the frames which support the floors. In this section, we develop a methodology for distributing a floor load to the frames which support the floor.

We model the building as a set of *rigid floors* supported by columns and braces between the floors. When subjected to horizontal loading, the floor plates displace horizontally, resulting in bending of the columns and shearing deformation in the braces. The horizontal load is resisted by the shear forces developed in the columns and braces. We know from the examples studied in Chaps. 9 and 10 that stiffness attracts force. Therefore, one should expect that the distribution of floor load to the supporting elements, i.e., the columns and braces, will depend on the relative stiffness of these elements.

14.3.1 Center of Twist: One Story Frame

We consider first the one story braced frame structure shown in Fig. 14.10a. The braces located at the midpoints of the sides provide the resistance to horizontal load. We represent the braces as simple shear springs. Figure 14.10b illustrates this modeling strategy. Each brace provides a force which acts in the plane of the wall that contains the brace.

We locate the origin of the $X-Y$ coordinate system at the geometric center of the floor and assume the floor is subjected to external forces P_x, P_y, M . Under the action of these forces, the floor will experience translation (u, v) and rotation ω about the origin. These displacements produce shear forces in the springs which oppose the motion. The free body diagram for the floor is shown in Fig. 14.11.

Noting the free body diagram shown above, the equilibrium equations expand to

$$+ \rightarrow \sum F_x = P_x - F_{Ax} - F_{Cx} = 0$$

$$+ \uparrow \sum F_y = P_y - F_{By} - F_{Dy} = 0$$

$$\sum M_0 = M + (F_{Cx} - F_{Ax}) \frac{B}{2} + (F_{Dy} - F_{By}) \frac{L}{2} = 0 \quad (14.13)$$

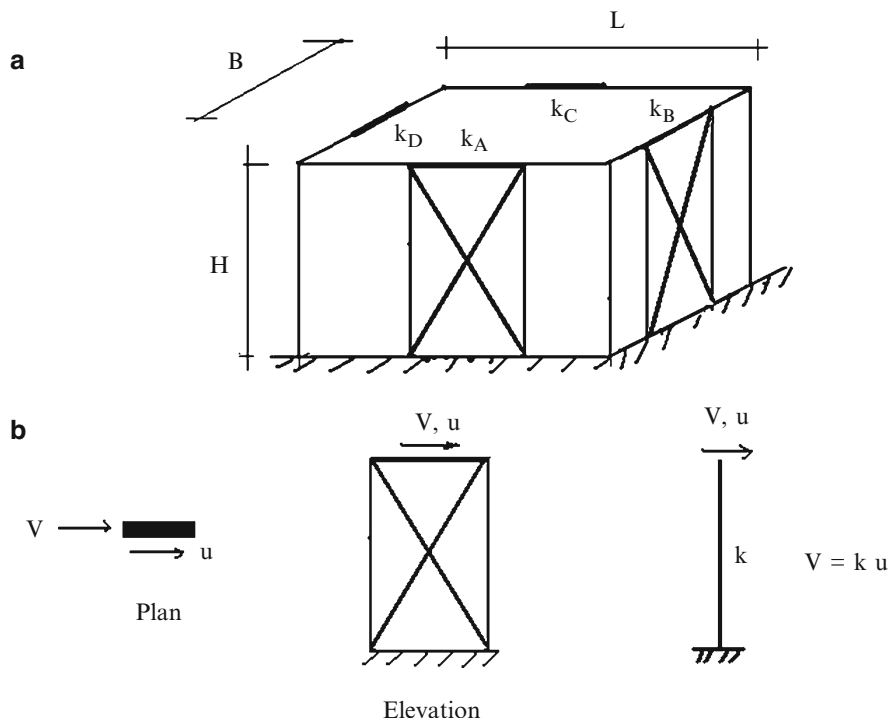
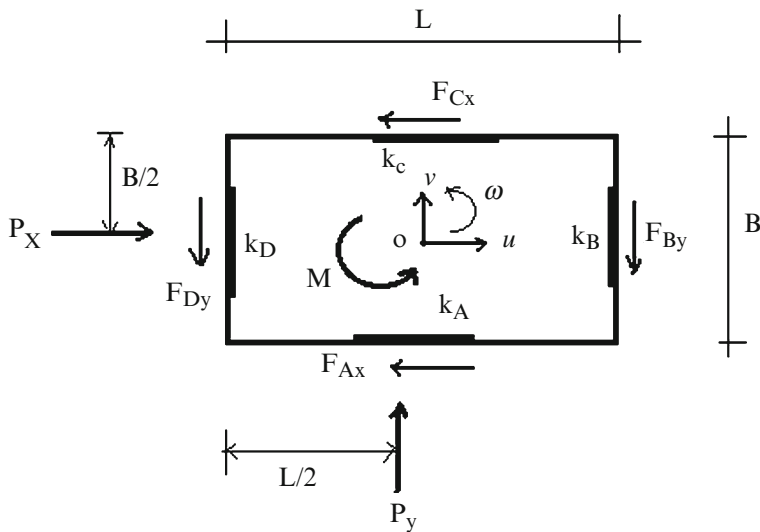


Fig. 14.10 (a) One story braced frame. (b) Shear spring model for brace

**Fig. 14.11** Plan view

Assuming the floor plate is rigid; the shear forces are related to the displacements by

$$\begin{aligned}
 F_{Ax} &= k_A \left(u + \frac{B}{2} \omega \right) \\
 F_{Cx} &= k_C \left(u - \frac{B}{2} \omega \right) \\
 F_{By} &= k_B \left(v + \frac{L}{2} \omega \right) \\
 F_{Dy} &= k_D \left(v - \frac{L}{2} \omega \right)
 \end{aligned} \tag{14.14}$$

Substituting for the forces in (14.13) leads to

$$\begin{aligned}
 P_x &= u(k_A + k_C) + \frac{B}{2}(k_A - k_C)\omega \\
 P_y &= v(k_B + k_D) + \frac{L}{2}(k_B - k_D)\omega \\
 M &= \frac{B}{2}(k_A - k_C)u + \frac{L}{2}(k_B - k_D)v + \left\{ \frac{B^2}{4}(k_A + k_C) + \frac{L^2}{2}(k_B + k_D) \right\}\omega = 0
 \end{aligned} \tag{14.15}$$

We see that the response depends on the relative stiffness of the braces. If $k_A = k_C = k_D \neq k_B$, the floor will experience rotation when only P_x or P_y is applied at the geometric center. Given the stiffness of the braces, one solves (14.15) for u, v, ω and evaluates the braces forces using (14.14).

Example 14.3

Given: The floor plan, dimensions and layout of the braces, and the brace stiffnesses shown in Fig. E14.3a.

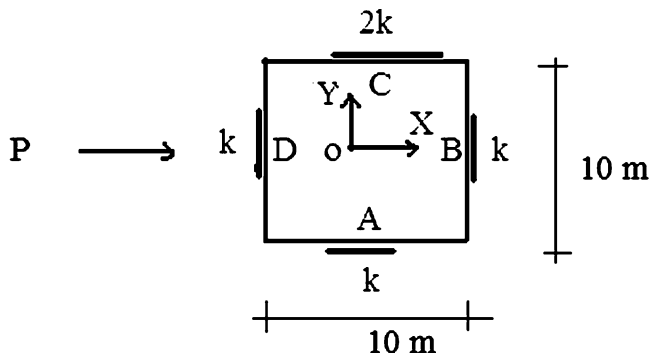


Fig. E14.3a Plan view

Determine: The response due to P_x .

Solution: We note that the braces at A, B, D have equal stiffnesses, and the brace at C is twice as stiff as the others. For convenience, we show these values as just k and $2k$. We set $P_y = M = 0$ in (14.15).

$$P_x = (3k)u + 5(-k)\omega = P$$

$$P_y = (2k)v = 0$$

$$M = 5(-k)u + \left(\frac{700}{4}k\right)\omega = 0$$

Solving these equations, we obtain

$$u = \frac{7P}{20k}$$

$$v = 0$$

$$\omega = \frac{P}{100k}$$

Finally, the brace forces are

$$F_{Ax} = k_A \left(u + \frac{B}{2} \omega \right) = P \left(\frac{7}{20} + \frac{5}{100} \right) = 0.4P$$

$$F_{Cx} = k_C \left(u - \frac{B}{2} \omega \right) = 2P \left(\frac{7}{20} - \frac{5}{100} \right) = 0.3P$$

$$F_{By} = k_B \left(v + \frac{L}{2} \omega \right) = P \left(\frac{5}{100} \right) = 0.05P$$

$$F_{Dy} = k_D \left(v - \frac{L}{2} \omega \right) = P \left(-\frac{5}{100} \right) = -0.05P$$

To avoid rotation, which is undesirable, one needs to modify either the stiffness at A or C. Taking $k_A = k_C = k$, the response is

$$u = \frac{P}{2k}$$

$$v = \omega = 0$$

$$F_A = F_C = \frac{P}{2}$$

The formulation described above can be generalized to deal with an arbitrary number of braces or shear walls oriented in either the X or Y direction. We shift to the notation shown in Fig. 14.12 to identify the various braces. Each brace is characterized by a stiffness magnitude (k) and the perpendicular distance from the tangent to the origin.

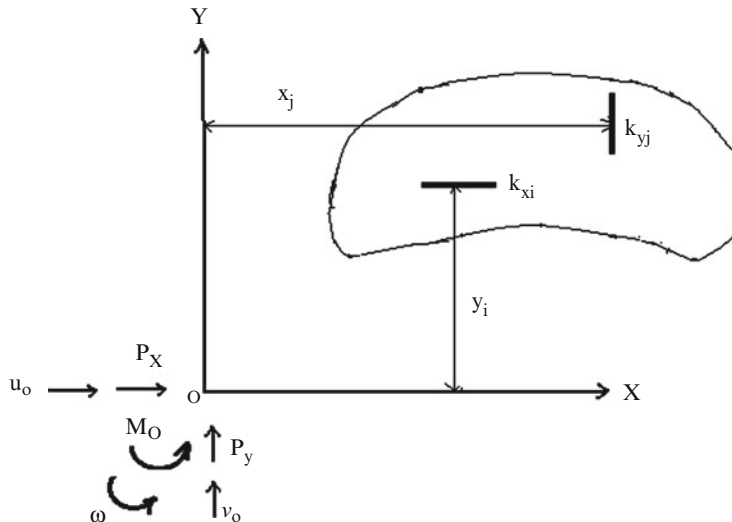


Fig. 14.12 Notation

Assuming the floor is rigid, the tangential motion for the X oriented braces due to a rigid body motion of the origin o is

$$+ \rightarrow u_i = u_o - y_i \omega \quad (14.16)$$

Similarly, the Y motion for brace j is given by

$$+ \uparrow v_j = v_o + x_j \omega \quad (14.17)$$

These motions produce shear forces which act to *oppose* the motion of the floor. The individual forces are

$$\begin{aligned} + \rightarrow F_{xi} &= -k_{xi}u_i = -k_{xi}u_o + k_{xi}y_i \omega \\ + \uparrow F_{yj} &= -k_{yj}v_j = -k_{yj}v_o - k_{yj}x_j \omega \end{aligned} \quad (14.18)$$

Summing forces and moments with respect to the origin leads to the equilibrium equations for the floor

$$\begin{aligned} + \rightarrow P_x - u_0 \left(\sum k_{xi} \right) + \omega \left(\sum y_i k_{xi} \right) &= 0 \\ + \uparrow P_y - v_0 \left(\sum k_{yj} \right) - \omega \left(\sum x_j k_{yj} \right) &= 0 \\ M_0 + u_0 \left(\sum y_i k_{xi} \right) - v_0 \left(\sum x_j k_{yj} \right) - \omega \left\{ \sum y_i^2 k_{xi} + \sum x_j^2 k_{yj} \right\} &= 0 \end{aligned} \quad (14.19)$$

where P_x, P_y, M_0 are the external loads on the floor.

We define the following terms

$$\begin{aligned} \sum k_{xi} &= K_{xx} \\ \sum k_{yj} &= K_{yy} \\ \sum y_i k_{xi} &= K_{xz} \\ \sum x_j k_{yj} &= K_{yz} \\ \sum y_i^2 k_{xi} + \sum x_j^2 k_{yj} &= K_o \end{aligned} \quad (14.20)$$

With this notation, (14.19) takes the following form

$$\begin{aligned} P_x &= K_{xx}u_0 - K_{xz}\omega \\ P_y &= K_{yy}v_0 + K_{yz}\omega \\ M_0 &= -K_{xz}u_0 + K_{yz}v_0 + K_o\omega \end{aligned} \quad (14.21)$$

Equation (14.21) applies for an arbitrary choice of origin. Note that forces applied at the origin will produce rotation when either $K_{xz} \neq 0$ or $K_{yz} \neq 0$. If the stiffness distribution is symmetrical, these terms vanish. Rotation of the floor is a torsional mode of response, which introduces an undesirable anti-symmetric deformation in the perimeter facades. Therefore, one approach is to always choose a symmetrical stiffness layout. Another approach is to shift the origin to some other point in the floor. Obviously, the most desirable point corresponds to $K_{xz} = K_{yz} = 0$.



Fig. 14.13 Floor geometry

Consider the floor geometry shown in Fig. 14.13. Point o denotes the initial origin and C some arbitrary point in the floor. We locate a new set of axes at C and express the forces in terms of the coordinates with respect to C.

$$\begin{aligned} u_i &= u_c - y'_i \omega \\ v_i &= v_c + x'_i \omega \end{aligned} \quad (14.22)$$

$$\begin{aligned} F_{xi} &= -k_{xi}u_c + k_{xi}y'_i \omega \\ F_{yi} &= -k_{yi}v_c - k_{yi}x'_i \omega \end{aligned} \quad (14.23)$$

The equilibrium equations referred to point C has the following form

$$\begin{aligned} P_{xc} - u_c \left(\sum k_{xi} \right) + \omega \left(\sum y'_i k_{xi} \right) &= 0 \\ P_{yc} - v_c \left(\sum k_{yj} \right) - \omega \left(\sum x'_j k_{yj} \right) &= 0 \end{aligned} \quad (14.24)$$

$$M_c + u_c \left(\sum y'_i k_{xi} \right) - v_c \left(\sum x'_j k_{yj} \right) + \omega \left(-\sum y'^2_i k_{xi} - \sum x'^2_j k_{yj} \right) = 0$$

We choose point C such that

$$\sum y'_i k_{xi} = \sum x'_j k_{yj} = 0 \quad (14.25)$$

These conditions define the coordinates of point C. Substituting for x' and y' using

$$x' = -x_C + x$$

$$y' = -y_C + y$$

Leads to

$$\begin{aligned} x_C &= \frac{\sum x_j k_{yj}}{\sum k_{yj}} \\ y_C &= \frac{\sum y_i k_{xi}}{\sum k_{xi}} \end{aligned} \quad (14.26)$$

The equilibrium equations referred to these new axes simplify to

$$\begin{aligned} P_x &= K_{xx} u_C = R_x \\ P_y &= K_{yy} v_C = R_y \\ M_C &= K_C \omega_C = M_z \end{aligned} \quad (14.27)$$

where

$$K_C = \sum y_i'^2 k_{xi} + \sum x_j'^2 k_{yj}$$

The external and internal forces are shown in Fig. 14.14.

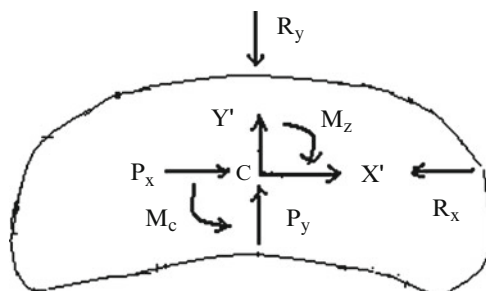


Fig. 14.14

Point C is called the “center of twist.” Figure 14.14 shows that the resultant of the “resisting” forces acts at the center of twist. External forces applied at the center of twist produce only translation; an external moment applied to the floor produces twist about the center of twist. We point out that the coordinates of the center of twist depend on the stiffness of the components located in the story. The location of the center of twist changes when either the position or magnitude of the stiffness components is changed.

Example 14.4

Given: The floor plan shown in Fig. E14.4a. The two shear walls are orthogonal and are located on the X and Y axes.

Determine: The center of twist.

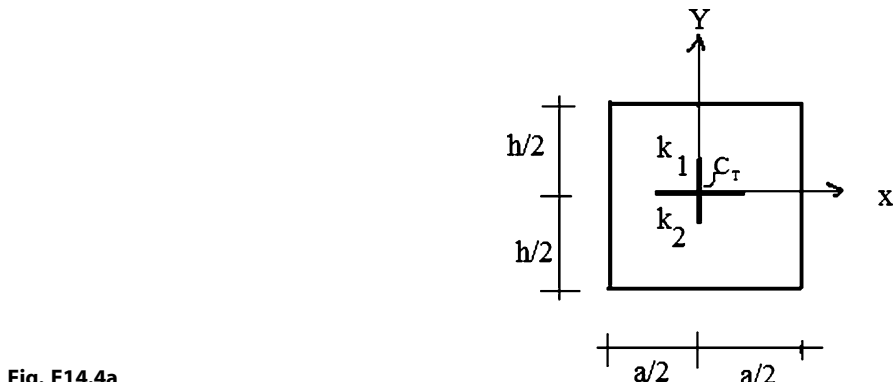


Fig. E14.4a

Solution: The center of stiffness lies on an axis of symmetry. In this case, there are two axes of symmetry and therefore the center of twist is at the origin.

Example 14.5

Given: The stiffness distribution shown in Fig. E14.5a.

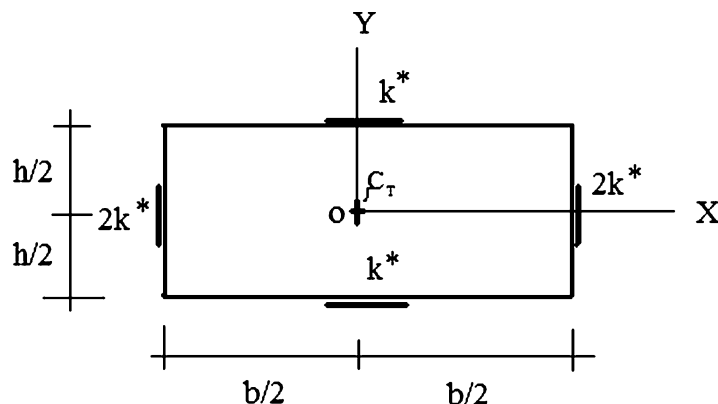


Fig. E14.5a

Determine: The center of twist.

Solution: The stiffness distributions are symmetrical with respect to the X and Y axes. Therefore,

$$X_{CT} = Y_{CT} = 0.$$

Example 14.6

Given: The stiffness distribution shown in Fig. E14.6a.

Determine: The center of twist.

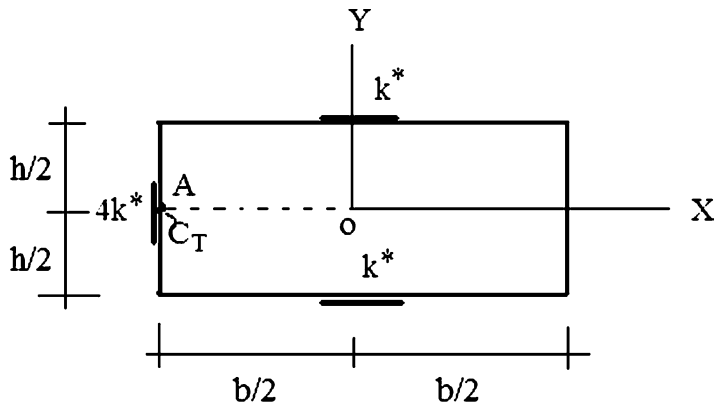


Fig. E14.6a

Solution: The center of twist (C_T) lies on the X -axis because the stiffness is symmetrical with respect to the X -axis. Summing moments about the origin leads to

$$x_{CT} = \frac{\sum x_i k_{yi}}{\sum k_{yi}} = \frac{4k^*(-(b/2))}{4k^*} = -\frac{b}{2}$$

Example 14.7

Given: The stiffness distribution and loading shown in Fig. E14.7a.

Determine: The rigid body motion.

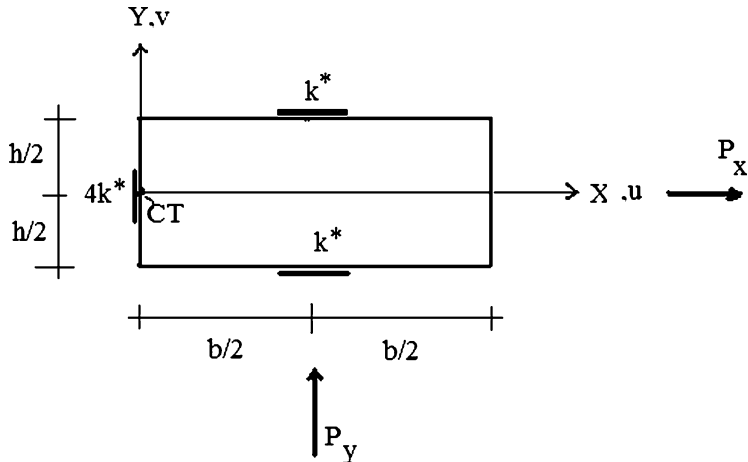


Fig. E14.7a

Solution: The floor will experience rotation as well as translation since there is a net moment with respect to the center of twist. We determine the motion measures using (14.27). The stiffness measures are

$$K_{xx} = \sum k_{xj} = 2k^* \rightarrow$$

$$K_{yy} = \sum k_{yj} = 4k^* \uparrow$$

$$K_C = \sum y_j^2 k_{xj} = 2 \left\{ \left(\frac{h}{2} \right)^2 k^* \right\} = \frac{h^2}{2} k^*$$

Then

$$u = \frac{P_x}{K_{xx}} = \frac{P_x}{2k^*}$$

$$v = \frac{P_y}{K_{yy}} = \frac{P_y}{4k^*}$$

$$\omega = \frac{P_y \left(\frac{b}{2} \right)}{K_C} = P_y \frac{\frac{b}{2}}{\frac{h^2}{2} k^*} = \frac{P_y}{k^*} \frac{b}{h^2}$$

The deformed configuration of the floor is shown in Fig. E14.7b.

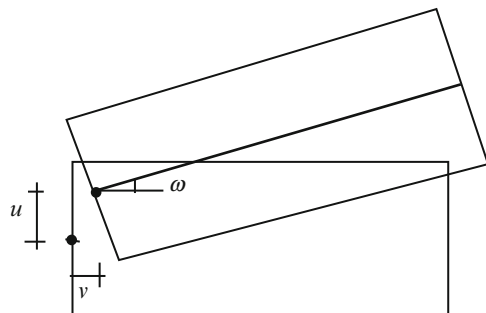


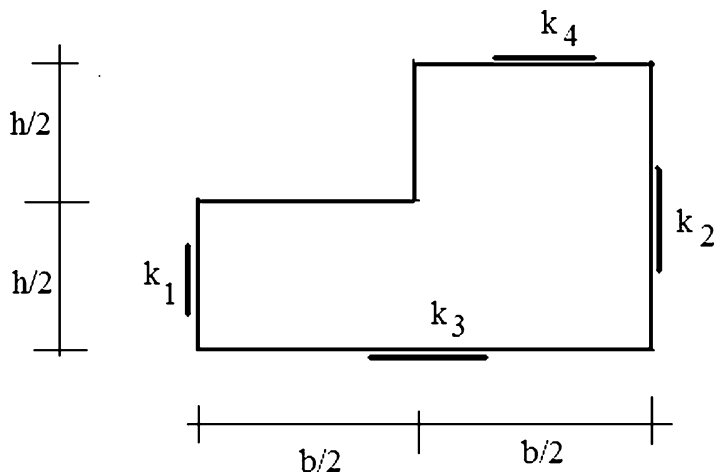
Fig. E14.7b

Example 14.8

Given: The stiffness distribution shown in Fig. E14.8a.

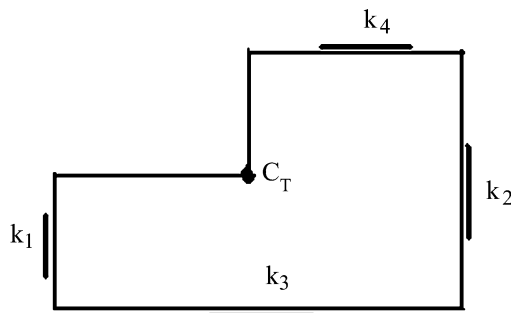
Determine: The center of twist for the following combination of stiffness factors:

- (a) $k_1 = k_2 = k_3 = k_4$
- (b) $k_4 = k_3 \quad k_1 > k_2$
- (c) $k_4 > k_3 \quad k_1 = k_2$
- (d) $k_4 > k_3 \quad k_1 > k_2$

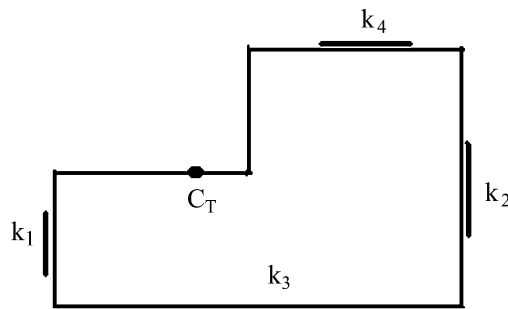
**Fig. E14.8a**

Solution: We view the problem as equivalent to finding the centroid of a set of areas, with area replaced by stiffness. We use qualitative reasoning to estimate the location of the center of twist.

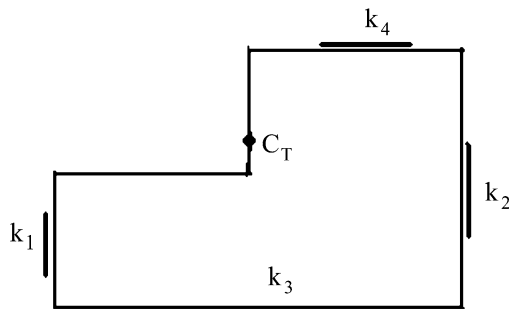
Case (a) $k_1 = k_2 = k_3 = k_4$



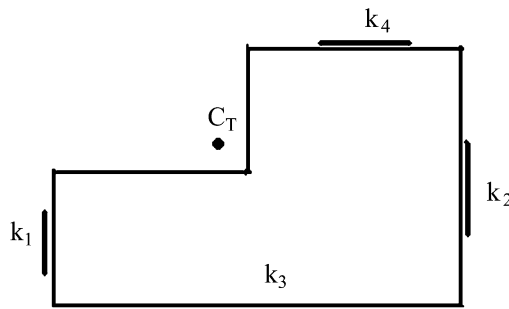
Case (b) $k_4 = k_3$ $k_1 > k_2$



Case(c) $k_4 > k_3$ $k_1 = k_2$



Case (d) $k_4 > k_3$ $k_1 > k_2$



We consider next the single inclined brace shown in Fig. 14.15. Introducing displacements u and v produces a longitudinal force F equal to ku' . Projecting F on the x and y axes leads to

$$\begin{aligned} F_x &= F \cos \theta = k \left[u(\cos \theta)^2 + v \cos \theta \sin \theta \right] \\ F_y &= F \sin \theta = k \left[u \sin \theta \cos \theta + v (\sin \theta)^2 \right] \end{aligned} \quad (14.28)$$

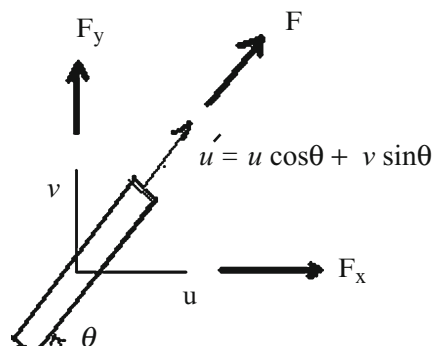


Fig. 14.15 Inclined brace

Summing these forces over the number of braces, the resultants are given by

$$\begin{aligned} R_x &= \sum F_x = u \sum k_i \cos^2 \theta + v \sum k_i \cos \theta \sin \theta \\ R_y &= \sum F_y = u \sum k_i \sin \theta \cos \theta + v \sum k_i \sin^2 \theta \end{aligned} \quad (14.29)$$

We write these equations as

$$\begin{aligned} R_x &= uK_{cc} + vK_{cs} \\ R_y &= uK_{cs} + vK_{ss} \end{aligned} \quad (14.30)$$

where

$$\begin{aligned} K_{cc} &= \sum k_i \cos^2 \theta \\ K_{cs} &= \sum k_i \cos \theta \sin \theta \\ K_{ss} &= \sum k_i \sin^2 \theta \end{aligned}$$

Note that when $\theta = 0^\circ$ or 90° , these expressions reduce to (14.27).

The line of action is determined by summing moments about O . Working first with the X direction (u) and then the Y direction (v), leads to the following pair of equations for x^* and y^* , the coordinates of the center of twist.

$$\begin{aligned} y^*K_{cc} - x^*K_{cs} &= \sum y_i k_i \cos^2 \theta - \sum x_i k_i \sin \theta \cos \theta \\ y^*K_{cs} - x^*K_{ss} &= \sum y_i k_i \sin \theta \cos \theta - \sum x_i k_i \sin^2 \theta \end{aligned} \quad (14.31)$$

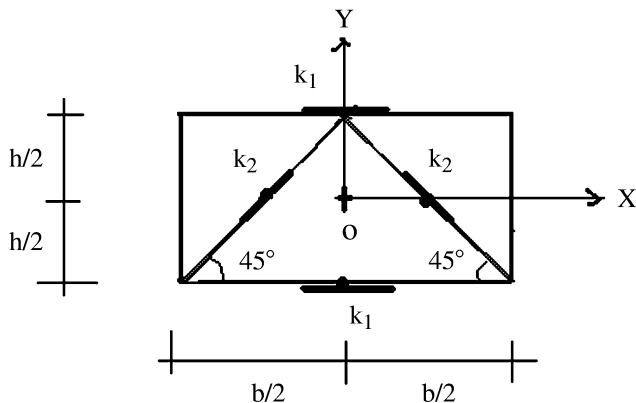
When the stiffness elements are parallel to either x or y , these equations reduce to

$$\begin{aligned} K_{cc} &= \sum k_x & K_{cs} &= 0 & K_{ss} &= \sum k_y \\ y^* &= \frac{\sum y k_x}{\sum k_x} & x^* &= \frac{\sum x k_y}{\sum k_y} \end{aligned}$$

Example 14.9

Given: The stiffness distribution shown in Fig. E14.9a. Two of the braces are inclined with respect to the x -axis.

Determine: The center of twist.

**Fig. E14.9a**

Solution: Evaluating (14.29) and (14.31), leads to

$$K_{cc} = \sum k_i \cos^2 \theta = 2k_1 + 2\left(\frac{1}{2}k_2\right) = 2k_1 + k_2$$

$$K_{ss} = \sum k_i \cos \theta \sin \theta = 2\left(\frac{1}{2}k_2\right) = k_2$$

$$K_{cs} = \sum k_i \sin^2 \theta = \frac{1}{2}k_2 + \left(-\frac{1}{2}k_2\right) = 0$$

$$\sum y_i k_i \cos^2 \theta = 0$$

$$\sum x_i k_i \sin \theta \cos \theta = k_2 \frac{b}{4} \sum (-1)\frac{1}{2} + (+1)\left(-\frac{1}{2}\right) = -k_2 \frac{b}{4}$$

$$\sum y_i k_i \sin \theta \cos \theta = \frac{h}{2}k_2\left(\frac{1}{2} - \frac{1}{2}\right) = 0$$

Then

$$y^* = \frac{1 + (bk_2/4)}{2k_1 + k_2} = \frac{b}{4} \left(\frac{k_2}{k_2 + 2k_1} \right)$$

$$x^* = 0$$

14.3.2 Center of Mass: One Story Frame

The center of twist for a one story frame is a property of the stiffness components located in the story below the floor. It defines the point of application of the interstory resistance forces acting on the floor. These forces depend on the translation and rotation of the floor produced by the applied loading, i.e., they are due to interstory deformation.

When the loading is dynamic, additional inertia forces are generated due to the acceleration of the masses located on the floor. In order to study the equilibrium of the floor, we need to establish the magnitude and location of the resultant of these inertia forces. In what follows, we describe the procedure for locating this resultant.

Figure 14.16 shows a typical plan view of a floor. We locate the origin at some arbitrary point in the floor, and suppose that there are masses located at discrete points in the floor. The center of mass is a particular point in the floor defined by the coordinates \bar{x} and \bar{y} , where

$$\begin{aligned}\bar{x} &= \frac{\sum x_i m_i}{\sum m_i} \\ \bar{y} &= \frac{\sum y_i m_i}{\sum m_i}\end{aligned}\quad (14.32)$$

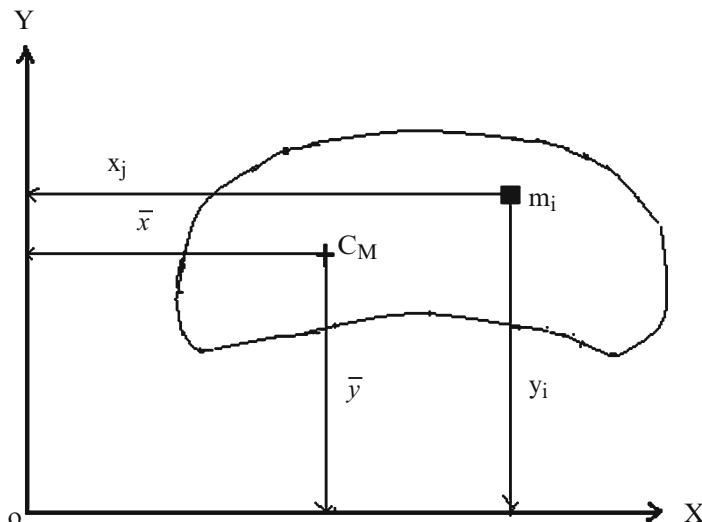
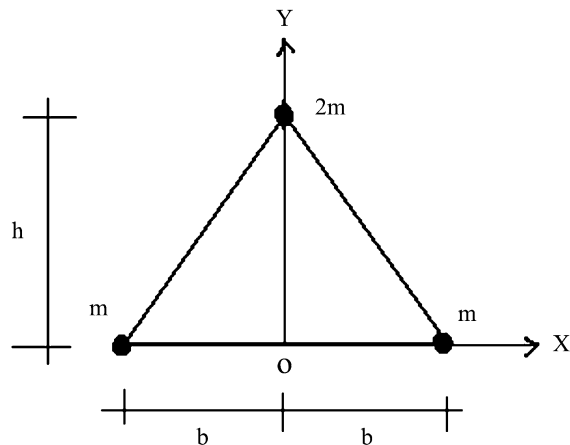


Fig. 14.16 Plan view of floor

Example 14.10

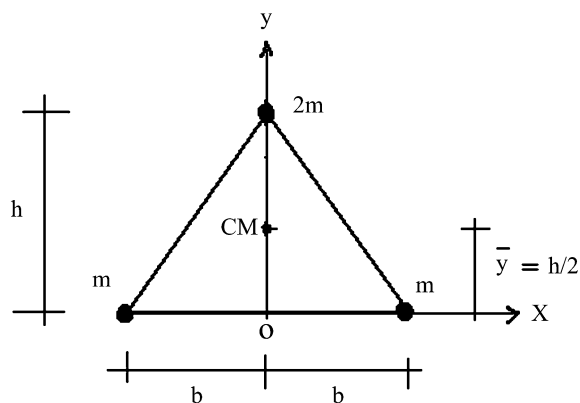
Given: The floor mass layout shown in Fig. E14.10a.

Determine: The center of mass.

Fig. E14.10a

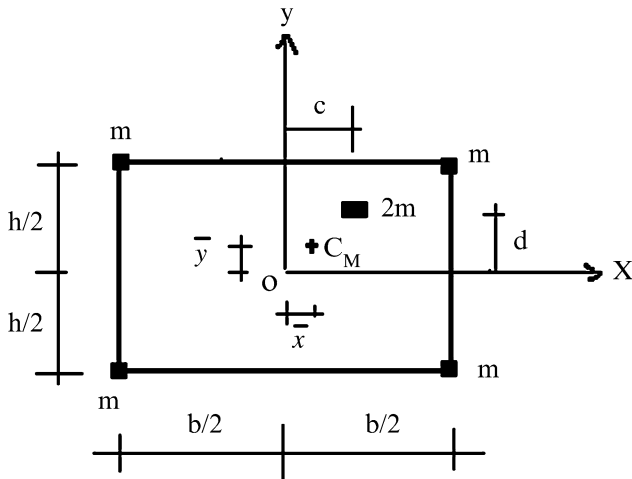
Solution: The center of mass is on the y -axis. In general, if the mass distribution is symmetrical, the center of mass lies on the axis of symmetry. We determine the y coordinate by summing moments about the x -axis (Fig. E14.10b).

$$\bar{y} = \frac{\sum y_i m_i}{\sum m_i} = \frac{(2m)h}{4m} = \frac{h}{2}$$

Fig. E14.10b**Example 14.11**

Given: The floor mass layout shown in Fig. E14.11a.

Determine: The center of mass.

**Fig. E14.11a**

Solution: Summing the moments leads to

$$\sum m_i = 6m$$

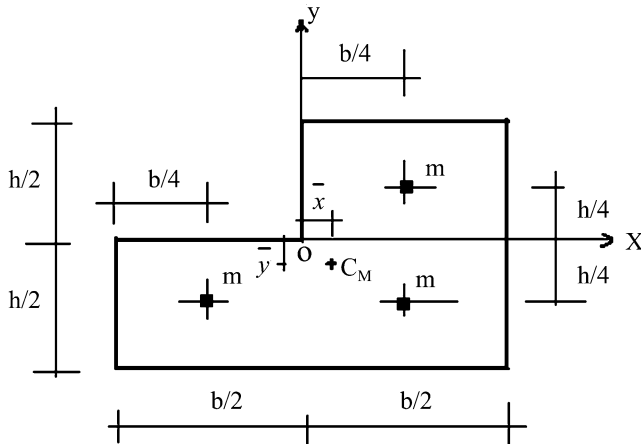
$$\bar{x} = \frac{2mc + 2m(b/2) + 2m(-b/2)}{6m} = \frac{c}{3}$$

$$\bar{y} = \frac{2md + 2m(h/2) + 2m(-h/2)}{6m} = \frac{d}{3}$$

Example 14.12

Given: The floor mass layout shown in Fig. E14.12a.

Determine: The center of mass.

**Fig. E14.12a**

Solution: We sum moments about the x and y axes and obtain

$$\bar{x} = \frac{m(b/4)}{3m} = \frac{b}{12}$$

$$\bar{y} = \frac{-m(h/4)}{3m} = -\frac{h}{12}$$

14.3.3 One Story Frame: General Response

We have shown that there are two key points in the floor, *the center of twist and the center of mass*. For quasi-static loading, we work with quantities referred to the center of twist. Noting (14.27), the response of the center of twist due to an arbitrary static loading is (Fig. 14.17)

$$u_c = \frac{P_x}{K_{xx}}$$

$$v_c = \frac{P_y}{K_{yy}}$$

$$\omega_c = \frac{M_c}{K_c} \quad (14.33)$$

Note that twist occurs only when there is an external moment with respect to the center of twist; forces applied at the center of twist produce only translation.

When the loading is dynamic, one needs to include the inertia forces. In this case, it is more convenient to place the origin at the center of mass and work with force and displacement quantities referred to the axes centered at the center of mass. Figure 14.18a illustrates this choice. Note that the resistance forces act at the center of twist and produce a moment about the center of mass. The displacements of the two centers are related by

$$u_{CT} = u_{CM} - y_{CT}\omega$$

$$v_{CT} = v_{CM} + x_{CT}\omega \quad (14.34)$$

$$\omega_{CT} = \omega_{CM}$$

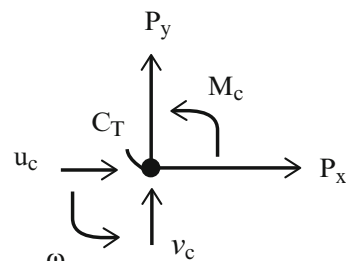


Fig. 14.17 Forces acting at the center of twist

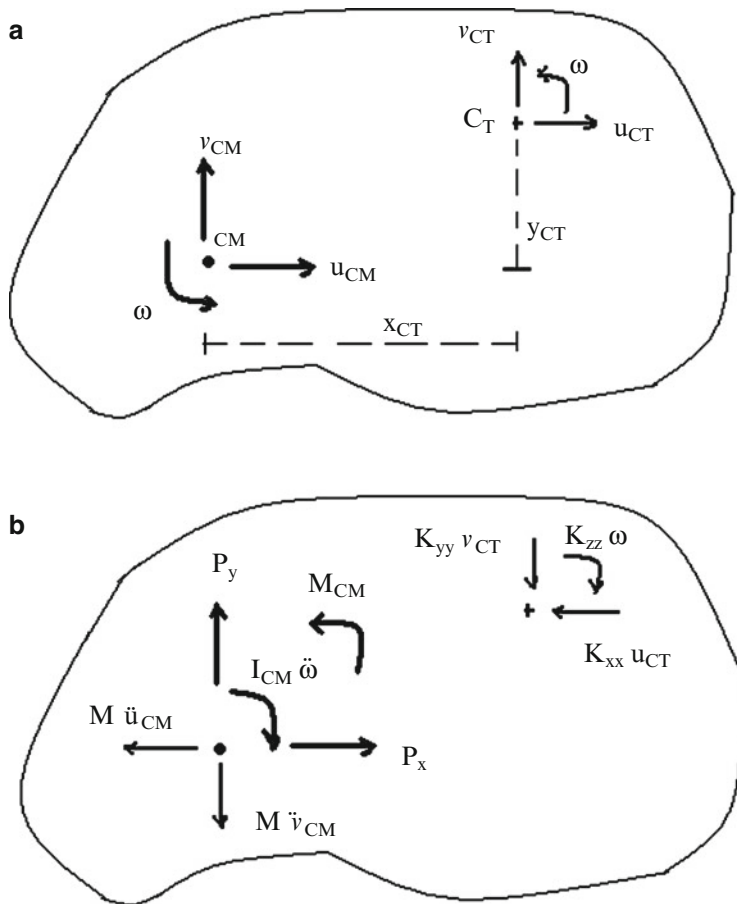


Fig. 14.18 Forces acting at the center of mass (a) Displacements. (b) Forces

The equilibrium equations referred to the center of mass have the following form

$$\begin{aligned}
 P_x &= m\ddot{u}_{CM} + K_{xx}(u_{CM} - y_{CT}\omega) \\
 P_y &= m\ddot{v}_{CM} + K_{yy}(v_{CM} + x_{CT}\omega) \\
 M_{CM} &= I_{CM}\ddot{\omega} + K_C\omega + x_{CT}K_{yy}(v_{CM} + x_{CT}\omega) - y_{CT}K_{xx}(u_{CM} - y_{CT}\omega) \\
 &= I_{CM}\ddot{\omega} + \omega\{K_C + x_{CT}^2K_{yy} + y_{CT}^2K_{xx}\} + x_{CT}K_{yy}v_{CM} - y_{CT}K_{xx}u_{CM}
 \end{aligned} \tag{14.35}$$

Equation (14.35) shows that the motion is coupled when the center of twist *does not* coincide with the center of mass. The center of mass is usually fixed by the mass distribution on the floor and one usually does not have any flexibility in shifting masses. Therefore, the most effective strategy is to adjust the location of the braces in the story below the floor such that the centers of mass and twist coincide, i.e., to take $x_{CT} = y_{CT} = 0$.

Example 14.13

Given: The mass and stiffness layout shown in Fig. E14.13a.

Determine: The magnitude of the stiffness elements k_1 and k_2 such that the centers of mass and twist coincide.

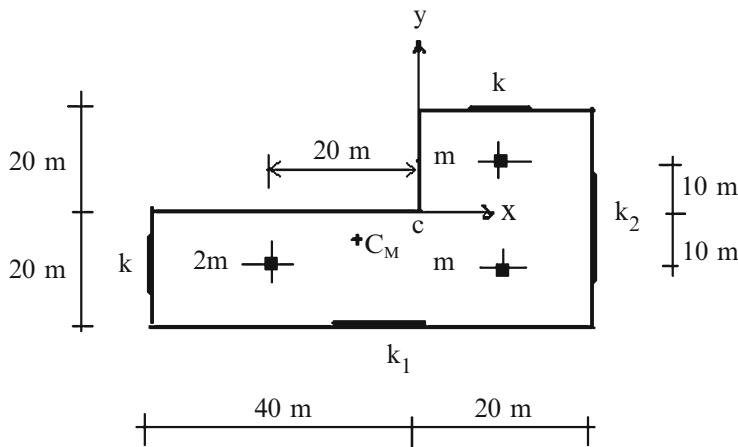


Fig. E14.13a

Solution: First, we locate the center of mass.

$$\sum m_i = 4 \text{ m}$$

$$\sum x_i m_i = 10(2 \text{ m}) - 20(2 \text{ m}) = -20 \text{ m}$$

$$\bar{x} = \frac{-20 \text{ m}}{4 \text{ m}} = -5 \text{ m}$$

Similarly,

$$\sum y_i m_i = 10(\text{m}) - 10(3 \text{ m}) = -20 \text{ m}$$

$$\bar{y} = \frac{-20 \text{ m}}{4 \text{ m}} = -5 \text{ m}$$

Next, we determine k_1 and k_2 by requiring the center of twist to coincide with the center of mass. The steps are

Step 1:

$$x_{CT} = \frac{\sum x_i k_y}{\sum k_y} = \frac{20k_2 - 40k}{k_2 + k} = -5 \text{ m}$$

↓

$$20k_2 - 40k = -5k - 5k_2$$

$$25k_2 = 35k$$

$$k_2 = 1.4k$$

Step 2:

$$y_{CT} = \frac{\sum y_i k_x}{\sum k_x} = \frac{20(k - k_1)}{k_1 + k} = -5 \text{ m}$$

↓

$$25k = 15k_1$$

$$k_1 = 1.67k$$

14.3.4 Multistory Response

A typical floor in a multistory structure is connected to the adjacent floors by stiffness elements such as columns, shear walls, and braces. When the floors displace, interstory deformation due to the relative motion between the floors is developed, resulting in self-equilibrating story forces which act on the adjacent floors. Figure 14.19 illustrates this mode of behavior. Floors i and $i + 1$ experience lateral displacements which produce shear deformations in the braces,

$$\gamma = u_{i+1} - u_i$$

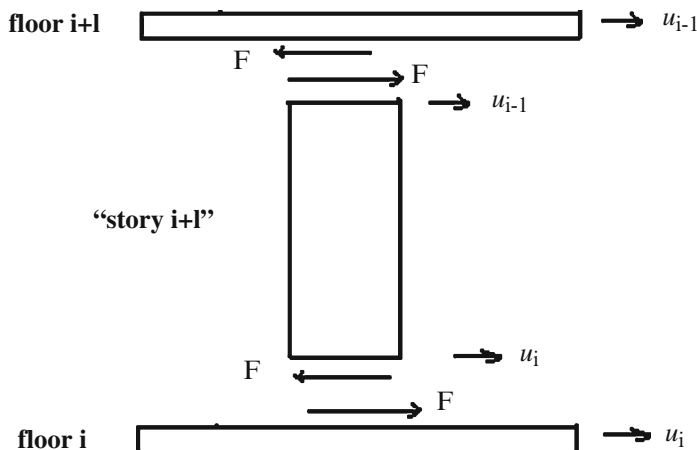


Fig. 14.19 Forces due to interstory deformation

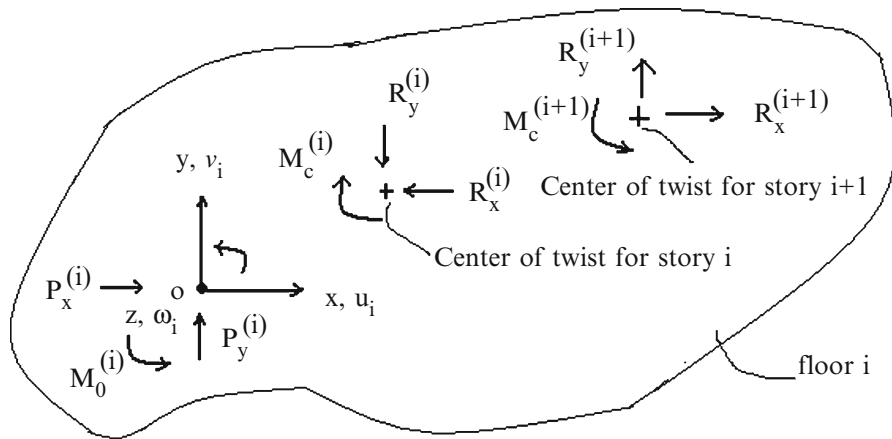


Fig. 14.20 Forces acting on floor i

and corresponding shear forces

$$F = k\gamma = k(u_{i+1} - u_i)$$

These forces act on both floors $i + 1$ and floor i ; the sense is reversed for the lower floor (this follows from Newton's law of action equal reaction).

In order to express these resistance forces in terms of displacements, we need to specify a common reference frame for all the floors. We suppose the floors translate and rotate, with respect to this common reference frame. We consider floor i . We determine the interstory displacement measures for the two centers of twist associated with the stories above and below floor i and apply (14.27). The resulting expressions for the resultant forces acting on floor i are listed below. Their sense is defined in Fig. 14.20. Note that the direction of the forces due to story $i + 1$ are opposite to those due to story i .

For story i :

$$\begin{aligned} R_x^{(i)} &= K_{xx}^{(i)} \left[\left\{ u_i - y_{CT}^{(i)} \omega_i \right\} - \left\{ u_{i-1} - y_{CT}^{(i)} \omega_{i-1} \right\} \right] \\ R_y^{(i)} &= K_{yy}^{(i)} \left[\left\{ v_i + x_{CT}^{(i)} \omega_i \right\} - \left\{ v_{i-1} + x_{CT}^{(i)} \omega_{i-1} \right\} \right] \\ M_C^{(i)} &= K_C^{(i)} [\omega_i - \omega_{i-1}] \end{aligned} \quad (14.36)$$

For story $i + 1$:

$$\begin{aligned} R_x^{(i+1)} &= K_{xx}^{(i+1)} \left[\left\{ u_{i+1} - y_{CT}^{(i+1)} \omega_{i+1} \right\} - \left\{ u_i - y_{CT}^{(i+1)} \omega_i \right\} \right] \\ R_y^{(i+1)} &= K_{yy}^{(i+1)} \left[\left\{ v_{i+1} + x_{CT}^{(i+1)} \omega_{i+1} \right\} - \left\{ v_i + x_{CT}^{(i+1)} \omega_i \right\} \right] \\ M_C^{(i+1)} &= K_C^{(i+1)} [\omega_{i+1} - \omega_i] \end{aligned} \quad (14.37)$$

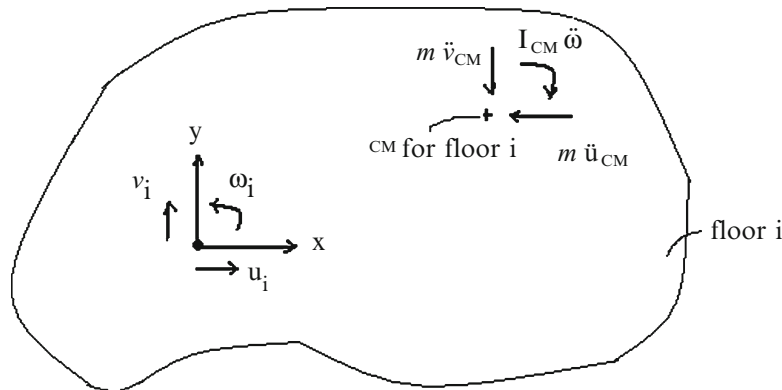


Fig. 14.21 Inertia forces for floor i

The inertia forces for a floor depend on the mass distribution and acceleration of the floor. They act at the center of mass, a property of the floor. Figure 14.21 shows the inertia force for floor i .

We require floor i to be in equilibrium. Summing forces with respect to the origin at O, results in the following equilibrium equations

$$\begin{aligned}
 P_x^{(i)} - m^{(i)}\ddot{u}_{i,CM} - R_x^{(i)} + R_x^{(i+1)} &= 0 \\
 P_y^{(i)} - m^{(i)}\ddot{v}_{i,CM} - R_y^{(i)} + R_y^{(i+1)} &= 0 \\
 M_0^{(i)} - I_{CM}^{(i)}\ddot{\omega} - M_C^{(i)} + M_C^{(i+1)} + m^{(i)}y_{CM}^{(i)}\ddot{u}_{i,CM} - m^{(i)}x_{CM}^{(i)}\ddot{v}_{i,CM} + y_{CT}^{(i)}R_x^{(i)} \\
 - x_{CT}^{(i)}R_y^{(i)} - y_{CT}^{(i+1)}R_x^{(i+1)} + x_{CT}^{(i+1)}R_y^{(i+1)} &= 0
 \end{aligned} \tag{14.38}$$

The form of (14.36) and (14.37) shows that the equilibrium equations for floor i involve the displacements for floor $i - 1$, i , and $i + 1$. Assuming there are n floors, there are n sets of equations similar in form to (14.38).

When the location of the center of mass is the same for all the floors; we take the origin at the “common” center of mass. If the center of twist also coincides with the center of mass, the equations simplify to

$$\begin{aligned}
 P_x^{(i)} &= m^{(i)}\ddot{u}_i + K_{xx}^{(i)}(u_i - u_{i-1}) - K_{xx}^{(i+1)}(u_{i+1} - u_i) \\
 P_y^{(i)} &= m^{(i)}\ddot{v}_i + K_{yy}^{(i)}(v_i - v_{i-1}) - K_{yy}^{(i+1)}(v_{i+1} - v_i) \\
 M_0^{(i)} &= I^{(i)}\ddot{\omega}_i + K_C^{(i)}(\omega_i - \omega_{i-1}) - K_C^{(i+1)}(\omega_{i+1} - \omega_i)
 \end{aligned} \tag{14.39}$$

where u , v , and ω are the displacement measures for the center of mass.

These equations are useful for qualitative reasoning about the behavior. In general, we want to avoid torsion, if possible. Therefore, we distribute the interstory stiffness elements such that the location of the center of twist is constant for all stories. In regions where the seismic loading is high, such as California, one needs to consider dynamic response. In this case, the goal in seismic design is to have the center of mass and center of twist coincide throughout the height of the structure.

The formulation obtained above can be interpreted as a “shear beam” formulation for a building system in the sense that the assumptions we introduced concerning the behavior of a floor are similar to those for a beam subjected to shearing and torsional action. These assumptions are applicable for low-rise buildings, where the aspect ratio, defined as the ratio of height to width, is of order 1. Most buildings are in this category. For tall buildings and for those structures having flexible floors, one creates idealized models consisting of 3D frame structures composed of columns, beams, shear walls, and floor plates. These models generally involve a large number of variables and require computer-based analysis methods to generate solutions. The advantage of simple models is that one can reason about behavior through examination of analytical solutions. Both approaches are necessary and each has a role.

14.3.5 Matrix Formulation: Shear Beam Model

In what follows, we introduce matrix notation and express the equations defined in the previous section in a form similar to the equations for a member system that are presented in Chap. 12. We number the floor and stories consecutively, and work with the common X - Y - Z reference frame shown in Fig. 14.22. The following notation is used for floor i :

$$\begin{aligned}\underline{U}_i^o &= \{u_i, v_i, \omega_i\} = \text{Floor displacement vector} \\ P_i &= \{P_{xi}, P_{yi}, M_{zi}\} = \text{External load vector}\end{aligned}\quad (14.40)$$

These quantities are referred to the common global reference frame located at point O.

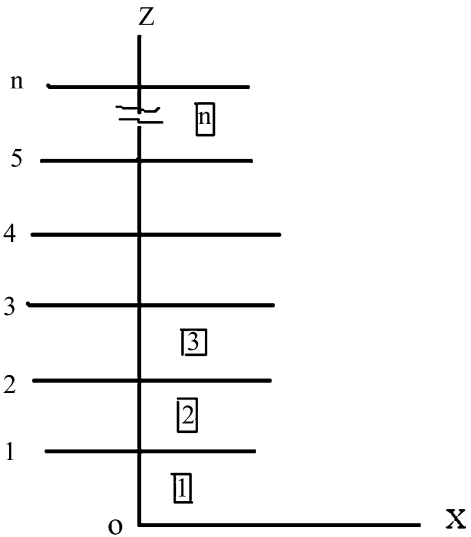
The interstory displacements at the center of twist for story i are expressed as a matrix product.

$$\Delta \underline{U}_{CT,i} = T_{CT,i} \{\underline{U}_i - \underline{U}_{i-1}\} \quad (14.41)$$

where T_{CT} has the following general form

$$T_{CT,i} = \begin{bmatrix} 1 & 0 & -y_{CT}^{(i)} \\ 0 & 1 & x_{CT}^{(i)} \\ 0 & 0 & 1 \end{bmatrix} \quad (14.42)$$

Fig. 14.22 Numbering scheme for floors and stories



The corresponding story resistance force matrices acting at the centers of twist are related to these interstory displacements by [see (14.27)]

$$\begin{aligned} \underline{R}_{CT,i} &= K_i \Delta \underline{U}_{CT,i} \\ \underline{R}_{CT,i+1} &= K_{i+1} \Delta \underline{U}_{CT,i+1} \end{aligned} \quad (14.43)$$

where \underline{K}_j depends on the stiffness properties for story j .

$$\underline{K}_j = \begin{bmatrix} K_{xx}^{(j)} & 0 & 0 \\ 0 & K_{yy}^{(j)} & 0 \\ 0 & 0 & K_C^{(j)} \end{bmatrix} \quad (14.44)$$

We need to transfer these forces from the center of twist to the origin of the common reference frame. This operation involves the transpose of \underline{T}_{CT} .

$$\begin{aligned} \underline{R}_{o,i} &= \underline{T}_{CT,i}^T \underline{R}_{CT,i} \\ \underline{R}_{o,i+1} &= \underline{T}_{CT,i+1}^T \underline{R}_{CT,i+1} \end{aligned} \quad (14.45)$$

Using (14.41) and (14.43), (14.45) expands to

$$\begin{aligned} \underline{R}_{o,i} &= \underline{K}_{o,i} (\underline{U}_i - \underline{U}_{i-1}) \\ \underline{R}_{o,i+1} &= \underline{K}_{o,i+1} (\underline{U}_{i+1} - \underline{U}_i) \end{aligned} \quad (14.46)$$

where \underline{K}_o is the stiffness matrix referred to the common origin, O.

$$\underline{K}_{o,j} = \underline{T}_{CT,j}^T \underline{K}_j \underline{T}_{CT,j} \quad (14.47)$$

One starts with the properties of the center of twist namely, K_{xx} , K_{yy} , K_C , x_{CT} , y_{CT} , and then generates \underline{K}_o for each story.

We consider next the inertia forces which act at the center of mass of the floor. The displacements are related by

$$\begin{aligned} \underline{U}_{CM,i} &= T_{CM,i} U_i \\ T_{CM,i} &= \begin{bmatrix} 1 & 0 & -y_{CM} \\ 0 & 1 & x_{CM} \\ 0 & 0 & 1 \end{bmatrix} \end{aligned} \quad (14.48)$$

The inertia force matrix acting at the center of mass is related to the acceleration matrix by

$$\underline{F}_{CM,i} = -\underline{m}_i \ddot{\underline{U}}_{CM,i} = -\underline{m}_i T_{CM,i} \ddot{\underline{U}}_i \quad (14.49)$$

where

$$\underline{m}_i = \begin{bmatrix} m^{(i)} & & \\ & m^{(i)} & \\ & & T_{CM}^{(i)} \end{bmatrix} \quad (14.50)$$

Translating these forces from the center of mass to the origin leads to

$$\begin{aligned} \underline{F}_{o,i} &= m_{o,i} \ddot{\underline{U}}_i \\ \underline{m}_{o,i} &= \underline{T}_{CM,i}^T \underline{m}_i \underline{T}_{CM,i} \end{aligned} \quad (14.51)$$

We interpret $\underline{m}_{o,i}$ as the effective mass matrix for floor i .

Finally, summing forces for floor i , the matrix equilibrium equation referred to the common reference frame has the form.

$$\underline{P}_{o,i} = m_{o,i} \ddot{\underline{U}}_i + \underline{R}_{o,i} - \underline{R}_{o,i+1} = 0 \quad (14.52)$$

Substituting for the internal resistance matrices, the expanded form for floor i is

$$\underline{P}_{o,i} = m_{o,i} \ddot{\underline{U}}_i + \underline{K}_{o,i}(U_i - U_{i-1}) - \underline{K}_{o,i+1}(U_{i+1} - U_i) \quad (14.53)$$

We suppose these are N floors and express the complete set of N equations as a single matrix equation,

$$\underline{P} = \underline{m}\ddot{\underline{U}} + \underline{K}\underline{U} \quad (14.54)$$

We assemble \underline{m} and \underline{K} in partitioned form (N rows and N columns). The entries follow from (14.53).

$$i = 1, 2, \dots, N$$

$m_{o,i}$ in partitioned row i and column i of \underline{m}

$$+ \underline{K}_{o,i} \left\{ \begin{array}{l} \text{in row } i \text{ and column } i \\ \text{in row } i - 1 \text{ and column } i - 1 \end{array} \right\} \text{of } \underline{K} \quad (14.55)$$

$$- \underline{K}_{o,i} \left\{ \begin{array}{l} \text{in row } i \text{ and column } i - 1 \\ \text{in row } i - 1 \text{ and column } i \end{array} \right\} \text{of } \underline{K}$$

$$P_{o,i} \quad \text{in row } i \text{ of } P$$

Note that this approach is *identical* to the procedure that we followed in Chap. 12 to assemble the system matrices for a member system. The following example illustrates the steps for a three story structure.

Example 14.14

Given: The three story structure shown in Fig. E14.14a. Assume the transformed mass and stiffness properties are known for each floor.

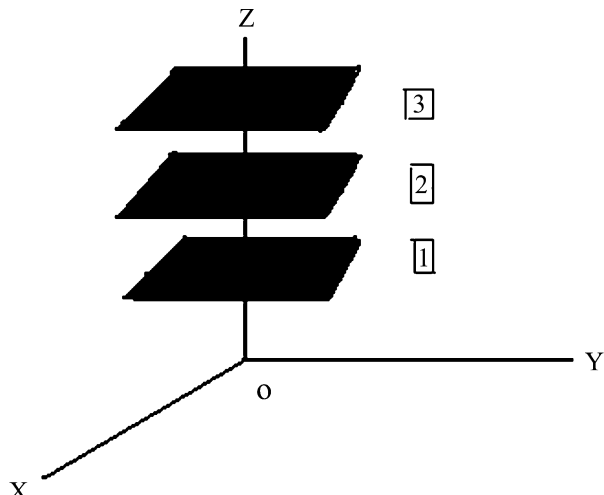


Fig. E14.14a

Determine: The non-zero entries in the system load, mass, and stiffness matrices.
Solution: $N = 3$ for this example. The partitioned form of the equations is listed below.

$$\begin{Bmatrix} P_{o,1} \\ P_{o,2} \\ P_{o,3} \end{Bmatrix} = \begin{bmatrix} \underline{m}_{o,1} & & \\ & \underline{m}_{o,2} & \\ & & \underline{m}_{o,3} \end{bmatrix} \begin{Bmatrix} \ddot{U}_1 \\ \ddot{U}_2 \\ \ddot{U}_3 \end{Bmatrix} + \begin{bmatrix} (\underline{K}_{o,1} + \underline{K}_{o,2}) & -\underline{K}_{o,2} & 0 \\ -\underline{K}_{o,2} & (\underline{K}_{o,2} + \underline{K}_{o,3}) & -\underline{K}_{o,3} \\ 0 & -\underline{K}_{o,3} & \underline{K}_{o,3} \end{bmatrix} \begin{Bmatrix} \underline{U}_1 \\ \underline{U}_2 \\ \underline{U}_3 \end{Bmatrix}$$

14.4 Response of Symmetrical Buildings

We consider the symmetrical structural system shown in Fig. 14.23. We locate the global reference frame on the symmetry axis. By definition, the center of mass and center of twist for all the floors are located on the Z-axis.

We suppose the external floor loading is applied in the X direction. This loading is resisted by the frames supporting the floors. Each frame displaces in the X direction and develops resistance through shearing action between the floors.

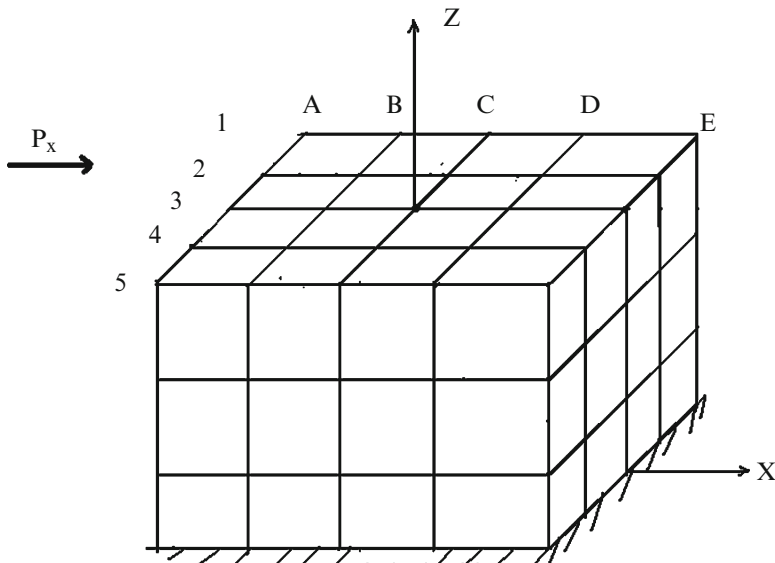


Fig. 14.23 Symmetrical building structure

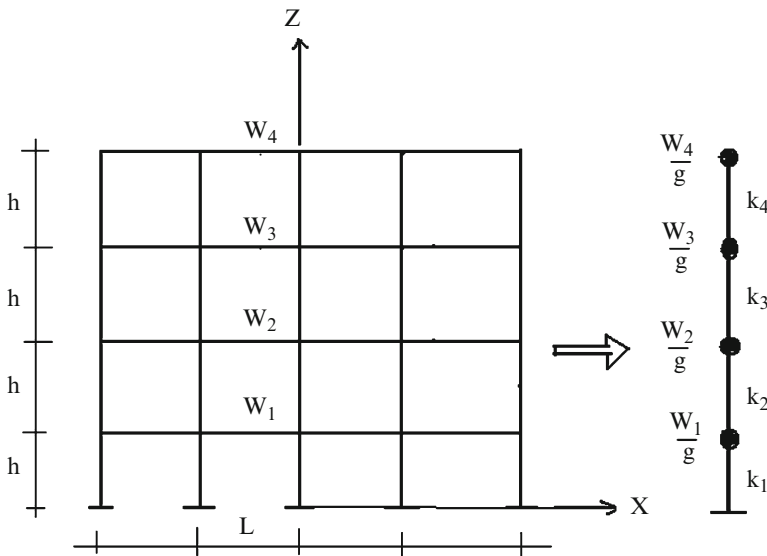


Fig. 14.24 Shear model of typical frame

We model a typical frame as a set of discrete masses supported by shear springs. Figure 14.24 illustrates this idealization. The shear spring stiffness for a story in a frame is determined by summing the contribution of the columns contained in the story. We developed an approximate method for estimating lateral stiffness for frames in Chap. 11. Applying this method, the equivalent shear stiffness for a story in a frame is estimated as

$$k_{\text{story } i} = \frac{12E}{h^3} \sum_{\text{inter col}} I_c \frac{1}{(1 + (r/2))} + \frac{12E}{h^3} \sum_{\text{exter col}} I_c \frac{1}{(1 + r)} \quad (14.56)$$

where r is the ratio of relative stiffness factors for the column and girder.

$$r = \frac{I_{\text{col}}/h}{I_{\text{girder}}/L}$$

We evaluate the story shear stiffness factors for each frame. When shear walls or braces are present in a story, we combine the stiffness terms corresponding to the braces according to

$$k|_{\text{story } i} = k_{\text{col}}|_{\text{story } i} + k_{\text{brace}}|_{\text{story } i} \quad (14.57)$$

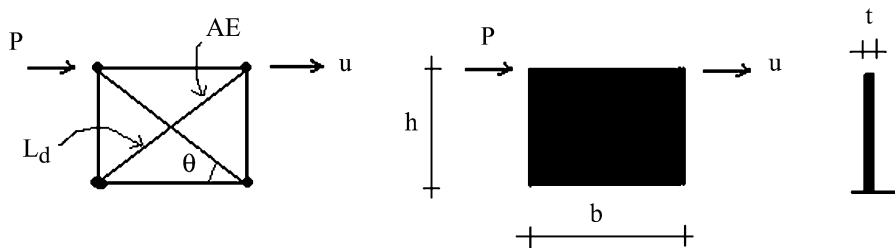


Fig. 14.25 Shear stiffness elements. (a) Steel brace. (b) Concrete shear wall

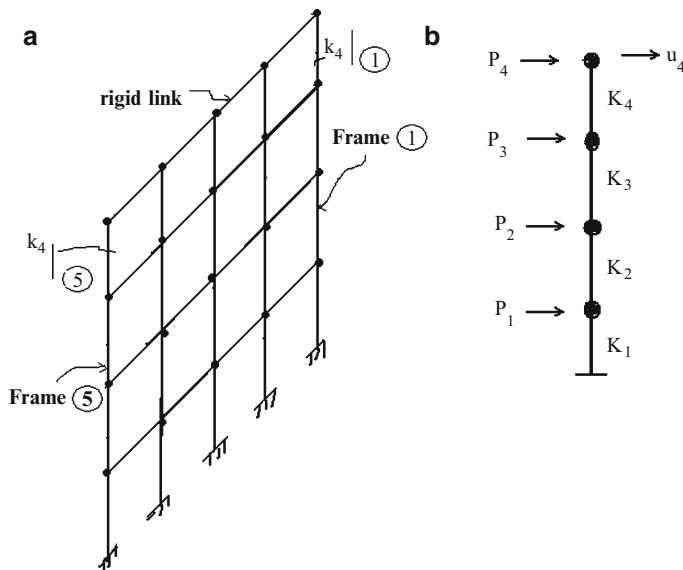


Fig. 14.26 Idealized building model. (a) Set of frames with rigid link. (b) Global loads and global story stiffnesses

The shear stiffness factors for the shear elements defined in Fig. 14.25 are

$$k_{\text{shearwall}} = \frac{h}{Gbt} \quad (14.58)$$

$$k_{\text{brace}} = \frac{2AE}{L_d} (\cos \theta)^2 \quad (14.59)$$

The complete building system is represented as a set of frames in parallel linked through the “rigid” floor slab. Figure 14.26 illustrates this idealization. At each

story level, *all frames experience the same lateral displacement*. It follows that the story shear force in a particular frame is proportional to the ratio of the frame story shear stiffness to the global story shear stiffness which is defined as

$$K_{\text{global, floor } i} = K_i = \sum_{\text{frames}} k_i \Big|_{\text{frame } j} \quad (14.60)$$

$$V_{\text{frame } j} = \frac{k_i|_{\text{frame } j}}{K_i} V_i|_{\text{global}}$$

Generalizing this result, we can state that the lateral global loads are distributed to the individual parallel frames in proportion to their relative stiffness.

Noting Fig. 14.26, the global shear for a story is equal to the sum of the loads acting on the floors above the particular floor. For example,

$$V_1|_{\text{global}} = P_1 + P_2 + P_3 + P_4 \quad (14.61)$$

$$V_2|_{\text{global}} = P_2 + P_3 + P_4$$

One first evaluates these global shear forces and then determines the individual frame story shears with (14.60).

Suppose the ratio of story stiffness to global story stiffness is constant for all stories in frame j

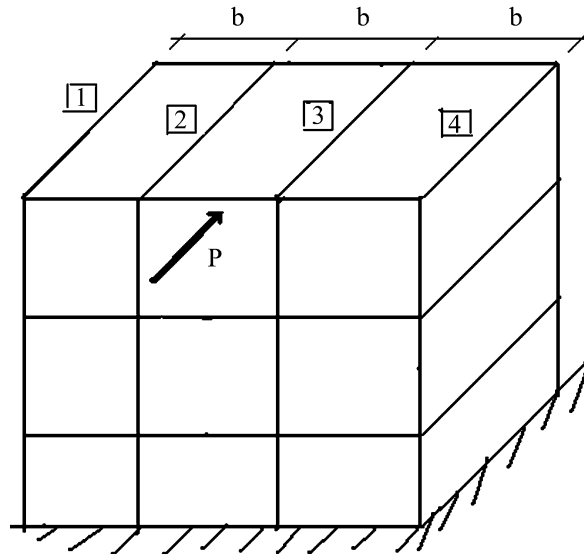
$$\frac{k_i|_{\text{frame } j}}{K_i} = \alpha_j \quad (14.62)$$

Then, it follows that frame j carries a fraction equal to α_j of the total applied load. This result is useful since it allows one to reason in a qualitative way about how global floor loads are distributed into the frames. For example, suppose that there are n frames having equal stiffness then, each frame carries $(1/n)$ of the total lateral load.

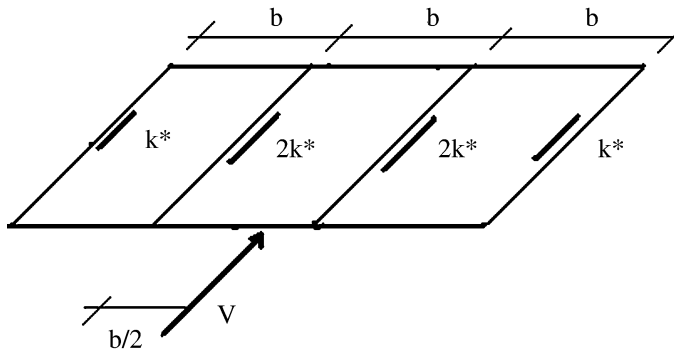
Example 14.15

Given: The symmetrical rigid frame structure shown in Fig. E14.15a. Assume the frame properties are constant throughout the building height and also assume the structure is uniformly loaded. (a) The columns in frames 2 and 3 are twice as stiff as the columns in frames 1 and 4 and the floor slab is rigid. (b) Assume equal frame stiffnesses and rigid floor slab. (c) Assume equal frame stiffnesses and a flexible floor slab.

Determine: The distribution of the total lateral load to the individual frames.

Fig. E14.15a**Solution:**

Part (a): A typical floor is shown in Fig. E14.15b. The equivalent story shear stiffness factors are defined as k^* and $2k^*$. The resultant global shear force acts at the midpoint of the side and there is no twist since the stiffness distribution is symmetrical.

**Fig. E14.15b** Typical floor

The total story stiffness is

$$\sum k_j = (k^*)(1 + 2 + 2 + 1) = 6k^*$$

According to (14.60), the fraction of the total story shear carried by an individual frame is equal to the ratio of the frame story stiffness to the total story stiffness. Then

For frames 1 and 4

$$V_1 = V_4 = V \frac{k^*}{6k^*} = \frac{1}{6}V$$

For frames 2 and 3

$$V_2 = V_3 = V \frac{2k^*}{6k^*} = \frac{1}{3}V$$

In this case, *the interior frames carry twice as much load as the exterior frames.*

Part (b): If the floor slab is rigid and equal frame stiffnesses are used, the frame load distribution shown in Fig. E14.15c is now applicable; the shear is assigned uniformly to the frames.

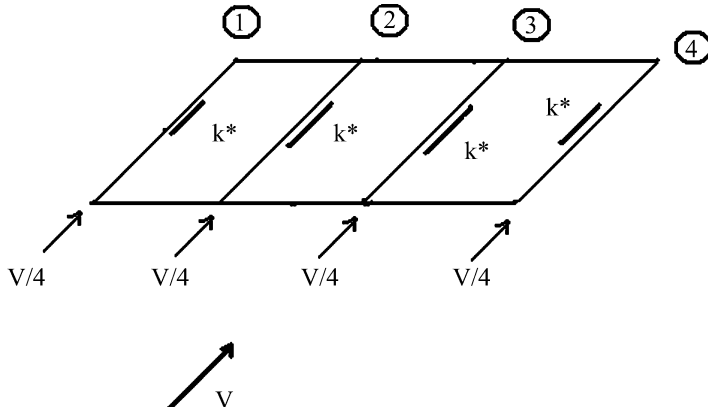


Fig. E14.15c Typical floor

Part (c): Suppose one generates an estimate for the global loading on an individual frame using the tributary areas for the frames. Consider the structure shown in Fig. E14.15a. We divide the façade area into area segments and associate these segmental areas with the frames adjacent to the areas as illustrated in Fig. E14.15d.

We note that the width for the segmental areas 1 and 4 is $\frac{1}{2}$ the width for the interior tributary areas. Therefore, assuming the external loading is constant over the width, it follows that the magnitude of the loads for frames 1 and 4 is $\frac{1}{2}$ the load for the interior frames. This breakdown is shown in Fig. E14.15e. This distribution is based on the assumption that the frames act independently, i.e., the floor slabs are flexible.

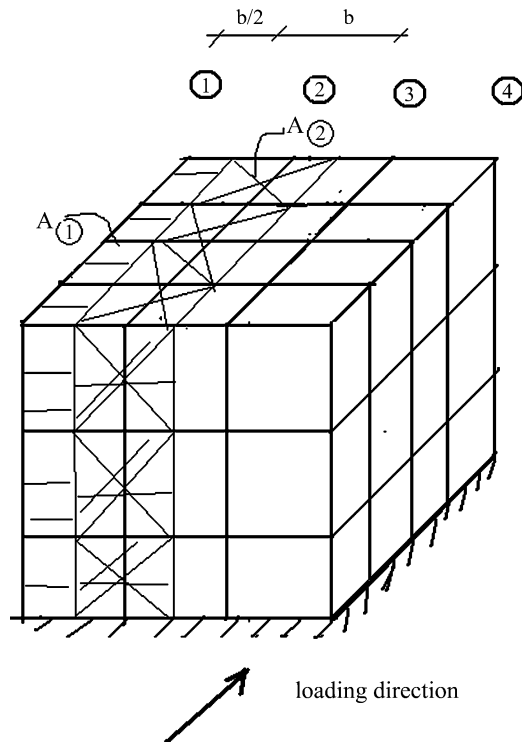


Fig. E14.15d

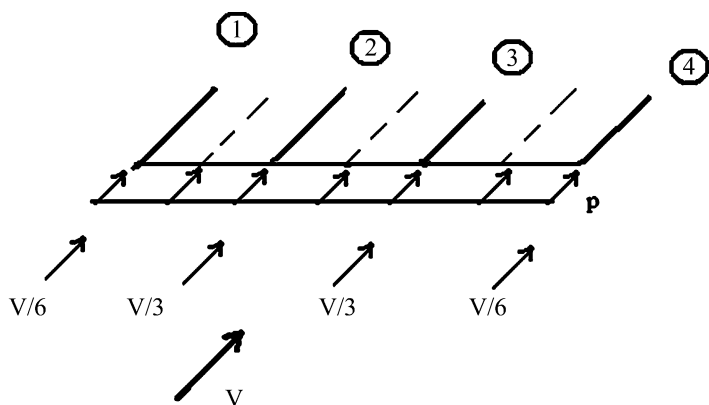


Fig. E14.15e

Example 14.16

Given: The five story symmetrical rigid frame building shown in Figs. E14.16a, b. Assume the building can be subjected to an earthquake in either the North–South or East–West directions. Take the spectral acceleration as $S_a = 0.15g$. Consider all the beams to be the same size and all the columns to be the same size. Assume $I_B = 4I_C$.

Determine: The maximum moments in the columns (a) for flexible floors and (b) for rigid floors.

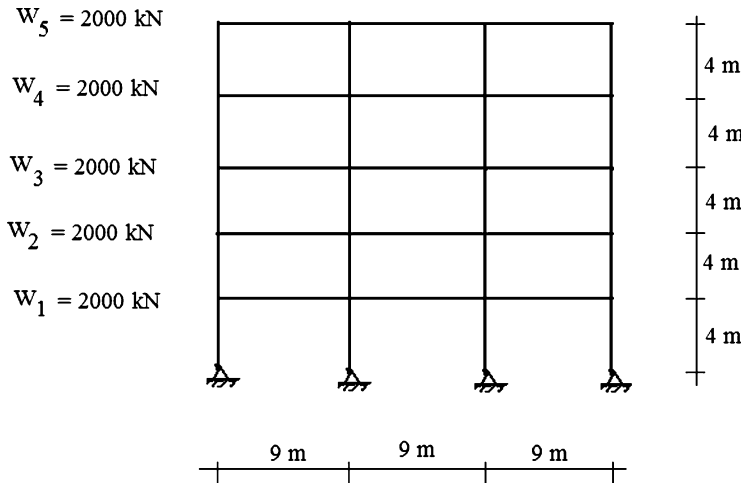


Fig. E14.16a Elevation

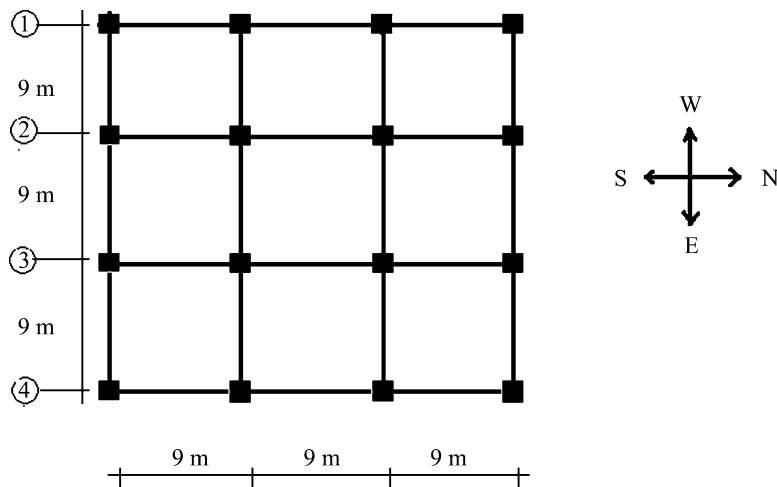


Fig. E14.16b Typical floor plan

Solution: We use (14.10). The base shear is given by

$$\begin{aligned} V|_{\text{base}} &= \frac{\left(\sum_{i=1}^5 Z_i W_i\right)^2}{\sum_{i=1}^5 W_i (Z_i)^2} S_a \\ &= \frac{(2,000(3) + 2,000(6) + 2,000(9) + 2,000(12) + 2,000(15))^2}{2,000(3)^2 + 2,000(6)^2 + 2,000(9)^2 + 2,000(12)^2 + 2,000(15)^2} (0.15) \\ &= 1,227 \text{kN} \end{aligned}$$

Then, applying (14.11), we obtain the individual floor loads (Fig. E14.16c).

$$P|_{\text{floor } i} = \left(\frac{W_i Z_i}{\sum W_i Z_i} \right) V|_{\text{base}}$$

$$\sum_{i=1}^5 W_i Z_i = 2,000(3) + 2,000(6) + 2,000(9) + 2,000(12) + 2,000(15)$$

$$= 90,000 \text{kN/m}$$

$$P|_{\text{floor 1}} = \frac{3(2,000)}{90,000} (1,227) = 81.8 \text{kN}$$

$$P|_{\text{floor 2}} = \frac{6(2,000)}{90,000} (1,227) = 163.6 \text{kN}$$

$$P|_{\text{floor 3}} = \frac{9(2,000)}{90,000} (1,227) = 245.4 \text{kN}$$

$$P|_{\text{floor 4}} = \frac{12(2,000)}{90,000} (1,227) = 327.2 \text{kN}$$

$$P|_{\text{floor 5}} = \frac{15(2,000)}{90,000} (1,227) = 409 \text{kN}$$

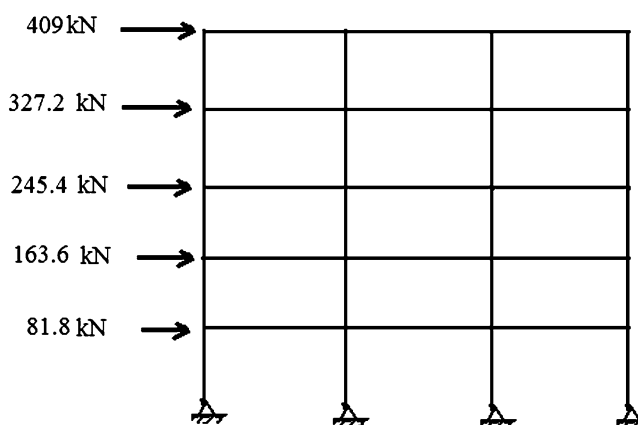


Fig. E14.16c Earthquake floor loads

It remains to distribute the floor loads to the frames. Since the structure is symmetrical, we need to consider only one direction, say the N–S direction (Fig. E14.16d).

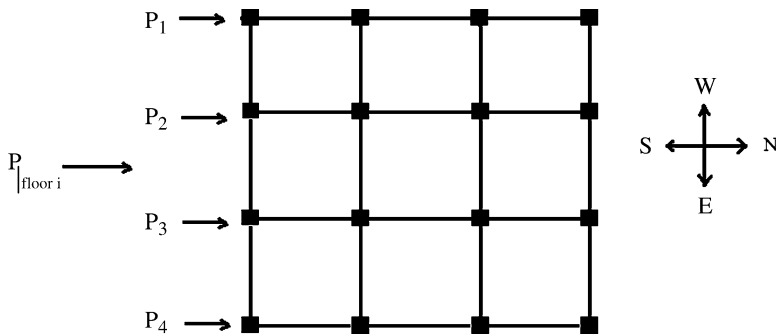


Fig. E14.16d Floor load distribution

When the floor slab is rigid, and the frame stiffnesses are equal, the floor load is distributed uniformly to the frames (Fig. E14.16e).

$$P_1 = P_2 = P_3 = P_4 = \frac{1}{4} P_{\text{floor } i}$$

Therefore

$$P_1 = P_2 = P_3 = P_4 = \begin{cases} 20.5 \text{ kN} \\ 40.9 \text{ kN} \\ 61.4 \text{ kN} \\ 81.8 \text{ kN} \\ 102.3 \text{ kN} \end{cases}$$

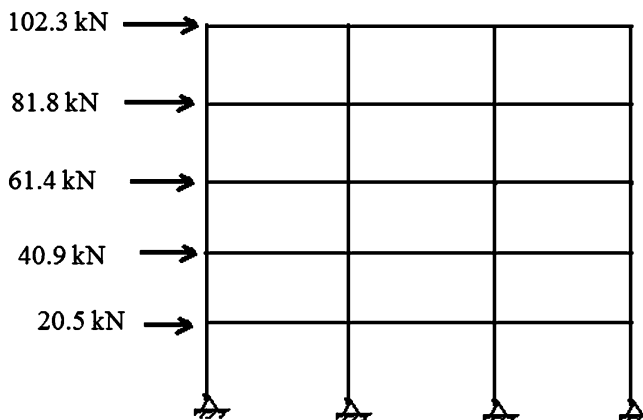


Fig. E14.16e Frame load—rigid floors

When the floor slab is flexible, the loads are proportioned to their tributary floor areas.

Then it follows that (Fig. E14.16f)

$$P_2 = P_3 = \frac{1}{3} P_{\text{floor}_i} = \begin{cases} 27.3 \text{ kN} \\ 54.5 \text{ kN} \\ 81.8 \text{ kN} \\ 109 \text{ kN} \\ 136.3 \text{ kN} \end{cases}$$

$$P_1 = P_4 = \frac{1}{6} P_{\text{floor}_i} = \begin{cases} 13.6 \text{ kN} \\ 27.3 \text{ kN} \\ 40.9 \text{ kN} \\ 54.5 \text{ kN} \\ 68.2 \text{ kN} \end{cases}$$

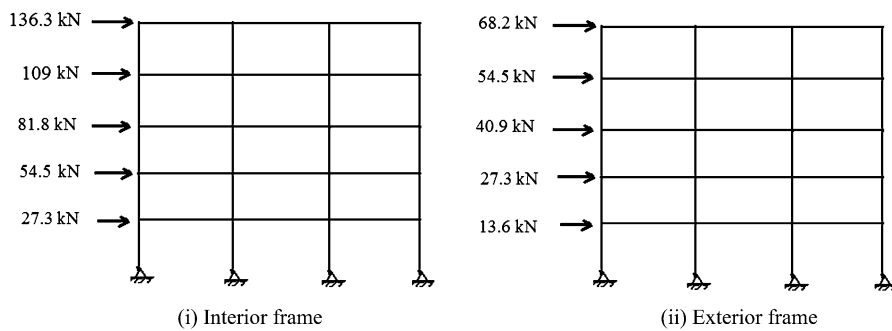


Fig. E14.16f Frame loads—flexible floors

We apply the stiffness method described in Chap. 11 to estimate the maximum moments in the column.

$$I_{C_{\text{ext}}} = I_C \text{ and } I_B = 4I_C \Rightarrow \frac{I_{C_{\text{ext}}}/h}{I_B/L} = \frac{I_C/h}{I_B/L} = \frac{(I_C/4)}{(4I_C/9)} = 0.5625$$

$$k_E = \frac{3EI_{CE}}{h^3} \left\{ \frac{1}{1 + \frac{1}{2} \left(\frac{I_{CE}/h}{I_b/L} \right)} \right\} = \frac{2.34EI_C}{h^3}$$

$$\Rightarrow \frac{k_E}{k_I} = 0.89$$

$$k_I = \frac{3EI_{CI}}{h^3} \left\{ \frac{1}{1 + \frac{1}{4} \left(\frac{I_{CI}/h}{I_b/L} \right)} \right\} = \frac{2.63EI_C}{h^3}$$

Noting that

$$\frac{V_E}{V_I} = \frac{k_E}{k_I}$$

we express the total shear as (Figs. E14.16g, h)

$$V_{\text{Total}} = 2V_E + 2V_I = 2\left(\frac{k_E}{k_I} + 1\right)V_I \Rightarrow V_I = 0.265V_{\text{Total}}$$

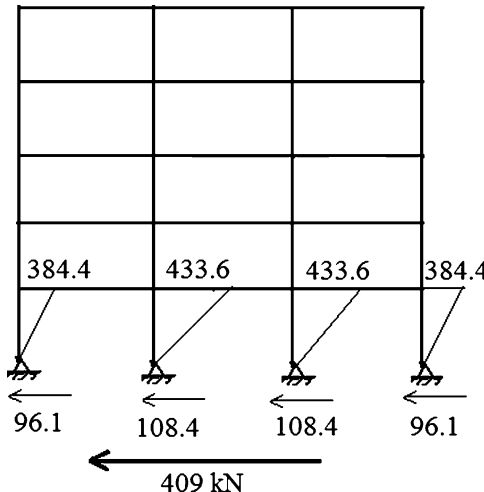


Fig. E14.16g Maximum column moments—rigid floors

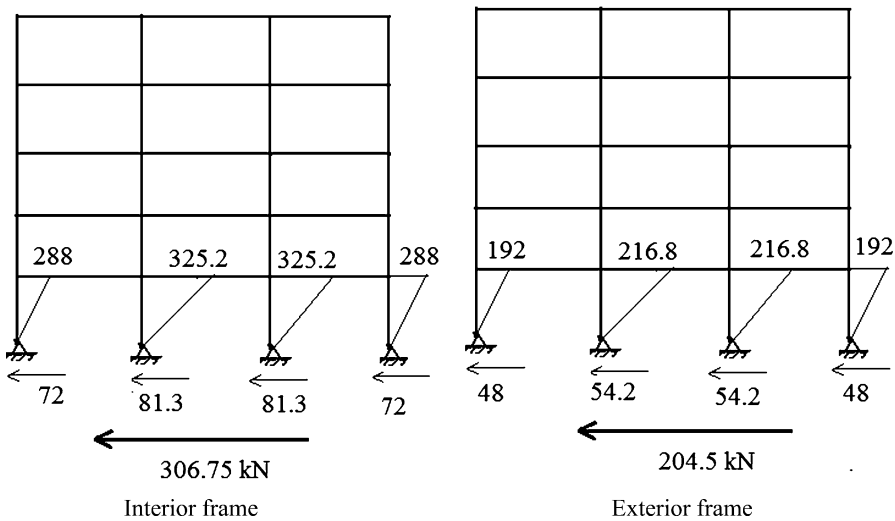


Fig. E14.16h Maximum column moments—flexible floors

Example 14.17

Given: The one story frame shown in Figs. E14.17a–c. Assume the cross-sections are equal.

Determine:

- The center of mass.
- The center of twist. Take $I_b = 2I_c$.
- The revised stiffness required on lines B-B and 2-2 so that the center of stiffness coincides with the center of mass.
- The translation and rotation of the center of twist for the structure determined in part (c) due to load P_1 .

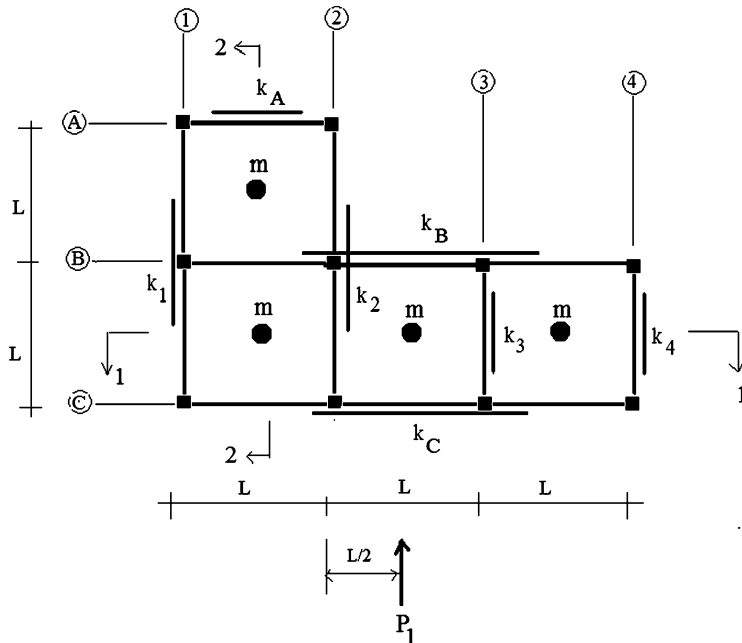


Fig. E14.17a Plan

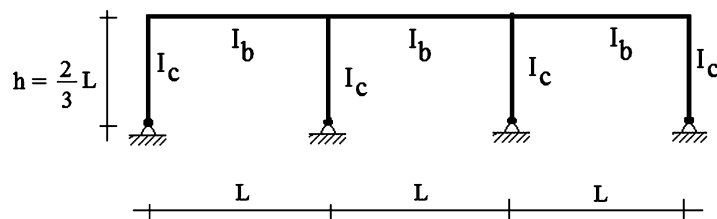
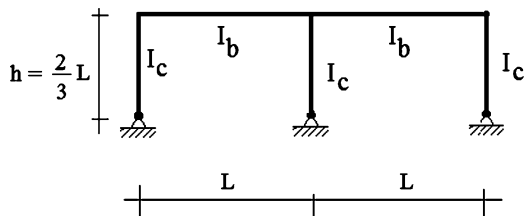


Fig. E14.17b Elevation—section 1-1

Fig. E14.17c Elevation—
section 2-2

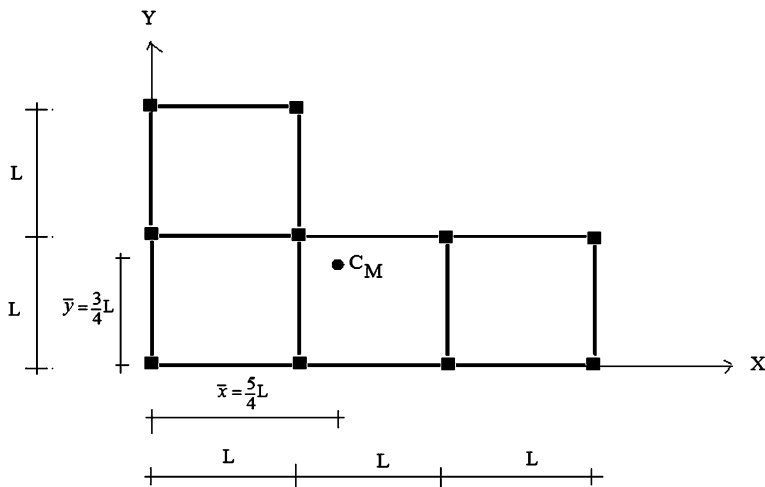


Solution:

(a) Locating the center of mass

$$\bar{x} = \frac{\sum x_i m_i}{\sum m_i} = \frac{(0.5L)2m + (1.5L)m + (2.5L)m}{4m} = \frac{5}{4}L$$

$$\bar{y} = \frac{\sum y_i m_i}{\sum m_i} = \frac{(0.5L)3m + (1.5L)m}{4m} = \frac{3}{4}L$$



(b) Locating the center of twist

$$I_{CE} = I_{CI} = I_c$$

$$I_b = 2I_c$$

$$\left(\frac{I_{CI}/h}{I_b/L} \right) = \left(\frac{I_{CE}/h}{I_b/L} \right) = \left(\frac{3I_c/2L}{2I_c/L} \right) = 0.75$$

Using the shear stiffness equations (11.11) and (11.12)

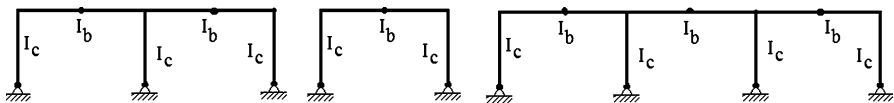
$$f_{BE} = \left\{ \frac{1}{1 + \frac{1}{2} \left(\frac{I_{CE}/h}{I_b/L} \right)} \right\} = 0.73$$

$$f_{BI} = \left\{ \frac{1}{1 + \frac{1}{4} \left(\frac{I_{CE}/h}{I_b/L} \right)} \right\} = 0.84$$

Let $(EI_c/h^3) = k$

$$k_{BE} = \frac{3EI_{CE}}{h^3} \left\{ \frac{1}{1 + \frac{1}{2} \left(\frac{I_{CE}/h}{I_b/L} \right)} \right\} = \frac{3EI_{CE}}{h^3} f_{BE} = 2.19k$$

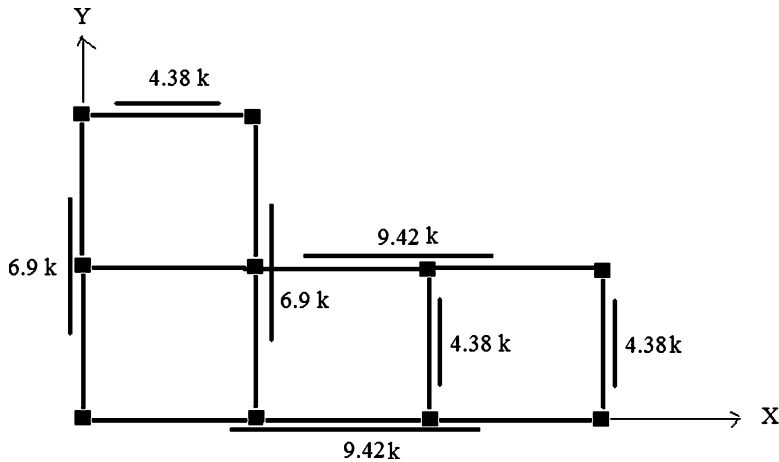
$$k_{BI} = \frac{3EI_{CI}}{h^3} \left\{ \frac{1}{1 + \frac{1}{4} \left(\frac{I_{CI}/h}{I_b/L} \right)} \right\} = \frac{3EI_{CI}}{h^3} f_{BI} = 2.52k$$



$$k_1 = k_2 = 2k_{BE} + k_{BI} = 6.9k$$

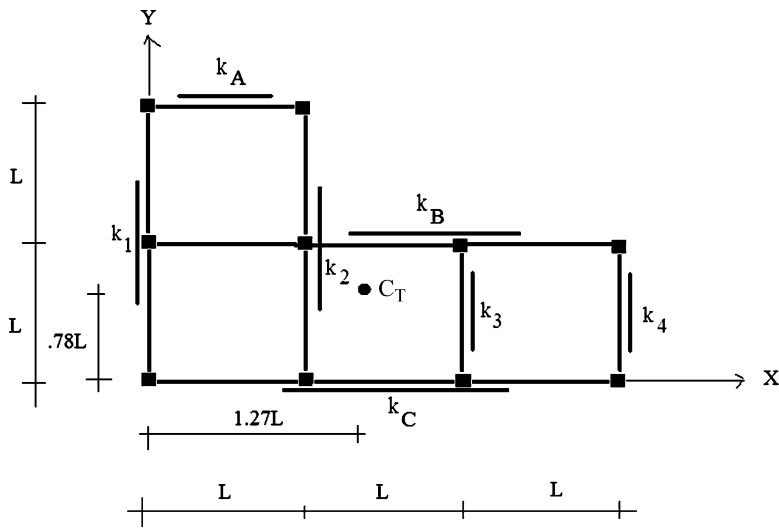
$$k_3 = k_4 = k_A = 2k_{BE} = 4.38k$$

$$k_B = k_C = 2k_{BE} + 2k_{BI} = 9.42k$$



$$x_{CT} = \frac{\sum x_j k_{yj}}{\sum k_{yj}} = \frac{6.9k(L) + 4.38k(2L) + 4.38k(3L)}{2(6.9k + 4.38k)} = 1.27L$$

$$y_{CT} = \frac{\sum y_i k_{xi}}{\sum k_{xi}} = \frac{9.42k(L) + 4.38k(2L)}{2(9.42k) + 4.38k} = 0.78L$$

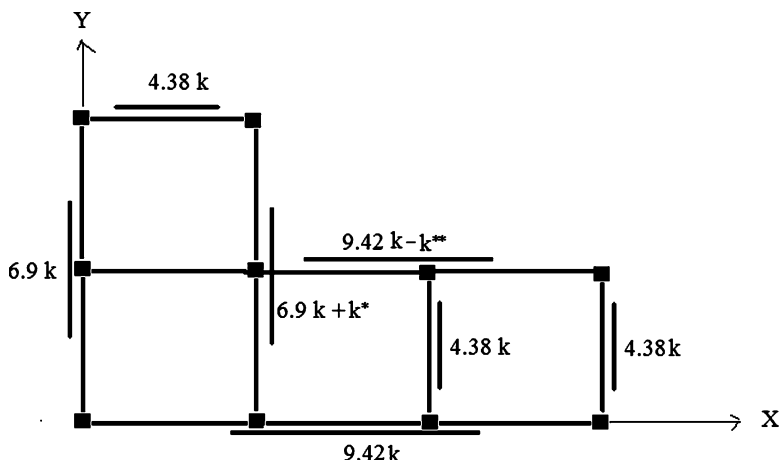


(c) The revised stiffness required on lines B-B and 2-2

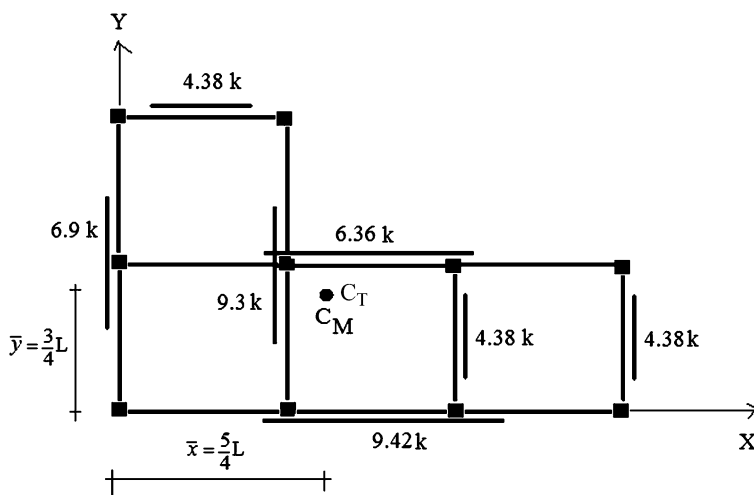
$$x_{CT} = \bar{x} = \frac{5}{4}L = \frac{(6.9k + k^*)(L) + 4.38k(2L) + 4.38k(3L)}{6.9k + (6.9k + k^*) + 2(4.38k)}$$

$$y_{CT} = \bar{y} = \frac{3}{4}L = \frac{(9.42k - k^{**})(L) + 4.38k(2L)}{9.42k + (9.42k - k^{**}) + 4.38k}$$

$$\therefore k^* = 2.4k \quad k^{**} = 3.06k$$



(d) The translation and rotation of the center of twist



Noting the result for part (c) and (14.20) specialized for the center of twist, the displacements of the center of twist due to P_1 are

$$K_{yy} = \sum k_{yj} = k\{6.9 + 9.3 + 2(4.38)\} = 24.96k$$

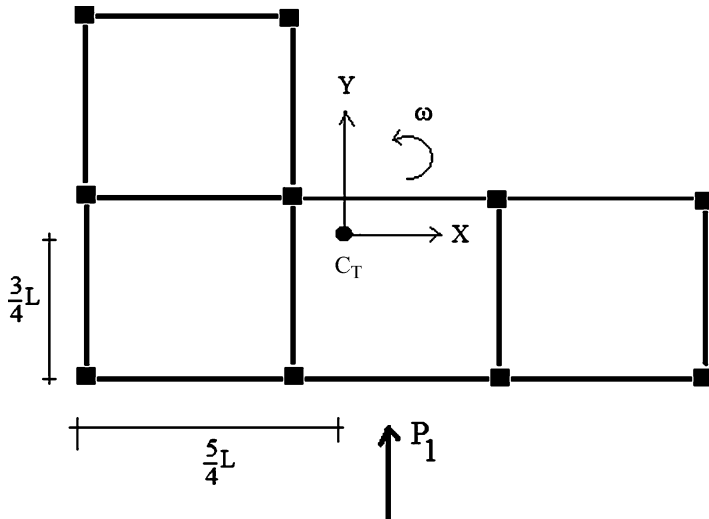
$$K_o = \sum y_i^2 k_{xi} + \sum x_j^2 k_{yj} = \left\{ 4.38k(1.25L)^2 + 9.42k(0.75L)^2 + 6.36k(0.25L)^2 \right\} + \left\{ 6.9k(1.25L)^2 + 9.3k(0.25L)^2 + 4.38k(0.75L)^2 + 4.38k(1.75L)^2 \right\} = 39.78kL^2$$

$$M_o = P_1 \left(\frac{L}{4} \right)$$

$$u = 0$$

$$v = \frac{P_y}{K_{yy}} = \frac{P_1}{24.96k}$$

$$\theta_z = \frac{M_0}{K_o} = \frac{P_1(L/4)}{39.78kL^2} = 0.00628 \frac{P_1}{kL}$$



14.5 Summary

14.5.1 Objectives

- To describe various idealized models that are used to represent building structures as an assemblage of plane frames and rigid floor slabs.
- To introduce procedures for generating wind and earthquake loads for building structures.

- To introduce the concepts of center of mass and center of stiffness and apply these concepts to typical building structures.
- To formulate the governing equations for a building idealized as a three-dimensional shear beam.
- To represent these equations using matrix notation.
- To specialize the formulation for symmetrical buildings.

14.5.2 Key Facts and Concepts

- The normal pressure due to wind varies as a power law ($p \sim z^{1/7}$) in the vertical direction.
- Seismic excitation is represented by a set of inertia forces acting at the floor levels.

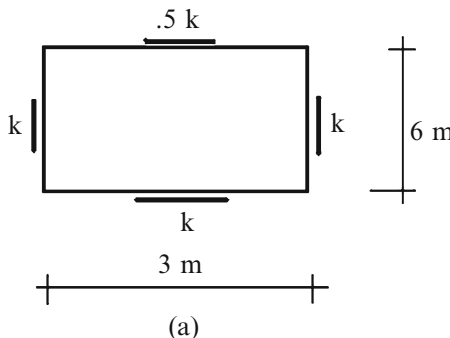
These forces are defined in terms of certain parameters that depend on the site and are specified by design codes. The vertical force distribution depends on the floor masses and increases with distance from the base.

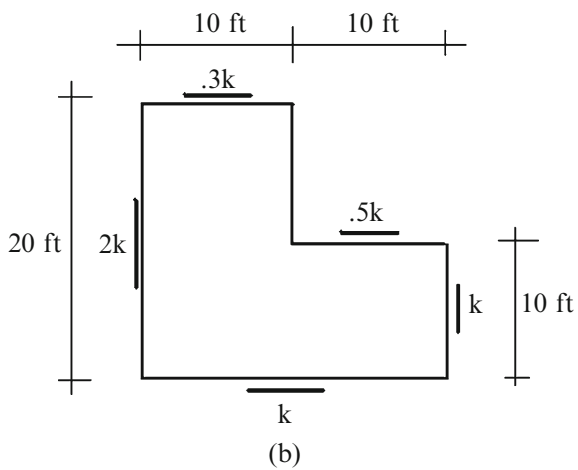
- The center of mass is a property of a floor, i.e., it depends on the mass distribution within the floor. It is important since the resultant of the inertia forces passes through the center of mass.
- The center of stiffness is a property of the lateral stiffness distribution in a story. Twisting of the floor slab will occur when the resultant force acting on a story does not pass through the center of stiffness. Ideally one positions the center of stiffness to coincide with the center of mass if dynamic loading is one of the design loading conditions.
- Given a set of parallel frames connected by a rigid diaphragm and subjected to a lateral load applied at the center of twist, the load carried by an individual frame is proportional to the relative stiffness of the frame.

14.6 Problems

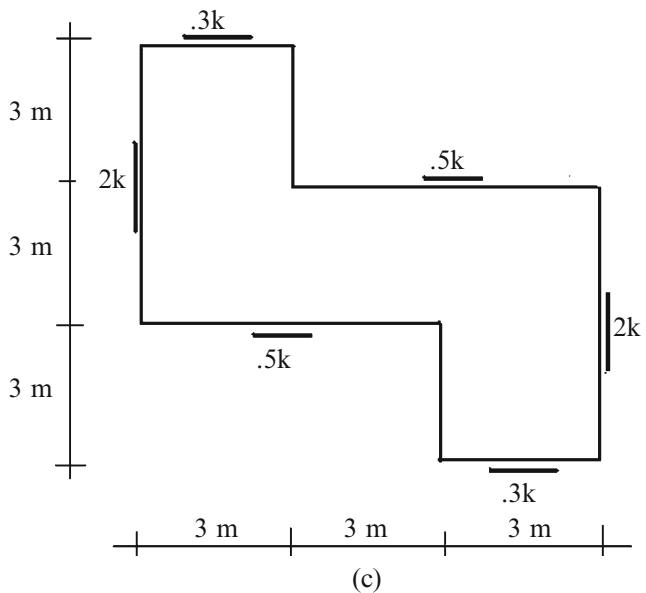
Problem 14.1

Consider the plan view of one story rigid frames shown below. Determine the center of twist corresponding to the brace stiffness patterns shown.

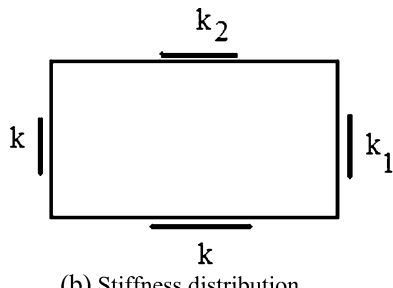
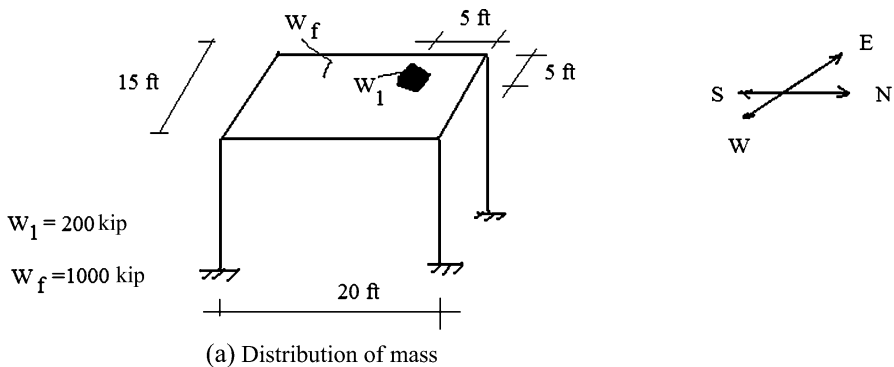




(b)



(c)

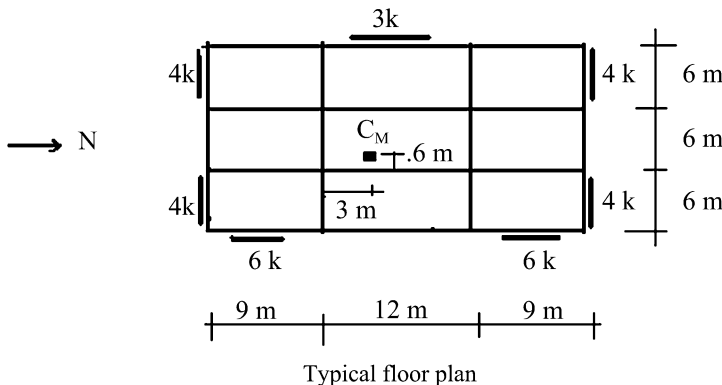
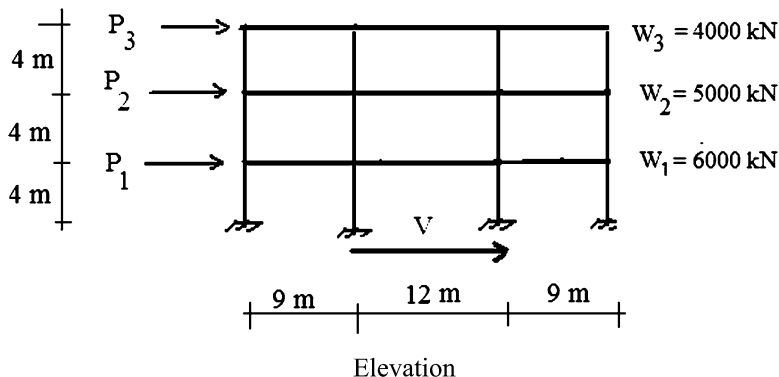
Problem 14.2

The one story frame shown has an unsymmetrical mass distribution.

- Determine the center of mass.
- Determine the stiffness parameters k_1 and k_2 such that the center of stiffness coincides with the center of mass.
- Determine the earthquake floor loads corresponding to $S_a = 0.3g$. Consider both directions, i.e., N-S and E-W.

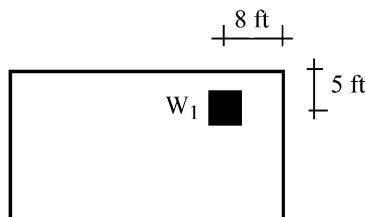
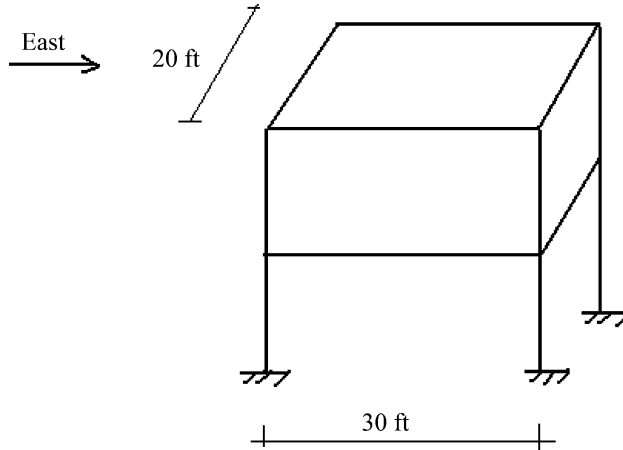
Problem 14.3

For the rigid frame shown below, determine (a) the center of twist (C_T) and (b) the seismic floor loads applied at the center of mass (C_M) for an N–S earthquake with $S_a = 0.3g$. Assume properties are equal for each floor.

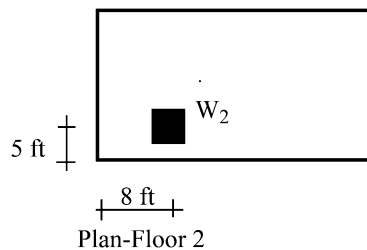


Problem 14.4

Consider the two story rigid frame defined below. Assume the weight of the floor slabs are equal to w_{floor} . Concentrated masses are located on each floor as indicated.



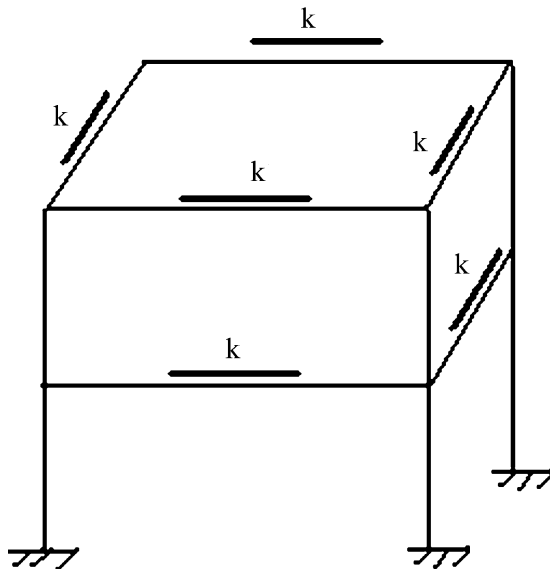
Plan-Floor 1



Plan-Floor 2

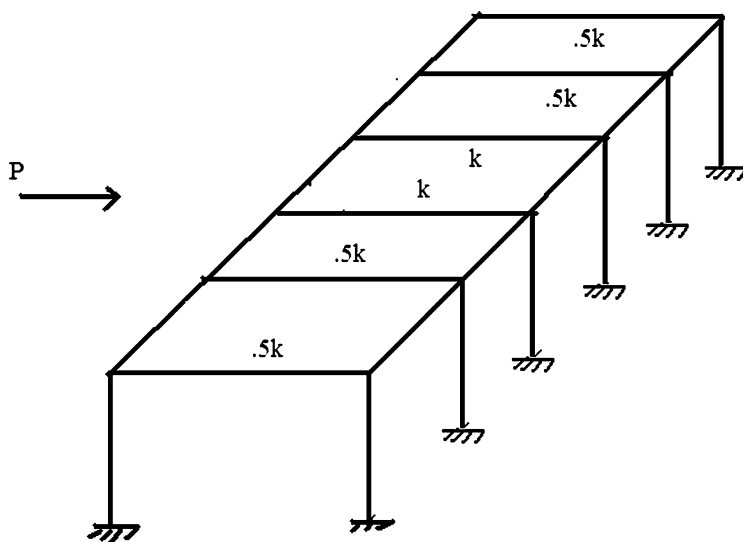
- Determine the position of the center of mass for each floor.
- Assume the structure is subjected to an earthquake acting in the east direction. Determine the earthquake forces for the individual floors. Assume $w_{\text{floor}} = 1000 \text{ kip}$, $w_1 = w_2 = 1000 \text{ kip}$, and $S_a = 0.3g$.

- (c) Suppose the story stiffness distribution shown below is used. Describe qualitatively how the structure will displace when subjected to an earthquake. Consider the stiffness distribution to be the same for each floor.



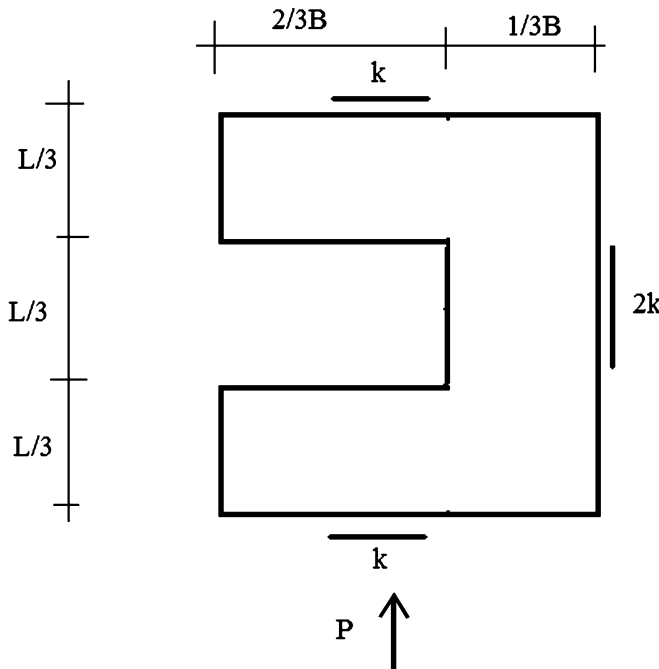
Problem 14.5

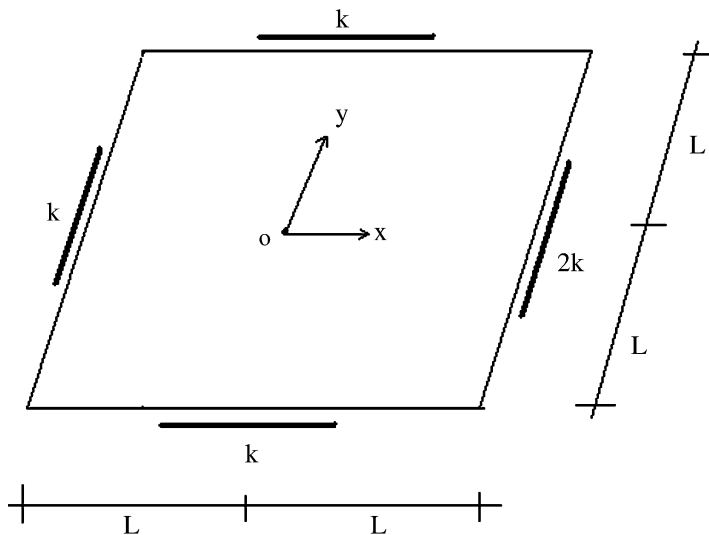
Consider the single story multi-frame structure shown below. Determine the lateral force in the frames due to a global load P . Consider both wind and earthquake loading. Assume the slab is rigid.



Problem 14.6

Consider the stiffness distribution for the one story rigid frame shown below. Determine the displaced configuration under the action of the loading shown. Assume the slab is rigid.

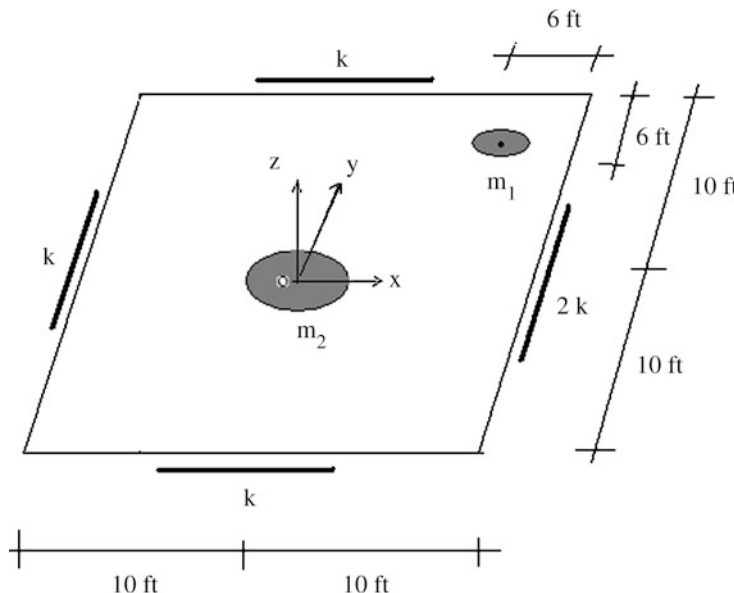


Problem 14.7

- (a) Determine the center of twist.
- (b) Using (14.47), determine K_0 .

Problem 14.8

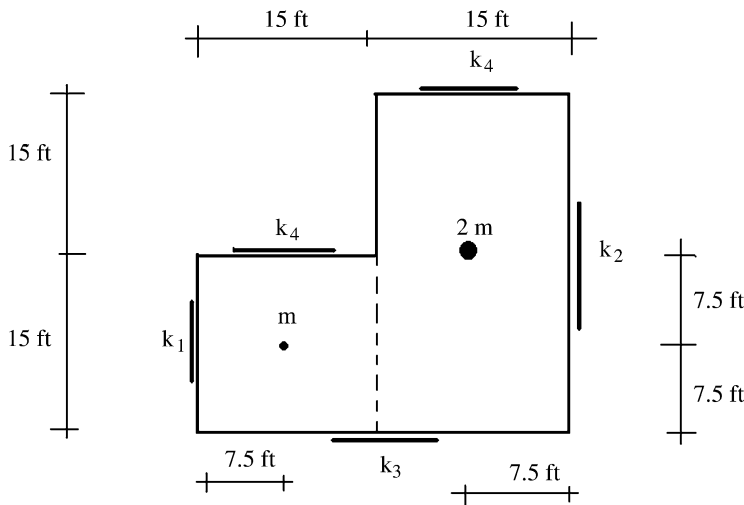
Consider the plan view of a one story frame shown below. Using the matrix formulation presented in Sect. 14.3.5, generate the equations of motion for the story. Take $m_1 = 1000 \text{ lb}$, $m_2 = 500 \text{ lb}$, and $k = 10 \text{ kip/in}$.



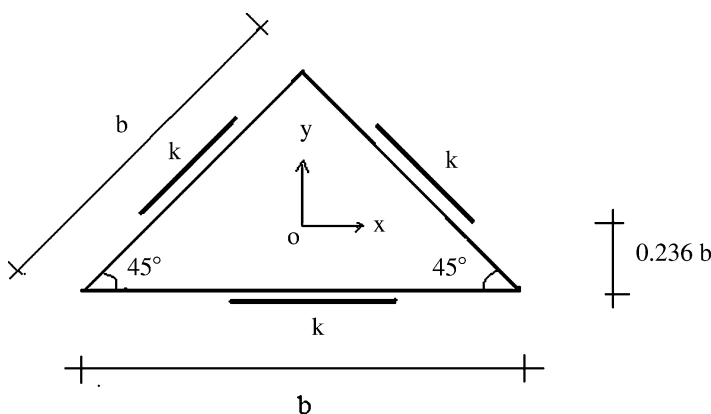
Problem 14.9

Consider the one story plan view shown below.

- Locate the center of mass.
- Locate the center of twist. Take $k_1 = k_2 = k_3 = k_4 = k$.
- Take $k_1 = k_3 = 10$. Suggest values for k_2 and k_4 such that the center of mass coincides with the center of twist.

**Problem 14.10**

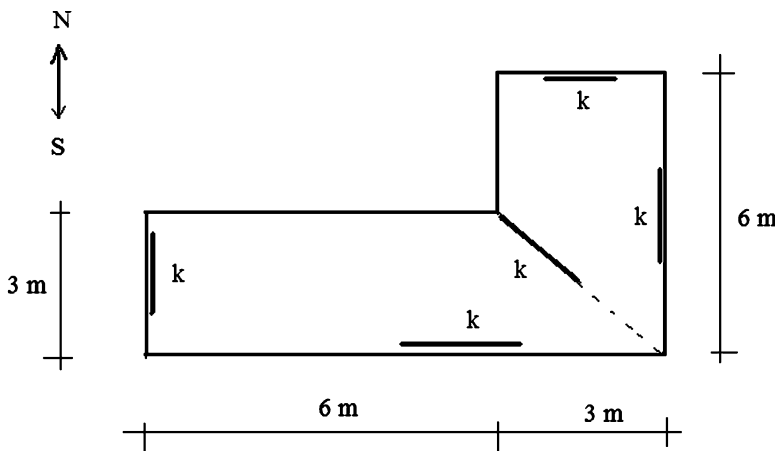
Consider the floor plan shown below. Assume the mass is uniformly distributed over the floor area. Establish the equations of motion referred to point O.



Problem 14.11

Consider the roof plan for a one story structure shown below. Assume the shear walls have equal stiffness and the roof dead load is uniform.

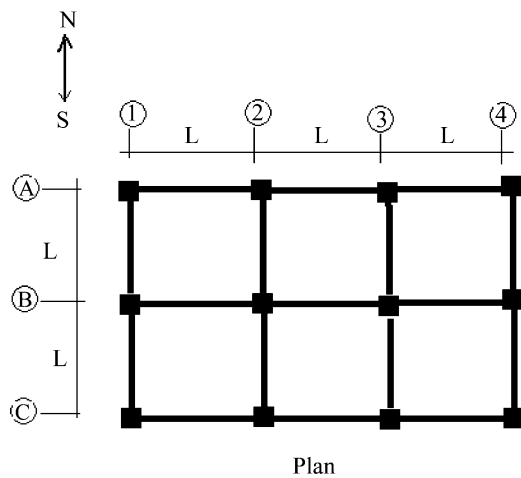
- Determine the center of mass and the center of stiffness.
- Describe how the structure responds to an earthquake in the N–S direction.



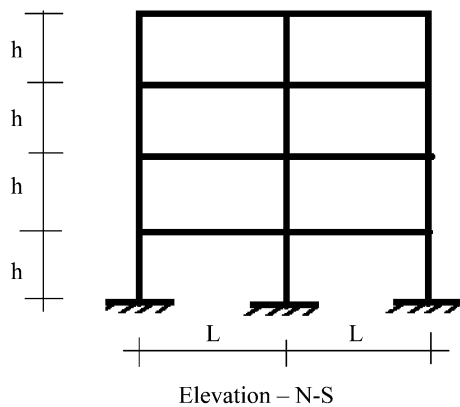
Problem 14.12

The framing shown below has identical rigid frames along column lines 1, 2, 3, and 4, and cross-bracing along lines A, B, and C. Consider all the beams and all the columns to be the same size. Assume $I_b = 3I_c$ and $L = 2h$.

- Assuming the roof slab is rigid with respect to the rigid frames, what part of the total seismic load due to a N–S earthquake is carried by frame 4.
- Repeat part (a) considering the roof slab to be flexible.



Plan



Elevation – N-S

Overview

The previous chapter dealt with issues related to the lateral loadings on building systems. In that chapter we described how one can represent the global lateral loading as loads acting on the individual frames contained in the building system (Fig. 15.1). We focus in this chapter on how one treats vertical loads such as gravity loads. Gravity loads applied to a floor slab are converted to distributed loads acting on the beams which support the slab. Since the floor slab loads involve both dead and live loads, one needs to investigate various floor slab loading patterns in order to establish the maximum values of the design parameters. We apply Müller-Breslau principle for this task. The last section of the chapter contains a case study which illustrates the application of these ideas to rigid and braced frame.

15.1 Loads on Frames

Figure 15.2 shows a typical makeup of a rectangular building; the structural system is composed of floor slabs that are supported by frames arranged in an orthogonal pattern. The action of wind and earthquake is represented by concentrated lateral loads applied to the nodes. Gravity loads acting on the floor slabs or roof are transferred to the beams and then to the columns. The nature of these beam loads (uniform, concentrated, triangular, trapezoidal) depends on the makeup of the flooring system. In this chapter, we examine first the mechanism by which the floor loads are transferred to the beams and then describe how to establish the critical loading pattern of beam loading that produces the peak values of moment in an individual frame. Given the peak moments, one can select appropriate cross sections.



Fig. 15.1 Multistory building

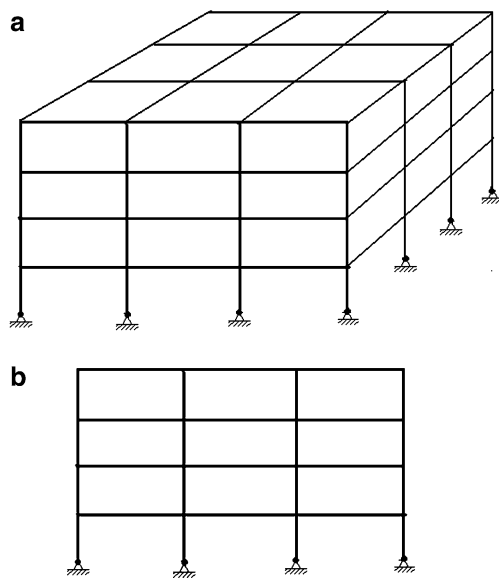
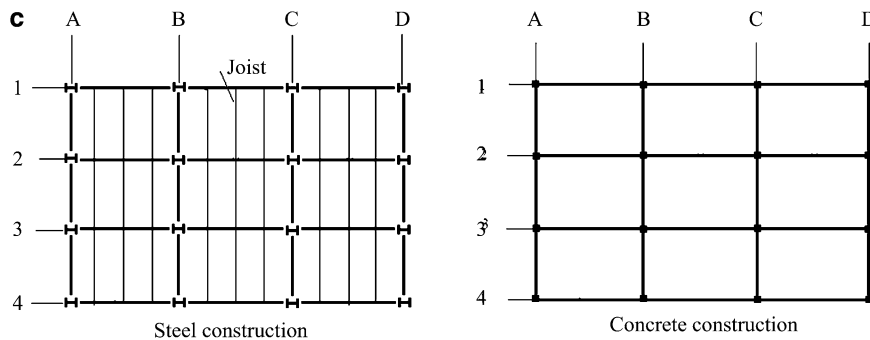
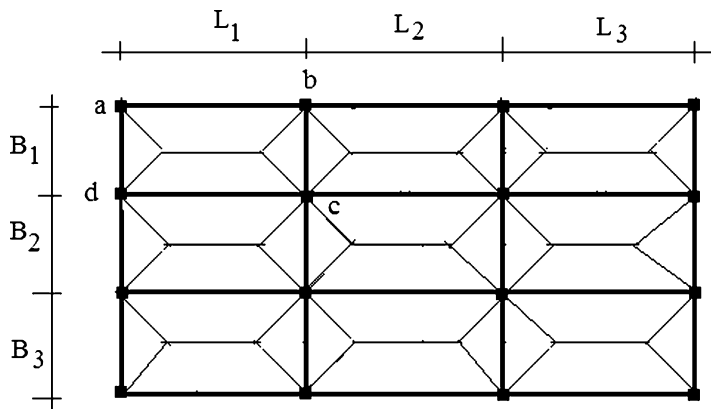


Fig. 15.2 Rectangular building. (a) Building frame. (b) Elevation view—individual frame. (c) Typical plan view—flooring system.

**Fig. 15.2** (continued)**Fig. 15.3** Slab-beam framing scheme—two-way action

15.2 Treatment of Gravity Floor Loads

Figure 15.3 shows a rectangular segment of the floor (abcd) bounded by columns at its corners and beams along its sides. In typical concrete construction, the floor slab and beams are framed simultaneously. The floor slab–beam system functions as a rectangular plate supported on all its sides. If the load is transmitted to all the sides, we refer to this behavior as two-way action. When the load tends to be transmitted primarily in one direction, this behavior is called one-way action.

Whether one-way or two-way action occurs depends on the dimensions and make up of the floor slab. The most common approach is to work with the tributary areas defined in Fig. 15.4. One constructs 45° lines and computes individual areas. The loading on an area is assigned to the adjacent beam. When the members are located in the interior, these areas are doubled to account for the adjacent panels. In general, the areas are either triangular or trapezoidal.

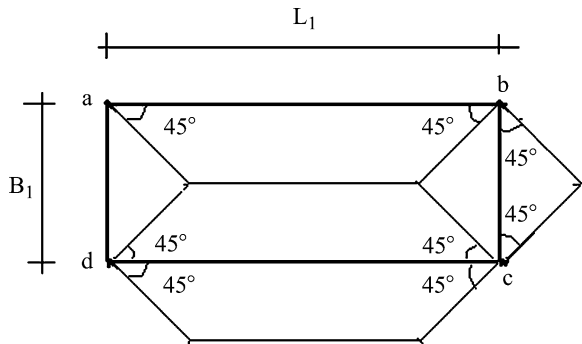


Fig. 15.4 Tributary areas for floor panel abcd

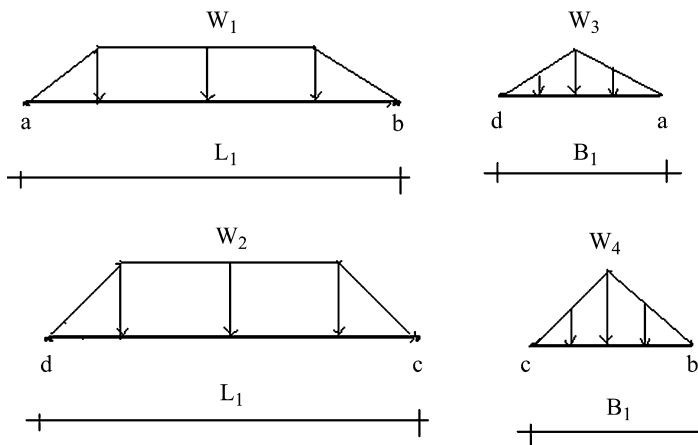


Fig. 15.5 Two-way action perimeter beam loadings for uniform floor loading—panel abcd

The floor loading is represented as a uniform load q (lb/ ft^2 or N/ m^2) applied to the floor slab. Using the concept of tributary areas, we convert this loading to a line loading w (lb/ ft or N/m) on the perimeter floor beams. The loading patterns for the beams supporting panel abcd and adjacent panels shown in Fig. 15.4 are listed below.

$$\begin{cases} w_1 = q\left(\frac{B_1}{2}\right) \\ w_2 = q\left(\frac{B_1}{2} + \frac{B_2}{2}\right) \\ w_3 = q\left(\frac{B_1}{2}\right) \\ w_4 = qB_1 \end{cases}$$

When steel members are used, the usual approach is to form the floor by first installing joists, then overlaying steel decking, and lastly casting a thin layer of

concrete. Loading applied to the floor is transferred through the decking to the joists and ultimately to the beams supporting the joists. For the geometry shown in Fig. 15.6, beams ab and cd carry essentially all the loads applied to the floor panel abcd. The loads on beams ad and bc are associated with the small tributary areas between the beams and the adjacent joists. Depending on the joist spacing, the beam loads are represented either as concentrated loads or as a uniformly distributed load (see Fig. 15.7).

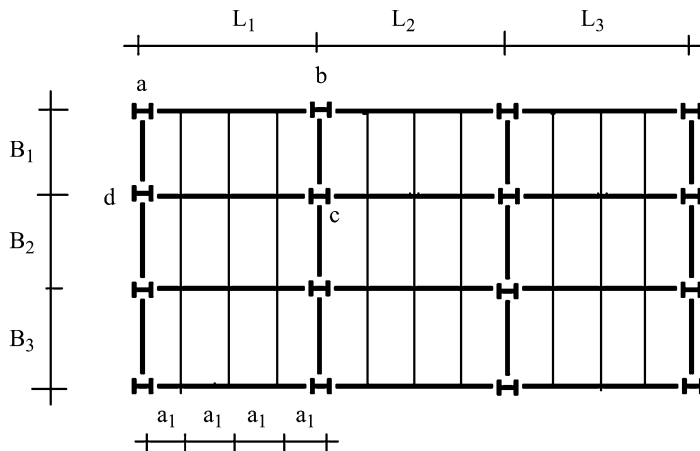


Fig. 15.6 Steel joist/beam framing scheme

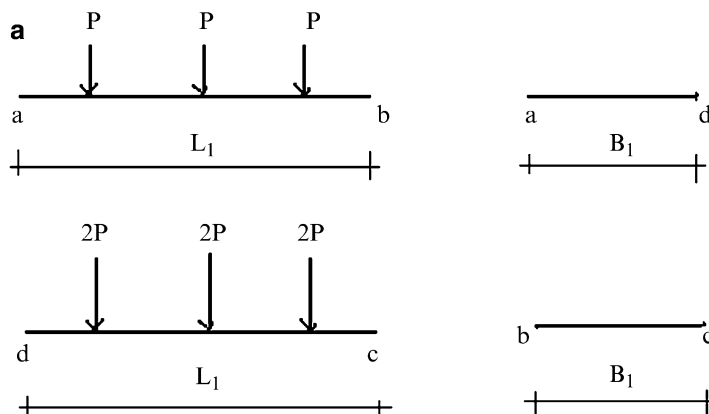


Fig. 15.7 One-way action beam loading for uniform floor loading q . (a) Large joist spacing. (b) Small joist spacing

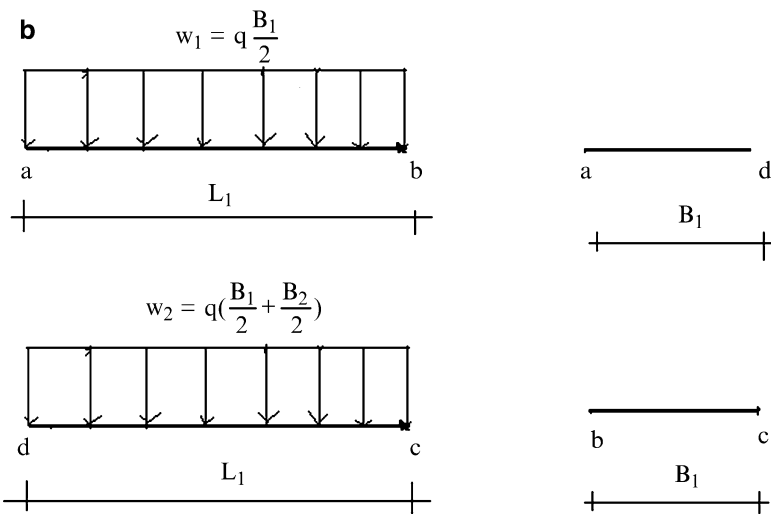


Fig. 15.7 (continued)

15.3 Live Load Patterns for Frame Structures

Gravity type loading is usually the dominant loading for low-rise multistory frames. It consists of both dead and live loading. Given a multistory frame, the first step is to establish the critical loading patterns for the individual members. Once the loading patterns are established, one can carry out an approximate analysis to generate peak force values which are used for the initial design. From then on, one iterates on member properties using an exact analysis method.

In this section, we describe how Müller-Breslau Principle can be employed to establish loading patterns for live gravity loading. We also describe some approximate techniques for estimating the peak positive and negative moments in beams.

Consider the frame shown in Fig. 15.8. We suppose the gravity live loading is a uniform distributed load, w , that can act on a portion of any member. Our objective here is to determine the loading patterns that produce the maximum positive moment at A and maximum negative moment at B.

To determine the positive moment at A, we insert a moment release at A and apply self-equilibrating couples as indicated in Fig. 15.9. According to Müller-Breslau Principle, one applies a downward load to those spans where the beam deflection is upward to produce the maximum positive moment at A. The corresponding loading pattern is shown in Fig. 15.10.

Referring back to Fig. 15.8, we establish the loading pattern for the negative moment at B by inserting a moment release at B and applying a negative moment. In this case, there are two possible deflected shapes depending upon whether one assumes the inflection points are in either the columns or the beams. These shapes are plotted in Figs. 15.11 and 15.12. The exact shape depends on the relative

Fig. 15.8 Multistory frame example

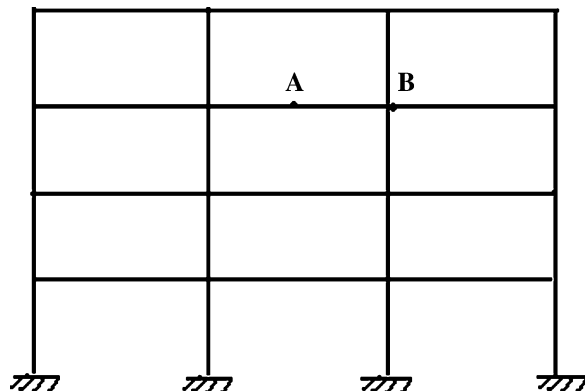


Fig. 15.9 Deflection pattern for positive moment at A

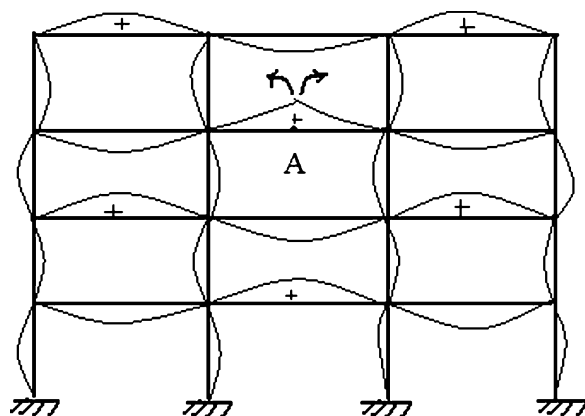
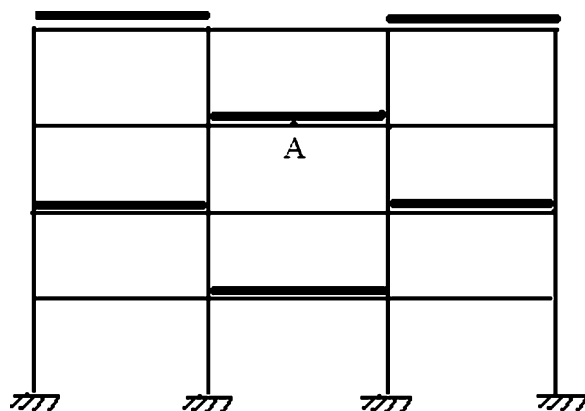


Fig. 15.10 Loading pattern for maximum positive moment at A



stiffness of the beams and columns which is not known at the preliminary design phase. Although there are cases where there is some ambiguity in the deflected shape, the Müller-Breslau Principle is a very useful tool for generating a qualitative first estimate of the loading pattern (Fig. 15.13). One can refine the estimate later using a structural analysis software system.

Fig. 15.11 Deflection pattern for negative moment at B—inflection points in beams

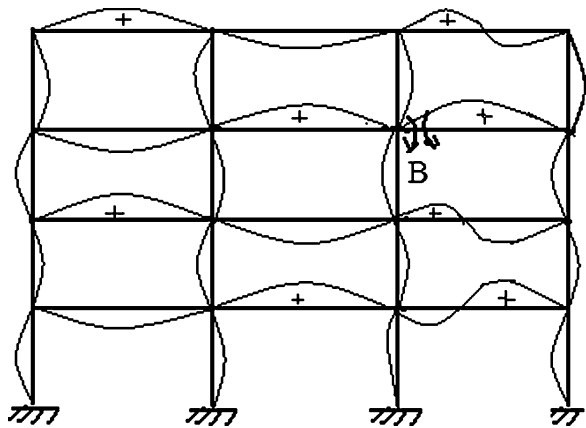


Fig. 15.12 Deflection pattern for negative moment at B—inflection points in columns

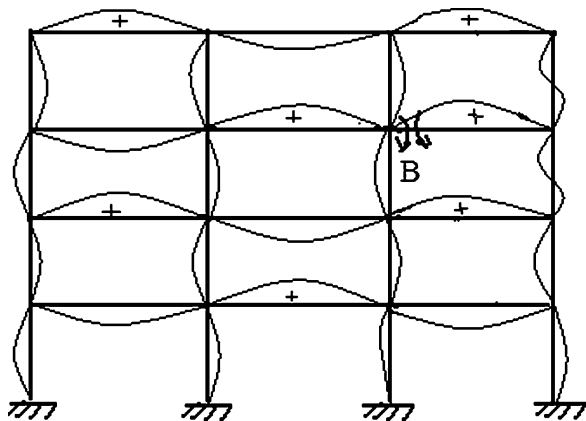
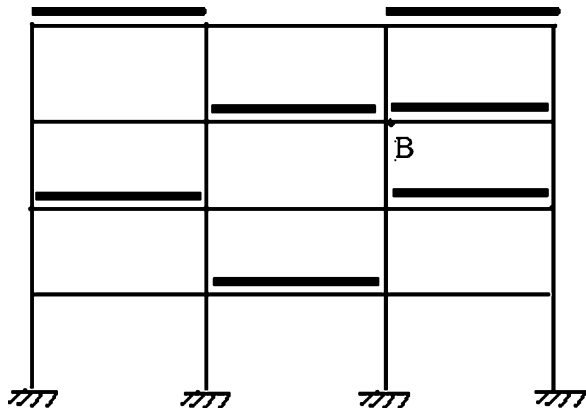


Fig. 15.13 Loading Pattern for Maximum negative moment at B—inflection points in columns



Example 15.1

Given: The rigid steel frame defined in Fig. E15.1a. Assume the member loading is a uniformly distributed live load.

Determine:

- Critical loading patterns for gravity live loading using Müller-Breslau Principle.
- Compare the maximum moment corresponding to the critical pattern loading to the results for a uniform loading on all members. Consider all the girders to be the same size and all the columns to be the same size.

Assume $L_1 = 6 \text{ m}$, $L_2 = 9 \text{ m}$, $h = 4 \text{ m}$, $w = 10 \text{kN/m}$, and $I_G = 3.5I_C$

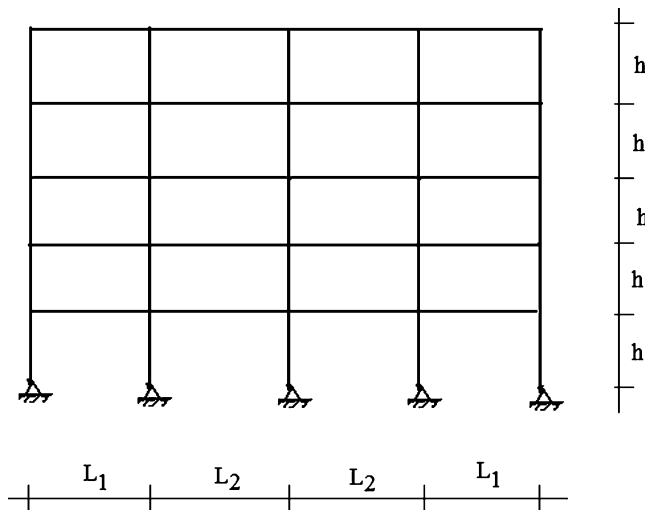


Fig. E15.1a

Solution:

Part (a): The process followed to determine the critical loading patterns for bending moment in the beams is described below.

Step 1: Positive Moment at mid-span of the beams.

There are two live load patterns for positive moment at the midpoint of the beams. They are listed in Fig. E15.1b.

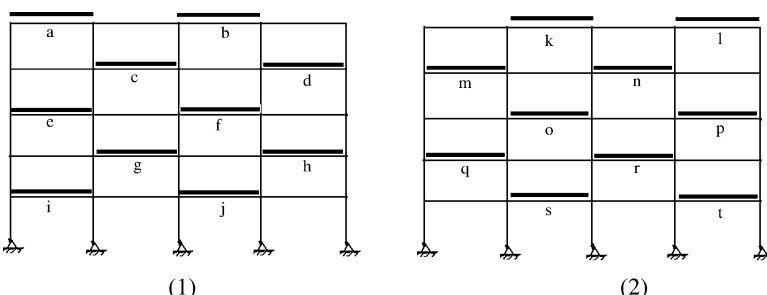


Fig. E15.1b Positive moment loading patterns

Step2: Negative moment at the end point of the beams

There are 15 patterns of uniform loading for negative moment. They are shown in Fig. E15.1c. One carries out analyses for these 15 different loading patterns, and then scans the individual results to determine the absolute maximum and minimum values of the end moments.

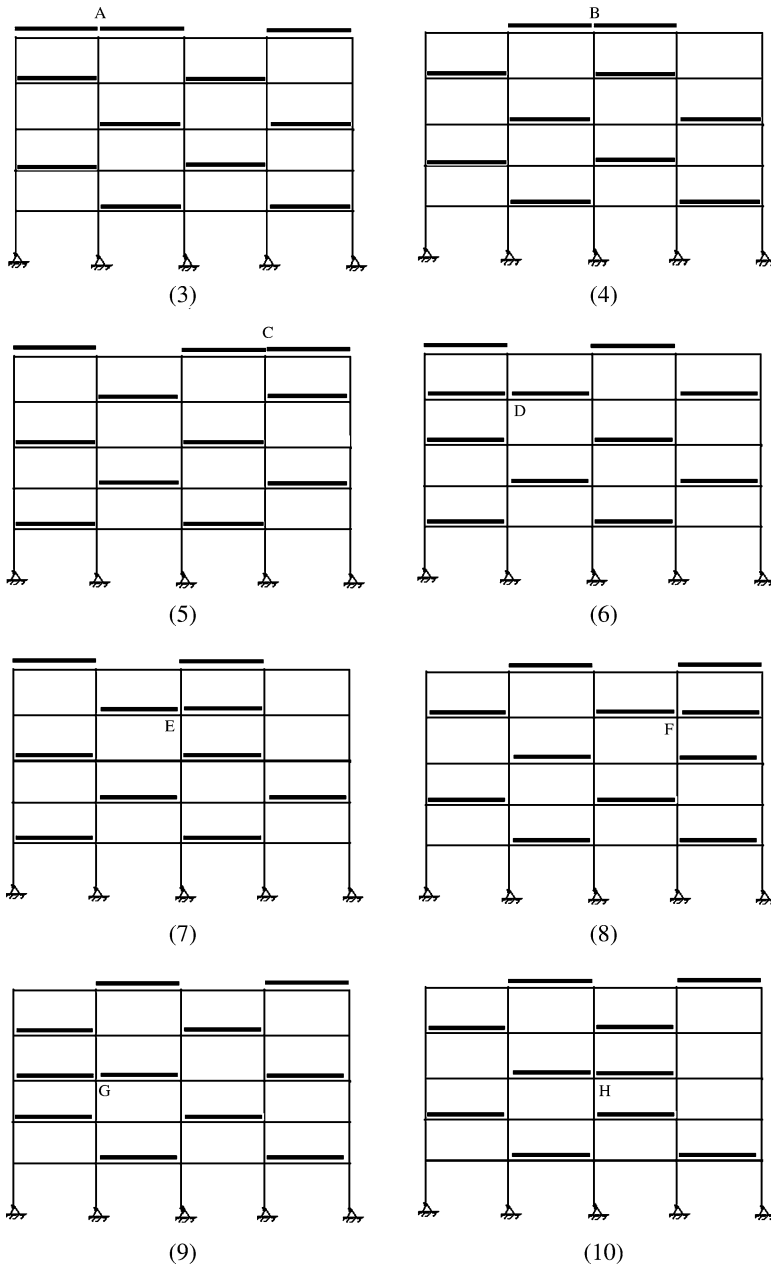


Fig. E15.1c Live load patterns for negative moment

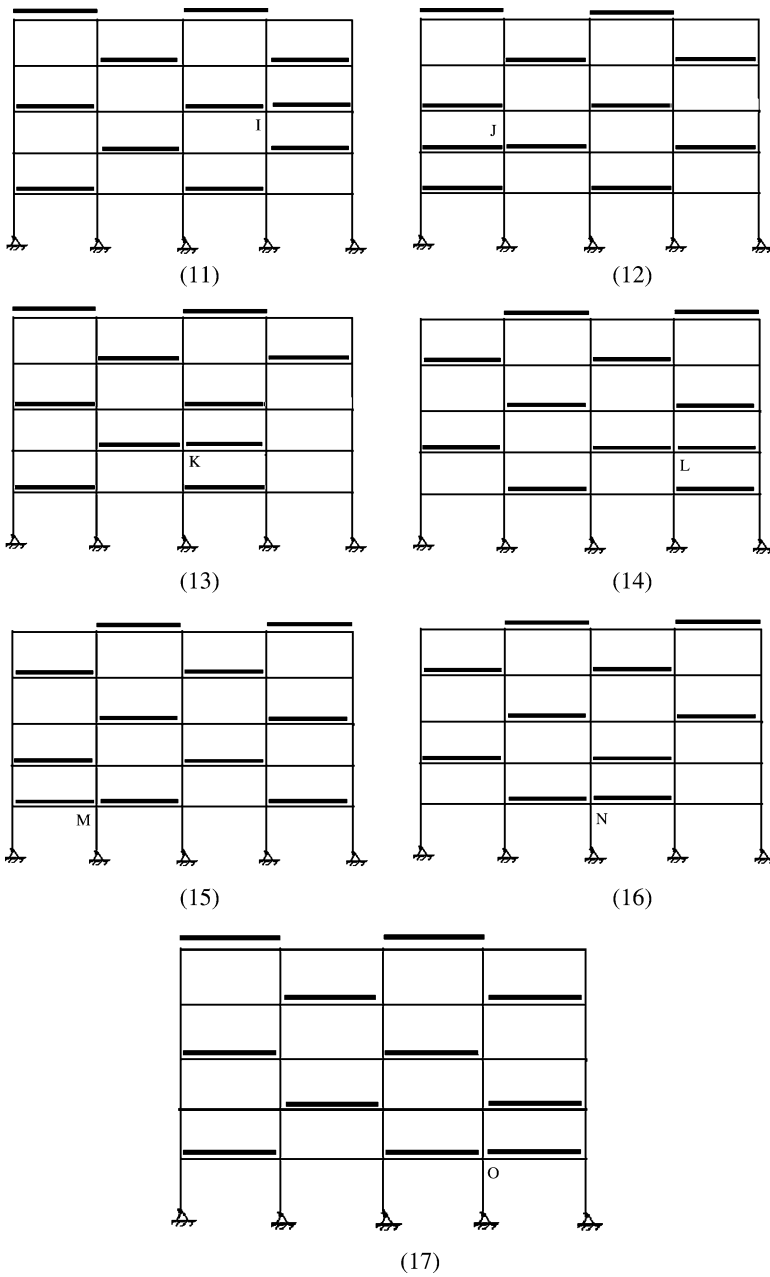


Fig. E15.1c (continued)

Part (b): The moment results for uniform loading and pattern loading are plotted in Figs. 15.1d, e. We note that the uniform loading produces results which under estimate the peak values (30% for positive moment, and 11% for negative moment). However, since the uniform loading case is easy to implement and provides reasonable results, it frequently is used to generate a first estimate.

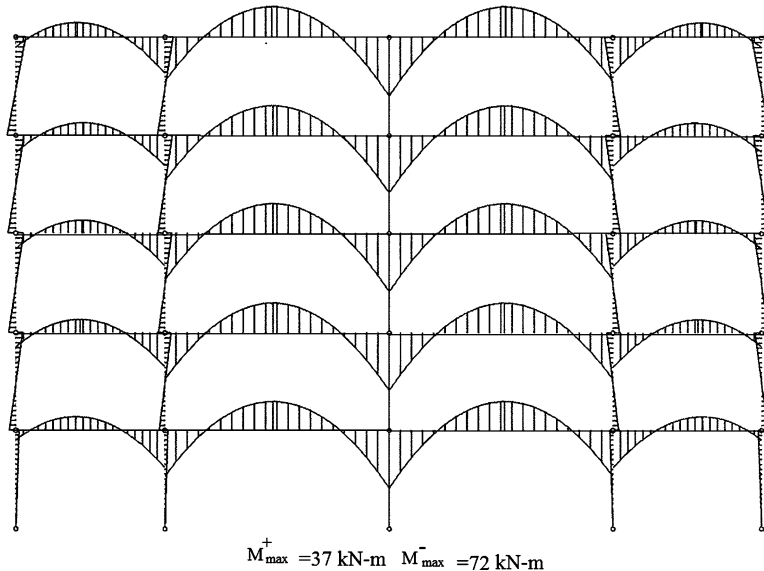


Fig. E15.1d Moment diagram for Uniform loading

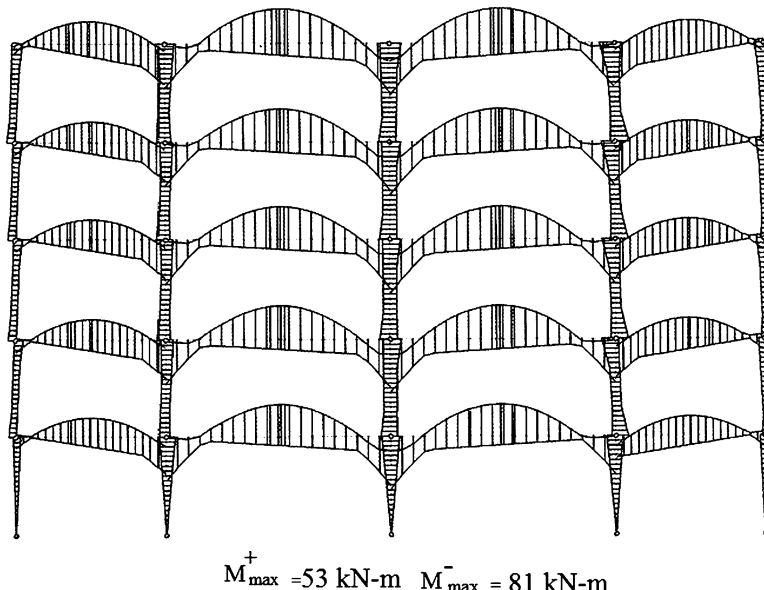
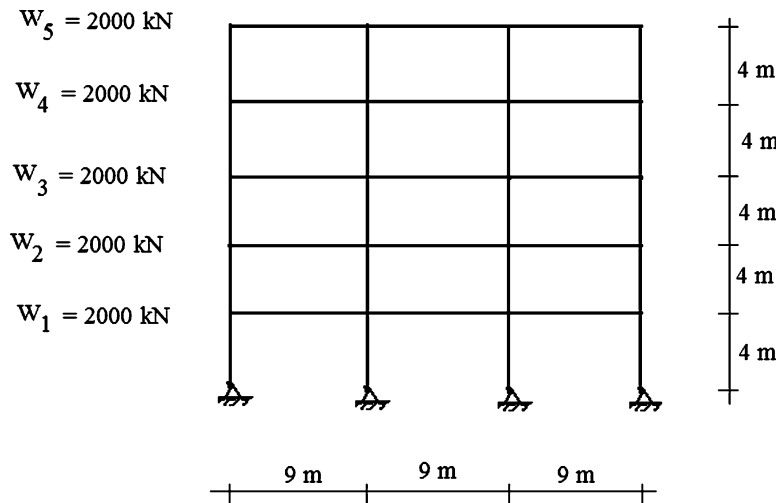
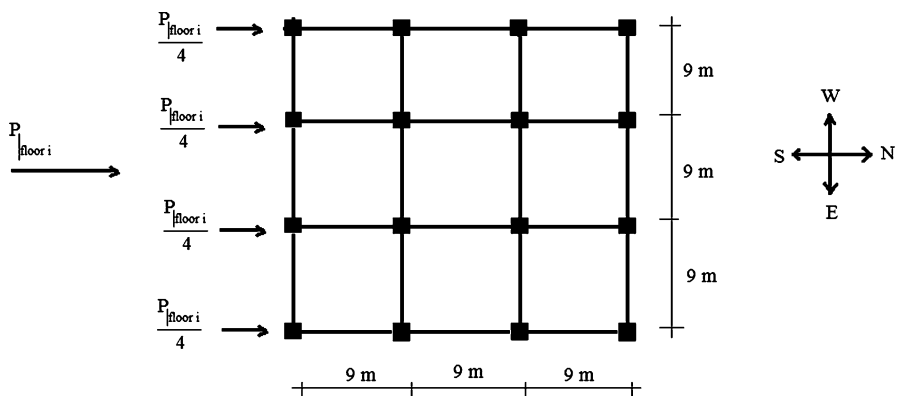


Fig. E15.1e Discrete moment envelope for pattern loading

Example 15.2

Given: The five story symmetrical rigid frame building shown in Figs. E15.2a–i. Assume the building is subjected to gravity loading and an earthquake in the North–south direction. Use the results of the earthquake analysis carried out in Example 14.16. Consider the floor load to be transmitted to all sides (two way action). Assume the floors are rigid with respect to lateral motion.

**Fig. E15.2a** Elevation**Fig. E15.2b** Typical floor plan

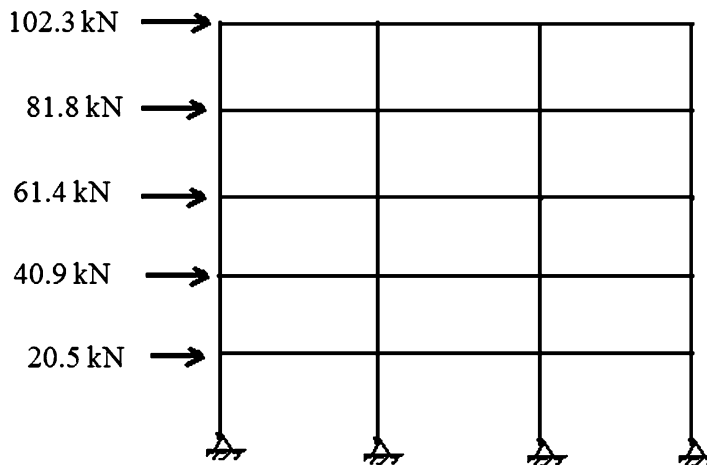


Fig. E15.2c Earthquake in N-S direction—floor loads on a typical frame

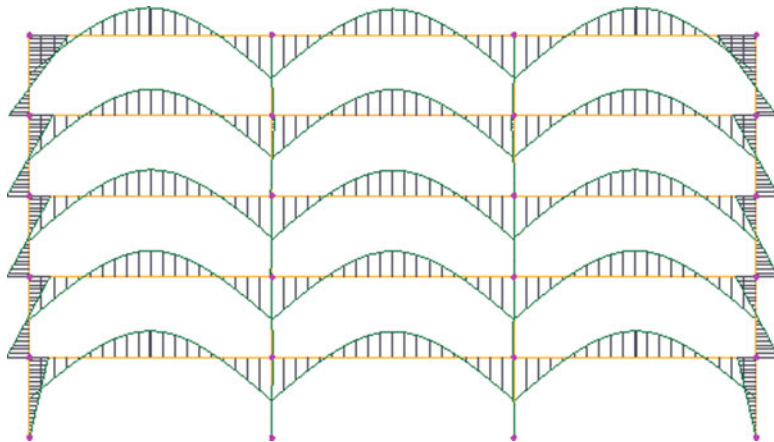
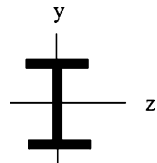
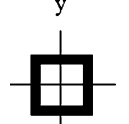


Fig. E15.2d Moment diagram—gravity

Determine: The maximum forces in the columns and beams using computer software. Also plot the lateral displacement of the floors. Assume all the beams to be the same size and all the columns to be the same size. We consider two cases: $I_b = 3I_c$ and $I_b = 1.44I_c$. The corresponding cross-sectional properties are

$$I \text{ shape beams} \left\{ \begin{array}{l} I_z = 445,146,750 \text{ mm}^4 \\ I_y = 22,798,170 \text{ mm}^4 \\ I_x = 1,135,750 \text{ mm}^4 \\ A = 12,320 \text{ mm}^2 \end{array} \right.$$



Hollow square columns	$\begin{cases} \text{case (1)} \\ \text{case (2)} \end{cases} \quad \begin{cases} I_z = 148,520,925 \text{ mm}^4 \\ I_y = 148,520,925 \text{ mm}^4 \\ I_x = 233,390,025 \text{ mm}^4 \\ A = 10,677 \text{ mm}^2 \\ I_z = 309,106,575 \text{ mm}^4 \\ I_y = 309,106,575 \text{ mm}^4 \\ I_x = 486,749,250 \text{ mm}^4 \\ A = 15,867 \text{ mm}^2 \end{cases}$	
-----------------------	---	--

Solution: The floor loading is uniformly applied to the floor slab. Using the concept of tributary areas, we convert this loading to line loadings w on the perimeter floor beams. Note that the N–S and E–W loading are identical because of the geometry.

$$W_{\text{floor total}} = 2,000 \text{ kN}$$

$$\frac{2,000}{(27)(27)} = 2.744 \text{ kN/m}^2$$

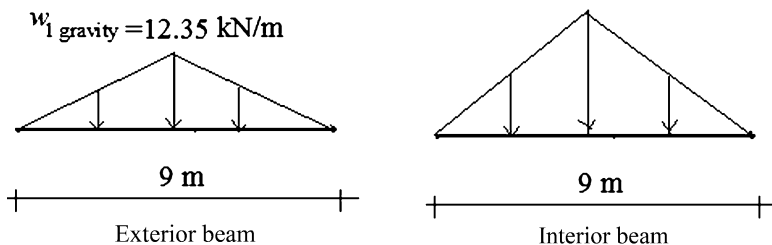
↓

$$w_1 \text{ gravity} = 2.744(4.5) = 12.35 \text{ kN/m}$$

$$w_2 \text{ gravity} = 2.744(9) = 24.7 \text{ kN/m}$$

The gravity line loading patterns for the perimeter floor beams are listed below.

$$w_2 \text{ gravity} = 24.7 \text{ kN/m}$$



Using computer software, we analyze the three-dimensional rigid frame for gravity and earthquake loading.

The beam and column forces are determined by scanning through the output file. The critical values for the column forces occur in the first story. Results for the beams, columns, and lateral displacement corresponding to $I_b = 3I_c$ and $I_b = 1.44I_c$ are listed below.

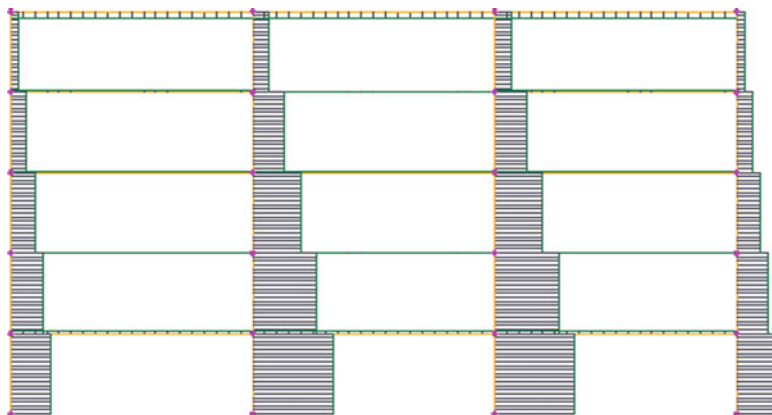


Fig. E15.2e Axial force diagram—gravity

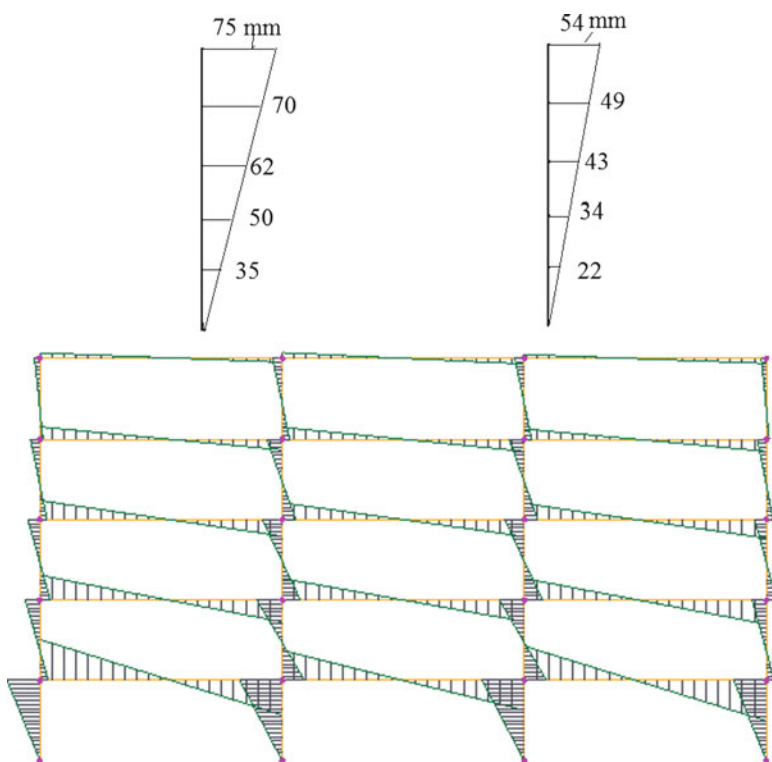
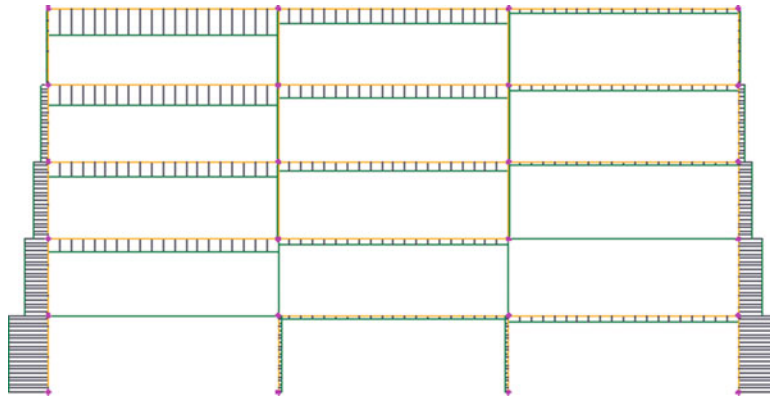


Fig. E15.2f Moment diagram—wind

Beam _{interior frame}	Gravity	$I_b = 3I_c$	$\begin{cases} P = 60 \text{ kN} \\ V = 120 \text{ kN} \\ M = 183 \text{ kNm} \end{cases}$	$I_b = 1.44I_c$	$\begin{cases} P = 68 \text{ kN} \\ V = 117 \text{ kN} \\ M = 180 \text{ kNm} \end{cases}$
	Earthquake	$I_b = 3I_c$	$\begin{cases} P \approx 0 \\ V = 52 \text{ kN} \\ M = 252 \text{ kNm} \end{cases}$	$I_b = 1.44I_c$	$\begin{cases} P = 2 \text{ kN} \\ V = 48 \text{ kN} \\ M = 228 \text{ kNm} \end{cases}$
Column _{Exterior}	Gravity	$I_b = 3I_c$	$\begin{cases} P = 527 \text{ kN} \\ M = 44 \text{ kNm} \end{cases}$	$I_b = 1.44I_c$	$\begin{cases} F = 539 \text{ kN} \\ M_{\max} = 55 \text{ kNm} \end{cases}$
	Earthquake	$I_b = 3I_c$	$\begin{cases} P = \pm 133 \text{ kN} \\ M = 202 \text{ kNm} \end{cases}$	$I_b = 1.44I_c$	$\begin{cases} F = \pm 197 \text{ kN} \\ M_{\max} = 130 \text{ kNm} \end{cases}$
Column _{Interior}	Gravity	$I_b = 3I_c$	$\begin{cases} P = 1140 \text{ kN} \\ M = 4.4 \text{ kNm} \end{cases}$	$I_b = 1.44I_c$	$\begin{cases} F = 1128 \text{ kN} \\ M_{\max} = 2.3 \text{ kNm} \end{cases}$
	Earthquake	$I_b = 3I_c$	$\begin{cases} P = \pm 24 \text{ kN} \\ M = 258 \text{ kNm} \end{cases}$	$I_b = 1.44I_c$	$\begin{cases} F = \pm 14 \text{ kN} \\ M_{\max} = 263 \text{ kNm} \end{cases}$

**Fig. E15.2g** Axial force diagram—wind

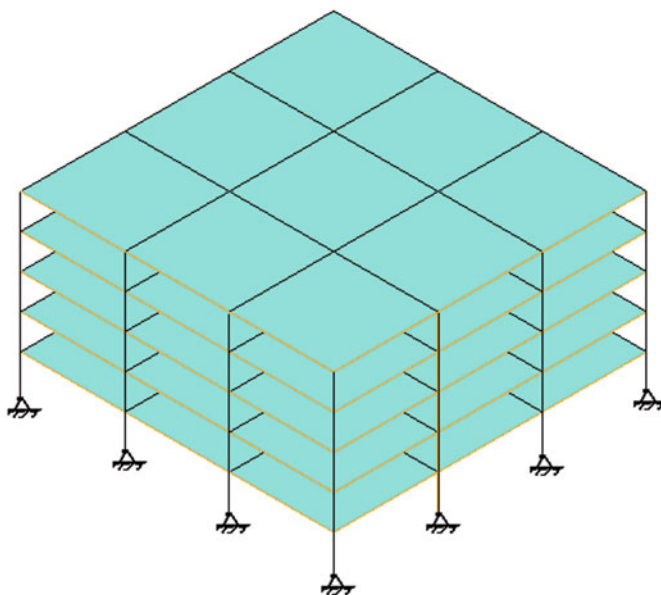
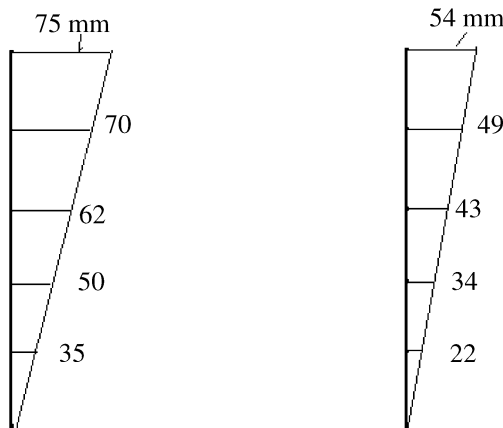


Fig. E15.2h 3D model



$$I_b = 3 I_c$$

$$I_b = 1.44 I_c$$

Fig. E15.2i Lateral displacement

15.4 A Case Study: Four-Story Building

In this section, we illustrate the computation of the design parameters for a typical building considering dead, live, and wind loadings. This example is intended to integrate the material presented in Chaps. 11, 12 and 14.

15.4.1 Building Details and Objectives

The building is a 4 story steel frame building with a green roof. Figure 15.14 shows the typical floor plan and elevation views. The rigid flooring system transmits the gravity load primarily in the E–W direction to the floor beams oriented in the N–S direction (one-way action).

The loading and member data are as follows:

- Floor dead load = 0.055 kip/ft²
- Floor live load = 0.07 kip/ft²
- Green roof
 - Self weight of roof material = 0.045 kip/ft²
 - Self weight of construction material = 15 psf = 0.015 kip/ft²

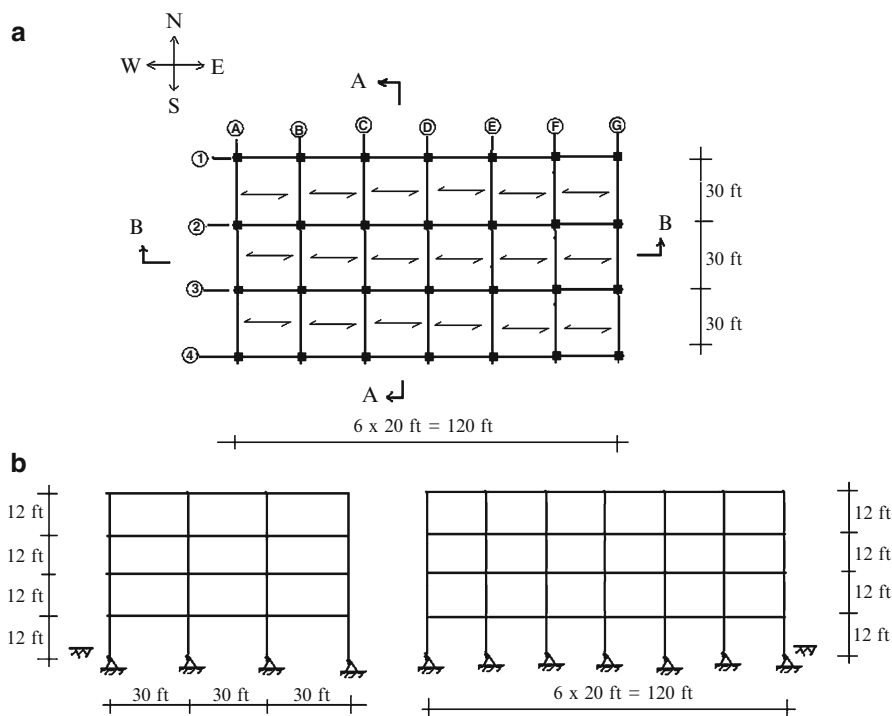


Fig. 15.14 Floor plan and elevation views—case study. (a) Plan. (b) N–S elevation—Section A–A. (c) E–W elevation—Section B–B

- Weight of soil = 0.12 kip/ft²
- Total roof dead load = 0.18 kip/ft²
- Roof live load = 0.02 kip/ft²
- Global wind loads acting in the N–S and E–W direction are defined in Fig. 15.15. They correspond to a peak wind speed of 80 mph for a building located in Boston, Massachusetts.
- The weight of exterior walls will be carried by the edge beams.
- Self weight of exterior walls + portion of the floor load = 1.1 kip/ft
- Based on economic considerations related to fabrication and construction, the choice of member sizes is restricted to the following:
 - All the roof beams in the N–S direction are the same size.
 - All the floor beams in the N–S direction are the same size.
 - All the floor/roof beams in the E–W direction are the same size.
 - All the columns have the same size.
 - All the braces have the same size.
- The following combinations of loads for strength design are to be considered:

$$w_u = \begin{cases} 1.4w_D \\ 1.2w_D + 1.6w_{L_{\text{floor}}} + 0.5w_{L_{\text{roof}}} \\ 1.2w_D + 0.5w_{L_{\text{floor}}} + 0.5w_{L_{\text{roof}}} + 1.6w_W \end{cases}$$

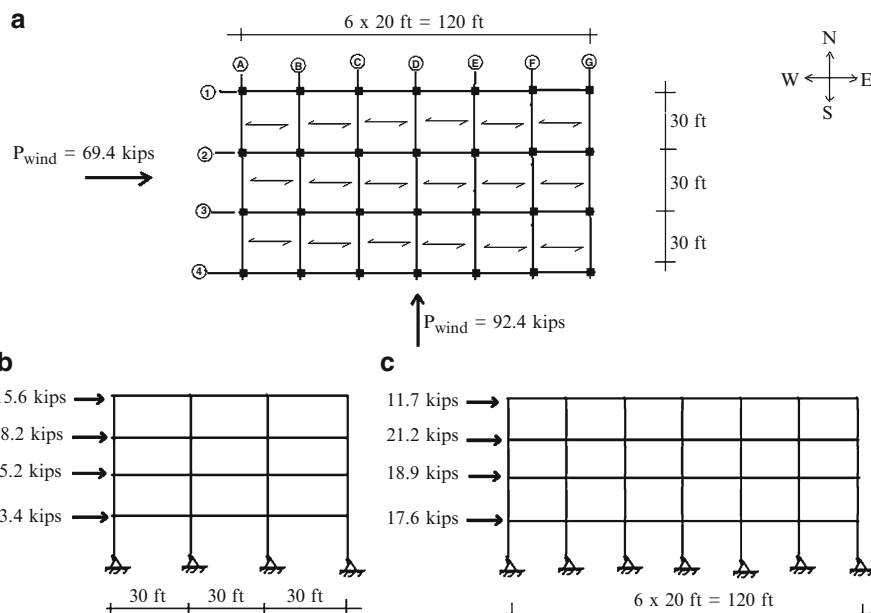


Fig. 15.15 Global Wind loads. (a) Plan. (b) N–S. (c) E–W

- The following limits are required by the serviceability constraint:

$$\text{Limit beam deflection to } \begin{cases} \frac{L_{\text{beam}}}{240} & \text{for (DL + LL)} \\ \frac{L_{\text{beam}}}{360} & \text{for LL} \end{cases}$$

$$\text{Limit building drift to } \frac{H_{\text{building}}}{300}$$

15.5 Analysis Procedures for Bracing Scheme

Our objectives are to describe the analysis procedures and to establish the peak design values for beams, columns, and braces corresponding to the following structural schemes:

Case (1): The structure is a braced frame, i.e., all the connections between beams and columns are pinned.

Case (2): The structure is a rigid frame in the N–S direction and a braced frame in the E–W direction. All the connections between beams and columns in the N–S direction are moment (rigid) connections; in the E–W direction, they remain pinned.

15.5.1 Case (1) Frames Are Braced in Both N–S and E–W Directions: Building Details

We suppose that since the connections between the beams and the columns are pin connections in both the N–S and E–W directions the lateral load (wind) is carried by the bracing. The brace layout is governed by architectural considerations. We use the K bracing schemes shown in Fig. 15.16. The braces have equal stiffnesses and the floors are rigid. Therefore the global wind load will be distributed equally between braces (see Chap. 14). The column load is purely axial since the members are pinned. We establish the column load per floor working with the tributary floor area associated with the column. The beams are simply supported, and the beam loading is based on one-way action (uniformly loaded).

Our objective here is to show how one generates the design values for beams, columns, and bracing elements. Details are presented in the following sections.

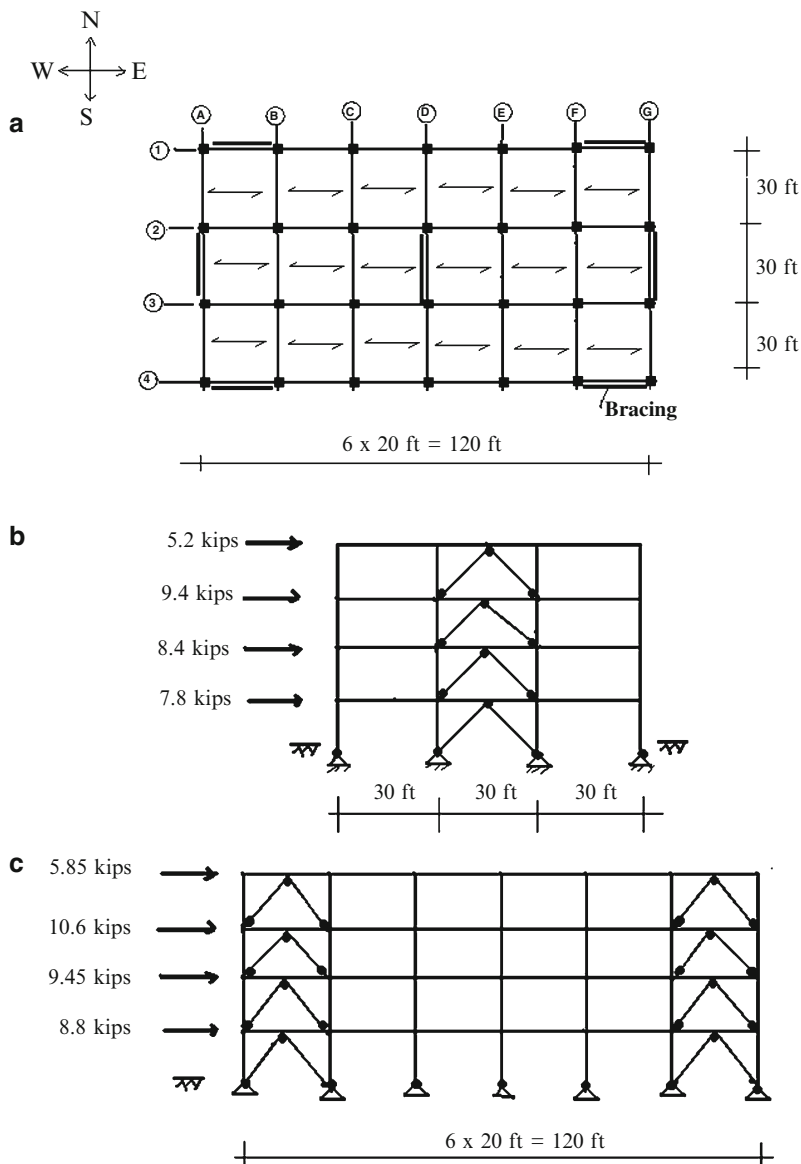
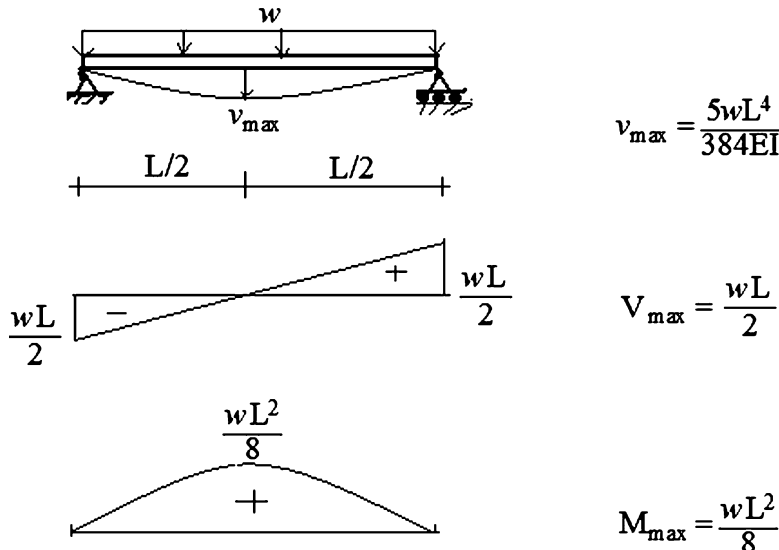


Fig. 15.16 Braced frame configuration. (a) Plan—braced in both directions. (b) N–S elevation—braced frames A–A, D–D, G–G. (c) E–W elevation braced frames 1–1, 4–4

15.5.2 Case (1) Beam Properties in the N-S and E-W Directions

The floor loading is transmitted by the floor slab to the beams oriented in the N-S direction, which function as simply supported beams, and the beam loading is based on one-way action (uniformly loaded). Selection of the beam cross section is controlled by both strength (moment and shear) and serviceability (deflection). Both the maximum moment and the deflection occur at mid-span. The cross section is determined by the mid-span bending moment, end shear, and the mid-span deflection as shown in Figure below.



15.5.2.1 Bending Moment and Shear

Interior Floor Beams (30 ft span):

$$w_{D_{\text{floor}}} = 0.055(20) = 1.1 \text{ kip/ft} \Rightarrow M_{D_{\text{floor}}} = \frac{w_DL^2}{8} = \frac{1.1(30)^2}{8} = 124 \text{ kip ft}$$

$$w_{L_{\text{floor}}} = 0.07(20) = 1.4 \text{ kip/ft} \Rightarrow M_{L_{\text{floor}}} = \frac{w_LL^2}{8} = \frac{1.4(30)^2}{8} = 157.5 \text{ kip ft}$$

$$w_u = \begin{cases} 1.4w_D = 1.54 \text{ kip/ft} \\ 1.2w_D + 1.6w_L = 3.56 \text{ kip/ft} \end{cases} \leftarrow$$

$$M_u = \frac{w_u L^2}{8} = \frac{3.56(30)^2}{8} = 400.5 \text{ kip ft}$$

$$V_u = \frac{w_u L}{2} = \frac{3.56(30)}{2} = 53.4 \text{ kip}$$

Interior Roof Beams (30 ft span):

$$w_{D_{\text{roof}}} = 0.18(20) = 3.6 \text{ kip/ft} \Rightarrow M_{D_{\text{roof}}} = \frac{w_D L^2}{8} = \frac{3.6(30)^2}{8} = 405 \text{ kip ft}$$

$$w_{L_{\text{roof}}} = 0.02(20) = 0.4 \text{ kip/ft} \Rightarrow M_{L_{\text{roof}}} = \frac{w_L L^2}{8} = \frac{0.4(30)^2}{8} = 45 \text{ kip ft}$$

$$M_{L_{\text{roof}}} = \frac{w_L L^2}{8} = \frac{0.4(30)^2}{8} = 45 \text{ kip ft}$$

$$w_u = \begin{cases} 1.4w_D = 5.04 \text{ kip/ft} & \leftarrow \\ 1.2w_D + 1.6w_L = 4.96 \text{ kip/ft} & \end{cases}$$

$$M_u = \frac{w_u L^2}{8} = \frac{5.04(30)^2}{8} = 567 \text{ kip ft}$$

$$V_u = \frac{w_u L}{2} = \frac{5.04(30)}{2} = 75.6 \text{ kip}$$

15.5.2.2 Deflection

The design is constrained by the deflection at mid-span.

$$\begin{aligned} v_{\max} &= \frac{5wL^4}{384EI} \\ &\leq \frac{L}{240} = \frac{30(12)}{240} = 1.5 \text{ in} \quad \text{for } (w = w_D + w_L) \\ &\leq \frac{L}{360} = \frac{30(12)}{360} = 1.0 \text{ in} \quad \text{for } (w = w_L) \end{aligned}$$

These constraints lead to the following conditions on the required I .

$$\text{Floor} \begin{cases} I_{(D+L)_{\text{req}}} = \frac{5(w_D + w_L)(30)^4(12)^3}{384(29,000)(1.5)} = 418.96(w_D + w_L) = 1,047 \text{ in.}^4 & \leftarrow \\ I_{L_{\text{req}}} = \frac{5(w_L)(30)^4(12)^3}{384(29,000)(1.0)} = 628.45(w_L) = 880 \text{ in.}^4 & \end{cases}$$

$$\text{Roof} \begin{cases} I_{(D+L)_{\text{req}}} = 418.96(3.6 + 0.4) = 1,676 \text{ in.}^4 & \leftarrow \\ I_{L_{\text{req}}} = 628.45(0.4) = 251 \text{ in.}^4 & \end{cases}$$

15.5.2.3 Beam Properties E-W Direction

Edge Roof/Floor Beams (20 ft span):

$$w_D = 1.1 \text{ kip/ft}$$

$$w_u = 1.4(1.1) = 1.54 \text{ kip/ft}$$

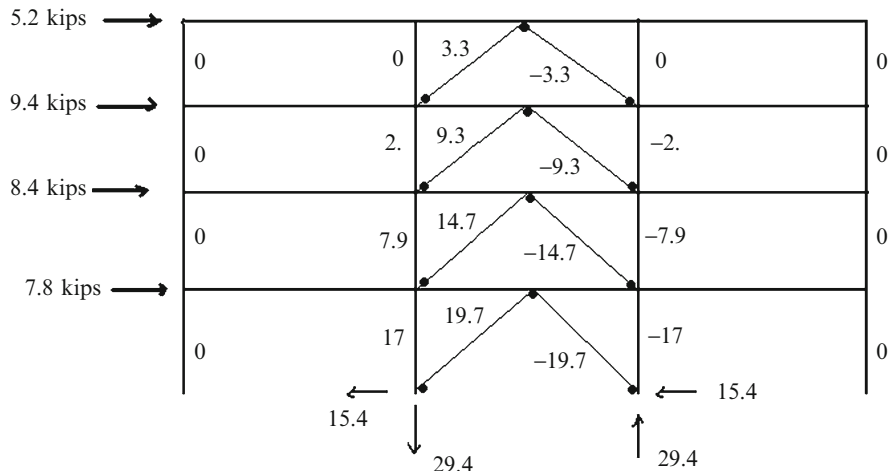
$$M_u = \frac{w_u L^2}{8} = \frac{1.54 (20)^2}{8} = 77 \text{ kip ft}$$

$$V_u = \frac{w_u L}{2} = \frac{1.54 (20)}{2} = 15.4 \text{ kip}$$

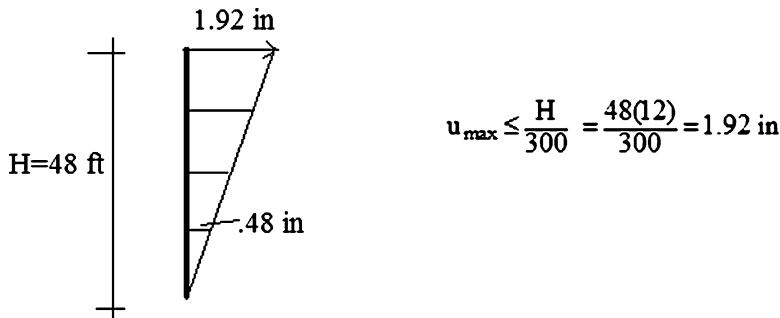
$$v_{\max} = \frac{5wL^4}{384EI} \leq \frac{L}{240} = \frac{20(12)}{240} = 1.0 \Rightarrow I_{\text{req}} = \frac{5(1.1)(20)^4(12)^3}{384(29,000)(1.0)} = 137 \text{ in.}^4$$

15.5.3 Case (1) Bracing Systems

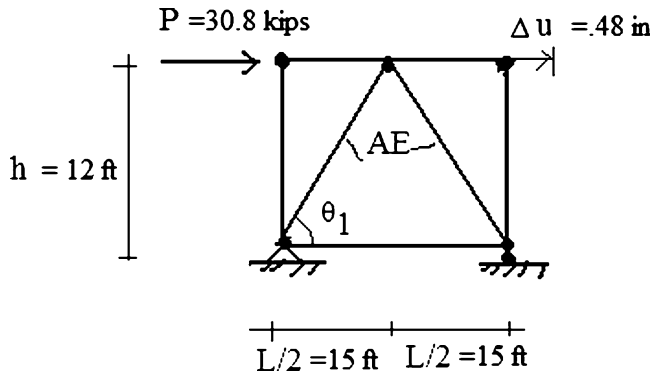
Next, we compute the axial forces in the N-S bracing. Since all the members are pinned, the total lateral wind load on a floor is carried by the bracing systems. The axial forces in a typical brace are shown on the sketch below. We assume the shear is equally distributed between the diagonals.



The constraint on the maximum lateral deflection at the top floor is $u_{\max} \leq H/300$:



We assume the inter-story displacement is constant for the stories and focus on the first story which has the maximum shear force.



N-S bracing—1st floor

Noting the equations presented in Sect. 11.4.3, we solve for the required area.

$$k_{\text{brace}} = \frac{2AE}{h} (\sin \theta_1 \cos^2 \theta_1)$$

$$P = k_{\text{brace}} \Delta u$$

$$\therefore P = \frac{2AE}{h} (\sin \theta_1 \cos^2 \theta_1) \Delta u \Rightarrow A = \frac{Ph}{2E(\sin \theta_1 \cos^2 \theta_1) \Delta u}$$

Substituting the prescribed values

$$\Delta u = 0.48 \text{ in.}$$

$$\theta_1 = \tan^{-1} \left(\frac{12}{15} \right) = 38.66^\circ$$

$$P = 30.8 \text{ kip}$$

leads to

$$A_{\text{required}} = \frac{(30.8)(12 \times 12)}{2(29,000)(\sin(38.66) \cos^2(38.66))(0.48)} = 0.42 \text{ in.}^2$$

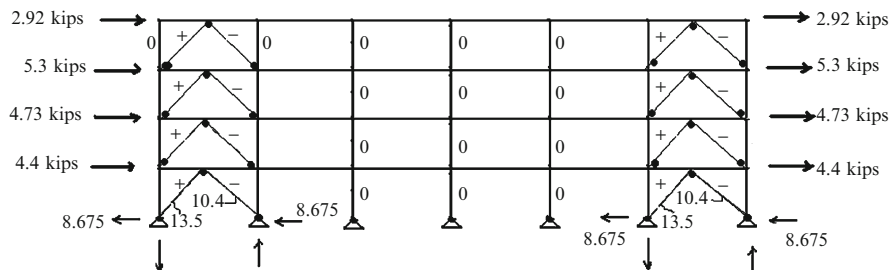
The diagonal elements may be subjected to either tension or compression loading depending on the direction of the wind. The maximum axial force due to wind in the bracing is 19.7 kip. Applying the appropriate load factor, the design value is $P_u = 19.7(1.6) = 31.5 \text{ kip}$.

$$N - S \text{ bracing} \begin{cases} P_{u_{\max}} = 19.7(1.6) = 31.5 \text{ kip} \\ L_{\text{bracing}} = \sqrt{12^2 + 15^2} = 19.2 \text{ ft} \\ \Delta u = 0.48 \text{ in.} \rightarrow A_{\text{req}} = 0.42 \text{ in.}^2 \end{cases}$$

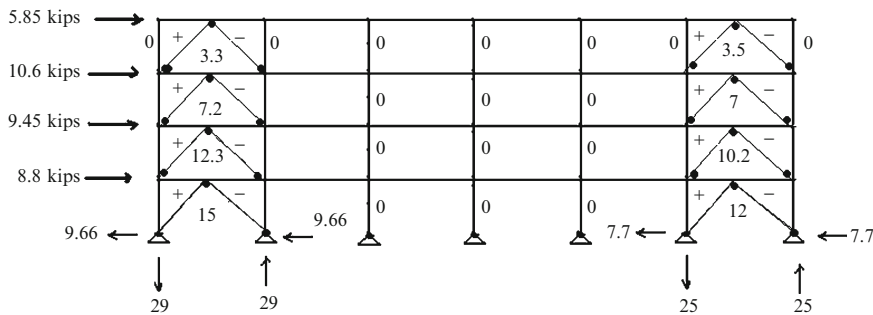
Based on the design axial load $P_u = 31.5 \text{ kip}$, an effective length of 19.2 ft, and the required area based on the lateral sway of .48 in., one selects a cross-sectional area and uses this section for all the brace members in the N-S direction.

15.5.3.1 E-W Bracing

We repeat the same type of analysis for the E-W bracing except that now the bracing system is indeterminate. We assume each of the braces carries $\frac{1}{2}$ the lateral load, and estimate the forces in the brace members by hand computations or use computer analysis. The force results are listed below.

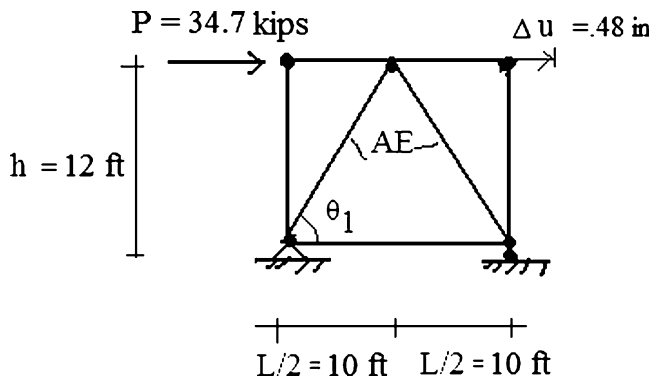


Approximate approach



Computer analysis

The maximum factored axial force in the bracing is $P_u = 15(1.6) = 24$ kip.



E-W bracing—1st floor

We compute the required brace area following the same approach used for the N-S bracing system. The loading and displacement values are

$$\Delta u = 0.48 \text{ in.}$$

$$\theta_1 = \tan^{-1} \left(\frac{12}{10} \right) = 50.19^\circ$$

$$P = 34.7 \text{ kip}$$

The required area is given by

$$A_{\text{required}} = \frac{(34.7)(12 \times 12)}{2(29,000)(\sin(50.19)\cos^2(50.19))(0.48)} = 0.57 \text{ in.}^2$$

The diagonal elements may be subjected to either tension or compression loading depending on the direction of the wind. The maximum axial force due to wind in the bracing is 15 kip. Applying the appropriate load factor, the design value is $P_u = 15(1.6) = 24$ kip.

$$N - S \text{ bracing} \left\{ \begin{array}{l} P_{u_{\max}} = 15(1.6) = 24 \text{ kip} \\ L_{\text{bracing}} = \sqrt{12^2 + 10^2} = 15.6 \text{ ft} \\ \Delta u = 0.48 \text{ in} \rightarrow A_{\text{req}} = 0.57 \text{ in.}^2 \end{array} \right.$$

Based on the design axial load $P_u = 24$ kip, an effective length of 15.6 ft, and the required area based on the lateral sway of .48 in., one selects a cross-sectional area and uses this section for all the brace members in the E-W direction.

15.5.4 Case (1) Interior Columns

The column load is purely axial since the members are pinned. We establish the column load per floor working with the tributary floor areas for dead and live loads, and the brace forces due to wind. The column on the first floor has the maximum axial force.

The loads in an interior column located in the first story are

$$P_D = 20(30)\{0.18 + .055(3)\} = 207 \text{ kip}$$

$$P_{L \text{ roof}} = 20(30)\{0.02\} = 12 \text{ kip}$$

$$P_{L \text{ floor}} = 20(30)\{0.07(3)\} = 126 \text{ kip}$$

$$P_{N-S \text{ Wind}} = 29.4 \text{ kip}$$

Evaluating the following load combinations

$$P_u = \left\{ \begin{array}{l} 1.4P_D = 290 \text{ kip} \\ 1.2P_D + 1.6P_L + 0.5P_{L_r} = 456 \text{ kip} \leftarrow \\ 1.2P_D + 0.5P_L + 0.5P_{L_r} + 1.6P_{\text{Wind}} = 364 \text{ kip} \end{array} \right.$$

leads to the design value of $P_u = 456$ kips. One selects a cross section based on $P_u = 456$ kips and an effective length of 12 ft.

15.5.5 Summary for Case (1)

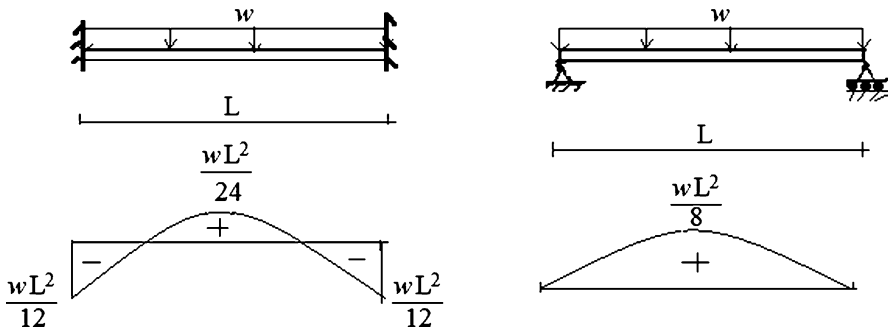
N-S roof beam	$M_u = 567 \text{ kips-ft}$	$I_{req} = 1676 \text{ in}^4$
N-S floor beam	$M_u = 400 \text{ kips-ft}$	$I_{req} = 1047 \text{ in}^4$
E-W beams	$M_u = 77 \text{ kips-ft}$	$I_{req} = 137 \text{ in}^4$
Columns	$P_u = 456 \text{ kips}$	
E-W braces	$P_u = 24 \text{ kips}$	$A_{min} > .57 \text{ in}^2$
N-S braces	$P_u = 31.5 \text{ kips}$	$A_{min} > .42 \text{ in}^2$

15.5.6 Case (2) Frames Are Rigid in the N-S Direction but Remain Braced in the E-W Direction

Figure 15.17 shows a plan view of this structural scheme. Our objective here is to generate the response of an individual rigid frame and to compare the design values for the braced vs. rigid frame structural concepts.

15.5.7 Strategy for N-S Beams and Columns

We specify moment connections between the beams and the columns in the N-S direction and assume that the lateral wind load will be carried equally by the seven rigid frames, because the floor slabs are rigid and the rigid frames have equal stiffnesses. The E-W direction remains the same as in Part (i), i.e., the beams in this direction are pin ended. Since the beams in the N-S direction are now rigidly connected to the columns, end moments will be developed in the beams. *The net effect is a reduction in the maximum moment in the beams.* For a first estimate, assuming full fixity, the peak moment reduces from $wL^2/8$ to $wL^2/12$, a reduction of 33 %. It follows that the beams will be *lighter*; however the columns will be *heavier* since they now must be designed for both axial force and moment.



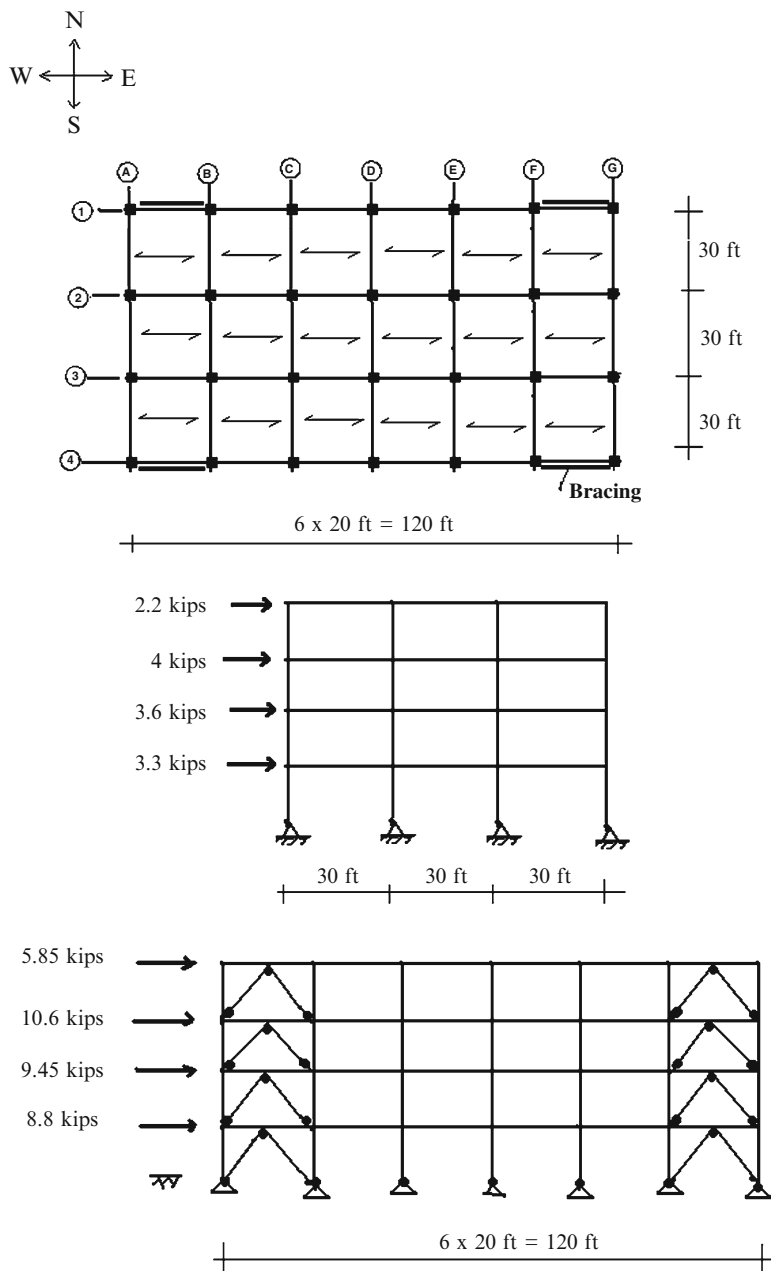
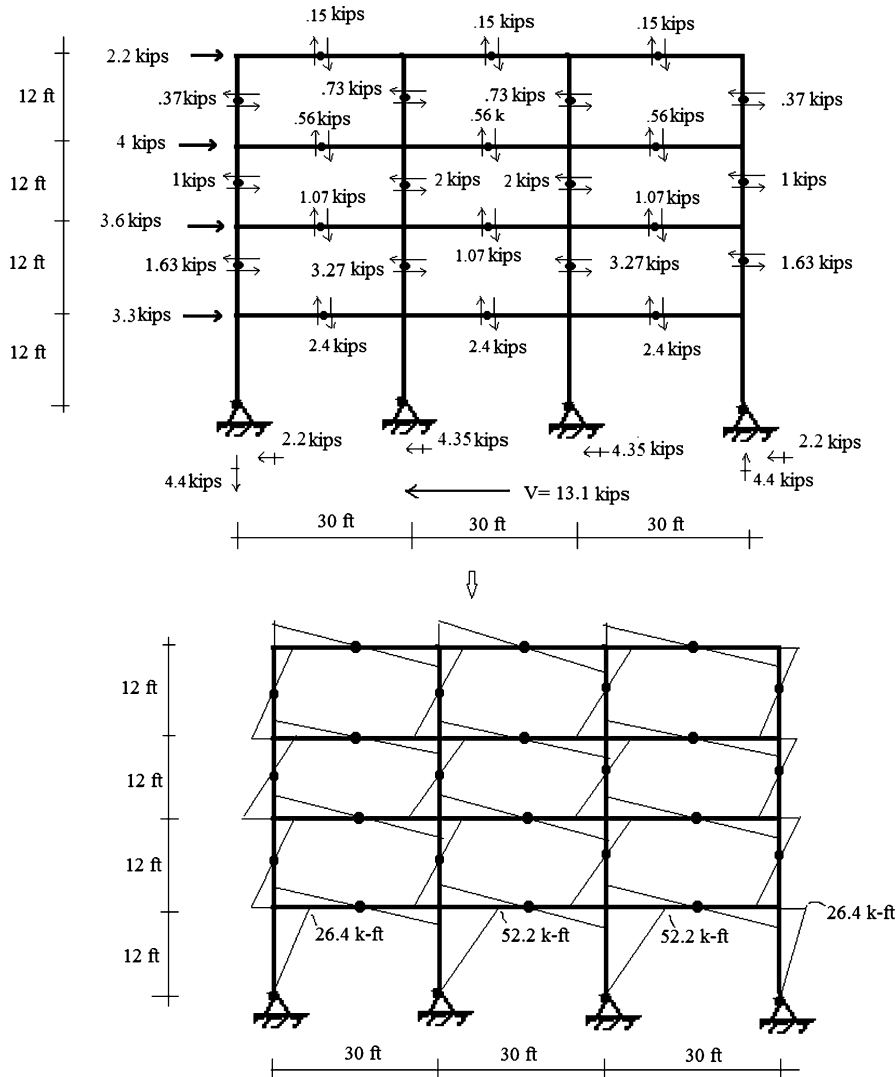


Fig. 15.17 Rigid frame N-S, Braced frame E—W. (a) Plan. (b)Typical rigid frame elevation—N-S. (c) E-W elevation braced frames 1-1, 4-4

Wind loading introduces end moments in the beams and columns. We use the portal method (see Chap. 11) to estimate these values. The results are shown on the sketch below. The peak column moment due to wind is 4.35 kip (12 ft) = 52.2 kip ft, the peak floor beam moment due to wind is 2.4 kip (15 ft) = 36 kip ft, and the peak roof beam moment due to wind is 0.15 kip (15 ft) = 2.25 kip ft.



Lateral load analysis-Portal Method

15.5.7.1 N-S Beams

We estimate the design moment for roof and floor beams based on the following combination of factored moments:

Roof:

$$M_u^- \approx \begin{cases} 1.4 \frac{w_D L^2}{12} = \frac{1.4(3.6)(30)^2}{12} = 378 \text{ kip ft} \leftarrow \\ (1.2w_D + 1.6w_L) \frac{L^2}{12} = \frac{(1.2(3.6) + 1.6(0.4))(30)^2}{12} = 372 \text{ kip ft} \\ (1.2w_D + 0.5w_L) \frac{L^2}{12} + 1.6M_{\text{wind}} = \frac{(1.2(3.6) + 0.5(0.4))(30)^2}{12} + 1.6(2.25) = 343 \text{ kip ft} \end{cases}$$

Floor:

$$M_u^- \approx \begin{cases} 1.4 \frac{w_D L^2}{12} = \frac{1.4(1.1)(30)^2}{12} = 115.5 \text{ kip ft} \\ (1.2w_D + 1.6w_L) \frac{L^2}{12} = \frac{(1.2(1.1) + 1.6(1.4))(30)^2}{12} = 267 \text{ kip ft} \leftarrow \\ (1.2w_D + 0.5w_L) \frac{L^2}{12} + 1.6M_{\text{wind}} = \frac{(1.2(1.1) + 0.5(1.4))(30)^2}{12} + (1.6)36 = 209 \text{ kip ft} \end{cases}$$

15.5.7.2 N-S Columns

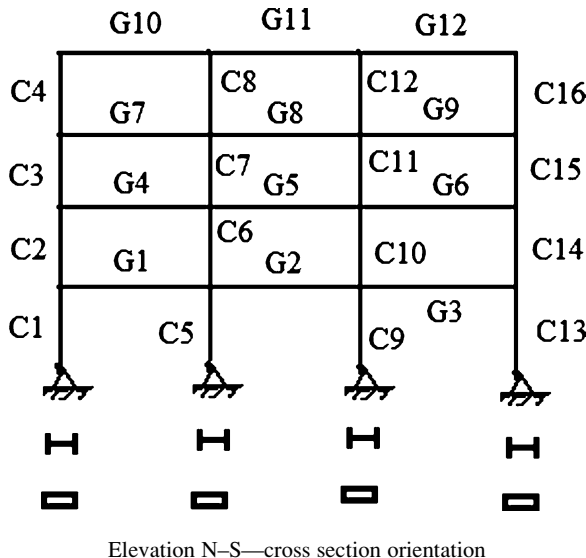
As a first estimate we use tributary areas to estimate the axial load in the columns due to dead and live loads. The most critical load combinations for the columns are

$$\begin{cases} P_u = 1.2P_D + 1.6P_W + 0.5P_{L_{\text{floors}}} + 0.5P_{L_{\text{roof}}} \approx 317 \text{ kip} \\ M_u \approx 1.6M_W \approx 1.6(52.2) \approx 84 \text{ kip ft} \\ \begin{cases} P_u = 1.2P_D + 1.6P_{L_{\text{floors}}} + 0.5P_{L_{\text{roof}}} \approx 461 \text{ kip} \\ M_u \approx 10 \text{ kip ft} \end{cases} \end{cases}$$

In what follows, we use estimated member properties based on the above estimated design values to compute the initial response due to the combination of pattern, dead and wind loadings. Determining the actual properties is an iterative process. We expect the beam sizes to decrease, and the column size to increase as the iteration proceeds due to the shift from braced frame to rigid frame. The estimated properties are

$$\begin{cases} I_{\text{col}} = 272 \text{ in.}^4 & A_{\text{col}} = 14.4 \text{ in.}^2 \\ I_{\text{beam/floor}} = 1,070 \text{ in.}^4 & A_{\text{beam/floor}} = 19.1 \text{ in.}^2 \\ I_{\text{beam/roof}} = 1,830 \text{ in.}^4 & A_{\text{beam/roof}} = 24.3 \text{ in.}^2 \end{cases}$$

We orient the cross sections such that the bending occurs about the strong axis as indicated on the sketch below.



15.5.8 Live Load Patterns

We determine the live load patterns for the maximum positive and negative moments for the beams and columns and then analyze the model under the combined dead, live, and wind loads. The wind loads are defined in Fig. 15.17b.

Live Load Patterns for Positive Moment—Beams:

There are two load patterns for maximum positive moment at mid-span of the beams.

Negative Moment Live Load Patterns—Beams:

There are eight loading patterns for maximum negative end moments of the beams.

Axial Force Live Load Patterns—Columns:

The following two load patterns establish the peak values of the column axial forces.

Figure 15.18 shows live load patterns for maximum moments in beams, and axial force in columns.

15.5.9 Moment Diagrams

Using the estimated initial properties and a computer software system, we analyze the rigid frame for the various loading patterns. The results are summarized below.

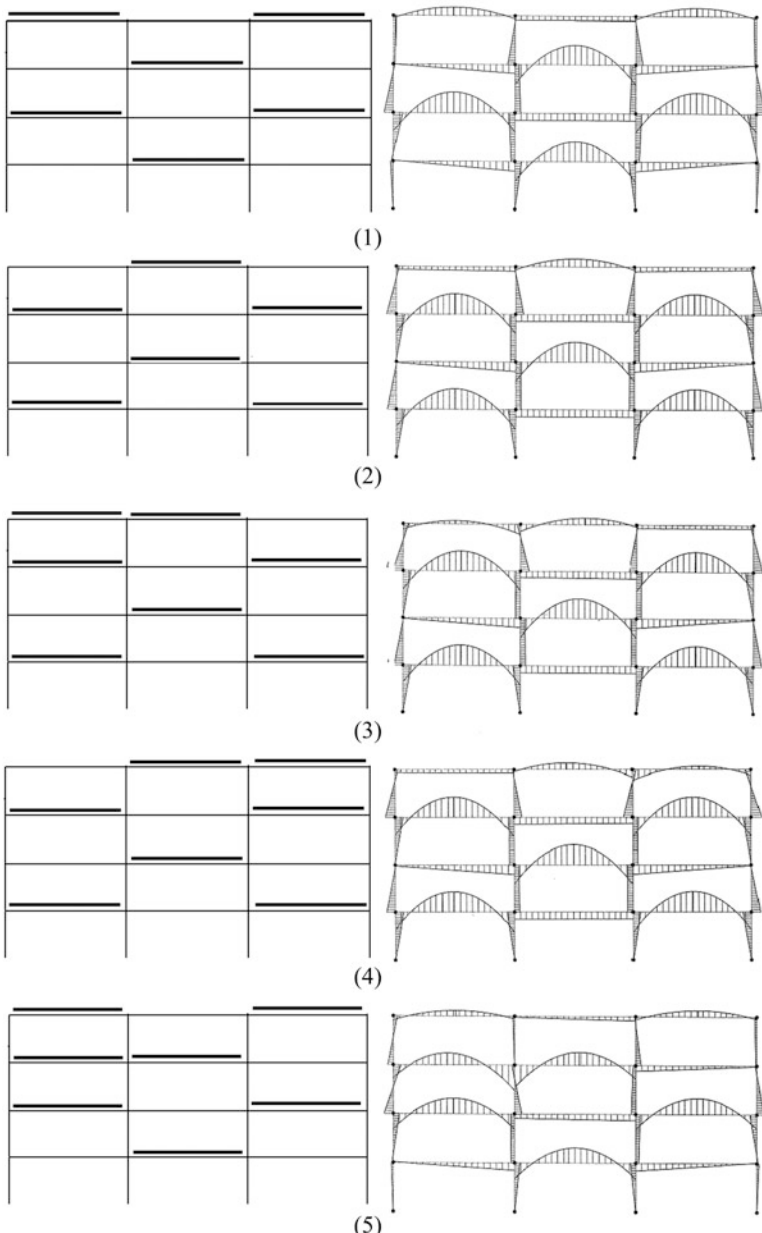


Fig. 15.18 (a) Positive live load (LL) moment patterns. (b) Negative live load (LL) moment patterns. (c) Live load patterns for axial force

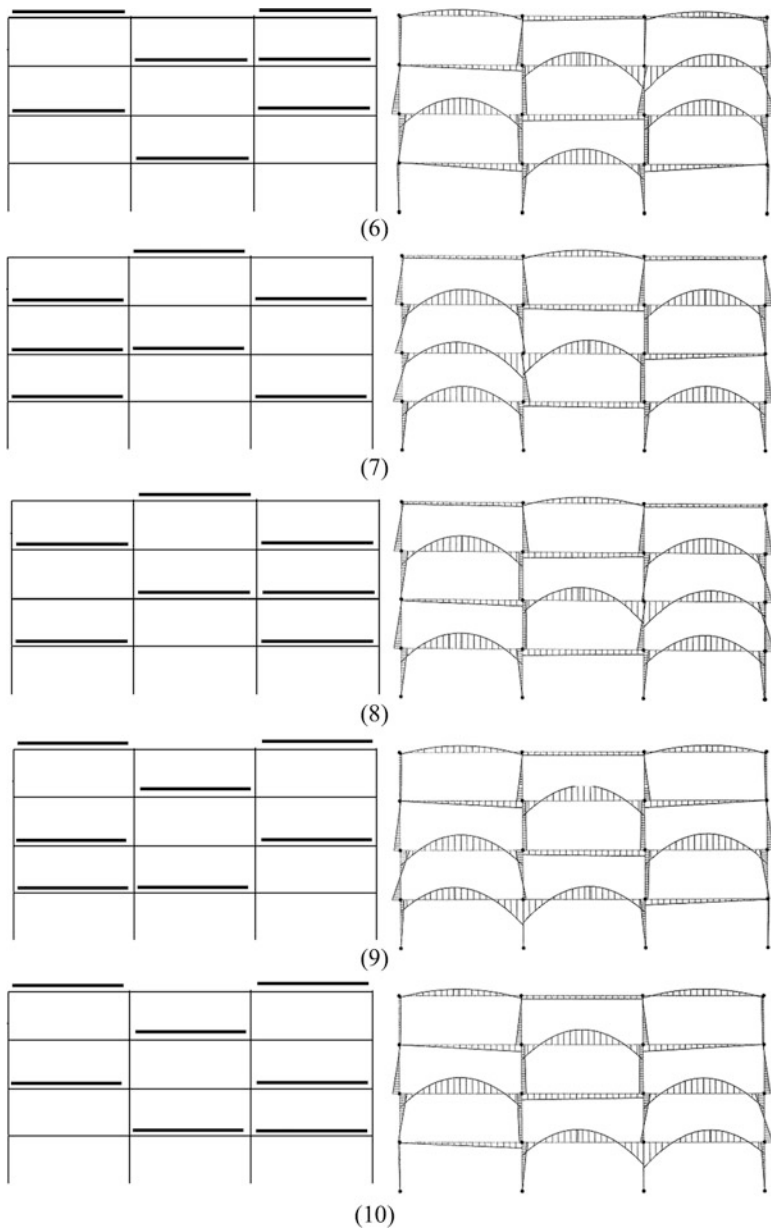


Fig. 15.18 (continued)

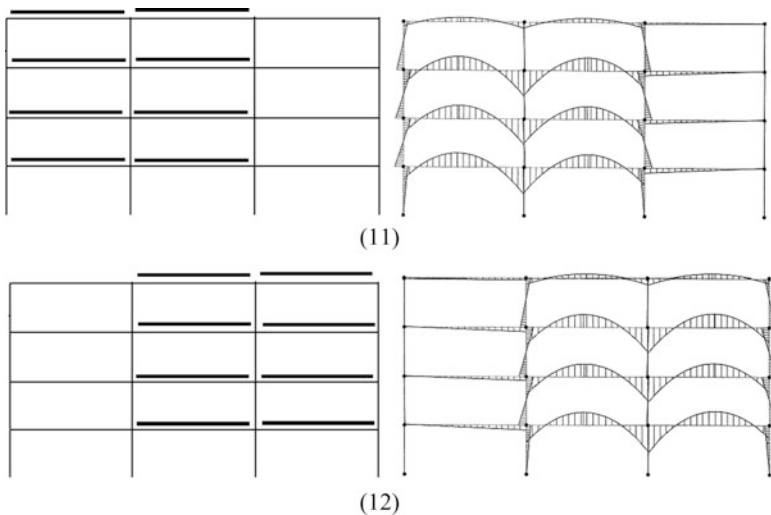


Fig. 15.18 (continued)

15.5.9.1 Dead Load

The moment diagrams due to dead loading for the individual beams are plotted in Fig. 15.19. The corresponding peak values for the braced frame are roof beam $M_D = 405$ kip ft and floor beam $M_D = 124$ kip ft. We note that the peak moment values for rigid frame are approximately 25 % less than the corresponding values for the braced frame. This reduction is due to including a rigid connection between the beams and columns.

15.5.9.2 Uniform Live Load

To provide an estimate of the peak values of live load moment, a uniform live load is applied to all the beams. Results are listed in Fig. 15.20. The corresponding braced frame results are roof beams: 45 kip ft and floor beams: 158 kip ft.

15.5.9.3 Wind Load N-S

The distribution of bending moment in the individual beams and columns due to wind loading is summarized in Fig. 15.21. There are significant moments in the columns located in the first floor. Note that there are **no** moments in the braced frame due to wind.

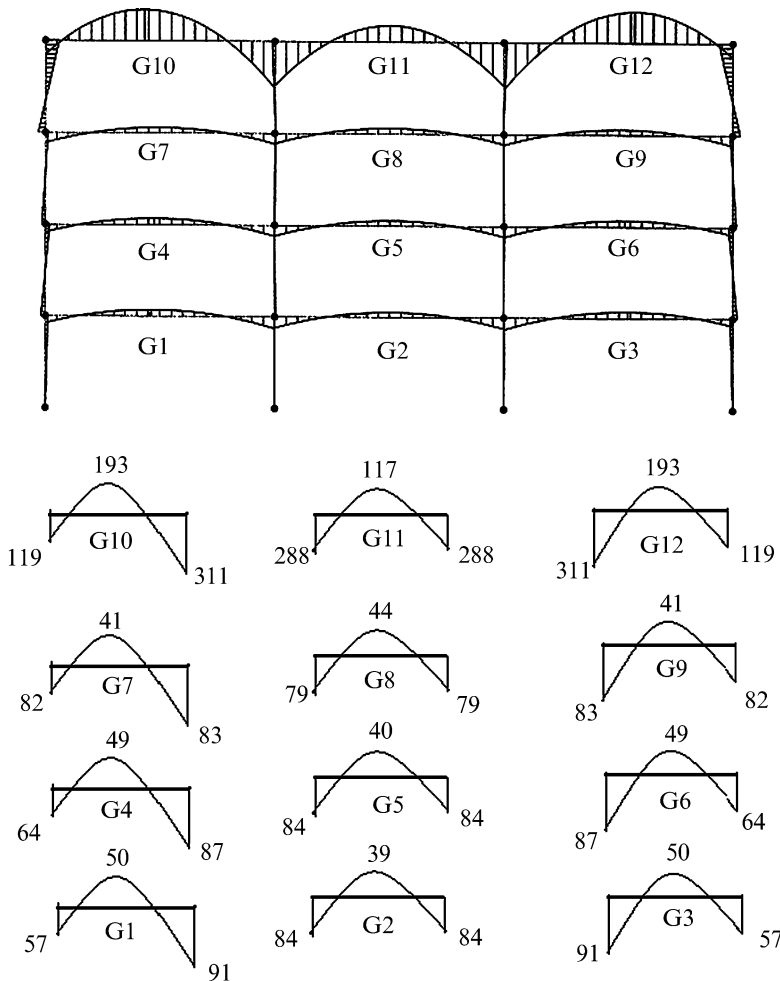


Fig. 15.19 Moment diagrams for beams—dead load (kip ft)

15.5.9.4 Maximum Positive and Negative Live Load Moments in the Beams

Results of the analyses for the ten live load patterns defined in Fig. 15.18a, b are used to construct the discrete moment envelope plots shown in Fig. 15.22. These plots show the *peak positive and negative moments at various sections along the spans generated by the ten different loading patterns*. The absolute peak values are summarized in Fig. 15.23. Comparing Fig. 15.23 with Fig. 15.20 shows that applying a uniform loading to all the beams tends to produce peak values of moment which are lower than the values of the pattern loading.

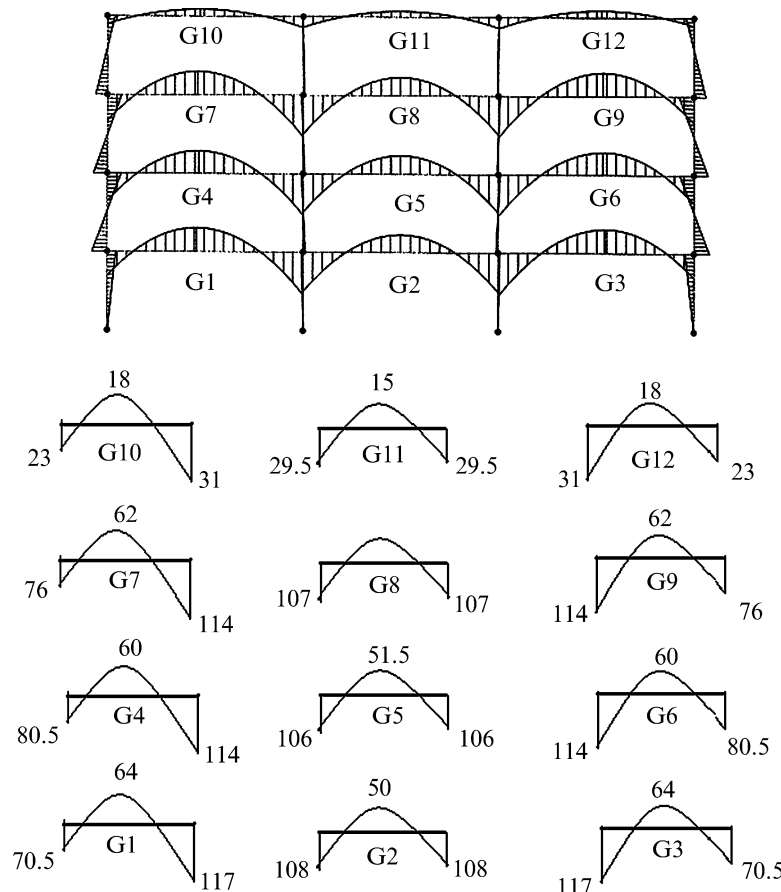


Fig. 15.20 Moment in beams—Uniform live loading (kip ft)

15.5.10 Design Values

The design values of moment, shear, and axial forces in the beams and columns are determined by generating discrete force envelopes based on the following loading combinations (Fig. 15.24):

$$\text{Factored load combination } \left\{ \begin{array}{l} (1) 1.4D \\ (2) 1.2D + 1.6L_{\text{floors}} + 0.5L_{\text{roof}} \\ (3) 1.2D + 1.6L_{\text{roof}} + 0.8W \\ (4) 1.2D + 0.5L_{\text{floors}} + 0.5L_{\text{roof}} + 1.6W \end{array} \right.$$

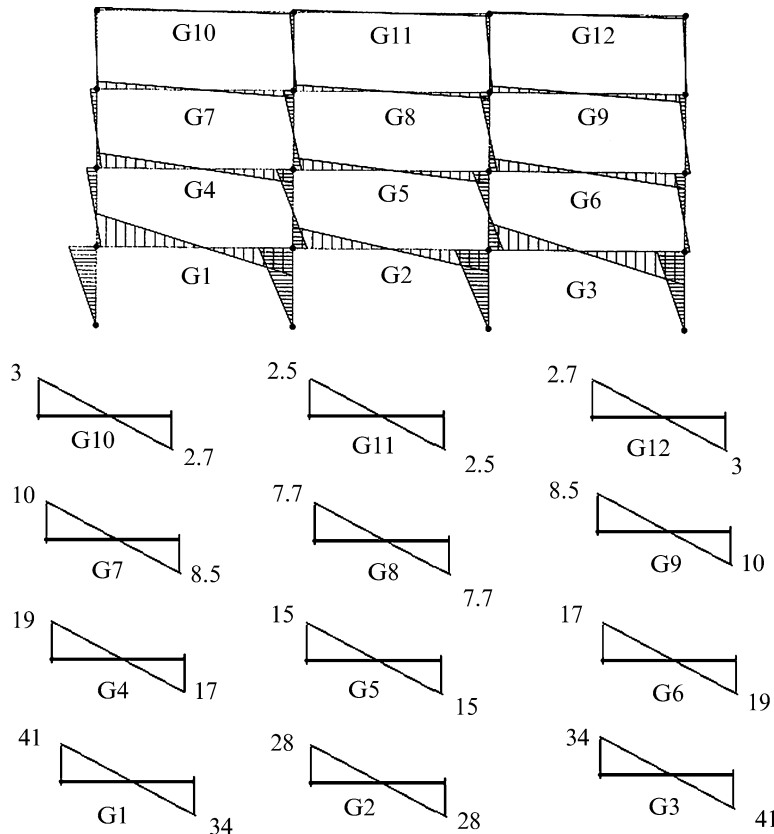


Fig. 15.21 Moment diagrams for beams—Wind loading (kip ft)

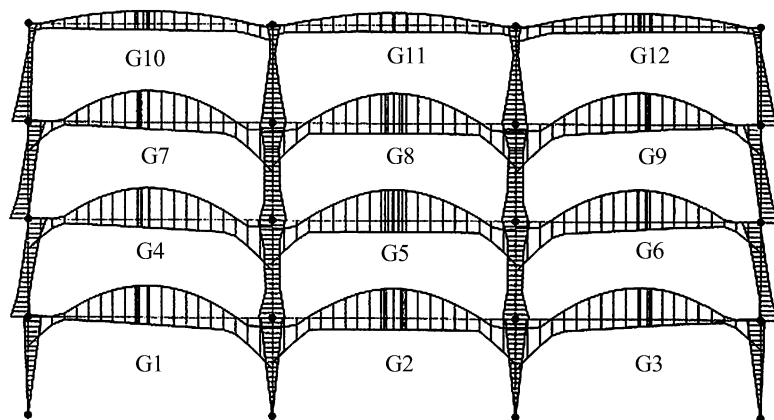


Fig. 15.22 Peak positive and negative discrete moment envelopes due to pattern live loading

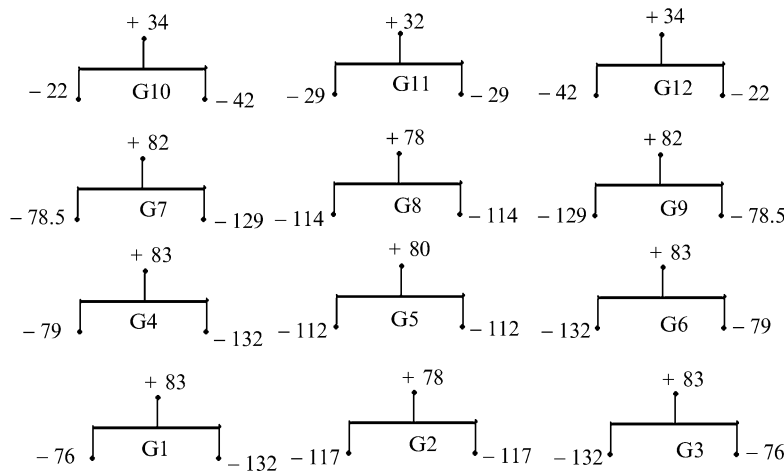


Fig. 15.23 Absolute Maximum positive and negative moments in the beams due to pattern live loading (kip ft)

We scan the discrete envelopes and identify which beam or column has the most critical combination, using this updated information, we determine revised values for the cross-sectional properties:

Revised values

$$\begin{cases} I_{\text{col}} = 341 \text{ in.}^4 & A_{\text{col}} = 17.7 \text{ in.}^2 \\ I_{\text{beam/floor}} = 890 \text{ in.}^4 & A_{\text{beam/floor}} = 16.2 \text{ in.}^2 \\ I_{\text{beam/roof}} = 1,140 \text{ in.}^4 & A_{\text{beam/roof}} = 16.2 \text{ in.}^2 \end{cases}$$

Then, using these properties, we generate updated values for the design moments shown in Fig. 15.25.

Since the columns are subjected to both axial action and bending, we need to scan the results for the individual loadings and identify the loadings that produce the maximum axial force and the maximum moment in the columns. Carrying out this operation, we identify the combinations for columns C1 and C5 listed in Fig. 15.26.

Given these design values, one generates new estimates for the cross-sectional properties. If these new estimates differ significantly from the original estimates, the analysis needs to be repeated since the results are based on the relative stiffness of the beams and columns. It turns out for this study that the initial estimates are sufficiently accurate.

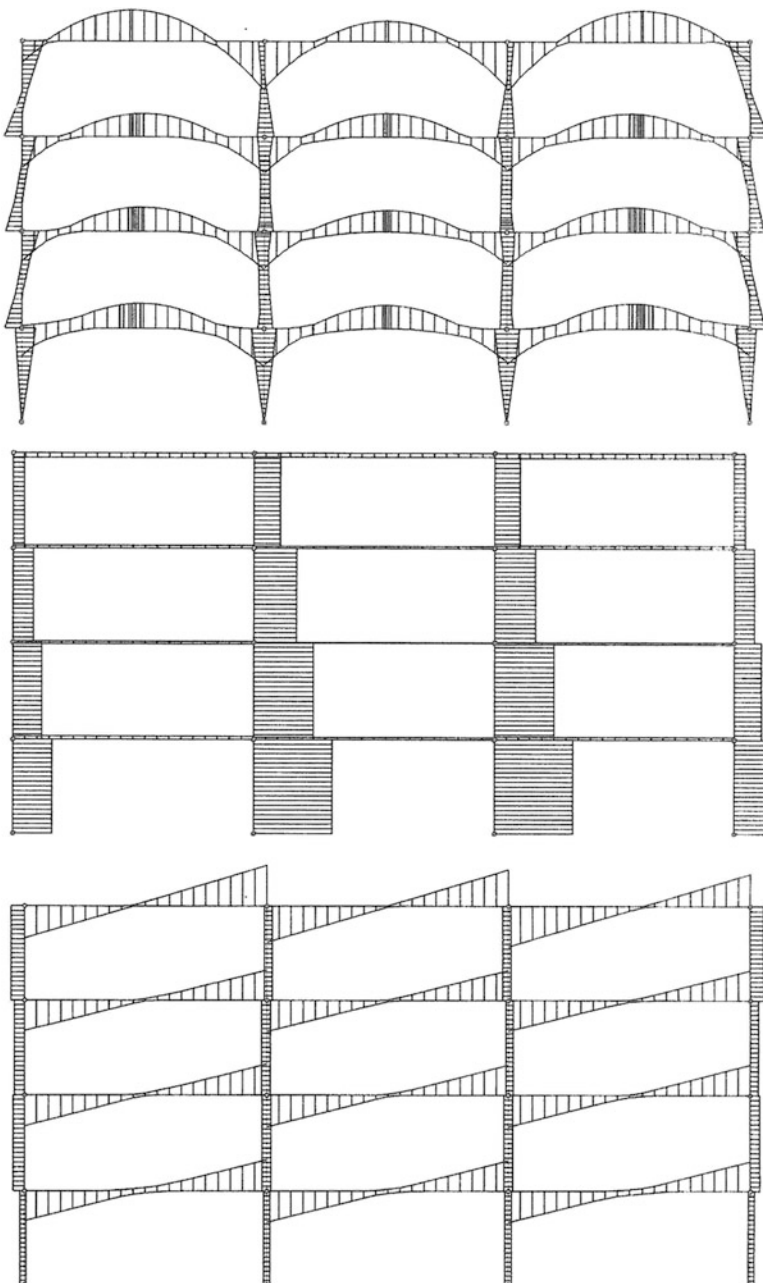
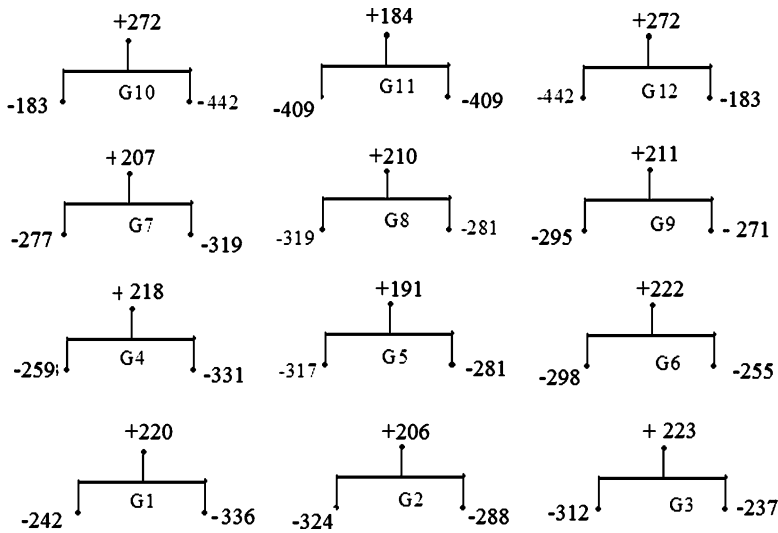
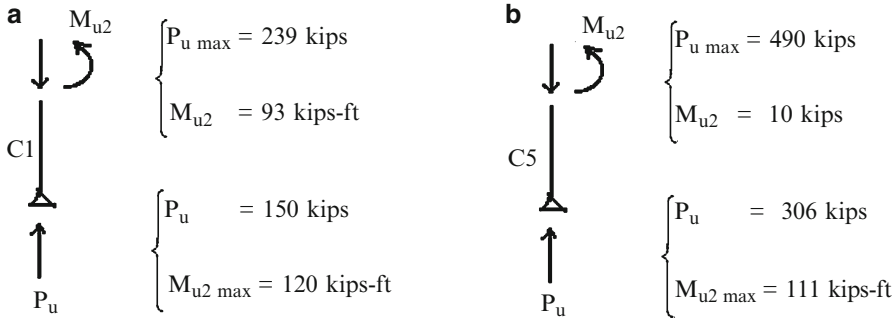


Fig. 15.24 (a) Discrete moment envelope-factored load combination. (b) Discrete axial force envelope-factored load combination. (c) Discrete Shear envelope-factored load combination

**Fig. 15.25** Maximum and minimum design moments (kip ft)**Fig. 15.26** Critical axial load-moment combinations for Columns C1 and C5. (a) Exterior column. (b) Interior column

15.5.11 Summary for Case (2)

N-S roof beam	$M_u = 442 \text{ kips-ft}$
N-S floor beam	$M_u = 336 \text{ kips-ft}$
E-W beams	same as part i
Columns	$\begin{cases} P_u = 490 \text{ kips} \\ M_u = 10 \text{ kips-ft} \end{cases} \text{ or } \begin{cases} P_u = 306 \text{ kips} \\ M_u = 111 \text{ kips-ft} \end{cases}$
E-W braces	same as part i

Comparing these values with the corresponding values for case (1), we see that the N-S rigid frame structure responds *more efficiently in the sense that its design values are less* and therefore the required cross sections are lighter.

15.6 Summary

15.6.1 Objectives

- To describe how gravity floor loading is transformed into distributed loading acting on the supporting beams.
- To show how Müller-Breslau principle can be applied to establish critical patterns of live gravity loading for the peak bending moments in rigid frames.
- To present a case study which integrates all the different procedures for dealing with dead, live, wind, and earthquake loads.

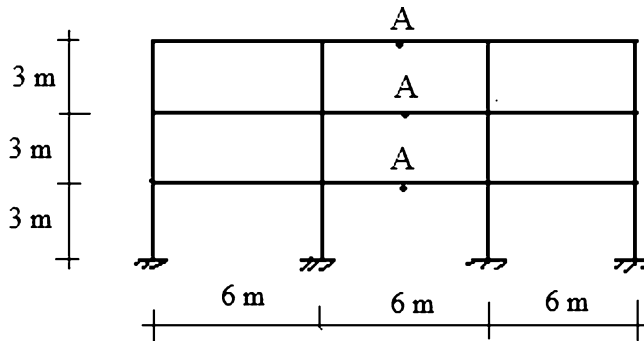
15.6.2 Key Concepts

- The floor slabs in concrete buildings are cast simultaneously with the supporting beams. The type of construction provides two possible load paths for gravity loads. Which path dominates depends on the relative magnitude of the side dimensions. The terms one-way and two-way actions are limiting cases where

- (1) one side is large with respect to the other side and (2) the sides are of the same order of magnitude.
- Gravity loading produces only positive moment in the beams of a braced frame.
 - Positive moment at mid-span in the beams of a rigid frame is due only to gravity loading.
 - Negative moment in the beams of a rigid frame is generated by both gravity and lateral loads.

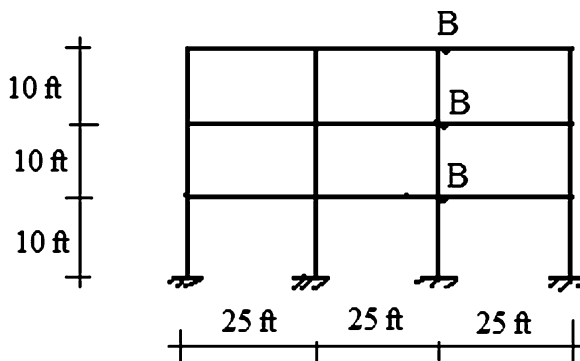
15.7 Problems

Problem 15.1



Using Müller-Breslau Principle, determine the loading patterns (uniformly distributed member load) that produce the peak values of positive moment at point A (mid-span) for each story.

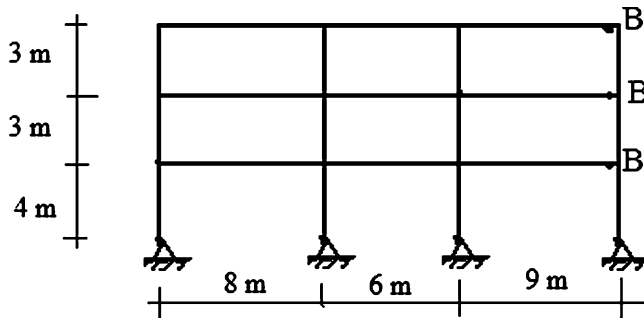
Problem 15.2



Using Müller-Breslau Principle, estimate the loading patterns (uniformly distributed member load) that produce the peak value of negative moment at B for each story. Check the results using a software package. Take $I_c = 150 \text{ in.}^4$ for all the columns and $I_g = 300 \text{ in.}^4$ for all the beams.

Problem 15.3

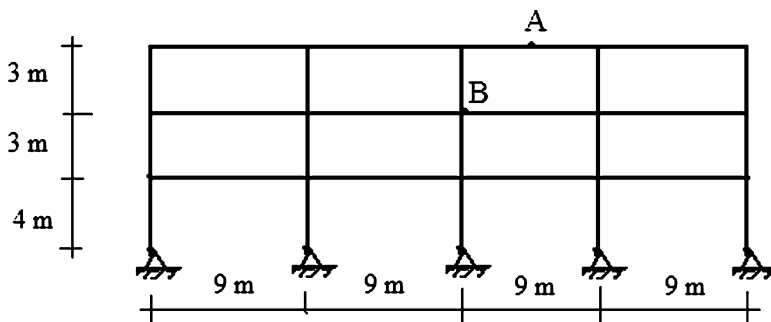
Using Müller-Breslau Principle, estimate the loading patterns (uniformly distributed member load) that produce the peak value of negative moment at B for each story. Check the results using a software package. Take $I_b = 300(10)^6 \text{ mm}^4$ for all the beams and $I_c = 100(10)^6 \text{ mm}^4$ for all the columns.



Problem 15.4

For the frame shown below

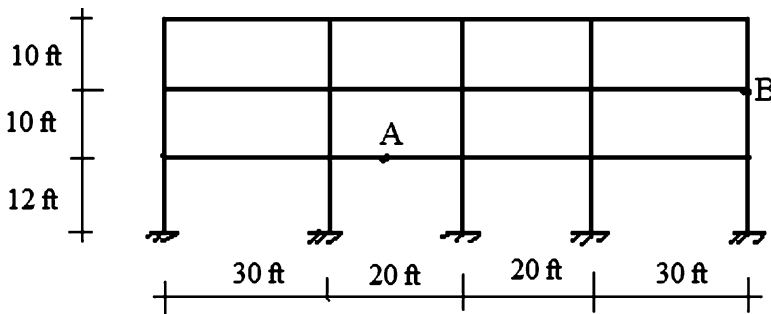
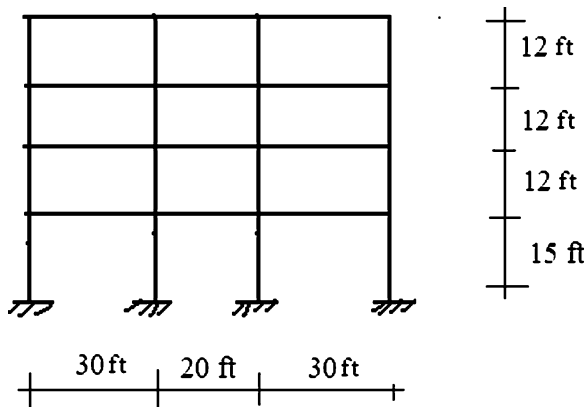
- Using Müller-Breslau Principle, sketch the influence lines for the positive moment at A and the negative moment at B.
- Use a software package to determine the maximum values of these quantities due to a uniformly distributed live load of 30 kN/m and a uniformly distributed dead load of 20 kN/m. Take $I_c = 100(10)^6 \text{ mm}^4$ for all the columns and $I_b = 200(10)^6 \text{ mm}^4$ for all the beams.



Problem 15.5

For the frame shown below,

- Using Müller-Breslau Principle, sketch the influence lines for the positive moment at A and the negative moment at B.
- Use a software package to determine the maximum values of these quantities due to a uniformly distributed live load of 1.8 kip/ft and a uniformly distributed dead load of 1.2 kip/ft. Take $I_c = 480 \text{ in.}^4$ for all the columns and $I_b = 600 \text{ in.}^4$ for all the beams.

**Problem 15.6**

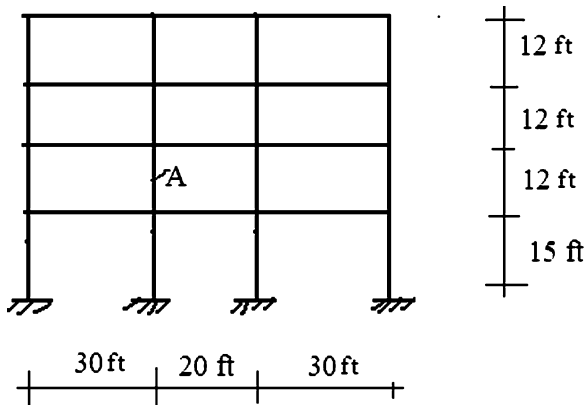
Consider the typical frame defined above. Assume the bay spacing is 20 ft.

- Determine the floor loads per bay due to an Earthquake of intensity $S_a = 0.3 \text{ g}$. Assume the following dead weights. Roof load = 0.08 kip/ft² and floor load = 0.06 kip/ft².
- Estimate the column shear forces due to this earthquake.
- Estimate the column shear forces due to both gravity and earthquake.

Problem 15.7

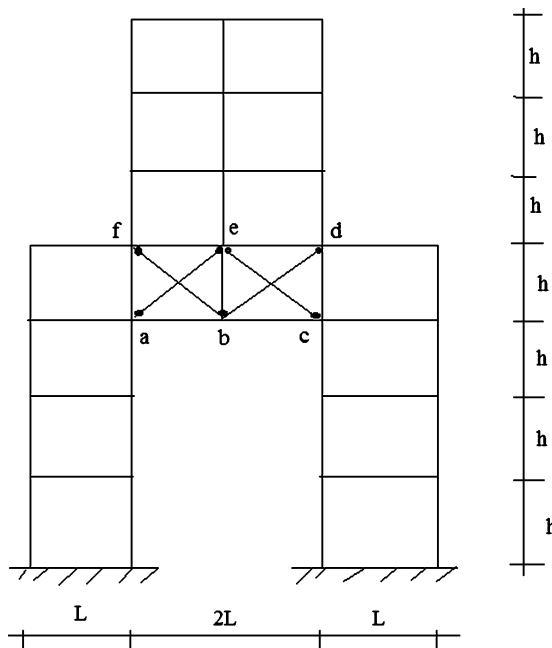
Consider the frame shown below. Assume a uniform gravity live loading for the beams.

- Describe how you would apply Müller-Breslau Principle to establish the loading pattern for the compressive axial load in column A.
- Compare the axial load in column A of the pattern loading to the uniform loading on all members. Consider all the girders to be of the same size and all the columns to be of the same size. Assume $I_{\text{beam}} = 2.5I_{\text{column}}$ and $w = 1.2 \text{ kip/ft}$. Use computer software.



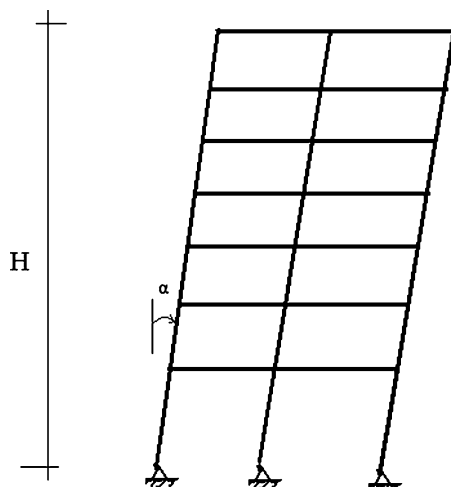
Problem 15.8

Discuss the function of the structure, abcdef. How would you determine the gravity loading acting on it? Assume uniform gravity loading for the beams.



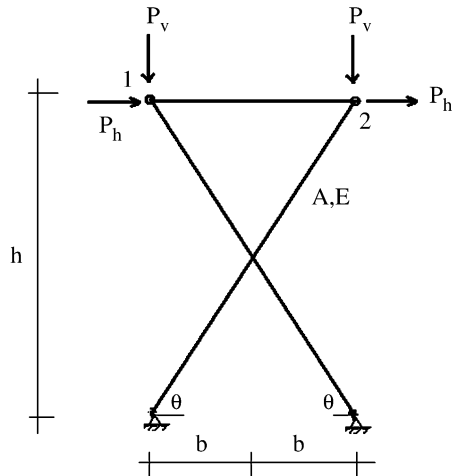
Problem 15.9

Consider a uniform floor gravity loading on the floors of the multistory rigid frame building shown below. Investigate how the internal forces vary with the angle α ranging from 0 to 20° , considering H constant. Is there a limiting value for α ?

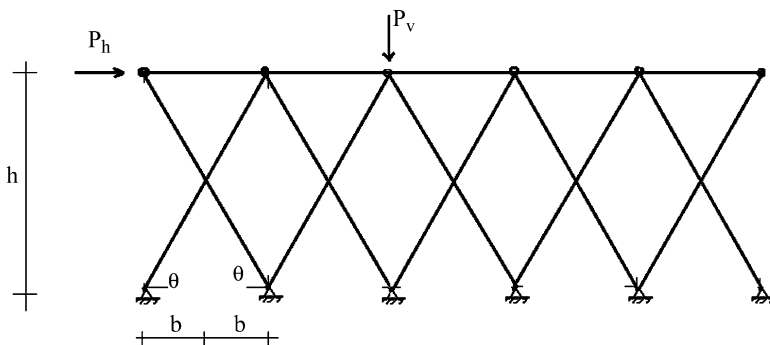


Problem 15.10

Consider the symmetrical structure shown below. All the members are pinned at their ends.



- Determine expression for the axial force in the diagonal members due to the vertical (P_v) and horizontal (P_h) loads.
- Determine the horizontal and vertical displacements of the nodes 1 and 2.
- Extend the analysis to the structure shown below. This structure is called a DIAGRID structure.

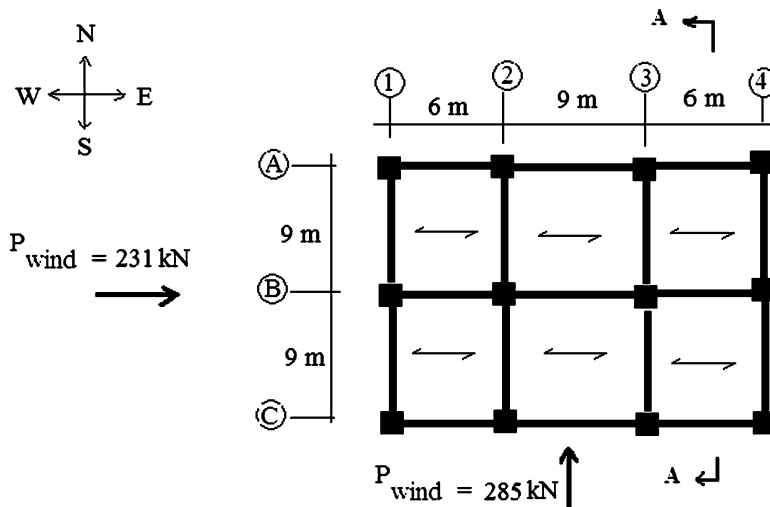


Problem 15.11

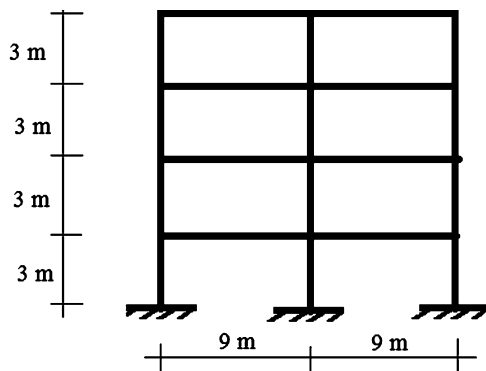
For the structure shown below, assume the floors are flexible and the flooring system transmits the gravity loading to the floor beams in the N–S direction (one-way action). Assume all beams are the same size and all the columns are the same size. $I_{\text{beam}} = 3I_{\text{column}}$, $\text{Floor}_{\text{gravity}} = 175 \text{ kN/m}^2$.

Compare the maximum forces in beams and columns caused by combination of gravity and wind for the following cases.

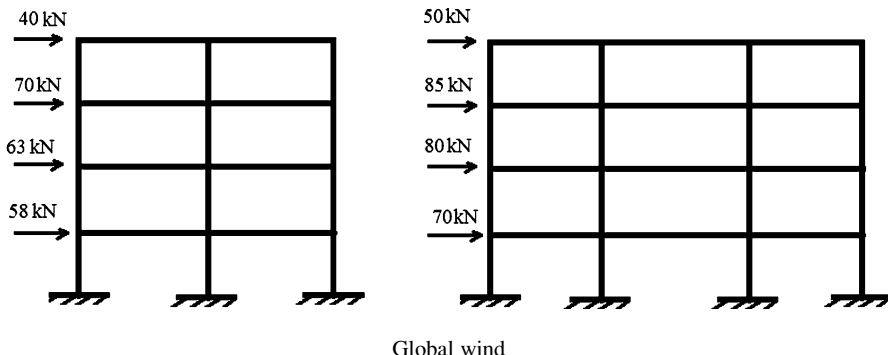
1. The structure is considered to be a braced frame, i.e., all the connections between beams and columns are pinned both in N–S and E–W direction. Assume the frames are suitably braced.
2. The structure is considered to be a rigid frame in the N–S direction and a braced frame in the E–W direction, i.e., all the connections between beams and columns are moment connections in N–S direction but pinned in the E–W direction remain pinned.



Typical plan



Elevation—Section A-A



Global wind

References

1. Schodek DL, Bechthold M. *Structures*. NJ: Pearson/Prentice Hall; 2008.
2. Hibbeler RC. *Engineering mechanics statics and dynamics*. 11th ed. NJ: Pearson/Prentice Hall; 2007.
3. Hibbeler RC. *Mechanics of materials*. NJ: Prentice Hall; 2008.
4. Gere JM. *Mechanics of materials*. 6th ed. Belmont, CA: Brooks/Coll; 2004.
5. Hibbeler RC. *Structural analysis*. 7th ed. NJ: Pearson-Prentice Hall; 2009.
6. Leet KM, Uang CM. *Fundamentals of structural analysis*. 2nd ed. NY: McGraw-Hill; 2005.
7. McCormac JC. *Structural analysis using classical and matrix methods*. Hoboken, NJ: Wiley; 2007.
8. Structural Engineering Institute, ASCE. ASCE/SEI 7-05, Minimum design loads for buildings and other structures. NY: ASCE; 2006.
9. American Institute of Steel Construction (AISC). AISC-ASD/LRFD Steel Construction Manual. 14th ed. Chicago, IL: AISC; 2011.
10. American Association of State Highway and Transportation Officials (AASHTO). AASHTO LRFD Bridge Design Specifications. 4th ed. Washington, DC: AASHTO; 2009.
11. American Concrete Institute (ACI). Building Code Requirements for Structural Concrete, ACI318M-08, Farmington Hills, MI; 2008.
12. International Code Council (ICC). International building code. Washington, DC: ICC; 2009.
13. Streeter VL. *Fluid mechanics*. NY: McGraw-Hill; 1966.
14. Federal Emergency Management Agency FEMA445, 2006, Next Generation Performance-based Design Guidelines, Washington, DC.
15. Heyman J. *The Science of structural engineering*. London, UK: Imperial College; 1999.
16. Tauchert TR. *Energy principles in structural mechanics*. NY: McGraw-Hill; 1974.
17. United States Geological Survey National Earthquake Information Center, Denver, Colorado. <http://earthquake.usgs.gov/earthquakes/shakemap/>
18. Terzaghi K, Peck RB. *Soil mechanics in engineering practice*. NY: Wiley; 1967.
19. Huntington WC. *Earth pressures and retaining walls*. NY: Wiley; 1957.
20. Lambe TW, Whitman RV. *Soil mechanics*. NY: Wiley; 1969.
21. Cross H. Analysis of continuous frames by distributing fixed-end moments. 1932. Transactions ASCE Volume 96, paper 1793.
22. Eurocode (1–9). British Standards Institute, London, UK; 2009.
23. Faraji S, Ting J, Crovo DS, Ernst H. Nonlinear Analysis of Integral Bridges: Finite Element Model, ASCE J. Geotechnical and Geo-Environmental Engineering. 2001; 127(5):454–461.
24. William T. Segui. *Steel design*, 4th ed. Thomson, Toronto, Ontario, Canada; 2007.
25. Wilbur JB, Noris CH. *Elementary structural analysis*. NY: McGraw-Hill; 1948.
26. Connor JJ. *Introduction to structural motion control*. NJ: Prentice Hall; 2003.
27. Strang G. *Linear algebra and its application*. NY: Academic; 1976.

28. Milne RJW. Structural engineering: history and development. London: E & FN Spon; 2010.
29. Matlab 7.13, Engineering calculations software
30. Mathcad 14.0, Engineering calculations software
31. GTSTRUDL® is developed and maintained in the CASE Center, School of Civil and Environmental Engineering, Georgia Institute of Technology, Atlanta, Georgia, USA.

Index

A

- AASHTO. *See* American Association of State Highway and Transportation Officials (AASHTO)
Active failure mode, 603, 607
Active soil pressure. *See* Rankine theory
A-frame
 description, 356
 indeterminate, 359–360
 loading, reactions and free body, 396–397, 398–399
 moment distribution, 397–399
 reactions and bending moment distribution, 432–433
Allowable soil pressure, 548, 549
American Association of State Highway and Transportation Officials (AASHTO), 19, 20
Analysis
 analytical tools (*see* Analytical tools, structural analysis)
 statically determinate plane frames
 angle-type frame segment, 364–366
 cantilever frame, 361–364
 moment, shear and axial force, 360–361
 portal frames (*see* Portal frames)
 sign convention, 360–361
Analytical solutions, multi span beams
 bending moment distribution, 676
 compatibility equation, 673
 lengths and moments, 673
 loading, 676, 677
 peak moments, 675–676
 static equilibrium equations, 674
 support settlement, continuous, 681–683
 uniform loading, continuous, 679–681
 variation, bending moment, 678–679
Analytical tools, structural analysis
 beam response, 39, 40
 concept of equilibrium, 32–34

- deformations and displacements, 38–39
description, 31–32
displacements
 deformation modes, 43
 description, 40
 reactions, cable tension and vertical displacement, 40–42
 rigid member, springs, 42
 spring forces, 43–45
 statically indeterminate beam, 45–47
FBD, 35
internal forces, 35–38
study of forces, 40
Anti-symmetry
 deflected shapes, 283–287
 shear and moment diagrams, 280–283
Approximate methods
 bending moment distribution
 approximate and exact results, 877
 axial force, shear force, 878–879
 members AC and FD, computer software system, 879
 qualitative reasoning, relative stiffness, 876–877
 bending type structures, 843
 column axial forces, 882–883
 column shears, 883–884
 high-rise rigid frames (*see* Cantilever method)
 multi-span beams (gravity loading), 844–848
 multistory rigid frames
 gravity loading, 847–849
 lateral loading, 849–870
 positive and negative moments,
 multistory steel frame, 878
 rigid steel frame, bracing, 884
 statically indeterminate structure, 843
 steel frame
 axial force, shear force and moments, 880–882
 portal and shear stiffness method, 880

- Arch bridges
 structures, 955–956
 two-hinged, 982
- Arches
 “false arch”, 490
 force method
 applied load, 685
 axial deformation, 684–685
 description, 683
 expressions, horizontal displacement, 684, 685
 integral expression, 688–689
 parabolic, 686–688
 structure, 684
 tension tie, 692–693
 two-hinged arch and loading, 689–692
 three-hinged (*see* Three-hinged arches)
- Arch structures
 historical development, 490
 models, 494–498
- Arc length
 differential and total, 465–466
 initial and loaded shapes, cable, 464–465
 maximum tension, determination, 477–478, 488
 sag profile and total arc length, 467–468
 sag ratio, 466
 temperature effect, 466–467, 487
- ASCE 7-05, 18, 19, 24, 25
- Axial force
 A-frame, 356
 compressive and maximum value, 510
 gable frame
 3-hinge, 389–391
 simply supported, 386–388
 graphical output, 415, 417
 shallow *vs.* deep parabolic curved members, 506, 509
 sign convention, 360–361
 and transverse shear, 523–524
 triangular rigid frame, 441
- Axial stiffness. *See* Equivalent axial stiffness
- Axial stress, 38, 61
- Axle load, 968, 970
- B**
- Backfill material
 fluid
 definition, 601
 horizontal and vertical components, 602
- H/3 units, 601–602
 hydrostatic forces, inclined surface, 601, 602
- granular
 active and passive failure states, 603
 angle of repose, 603
 dry loose sand, 603
 shear stress, 603
 theories, soil pressure distribution, 604
- Rankine theory (*see* Rankine theory)
- Base shear, 861, 1008, 1047
- Beam formulation
 loading, 928–930
 member end forces and displacements, 923–924
 nodes, 926–928
 spring support, 932–935
 stiffness matrices, 925–926
 support settlement, 930–931
 two-span beam, 924–925
- Beams
 deep beams, deformation and displacement relations, 274–277
 differential equations, equilibrium, 213–235
 displacement process, 39, 40
 external loads, 329
 forced envelope, 330
 force method
 fixed-ended beams (*see* Fixed-end beams)
 multi-span beams (*see* Multi-span beams)
 single-span beams, analyzing frames, 647–654
 yielding supports, 654–668
 influence line, 330
 internal force (*see* Internal forces)
 mass system, 28–29
 objectives, 329
 planar bending, 329–330
 prismatic beams (*see* Prismatic beams)
 problems
 computer software, 351–353
 conjugate beam method, 338–339
 deflected shape, 343–345
 influence lines, 348–350
 loading system, span, 350–351
 rotation, cross-section, 347–348
 shear and moment diagrams, 330–337
 single concentrated load, 350
 trapezoidal rule, 347
 vertical deflection, 345–347
 virtual force method, 340–343

- reactions (*see* Reactions)
 slender beams displacement and deformation (*see* Slender beams)
 stability and determinacy (*see* Stability)
 statically determinate beams (*see* Statically determinate beams)
 statically indeterminate, 45–47
 symmetry and anti-symmetry
 - deflected shapes, 283–287
 - shear and moment diagrams, 280–283
 torsion, prismatic members, 277–280
 transverse displacement, 330
 two span beams, displacement method
 - chord rotations, 750
 - decomposition, 747, 748
 - end actions, shear and moment, 751–754
 - end shears, 749–750
 - geometry and support settlements, 750
 - moment releases, 764–766
 - nodal moment equilibrium, 748–749
 - nodal rotations, 751
 - overhang, modified slope-deflection equations, 759–764
 - symmetrical beam, supports settlement, 754–759
 - three span beam, 766–773
 - uniformly loaded three span symmetrical beam, 773–775
 Behavior
 - brittle, 12
 - “combined bending and torsion”, 186
 - ductile, 12–13
 - planar bending (*see* Planar bending)
 - portal frames
 - gravity loading, 373–374
 - 3-hinge, 376–378
 - lateral loading, 375
 Bending moment
 - distribution
 - approximate and exact results, 877
 - axial force, shear force, 878–879
 - beams and columns, portal method, 850–857
 - lateral loading, 870
 - members AC and FD, computer software system, 879
 - mid-height, first story, 875
 - multi-span beams and multi-bay frames, 876
 - qualitative reasoning, relative stiffness, 876–877
 - transverse shear, 870
 - horizontal thrust force, 528–529
 influence line, 290–291
 reactions and shear distributions, 227–235
 uniform loading, parabolic, 328
 Braced frames
 - definition, 869–870
 - multistory, 355–356
 - N-S and E-W directions (*see* Multistory buildings)
 Braced rigid frame
 - analytical expressions, schemes, 865
 - column shear forces, 867
 - definition, one-story, 866
 - individual systems, defined, 863–864
 - one-story structure, 863, 864
 - shear force distribution
 - base story sub-element, 868
 - brace stiffness, 866
 - column shear forces, 867
 - frame stiffness, 866
 - inter-story displacement, 869–870
 - lateral forces, 867–868
 - one-story frame, 866
 - upper story sub-element, 868
 - value, lower floor controls, 870
 Bridge
 - gravity live loads, 19
 - segmented long-span, 15–16
 - structure
 - geometric arrangement, 77
 - and gravity, 15
 - iron truss bridge, USA, 57
 - plane bridge truss, 117, 118
 - steel truss bridges, 59
 - wooden bridge truss, 55, 56
 Brittle, 12, 13, 17, 48
 Buckling, 3, 13–14, 48
 Building
 - design, 15
 - effect, wind, 20
 - gravity live loads, 19
 - ground motion, 28
 - low-rise, 24, 25
 - vortex shedding, 26
 Building codes, 14
 Building systems
 - multistory (*see* Multistory buildings, systems)
 - “shear beam” formulation, 1035

C

- Cable length, 445, 466–467, 479
 Cable length equivalent axial stiffness, 468–471

- Cables, 4, 7, 17, 40–42
 Cable stayed
 bridges, 443, 466, 471
 schemes
 beam displacement, 659, 661
 composition, 659, 660
 elongation, 659, 661
 stiffen beams, 661
 vertical displacement, cable and beam, 664–668
 structures, 444, 464
 Cable stayed bridges
 configuration, 986, 987
 displacement profile of girder, 991
 estimated areas, 989
 force and displacement profiles, 989–990
 idealized scheme, 987–988
 tributary area, 988
 Cable structures
 arc length (*see* Arc length)
 Brooklyn Bridge, USA, 443–445
 cable-strand arrangements, 443, 444
 Clifton Suspension Bridge, England, 443, 444
 concentrated load (*see* Concentrated load)
 coordinates, lowest point, 485
 deflected shape, 485, 486
 distributed load (*see* Distributed load)
 doubly curved single-layer cable net, 444, 447
 equivalent axial stiffness (*see* Equivalent axial stiffness)
 guyed tower, 487
 maximum tension, 482–484
 Normandy Bridge, France, 444, 446
 peak values, cable tension, 486
 reactions and tension, 479–482
 self weight (*see* Catenary shape)
 Cantilever frame
 symmetrical, 363–364
 unsymmetrical, 361–362
 Cantilever method
 applied moment, 872
 bending moment, axial forces, columns, 875
 column-beam model, 871, 872
 deformation, relative rotation, 872
 description, 870
 lateral deflections, 870, 871
 reference axis, 871
 stiff belt type trusses, 873
 symmetrical plane frame, 874–875
 symmetrical 42-story plane frame, 873–874
 tall building model, 870, 871
 Cantilever walls. *See* Vertical retaining wall structures
 Catenary shape
 arc length and tension, 477–478
 equilibrium and vertical loading, 474–475
 horizontal projection, 474
 iteration and sag ratio, 476
 symmetrical case, 475–476
 Center of mass
 description, 1026
 floor
 mass layout, 1027–1029
 plan view, 1026
 Center of twist
 braces, 1024–1025
 external and internal forces, 1018
 floor
 configuration, 1021
 geometry, 1017
 free body diagram, floor, 1012–1013
 rigid body motion, 1016
 shear spring model, 1012
 stiffness
 braces, 1014–1015
 distribution, 1019–1020
 factors, 1021–1024
 symmetry axes, 1019
 Centroid
 dimension square/rectangular footings, 560
 single footing, 550–553
 structure, 547, 549
 Chord
 horizontal, 449, 454, 458
 inclined, 453, 455, 462
 Circular curved members
 deflection, light pole, 516–518
 geometry-circular arch, 515
 slender and retain, 515
 Clamped end model, 848
 Clamped/hinged model, 848
 Clay soil
 allowable pressure, 548, 549
 pressure distributions, 547, 548
 Combined footings
 description, 565
 factored loads, 566
 peak moment values, 566
 shear and moment, 566
 soil pressure distribution, 566, 567
 square columns, 568–574
 Complex trusses
 corresponding nodal force equilibrium equations, 99
 definition, 53, 94

- equilibrium at joints, 98
geometrically stable, 99–100
individual nodal force systems, 99
matrix form, 98
planar, 157–158
planar truss, 95–97
stability criterion, 66–67
static determinacy, 94
- Compound trusses, 53, 66, 67, 94
- Compression, 361, 364
- Computation of displacements
and deformation relations, 155
matrix equilibrium equations, 156
nodal displacement, 155, 156
planar complex truss, 157–158
scalar equation, 157
space truss, 159–160
“static-geometric” analogy, 155–156
- Computer based analysis
displacement method
bending moment distribution, 837
frame structures, 818–821
and member forces, truss, 827
- plane frames
gable, 415, 416
graphical output, 415, 417
- Concentrated load
horizontal cables
free body diagram, segment, 445, 447
moment distribution, 449
moments and sag, 445–447
multiple concentrated loads, 449–453
tension, 448–449
transverse loading, pretensioned cable, 445, 447
- inclined cables
description, 453–454
reactions and horizontal force, 454–455
sag determination, 455–458
- Concept of equilibrium
concurrent force system, 32
non-concurrent force system, 33–34
- Conjugate beam method, 256–258, 338–339
- Construction loading, 15–16
- Containments, 4, 15
- Corbel arch, 490
- Critical loading
plan, rectangular area, 552, 553
pressure distributions, 551, 552
- Critical sections for design, cantilever walls, 623–627
- Cross, H., 789
- Cross section
beam, 186
“combined bending and torsion”, 186
properties, 287
- Curvature
positive and negative, deflected shapes, 238, 239
relationship, 237–238
- Curved members, statically determinate. *See*
Statically determinate curved
members
- D**
- Deck
and beam system, 117
segments, 117
slab, 54
- Deep beams, deformation and displacement
relations, 274–277
- Deep curved members, 534
- Deflected shape
moment area theorems (*see* Moment area
theorems, slender beams)
qualitative reasoning (*see* Qualitative
reasoning, deflected shapes)
symmetry and anti-symmetry, 283–287
- Deflection profiles
curvature, 412
gable frames, 413, 414
lateral loading, 413–415
peak deflection, estimation, 438
portal and 3-hinge frame, 413
- Deflections
computation
deformation–displacement relations, 102–105
description, 100
force–deformation relationship, 100–102
virtual forces method, 105–116
- frames, principle of virtual forces (*see*
Principle of virtual forces)
- Deformations
and displacements, 38–39
inelastic, 13, 14, 31
modes, 43
slender beams (*see* Slender beams)
spring forces, 43–45
- Design codes, 18, 24, 49
- Design philosophy, 30–31
- Design strategies, N-S beams and columns, 1098–1102

- Determinacy, stability. *See Stability*
- Determinate, truss structures. *See Truss structures*
- Differential equations of equilibrium, planar loading
- arbitrary distributed loading, differential element, 213
 - cantilever beam triangular loading, 216–218
 - distributed and concentrated loads, 218–222
 - extreme value, moment, 215
 - integral forms, 215
 - jump conditions, 216
 - moment summation, 214
 - reactions, shear, and bending moment distributions, 227–235
 - shear and moment, interpretation, 215
 - uniform loading, end moments, 222–227
- Dimensions
- design code, 623
 - optimal geometry, 612
 - pressure distributions, 604
 - wall footing, 628
- Direct stiffness method, 939–945, 950, 951
- Displacement method
- beam structures, two span beams (*see Beams*)
 - description, 737
 - displacements and member forces, truss, 827
 - end moments and horizontal displacement, 841–842
 - frame structures
 - member equations, 742–747
 - moment distribution, sideway (*see Sideway*)
 - member end moments
 - moment distribution, 834–840
 - slope-deflection equations, 828–834
 - member forces, truss, 827–828
 - moment distribution, multi-span beams (*see Moment distribution*)
 - out of plane loading, slope-deflection equations (*see Out of plane loading*)
 - planar
 - beam-type structures, 737, 738
 - frame-type structures, 737–738
 - truss, 737, 738
 - plane truss
 - axial loaded member, 740
 - force-equilibrium equations, 741
 - vs. force method, 741
 - horizontal and vertical translations, 739
 - nodal displacements and member forces, 739–740

- rigid frame (*see Rigid frame*)
 - rotation and end moments, analytic expression, 841
 - steps, 738–739
- Distributed load
- horizontal cable
 - description, 458–459
 - tension determination, 459–460
 - inclined cables
 - arbitrary loading, 460–461
 - sag expression and lowest point, 462
 - tension determination, 463–464
 - total moment, 461
 - uniform load, 462–463
- Ductile, 12–13, 48

E

- Earthquake loading
- base shear, 1008–1009
 - elevation, 1008
 - floor forces, 1010–1011
 - ground acceleration time history, 1003–1005
 - ground motion, 28
 - lateral displacement profile, 1006
 - low-rise rigid frame, 1005
 - peak acceleration *vs.* structural period, 1007–1008
 - peak lateral inertia force, 29
 - seismic lateral load profile, 30
 - seismic loading, 1003, 1004
 - single degree-of-freedom model, 28–29

Engineering process

- bridge structures, 955–956
- loading, 957
- objective, 955

Equivalent axial stiffness

- horizontal cable
 - actual and perturbed configurations, 468, 469
 - deflection patterns, 468–469
 - modified elastic modulus, 470–471
 - net motion, 469–470
 - sag ratio, 471

inclined cable

- Ernst's formula, 473
- guyed tower modeling, 471–472
- Millau Viaduct Bridge, France, 471
- modified elastic modulus, 472–473
- steel cable, 473–474

Equivalent single degree of freedom system, 1007

- Extensional strain, 12, 38
External loading
 creation, 205
 displacements, 636, 637
 primary structure, 638, 640
 produce reaction forces, 204
 shear and bending moment, beams, 289
 structure, 196
 and three force redundants, 642
 and unit load results, 648
- F**
- Factored load
 description, 1107
 discrete moment, axial force and shear envelope, 1107, 1110
Factored soil pressure, 555, 558
Factor of safety
 defined, 606
 requirements, 601
 vs. sliding and overturning, 607
Failure mode, buckling, 13–14
FBD. *See* Free body diagram (FBD)
Finite element method
 beam structures, 923–935
 bending moment and deflection profiles, 947–948
 description, 885
 direct stiffness method, 939–945, 950, 951
 horizontal displacements, 949
 local and global reference frames, 890–893
 matrix formulation for rigid frames, 887–889
 nodal equilibrium equations (*see* Nodal equilibrium equations)
 nodal supports
 displacement constraints, 901–902, 908–909
 end member forces, 902–903
 fixed and global end actions, 912
 fully fixed supports, 900
 geometric data, 905–906
 loading conditions, 902, 909–910
 local end actions, 912–913
 matrix displacement formulation, 905
 member forces, local coordinates, 911
 member plane frame, 905
 movement, 903
 rearranged system matrices, 903–904
 reduced system matrices, 901
 stiffness matrices, 906–907, 909
 system stiffness matrix, 914–915
 unknown force and displacements, 910–911
 spring stiffness, 946–947
 steps, 886–887
 three dimensional (3D) formulation, 935–938
 truss structures, 917–923
Fixed-end beams
 compatibility equations, 669
 fully fixed, 673
 partially fixed, 673, 674
 single concentrated force, 671–672
 structure, 668
 uniformly distributed loading, 670–671
Fixed support
 planar loading, 190
 three dimensional, 192
Flexibility coefficients
 description, 640
 pitched roof frames, 708
 plane frame, 694
 Principle of Virtual Forces, 642
 symbolic/numerical integration, 686
Flexibility method, 46
Floor loads
 gravity (*see* Gravity floor loads)
 wind load, 1003
Footings
 combined (*see* Combined footings)
 single (*see* Single footings)
 strap (*see* Strap footings)
Force envelopes
 axial, 1107, 1110
 definition, 289
 discrete, 1107
 multiple concentrated loads (*see* Multiple concentrated loads)
 single concentrated force
 absolute maximum shear force, 317
 apply at mid-span, 317
 construction, moment envelope, 318
 load, 316, 317
Force envelopes, two-hinged arches, 982
Force method
 arch-type structures (*see* Arches)
 axial, shear forces and bending moment, 725
 beam-type structures (*see* Beams)
 behavioral differences, 731–732
 computer software system, use, 725–728, 730–731
 description, 635–636
 forces, cables, 723

Force method (*cont.*)

- frame-type structures (*see* Frames)
- horizontal reaction, 728
- indeterminate trusses (*see* Indeterminate, trusses)
- Maxwell's law, reciprocal displacements (*see* Maxwell's law)
- parabolic arch, 724
- peak positive and negative moments, 728–729
- properties and loadings, 721–722
- reactions and member forces, 733–735
- structure and steps
 - actual, 636
 - choices, primary, 638, 639
 - external loading, displacements, 636–639
 - flexibility coefficients, 640–641
 - force redundants, 641–642
 - “geometric compatibility equation”, 637
 - internal forces, 642–643
 - matrix form, 642
 - multi-bay multistory frame, 643
 - multi-span beam-type, 643
 - primary, 636
 - reaction force, displacements, 636, 637
 - redundant reactions, 638, 641
 - truss-type, 643–645
- vertical reaction, 720–721

Frames

- braced, 25
- force method
 - arbitrary-shaped single bay frame structure, 694
 - axial deformation, 694
 - compatibility equation, 694
 - description, 693
 - flexibility matrix, 695
 - matrix equations, 694
 - pitched roof (*see* Pitched roof frames)
 - portal (*see* Portal frames)
- three-story, 28–29

Frame type structures, member equations

- deformation and end actions, 742, 743
- description, 742
- equilibrium conditions, 744, 745
- fixed end actions, 743–744
- moment and shear quantities, 746–747
- nodal displacement, 743
- slope-deflection equations, 747
- superposition, 744, 745

Free body diagram (FBD)

beam

- construction, 196, 200
- member FG, 203
- segment AB, 201, 227, 229–230
- segment EF, 202
- statically indeterminate, 46
- statically determinate plane frames
 - A-frames, 396–397, 399
 - forces acting, node B, 358–359
 - member forces, 358
- structural analysis, 35

Fully fixed arch, 497

G

Gable frame

- bending moment distributions, 428–432
- deflection profiles, 413, 414
- 3-hinge
 - lateral load, 389–391
 - shear and moment, 393–396
- simply supported
 - lateral load, 386–388
 - unsymmetrical loading, 391–393

Geometric compatibility

- description, 637
- flexibility coefficients, 640
- flexibility matrix, 644
- matrix equations, 694–695
- member forces, 715, 718

Girder, 7, 17, 48

Girder bridge system, 976

Global force equilibrium equations, planar loading, 196

Global reference frame

- local reference frame (*see* Local reference frame)
- quantities, 1035
- symmetry axis, 1039

Granular material, 599, 603–604

Gravity floor loads

- floor slab-beam system, 1071
- loading patterns, 1072–1073
- one-way action beam loading, 1073–1074
- steel joist/beam framing, 1073
- tributary areas, 1071, 1072

Gravity load, 15, 19–20, 25

Gravity walls

- concrete and soil backfill, 610–611
- description, 600–601
- retaining analysis, 607–610

Grid structures, 824–825

Guyed towers, 464, 466, 471, 472, 487

H

Heyman, J., 32
High rise rigid frame. *See* Cantilever method
High strength steel, 443, 444, 471
Hinged model, 848
Hinged support
 3-D, 192
 planar loading, 190
3-Hinge frames
 deflection profiles, 413–415
 description, 358
 gable
 lateral loading, 389–391
 shear and moment, 393–396
 gravity loading, 382, 384
 lateral loading, 382, 386
 portal
 gravity loading, 376
 lateral loading, 377
 shear and moment distributions, 368–371
 variable cross-section, 377–378
Horizontal cables
 concentrated load (*see* Concentrated load)
 distributed load
 description, 458–459
 tension determination, 459–460
 equivalent axial stiffness
 actual and perturbed configurations, 468, 469
 deflection patterns, 468–469
 modified elastic modulus, 470–471
 net motion, 469–470
 sag ratio, 471
Horizontal projection
 catenary shape, 474
 distributed loading, 458–460
Horizontal structures. *See* Multi-span horizontal structures
Huntington, W.C., 604

I

Idealized dead loading, 497
Idealized model
 defined, 857, 982
 integral abutment bridge, 965
 loading-idealized model, 984
 low-rise frame story, 858
 story stiffness, 860
 sub-elements, 858
 three-span arch, 986
Impact magnification factor, 971

Inclined cables

cable-stayed schemes, 659
concentrated load
 description, 453–454
 reactions and horizontal force, 454–455
 sag determination, 455–458
distributed load (*see* Distributed load)
equivalent axial stiffness
 Ernst's formula, 473
 guyed tower modeling, 471–472
 Millau Viaduct Bridge, France, 471
 modified elastic modulus, 472–473
 steel cable, 473–474

Indeterminate

arches, 684, 689
beams
 first degree, 647, 650, 662
 second degree, 652, 664, 668
frames
 first degree, 694, 698
 second degree, 705
pitched roof trusses, frames (*see* Pitched roof frames)
plane truss, 63
portal frames, 698–699
trusses
 internal force distribution, 714–715
 member forces, determination, 715–719
 principle of virtual forces, 712–713
 structures, 712, 713
 three member truss, 712, 714

Influence lines

actual loading distribution, 120
bending moment, 290–291
cf vs. af, 120
chord forces, 123
deck-beam system, 117
deck segments gf and fe, 117, 119
diagonal members, function, 120
force parameters, 961–962
live load analysis, gable roof structure, 124–131
loading, 117
loading zones, moment at A, 958, 959
load positions and corresponding member forces, 117, 118
member ab and fg, 124
Müller-Breslau principle application, 957–958
peak value, member force, 120
positive moment at D, 958, 959
“shear”, 120
shear force, 291–297

- Influence lines (*cont.*)
- slender members, compression *vs.* tension, 121–122
 - span beam, 960
 - structure and truck loading, 124
 - truss geometry, 117, 118
 - virtual work, principle
 - arbitrary virtual displacement patterns, 298–299
 - cantilever construction-concentrated loading, 310–312
 - construction, 304–309
 - equilibrium equations, 299–300
 - internal moment, 301–302
 - internal shear, 301–304
 - uniform design loading-cantilever construction, 313–316
- Integral abutment bridges
- elevation—three-span, 963, 964
 - idealized models, 963, 965
- Internal bending moment, 205
- Internal forces
- free body diagram
 - segment ABD, at D, 199
 - segment ABE and FCD, at E and F, 202
 - segment BC, at B, 227
 - segment BCDE, at B, 201
 - segment BCDEF, at B, 230
 - planar loading
 - beam and eccentric lateral load, 210–212
 - cantilever beam and multiple concentrated loads, 207–209
 - internal shear and moment, 205
 - maximum bending moment and shear force, 206
 - “shear” and “moment” diagrams, 206
 - sign convention, 205–206
 - uniform loading and cantilever beam, 209–210
 - structural analysis, 35–38
- J**
- Joints
- definition, 51
 - deflections, 100
 - 3-D trusses
 - analysis process, 141
 - direction cosines, 140
 - displacement computation, 147–149
 - force equilibrium equations, 139
 - resolution, force, 140
- tetrahedron, analysis, 144–147
- tripod structure, analysis, 141–143
- equilibrium, 93–94
- method (*see* Method of joints)
- pin joint connections, 59
- K**
- Keystone arch construction, 490
- Kirchoff's hypothesis, 235
- K-type truss, 89–91
- L**
- Lambe, T.W., 604
- Lane load, 19, 20
- Lateral loading
- building response
 - center of mass, 1026–1029
 - center of twist (*see* Center of twist)
 - description, 1011
 - forces acting, center of mass, 1030
 - matrix formulation (*see* Matrix formulation)
 - multistory response, 1032–1035
 - stiffness elements, 1031–1032
 - center of mass, 1061–1062
 - center of twist, 1064
 - center of twist and seismic floor loads, 1060
 - deflection profiles, 413–415
 - displaced configuration, 1063
 - frames, 1066–1067
 - 3-hinge gable frame, 389–391
 - lateral force, 1062–1063
 - multistory building systems, 999–1001
 - one story plan view, 1065
 - pitched roof frames, 382, 385–386
 - portal frames, 375, 377
 - story rigid frames, 1057–1059
 - symmetrical buildings (*see* Symmetrical buildings)
 - treatment
 - earthquake loading, 1003–1011
 - rectangular buildings, 1001–1002
 - wind loading, 1002–1003
- Line elements, 4, 7, 236
- Live load gravity, 19–20
- Live load patterns
- deflection pattern
 - beams, negative moment, 1074, 1076
 - columns, negative moment, 1074, 1076
 - positive moment, 1074, 1075
 - earthquake analysis, 1081–1086

- gravity type loading, 1074
loading pattern
 columns, maximum negative moment, 1075, 1076
 maximum positive moment, 1074, 1075
multistory frame, 1074, 1075
uniformly distributed live load, 1077–1080
- Live loads, bridges
 transverse distribution, truck load
 (see *Transverse distribution, truck loading*)
 truck loading and span discretization, 968, 969
 uniform live load, 971–972
- Loading pattern
 computer-based analysis, 978
 dead load, 978–979
 span discretization, 978, 979
- Loadings
 codes and technical societies, 14
 earthquake (see *Earthquake loading*)
 gravity live loads, 19–20
 properties
 importance factor, values, 18–19
 occupancy categories, 18
 quasi-static loading, 17–18
 temporal variation, 17
 snow, 26–28
 source
 construction, 15–16
 function, 15
 interaction, environment, 15
 terrorist loads, 16
 wind (see *Wind load*)
- Local reference frame
 member and nodes, 890, 891
 nodal forces, 893
 rotation matrices, 892
 rotation of axes, 890, 891
 structure, 890
- Low-rise rigid frames
 bracing, 863–870
 shear stiffness method, 857–863
- M**
- Mass, 15, 17, 22, 28–30
- Matrix formulation
 displacements, computation, 154–160
 floors and stories, 1035–1036
 force equilibrium equations, 152–154
 inertia forces, 1037
 manual techniques, 150
- member-node incidence, 152
notation, 150–151
- Rigid frames
 end forces and displacements, 887
 fixed end forces, 889
 linearly loaded beam, 889
 member stiffness matrices, 888–889
stability, 154
story structure, 1038
system load, mass and stiffness matrices, 1039
- Maxwell's law
 compatibility equations, 647
 definition, 644
 reciprocal loading conditions, 644–646
- Member equations
 frame-type structures (see *Frame type structures, member equations*)
 matrix formulation for rigid frames (see *Matrix formulation, rigid frames*)
- Method of joints
 application, 68
 cantilever truss analysis, 78–80
 five member truss, 71–77
 force components, 67, 68
 gable roof truss analysis, 80–83
 plane truss, 67
 three member truss analysis, 68–71
 zero force member, 68
- Method of sections
 chord trusses, 85
 design, 161
 equilibrium equations, 83–84
 hybrid analysis strategy, 91–94
 joints, 83
 K-type trusses, analysis, 89–91
 parallel chord truss, 85–87
 roof truss, 87–89
 “shear” forces, 85
- Method of virtual forces
 bending, slender beams, 259
 deflection computation, 260–270
 displacement, roller support, 436
 horizontal deflection determination, 434–437
 horizontal displacement, 436
 vertical deflection determination, 434, 435, 438
- Modern cables, 443
- Modulus of elasticity, 38, 49
- Moment area theorems, slender beams
 cantilever beam, 246–249
 cross-sectional rotation and deflection, 243

- Moment area theorems (*cont.*)
 - double integral, 244
 - “First Moment Area” theorem, 244
 - integration, x_1 and x_2 , 244
 - “Second Moment Area Theorem”, 245–246
 - simply supported beam, 249–254
- Moment distribution
 - frame structures (*see* Sideway)
 - multi-span beams
 - dimensionless factor (DF), 790
 - incremental moments, 791
 - iteration cycle, 789
 - method, 789
 - moment equilibrium, 790
 - moment release, two span beam, 793–795
 - multiple free nodes, 795
 - reduced relative rigidity factor, 793
 - solution procedure, 788–789
 - three span beam, 795–799
 - two span beam, 791–793
 - unbalanced clockwise nodal moment, 789–790
- Moment envelopes for bridges. *See* Live loads, bridges
- Müller-Breslau principle
 - influence lines (*see* Influence lines)
 - live load patterns (*see* Live load patterns)
- Multi-bay
 - masonry frames, 643
 - portal frame, 356
- Multiple concentrated loads
 - force envelopes
 - absolute maximum moment, 322
 - computation, maximum moments, 322–326
 - critical truck loading position, 327
 - dead + truck loading, 328
 - forces, 319
 - M_1 and M_2 , maximum value, 320
 - maximum bending moments, 321
 - moment diagram-arbitrary position, loading, 319, 320
 - truck moving across, span, 327
 - internal forces, cantilever beam, 207–209
- Multi-span beams (gravity loading)
 - data-moment diagrams
 - single-span, 844
 - three-span, 844, 845–846
 - two-span, 844
 - quantitative reasoning, relative stiffness, 844–848
- Multi-span beams force method
 - analytical solutions (*see* Analytical solutions, multi span beams)
 - structures, 643
- Multi-span bridges
 - geometric configurations
 - elevation—multi-span bridge, 962, 964
 - idealized models, 963, 965
 - integral abutment bridge, 963, 964
 - span arrangements, 962, 963
 - live loads, bridge (*see* Live loads, bridges)
 - span lengths
 - bending moment distribution, 965–966
 - symmetrical scheme, 965, 967
 - support settlements (*see* Support settlements)
- Multi-span horizontal structures
 - cable-stayed
 - bridge, 986–991
 - structure, 997–998
 - engineering process, girders, 955–957
 - global deflection, 995
 - idealized tied arch, 996
 - influence lines, 957–962, 992–993
 - internal forces, 995
 - multi span bridges (*see* Multi span bridges)
 - single span bridge, 993
 - span lengths, 993–994
 - symmetrical cable structure, 998
 - three-span continuous girder bridge
 - (*see* Three-span continuous girder bridge)
 - three-span parabolic arch response, 985–987
 - two-hinged parabolic arch response, 982–985
- Multistory buildings
 - braced frames, N-S and E-W directions
 - beam properties E-W direction, 1093
 - bending moment and shear, 1091–1092
 - bracing systems, 1093–1097
 - configuration, 1091
 - deflection, 1092
 - floor loading, 1091
 - interior columns, 1097
 - result, 1098
 - four-story building
 - floor plan and elevation structure, 1087
 - global wind loads, 1088
 - loading and member data, 1087
 - gravity floor loads, treatment (*see* Gravity floor loads)

- live load patterns (*see* Live load patterns)
loading patterns estimation,
 Müller–Breslau principle,
 1113–1120
load paths, 1112–1113
loads, frames
 rectangular building, 1069–1071
 structure, 1069, 1070
 system, 1069
rigid frames, N-S and E-W direction
 beams, N-S, 1101
 braced *vs.* rigid frame, 1098, 1099
 columns, N-S, 1101
 connection, N-S beams
 and columns, 1098
 dead load, 1105, 1106
 design values, 1107–1111
 live load moments, 1106–1107
 live load patterns, 1102
 moment diagrams, 1102–1105
 result, 1112
 uniform live load, 1105, 1107
 wind load N-S, 1105, 1108
systems
 braced frame structure, 1000–1001
 lateral stiffness systems, 1001
 low-rise building, 999–1000
- Multistory response
forces
 floor, 1033
 inertia, 1034
 interstory deformation, 1032
 shear beam, 1035
- Multistory rigid and braced frame, 356
- Multistory rigid frames
gravity loading, 848–849
lateral loading
 approaches, estimation, 850
 inflection points, 849
 low-rise, bracing, 863–870
 portal method, 850–857
 shear stiffness method, 857–863
- N**
- Nodal equilibrium equations
direct stiffness method, 898
equilibrium equations, 897
member end actions, 894–895
member node incidence, 893–894
member reaction forces, 896
positive/negative end, 893
system matrices, 899–900
- Nodes
concurrent force system, 62
description, 51
horizontal displacement, 107–109
member af and cf, extreme values, 120
and member incidence, 152
plane trusses, 137
positive and negative, member *n*, 150
scalar equilibrium equations, 62
- Non prismatic members, 270–274
- O**
- Optimal shape
parabolic arch, 503
statically determinate arch, 532–533
- Out of plane bending, 826
- Out of plane loading
end actions, 821–822
equilibrium equations, 824
free body diagrams, 822–823
grid structure, 824–825
plane frames
 displacement and rotation, 416, 419
 3-D system, 415, 418
 free body diagram, 416, 418
 gravity load, 415–416
 highway signpost, 416, 418
 transversely loaded
 grid structure, 419
 prismatic member, 821
- Overturning
base pressure distribution, 628
defined, 606
vs. safety, 618
stability, 627
toe and sliding, 605
- P**
- Parabolic geometry
notation, parabolic shape function, 502, 503
 O_{\max} *vs.* h/L tabulation, 504
shallow *vs.* deep parabolic curved
members, 505–510
- Passive soil pressure, 605
- Pattern loading
three-span system, 971, 972
uniform dead and lane, 978
- Peak acceleration, 28–30
- Peak pressure, 551, 552, 574
- Peck, R.B., 549, 604
- Piles/caissons, 546, 621

- Pitched roof frames
 analytical solutions
 gable frame (*see* Gable frame)
 gravity loading, 381–384
 lateral loading, 382, 385–386
 displacement profiles, shear and moment diagrams, 439
 expression, horizontal reaction, 709
 flexibility coefficients, 708
 member loads
 equivalent vertical loading, 380
 inclined member, 378–379
 normal and tangential directions, 380–382
 reactions, 379–380
 peak negative and positive moments, 711
 primary structure, 707, 709
 relative stiffness factors, 708–709
 structures, 378
 three-hinge solution, 711
 total bending moment distribution, 709–711
 two *vs.* three-hinge solution, 712
- Planar beam systems, 193
- Planar bending
 definition, 186
 stability and determinacy, beams (*see* Stability)
 transverse displacement, 329–330
- Planar loading, beams. *See* Beams
- Planar trusses
 analysis
 axial force, 61
 complex trusses (*see* Complex trusses)
 equilibrium considerations, 61–62
 joints (*see* Joints)
 sections (*see* Sections)
 stability criterion (*see* Stability)
 statically determinate, 62–63
 bottom and top nodes, 54
 complex and compound, 53
 simple planar truss construction, 52
 structure, 102
 two member, 102, 103
- Plane frames
 statically determinate (*see* Statically determinate plane frames)
 transverse deformation, 694
- Plane trusses
 2-D, 137
 definition, 51
 member forces, 164–170
 node, 61
 statical determinacy, 161
- Platforms, 3, 4, 15
- Portal frames
 anti-symmetrical loading, displacement method
 chord rotation, 781
 frame with no sideway, 783–785
 frame with sideway, 785–788
 moments and shear, 782–783
 slope-deflection equations, 782
 behavior (*see* Behavior)
 bending moment distribution, 703–705
 expression, displacement, 695
 gravity-loading
 anti-symmetrical model, 700, 701
 bending moment distributions, 702
 compatibility equation, 701–702
 decomposition, loading, 699, 700
 horizontal reaction, 702
 net bending moment distribution, 703
 peak moments, 703
 symmetrical model, 700, 701
 two-hinged, 699, 700
 lateral loading symmetrical bending moment
 distribution, 699, 700
 displacement, 697
 models, 699
 two-hinged, 698–699
 overhang, 371–373
 reaction, gravity loading, 695, 696
 simply supported, 366–368
 structure, 695, 696
 symmetrical
 anti-symmetrical loading, 705–706
 bending moment distribution, two-hinged frame, 706, 707
 displacement, 705
 hinged and fixed supports, bending moment distribution, 707, 708
 structures, 705
 symmetrical loading, displacement method
 description, 779, 780
 moment equilibrium, 780–781
 three-hinge (*see* 3-Hinge frames)
- Portal method
 axial and shear forces, 851, 853, 854, 856
 bending moment distribution
 beams, 851, 852, 854, 856
 columns, 851, 852, 854, 855
 description, 850, 876
 moments, joints, 851, 852, 854, 855

- reactions, shear forces and moment distribution, 851, 853, 854, 857
- rigid frame, 850, 854
- shear distribution
 beams, 851, 853, 854, 856
 columns, 851, 854
- steel frame, 880
- Positive sense, bending, 361
- Primary structure
 description, 636
 displacement, 639, 653
 fixed end moments, 670
 flexibility
 coefficients, 640
 matrix, 695
 force redundants, 641–642
 geometric compatibility equation, 637
 multi-span beam, 643
 pitched roof frames, 707–709
 redundant moment, 682
 vertical restraints, 638
- Principle of virtual forces
 axial and shear forces, 400
 deflections, computation
 cantilever-type structure, 400–403
 horizontal displacements and rotation, 403–406
 non-prismatic member, 408–412
 steel structure, 406–408
 low-rise frames, 400
 planar frame structure, 399–400
- Prismatic beams
 “combined bending and torsion”, 186, 188
 cross-sections and bending mode, 185, 186
 geometrical parameters and notation, 185, 187
- Mechanics Theory, 188
- planar bending, 186, 187
- Q**
- Qualitative reasoning, deflected shapes
 beam and moment release, 242–243
 cantilever beam, 241–242
 moments, positive and negative, 238, 239
 overhang and beam, 242
 positive and negative curvature, 238, 239
 shape transition at inflection point, 239
 supports-displacement measures, types, 239, 240
- uniformly loaded and simply supported beam, 240–241
- R**
- Rankine theory
 defined, magnitude per unit wide strip, 604–605
 distribution, soil pressure, 604
 horizontal forces, 605
 soil pressure, surcharge, 605
- Reactions
 planar loading
 beam and two overhangs, 196–197
 beam free body diagram, construction, 200
 horizontal beam supports, vertical sign, 203–204
 segment BCDE, 201
 simply supported beam, 197–198
 statically determinate and indeterminate structure, 196
 three-span beam and two moment releases, 202
 two-span beam and moment release, 198–200
 structural engineering forces, 35, 36
 statically indeterminate beam, 46–47
 supports, planar structures, 10, 11
- Redundant
 cable force, 659
 displacements, primary structure, 665–666
 external loading, 653
 force
 expression, primary structure, 642
 reaction, 638, 641
 steps, 636
 internal force, 643
 matrix equations, 694–695
 tension, tie, 691
 three-span beam, 652
- Relative stiffness
 bending moment distribution, 676
 clamped/hinged model, 848
 DF_{BC} vs. DF_{BA} , 847
 end moments estimation, 850
 flexibility coefficients, 708–709
 hinged and clamped end model, 848
 internal force distribution, 715
 member distribution factors, 845
 multi-span beam, 845, 846
 qualitative reason, 876–877
 two-span beam, 678
- Resultant
 centroid, 551
 combined footings, 565

- R**
- Resultant (*cont.*)
 - factored loads, 566
 - force, 550
 - line of action, 552, 564
 - pressure distributions, 578
 - Retaining walls. *See* Vertical retaining wall structures
 - Rigid body motion
 - prevent
 - arranged, 64
 - insufficient, 65–66
 - order, 133
 - reactions, 95–96
 - required, 62
 - respect, 132
 - supported, 52
 - restraining, 133–137
 - Rigid frame
 - displacement method
 - anti-symmetrical loading, portal frames, 781–788
 - description, 775
 - free body diagrams, members and nodes, 777, 778
 - moment equilibrium, 777–778
 - sideway, 776
 - slope-deflection equations, 779
 - symmetrical loading, portal frames, 779–781
 - five story symmetrical rigid frame building, 1081–1086
 - lateral loading, 382, 385
 - masonry, 356
 - N-S and E-W directions (*see* Multistory buildings)
 - pitched roof frames, 378
 - simply supported gable, 382–383
 - triangular, 441
 - Roller support, 191, 192
 - Rotation, 360, 400–401, 403, 406, 415, 419, 434–436
- S**
- Sag
 - arc length, 464–468
 - concentrated loads, horizontal cables
 - angle of inclination, relationship, 448
 - downward vertical, 451
 - expression, 445–446, 449
 - profile, 452, 453
 - distributed loading, 458, 459, 462
 - equivalent axial stiffness, 469, 471
 - inclined cables and concentrated loading, 455–458
 - Sandy soil
 - allowable pressures, 548, 549
 - pressure distributions, 547, 548
 - Sections
 - cantilever walls design, 623–627
 - method (*see* Method of sections)
 - Shallow curved members
 - vs. deep, 514–515
 - non-shallow curved member, 513–514
 - trigonometric measures, 504
 - Shallow foundations
 - allowable soil pressure, 589
 - combined footing, 593
 - dimensioning, combined footings (*see* Combined footings)
 - dimensions, square/rectangular, 591–593
 - pad footing, 596
 - service loads, 589
 - single rectangular footing, dimensioning (*see* Single footings)
 - soil pressure distribution (*see* Soil pressure distributions)
 - square columns, 591–593
 - strap footing, 594–595
 - strap footings, dimensioning (*see* Strap footings)
 - types
 - combined footing, 547
 - footings, 546
 - single footing, 546
 - strap footing, 547, 548
 - structure, 545, 546
 - superstructure, 545
 - Shear beam models, matrix formulation.
 - See* Matrix formulation
 - Shear force
 - influence line
 - construction, 293–297
 - cross-section location, 291, 293
 - at location x_1 , 292
 - single concentrated force, 291, 292
 - maximum bending moment, 206
 - maximum moment occurs at mid-span, 510
 - transverse, 275
 - Shear stiffness method
 - approximate analysis, 862–863
 - bottom story-fixed support, transverse shear model, 860
 - definition, idealized model, 857
 - description, 876

- elements, 1041
exterior and interior element—upper story, 859
factors, 1040, 1041
low-rise frame, 857, 858
parameter, 863
ratios
 lowest story, 861
 upper stories, 859
slope-deflection equations, 859
steel frame, 880
sub-elements, base story
 fixed support, 860
 hinged support, 861
total transverse shear, 857
- Shear walls, concrete frame, 1000
- Shell, 4, 7
- Sideway
 with sideway, frame's moment distribution
 computer-based analysis, frame with inclined legs, 818–821
 fixed end moments, 809–810
 frame with inclined legs, 813–817
 “holding” forces, 809
 portal bent, 810–813
 without sideway, frame's moment distribution
 end actions, 800–802
 support settlement, two-bay portal frame, 804–806
 symmetrical loading, two-bay portal frame, 802–804
 temperature increase, two-bay portal frame, 806–809
- Sign convention
matrix formulation, beam bending problem, 205–206
positive directions, 205
- Simple planar truss, 52, 54
- Simple space truss, 52
- Single footings
 column position, 554
 dowels use, 557
 effective soil pressure, 554
 procedure, 555
 service loads, 557–559
 shear and moment, 555–556
 shear, location, 555, 556
 square/rectangular, 560–564
 steel reinforcement, 556, 557
- Slender beams
centroidal axis, strain, 236
conjugate beam method, 254–259
- cross section rotation angle, 237
curvature relationship, moment, 237–238
differential elements, 236, 237
express and curvature, extensional strain, 237
homogeneous beam, 235, 236
Kirchoff's hypothesis, 235
moment area theorems, 243–254
non-prismatic members, 270–274
qualitative reasoning, deflected shapes
 (*see* Qualitative reasoning, deflected shapes)
virtual forces method, 259–270
- Sliding
defined, 606, 608
vs. safety, 607
stability, 627
- Slope deflection equations, out of plane loading
 See Out of plane loading
- Snow load
drift profiles, 28
flat and sloped roof, 26–28
- Soil friction angle, 627
- Soil pressure distributions
allowable pressures, 548, 549
analytical method
 equilibrium, 550
 line of action, 552
 peak pressure, 551–552
 plan, rectangular area, 552, 553
 single footing, 550
 trapezoidal, 551
concentric load, 547, 548
description, 547
determination, 587–588
dimensions, footing, 547–549
footing/wall base, 612
Rankine theory, 604–605
- Spectral acceleration, 1007–1008
- Stability
and determinacy, beams
concurrent displacement constraints, 188, 189
3-D fixed support, 192
3-D hinged support, 192
3-D roller support, 192
fixed and hinged support, 190
moment release, 194–195
multiple supports, 193–194
planar rigid body motions, 188, 189
roller support, 191
static determinacy, 193
unstable support arrangements, 193
X-Y plane, 188

- Stability (cont.)**
- 3-D trusses, equilibrium analysis
 - Cramer's rule, 154
 - requirement, 154
 - planar truss
 - complex truss, 66–67
 - compound truss, 66
 - equilibrium equations, 64
 - "initial instability", 64
 - plane truss, 63
 - simple and compound trusses, 67
 - simple trusses, 64–66
 - suitably restrain, 64
 - unstable, motion restraints, 64
 - structural engineering
 - initial, 10–12
 - loss and material failure, 12–13
 - priorities, 14
 - vertical retaining wall structures (*see* Vertical retaining wall structures)
- Stabilizing effect, 601**
- Statical determinacy**
- beams (*see* Beams)
 - plane frames (*see* Statically determinate plane frames)
- Statically determinate beams**
- engineering process, 287–289
 - force envelopes (*see* Force envelopes)
 - influence lines (*see* Influence lines)
- Statically determinate curved members**
- arch-type structures, 489–494
 - factors and concepts, 534
 - internal forces, 498–503
 - models, arch structures, 494–498
 - objectives, 533
 - parabolic geometry, 503–510
 - problems, parabolic member, 534–544
 - three-hinged arches, analysis, 518–533
 - virtual forces
 - circular, 515–518
 - displacements, 510–511
 - non-shallow slender, 511
 - shallow slender, 511–515
- Statically determinate plane frames**
- A-frame (*see* A-frame)
 - analysis (*see* Analysis)
 - axial forces and end moments, 441
 - beams and columns, 355
 - bending moment distributions, 428–432
 - computer-based analysis, 415–417
 - deflection profiles (*see* Deflection profiles)
 - displacement determination, 442
- out of plane loading (*see* Out of plane loading)**
- pitched roof frames (*see* Pitched roof frames)**
- planar loading**
- adequate support schemes, 357
 - indeterminate portal and A-frames, 359–360
 - indeterminate support schemes, 357–358
 - nodal forces and rigid plane frames, 358–359
 - three-hinge plane frames, 358
- reactions, shear and moment distributions, 420–428**
- rigid plane frames, 355–356**
- steel material, 440**
- virtual force**
- method, 434–438
 - principle (*see* Principle of virtual forces)
- Static determinacy**
- 2-D plane trusses, 137
 - stable determinate structure, 137–138
 - structure, 137
 - unstable structure, 138–139
- Steel base plate, 556, 557**
- Stiffness**
- definition, 39
 - material, 31
 - method, 45
- Stiffness factor, 44**
- Straight members**
- "equivalent", 472
 - slender, 511
- Strand, 444, 471**
- Strap footings**
- description, 575
 - design approach, 578–580
 - equilibrium, 576–577
 - notation and pressure
 - distribution, 575, 576
 - parallel axis theorem, 577
 - reinforcing pattern, 578, 580
 - soil pressure profile, 581–586
 - summing moments, 578
- Structural components, 3, 4, 11, 13, 35, 47**
- Structural engineering**
- analytical tools (*see* Analytical tools, structural analysis)
 - buckling failure mode, 13–14
 - components and types, 4–9
 - description, 3

- design
 loading, 7, 10
 philosophy, 30–31
 load, types (*see* Loadings)
 reactions, 10, 11
 stability
 initial, 10–12
 loss and material failure, 12–13
 priorities, 14
 Structural idealization, 54
 Structural types
 function, 4–6
 makeup, 4, 7–9
 Superposition, 744, 745
 Support constraints, 886
 Support settlements
 moments, 974
 resulting moments, 975–976
 three-span beam, 975
 Surcharge, soil pressure, 605, 627
 Surface elements, 4, 7
 Symmetrical buildings
 earthquake floor loads, 1047
 floor load distribution, 1048
 frame load-rigid and flexible floors, 1048–1049
 idealized building model, 1041–1042
 maximum column moments-rigid and flexible floors, 1050
 one story frame, 1051–1056
 rigid frame building, 1046
 rigid frame structure, 1042–1043
 segmental areas, 1044–1045
 shear stiffness factors, 1041
 structure, 1039
 total story stiffness, 1043–1044
 typical floor, 1043
 typical frame, 1040
 Symmetry and anti-symmetry
 deflected shapes, 283–287
 shear and moment diagrams, 280–283
- T**
- Tall building
 lateral deflections, 870, 871
 quantities, M_{i+1} and V_{Ti+1} , 870
 segment, 871
- Tandem, 19, 20
- Temperature change
 effect, 115
 total extension, 101
- Tension
 cable-stayed structures, 444
- concentrated loads
 horizontal cables, 448–450, 452
 inclined cables, 456–458
- determination
 catenary equations, 477–478
 maximum tension, 482–484, 488
 peak values, 486
 segment, cable, 479–482
- distributed loading
 horizontal cables, 459–460
 inclined cables, 463–464
 equivalent axial stiffness, 470–472
- Terrorist loads, 16
- Terzaghi, K., 549, 604
- Thermal loading, 15
- Three-dimensional (3D) formulation
 displacement measures, 936–938
 notation, 935–936
- Three-dimensional (3D) trusses
 equilibrium analysis, 132
 joints, 139–149
 restraining rigid body motion, 133–137
 restraints, rigid object, 133
 space truss structures, 132
 static determinacy, 137–139
 tetrahedron units, 3-D trusses, 132
- Three-hinged arches
 and geometry and reactions, 519
 one degree indeterminate, 497
 optimal shape, statically determinate arch, 532–533
- parabolic arch
 concentrated load, mid-span, 526–529
 force equilibrium, 520–521
 horizontal and vertical loads, 530–532
 moments, A and C, 520
 uniform vertical loading, 521–525
 R_{Bx} and R_{By} , 519
- Three-span arch study
 discrete force envelopes, 985, 987
 idealized model, 985–986
- Three-span continuous girder bridge
 axle loading, 977
 cross-section, 976–977
 loading patterns, 978
 support settlement, 981, 983
 truck loading, 980–982
 uniform lane load, 980
- Three-span parabolic arch response, 985–987
- Thrust, 691, 692
- Tied arches, 691

- Torsional response
 floor rotation, 1017
 shearing, 1035
- Tower, 3, 4, 16
- Transverse distribution, truck loading
 axle distribution factor, 971
 loading, 971
 slab-stringer bridge deck cross-sections, 968, 970
 vehicle wheel loads, 968, 970
- Trapezoidal rule, 272
- Truck load, 19, 20
- Truss *See also* Truss structures
 defined, 7
 formulation
 fixed end actions—members and joints, 922
 force and displacement, 917
 load vectors, 921
 local and global frames, 918
 stiffness matrix and displacement vector, 920
 topological and geometric information, 919
 unknown displacements, 922–923
 indeterminate (*see* Indeterminate, trusses)
- Truss structures
 deflections, computation (*see* Deflections)
 facts and concepts, 161–162
Influence lines (*see* Influence lines)
 matrix formulation
 displacements, computation, 154–160
 force equilibrium equations, 152–154
 manual techniques, 150
 member–node incidence, 152
 notation, 150–151
 stability, 154
 objectives, 161
 planar trusses, analysis
 complex trusses, 94–100
 3-D space structures, 61
 equilibrium considerations, 61–62
 joints, method, 67–83
 sections, method, 83–94
 stability criterion, 63–67
 statically determinate planar trusses, 62–63
 problems
 computer software, 175–177
 cross-sectional area, 174–175
 interior truss, quantities, 180–183
 and loading, 177–180
 member forces, plane trusses, 164–170
- plane trusses, classification, 162–164
 virtual forces, 170–174
- three-dimensional trusses (*see* Three-dimensional trusses)
- types
 complex planar, 53
 compound planar, 53
 compression elements, 57
 covered wood bridges, 55, 56
 Egyptian boat built, 54–55
 flourishing industry, New England, 55
 force parallelogram, 55
 high-strength bolts and welding, 58
 iron trusses, 57–59
 pin joint connections, 58, 59
 “plane” and “joints”, 51
 simple planar and space, construction, 52
 single span truss bridge system, 54
 steel, 57–58
 structural systems, 54
 three-dimensional truss roof system, 60
 wooden bridge truss structures, 55
- Two-hinged arch
 and one degree indeterminate, 497
 structure, 494
- Two-hinged parabolic arch response
 discrete force envelopes—truck loading, 982, 984–985
 idealized model, 982, 984
- Type of foundations
 footings
 combined, 547
 description, 545–546
 single, 546
 strap, 547, 548
 structure, 545, 546
 superstructure, 545
- U**
- Ultimate
 rectangular footing, 568
 shear and moment, 555–556
- Unstable
 initially, 65–66
 structure, 138–139
- V**
- Vertical retaining wall structures
 backfill material (*see* Backfill material)
 cantilever, 601, 618–620

- concrete piles, 621–623
design, cantilever walls, 623–627
with footing, 612–618
gravity, 600–601
gravity wall, 607, 611
peak pressures, 611
stability analysis
 cantilever and gravity, 607
 concrete gravity wall and soil backfill, 607–611
 defined, safety for sliding, 606
 equilibrium, 605
 force summation, 606
 gravity wall, 605, 606
 overturning, 606
types, 599–600
- Virtual forces method
 and actual force, 112
application, 161
curved members
 circular, 515–518
 displacements, 510–511
 non-shallow
 slender, 511
 shallow slender, 511–515
definition, 105
deflection, computation, 106–111
diagonal pattern reversed, 114
matrix equilibrium equations, 156
principle, 115, 170–175, 183
procedure, 105
- W**
Whitman, R.V., 604
Wind load
 pressure
 distribution, 20–21
 profiles, 22–25
 vortex shedding, 26
 velocity distribution, 22, 23
Wind loading, 1002–1003
Wind pressure
 distribution, 20–21
 profiles
 Bernoulli's equation, 22
 low-rise gable roof structure, 24–25
 stagnation and design pressure, 23–24
 vortex shedding, 26
Wind speed, 22, 23
Wind velocity, 22
- Y**
Yielding support, beam
 axial force, 661–663
 cable-stayed schemes (*see* Cable stayed)
 deflection, 656–657
 external concentrated loading, 658–659
 force redundant and displacement profiles, 655, 656
 force redundant system, primary structure, 657–658
 linear elastic behavior, 655–656
 supporting members, 654–655
 vertical restraint, 655